



Section III

STATE OF AIR, LAND, AND WATER

These chapters present carbon cycle fluxes and processes in different physical and ecological domains, including the atmosphere, soils, inland and coastal waters, and the coastal ocean, as well as in terrestrial ecosystems such as forests, grasslands, and those in Arctic regions. Understanding these ecosystems is fundamental to assessing and predicting net carbon sources and sinks, including feedbacks to and from the climate system. These ecosystems also represent key carbon reservoirs with sensitivity to changes in climate and atmospheric composition.

Chapter 8

Observations of Atmospheric Carbon Dioxide and Methane

Chapter 9

Forests

Chapter 10

Grasslands

Chapter 11

Arctic and Boreal Carbon

Chapter 12

Soils

Chapter 13

Terrestrial Wetlands

Chapter 14

Inland Waters

Chapter 15

Tidal Wetlands and Estuaries

Chapter 16

Coastal Ocean and Continental Shelves



8 Observations of Atmospheric Carbon Dioxide and Methane

Lead Authors

Andrew R. Jacobson, University of Colorado, Boulder, and NOAA Earth System Research Laboratory;
John B. Miller, NOAA Earth System Research Laboratory

Contributing Authors

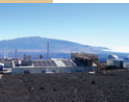
Ashley Ballantyne, University of Montana; Sourish Basu, University of Colorado, Boulder, and NOAA Earth System Research Laboratory; Lori Bruhwiler, NOAA Earth System Research Laboratory; Abhishek Chatterjee, Universities Space Research Association and NASA Global Modeling and Assimilation Office; Scott Denning, Colorado State University; Lesley Ott, NASA Goddard Space Flight Center

Acknowledgments

Richard Birdsey (Science Lead), Woods Hole Research Center; Nathaniel A. Brunsell (Review Editor), University of Kansas; James H. Butler (Federal Liaison), NOAA Earth System Research Laboratory

Recommended Citation for Chapter

Jacobson, A. R., J. B. Miller, A. Ballantyne, S. Basu, L. Bruhwiler, A. Chatterjee, S. Denning, and L. Ott, 2018: Chapter 8: Observations of atmospheric carbon dioxide and methane. In *Second State of the Carbon Cycle Report (SOCCR2): A Sustained Assessment Report* [Cavallaro, N., G. Shrestha, R. Birdsey, M. A. Mayes, R. G. Najjar, S. C. Reed, P. Romero-Lankao, and Z. Zhu (eds.)]. U.S. Global Change Research Program, Washington, DC, USA, pp. 337-364, <https://doi.org/10.7930/SOCCR2.2018.Ch8>.



KEY FINDINGS

1. Global concentrations of carbon dioxide (CO₂) and methane (CH₄) have increased almost linearly since the *First State of the Carbon Cycle Report* (CCSP 2007; see Figure 8.1, p. 339). Over the period 2004 to 2013, global growth rates estimated from the National Oceanic and Atmospheric Administration's marine boundary layer network average 2.0 ± 0.1 parts per million (ppm) per year for CO₂ and 3.8 ± 0.5 parts per billion (ppb) per year for CH₄. Global mean CO₂ abundance as of 2013 was 395 ppm (compared to preindustrial levels of about 280 ppm), and CH₄ stands at more than 1,810 ppb (compared to preindustrial levels of about 720 ppb) (*very high confidence*).
2. Inverse model analyses of atmospheric CO₂ data suggest substantial interannual variability in net carbon uptake over North America. Over the period 2004 to 2013, North American fossil fuel emissions from inventories average $1,774 \pm 24$ teragrams of carbon (Tg C) per year, partially offset by the land carbon sink of 699 ± 82 Tg C per year. Additionally, inversion models suggest a trend toward an increasing sink during the period 2004 to 2013. These results contrast with the U.S. land sink estimates reported to the United Nations Framework Convention on Climate Change, which are smaller and show very little trend or interannual variability.
3. During most of the study period covered by the *Second State of the Carbon Cycle Report* (2004 to 2012), inverse model analyses of atmospheric CH₄ data show minimal interannual variability in emissions and no robust evidence of trends in either temperate or boreal regions. The absence of a trend in North American CH₄ emissions contrasts starkly with global emissions, which show significant growth since 2007. Methane emissions for North America over the period 2004 to 2009 estimated from six inverse models average 66 ± 2 Tg CH₄ per year. Over the same period, CH₄ emissions reported by the U.S. Environmental Protection Agency equate to a climate impact of 13% of CO₂ emissions, given a 100-year time horizon.

Note: Confidence levels are provided as appropriate for quantitative, but not qualitative, Key Findings and statements.

8.1 Introduction

Atmospheric carbon dioxide (CO₂) and methane (CH₄) are the primary contributors to anthropogenic radiative forcing. Atmospheric concentration measurements of these two species provide fundamental constraints on sources and sinks, quantities that need to be monitored and understood in order to guide societal responses to climate change. These atmospheric observations also have provided critical insights into the global carbon cycle and carbon stocks and flows among major reservoirs on land and in the ocean. This chapter discusses atmospheric CO₂ and CH₄ measurements and their use in inverse modeling.

After decades of steady growth in anthropogenic carbon emissions associated with fossil fuel consumption, global emissions began to stabilize in

2014 and 2015 (BP 2016). Global emissions nearly doubled from 5,000 teragrams of carbon (Tg C) per year in 1980 to around 10,000 Tg C per year in 2015. In North America, emissions recently have been decreasing: in Canada from 151 to 141 Tg C per year between 2004 to 2013, and in the United States from 1,570 to 1,407 Tg C per year over the same time period (Boden et al., 2017). Nevertheless, the global atmospheric CO₂ concentration has passed the 400 parts per million (ppm) milestone (a part per million represents the mole fraction of CO₂ in dry air and is equivalently expressed as $\mu\text{mol per mol}$). Given the long lifetime of atmospheric CO₂, this global burden will continue to rise as long as net emissions remain positive.

The global atmospheric growth rate of CO₂ has averaged around half the rate of CO₂ input from fossil fuel combustion over the last 50 years, rising

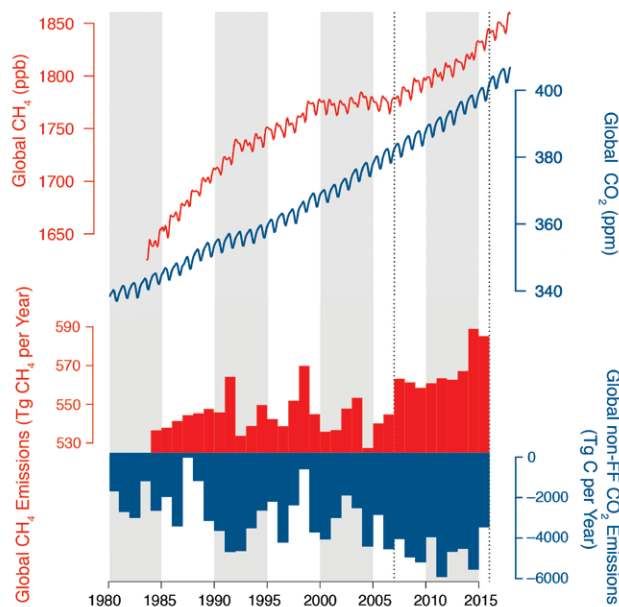


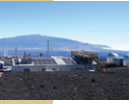
Figure 8.1. Global Monthly Mean Concentrations of Methane (CH₄; red line) and Carbon Dioxide (CO₂; blue line) and Global Annual Emissions of CH₄ (red bars) and Nonfossil Fuel Annual Emissions of CO₂ (blue bars). Global CH₄ and CO₂ concentrations (in parts per billion [ppb] and parts per million [ppm], respectively) are from the National Oceanic and Atmospheric Administration’s Marine Boundary Layer product. Methane emissions were generated from annual growth rates of marine boundary layer CH₄, assuming a CH₄ lifetime of 9.1 years. Carbon dioxide emissions were generated from annual growth rates of marine boundary layer CO₂, converted to emissions using a factor of 2,128 teragrams of carbon (Tg C) per year per ppm and removing anthropogenic fossil fuel emissions. From 1980 to 2016, these global fossil fuel emissions grew steadily from about 5,000 Tg C per year to about 9,200 Tg C per year (Boden et al., 2017). Dotted vertical lines in 2007 and 2016 represent approximate reference times for publication of the first and second *State of the Carbon Cycle* reports.

from less than 1 ppm per year in the early 1960s to around 2.5 ppm per year between 2010 and 2015 (see Figure 8.1, this page; Ballantyne et al., 2015). Although the growth rate varies substantially from year to year, mainly in response to the El Niño–Southern Oscillation (Bacastow 1976; Sarmiento et al., 2010), the trend in net CO₂ absorption by the terrestrial biosphere and the ocean has increased from around 2,000 Tg C per year in 1960 to nearly

5,000 Tg C per year in 2015 (see Figure 8.1, this page; Ballantyne et al., 2015). Although the total sink is well constrained, now limited mainly by the ~5% to 10% uncertainty on global fossil fuel emissions, its partitioning between land and ocean and on land between continents is still uncertain. Accordingly, there is no consensus on the fraction of the global sink in North America, although almost all inventory, biospheric model, and atmospheric studies show it to be a sink (King et al., 2015).

The global abundance of CH₄ grew significantly from 1984 to 1996, but between 1997 and 2006 there was no significant change in global burden (see Figure 8.1, this page). This quasi-asymptotic behavior can be explained as an approach to steady-state concentrations (Dlugokencky et al., 1998). The balance between surface sources and atmospheric chemical loss, which is mainly due to oxidation by hydroxyl radicals, can be explained by constant emissions and a constant atmospheric CH₄ lifetime. For the emissions calculations reported in this chapter, a value of 9.1 years was used for this lifetime (Montzka et al., 2011). Indeed, global net emissions exhibited variability but no significant trend between 1984 and 2006 (Dlugokencky et al., 2011; see Figure 8.1, this page). After 2007, however, global CH₄ abundance began to rise rapidly (e.g., Dlugokencky et al., 2009; Nisbet et al., 2016), implying an increase in global emissions from 541 ± 8 Tg CH₄ per year (1999 to 2006) to 569 ± 12 Tg CH₄ per year (2008 to 2015). Emissions in 2014 and 2015 are particularly large, with a mean of 587 ± 3 Tg CH₄ per year. Analysis of trends in the ¹³C:¹²C content of CH₄ (δ¹³C) indicates that, at global scales, the rise since 2007 resulted predominantly from changes in microbial emissions (e.g., wetlands, livestock, and agriculture) and not fossil fuel–related emissions (Schaefer et al., 2016; Schwietzke et al., 2016). Moreover, because the recent CH₄ trend displays no significant meridional gradient, much of this new emissions increment likely originated in the tropics (Nisbet et al., 2016) and not in the northern midlatitudes.

Global total emissions of CO₂ and CH₄ are well constrained by available atmospheric measurements;



however, using these measurements to attribute to sources and sinks (e.g., fossil emissions versus terrestrial biosphere uptake) or partitioning between land and ocean regions remains difficult. In fact, even at smaller scales (i.e., continental regions as large as North America), substantial uncertainty remains about net contributions by terrestrial and aquatic ecosystems. The ability to use CO₂ and CH₄ time and space gradients to constrain North American sources and sinks is limited by current knowledge of atmospheric mixing and by the time and space density of calibrated observations (see Section 8.6, p. 349).

8.2 Historical Context

From the late 1950s through mid-1990s, measurements of atmospheric CO₂ and CH₄ concentrations were mostly targeted at understanding variations in “background” marine air, remote from the complex signals found over continents. Motivated largely by the finding of Tans et al. (1990) that Northern Hemisphere extratropical land regions were very likely a significant CO₂ sink, new attention was placed on understanding the role played by terrestrial ecosystems. New measurement sites were established on land, with an emphasis on platforms extending well into the daytime planetary boundary layer or higher, in an attempt to capture signals of regional (approximately 1,000 km) surface exchange (Gloor et al., 2001). This effort included observations on towers extending far above the ecosystem canopy (typically >300 m above ground level) and from light aircraft flying well into the free troposphere (typically >6 km above sea level).

The availability of calibrated, comparable observations of atmospheric CO₂ mole fractions on a common scale has made it possible to estimate surface exchange via inversion of atmospheric transport. Studies including Enting and Mansbridge (1991), Fan et al. (1998), and the ensuing Atmospheric Tracer Transport Model Intercomparison Project (TransCom) model intercomparisons (e.g., Baker et al., 2006; Gurney et al., 2002) reported widely ranging values of mean sinks for continental-scale

land regions. These results demonstrated that, in the face of highly variable surface fluxes, uncertainties and biases in atmospheric transport models (e.g., Stephens et al., 2007), coupled with the sparseness of available observations, render the estimation of mean surface fluxes strongly underconstrained. In the context of a common estimation methodology, interannual variability in surface fluxes can be strikingly coherent between inversion models (Baker et al., 2006; Peylin et al., 2013), suggesting that standing biases in transport models may drive differences in the mean flux estimated by global inverse models.

At the time of the *First State of the Carbon Cycle Report* (SOCCR1; CCSP 2007), there was agreement within large uncertainty bounds between “bottom-up” estimates from terrestrial biomass inventories and “top-down” atmospheric studies (Pacala et al., 2001; see Ch. 2 and Ch. 3 in SOCCR1) on the size of the terrestrial CO₂ sink in North America. Atmospheric inverse modeling was discussed in SOCCR1, but the final fluxes reported for North America excluded estimates from those techniques. These estimates were brought together for the first time at the continental scale for the North American Carbon Program (NACP) interim regional synthesis project (Hayes et al., 2012; Huntzinger et al., 2012).

8.3 Current Understanding of Carbon Fluxes and Stocks

The global average atmospheric CO₂ concentration in 2015 of about 401 ppm (see Figure 8.1, p. 339) is roughly 20 ppm (5%) higher than in 2007. The anthropogenic excess of CO₂—the concentration in the atmosphere above the preindustrial level of about 280 ppm—has grown by 20% in just the 8 years since 2007. The 2015 global average concentration of CH₄ was about 1,833 parts per billion (ppb), which is 3% higher than in 2007 (a 5% increase in the anthropogenic excess).

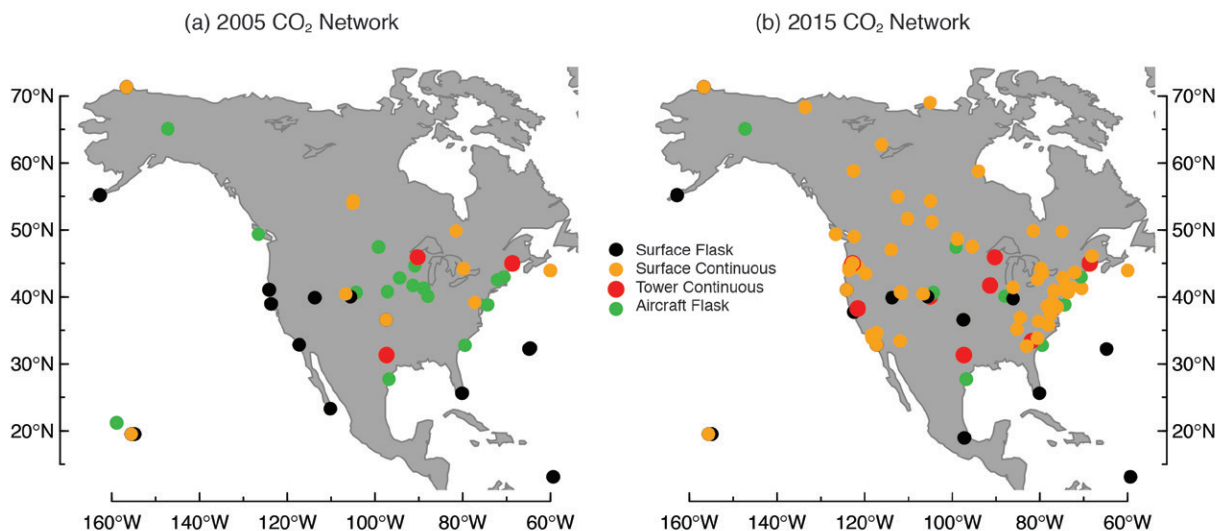


Figure 8.2. Growth of the North American Carbon Dioxide (CO₂) Monitoring Network from (a) 2005 to (b) 2015. Many National Oceanic and Atmospheric Administration aircraft sites were terminated after 2005. Unlike “surface” sites, “tower” sites generally have inlets 100 m to 400 m above the surface and sometimes sample air above the planetary boundary layer. About 90% of both tower and surface sites also report methane measurements.

8.3.1 Advances in Atmospheric Measurements and Platforms

Surface Networks

The observation network for atmospheric CO₂ and CH₄ has grown dramatically since SOCCR1 (see Figure 8.2, this page). Networks are now run by 1) governmental institutions such as the National Oceanic and Atmospheric Administration (NOAA), Environment and Climate Change Canada, U.S. Department of Energy, and California Air Resources Board; 2) research institutions including the National Center for Atmospheric Research (NCAR) and National Ecological Observatory Network (NEON); 3) universities such as Scripps Institution of Oceanography, The Pennsylvania State University, Oregon State University, and Red Universitaria de Observatorios Atmosfericos in Mexico; and 4) corporations (e.g., Earth Networks). Platforms and measurement techniques for observing greenhouse gas (GHG) distributions also have grown and become more diverse. In 2005, the North American CO₂ and CH₄ surface network mainly consisted of weekly surface flask–air

sampling at a handful of sites and continuous observations at several observatories and three tall towers (see Figure 8.2, this page). Sustained records are now available from many more towers, especially those of intermediate (~ 100 m) height. As the density of the North American GHG measurement network has grown, the emissions sensitivity of observations has moved from hemispheric scales (using background marine boundary layer observations), to regional scales (using tower and aircraft observations), and, more recently, to local scales from urban networks and oil and gas measurement campaigns. These new *in situ* measurements of CO₂ and CH₄ (see Figure 8.2, this page) have been enabled by better availability of higher-precision, stable laser spectroscopic analyzers that require less-frequent calibration, although traceability to a common CO₂ reference scale is critical for this collection of networks to be unified. Currently, about 90% of the CO₂ network sites also report CH₄ measurements.

Remote Sensing

New remote-sensing approaches have emerged such as the international Total Carbon Column



Observing Network (TCCON), which now has six sites in North America among about 20 worldwide. TCCON measurements are made using high-resolution solar-tracking Fourier transform spectrometers (FTSs; Wunch et al., 2011), which are sensitive to the total CO₂ content of the atmospheric column, can provide constraints on large-scale carbon fluxes (Chevallier et al., 2011; Keppel-Aleks et al., 2012), and also help identify biases in satellite-based remote sensors (e.g., Wunch et al., 2016). Since SOCCRI, first-generation CO₂- and CH₄-dedicated near-infrared space-based spectrometers have been deployed aboard the Greenhouse Gases Observing Satellite (GOSAT; Japan Aerospace Exploration Agency) and the Orbiting Carbon Observatory-2 (OCO-2; National Aeronautics and Space Administration [NASA]) satellites. Numerous carbon cycle data assimilation systems are attempting to assimilate these CH₄ (GOSAT) and CO₂ (GOSAT and OCO-2) column averages to derive surface fluxes. These efforts are challenged by small but spatially and temporally coherent biases in the data (Basu et al., 2013; Feng et al., 2016; Lindqvist et al., 2015). Estimating emissions anomalies (as opposed to absolute emissions), such as carbon flux variability driven by climate events, has proved to be more successful (Basu et al., 2014; Guerlet et al., 2013; Reuter et al., 2014; Turner et al., 2017). Assimilating column-average GHG data from both ground- and space-based instruments into carbon cycle models is still a rather new activity that requires modifications in traditional atmospheric inverse models. They need to be modified to handle a much larger data volume, extract information from full-column averages, and assimilate retrievals contaminated by coherent biases, which can masquerade as atmospheric gradients arising from surface exchange.

Another remote-sensing approach for CO₂ uses light detection and ranging (LIDAR), which has been deployed at surface sites to measure the mean CO₂ along horizontal paths (Gibert et al., 2008, 2011) and aboard aircraft to measure partial-column integrals (Dobler et al., 2013). Space-based LIDAR total column CO₂ and CH₄ measurements are under

development (Ehret et al., 2008), and a CH₄ system will be deployed on the MERLIN satellite sensor. LIDAR instruments have narrow beams and thus can often obtain data in partly cloudy regions that confound passive sensors. Because they are active, LIDAR instruments can obtain data in the absence of sunlight (at high latitudes or at night). Despite this appealing feature, LIDAR instruments are not yet broadly distributed for atmospheric research.

Vertical In Situ

Calibrated CO₂ and CH₄ total column values can be measured using *in situ* approaches. The AirCore is a thin steel tube that samples an air profile, typically during a balloon flight (Karion et al., 2010). Profiles (and thus column integrals) of CO₂ and CH₄ (Karion et al., 2010) extend to altitudes that allow sampling of nearly 99% of the atmospheric column of air. In addition to defining the vertical structure of CO₂ and CH₄ in both the troposphere and stratosphere, these data provide calibrated total columns that can be directly compared to remotely sensed soundings from space (e.g., OCO-2 and GOSAT) and the ground (TCCON). Time series of AirCore measurements are being established at Sodankylä, Finland; Orleans, France; Lamont, Oklahoma; and Boulder, Colorado. While not sampling the total column, *in situ* measurements taken aboard light aircraft flying between the surface and 6 to 8 km above sea level also are ongoing. These regular (biweekly to monthly) measurements capture the seasonal and interannual distribution of CO₂, CH₄, and other GHGs throughout North America (Sweeney et al., 2015; see Figure 8.2, p. 341). Although the number of air samples collected has not significantly increased since 2007, the number of gases measured has increased from eight to more than 50, including gases like carbonyl sulfide (COS) and the ¹⁴C:C ratio of CO₂ (Δ¹⁴CO₂) that are tracers for biogenic and fossil fuel emissions.

Other Species

Carbon monoxide (CO) retrievals from the Measurements Of Pollution In The Troposphere (MOPITT) and Infrared Atmospheric Sounding Interferometer (IASI) satellite instruments have



been used to constrain biomass burning GHG emissions and help separate intact ecosystem carbon uptake from biomass burning emissions (e.g., van der Laan-Luijkx et al., 2015). Although CO retrievals from these platforms can be biased by 10% or more (De Wachter et al., 2012; Deeter et al., 2016; George et al., 2009), robust signals can still be gleaned since the variation in CO from large biomass burning events can be up to 500% of the background. While not a GHG measurement, solar-induced fluorescence (SIF), a direct by-product of photosynthesis, can be measured from space and is emerging as an important marker of terrestrial gross primary production (Frankenberg et al., 2011; Joiner et al., 2011) and complement to remotely sensed CO₂. Direct estimation of gross primary production from SIF retrievals remains an area of active research.

Process Tracers

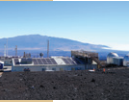
Concentrations and isotopic ratios of carbon cycle process tracers such as COS, CO, $\Delta^{14}\text{CO}_2$, halogenated species, ¹³CO₂, ¹³CH₄, propane, and ethane are now being regularly analyzed in North American air and as part of the NOAA tower and aircraft networks and targeted regional and local measurement campaigns. These include programs such as the Mid-Continent Intensive (MCI; NACP) campaign, Carbon in Arctic Reservoirs Vulnerability Experiment (CARVE; NASA), Atmospheric Carbon and Transfer-America (ACT-America) program (NASA), Indianapolis Flux Experiment (INFLUX), and Los Angeles megacities effort (see Section 8.3.2, this page). These process tracers allow for constraints on carbon cycle processes such as photosynthetic CO₂ fixation, fossil fuel emissions, and transport model fidelity.

8.3.2 Atmosphere-Based Fluxes from Local to Continental Scales

Short-Term and Regional to Local Emissions

Since SOCCR1 (CCSP 2007), studies of the carbon cycle have expanded to include regional campaigns designed to understand and quantify ecosystem and anthropogenic sources and sinks in particular regions and seasons. The NACP MCI campaign

intensively sampled the atmosphere above the Midwest agricultural region during 2007 and 2008 and compared sources and sinks derived from atmospheric CO₂ data to those based on bottom-up inventories. The results showed a high degree of convergence between surface fluxes inferred from three atmospheric inversions and bottom-up inventories (Ogle et al., 2015; Schuh et al., 2013). CARVE studied boreal and Arctic ecosystem carbon cycling in Alaska using aircraft and tower CO₂ and CH₄ measurements between 2012 and 2015 (e.g., Chang et al., 2014). One significant finding was that an ensemble of process-based wetland emission models (Melton et al., 2013) systematically underestimated atmospherically constrained CH₄ emissions from tundra ecosystems on Alaska's North Slope (Miller et al., 2016). Recently launched regional studies also should provide new insights into North American carbon cycling. The ACT-America (2015 to 2019) program is designed to explore the structure of GHG distributions within synoptic weather systems and reduce atmospheric transport error in inverse flux estimates using a variety of aircraft observations. The new NASA CARBON Atmospheric Flux Experiment (CARAFE) airborne payload, which is designed for validation of regional carbon flux estimates, was recently deployed to collect airborne eddy covariance measurements for CO₂ and CH₄ (Wolfe et al., 2015). Other studies such as NASA's Deriving Information on Surface Conditions from Column and Vertically Resolved Observations Relevant to Air Quality (DISCOVER-AQ) and Arctic Research of the Composition of the Troposphere from Aircraft and Satellites (ARCTAS), as well as the Texas Air Quality Study (TexAQS), have focused primarily on reactive gas compounds and air quality research but also have measured and interpreted CO₂ and CH₄ data (e.g., Brioude et al., 2012; Townsend-Small et al., 2016; Vay et al., 2011). At much larger scales, the HIAPER (High-Performance Instrumented Airborne Platform for Environmental Research) Pole-to-Pole Observations (HIPPO; 2009 to 2011) and the Atmospheric Tomography Mission (ATom; 2016 to 2018) projects have measured atmospheric trace gas species, including CO₂



and CH₄, along north-south transects in the Pacific and Atlantic oceans. These measurements are not significantly sensitive to North American emissions, but they are expected to help constrain large-scale carbon fluxes and atmospheric transport and, by extension, improve understanding of the North American carbon balance.

Many studies at more local scales have been designed to provide constraints on urban CH₄ and CO₂ emissions. A large global trend in urban migration is making cities loci of both emissions and their mitigation, thus driving interest in atmospheric measurement approaches to inform decision making (e.g., Duren and Miller 2012). There have been projects outside of North America (e.g., Bréon et al., 2015; Levin et al., 2011); some North American urban carbon balance studies include those in Indianapolis (INFLUX; Davis et al., 2017), Los Angeles (Feng et al., 2016; Wong et al., 2015; Wunch et al., 2009), Salt Lake City (McKain et al., 2012), and Boston (McKain et al., 2015). In general, these studies have deployed small networks of GHG sensors in and around cities and used the observed gradients, in conjunction with high-resolution atmospheric transport models and bottom-up inventories, to determine urban CH₄ and net CO₂ emissions (fossil and biogenic). Comparisons between atmospherically derived and bottom-up CO₂ emissions show varying degrees of agreement, even in the same city. In Indianapolis, a CO₂ flux calculation using tower observations and a high-resolution (1-km) atmospheric inversion system (Lauvaux et al., 2016) yielded emissions about 20% larger than either the Hestia Project (Gurney et al., 2012; Arizona State University) or Open-source Data Inventory for Anthropogenic CO₂ (ODIAC; Oda and Maksyutov 2011) inventory products, while aircraft mass-balance fluxes (Heimbürger et al., 2017) were about 20% lower than the inventories. Indianapolis airborne mass balance CH₄ emissions were about 30% higher than a custom-made urban inventory, and the tower-based inversion suggested CH₄ emissions twice as large as the aircraft mass balance estimate. In Salt Lake City, another atmospheric inversion approach using high-resolution

(1.3-km) meteorology also showed a high level of correspondence with the Vulcan Project. The California Research at the Nexus of Air Quality and Climate Change (CalNex) mission, which sampled CO₂ above Los Angeles, derived emissions 20% to 30% higher than ODIAC and Vulcan (Brioude et al., 2013; Gurney et al., 2012). In the Los Angeles megacities experiment and INFLUX, additional biogenic and anthropogenic process tracers like CO, Δ¹⁴CO₂, and numerous hydro- and halocarbons also have been measured (Newman et al., 2016; Turnbull et al., 2015). These data could enable partitioning the net CO₂ signals into anthropogenic and biogenic components.

Local studies also have been undertaken in and around oil and gas extraction fields. Between 2005 and 2016, U.S. natural gas extraction increased by over 38% (U.S. Energy Information Administration, www.eia.gov/dnav/ng/hist/n9010us2m.htm). The fraction of CH₄ that leaks during extraction and distribution is highly uncertain and is driving research on both bottom-up and top-down methods. Alvarez et al. (2012) estimated that if this CH₄ leak rate is greater than about 3%, the climate impact of natural gas combustion could equal or exceed that of coal on a per-unit energy basis. Some recent studies of CH₄ emissions from oil and gas production (e.g., Brandt et al., 2014) have found higher emissions compared to estimates from past U.S. Environmental Protection Agency (EPA) inventories. Field studies also have shown considerable variation among regions. For example, Karion et al. (2013) found that emissions from the Uintah Basin in Utah were about 9% of production, while Peischl et al. (2015) found leak rates well under 3% of production for the Haynesville, Fayetteville, and Marcellus shale regions. Based on a variety of studies at scales ranging from individual pieces of equipment to regional scales, Brandt et al. (2014) concluded that leakage rates are unlikely to be large enough to make the climate impact of natural gas as large as that of coal.

The answer to the question of why field studies suggest higher emissions than official inventories is likely related to the existence of a small number

of “super emitters” that are difficult to capture in inventory-based approaches, but whose atmospheric signatures are often seen in measurements (Brandt et al., 2014; Schwietzke et al., 2017; Kort et al., 2014). For example, Zavala-Araiza et al. (2015) found that half of CH₄ emissions from the Barnett Shale region were due to just 2% of oil and gas facilities, and the study achieved closure within error bounds between atmospheric methods and an inventory product derived from local emissions measurements. Although small in area and duration, these measurement campaigns have provided policy-relevant information using atmospheric CH₄ concentration data.

Interannual and Continental Emissions

Inverse models such as CarbonTracker have been continuously improved and upgraded to exploit the improved density of atmospheric CO₂ and CH₄ observations (Bruhwiler et al., 2014). Global inversions with regularly updated flux estimates include CarbonTracker (Peters et al., 2007; carbontracker.noaa.gov), the European Union’s Copernicus Atmospheric Monitoring Service (CAMS; atmosphere.copernicus.eu; formerly MACC), Max Planck Institute Jena CarboScope project (Rödenbeck et al., 2003; www.bgc-jena.mpg.de/CarboScope), and CarbonTracker-Europe from Wageningen University (Peters et al., 2010; www.carbontracker.eu). These products constitute the ensemble of inverse models used in this chapter to estimate North American CO₂ fluxes.

Mean annual CO₂ fluxes over North America from this ensemble are shown in Figure 8.3, this page, and listed in Table 8.1, p. 346. These inverse model flux estimates show some level of agreement about mean fluxes and patterns of interannual variability. However, they also manifest notable differences. These differences remain one of the most important indicators of the overall uncertainty in inverse model fluxes. The uncertainty in fluxes derived from inverse models has proven to be a difficult quantity to estimate directly, since those models depend on results from upstream analyses with complicated, unknown uncertainties. For instance,

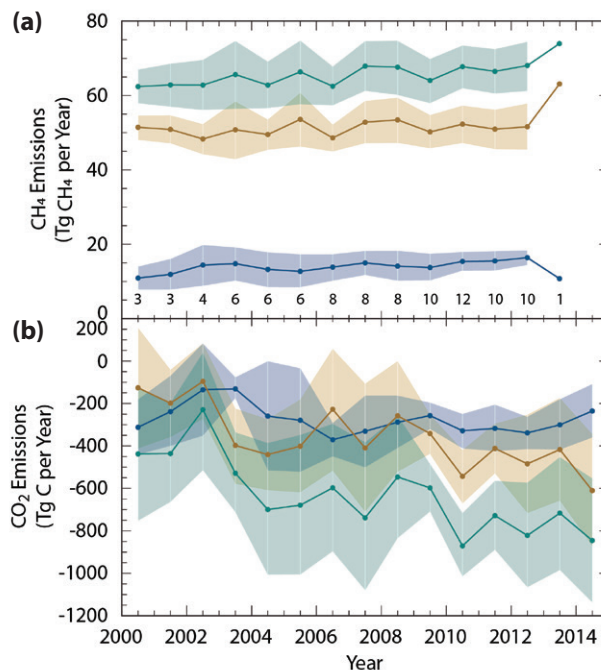


Figure 8.3. Inverse Model Estimates of Annual Emissions of (a) Methane (CH₄) and (b) Nonfossil Fuel Carbon Dioxide (CO₂) from 2000 to 2014. Estimates are given in teragrams (Tg) for North America (green), boreal North America (blue), and temperate North America (beige) based on the across-model mean of inverse models. Error bands represent one-sigma across-model spread taken as a proxy for model uncertainty. Methane emissions data are from the Global Carbon Project (GCP) inverse model collection of Saunio et al. (2016), with the number of models contributing to each annual mean shown in black. Carbon dioxide emissions are the across-model mean of the four inverse models collected for this report. Negative emissions represent a sink.

some of the overall difference in inverse model fluxes can be attributed to differing atmospheric transport among the models, which assume that the winds and diffusive mixing of the transport model are unbiased and subject only to random error. Another element of overall uncertainty comes from the structure of the flux estimation scheme in each inverse model. This structure includes the choice of prior emissions from the burning of fossil fuels, terrestrial biosphere, and the ocean used in the model. The interpretation of results from inverse models is further complicated by the fact that these

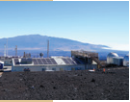


Table 8.1. Estimates of Annual, North American, Land Biosphere Carbon Dioxide (CO₂) Fluxes (Including Fire) Derived from Atmospheric CO₂ Measurements Using Inverse Models and the U.S. Environmental Protection Agency (EPA) Inventory over the Period 2004 to 2013

	CT2015	CAMS ^a	CTE2015	CarboScope ^b	Inverse Models	EPA	Fossil Fuel Emissions
Boreal North America	-160 ± 77	-356 ± 61	-302 ± 50	-407 ± 64	-306 ± 43		30 ± 1
Temperate North America	-352 ± 111	-602 ± 95	-252 ± 126	-365 ± 109	-393 ± 67	-202 ± 5 ^c	1744 ± 37
North America	-511 ± 106	-959 ± 117	-555 ± 147	-773 ± 107	-699 ± 82		1774 ± 24

Emissions in teragrams of carbon (Tg C) per year are listed for the Atmospheric Tracer Transport Model Intercomparison Project's (TransCom) temperate and boreal North American regions (Gurney et al., 2002). The "inverse models" column averages across the four inverse models (CarbonTracker [CT], Copernicus Atmospheric Monitoring Service [CAMS], CarbonTracker-Europe [CTE], and CarboScope) and represents the best estimate from this ensemble. Fossil fuel emissions are derived from Boden et al. (2017). Values reported are the 2004 to 2013 mean plus or minus a measure of interannual and across-model variability (twice the standard error of the mean of annual emissions). Negative emissions represent a sink.

Notes

a) Version v15r4, atmosphere.copernicus.eu.

b) Version v3.8.

c) U.S. EPA (2017) estimates correspond to "managed lands" in the United States, which largely corresponds to the TransCom temperate North American region.

models retrieve spatiotemporal patterns of CO₂ and CH₄ fluxes that do not necessarily correspond with patterns expected from differing theories about ecosystem carbon exchange; therefore, they do not map directly onto improvements in process knowledge. Despite these limitations, inverse model results are important because their net carbon flux estimates are by construction consistent with atmospheric data constraints. Ensembles of inverse models using different transport, structure, data inputs, and priors are particularly useful since they mitigate some of these limitations.

Previous comparisons of inverse models such as Baker et al. (2006) and Peylin et al. (2013) indicated that, while each inversion manifests a different long-term mean flux estimate, the patterns of interannual variability tend to have better agreement. There is some indication of interannual variation coherence in the present collection of models, but with some significant disagreement, mainly from the Jena CarboScope model. Averaging across the

inversions, the land biosphere sink in North America, including fire emissions, averaged over 2004 to 2013 is 699 ± 82 Tg C per year (mean \pm two standard errors of the mean of the interannual and intermodel variability). This sink offsets about 39% of the fossil fuel emissions of $1,774 \pm 24$ Tg C per year for the same geographic area, although 98% of these anthropogenic emissions come from just the temperate North American region. Disagreement remains among these inversions about the average size of the North American sink, but they all estimate significant interannual variability in that sink. Over the temperate North American region, these inverse models estimate interannual variability (one sigma) of between 163 and 277 Tg C per year, equivalent to 45% to 83% of each model's mean flux.

The level of interannual variability from inverse models stands in stark contrast to the annual Inventory of U.S. Greenhouse Gas Emissions and Sinks, prepared by the U.S. EPA. EPA's U.S. GHG inventory estimates land use, land-use change, and

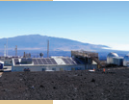


forestry (LULUCF) sector emissions on managed lands. Managed lands represent about 95% of total U.S. land cover and more than 99% of the conterminous United States, which corresponds well to the net biosphere fluxes estimated by inversion models for temperate North America. EPA's LULUCF CO₂ sink estimate has a 2004 to 2013 mean of 202 ± 5 Tg C per year (U.S. EPA 2017; mean plus or minus two standard errors of the mean). The small interannual variability in the EPA inventory of just 5 Tg C per year stands in contrast to all the inverse models. This low apparent variability may arise from the historical 5- to 14-year frequency at which U.S. Forest Service Forest Inventory and Analysis (FIA) plots have been resampled. Comparing the interannual variability of inventories and inversions is inherently difficult due to the mismatch in their temporal sensitivities.

Various estimates of North American surface CO₂ emissions were collected as part of the recent NACP regional interim synthesis (Hayes et al., 2012; Huntzinger et al., 2012) and REgional Carbon Cycle Assessment and Processes (RECCAP) effort (Canadell et al., 2011; King et al., 2015). The RECCAP North America study included a suite of inverse models collected by Peylin et al. (2013) with a 2000 to 2009 mean CO₂ sink of 890 ± 400 Tg C per year (mean and one sigma standard deviation), implying a larger sink than either inventory (270 Tg C per year) or terrestrial biosphere model (359 ± 111 Tg C per year) estimates (King et al., 2015). The current suite of inverse models collected for this report (see Table 8.1, p. 346) suggests North American biosphere emissions of 699 ± 82 Tg C per year averaged over 2000 to 2014. The models collected for this chapter also supplied results from their earlier versions to the RECCAP ensemble of Peylin et al. (2013). That report showed a wide range of North American flux estimates, but the subset of models used in this chapter all manifested sinks smaller than 500 Tg C per year for North America over the reporting period 2001 to 2004, whereas the other models all estimated greater sinks between about 500 and 1,500 Tg C per year.

The North American sink estimated from the suite of inverse models collected for this report agrees well with previous bottom-up estimates. SOCCR1 (Pacala et al., 2007) reported a sink of 666 ± 250 Tg C per year for 2003. This estimate was derived from bottom-up inventories and models and did not include information from atmospheric inverse models. Hayes et al. (2012) attempted to reconcile net biosphere emissions estimates from inventories, terrestrial biosphere models, and atmospheric inverse models averaged over 2000 to 2006 for North America. That study found a sink of 511 Tg C per year simulated by terrestrial biosphere models and an inventory-based sink estimate of 327 Tg C per year (with an estimate of additional noninventoried fluxes that brings the total sink estimate to 564 Tg C per year). The collection of inverse models used in that study manifested significantly larger sinks (981 Tg C per year) than the current collection. See Ch. 2: The North American Carbon Budget, p. 71, for an assessment of the overall agreement of these various estimates of North American surface CO₂ exchange with the atmosphere.

The use of regional models of CO₂ and CH₄ has become more common since SOCCR1. These models have focused, for example, on continental-scale processes (Butler et al., 2010; Gourdji et al., 2012; Schuh et al., 2010) or at the scale of the mid-continent (Lauvaux et al., 2012b; Schuh et al., 2013). Regional model CO₂ flux estimates for North America so far have been published for periods of up to 1 year, with multi-year analyses only available from global inversion approaches. One prominent result from regional inverse CO₂ studies is the sensitivity of the annual net CO₂ flux to defining the inflow of atmospheric CO₂ into the study region (Gourdji et al., 2012; Schuh et al., 2010). Lauvaux et al. (2012b) demonstrated that this sensitivity could be minimized with observations at the inflow boundaries. This finding highlights the importance of global-scale measurement networks and carbon reanalysis systems for understanding North American carbon fluxes. More recently, CH₄ has received more attention with regional inversions for the continent (Kort et al.,



2008; Miller et al., 2013), California (Jeong et al., 2013), and Alaska (Chang et al., 2014; Miller et al., 2016). Additional uncertainties in inverse modeling approaches arise from sparse data coverage. When the observational network is not strongly sensitive to particular land regions, inverse modeling systems must make assumptions about spatial and temporal patterns of emissions. As with the issue of boundary inflow, mitigating this sensitivity necessitates building a denser, intercalibrated measurement network.

8.4 Indicators, Trends, and Feedbacks

Atmospheric CH₄ and CO₂ levels continue to increase. In the case of CO₂, this increase is unambiguously a result of anthropogenic emissions, primarily from fossil fuel combustion, with North America accounting for about 20% of global emissions. The recent rise in global CH₄ concentrations (see Figure 8.1, p. 339), on the other hand, has been attributed primarily to biological, not fossil, processes on the basis of a concomitant decrease in the global mean ¹³C:¹²C ratio and the tropical origin of the increase (Nisbet et al., 2016; Schaefer et al., 2016; Schwietzke et al., 2016). Two recent analyses render the causes of recent CH₄ growth rate changes less clear. First, studies have pointed out that the tropospheric CH₄ sink may not have been constant over recent years as had been assumed (Rigby et al., 2017; Turner et al., 2017). Secondly, Worden et al. (2017) suggest that atmospheric δ¹³C of CH₄ may have decreased because of less biomass burning, thus allowing for an increase in isotopically heavier fossil fuel CH₄ sources. Nonetheless, these results mostly pertain to the global mean and do not directly bear on potential trends in North American emissions. Despite the recent increase in oil and gas production due to new extraction technologies, both inventories and atmospheric inversions do not reveal an increase in North American CH₄ emissions (Bruhwiler et al., 2014; Miller et al., 2013; U.S. EPA 2016; see Figure 8.3, p. 345). Normalizing CH₄ and CO₂ emissions using a 100-year global warming potential (GWP) indicates that U.S. radiative forcing from CH₄ emissions from 2000 to 2013 equates to just

13% of that from CO₂. Changes in U.S., Canadian, and Mexican energy systems will affect the atmospheric trends of anthropogenic CO₂ and CH₄, but U.S. GHG emissions currently are dominated by CO₂ and are likely to remain so for the foreseeable future.

Much less certain than anthropogenic CO₂ sources is the balance of biogenic sources (respiration and fire) and sinks (photosynthesis). There is general agreement that the terrestrial biosphere of the United States, and North America as a whole, acts as a CO₂ sink (see Figure 8.3, p. 345, and Table 8.1, p. 346; Hayes et al., 2012; King et al., 2015), but there is substantial uncertainty about the location of and reasons for the sinks. There is evidence that their interannual variability is driven largely by climatic factors. For example, Peters et al. (2007) presented evidence for a direct effect of drought on the North American sink. Understanding the spatial and temporal variability of sinks is critical, because positive feedbacks between net ecosystem CO₂ exchange and climate represent a first-order uncertainty in climate projections (Bodman et al., 2013; Booth et al., 2012; Friedlingstein et al., 2006, 2014; Huntingford et al., 2009; Wenzel et al., 2014; Wieder et al., 2015). At hemispheric and global scales, atmospheric CO₂ data have proved to be a powerful constraint on the representation of the carbon cycle (including, to some measure, feedbacks) in climate models (e.g., Cox et al., 2013; Graven et al., 2013; Keppel-Aleks et al., 2013; Randerson et al., 2009). The present generation of global atmospheric inverse models is limited by the accuracy and resolution (generally about 1° × 1°) of meteorological transport, availability and accuracy of prior flux emissions, uncertainty about the spatial coherence of prior flux errors, and the limited set of observation sites shown in Figure 8.2, p. 341. Together, these limitations mean that, at present, global atmospheric inverse models cannot unambiguously resolve source-sink patterns below the scale of 5 to 10 million km². A new generation of regional and local models using much higher resolution meteorology (e.g., approaching the approximately 1- to 4-km resolution used by Lauvaux et al. [2016] and McKain et al. [2015]) will be more



capable of assimilating data from the sites in Figure 8.2, p. 341. Without quantitative knowledge of the spatial structure of flux uncertainties (Cooley et al., 2012; Ogle et al., 2015) and atmospheric transport errors (Díaz Isaac et al., 2014; Lauvaux and Davis 2014), these high-resolution inverse systems will have limited ability to determine the spatial structure of fluxes (Lauvaux et al., 2012a, 2016). Nonetheless, these improved inversion systems should enable better understanding of the climate-carbon relationship in North America.

8.5 Societal Drivers, Impacts, and Carbon Management

In a potential future when carbon emissions have a significant economic cost and international agreements to control emissions are in place, verifying claims of emissions mitigation and assessing the efficacy of mitigation strategies will be necessary. In addition to international agreements, 18 states have plans in place to reduce GHG emissions. Bottom-up methods based on economic, agricultural, and forest inventories provide much of the basis for these calculations. These methods are susceptible to systematic errors, including incomplete sectoral coverage, misreporting, and the use of uncertain emissions factors. Top-down methods derive emissions budgets consistent with atmospheric concentrations of GHGs, but they also contain systematic errors resulting from imperfect knowledge of atmospheric transport and lack of observations. Although these uncertainties place limits on the accuracy of top-down emissions estimates, atmospheric data still provide strong constraints on GHG emissions from local to global scales (e.g., Levin et al., 2010). As shown by the example of Brandt et al. (2014), natural gas super emitters can be localized from *in situ* observations even when they have not previously been identified by inventories. As described in this chapter, both existing and new technologies can provide independent and complementary information and help reconcile emissions estimates from the bottom-up and top-down approaches. From a carbon management and decision perspective, collecting and utilizing information from atmospheric data

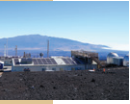
could provide additional information in regions and sectors where uncertainties in bottom-up inventories are large. Top-down emissions estimates can be produced with low latency and with robust uncertainty quantification. Together, these two methods can provide robust observational constraints on emissions at a variety of scales.

8.6 Synthesis, Knowledge Gaps, and Outlook

8.6.1 Findings from Atmospheric Inversions and Related Analyses

The present collection of atmospheric CO₂ inversions shows no clear trend in the boreal North American sink, but it does suggest the possibility of an increasing sink in temperate latitudes. A more robust feature of atmospheric inversions is that they show that the North American CO₂ sink is more highly variable and sensitive to drought and temperature stress than bottom-up biosphere models (King et al., 2015; Peters et al., 2007). Inversions also produce a larger mean sink and a deeper annual cycle than terrestrial biosphere models. Significant uncertainty remains about the magnitude of the mean North American carbon sink, in part because models disagree about the partitioning of the net sink between northern and tropical land regions. The mechanisms behind the land sink cannot be understood fully without more agreement on its location. Notably, distinguishing between a potentially short-lived sink due to recovery from past land-use practices (mainly a temperate Northern Hemisphere phenomenon) and a longer-term sink due to CO₂ fertilization remains elusive. Moreover, the role of carbon-climate feedback processes in North America, both negative (e.g., extended growing seasons and tree-line migration) and positive (e.g., permafrost carbon release and insect outbreaks), is poorly understood at present. Atmospheric measurements can impose significant constraints on these processes (e.g., Sweeney et al., 2015), and continued and expanded measurements, especially in sensitive Arctic and boreal regions, will be critical moving forward.

Inventories suggest that fossil fuel CO₂ emissions are stabilizing and even decreasing for certain



regions and sectors of the global and North American economy. This finding is difficult to verify given the *ad hoc* nature of the GHG observation network, lack of integration among programs, and sparse measurements of anthropogenic emissions tracers such as $\Delta^{14}\text{CO}_2$ and CO.

Individual atmospheric CH_4 inversions consistently show no trend and little interannual variability in total CH_4 emissions (natural and anthropogenic) for both the temperate (largely the United States) and boreal regions and the continent as a whole (see Figure 8.3, p. 345). These results suggest that North American emissions have not contributed significantly to the global upward trend that started in 2007. Increasing oil and gas production in North America could result in increased CH_4 emissions, a result apparently confirmed by Turner et al. (2016) on the basis of comparing inverse model estimates from different time periods. This conclusion has been called into question by Bruhwiler et al. (2017), who argue that robust trend detection is limited by interannual variability, the sparse *in situ* measurement network, and biased satellite CH_4 retrievals. Recent increases in atmospheric ethane and propane suggest increased CH_4 emissions from fossil fuel production, although there is uncertainty in this conclusion due to poorly quantified emissions ratios (Helmig et al., 2016). As with CO_2 though, little reliable spatial information is available from the current suite of CH_4 inverse models. This limitation hampers attribution to specific mechanisms including CH_4 -climate feedbacks, especially in the boreal zone where permafrost degradation plays a key role in changing CH_4 and CO_2 fluxes (McGuire et al., 2016; see also Ch. 11: Arctic and Boreal Carbon, p. 428).

8.6.2 Future Atmospheric Measurement Challenges and Strategies for North America

Compatibility Among Networks

As the community expands research into new domains and with new measurement strategies, new challenges are emerging. Compatibility of measurements among existing and future networks is a concern, as there is ample history of calibration

difficulties from the decades of *in situ* measurement experience (e.g., Brailsford et al., 2012). This challenge is being addressed by careful attention to calibration and participation in laboratory and field intercomparison activities (Masarie et al., 2011; www.esrl.noaa.gov/gmd/ccgg/wmorr/). Much more challenging is linking ground- and space-based remote-sensing measurements to each other and to the calibrated *in situ* networks. Concentrations derived from any remote-sensing gas measurement, whether ground- or space-based, cannot be formally calibrated because the measurement instrument cannot be “challenged” by a reference sample with a known concentration. Thus, identification and correction of biases remain a significant challenge. With the OCO-2 and GOSAT programs, the primary strategy has been to compare the satellite-based retrievals with TCCON retrievals. The TCCON retrievals of column CO_2 are themselves remote-sensing products that have been statistically linked to the World Meteorological Organization CO_2 calibration scale using aircraft *in situ* partial column CO_2 and CH_4 extrapolated to the top of the atmosphere (Wunch et al., 2011). This linkage remains uncertain due to the limited number of *in situ* profiles used and their limited maximum altitude. A limited number of nearly total column AirCore (Karion et al., 2010) measurements also have been compared with TCCON columns.

Bias correction of satellite retrievals remains challenging due to the limited number of TCCON stations (currently less than 20) and because estimates of the TCCON site-to-site bias of 0.4 ppm (one-sigma; Wunch et al., 2016) are significant for carbon cycle studies. As an example of the importance of small biases, Reuter et al. (2014) demonstrated that a gradient of 0.5 ppm in column CO_2 across Europe was associated with a change in flux over that region of about $-500 \text{ Tg C per year}$. This increased sink over Europe using a regional model is consistent with the inversion intercomparison of Houweling et al. (2015), who found that assimilating GOSAT column CO_2 retrievals in global inversion models caused an increase of about $700 \text{ Tg C per year}$ in the European sink, with a compensating increase



in the northern Africa source of about 900 Tg C per year. These shifts in emissions were associated with degraded agreement with unassimilated *in situ* observations from both surface observation sites and aircraft campaigns. For comparison, the *in situ* assimilation models collected for this chapter estimate a modest sink of 219 ± 405 Tg C per year in Europe and a negligible source of 13 ± 281 Tg C per year in northern Africa over the 2004 to 2013 period. These uncertainties, which comprise both interannual variability and intermodel differences in the inversions, are relatively large but still appear inconsistent with the GOSAT-driven flux increments reported in Houweling et al. (2015). In the relatively short time that GOSAT and OCO-2 have been collecting data, significant progress has been made in identifying and correcting biases in those datasets. Progress also is needed in understanding the time and space scales of remote-sensing data least susceptible to bias and how to assimilate these retrievals jointly with *in situ* data having less bias. Moving forward, more measurements will be key, including expansion of AirCore (Karion et al., 2010) and commercial aircraft observations (Basu et al., 2014) that will enable better assessment and utilization of both ground- and space-based total column CO₂ and CH₄ remote-sensing data.

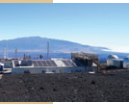
Next-Generation Measurements

Atmospheric measurements will play an important role in addressing these critical questions on the present and future state of both anthropogenic and biogenic components of the North American carbon cycle. The following is a list of potential, yet achievable, atmospheric measurement approaches that could dramatically change the current view of the North American (and global) carbon cycle.

A. Commercial Aircraft CO₂ and CH₄ Observations. The Comprehensive Observation Network for Trace gases by Airliner (CONTRAIL) program has measured GHGs from commercial aircraft for nearly two decades (Matsueda et al., 2008). A similar European effort, In-service Aircraft for a Global Observing System (IAGOS) project (Filges et al., 2015), is not yet fully

operational for GHG measurements. The technology exists for unattended, high-accuracy airborne CO₂ and CH₄ measurements (Karion et al., 2013), and deploying instruments aboard 40 domestic U.S. commercial aircraft could result in approximately 500 vertical profiles per day, radically changing CO₂ and CH₄ data density over North America.

- B. Greatly Expanded $\Delta^{14}\text{CO}_2$ Measurements.** Recently, Basu et al. (2016) demonstrated that expanding the U.S. network of $\Delta^{14}\text{CO}_2$ measurements from about 800 per year to 5,000 per year, as recommended by the U.S. National Research Council (Pacala et al., 2010), could allow for atmospherically based determination of U.S. fossil fuel CO₂ emissions to within 5%, complementing official U.S. EPA inventory-based estimates. In addition to $^{14}\text{CO}_2$, other tracers such as CO, non-methane hydrocarbons, halogenated species, and $^{14}\text{CH}_4$ (for fossil CH₄ identification) can serve as powerful constraints on emissions, both in total and by sector.
- C. Upcoming Satellite-Based CO₂ and CH₄ Sensors.** These sensors, including GOSAT-2, OCO-3, TanSat (China), Geostationary Carbon Cycle Observatory (GeoCARB; NASA), MERLIN (France and Germany), TROPOMI (European Space Agency), and others (Ciais et al., 2014) likely will enable dramatically increased spatial coverage of total column CO₂, CH₄, and other gases. For the utility of these data to be maximized, existing challenges associated with aerosols, characterization of the ocean and land surface, clouds, daylight, and, more generally, the linkage to formal gas concentration scales must be overcome. GOSAT and OCO-2, and particularly their planned successors, also will yield information on chlorophyll fluorescence (SIF), which has potential as a marker of time and space patterns of plant photosynthesis.
- D. NEON.** If built out as planned, NEON (National Science Foundation) will provide calibrated CO₂ measurements on towers over a variety of North American biomes that will add



significantly to the North American CO₂ observational dataset.

- E. Additional Gas Tracers.** As with anthropogenic ancillary tracers (see B), numerous gases can serve as tracers of terrestrial ecosystem processes. Gross primary production fluxes are closely linked to atmospheric gradients in COS and $\Delta^{17}\text{O}$ (anomalies in the $^{18}\text{O}:^{17}\text{O}$ ratio of CO₂; e.g., Campbell et al., 2008; Thiemens et al., 2014). Atmospheric $\delta^{13}\text{CO}_2$ is sensitive to the impact of regional-scale moisture stress on terrestrial photosynthesis (Ballantyne et al., 2010) and can distinguish C₃ and C₄ plant productivity. Schwietzke et al. (2016) showed the potential for $\delta^{13}\text{CH}_4$ observations to distinguish fossil fuel CH₄ emissions from other sources. Measurements of the $\delta^{18}\text{O}$ of CO₂ reflect both biospheric processes and changes in the hydrological cycle (Ciais et al., 1997; Flanagan et al., 1997; Miller et al., 1999).
- F. Measurements to Improve Atmospheric Transport Simulation.** Such measurements are critical for fully extracting the information content of atmospheric CO₂ and CH₄ data. Better understanding and parameterizing of atmospheric transport are critical. Near-surface GHG

concentrations are a sensitive function of the planetary boundary-layer mixing height, wind speed, and wind direction. Measurements of the vertical wind structure and boundary-layer depth using rawinsonde, LIDAR, and radar, and assimilating these data into atmospheric transport models, can improve atmospheric transport significantly (Deng et al., 2017). Simulated CO₂ transport is sensitive to boundary-layer mixing, convective cloud transport, synoptic weather patterns, and the surface energy balance, all of which can be difficult to simulate with the high accuracy and precision required for atmospheric inversions. Fortunately, decades of weather forecasting research provide a strong foundation for improving the meteorological reanalyses used in atmospheric inversions. Observational programs that merge meteorological measurements with high-density GHG data (e.g., ACT-America) are aimed at advancing this aspect of atmospheric inverse modeling. In addition, measurements of tracers such as water vapor isotopic ratios, sulfur hexafluoride (SF₆), and even $^{14}\text{CO}_2$, where emissions are relatively well known (Turnbull et al., 2008), also can constrain simulated transport (Denning et al., 1999; Patra et al., 2011; Peters et al., 2004).



SUPPORTING EVIDENCE

KEY FINDING 1

Global concentrations of carbon dioxide (CO₂) and methane (CH₄) have increased almost linearly since the *First State of the Carbon Cycle Report* (CCSP 2007; see Figure 8.1, p. 339). Over the period 2004 to 2013, global growth rates estimated from the National Oceanic and Atmospheric Administration's (NOAA) marine boundary layer network average 2.0 ± 0.1 parts per million (ppm) per year for CO₂ and 3.8 ± 0.5 parts per billion (ppb) per year for CH₄. Global mean CO₂ abundance as of 2013 was 395 ppm (compared to preindustrial levels of about 280 ppm), and CH₄ stands at more than 1,810 ppb (compared to preindustrial levels of about 720 ppb); (*very high confidence*).

Description of evidence base

Global mean atmospheric growth rates and abundances of CO₂ and CH₄ are derived from publicly available tables on NOAA websites: 1) www.esrl.noaa.gov/gmd/ccgg/trends/global.html and 2) www.esrl.noaa.gov/gmd/ccgg/trends_ch4/.

Major uncertainties

The averages were calculated from the regularly updated marine boundary layer sites of NOAA's Global Greenhouse Gas Reference Network. These averages are not associated with any recent literature. The methodology used to construct the global "surfaces" from which the global averages are computed is described in Masarie and Tans (1995). The uncertainties originate primarily from the incomplete sampling of the marine boundary layer by the NOAA network and the uncertainty associated with smoothing the raw data prior to creating the global surface. Measurement uncertainty of CO₂ and CH₄ is a minor component. Uncertainty calculations are described in detail at: www.esrl.noaa.gov/gmd/ccgg/mb/mb.html. While the atmospheric CO₂ growth rate is relatively stable, there is strong decadal and interannual variability of CH₄ emissions, making computation of an average inherently sensitive to the choice of time period. For instance, the CH₄ growth rate averaged over 1997 to 2006 was 2.8 ppb per year, whereas over 2007 to 2015, it was instead 7.0 ppb per year.

Assessment of confidence based on evidence and agreement, including short description of nature of evidence and level of agreement

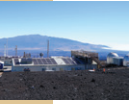
NOAA data are the gold standard for determining global growth rates and abundances because of extensive global coverage and high internal network compatibility, including high measurement precision. The trends and growth rates also agree well with estimates from other laboratories.

Summary sentence or paragraph that integrates the above information

NOAA CO₂ and CH₄ trends and abundances are publicly available, fully traceable, and represent the most comprehensive description of global CO₂ and CH₄.

KEY FINDING 2

Inverse model analyses of atmospheric CO₂ data suggest substantial interannual variability in net carbon uptake over North America. Over the period 2004 to 2013, North American fossil fuel emissions from inventories average $1,774 \pm 24$ teragrams of carbon (Tg C) per year, partially offset by the land carbon sink of 699 ± 82 Tg C year. Additionally, inversion models suggest a trend



toward an increasing sink during the period 2004 to 2013. These results contrast with the U.S. land sink estimates reported to the United Nations Framework Convention on Climate Change, which are smaller and show very little trend or interannual variability.

Description of evidence base

Fossil fuel emissions are from Carbon Dioxide Information Analysis Center (CDIAC) estimates (available from the U.S. Department of Energy's Environmental Systems Science Data Infrastructure for a Virtual Ecosystem [ESS-DIVE] data archive, ess-dive.lbl.gov). The land carbon sink is based on the 10-year average of North American annual fluxes from four global inverse models, specified in the text. The error reported is twice the standard error of the mean of the 10 years and for the four models and mostly represents the amount of interannual variability. The evidence for a trend is based on a linear least-squares regression. The comparison of variability with the U.S. Environmental Protection Agency's (EPA) estimate of the U.S. land sink is based on EPA data accessed at www.epa.gov/ghgemissions/inventory-us-greenhouse-gas-emissions-and-sinks-1990-2015.

Major uncertainties

Fossil fuel emissions uncertainty is very low (see Appendix E: Fossil Fuel Emissions Estimates for North America, p. 839). Long-term means of CO₂ sources and sinks derived from a given inverse model are highly uncertain. However, the interannual variability of fluxes from different models tends to agree well, suggesting lower uncertainty. EPA land flux estimates may not exhibit enough variability due to the U.S. Forest Service methodology, upon which EPA's estimates are largely based.

Assessment of confidence based on evidence and agreement, including short description of nature of evidence and level of agreement

Fossil fuel uncertainty at the national, annual scale has the smallest uncertainty because it can be constrained by highly accurate information on imports and exports and internal usage. Inverse model-based estimates of CO₂ sources and sinks contain numerous random and systematic errors including biases associated with wind fields and parameterization of vertical mixing. Because models exhibit different mean atmospheric transport, their long-term average fluxes can differ significantly. However, the interannual variability of fluxes among inverse models is much more similar, meaning that the difference between the inverse model and EPA flux variability is likely to be robust.

Estimated likelihood of impact or consequence, including short description of basis of estimate

The contrast between variability exhibited in the inverse model and the EPA estimates of land sink variability could cause EPA to reexamine its methodologies. Additionally, the emerging evidence that the North American CO₂ sink is growing also could spur research in the "bottom-up" community and impact policy decisions.

Summary sentence or paragraph that integrates the above information

Regularly produced inverse modeling estimates of CO₂ sources and sinks over North America are beginning to provide valuable information at least on interannual variability of terrestrial ecosystem fluxes.



KEY FINDING 3

During most of the study period covered by the *Second State of the Carbon Cycle Report* (2004 to 2012), inverse model analyses of atmospheric CH₄ data show minimal interannual variability in emissions and no robust evidence of trends in either temperate or boreal regions. The absence of a trend in North American CH₄ emissions contrasts starkly with global emissions, which show significant growth since 2007. Methane emissions for North America over the period 2004 to 2009 estimated from six inverse models average 66 ± 2 Tg CH₄ per year. Over the same period, EPA-reported CH₄ emissions equate to a climate impact of 13% of CO₂ emissions, given a 100-year time horizon.

Description of evidence base

The conclusions of minimal interannual variability (standard deviation), trend (slope and its uncertainty), and mean flux are all based on fluxes from 14 inverse models used in the global CH₄ budget analysis of the Global Carbon Project (Saunois et al., 2016). The 13% ratio of CH₄ to CO₂ warming impact is based on EPA CH₄ and CO₂ emission estimates using a 100-year global warming potential (GWP) value of 28.

Major uncertainties

Total CH₄ emissions for North America include the inversely derived value of 60 Tg CH₄ per year and the EPA anthropogenic emissions estimate for the United States, which would impact the 13% ratio. Inverse models are subject to poorly known uncertainties stemming from the use of biased priors, imperfect models of atmospheric transport, and the sparse network of *in situ* measurements.

Assessment of confidence based on evidence and agreement, including short description of nature of evidence and level of agreement

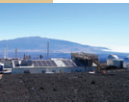
Total emissions have a high uncertainty (not reflected in the variability value stated in the Key Finding); note that EPA does not provide an uncertainty for its estimate. The absence of any trend has higher confidence, because numerous models with different methodologies contributed to this finding. However, the models used in the comparison did not uniformly cover the 2000 to 2013 period, making the conclusion less robust than that for CO₂. On the other hand, the smaller variability relative to CO₂ is consistent across models and is more robust. The 13% value is uncertain because of EPA's CH₄ emissions estimate and, to a lesser extent, the GWP uncertainty.

Estimated likelihood of impact or consequence, including short description of basis of estimate

The finding that CH₄ is unlikely to have a temperate North American trend different from zero is significant, because there is great interest in the cumulative radiative forcing impact of CH₄ emissions from the oil and gas sector. Moreover, while not a new finding, the simple calculation of CH₄ having only 13% of the warming impact as CO₂ should remind policymakers and scientists that CO₂ emissions are substantially more important.

Summary sentence or paragraph that integrates the above information

The global and North American emissions were derived using atmospheric CH₄ data assimilated in a wide variety of CH₄ inverse models using both *in situ* and remote-sensing data. Although a consistent picture is emerging, the results are more uncertain than those for CO₂, because estimates are not produced regularly over consistent timescales.

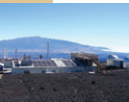


REFERENCES

- Alvarez, R. A., S. W. Pacala, J. J. Winebrake, W. L. Chameides, and S. P. Hamburg, 2012: Greater focus needed on methane leakage from natural gas infrastructure. *Proceedings of the National Academy of Sciences USA*, **109**(17), 6435-6440, doi: 10.1073/pnas.1202407109.
- Bacastow, R. B., 1976: Modulation of atmospheric carbon dioxide by the Southern oscillation. *Nature*, **261**(5556), 116-118, doi: 10.1038/261116a0.
- Baker, D. F., R. M. Law, K. R. Gurney, P. Rayner, P. Peylin, A. S. Denning, P. Bousquet, L. Bruhwiler, Y. H. Chen, P. Ciais, I. Y. Fung, M. Heimann, J. John, T. Maki, S. Maksyutov, K. Masarie, M. Prather, B. Pak, S. Taguchi, and Z. Zhu, 2006: TransCom 3 inversion intercomparison: Impact of transport model errors on the interannual variability of regional CO₂ fluxes, 1988-2003. *Global Biogeochemical Cycles*, **20**(1), doi: 10.1029/2004gb002439.
- Ballantyne, A. P., J. B. Miller, and P. P. Tans, 2010: Apparent seasonal cycle in isotopic discrimination of carbon in the atmosphere and biosphere due to vapor pressure deficit. *Global Biogeochemical Cycles*, **24**(3), doi: 10.1029/2009GB003623.
- Ballantyne, A. P., R. Andres, R. Houghton, B. D. Stocker, R. Wanninkhof, W. Anderegg, L. A. Cooper, M. DeGrandpre, P. P. Tans, J. B. Miller, C. Alden, and J. W. C. White, 2015: Audit of the global carbon budget: Estimate errors and their impact on uptake uncertainty. *Biogeosciences*, **12**(8), 2565-2584, doi: 10.5194/bg-12-2565-2015.
- Basu, S., J. B. Miller, and S. Lehman, 2016: Separation of biospheric and fossil fuel fluxes of CO₂ by atmospheric inversion of CO₂ and ¹⁴CO₂ measurements: Observation system simulations. *Atmospheric Chemistry and Physics*, **16**(9), 5665-5683, doi: 10.5194/acp-16-5665-2016.
- Basu, S., M. Krol, A. Butz, C. Clerbaux, Y. Sawa, T. Machida, H. Matsueda, C. Frankenberg, O. P. Hasekamp, and I. Aben, 2014: The seasonal variation of the CO₂ flux over tropical Asia estimated from GOSAT, CONTRAIL, and IASI. *Geophysical Research Letters*, **41**(5), 1809-1815, doi: 10.1002/2013gl059105.
- Basu, S., S. Guerlet, A. Butz, S. Houweling, O. Hasekamp, I. Aben, P. Krummel, P. Steele, R. Langenfelds, M. Torn, S. Biraud, B. Stephens, A. Andrews, and D. Worthy, 2013: Global CO₂ fluxes estimated from GOSAT retrievals of total column CO₂. *Atmospheric Chemistry and Physics*, **13**(17), 8695-8717, doi: 10.5194/acp-13-8695-2013.
- Boden, T. A., G. Marland, and R. J. Andres, 2017: *Global, Regional, and National Fossil-Fuel CO₂ Emissions*. Carbon Dioxide Information Analysis Center, U.S. Department of Energy, Oak Ridge National Laboratory, Oak Ridge, Tenn., USA, doi: 10.3334/CDIAC/00001_V2017. [http://ess-dive.lbl.gov/2017/12/19/cdiac/]
- Bodman, R. W., P. J. Rayner, and D. J. Karoly, 2013: Uncertainty in temperature projections reduced using carbon cycle and climate observations. *Nature Climate Change*, **3**(8), 725-729, doi: 10.1038/nclimate1903.
- Booth, B. B. B., C. D. Jones, M. Collins, I. J. Totterdell, P. M. Cox, S. Sitch, C. Huntingford, R. A. Betts, G. R. Harris, and J. Lloyd, 2012: High sensitivity of future global warming to land carbon cycle processes. *Environmental Research Letters*, **7**(2), 024002, doi: 10.1088/1748-9326/7/2/024002.
- BP, 2016: *BP Statistical Review of World Energy June 2016*. BP. [https://www.bp.com/en/global/corporate/energy-economics/statistical-review-of-world-energy.html]
- Brailsford, G. W., B. B. Stephens, A. J. Gomez, K. Riedel, S. E. Mikaloff Fletcher, S. E. Nichol, and M. R. Manning, 2012: Long-term continuous atmospheric CO₂ measurements at Baring Head, New Zealand. *Atmospheric Measurement Techniques*, **5**(12), 3109-3117, doi: 10.5194/amt-5-3109-2012.
- Brandt, A. R., G. A. Heath, E. A. Kort, F. O'Sullivan, G. Petron, S. M. Jordaan, P. Tans, J. Wilcox, A. M. Gopstein, D. Arent, S. Wofsy, N. J. Brown, R. Bradley, G. D. Stucky, D. Eardley, and R. Harriss, 2014: Methane leaks from North American natural gas systems. *Science*, **343**(6172), 733-735, doi: 10.1126/science.1247045.
- Bréon, F. M., G. Broquet, V. Puygrenier, F. Chevallier, I. Xueref-Remy, M. Ramonet, E. Dieudonné, M. Lopez, M. Schmidt, O. Perrussel, and P. Ciais, 2015: An attempt at estimating Paris area CO₂ emissions from atmospheric concentration measurements. *Atmospheric Chemistry and Physics*, **15**(4), 1707-1724, doi: 10.5194/acp-15-1707-2015.
- Brioude, J., G. Petron, G. J. Frost, R. Ahmadov, W. M. Angevine, E. Y. Hsie, S. W. Kim, S. H. Lee, S. A. McKeen, M. Trainer, F. C. Fehsenfeld, J. S. Holloway, J. Peischl, T. B. Ryerson, and K. R. Gurney, 2012: A new inversion method to calculate emission inventories without a prior at mesoscale: Application to the anthropogenic CO₂ emission from Houston, Texas. *Journal of Geophysical Research: Atmospheres*, **117**(D5), doi: 10.1029/2011jd016918.
- Brioude, J., W. M. Angevine, R. Ahmadov, S. W. Kim, S. Evan, S. A. McKeen, E. Y. Hsie, G. J. Frost, J. A. Neuman, I. B. Pollack, J. Peischl, T. B. Ryerson, J. Holloway, S. S. Brown, J. B. Nowak, J. M. Roberts, S. C. Wofsy, G. W. Santoni, T. Oda, and M. Trainer, 2013: Top-down estimate of surface flux in the Los Angeles Basin using a mesoscale inverse modeling technique: Assessing anthropogenic emissions of CO, NO_x and CO₂ and their impacts. *Atmospheric Chemistry and Physics*, **13**(7), 3661-3677, doi: 10.5194/acp-13-3661-2013.



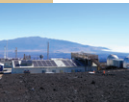
- Bruhwyler, L. M., S. Basu, P. Bergamaschi, P. Bousquet, E. Dlugokencky, S. Houweling, M. Ishizawa, H.-S. Kim, R. Locatelli, S. Maksyutov, S. Montzka, S. Pandey, P. K. Patra, G. Petron, M. Saunio, C. Sweeney, S. Schwietzke, P. Tans, and E. C. Weatherhead, 2017: U.S. CH₄ emissions from oil and gas production: Have recent large increases been detected? *Journal of Geophysical Research: Atmospheres*, **122**(7), 4070-4083, doi: 10.1002/2016JD026157.
- Bruhwyler, L., E. Dlugokencky, K. Masarie, M. Ishizawa, A. Andrews, J. Miller, C. Sweeney, P. Tans, and D. Worthy, 2014: CarbonTracker-CH₄: An assimilation system for estimating emissions of atmospheric methane. *Atmospheric Chemistry and Physics*, **14**(16), 8269-8293, doi: 10.5194/acp-14-8269-2014.
- Butler, M. P., K. J. Davis, A. S. Denning, and S. R. Kawa, 2010: Using continental observations in global atmospheric inversions of CO₂: North American carbon sources and sinks. *Tellus B: Chemical and Physical Meteorology*, **62**(5), 550-572, doi: 10.1111/j.1600-0889.2010.00501.x.
- Campbell, J. E., G. R. Carmichael, T. Chai, M. Mena-Carrasco, Y. Tang, D. R. Blake, N. J. Blake, S. A. Vay, G. J. Collatz, I. Baker, J. A. Berry, S. A. Montzka, C. Sweeney, J. L. Schnoor, and C. O. Stanier, 2008: Photosynthetic control of atmospheric carbonyl sulfide during the growing season. *Science*, **322**(5904), 1085-1088, doi: 10.1126/science.1164015.
- Canadell, J. G., P. Ciais, K. Gurney, C. Le Quéré, S. Piao, M. R. Raupach, and C. L. Sabine, 2011: An international effort to quantify regional carbon fluxes. *Eos, Transactions American Geophysical Union*, **92**(10), 81, doi: 10.1029/2011eo100001.
- CCSP, 2007: *First State of the Carbon Cycle Report (SOCCR): The North American Carbon Budget and Implications for the Global Carbon Cycle. A Report by the U.S. Climate Change Science Program and the Subcommittee on Global Change Research*. [A. W. King, L. Dilling, G. P. Zimmerman, D. M. Fairman, R. A. Houghton, G. Marland, A. Z. Rose, and T. J. Wilbanks (eds.)]. National Oceanic and Atmospheric Administration, National Climatic Data Center, Asheville, NC, USA, 242 pp.
- Chang, R. Y., C. E. Miller, S. J. Dinardo, A. Karion, C. Sweeney, B. C. Daube, J. M. Henderson, M. E. Mountain, J. Eluszkiewicz, J. B. Miller, L. M. Bruhwiler, and S. C. Wofsy, 2014: Methane emissions from Alaska in 2012 from CARVE airborne observations. *Proceedings of the National Academy of Sciences USA*, **111**(47), 16694-16699, doi: 10.1073/pnas.1412953111.
- Chevallier, F., N. M. Deutscher, T. J. Conway, P. Ciais, L. Ciattaglia, S. Dohe, M. Fröhlich, A. J. Gomez-Pelaez, D. Griffith, F. Hase, L. Haszpra, P. Krummel, E. Kyrö, C. Labuschagne, R. Langenfelds, T. Machida, F. Maignan, H. Matsueda, I. Morino, J. Notholt, M. Ramonet, Y. Sawa, M. Schmidt, V. Sherlock, P. Steele, K. Strong, R. Sussmann, P. Wennberg, S. Wofsy, D. Worthy, D. Wunch, and M. Zimnoch, 2011: Global CO₂ fluxes inferred from surface air-sample measurements and from TCCON retrievals of the CO₂ total column. *Geophysical Research Letters*, **38**(24), doi: 10.1029/2011gl049899.
- Ciais, P., A. S. Denning, P. P. Tans, J. A. Berry, D. A. Randall, G. J. Collatz, P. J. Sellers, J. W. C. White, M. Trolier, H. A. J. Meijer, R. J. Francey, P. Monfray, and M. Heimann, 1997: A three-dimensional synthesis study of δ¹⁸O in atmospheric CO₂: 1. Surface fluxes. *Journal of Geophysical Research: Atmospheres*, **102**(D5), 5857-5872, doi: 10.1029/96JD02360.
- Ciais, P., A. J. Dolman, A. Bombelli, R. Duren, A. Peregon, P. J. Rayner, C. Miller, N. Gobron, G. Kinderman, G. Marland, N. Gruber, F. Chevallier, R. J. Andres, G. Balsamo, L. Bopp, F. M. Bréon, G. Broquet, R. Dargaville, T. J. Battin, A. Borges, H. Bovensmann, M. Buchwitz, J. Butler, J. G. Canadell, R. B. Cook, R. DeFries, R. Engelen, K. R. Gurney, C. Heinze, M. Heimann, A. Held, M. Henry, B. Law, S. Luyssaert, J. Miller, T. Moriyama, C. Moulin, R. B. Myneni, C. Nussli, M. Obersteiner, D. Ojima, Y. Pan, J. D. Paris, S. L. Piao, B. Poulter, S. Plummer, S. Quegan, P. Raymond, M. Reichstein, L. Rivier, C. Sabine, D. Schimel, O. Tarasova, R. Valentini, R. Wang, G. van der Werf, D. Wickland, M. Williams, and C. Zehner, 2014: Current systematic carbon-cycle observations and the need for implementing a policy-relevant carbon observing system. *Biogeosciences*, **11**(13), 3547-3602, doi: 10.5194/bg-11-3547-2014.
- Cooley, D., F. J. Breidt, S. M. Ogle, A. E. Schuh, and T. Lauvaux, 2012: A constrained least-squares approach to combine bottom-up and top-down CO₂ flux estimates. *Environmental and Ecological Statistics*, **20**(1), 129-146, doi: 10.1007/s10651-012-0211-6.
- Cox, P. M., D. Pearson, B. B. Booth, P. Friedlingstein, C. Huntingford, C. D. Jones, and C. M. Luke, 2013: Sensitivity of tropical carbon to climate change constrained by carbon dioxide variability. *Nature*, **494**(7437), 341-344, doi: 10.1038/nature11882.
- Davis, K. J., A. Deng, T. Lauvaux, N. L. Miles, S. J. Richardson, D. P. Sarmiento, K. R. Gurney, R. M. Hardesty, T. A. Bonin, W. A. Brewer, B. K. Lamb, P. B. Shepson, R. M. Harvey, M. O. Cambaliza, C. Sweeney, J. C. Turnbull, J. Whetstone, and A. Karion, 2017: The Indianapolis flux experiment (INFLUX): A test-bed for developing urban greenhouse gas emission measurements. *Elementa: Science of the Anthropocene*, **5**(0), 21, doi: 10.1525/elementa.188.
- De Wachter, E., B. Barret, E. Le Flochmoën, E. Pavelin, M. Matricardi, C. Clerbaux, J. Hadji-Lazaro, M. George, D. Hurtmans, P. F. Coheur, P. Nedelec, and J. P. Cammas, 2012: Retrieval of MetOp-A/IASI CO profiles and validation with MOZAIC data. *Atmospheric Measurement Techniques*, **5**(11), 2843-2857, doi: 10.5194/amt-5-2843-2012.
- Deeter, M. N., S. Martínez-Alonso, L. V. Gatti, M. Gloor, J. B. Miller, L. G. Domingues, and C. S. C. Correia, 2016: Validation and analysis of MOPITT CO observations of the Amazon Basin. *Atmospheric Measurement Techniques*, **9**(8), 3999-4012, doi: 10.5194/amt-9-3999-2016.
- Deng, A., T. Lauvaux, K. J. Davis, B. J. Gaudet, N. Miles, S. J. Richardson, K. Wu, D. P. Sarmiento, R. M. Hardesty, T. A. Bonin, W. A. Brewer, and K. R. Gurney, 2017: Toward reduced transport errors in a high resolution urban CO₂ inversion system. *Elementa: Science of the Anthropocene*, **5**(0), 20, doi: 10.1525/elementa.133.



- Denning, A. S., M. Holzer, K. R. Gurney, M. Heimann, R. M. Law, P. J. Rayner, I. Y. Fung, S.-M. Fan, S. Taguchi, P. Friedlingstein, Y. Balkanski, J. Taylor, M. Maiss, and I. Levin, 1999: Three-dimensional transport and concentration of SF₆. A model intercomparison study (TransCom 2). *Tellus B: Chemical and Physical Meteorology*, **51**(2), 266-297, doi: 10.3402/tellusb.v51i2.16286.
- Díaz Isaac, L. I., T. Lauvaux, K. J. Davis, N. L. Miles, S. J. Richardson, A. R. Jacobson, and A. E. Andrews, 2014: Model-data comparison of MCI field campaign atmospheric CO₂ mole fractions. *Journal of Geophysical Research: Atmospheres*, **119**(17), 10536-10551, doi: 10.1002/2014JD021593.
- Dlugokencky, E. J., E. G. Nisbet, R. Fisher, and D. Lowry, 2011: Global atmospheric methane: Budget, changes and dangers. *Philosophical Transactions of the Royal Society A: Mathematical, Physical and Engineering Sciences*, **369**(1943), 2058-2072, doi: 10.1098/rsta.2010.0341.
- Dlugokencky, E. J., K. A. Masarie, P. M. Lang, and P. P. Tans, 1998: Continuing decline in the growth rate of the atmospheric methane burden. *Nature*, **393**, 447, doi: 10.1038/30934.
- Dlugokencky, E. J., L. Bruhwiler, J. W. C. White, L. K. Emmons, P. C. Novelli, S. A. Montzka, K. A. Masarie, P. M. Lang, A. M. Crowell, J. B. Miller, and L. V. Gatti, 2009: Observational constraints on recent increases in the atmospheric CH₄ burden. *Geophysical Research Letters*, **36**(18), doi: 10.1029/2009GL039780.
- Dobler, J. T., F. W. Harrison, E. V. Browell, B. Lin, D. McGregor, S. Kooi, Y. Choi, and S. Ismail, 2013: Atmospheric CO₂ column measurements with an airborne intensity-modulated continuous wave 1.57 μm fiber laser LIDAR. *Applied Optics*, **52**(12), 2874-2892, doi: 10.1364/AO.52.002874.
- Duren, R. M., and C. E. Miller, 2012: Measuring the carbon emissions of megacities. *Nature Climate Change*, **2**(8), 560-562, doi: 10.1038/nclimate1629.
- Ehret, G., C. Kiemle, M. Wirth, A. Amediek, A. Fix, and S. Houweling, 2008: Space-borne remote sensing of CO₂, CH₄, and N₂O by integrated path differential absorption LIDAR: A sensitivity analysis. *Applied Physics B*, **90**(3-4), 593-608, doi: 10.1007/s00340-007-2892-3.
- Enting, I. G., and J. V. Mansbridge, 1991: Latitudinal distribution of sources and sinks of CO₂: Results of an inversion study. *Tellus B: Chemical and Physical Meteorology*, **43**(2), 156-170, doi: 10.1034/j.1600-0889.1991.00010.x.
- Fan, S., M. Gloor, J. Mahlman, S. Pacala, J. Sarmiento, T. Takahashi, and P. Tans, 1998: A large terrestrial carbon sink in North America implied by atmospheric and oceanic carbon dioxide data and models. *Science*, **282**(5388), 442, doi: 10.1126/science.282.5388.442.
- Feng, S., T. Lauvaux, S. Newman, P. Rao, R. Ahmadov, A. Deng, L. I. Diaz-Isaac, R. M. Duren, M. L. Fischer, C. Gerbig, K. R. Gurney, J. Huang, S. Jeong, Z. Li, C. E. Miller, D. Keeffe, R. Patara-suk, S. P. Sander, Y. Song, K. W. Wong, and Y. L. Yung, 2016: Los Angeles megacity: A high-resolution land-atmosphere modelling system for urban CO₂ emissions. *Atmospheric Chemistry and Physics*, **16**(14), 9019-9045, doi: 10.5194/acp-16-9019-2016.
- Filges, A., C. Gerbig, H. Chen, H. Franke, C. Klaus, and A. Jordan, 2015: The IAGOS-core greenhouse gas package: A measurement system for continuous airborne observations of CO₂, CH₄, H₂O and CO. *Tellus B: Chemical and Physical Meteorology*, **67**(1), 27989, doi: 10.3402/tellusb.v67.27989.
- Flanagan, L. B., J. R. Brooks, G. T. Varney, and J. R. Ehleringer, 1997: Discrimination against C¹⁸O¹⁶O during photosynthesis and the oxygen isotope ratio of respired CO₂ in boreal forest ecosystems. *Global Biogeochemical Cycles*, **11**(1), 83-98, doi: 10.1029/96GB03941.
- Frankenberg, C., J. B. Fisher, J. Worden, G. Badgley, S. S. Saatchi, J.-E. Lee, G. C. Toon, A. Butz, M. Jung, A. Kuze, and T. Yokota, 2011: New global observations of the terrestrial carbon cycle from GOSAT: Patterns of plant fluorescence with gross primary productivity. *Geophysical Research Letters*, **38**(17), doi: 10.1029/2011gl048738.
- Friedlingstein, P., M. Meinshausen, V. K. Arora, C. D. Jones, A. Anav, S. K. Liddicoat, and R. Knutti, 2014: Uncertainties in CMIP5 climate projections due to carbon cycle feedbacks. *Journal of Climate*, **27**(2), 511-526, doi: 10.1175/jcli-d-12-00579.1.
- Friedlingstein, P., P. Cox, R. Betts, L. Bopp, W. von Bloh, V. Brovkin, P. Cadule, S. Doney, M. Eby, I. Fung, G. Bala, J. John, C. Jones, F. Joos, T. Kato, M. Kawamiya, W. Knorr, K. Lindsay, H. D. Matthews, T. Raddatz, P. Rayner, C. Reick, E. Roeckner, K. G. Schnitzler, R. Schnur, K. Strassmann, A. J. Weaver, C. Yoshikawa, and N. Zeng, 2006: Climate-carbon cycle feedback analysis: Results from the C⁴MIP model intercomparison. *Journal of Climate*, **19**(14), 3337-3353, doi: 10.1175/jcli3800.1.
- George, M., C. Clerbaux, D. Hurtmans, S. Turquety, P. F. Coheur, M. Pommier, J. Hadji-Lazaro, D. P. Edwards, H. Worden, M. Luo, C. Rinsland, and W. McMillan, 2009: Carbon monoxide distributions from the IASI/METOP mission: Evaluation with other space-borne remote sensors. *Atmospheric Chemistry and Physics*, **9**(21), 8317-8330, doi: 10.5194/acp-9-8317-2009.
- Gibert, F., G. J. Koch, J. Y. Beyon, T. W. Hilton, K. J. Davis, A. Andrews, P. H. Flamant, and U. N. Singh, 2011: Can CO₂ turbulent flux be measured by LIDAR? A preliminary study. *Journal of Atmospheric and Oceanic Technology*, **28**(3), 365-377, doi: 10.1175/2010jtecha1446.1.



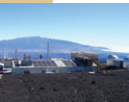
- Gibert, F., I. Xuéref-Rémy, L. Joly, M. Schmidt, J. Cuesta, K. J. Davis, M. Ramonet, P. H. Flamant, B. Parvite, and V. Zéninari, 2008: A case study of CO₂, CO and particles content evolution in the suburban atmospheric boundary layer using a 2- μ m Doppler DIAL, a 1- μ m backscatter LIDAR and an array of in-situ sensors. *Boundary-Layer Meteorology*, **128**(3), 381-401, doi: 10.1007/s10546-008-9296-8.
- Gloor, M., P. Bakwin, D. Hurst, L. Lock, R. Draxler, and P. Tans, 2001: What is the concentration footprint of a tall tower? *Journal of Geophysical Research: Atmospheres*, **106**(D16), 17831-17840, doi: 10.1029/2001jd900021.
- Gourdji, S. M., K. L. Mueller, V. Yadav, D. N. Huntzinger, A. E. Andrews, M. Trudeau, G. Petron, T. Nehrkorn, J. Eluszkiewicz, J. Henderson, D. Wen, J. Lin, M. Fischer, C. Sweeney, and A. M. Michalak, 2012: North American CO₂ exchange: Inter-comparison of modeled estimates with results from a fine-scale atmospheric inversion. *Biogeosciences*, **9**(1), 457-475, doi: 10.5194/bg-9-457-2012.
- Graven, H. D., R. F. Keeling, S. C. Piper, P. K. Patra, B. B. Stephens, S. C. Wofsy, L. R. Welp, C. Sweeney, P. P. Tans, J. J. Kelley, B. C. Daube, E. A. Kort, G. W. Santoni, and J. D. Bent, 2013: Enhanced seasonal exchange of CO₂ by northern ecosystems since 1960. *Science*, **341**(6150), 1085-1089, doi: 10.1126/science.1239207.
- Guerlet, S., S. Basu, A. Butz, M. Krol, P. Hahne, S. Houweling, O. P. Hasekamp, and I. Aben, 2013: Reduced carbon uptake during the 2010 Northern Hemisphere summer from GOSAT. *Geophysical Research Letters*, **40**(10), 2378-2383, doi: 10.1002/grl.50402.
- Gurney, K. R., I. Razlivanov, Y. Song, Y. Zhou, B. Benes, and M. Abdul-Massih, 2012: Quantification of fossil fuel CO₂ emissions on the building/street scale for a large U.S. city. *Environmental Science and Technology*, **46**(21), 12194-12202, doi: 10.1021/es3011282.
- Gurney, K. R., R. M. Law, A. S. Denning, P. J. Rayner, D. Baker, P. Bousquet, L. Bruhwiler, Y. H. Chen, P. Ciais, S. Fan, I. Y. Fung, M. Gloor, M. Heimann, K. Higuchi, J. John, T. Maki, S. Maksyutov, K. Masarie, P. Peylin, M. Prather, B. C. Pak, J. Randerson, J. Sarmiento, S. Taguchi, T. Takahashi, and C. W. Yuen, 2002: Towards robust regional estimates of CO₂ sources and sinks using atmospheric transport models. *Nature*, **415**(6872), 626-630, doi: 10.1038/415626a.
- Hayes, D. J., D. P. Turner, G. Stinson, A. D. McGuire, Y. X. Wei, T. O. West, L. S. Heath, B. Dejong, B. G. McConkey, R. A. Birdsey, W. A. Kurz, A. R. Jacobson, D. N. Huntzinger, Y. D. Pan, W. Mac Post, and R. B. Cook, 2012: Reconciling estimates of the contemporary North American carbon balance among terrestrial biosphere models, atmospheric inversions, and a new approach for estimating net ecosystem exchange from inventory-based data. *Global Change Biology*, **18**(4), 1282-1299, doi: 10.1111/j.1365-2486.2011.02627.x.
- Heimburger, A. M. F., R. M. Harvey, P. B. Shepson, B. H. Stirm, C. Gore, J. Turnbull, M. O. L. Cambaliza, O. E. Salmon, A.-E. M. Kerlo, T. N. Lavoie, K. J. Davis, T. Lauvaux, A. Karion, C. Sweeney, W. A. Brewer, R. M. Hardesty, and K. R. Gurney, 2017: Assessing the optimized precision of the aircraft mass balance method for measurement of urban greenhouse gas emission rates through averaging. *Elementa: Science of the Anthropocene*, **5**(0), 26, doi: 10.1525/elementa.134.
- Helmig, D., S. Rossabi, J. Hueber, P. Tans, S. A. Montzka, K. Masarie, K. Thoning, C. Plass-Duelmer, A. Claude, L. J. Carpenter, A. C. Lewis, S. Punjabi, S. Reimann, M. K. Vollmer, R. Steinbrecher, J. W. Hannigan, L. K. Emmons, E. Mahieu, B. Franco, D. Smale, and A. Pozzer, 2016: Reversal of global atmospheric ethane and propane trends largely due to US oil and natural gas production. *Nature Geoscience*, **9**, 490, doi: 10.1038/ngeo2721.
- Houweling, S., D. Baker, S. Basu, H. Boesch, A. Butz, F. Chevallier, F. Deng, E. J. Dlugokencky, L. Feng, A. Ganshin, O. Hasekamp, D. Jones, S. Maksyutov, J. Marshall, T. Oda, C. W. O'Dell, S. Oshchepkov, P. I. Palmer, P. Peylin, Z. Poussi, F. Reum, H. Takagi, Y. Yoshida, and R. Zhuravlev, 2015: An intercomparison of inverse models for estimating sources and sinks of CO₂ using GOSAT measurements. *Journal of Geophysical Research: Atmospheres*, **120**(10), 5253-5266, doi: 10.1002/2014JD022962.
- Huntingford, C., J. A. Lowe, B. B. Booth, C. D. Jones, G. R. Harris, L. K. Gohar, and P. Meir, 2009: Contributions of carbon cycle uncertainty to future climate projection spread. *Tellus B: Chemical and Physical Meteorology*, **61**(2), 355-360, doi: 10.1111/j.1600-0889.2009.00414.x.
- Huntzinger, D. N., W. M. Post, Y. Wei, A. M. Michalak, T. O. West, A. R. Jacobson, I. T. Baker, J. M. Chen, K. J. Davis, D. J. Hayes, F. M. Hoffman, A. K. Jain, S. Liu, A. D. McGuire, R. P. Neilson, C. Potter, B. Poulter, D. Price, B. M. Raczka, H. Q. Tian, P. Thornton, E. Tomelleri, N. Viovy, J. Xiao, W. Yuan, N. Zeng, M. Zhao, and R. Cook, 2012: North American Carbon Program (NACP) regional interim synthesis: Terrestrial biospheric model intercomparison. *Ecological Modelling*, **232**, 144-157, doi: 10.1016/j.ecolmodel.2012.02.004.
- Jeong, S., Y.-K. Hsu, A. E. Andrews, L. Bianco, P. Vaca, J. M. Wilczak, and M. L. Fischer, 2013: A multitower measurement network estimate of California's methane emissions. *Journal of Geophysical Research: Atmospheres*, **118**(19), 11,339-311,351, doi: 10.1002/jgrd.50854.
- Joiner, J., Y. Yoshida, A. P. Vasilkov, Y. Yoshida, L. A. Corp, and E. M. Middleton, 2011: First observations of global and seasonal terrestrial chlorophyll fluorescence from space. *Biogeosciences*, **8**(3), 637-651, doi: 10.5194/bg-8-637-2011.
- Karion, A., C. Sweeney, P. Tans, and T. Newberger, 2010: AirCore: An innovative atmospheric sampling system. *Journal of Atmospheric and Oceanic Technology*, **27**(11), 1839-1853, doi: 10.1175/2010jtecha1448.1.



- Karion, A., C. Sweeney, S. Wolter, T. Newberger, H. Chen, A. Andrews, J. Kofler, D. Neff, and P. Tans, 2013: Long-term greenhouse gas measurements from aircraft. *Atmospheric Measurement Techniques*, **6**(3), 511-526, doi: 10.5194/amt-6-511-2013.
- Keppel-Aleks, G., J. T. Randerson, K. Lindsay, B. B. Stephens, J. Keith Moore, S. C. Doney, P. E. Thornton, N. M. Mahowald, F. M. Hoffman, C. Sweeney, P. P. Tans, P. O. Wennberg, and S. C. Wofsy, 2013: Atmospheric carbon dioxide variability in the Community Earth System Model: Evaluation and transient dynamics during the twentieth and twenty-first centuries. *Journal of Climate*, **26**(13), 4447-4475, doi: 10.1175/jcli-d-12-00589.1.
- Keppel-Aleks, G., P. O. Wennberg, R. A. Washenfelder, D. Wunch, T. Schneider, G. C. Toon, R. J. Andres, J. F. Blavier, B. Connor, K. J. Davis, A. R. Desai, J. Messerschmidt, J. Notholt, C. M. Roehl, V. Sherlock, B. B. Stephens, S. A. Vay, and S. C. Wofsy, 2012: The imprint of surface fluxes and transport on variations in total column carbon dioxide. *Biogeosciences*, **9**(3), 875-891, doi: 10.5194/bg-9-875-2012.
- King, A. W., R. J. Andres, K. J. Davis, M. Hafer, D. J. Hayes, D. N. Huntzinger, B. de Jong, W. A. Kurz, A. D. McGuire, R. Vargas, Y. Wei, T. O. West, and C. W. Woodall, 2015: North America's net terrestrial CO₂ exchange with the atmosphere 1990–2009. *Biogeosciences*, **12**(2), 399-414, doi: 10.5194/bg-12-399-2015.
- Kort, E. A., C. Frankenberg, K. R. Costigan, R. Lindenmaier, M. K. Dubey, and D. Wunch, 2014: Four Corners: The largest US methane anomaly viewed from space. *Geophysical Research Letters*, **41**(19), 6898-6903, doi: 10.1002/2014GL061503.
- Kort, E. A., J. Eluszkiewicz, B. B. Stephens, J. B. Miller, C. Gerbig, T. Nehrkorn, B. C. Daube, J. O. Kaplan, S. Houweling, and S. C. Wofsy, 2008: Emissions of CH₄ and N₂O over the United States and Canada based on a receptor-oriented modeling framework and COBRA-NA atmospheric observations. *Geophysical Research Letters*, **35**(18), doi: 10.1029/2008gl034031.
- Lauvaux, T., A. E. Schuh, M. Bocquet, L. Wu, S. Richardson, N. Miles, and K. J. Davis, 2012a: Network design for mesoscale inversions of CO₂ sources and sinks. *Tellus B: Chemical and Physical Meteorology*, **64**(1), 17980, doi: 10.3402/tellusb.v64i0.17980.
- Lauvaux, T., A. E. Schuh, M. Uliasz, S. Richardson, N. Miles, A. E. Andrews, C. Sweeney, L. I. Diaz, D. Martins, P. B. Shepson, and K. J. Davis, 2012b: Constraining the CO₂ budget of the corn belt: Exploring uncertainties from the assumptions in a mesoscale inverse system. *Atmospheric Chemistry and Physics*, **12**(1), 337-354, doi: 10.5194/acp-12-337-2012.
- Lauvaux, T., and K. J. Davis, 2014: Planetary boundary layer errors in mesoscale inversions of column-integrated CO₂ measurements. *Journal of Geophysical Research: Atmospheres*, **119**(2), 490-508, doi: 10.1002/2013JD020175.
- Lauvaux, T., N. L. Miles, A. Deng, S. J. Richardson, M. O. Cambaliza, K. J. Davis, B. Gaudet, K. R. Gurney, J. Huang, D. O'Keefe, Y. Song, A. Karion, T. Oda, R. Patarasuk, I. Razlivanov, D. Sarmiento, P. Shepson, C. Sweeney, J. Turnbull, and K. Wu, 2016: High-resolution atmospheric inversion of urban CO₂ emissions during the dormant season of the Indianapolis Flux Experiment (INFLUX). *Journal of Geophysical Research: Atmospheres*, **121**(10), 5213-5236, doi: 10.1002/2015jd024473.
- Levin, I., S. Hammer, E. Eichelmann, and F. R. Vogel, 2011: Verification of greenhouse gas emission reductions: The prospect of atmospheric monitoring in polluted areas. *Philosophical Transactions. Series A, Mathematical, Physical, and Engineering Sciences Royal Society (Great Britain)*, **369**(1943), 1906-1924, doi: 10.1098/rsta.2010.0249.
- Levin, I., T. Naegler, R. Heinz, D. Osusko, E. Cuevas, A. Engel, J. Ilmberger, R. L. Langenfelds, B. Neining, C. v. Rohden, L. P. Steele, R. Weller, D. E. Worthy, and S. A. Zimov, 2010: The global SF₆ source inferred from long-term high precision atmospheric measurements and its comparison with emission inventories. *Atmospheric Chemistry and Physics*, **10**(6), 2655-2662, doi: 10.5194/acp-10-2655-2010.
- Lindqvist, H., C. W. O'Dell, S. Basu, H. Boesch, F. Chevallier, N. Deutscher, L. Feng, B. Fisher, F. Hase, M. Inoue, R. Kivi, I. Morino, P. I. Palmer, R. Parker, M. Schneider, R. Sussmann, and Y. Yoshida, 2015: Does GOSAT capture the true seasonal cycle of carbon dioxide? *Atmospheric Chemistry and Physics*, **15**(22), 13023-13040, doi: 10.5194/acp-15-13023-2015.
- Masarie, K. A., and P. P. Tans, 1995: Extension and integration of atmospheric carbon dioxide data into a globally consistent measurement record. *Journal of Geophysical Research: Atmospheres*, **100**(D6), 11593-11610, doi: 10.1029/95JD00859.
- Masarie, K. A., G. Pétron, A. Andrews, L. Bruhwiler, T. J. Conway, A. R. Jacobson, J. B. Miller, P. P. Tans, D. E. Worthy, and W. Peters, 2011: Impact of CO₂ measurement bias on CarbonTracker surface flux estimates. *Journal of Geophysical Research: Atmospheres*, **116**(D17), doi: 10.1029/2011JD016270.
- Matsueda, H., T. Machida, Y. Sawa, Y. Nakagawa, K. Hirotoni, H. Ikeda, N. Kondo, and K. Goto, 2008: Evaluation of atmospheric CO₂ measurements from new flask air sampling of JAL airliner observations. *Papers in Meteorology and Geophysics*, **59**, 1-17, doi: 10.2467/mripapers.59.1.
- McGuire, A. D., C. Koven, D. M. Lawrence, J. S. Clein, J. Xia, C. Beer, E. Burke, G. Chen, X. Chen, C. Delire, E. Jafarov, A. H. MacDougall, S. Marchenko, D. Nicolsky, S. Peng, A. Rinke, K. Saito, W. Zhang, R. Alkama, T. J. Bohn, P. Ciais, B. Decharme, A. Ekici, I. Gouttevin, T. Hajima, D. J. Hayes, D. Ji, G. Krinner, D. P. Lettenmaier, Y. Luo, P. A. Miller, J. C. Moore, V. Romanovsky, C. Schädel, K. Schaefer, E. A. G. Schuur, B. Smith, T. Sueyoshi, and Q. Zhuang, 2016: Variability in the sensitivity among model simulations of permafrost and carbon dynamics in the permafrost region between 1960 and 2009. *Global Biogeochemical Cycles*, **30**(7), 1015-1037, doi: 10.1002/2016gb005405.



- McKain, K., A. Down, S. M. Raciti, J. Budney, L. R. Hutyrá, C. Floerchinger, S. C. Herndon, T. Nehrkorn, M. S. Zahniser, R. B. Jackson, N. Phillips, and S. C. Wofsy, 2015: Methane emissions from natural gas infrastructure and use in the urban region of Boston, Massachusetts. *Proceedings of the National Academy of Sciences USA*, **112**(7), 1941-1946, doi: 10.1073/pnas.1416261112.
- McKain, K., S. C. Wofsy, T. Nehrkorn, J. Eluszkiewicz, J. R. Ehleringer, and B. B. Stephens, 2012: Assessment of ground-based atmospheric observations for verification of greenhouse gas emissions from an urban region. *Proceedings of the National Academy of Sciences USA*, **109**(22), 8423-8428, doi: 10.1073/pnas.1116645109.
- Melton, J. R., R. Wania, E. L. Hodson, B. Poulter, B. Ringeval, R. Spahni, T. Bohn, C. A. Avis, D. J. Beerling, G. Chen, A. V. Eliseev, S. N. Denisov, P. O. Hopcroft, D. P. Lettenmaier, W. J. Riley, J. S. Singarayer, Z. M. Subin, H. Tian, S. Zürcher, V. Brovkin, P. M. van Bodegom, T. Kleinen, Z. C. Yu, and J. O. Kaplan, 2013: Present state of global wetland extent and wetland methane modelling: Conclusions from a model inter-comparison project (WET-CHIMP). *Biogeosciences*, **10**(2), 753-788, doi: 10.5194/bg-10-753-2013.
- Miller, J. B., D. Yakir, J. W. C. White, and P. P. Tans, 1999: Measurement of $^{18}\text{O}/^{16}\text{O}$ in the soil-atmosphere CO_2 flux. *Global Biogeochemical Cycles*, **13**(3), 761-774, doi: 10.1029/1999GB900028.
- Miller, S. M., C. E. Miller, R. Commane, R. Y. W. Chang, S. J. Dinardo, J. M. Henderson, A. Karion, J. Lindaas, J. R. Melton, J. B. Miller, C. Sweeney, S. C. Wofsy, and A. M. Michalak, 2016: A multiyear estimate of methane fluxes in Alaska from CARVE atmospheric observations. *Global Biogeochemical Cycles*, **30**(10), 1441-1453, doi: 10.1002/2016GB005419.
- Miller, S. M., S. C. Wofsy, A. M. Michalak, E. A. Kort, A. E. Andrews, S. C. Biraud, E. J. Dlugokencky, J. Eluszkiewicz, M. L. Fischer, G. Janssens-Maenhout, B. R. Miller, J. B. Miller, S. A. Montzka, T. Nehrkorn, and C. Sweeney, 2013: Anthropogenic emissions of methane in the United States. *Proceedings of the National Academy of Sciences USA*, **110**(50), 20018-20022, doi: 10.1073/pnas.1314392110.
- Montzka, S. A., M. Krol, E. Dlugokencky, B. Hall, P. Jockel, and J. Lelieveld, 2011: Small interannual variability of global atmospheric hydroxyl. *Science*, **331**(6013), 67-69, doi: 10.1126/science.1197640.
- Newman, S., X. M. Xu, K. R. Gurney, Y. K. Hsu, K. F. Li, X. Jiang, R. Keeling, S. Feng, D. O'Keefe, R. Patarasuk, K. W. Wong, P. Rao, M. L. Fischer, and Y. L. Yung, 2016: Toward consistency between trends in bottom-up CO_2 emissions and top-down atmospheric measurements in the Los Angeles megacity. *Atmospheric Chemistry and Physics*, **16**(6), 3843-3863, doi: 10.5194/acp-16-3843-2016.
- Nisbet, E. G., E. J. Dlugokencky, M. R. Manning, D. Lowry, R. E. Fisher, J. L. France, S. E. Michel, J. B. Miller, J. W. C. White, B. Vaughn, P. Bousquet, J. A. Pyle, N. J. Warwick, M. Cain, R. Brownlow, G. Zazzeri, M. Lanoisellé, A. C. Manning, E. Gloor, D. E. J. Worthy, E. G. Brunke, C. Labuschagne, E. W. Wolff, and A. L. Ganesan, 2016: Rising atmospheric methane: 2007-2014 growth and isotopic shift. *Global Biogeochemical Cycles*, **30**(9), 1356-1370, doi: 10.1002/2016gb005406.
- Oda, T., and S. Maksyutov, 2011: A very high-resolution (1 km \times 1 km) global fossil fuel CO_2 emission inventory derived using a point source database and satellite observations of nighttime lights. *Atmospheric Chemistry and Physics*, **11**(2), 543-556, doi: 10.5194/acp-11-543-2011.
- Ogle, S. M., K. Davis, T. Lauvaux, A. Schuh, D. Cooley, T. O. West, L. S. Heath, N. L. Miles, S. Richardson, F. J. Breidt, J. E. Smith, J. L. McCarty, K. R. Gurney, P. Tans, and A. S. Denning, 2015: An approach for verifying biogenic greenhouse gas emissions inventories with atmospheric CO_2 concentration data. *Environmental Research Letters*, **10**(3), 034012, doi: 10.1088/1748-9326/10/3/034012.
- Pacala, S. W., C. Breidenich, P. G. Brewer, I. Fung, M. R. Gunson, G. Heddle, G. Marland, K. Paustian, M. Prather, J. T. Randerson, P. Tans, and S. C. Wofsy, 2010: *Verifying Greenhouse Gas Emissions: Methods to Support International Climate Agreements*. Committee on Methods for Estimating Greenhouse Gas Emissions, Washington, DC. [<http://www.nap.edu/catalog/12883/verifying-greenhouse-gas-emissions-methods-to-support-international-climate-agreements>]
- Pacala, S. W., G. C. Hurtt, D. Baker, P. Peylin, R. A. Houghton, R. A. Birdsey, L. Heath, E. T. Sundquist, R. F. Stallard, P. Ciais, P. Moorcroft, J. P. Caspersen, E. Shevliakova, B. Moore, G. Kohlmaier, E. Holland, M. Gloor, M. E. Harmon, S. M. Fan, J. L. Sarmiento, C. L. Goodale, D. Schimel, and C. B. Field, 2001: Consistent land- and atmosphere-based U.S. carbon sink estimates. *Science*, **292**(5525), 2316-2320, doi: 10.1126/science.1057320.
- Pacala, S., R. A. Birdsey, S. D. Bridgman, R. T. Conant, K. Davis, B. Hales, R. A. Houghton, J. C. Jenkins, M. Johnston, G. Marland, and K. Paustian, 2007: The North American carbon budget past and present. In: *First State of the Carbon Cycle Report (SOCCR): The North American Carbon Budget and Implications for the Global Carbon Cycle. A Report by the U.S. Climate Change Science Program and the Subcommittee on Global Change Research*. [A. W. King, L. Dilling, G. P. Zimmerman, D. M. Fairman, R. A. Houghton, G. Marland, A. Z. Rose, and T. J. Wilbanks (eds.)]. National Oceanic and Atmospheric Administration, National Climatic Data Center, Asheville, NC, USA, 29-36 pp.



- Patra, P. K., S. Houweling, M. Krol, P. Bousquet, D. Belikov, D. Bergmann, H. Bian, P. Cameron-Smith, M. P. Chipperfield, K. Corbin, A. Fortems-Cheiney, A. Fraser, E. Gloor, P. Hess, A. Ito, S. R. Kawa, R. M. Law, Z. Loh, S. Maksyutov, L. Meng, P. I. Palmer, R. G. Prinn, M. Rigby, R. Saito, and C. Wilson, 2011: TransCom model simulations of CH₄ and related species: Linking transport, surface flux and chemical loss with CH₄ variability in the troposphere and lower stratosphere. *Atmospheric Chemistry and Physics*, **11**(24), 12813-12837, doi: 10.5194/acp-11-12813-2011.
- Peischl, J., T. B. Ryerson, K. C. Aikin, J. A. de Gouw, J. B. Gilman, J. S. Holloway, B. M. Lerner, R. Nadkarni, J. A. Neuman, J. B. Nowak, M. Trainer, C. Warneke, and D. D. Parrish, 2015: Quantifying atmospheric methane emissions from the Haynesville, Fayetteville, and northeastern Marcellus shale gas production regions. *Journal of Geophysical Research: Atmospheres*, **120**(5), 2119-2139, doi: 10.1002/2014jd022697.
- Peters, W., A. R. Jacobson, C. Sweeney, A. E. Andrews, T. J. Conway, K. Masarie, J. B. Miller, L. M. Bruhwiler, G. Petron, A. I. Hirsch, D. E. Worthy, G. R. van der Werf, J. T. Randerson, P. O. Wennberg, M. C. Krol, and P. P. Tans, 2007: An atmospheric perspective on North American carbon dioxide exchange: CarbonTracker. *Proceedings of the National Academy of Sciences USA*, **104**(48), 18925-18930, doi: 10.1073/pnas.0708986104.
- Peters, W., M. C. Krol, E. J. Dlugokencky, F. J. Dentener, P. Bergamaschi, G. Dutton, P. v. Velthoven, J. B. Miller, L. Bruhwiler, and P. P. Tans, 2004: Toward regional-scale modeling using the two-way nested global model TMS: Characterization of transport using SF₆. *Journal of Geophysical Research: Atmospheres*, **109**(D19), doi: 10.1029/2004JD005020.
- Peters, W., M. C. Krol, G. R. van der Werf, S. Houweling, C. D. Jones, J. Hughes, K. Schaefer, K. A. Masarie, A. R. Jacobson, J. B. Miller, C. H. Cho, M. Ramonet, M. Schmidt, L. Ciattaglia, F. Apadula, D. Heltai, F. Meinhardt, A. G. Di Sarra, S. Piacentino, D. Sferlazzo, T. Aalto, J. Hatakka, J. Ström, L. Haszpra, H. A. J. Meijer, S. Van Der Laan, R. E. M. Neubert, A. Jordan, X. Rodó, J. A. Morguá, A. T. Vermeulen, E. Popa, K. Rozanski, M. Zimnoch, A. C. Manning, M. Leuenberger, C. Uglietti, A. J. Dolman, P. Ciais, M. Heimann, and P. P. Tans, 2010: Seven years of recent European net terrestrial carbon dioxide exchange constrained by atmospheric observations. *Global Change Biology*, **16**(4), 1317-1337, doi: 10.1111/j.1365-2486.2009.02078.x.
- Peylin, P., R. M. Law, K. R. Gurney, F. Chevallier, A. R. Jacobson, T. Maki, Y. Niwa, P. K. Patra, W. Peters, P. J. Rayner, C. Rodenbeck, I. T. van der Laan-Luijkx, and X. Zhang, 2013: Global atmospheric carbon budget: Results from an ensemble of atmospheric CO₂ inversions. *Biogeosciences*, **10**(10), 6699-6720, doi: 10.5194/bg-10-6699-2013.
- Randerson, J. T., F. M. Hoffman, P. E. Thornton, N. M. Mahowald, K. Lindsay, Y.-H. Lee, C. D. Nevison, S. C. Doney, G. Bonan, R. Stöckli, C. Covey, S. W. Running, and I. Y. Fung, 2009: Systematic assessment of terrestrial biogeochemistry in coupled climate-carbon models. *Global Change Biology*, **15**(10), 2462-2484, doi: 10.1111/j.1365-2486.2009.01912.x.
- Reuter, M., M. Buchwitz, M. Hilker, J. Heymann, O. Schneising, D. Pillai, H. Bovensmann, J. P. Burrows, H. Bösch, R. Parker, A. Butz, O. Hasekamp, C. W. O'Dell, Y. Yoshida, C. Gerbig, T. Nehr Korn, N. M. Deutscher, T. Warneke, J. Notholt, F. Hase, R. Kivi, R. Sussmann, T. Machida, H. Matsueda, and Y. Sawa, 2014: Satellite-inferred European carbon sink larger than expected. *Atmospheric Chemistry and Physics*, **14**(24), 13739-13753, doi: 10.5194/acp-14-13739-2014.
- Rigby, M., S. A. Montzka, R. G. Prinn, J. W. C. White, D. Young, S. O'Doherty, M. F. Lunt, A. L. Ganesan, A. J. Manning, P. G. Simmonds, P. K. Salameh, C. M. Harth, J. Muhle, R. F. Weiss, P. J. Fraser, L. P. Steele, P. B. Krummel, A. McCulloch, and S. Park, 2017: Role of atmospheric oxidation in recent methane growth. *Proceedings of the National Academy of Sciences USA*, **114**(21), 5373-5377, doi: 10.1073/pnas.1616426114.
- Rödenbeck, C., S. Houweling, M. Gloor, and M. Heimann, 2003: CO₂ flux history 1982–2001 inferred from atmospheric data using a global inversion of atmospheric transport. *Atmospheric Chemistry and Physics*, **3**(6), 1919-1964, doi: 10.5194/acp-3-1919-2003.
- Sarmiento, J. L., M. Gloor, N. Gruber, C. Beaulieu, A. R. Jacobson, S. E. Mikaloff Fletcher, S. Pacala, and K. Rodgers, 2010: Trends and regional distributions of land and ocean carbon sinks. *Biogeosciences*, **7**(8), 2351-2367, doi: 10.5194/bg-7-2351-2010.
- Saunio, M., P. Bousquet, B. Poulter, A. Peregón, P. Ciais, J. G. Canadell, E. J. Dlugokencky, G. Etiope, D. Bastviken, S. Houweling, G. Janssens-Maenhout, F. N. Tubiello, S. Castaldi, R. B. Jackson, M. Alexe, V. K. Arora, D. J. Beerling, P. Bergamaschi, D. R. Blake, G. Brailsford, V. Brovkin, L. Bruhwiler, C. Crevoisier, P. Crill, K. Covey, C. Curry, C. Frankenberg, N. Gedney, L. Höglund-Isaksson, M. Ishizawa, A. Ito, F. Joos, H.-S. Kim, T. Kleinen, P. Krummel, J.-F. Lamarque, R. Langenfelds, R. Locatelli, T. Machida, S. Maksyutov, K. C. McDonald, J. Marshall, J. R. Melton, I. Morino, V. Naik, amp, apos, S. Doherty, F.-J. W. Parmentier, P. K. Patra, C. Peng, S. Peng, G. P. Peters, I. Pison, C. Prigent, R. Prinn, M. Ramonet, W. J. Riley, M. Saito, M. Santini, R. Schroeder, I. J. Simpson, R. Spahni, P. Steele, A. Takizawa, B. F. Thornton, H. Tian, Y. Tohjima, N. Viovy, A. Voulgarakis, M. van Weele, G. R. van der Werf, R. Weiss, C. Wiedinmyer, D. J. Wilton, A. Wiltshire, D. Worthy, D. Wunch, X. Xu, Y. Yoshida, B. Zhang, Z. Zhang, and Q. Zhu, 2016: The global methane budget 2000–2012. *Earth System Science Data*, **8**(2), 697-751, doi: 10.5194/essd-8-697-2016.



- Schaefer, H., S. E. Mikaloff Fletcher, C. Veidt, K. R. Lassey, G. W. Brailsford, T. M. Bromley, E. J. Dlugokencky, S. E. Michel, J. B. Miller, I. Levin, D. C. Lowe, R. J. Martin, B. H. Vaughn, and J. W. White, 2016: A 21st-century shift from fossil-fuel to biogenic methane emissions indicated by $^{13}\text{CH}_4$. *Science*, **352**(6281), 80-84, doi: 10.1126/science.aad2705.
- Schuh, A. E., A. S. Denning, K. D. Corbin, I. T. Baker, M. Uliasz, N. Parazoo, A. E. Andrews, and D. E. J. Worthy, 2010: A regional high-resolution carbon flux inversion of North America for 2004. *Biogeosciences*, **7**(5), 1625-1644, doi: 10.5194/bg-7-1625-2010.
- Schuh, A. E., T. Lauvaux, T. O. West, A. S. Denning, K. J. Davis, N. Miles, S. Richardson, M. Uliasz, E. Lokupitiya, D. Cooley, A. Andrews, and S. Ogle, 2013: Evaluating atmospheric CO_2 inversions at multiple scales over a highly inventoried agricultural landscape. *Global Change Biology*, **19**(5), 1424-1439, doi: 10.1111/gcb.12141.
- Schwietzke, S., G. Petron, S. Conley, C. Pickering, I. Mielke-Maday, E. J. Dlugokencky, P. P. Tans, T. Vaughn, C. Bell, D. Zimmerle, S. Wolter, C. W. King, A. B. White, T. Coleman, L. Bianco, and R. C. Schnell, 2017: Improved mechanistic understanding of natural gas methane emissions from spatially resolved aircraft measurements. *Environmental Science and Technology*, **51**(12), 7286-7294, doi: 10.1021/acs.est.7b01810.
- Schwietzke, S., O. A. Sherwood, L. M. P. Bruhwiler, J. B. Miller, G. Etiope, E. J. Dlugokencky, S. E. Michel, V. A. Arling, B. H. Vaughn, J. W. C. White, and P. P. Tans, 2016: Upward revision of global fossil fuel methane emissions based on isotope database. *Nature*, **538**(7623), 88-91, doi: 10.1038/nature19797.
- Stephens, B. B., K. R. Gurney, P. P. Tans, C. Sweeney, W. Peters, L. Bruhwiler, P. Ciais, M. Ramonet, P. Bousquet, T. Nakazawa, S. Aoki, T. Machida, G. Inoue, N. Vinnichenko, J. Lloyd, A. Jordan, M. Heimann, O. Shibistova, R. L. Langenfelds, L. P. Steele, R. J. Francey, and A. S. Denning, 2007: Weak northern and strong tropical land carbon uptake from vertical profiles of atmospheric CO_2 . *Science*, **316**(5832), 1732-1735, doi: 10.1126/science.1137004.
- Sweeney, C., A. Karion, S. Wolter, T. Newberger, D. Guenther, J. A. Higgs, A. E. Andrews, P. M. Lang, D. Neff, E. Dlugokencky, J. B. Miller, S. A. Montzka, B. R. Miller, K. A. Masarie, S. C. Biraud, P. C. Novelli, M. Crotwell, A. M. Crotwell, K. Thoning, and P. P. Tans, 2015: Seasonal climatology of CO_2 across North America from aircraft measurements in the NOAA/ESRL Global Greenhouse Gas Reference Network. *Journal of Geophysical Research: Atmospheres*, **120**(10), 5155-5190, doi: 10.1002/2014jd022591.
- Tans, P. P., I. Y. Fung, and T. Takahashi, 1990: Observational constraints on the global atmospheric CO_2 budget. *Science*, **247**(4949), 1431-1438, doi: 10.1126/science.247.4949.1431.
- Thiemens, M. H., S. Chakraborty, and T. L. Jackson, 2014: Decadal $\Delta^{17}\text{O}$ record of tropospheric CO_2 : Verification of a stratospheric component in the troposphere. *Journal of Geophysical Research: Atmospheres*, **119**(10), 6221-6229, doi: 10.1002/2013JD020317.
- Townsend-Small, A., E. C. Botner, K. L. Jimenez, J. R. Schroeder, N. J. Blake, S. Meinardi, D. R. Blake, B. C. Sive, D. Bon, J. H. Crawford, G. Pfister, and F. M. Flocke, 2016: Using stable isotopes of hydrogen to quantify biogenic and thermogenic atmospheric methane sources: A case study from the Colorado Front Range. *Geophysical Research Letters*, **43**(21), 11,462-411,471, doi: 10.1002/2016gl071438.
- Turnbull, J. C., C. Sweeney, A. Karion, T. Newberger, S. J. Lehman, P. P. Tans, K. J. Davis, T. Lauvaux, N. L. Miles, S. J. Richardson, M. O. Cambaliza, P. B. Shepson, K. Gurney, R. Patarasuk, and I. Razlivanov, 2015: Toward quantification and source sector identification of fossil fuel CO_2 emissions from an urban area: Results from the INFLUX experiment. *Journal of Geophysical Research: Atmospheres*, **120**(1), 292-312, doi: 10.1002/2014jd022555.
- Turnbull, J. C., J. B. Miller, S. J. Lehman, D. Hurst, P. P. Tans, J. Southon, S. Montzka, J. Elkins, D. J. Mondeel, P. A. Romashkin, N. Elansky, and A. Skorokhod, 2008: Spatial distribution of $\Delta^{14}\text{CO}_2$ across Eurasia: Measurements from the TROICA-8 expedition. *Atmospheric Chemistry and Physics Discussions*, **8**(4), 15207-15238, doi: 10.5194/acpd-8-15207-2008.
- Turner, A. J., C. Frankenberg, P. O. Wennberg, and D. J. Jacob, 2017: Ambiguity in the causes for decadal trends in atmospheric methane and hydroxyl. *Proceedings of the National Academy of Sciences USA*, **114**(21), 5367-5372, doi: 10.1073/pnas.1616020114.
- Turner, A. J., D. J. Jacob, J. Benmergui, S. C. Wofsy, J. D. Maa-sackers, A. Butz, O. Hasekamp, and S. C. Biraud, 2016: A large increase in U.S. methane emissions over the past decade inferred from satellite data and surface observations. *Geophysical Research Letters*, **43**(5), 2218-2224, doi: 10.1002/2016GL067987.
- U.S. EPA, 2016: *Inventory of U.S. Greenhouse Gas Emissions and Sinks: 1990-2014*. [<https://www.epa.gov/ghgemissions/inventory-us-greenhouse-gas-emissions-and-sinks-1990-2014>]
- U.S. EPA, 2017: *Inventory of U.S. Greenhouse Gas Emissions and Sinks: 1990-2015*. United States Environmental Protection Agency, EPA 430-P-17-001. [<https://www.epa.gov/ghgemissions/inventory-us-greenhouse-gas-emissions-and-sinks-1990-2015>]
- van der Laan-Luijkx, I. T., I. R. van der Velde, M. C. Krol, L. V. Gatti, L. G. Domingues, C. S. C. Correia, J. B. Miller, M. Gloor, T. T. van Leeuwen, J. W. Kaiser, C. Wiedinmyer, S. Basu, C. Clerbaux, and W. Peters, 2015: Response of the Amazon carbon balance to the 2010 drought derived with CarbonTracker South America. *Global Biogeochemical Cycles*, **29**(7), 1092-1108, doi: 10.1002/2014gb005082.
- Vay, S. A., Y. Choi, K. P. Vadrevu, D. R. Blake, S. C. Tyler, A. Wisthaler, A. Hecobian, Y. Kondo, G. S. Diskin, G. W. Sachse, J. H. Woo, A. J. Weinheimer, J. F. Burkhart, A. Stohl, and P. O. Wennberg, 2011: Patterns of CO_2 and radiocarbon across high northern latitudes during International Polar Year 2008. *Journal of Geophysical Research*, **116**(D14), doi: 10.1029/2011jd015643.



- Wenzel, S., P. M. Cox, V. Eyring, and P. Friedlingstein, 2014: Emergent constraints on climate-carbon cycle feedbacks in the CMIP5 Earth system models. *Journal of Geophysical Research: Biogeosciences*, **119**(5), 794-807, doi: 10.1002/2013jg002591.
- Wieder, W. R., C. C. Cleveland, D. M. Lawrence, and G. B. Bonan, 2015: Effects of model structural uncertainty on carbon cycle projections: Biological nitrogen fixation as a case study. *Environmental Research Letters*, **10**(4), 044016, doi: 10.1088/1748-9326/10/4/044016.
- Wolfe, G. M., T. F. Hanisco, H. L. Arkinson, T. P. Bui, J. D. Crouse, J. Dean-Day, A. Goldstein, A. Guenther, S. R. Hall, G. Huey, D. J. Jacob, T. Karl, P. S. Kim, X. Liu, M. R. Marvin, T. Mikoviny, P. K. Misztal, T. B. Nguyen, J. Peischl, I. Pollack, T. Ryerson, J. M. St. Clair, A. Teng, K. R. Travis, K. Ullmann, P. O. Wennberg, and A. Wisthaler, 2015: Quantifying sources and sinks of reactive gases in the lower atmosphere using airborne flux observations. *Geophysical Research Letters*, **42**(19), 8231-8240, doi: 10.1002/2015gl065839.
- Wong, K. W., D. Fu, T. J. Pongetti, S. Newman, E. A. Kort, R. Duren, Y. K. Hsu, C. E. Miller, Y. L. Yung, and S. P. Sander, 2015: Mapping CH₄ : CO₂ ratios in Los Angeles with CLARS-FTS from Mount Wilson, California. *Atmospheric Chemistry and Physics*, **15**(1), 241-252, doi: 10.5194/acp-15-241-2015.
- Worden, J. R., A. A. Bloom, S. Pandey, Z. Jiang, H. M. Worden, T. W. Walker, S. Houweling, and T. Röckmann, 2017: Reduced biomass burning emissions reconcile conflicting estimates of the post-2006 atmospheric methane budget. *Nature Communications*, **8**(1), 2227, doi: 10.1038/s41467-017-02246-0.
- Wunch, D., G. C. Toon, J. F. Blavier, R. A. Washenfelder, J. Notholt, B. J. Connor, D. W. Griffith, V. Sherlock, and P. O. Wennberg, 2011: The total carbon column observing network. *Philosophical Transactions of the Royal Society A: Mathematical, Physical and Engineering Sciences*, **369**(1943), 2087-2112, doi: 10.1098/rsta.2010.0240.
- Wunch, D., P. O. Wennberg, G. C. Toon, G. Keppel-Aleks, and Y. G. Yavin, 2009: Emissions of greenhouse gases from a North American megacity. *Geophysical Research Letters*, **36**(15), doi: 10.1029/2009gl039825.
- Wunch, D., P. O. Wennberg, G. Osterman, B. Fisher, B. Naylor, C. M. Roehl, C. Dell, L. Mandrake, C. Viatte, D. W. Griffith, N. M. Deutscher, V. A. Velasco, J. Notholt, T. Warneke, C. Petri, M. De Maziere, M. K. Sha, R. Sussmann, M. Rettinger, D. Pollard, J. Robinson, I. Morino, O. Uchino, F. Hase, T. Blumenstock, M. Kiel, D. G. Feist, S. G. Arnold, K. Strong, J. Mendonca, R. Kivi, P. Heikkinen, L. Iraci, J. Podolske, P. W. Hillyard, S. Kawakami, M. K. Dubey, H. A. Parker, E. Sepulveda, O. E. Garcia, Y. Te, P. Jeseck, M. R. Gunson, D. Crisp, and A. Eldering, 2016: Comparisons of the Orbiting Carbon Observatory-2 (OCO-2) X_{CO2} measurements with TCCON. *Atmospheric Measurement Techniques Discussions*, 1-45, doi: 10.5194/amt-2016-227.
- Zavala-Araiza, D., D. R. Lyon, R. A. Alvarez, K. J. Davis, R. Harriss, S. C. Herndon, A. Karion, E. A. Kort, B. K. Lamb, X. Lan, A. J. Marchese, S. W. Pacala, A. L. Robinson, P. B. Shepson, C. Sweeney, R. Talbot, A. Townsend-Small, T. I. Yacovitch, D. J. Zimmerle, and S. P. Hamburg, 2015: Reconciling divergent estimates of oil and gas methane emissions. *Proceedings of the National Academy of Sciences USA*, **112**(51), 15597-15602, doi: 10.1073/pnas.1522126112.



9 Forests

Lead Authors

Grant Domke, USDA Forest Service; Christopher A. Williams, Clark University

Contributing Authors

Richard Birdsey, Woods Hole Research Center; John Coulston, USDA Forest Service; Adrien Finzi, Boston University; Christopher Gough, Virginia Commonwealth University; Bob Haight, USDA Forest Service; Jeff Hicke, University of Idaho; Maria Janowiak, USDA Forest Service; Ben de Jong, El Colegio de la Frontera Sur; Werner A. Kurz, Natural Resources Canada, Canadian Forest Service; Melissa Lucash, Portland State University; Stephen Ogle, Colorado State University; Marcela Olguín-Álvarez, Consultant, SilvaCarbon Program; Yude Pan, USDA Forest Service; Margaret Skutsch, Centro de Investigaciones en Geografía Ambiental; Carolyn Smyth, Natural Resources Canada, Canadian Forest Service; Chris Swanston, USDA Forest Service; Pamela Templer, Boston University; Dave Wear, USDA Forest Service; Christopher W. Woodall, USDA Forest Service

Acknowledgments

Richard Birdsey (Science Lead), Woods Hole Research Center; Marc G. Kramer (Review Editor), Washington State University, Vancouver; John Schade (Federal Liaison) National Science Foundation; Anne Marsh (Federal Liaison), USDA Forest Service; Karina V. R. Schäfer (former Federal Liaison), National Science Foundation

Recommended Citation for Chapter

Domke, G., C. A. Williams, R. Birdsey, J. Coulston, A. Finzi, C. Gough, B. Haight, J. Hicke, M. Janowiak, B. de Jong, W. A. Kurz, M. Lucash, S. Ogle, M. Olguín-Álvarez, Y. Pan, M. Skutsch, C. Smyth, C. Swanston, P. Templer, D. Wear, and C. W. Woodall, 2018: Chapter 9: Forests. In *Second State of the Carbon Cycle Report (SOCCR2): A Sustained Assessment Report* [Cavallaro, N., G. Shrestha, R. Birdsey, M. A. Mayes, R. G. Najjar, S. C. Reed, P. Romero-Lankao, and Z. Zhu (eds.)]. U.S. Global Change Research Program, Washington, DC, USA, pp. 365-398, <https://doi.org/10.7930/SOCCR2.2018.Ch9>.



KEY FINDINGS

1. Net uptake of 217 teragrams of carbon (Tg C) per year by the forest sector in North America is well documented and has persisted at about this level over the last decade. The strength of net carbon uptake varies regionally, with about 80% of the North American forest carbon sink occurring within the United States (*high confidence, very likely*).
2. Forest regrowth following historical clearing plays a substantial role in determining the size of the forest carbon sink, but studies also suggest sizeable contributions from growth enhancements such as carbon dioxide fertilization, nitrogen deposition, or climate trends supporting accelerated growth (*medium confidence*). Resolving each factor's contribution is a major challenge and critical for developing reliable predictions.
3. Annual harvest removals from forestry operations in select regions decrease forest carbon stocks, but this decline in stocks is balanced by post-harvest recovery and regrowth in forestlands that were harvested in prior years. Removal, processing, and use of harvested biomass causes carbon emissions outside of forests, offsetting a substantial portion (about half) of the net carbon sink in North American forests (*high confidence*).
4. Recent trends in some disturbance rates (e.g., wildfires and insects) have diminished the strength of net forest carbon uptake across much of North America. Net loss of forest carbon stocks from land conversions reduced sink strength across the continent by 11 Tg C per year, with carbon losses from forest conversion exceeding carbon gains from afforestation and reforestation (*medium confidence*).
5. Several factors driving the carbon sink in North American forests are expected to decline over coming decades, and an increasing rate of natural disturbance could further diminish current net carbon uptake (*medium confidence*).

Note: Confidence levels are provided as appropriate for quantitative, but not qualitative, Key Findings and statements.

9.1 Introduction

The forest land area of North America increased from an estimated 719 million hectares (ha) in 2005 to more than 723 million ha in 2015 and now represents 36% of the land area in North America and 18% of the world's forest land area (FAO 2016b). The increase in forest land area over the last decade was driven entirely by gains in the United States, while Canada and Mexico both lost forestland (see Table 9.1, p. 367). The area of other wooded lands also increased in North America over the last decade, with substantial gains in the United States, no change in Canada, and loss in Mexico.

Forest ecosystems are the largest terrestrial carbon sink on Earth, and their management has been recognized as a relatively cost-effective strategy for offsetting greenhouse gas (GHG) emissions

(Canadell and Schulze 2014). In North America, forests—including urban forests, woodlands, and the products obtained from them—play a major role in the carbon cycle (Goodale et al., 2002). Since this report includes forestland from Canada, Mexico, and the United States, forestland is defined according to the Global Forest Resource Assessments from the United Nations Food and Agricultural Organization (FAO 2010, 2016b). This definition also is widely used for land representation in GHG reporting to the United Nations Framework Convention on Climate Change (UNFCCC; see U.S. EPA 2018) to ensure consistency and comparability in national reporting. Forest area is defined as land spanning greater than 0.5 ha with trees higher than 5 m and canopy cover of more than 10%, or trees able to reach these thresholds *in situ*. Other wooded lands are



defined as land not classified as forest, spanning greater than 0.5 ha with 1) trees higher than 5 m and a canopy cover of 5% to 10%; 2) trees able to reach these thresholds *in situ*; or 3) land with a combined cover of shrubs, bushes, and trees above 10%. Forests and other wooded land do not include land predominantly used for agriculture or urban purposes (FAO 2010). For this reason, urban forests are not included in this chapter, but their contribution to total carbon stocks and stock changes is described.

Forests' capacity to uptake and store carbon is influenced by many socioeconomic and biophysical factors (Caspersen et al., 2000; Joos et al., 2002; Birdsey et al., 2006; Zhang et al., 2012). Sustained investment in afforestation, reforestation, and improved forest management is an option for elevating the role forests play in future climate mitigation. This chapter presents the most recent estimates of carbon stocks and stock changes across the continuum of land with trees in North America and highlights advances in forest carbon cycle science since the *First State of the Carbon Cycle Report* (SOCCR1; CCSP 2007).

9.2 Historical Context

Forestland, and thus forest carbon, has changed substantially in North America over the last several hundred years. In the United States, for example, forestland amounts to an estimated 72% of the area that was forested in 1630, with roughly 120 million ha converted to other uses (mainly agricultural) primarily from 1850 to 1910 (Smith et al., 2009). National assessments of forest land area and carbon dynamics have been conducted in Canada, Mexico, and the United States, but the motivation for these reports and the methods and data sources they use differ substantially among countries. In recent decades, official government estimates of forest land area, forest carbon stocks, and stock changes have been compiled following guidelines from the Intergovernmental Panel on Climate Change (IPCC 2003, 2006). However, the methods for estimating carbon stocks and their changes (e.g., stock difference versus gain-loss) still differ based on country-specific circumstances, but estimation approaches have evolved as new and better information has become available in each country. Of the numerous key findings SOCCR1 identified on the

Table 9.1. Estimated Area (in Thousands of Hectares) of Forest and Other Wooded Land in North America in 2005 and 2015

Country ^a	Forestland ^b		Other Wooded Land ^c	
	2005	2015	2005	2015
Canada	347,576	347,069	40,866	40,866
Mexico	67,083	66,040	20,378	19,715
United States	304,757	310,095	15,452	21,279
Total^d	719,416****	723,204****	76,696****	81,860****

Notes

a) Estimates based on FAO (2016b).

b) Defined as land spanning greater than 0.5 hectare (ha) with trees higher than 5 m and a canopy cover of more than 10%, or trees able to reach these thresholds *in situ* (FAO 2010).

c) Defined as land not classified as forest, spanning greater than 0.5 ha with trees higher than 5 m and a canopy cover of 5% to 10%; or trees able to reach these thresholds *in situ*; or with a combined cover of shrubs, bushes, and trees above 10% (FAO 2010).

d) Uncertainty estimates (noted by asterisks) follow the convention described in Treatment of Uncertainty in SOCCR2, p. 16, in the Preface.



role of forests in the North American carbon cycle, many (e.g., land-use change) continue to be relevant 10 years later, along with several emerging topics (e.g., climate feedbacks).

9.3 Current Understanding of Carbon Fluxes and Stocks

9.3.1 Carbon Stocks and Pools

Forests

Carbon is continuously cycled among the atmosphere and ecosystem carbon storage pools (i.e., above- and belowground biomass, dead wood, litter, and soil). This cycling is driven by biogeochemical processes in forests (e.g., photosynthesis, respiration, decomposition, and disturbances such as fires or pest outbreaks) and anthropogenic activities (e.g., harvesting, thinning, and replanting).

As trees photosynthesize and allocate a portion of this carbon to growth, carbon is removed from the atmosphere and stored in living tree biomass. As live biomass dies, litter and dead wood are deposited on the forest floor and in the soil below ground (e.g., dead roots). The carbon in these dead components is either stored as soil organic matter or released to the atmosphere or water through decomposition by microorganisms. When forests are harvested, some of the biomass carbon is transferred to harvested wood products from which it may be lost to the atmosphere (burned) in the year

of the harvest (e.g., fuelwood [including pellets] and mill residues) or stored for a few years (e.g., paper products) to centuries (e.g., sawnwood or panels used in buildings) (IPCC 2006; Skog 2008).

Carbon stocks in North American forests have continued to increase over the last decade to an estimated 103,110 teragrams of carbon (Tg C), of which 32% is in live biomass and 68% is in dead organic matter (see Table 9.2, this page; Stinson et al., 2011; Köhl et al., 2015; FAO 2010, 2016b; U.S. EPA 2018). The increase in total carbon stocks is largely due to increases in aboveground biomass in the eastern United States, even as carbon stocks in Canada decreased slightly in recent years because of natural disturbances such as insects and wildfire (Stinson et al., 2011; Köhl et al., 2015; FAO 2010, 2016b; U.S. EPA 2018; ECCC 2016).

Carbon density (i.e., the amount of carbon stored per unit of land area) is highly variable (e.g., see Figure 9.1, p. 369, for the distribution of aboveground live biomass density on forestland in North America). The estimated carbon density in North American forests is 142.4 megagrams of carbon (Mg C) per hectare. In Canada, the largest carbon densities are in boreal and cordilleran forests (ECCC 2016; Kurz et al., 2013). In the United States, forests of the Northeast, upper Midwest, Pacific Coast, and Alaska continue to store the most

Table 9.2. Forest Carbon Stocks (in Teragrams of Carbon) by Carbon Pool in North America

Country	Aboveground Biomass	Belowground Biomass	Dead Wood	Litter	Soil
Canada ^a	11,162	2,746	4,683	11,666	19,729
Mexico ^b	1,597	396	2	NA ^c	NA
United States ^d	14,182	2,923	2,570	2,680	28,774
Total^e	26,941****	6,065****	7,255****	14,346****	48,503****

Notes

a) Estimates based on FAO (2010).

b) Estimates based on FAO (2016b).

c) Not applicable.

d) Estimates based on U.S. EPA (2018).

e) Uncertainty estimates (noted by asterisks) follow the convention described in Treatment of Uncertainty in SOCCR2, p. 16, in the Preface.

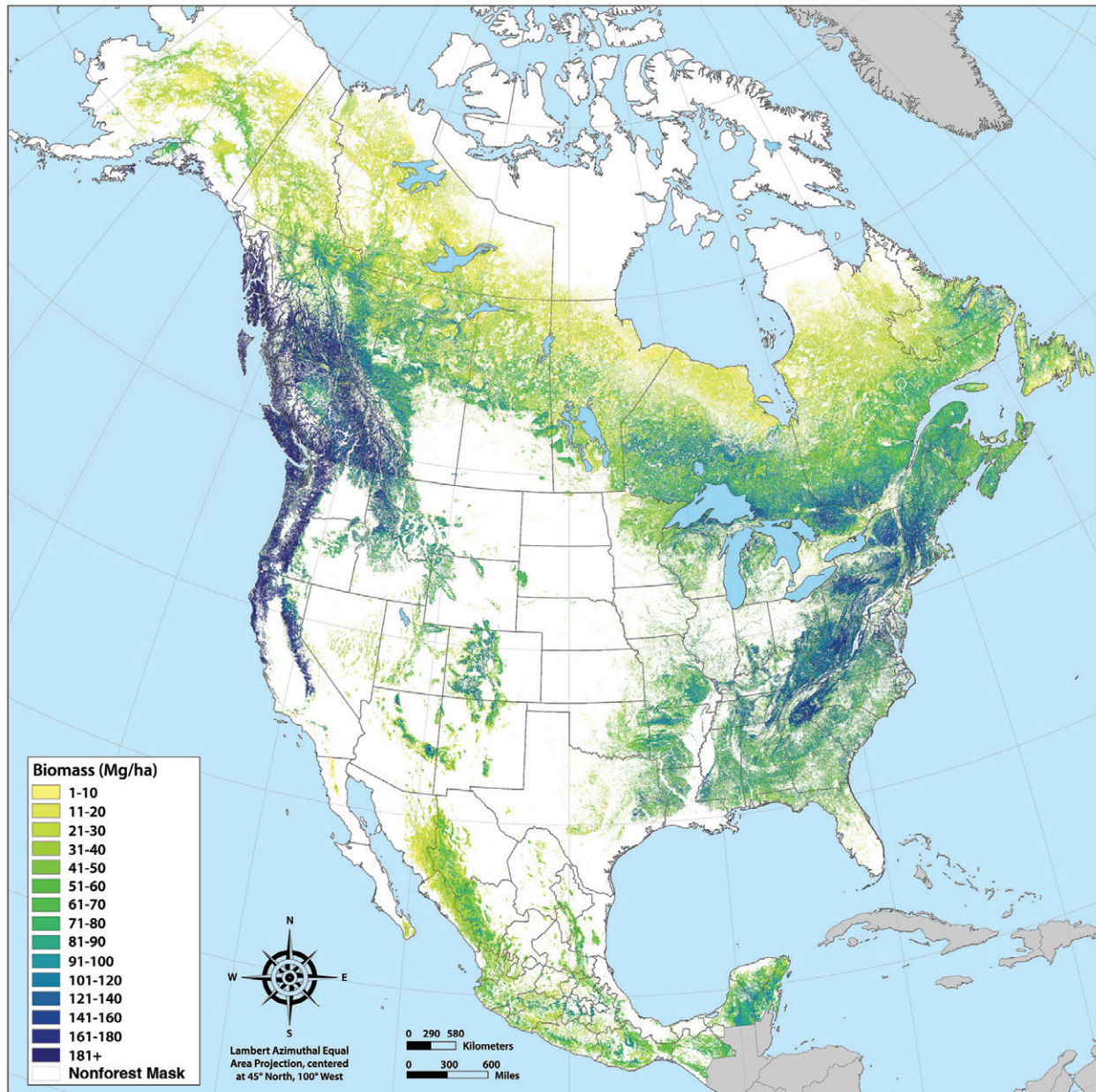


Figure 9.1. Hectares (ha) of Aboveground Forest Biomass Across North America. This comprehensive map combines four independently developed maps of biomass for Canada, Alaska, the conterminous United States, and Mexico (Beaudoin et al., 2014; Blackard et al., 2008; Wilson et al., 2013; MREDD+ Alliance 2013). A common legend, map projection, and spatial resolution of 250 m were applied to the individual maps with no attempt to harmonize the methods used for each of the original map products. Biomass of nonforest areas is masked by including only land-cover and land-use categories 1–6 from the North American Land Change Monitoring System (NALCMS 2018). Base years of the original maps are Canada, 2001; Alaska, 2004; conterminous United States, 2000–2009; and Mexico, 2007. [Figure source: Kevin McCullough, U.S. Forest Service. North American Biomass and Disturbance Mapping Working Group, 2014.]



carbon (U.S. EPA 2018; see Figure ES.1, p. 23, for a description of the areal extent of regions in the United States). In Mexico, forest carbon stocks are split fairly evenly among temperate, tropical, and semiarid forests (INECC/SEMARNAT 2015).

Woodlands

Woodlands are areas with tree coverage that falls between savanna and forest biomes. In the United States, for example, tree cover for woodlands does not meet the criteria for forestlands or agroforestry. Most woodlands occur in a matrix of grass vegetation and have been expanding in recent decades as trees and woody shrubs encroach on grasslands around the world, including in the western United States (Archer 1994; Briggs et al., 2002; Weisberg et al., 2007). For example, Asner et al. (2003) estimated a 10% increase in woody plant cover over a 40,000 ha area of northern Texas from 1937 to 1999 and an associated biomass carbon stock increase of 120 grams of carbon (g C) per m². In the Intermountain West, woodland areas increased by about 1.3 million ha from 2005 to 2010 and resulted in an estimated net carbon stock increase of 6,439 Mg in biomass, litter, and dead wood (Coulston et al., 2016; Ogle and Zeigler 2016). Woody encroachment also could affect soil carbon stocks (Hibbard et al., 2001), although this may not be the case in all woodland systems (Hughes et al., 2006) and may vary depending on the climate (Jackson et al., 2002).

9.3.2 Fluxes

North American forests currently act as a net sink for atmospheric carbon dioxide (CO₂; Hayes et al., 2012; King et al., 2015). A summary of data reported in recent GHG inventories (ECCC 2016; INECC/SEMARNAT 2015; U.S. EPA 2018) suggests that the North American carbon sink in forestland remaining forestland was about 325 Tg C per year over the last decade, with U.S. forests accounting for most of the sink (see Table 9.3, p. 371, and Box 9.1, Clarifying Forest Carbon Flows and Their Relation to Emissions or Removals of Atmospheric Carbon, p. 372, for an explanation of associated terms). This sink results from photosynthetic uptake that exceeds the releases of forest carbon by plant and

heterotrophic respiration and from fire. A sizeable portion of the net uptake of atmospheric carbon within forestlands is offset by harvest-related emissions. These emissions include wood processing—from log removal to product generation—as well as the decay and combustion of harvested wood products, which together release about 124 Tg C per year. Thus, the net forest sector–atmosphere flux for North America is estimated to be a sink of 217 Tg C per year over roughly the last decade. Urban trees are estimated to uptake another 27 Tg C per year in the United States and Canada. Note that the fluxes reported here represent contemporary rates in recent years, spatially integrated to the country scale. Future legacies resulting from contemporary or historical drivers of forest carbon dynamics are not included. Such trends are particularly important if those drivers exhibit long-term trends, as in a decline or increase in harvest or natural disturbance rates, which would lead to trends in carbon fluxes.

Net forest carbon gain and loss constitute a source of 11 Tg C per year in North America. In the United States, net emissions from forest carbon losses encompass losses of aboveground biomass from conversion to croplands, grasslands, and settlements and include both prompt and residual legacy emissions from conversions that occurred over a 20-year time frame. Canada adopted a similar approach for quantifying emissions but accounted for conversions to croplands, settlements, and wetlands. The U.S. and Canadian estimated flux from forest carbon gains and losses includes all live biomass, dead organic matter, and soil carbon components.

Forests are generally believed to neither release nor absorb substantial quantities of methane (CH₄), though upland soils can act as modest sinks and forested wetlands can be CH₄ sources. However, forest fires release CH₄, contributing a 25-year global warming potential (GWP) of 9 Tg of CO₂ equivalent¹ (CO₂e) per year in Canada and releasing 0.22 Tg CH₄

¹ Carbon dioxide equivalent (CO₂e): Amount of CO₂ that would produce the same effect on the radiative balance of Earth's climate system as another greenhouse gas, such as methane (CH₄) or nitrous oxide (N₂O), on a 25-year timescale. For comparison to units of carbon, each kg CO₂e is equivalent to 0.273 kg C (0.273 = 1/3.67). See Box P.2, p. 12, in the Preface for details.



Table 9.3. Net Emissions of Carbon Dioxide Equivalent (CO₂e)^a for Forestlands from Net Forest Gain and Loss, Tree Growth in Urbanized Settlements, and Harvested Wood Products of Domestic Origin, by Country and Expressed in Teragrams of Carbon (Tg C) per Year

Tg C per Year	Canada ^b	United States ^c	Mexico ^d	Total ^k
1. Net Ecosystem Exchange for Forestland Remaining Forestland ^e	-18	-267	-41	-325****
Stock Change for Forestland Remaining Forestland ^e (Δ Forest C)	-27	154	ND ^j	127
2. Net Flux Due to Forest Area Gain and Loss ($A_{\text{Loss}} + A_{\text{Gain}}$)	3	0	9	11***
Emissions from Forest Area Loss ^f (A_{Loss})	3	23	12	38
Emissions from Forest Area Gain ^g (A_{Gain})	0	-23	-3	-27
3. Settlements Remaining Settlements ^h (Urban; Net Ecosystem Production _{settled})	-3	-24	ND	-27***
4. Emissions from Biomass Removal and Use ⁱ (F_{HWP})	35	89	ND	124***
Harvest Removals of Forest Carbon (Harv)	43	113	ND	155
Stock Change for Wood Products (from Harvest Removals - 4)	8	23	ND	31
5. Forest Sector-Atmosphere Exchange (from 1 + 2 + 3 + 4; Δ Atmos. C)	16	-201	-32	-217****

Emissions are from 2000 to 2014 for the United States, from 2006 to 2015 for Canada, and the 2000s for Mexico. Exchanges with the atmosphere (e.g., terms 1, 2, 3, 4, 5) are assigned a negative sign for transfers out of the atmosphere (also known as removals or sinks), but the negative sign is dropped in the text when the direction of transfer is specified with terminology. Stock changes in forestlands and in wood products are assigned a positive sign if they are increasing (see Box 9.1, Clarifying Forest Carbon Flows and Their Relation to Emissions or Removals of Atmospheric Carbon, p. 372, for a review of associated terms).

Notes

- a) Carbon dioxide equivalent (CO₂e): Amount of CO₂ that would produce the same effect on the radiative balance of Earth's climate system as another greenhouse gas, such as methane (CH₄) or nitrous oxide (N₂O), on a 25-year timescale. For comparison to units of carbon, each kg CO₂e is equivalent to 0.273 kg C (0.273 = 1/3.67). See Box P.2, p. 12, in the Preface for more details.
- b) ECCC (2017). Only includes Canada's managed forests for the 10-year period 2006 to 2015.
- c) U.S. EPA (2018). Does not include U.S. territories, Hawai'i, or a large portion of interior Alaska (19.7 million hectares), which are not yet fully integrated into the U.S. national inventory program.
- d) INECC/SEMARNAT (2015). Includes effects of forest loss and cyclical uses, which account for some of the emissions that would otherwise appear as releases from harvested wood products.
- e) Includes net exchange between the atmosphere and forestland remaining forestland, including disturbance emissions that occur within forests such as those from fire combustion and onsite decay of harvest residues. For the United States, this estimate has been calculated from stock change (see c), plus average harvest removals of about 113 Tg C per year (U.S. EPA 2018).
- f) Includes emissions from forest conversion to croplands, wetlands, grasslands, and settlements when reported, and including residual emissions for decades after conversion; overlaps with reporting in other land use, land-use change, and forestry (LULUCF) categories.
- g) Includes emissions (and removals) from all lands converted to forestland through direct human activity; overlaps with reporting in other LULUCF categories.
- h) Also referred to as net growth of urban trees; overlaps with reporting in other LULUCF categories.
- i) Includes emissions from harvesting removals of biomass of domestic origin and its use in a range of forest products.
- j) No data.
- k) Uncertainty estimates (noted by asterisks) follow the convention described in Treatment of Uncertainty in SOCCR2, p. 16, in the Preface.



Box 9.1: Clarifying Forest Carbon Flows and Their Relation to Emissions or Removals of Atmospheric Carbon

Forests tend to accumulate carbon over time, absorbing carbon dioxide (CO_2) from the atmosphere and storing it as carbon in living biomass, dead organic matter, and mineral soil. The net effect of forests on the atmosphere's store of carbon is reflected in the term "forest net ecosystem production" ($\text{NEP}_{\text{forest}}$) or net ecosystem exchange (NEE), which principally represents a forest's metabolic balance between its rate of carbon uptake through photosynthesis and its rate of carbon release as CO_2 through respiration. NEP tends to be positive in forests free of recent disturbance, though climate extremes such as droughts can cause intermittent net carbon releases ($\text{NEP} < 0$).

Disturbance events typically diminish photosynthetic carbon uptake, promptly reducing NEP. Disturbances, including fire and harvesting, also destroy biomass and impose residual respiration releases of carbon from dead biomass as it decays within forests, further decreasing NEP. Fire disturbances (i.e., wildfires and prescribed burns) involve combustion emissions that directly release carbon to the atmosphere, mostly as CO_2 but also as methane, carbon monoxide, volatile organic compounds, and black carbon (see "fire" in Figure 9.2, p. 373).

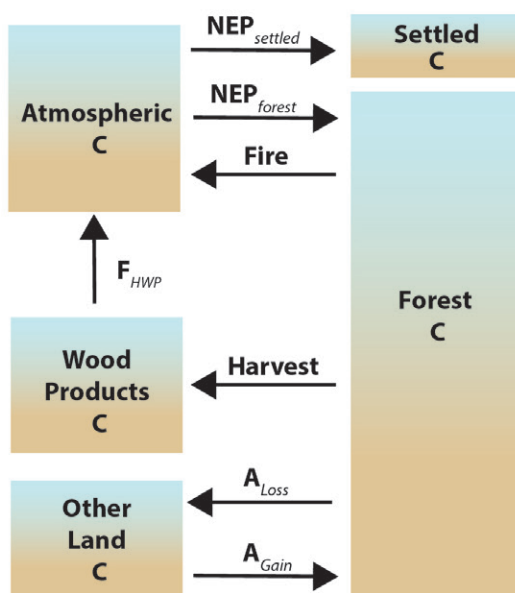
Harvesting introduces an additional release of forest carbon to the atmosphere through the immediate processing of harvest removals to generate wood products and energy as well as through the combustion and decay of wood products in use. The term F_{HWP} represents the sum of these harvest-related release processes. Some of the harvested biomass (see "harvest" in Figure 9.2, p. 373) is transferred to wood products, a portion of which can reside for decades to centuries either in use (e.g., houses and buildings) or in waste deposits (e.g., landfills). The transfer of forest carbon to long-lived wood products is not itself a direct sink of atmospheric carbon; the sink occurs upstream as part of NEP. Similarly, an increase of carbon stored in wood products should not be interpreted as a sink of atmospheric carbon, but rather the result of a transfer of forest carbon to wood products that exceeds the rate of release of carbon from combustion and decay of legacy wood products. However, if the carbon stocks within a harvested forest recover to their preharvest level faster than releases of the harvested carbon through F_{HWP} plus respiration, a "transient" sink of atmospheric carbon can be created as part of NEP. This sink is transient because it lasts only as long as the excess carbon is stored

in wood products, where excess carbon refers to the amount of the originally harvested carbon that has since been recovered by forest regrowth minus the cumulative release of harvested carbon. Correspondingly, shifting harvest removals toward longer-lived wood products can slow F_{HWP} , resulting in an avoided (or delayed) emission of carbon from wood products.

Forest carbon stocks respond not only to the previously mentioned carbon fluxes (e.g., $\text{NEP}_{\text{forest}}$, fire, and harvest), but also to gross losses and gains of carbon due to land conversions (AGain and ALoss). Although the reclassification of lands from nonforest to forest (or vice versa) does not itself involve emissions or removals of atmospheric carbon, the processes underlying such reclassifications invariably do. Most important is the residual emission of forest carbon that typically occurs when lands are converted from forest to nonforest. National inventory reports typically include such emissions for 20 years after forest loss, consistent with the estimates in Table 9.3, p. 371, but with methodological differences between countries. Land conversions also complicate agreement between NEE and stock change estimates. For example, NEE for Canada in this chapter was calculated



as the average of the annual fluxes on lands classified as forestland remaining forestland (FLFL) in each reporting year, while the stock change was calculated as the carbon stocks on all FLFL lands in 2015 minus the carbon stocks on all FLFL lands in 2006. Because FLFL area decreased over this interval, carbon stocks in FLFL decreased accordingly, with some of the carbon loss appearing as harvest removals, some involving transfer to other land categories, and neither involving immediate emission to the atmosphere (and thus not included in forestland NEE). For the United States, the estimated stock change presented in this chapter only considers lands that persisted as FLFL for the duration of the reporting interval. This estimate was then used to infer an associated NEE in



Stock Change in Forestlands:

$$\Delta \text{Forest C} = NEP_{\text{forest}} - \text{Harvest} - \text{Fire} + A_{\text{Gain}} - A_{\text{Loss}}$$

Net Atmosphere – Forest Sector Exchange:

$$\Delta \text{Atmospheric C} = \text{Fire} + F_{\text{HWP}} - NEP_{\text{forest}} - NEP_{\text{settled}}$$

Figure 9.2. Flow Diagram of Active Carbon Exchanges and Stores Between the Atmosphere and the Forest Sector.

FLFL after accounting for losses from harvest and fire, but at the risk of omitting NEE associated with lands that entered or left the

FLFL category during the reporting interval. Methods of assessing carbon transfers, emissions, and removals associated with lands entering or leaving the forestland class are improving and will continue to subtly adjust the larger picture.

The store of carbon in the atmosphere responds to NEP-forest and wooded portions of settled lands (NEP_{settled} ; see Ch. 4: Understanding Urban Carbon Fluxes, p. 189), plus direct fire emissions from forests and emissions from the decay and combustion of harvest removals (FHWP). The atmosphere does not directly experience the effects of reclassified lands, nor the flow of carbon from

forests to the wood products sector, though both have implications for atmospheric carbon as previously noted.

per year (ECCC 2016). In the United States, CH_4 emissions from forest fires equate to a 100-year GWP of 8.3 Tg CO_2e per year, or a 25-year GWP of about 33 Tg CO_2e per year (U.S. EPA 2018).

The Canadian forest sector constituted a near-zero carbon exchange with the atmosphere from 2006

to 2015 as net carbon uptake in intact forests was largely balanced by releases from harvested wood products (ECCC 2017; see Table 9.3, p. 371). Intact Canadian forests took up about 18 Tg C per year over this period, but with large interannual variability ranging from a sink of 248 Tg C to a source of 3.5 Tg C per year. This variability was



driven principally by variability in wildfire emissions, ranging from 3 to 75 Tg C per year from 1990 to 2014 (ECCC 2016). Emissions from harvested wood products were about 43 Tg C per year. These estimates pertain solely to Canada's managed forests, which represent about 66% of the country's total forested area (Stinson et al., 2011). In addition, Canada's urban forests contributed a small sink of 3 Tg C per year while land conversions released 3 Tg C per year, with emissions from forest losses exceeding removals from forest gains (ECCC 2016).

U.S. forests took up atmospheric carbon at a rate of about 267 Tg C per year from 2000 to 2015, contributing to a stock change of 154 Tg C per year (U.S. EPA 2018) after harvest removals of about 113 Tg C per year (U.S. EPA 2018; see Table 9.3, p. 371). This estimate accounts for about 77% of the atmospheric carbon sink in North American forests and includes all managed forestlands in the United States, except for those in interior Alaska (19.7 million ha; U.S. EPA 2018), Hawai'i, and the U.S. territories, all of which are not yet fully integrated into the U.S. national inventory program (U.S. Forest Service 2018). Most of the net sink for atmospheric carbon in U.S. forests is in aboveground carbon pools (U.S. EPA 2018). Urban trees are estimated to uptake another 24 Tg C per year. Net uptake in U.S. forestlands (a sink of 267 Tg C per year) substantially exceeds emissions from harvested wood products estimated at 113 Tg C and the net effect of land conversions, estimated at 0 Tg C per year (U.S. EPA 2018). Interannual variability in U.S. fluxes is reportedly small but may be underestimated by current methods.

Mexico's forests are estimated to uptake about 41 Tg C per year, overwhelming the net effects of land conversion estimated to release 9 Tg C per year (INECC/SEMARNAT 2015). Carbon releases from land clearing still exceed carbon uptake from reforestation, but their net effect is more than offset by carbon uptake in intact and degraded forestlands. This assessment departs from SOCCR1, which reported a sizeable net carbon release from Mexico's forests based on a gain-loss analysis that emphasized land

change but omitted consideration of carbon accumulation rates in both intact forests and degraded forests, with a corresponding net uptake of atmospheric carbon. Although a complete methodological description is unavailable, the new data sources and methods used in Mexico's national reporting are believed to provide an improved account of the net carbon uptake in forestlands, which was previously underestimated. Estimates are not available for Mexico's carbon release from harvested wood products and carbon uptake by urban trees.

Net carbon uptake in North American forests as documented in national reports is in broad agreement with results from a wide range of sources (Hayes et al., 2012; King et al., 2015), including 1) atmospheric inversion models (Peylin et al., 2013), 2) syntheses of forest inventory and land-change data (Pan et al., 2011), 3) measurements of forest-atmosphere carbon exchange with eddy covariance (Amiro et al., 2010), and 4) ecosystem process models (Sitch et al., 2015). Regions differ widely in their source and sink patterns and drivers. For example, in the United States, the Northeast has a prevailing legacy of carbon uptake from historical land clearing; in the Southeast, carbon uptake is dominated by regrowth from contemporary harvesting; and carbon releases in the West are increasing because of the recent rise in disturbances and environmental stresses (e.g., droughts, insects, and pathogens; Williams et al., 2016). Fluxes also exhibit large spatial variability at landscape scales (Turner et al., 2016; Williams et al., 2016), with neighboring stands ranging from sources to sinks due to a host of factors including time since disturbance, disturbance type and severity, forest type, local climate, site fertility, topographic position, and other edaphic factors.

9.3.3 Harvested Wood Products

Carbon storage and emissions from harvested wood products (including products in use and in landfills) substantially contribute to overall carbon stocks and fluxes from the forest sector (UNFCCC 2003). Although the contribution of harvested wood products is uncertain, some studies suggest that the



worldwide net increase in harvested wood products amounts to about 8% (189 Tg C per year) of the established global forest sink (Pan et al., 2011; Skog et al., 2004). However, wood product accumulation is the result of harvested wood inputs from forests that exceed releases from the decay and combustion of wood products in use. As such, the wood products pool cannot act as a direct sink for atmospheric carbon, but the store's losses do act as a direct source of atmospheric carbon (see Box 9.1, Clarifying Forest Carbon Flows and Their Relation to Emissions or Removals of Atmospheric Carbon, p. 372). Nonetheless, in the United States, Skog (2008) indicates that the amount of carbon in harvested wood products grew at a rate of 25 to 36 Tg C per year from 1990 to 2005. Canada reports an increase in wood products of about 12 to 17 Tg C per year over the same time period, slowing to about 8 Tg C per year from 2006 to 2015 (ECCC 2017). These net increases result from inputs exceeding losses. For example, in the United States, 76% of the annual domestic harvest input to the wood products pool in 2015 (110 Tg C per year) was offset by releases (84 Tg C per year), yielding a corresponding increase in wood products of 26 Tg C (U.S. EPA 2018, Annex 3b, Table A-240). Importantly, the net increase in the harvested wood products pool is contingent upon a sustained or growing rate of harvest removals of forest carbon, or a shift toward products that have a longer residence time. If harvest rates decline (as they did during the economic recession of 2008), net additions to harvested wood products may be lower than emissions from wood harvested in prior years, as was the case in the eastern United States (U.S. EPA 2018).

In 2009, the annual increase in harvested wood products slowed to 15 Tg C and 0 Tg C per year for the United States and Canada, respectively, driven by slowing economic markets, particularly housing. As economies recover, additions to the harvested wood products pool are now returning to prerecession levels, indicating the pool's strong sensitivity to markets. Looking ahead, carbon storage in harvested wood products is expected to increase by about 7 to 8 Tg C per year over the next 25 years (U.S. Department of State 2016).

9.4 Attribution and Trends

9.4.1 Overview

Many of the factors identified in SOCCR1 (CCSP 2007) continue to be important drivers of change in carbon stocks of forest ecosystems and wood products (CCSP 2007). North American forests are highly diverse, and many are changing rapidly. Management (e.g., timber harvesting and cyclical forest uses) is a major driver of carbon dynamics. Land conversions may cause net carbon emissions in North America, even in the United States where gross gains in forestland exceed gross losses. The changing climate and atmospheric chemistry (e.g., nitrogen deposition, tropospheric ozone, and rising atmospheric CO₂ concentrations) are modifying forest growth rates, growth potential, and mortality. Natural disturbances (e.g., wind, fire, and insects and disease) are generally accelerating mortality and modifying forest composition. All these drivers, and their ongoing trends, have important implications for forest carbon policy and management.

9.4.2 Land Use and Land-Use Change

Land use and land-use change can have major implications for land carbon stocks and fluxes and thus are key requirements for UNFCCC reporting. Land-use change, including conversion of nonforestland to forestland, in European nations (Nabuurs et al., 2013) and the United States (Woodall et al., 2015), has taken up a sizeable amount of atmospheric CO₂ since 1990, but this effect is expected to slow in the near future (Coulston et al., 2015; Nabuurs et al., 2013).

The current rate of land-use change in Canada is small, with about 0.02% of Canada's forest area lost each year through deforestation (Dyk et al., 2015; ECCC 2016) or about 30,000 ha of forest lost per year from 2006 to 2015 (ECCC 2017). The gain in forest area through afforestation, vegetation thickening, and expansion of tree lines northward and to higher elevations is not known, so the net balance of forest area change cannot be determined.

In Mexico, land converted to forest contributes a sink of atmospheric carbon of 3.4 Tg C per year.



This sink is more than offset by carbon losses from forest conversion, leading to net carbon emissions of about 8.8 Tg C per year from the balance of forest gains and losses in Mexico (see Table 9.3, p. 371; INECC/SEMARNAT 2015).

Deforestation in the United States occurs at a rate of about 0.12% per year, or 355,000 ha per year (Masek et al., 2011), but is more than offset by forest gain from afforestation. The net effect is a gain in U.S. forest land area of about 0.15% per year, or 430,000 ha per year (Smith et al., 2009; U.S. EPA 2018) between 2006 and 2015, largely converted from grasslands and croplands (U.S. EPA 2018). This nationwide assessment of net changes in forest area masks important region-specific patterns, with the North and Rocky Mountains seeing net gains in forest land area over the past couple decades and the Pacific Coast and South seeing net losses (Smith et al., 2009). The estimated net carbon flux in the United States associated with forestland conversion is approximately zero, with gains in forestland constituting a sink of atmospheric carbon of 23 Tg C per year and losses resulting in emissions of 23 Tg C per year (see Table 9.3, p. 371; U.S. EPA 2018).

9.4.3 Forest Management

Nearly two-thirds of Canada's forests and nearly all forests in the conterminous United States are considered managed lands. Human activities directly influence these lands, and management is mainly for wood products, water, and recreation services, with carbon uptake a secondary outcome. In many of these regions, forest carbon stocks are recovering from historical clearing and thinning dating back to as early as the 1600s. This recovery stimulates forest carbon uptake from both afforestation and carbon accumulation in still-maturing stands. Forest management also has 1) altered forest species composition (e.g., with the establishment of plantations); 2) generally accelerated carbon accumulation rates (Erb et al., 2013); and 3) modified forest soil fertility, both through nutrient gains from fertilizer application and nutrient losses from erosion caused by some harvesting practices. The net effect of such activities on forest carbon stocks and fluxes

is unclear. Fire suppression activities have tended to increase forest carbon stocks, and, along with grazing practices, may contribute to woody encroachment. Fuel reduction treatments (e.g., prescribed fire and thinning) often are intended to lower the risk of severe wildfire by reducing crown density, thinning the understory, and reducing fuel loads, all of which may contribute to short-term carbon losses. However, these treatments often lead to carbon storage in wood products, protection of residual trees, and increased growth through reduction of resource competition. Collectively, therefore, fuel reduction treatments may contribute to greater long-term carbon storage than untreated stands (Hurteau et al., 2008; Loudermilk et al., 2016).

9.4.4 Climate and Atmospheric Chemistry

Climate change and extreme weather events, as well as changes in atmospheric chemistry (e.g., nitrogen deposition, tropospheric ozone, and rising atmospheric CO₂ concentrations), affect carbon cycling in forests (Ollinger et al., 2002; Sun et al., 2015; Templer et al., 2012). In general, rising temperatures (Melillo et al., 2011) and atmospheric CO₂ concentrations (Norby et al., 2005) stimulate forest productivity, but the magnitude of these effects depends on soil fertility, particularly nitrogen and phosphorous availability, and the composition of the soil microbial community (Drake et al., 2011; Finzi and Schlesinger 2002; Terrer et al., 2016). Atmospheric nitrogen deposition can increase soil fertility (Thomas et al., 2010), counteract soil resource limitations (e.g., Johnson et al., 1998; Oren et al., 2001), and directly enhance tree growth (Thomas et al., 2010). Climate-induced changes in precipitation may alter soil carbon dynamics and vegetation carbon uptake during periods of inundation, lead to flooding-related tree mortality, and cause soil erosion with losses of particulate and dissolved organic carbon from forests (Frank et al., 2015).

Although some climatic and atmospheric changes can stimulate productivity, they also can negatively affect forest carbon sinks. High temperatures can induce heat-related stress in plants (Peng et al., 2011), worsen drought conditions (Diffenbaugh



et al., 2015), and lead to higher mortality and lower productivity in ecosystems (Anderegg et al., 2015a; Birdsey and Pan 2011). Climate warming also increases night-time ecosystem respiration and reduces net ecosystem production (NEP; Anderegg et al., 2015b). Similarly, the positive effect of rising atmospheric CO₂ and nitrogen availability on net primary production (NPP) can be moderated by elevated tropospheric ozone, which damages plants, reducing their health and productivity (Karnosky et al., 2003; Loya et al., 2003; Pan et al., 2009). Rates of sulfur deposition have declined in recent years, but acid deposition from excess nitrogen remains elevated and contributes to lower soil pH; depletion of labile cations, such as calcium, needed for plant growth (Likens et al., 1996, 2001); and mobilization of aluminum, which is toxic to plants (Aber et al., 1998). The effects of acid deposition on forest carbon storage are mediated through stand age, soil type (e.g., cation-poor sandstones versus calcium-rich limestone), and ultimately the fate of deposited nitrogen. Excess nitrogen deposition can result in nitrogen saturation of biotic and abiotic sinks, altering ecosystem carbon allocation, and lead to a cascade of negative effects on water and air quality that decrease forest productivity. The United States is a global hotspot of nitrogen emissions and deposition, with a steady rate of wet deposition of dissolved inorganic nitrogen from 1985 to 2012. However, the contribution from ammonium has increased relative to nitrate, and deposition is higher in the Midwest and Northeast than in the South and West (Du et al., 2014).

Stimulatory effects of rising CO₂ on aboveground forest productivity have not been matched by a concomitant increase in soil carbon, the largest carbon pool in forests and one that does not turn over very quickly (Lichter et al., 2008; van Groenigen et al., 2014). Thus, larger litter inputs to soils without an increase in soil carbon stocks implies an accelerated rate of carbon cycling in global forest ecosystems (Pan et al., 2013). Moreover, GHGs are returned to the atmosphere through emissions of CO₂ from harvested products; emissions of CO₂, CH₄, and nitrous oxide (N₂O) from biomass burning; and

evasion of CO₂ from streams and rivers (Kim and Tanaka 2003; Turner et al., 2013). These emissions are expected to offset a portion of the gains in productivity from afforestation following disturbance and climatic and atmospheric changes (Turner et al., 2013). Furthermore, severe warming of forest soils has been shown to accelerate soil organic matter decay and result in net loss of soil carbon emitted as CO₂ (Melillo et al., 2017). Given the wide range of forest responses, better understanding of the effects of climatic and atmospheric changes continues to be a high research priority in the United States.

9.4.5 Natural Disturbances

Natural disturbances are widespread across North America (see Figure 9.3, p. 378) and play an important role in the forest carbon cycle (Hicke et al., 2012; Odum 1969; Williams et al., 2016), affecting NPP and heterotrophic respiration, transferring carbon from live to dead pools, and involving direct emissions (e.g., from fires [French et al., 2011; Ghimire et al., 2012]). These disturbances include wildfires, insects and pathogens, droughts, floods, and severe wind events (Frank et al., 2015; Tian et al., 2015). Severe disturbances typically cause an immediate reduction in stand-level productivity, transfer carbon from live to dead stores, and increase decomposition. These effects generally are followed by a gradual increase in productivity and decrease in decomposition as the stand recovers. Initial net carbon release immediately after severe disturbances gives way to net carbon uptake as a forest regrows, but the full effect on atmospheric CO₂ depends also on the timing of disturbance-induced CO₂ releases. Carbon impacts of disturbance vary with several key features including disturbance type and severity, temporal sequence of events, and biotic and climatic conditions of regeneration (Hicke et al., 2012; Williams et al., 2016).

The extent, severity, and frequency of natural disturbances have increased in recent decades (Allen et al., 2010; Hicke et al., 2013; see Figure 9.4, p. 379), likely influenced by recent climate change and human activities. Western regions of Canada and the United States have experienced substantial die-offs recently from wildfire, insect outbreak,

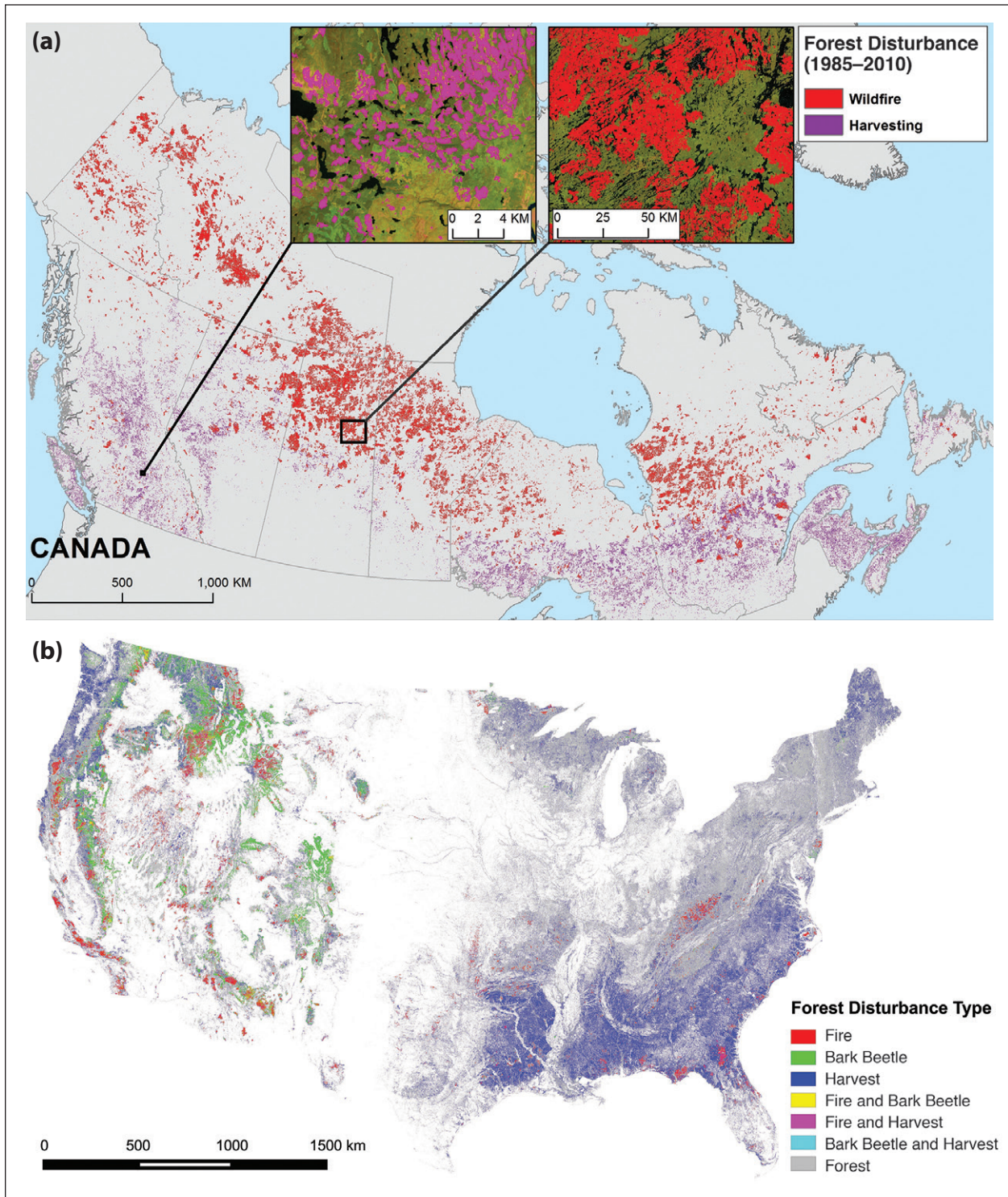


Figure 9.3. Satellite-Derived Distribution of Major Forest Disturbances by Type for Canada (a) and the United States (b). Canadian disturbance data, spanning 1985 to 2010, are based on Hermosilla et al. (2016) and White et al. (2017). U.S. disturbance data (based on Williams et al., 2016) include harvests from 1986 to 2010, fires from 1984 to 2014, and bark beetles from 1997 to 2014. [Figure sources: (a) Mike Wulder and Joanne White, Canadian Forest Service, Natural Resources Canada. (b) Reprinted from Williams et al., 2016, copyright Elsevier, used with permission.]



and drought disturbances. These events have led to widespread tree mortality, with fire and insects alone affecting up to 9% of the live tree carbon stocks in western U.S. forests (Ghimire et al., 2012, 2015; Hicke et al., 2013) and with insects also having a substantial and prolonged effect in British Columbia (Kurz et al., 2008a, 2008b). Disturbance impacts on region-wide carbon dynamics can be large and result in sizeable interannual variability in the forest carbon balance (see Figure 9.5, p. 380), and landscapes often contain offsetting effects of large carbon releases in small areas that recently experienced severe disturbance and modest carbon uptake in larger areas at various stages of recovery from prior disturbance. In eastern North America, native and invasive forest insects play important roles locally (Clark et al., 2010) and regionally (Kurz and Apps 1999). Insect damage in the United States is estimated to result in the loss of about 20 Tg of live carbon stocks per year, though release to the atmosphere through decomposition can be delayed for decades. Similar, if not larger, losses have been reported for Canada (Kurz et al., 2008a, 2008b). U.S. wildfires lead to emissions of about 40 Tg C per year, with large year to year variability. Windstorms cause an average annual loss of about 35 Tg of live carbon stocks in the United States alone (Williams et al., 2016), largely from hurricanes in the Southeast that have major individual impacts (Chambers et al., 2007; Fisk et al., 2013). Windstorm losses of live biomass are released to the atmosphere only gradually and typically are offset by forest regrowth, leading to a steady long-term effect on atmospheric carbon (Fisk et al., 2013; Zeng et al., 2009). Droughts in the United States and Canada have resulted in punctuated and widespread reductions in forest productivity (Schwalm et al., 2010) as well as tree mortality (Anderegg et al., 2013a, 2013b; Hogg et al., 2008; Michaelian et al., 2011; Peng et al., 2011; Potter 2016; van Mantgem et al., 2009) that together can cause sizeable declines in NEP and the strength of the forest carbon sink (Brzostek et al., 2014; Ma et al., 2012; Schwalm et al., 2012).

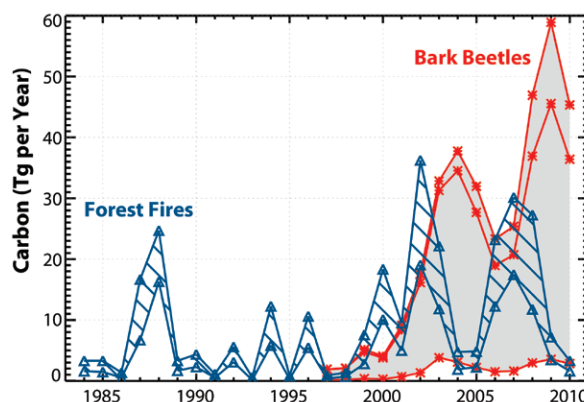


Figure 9.4. Teragrams (Tg) of Carbon in Western U.S. Trees Killed by Disturbances. The impacts of major bark beetle disturbances (1997 to 2010; red lines represent upper, middle, and lower estimates; gray shading indicates range between upper and lower estimates) and forest fires (1984 to 2010; blue lines represent moderate and moderate plus high-severity burned areas; hatching indicates range between moderate and moderate plus high-severity burned areas) are shown. [Figure source: Redrawn from Hicke et al., 2013, used with permission under a Creative Commons license (CC_By_3.0).]

9.4.6 Projections

Accounting for land-use change, management, disturbance, and forest aging, some models project that U.S. forests will continue taking up carbon but at declining rates, largely because of land-use dynamics and aging forests (USDA-OCE 2016; Wear and Coulston 2015). After 20 years of net gains, forest area is projected to level and then decline gradually after 2030 due to ongoing population growth and declining afforestation on agricultural lands (U.S. Forest Service 2012; Wear and Coulston 2015), though projections differ depending on assumptions about how macroeconomic and market trends will drive land use. In the western United States, aging forests coupled with disturbance dynamics are projected to diminish carbon uptake to negligible levels by midcentury. In the East, younger productive forests are expected to have high carbon uptake rates, though harvest-related emissions substantially reduce the net effect on atmospheric carbon.

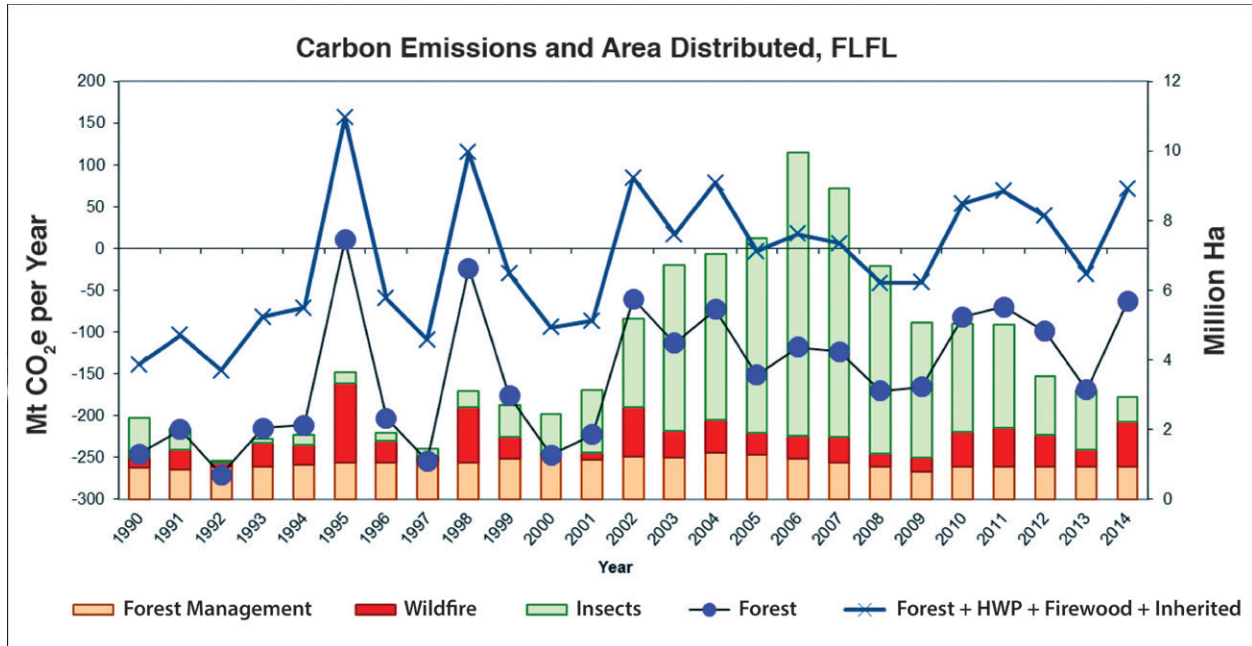


Figure 9.5. Effects of Natural Disturbances on Carbon Dynamics in Canada’s Managed Forests. Disturbances such as wildfire and insects contribute to very large interannual variability in greenhouse gas (GHG) emissions and removals on the hectares (ha) of Canadian forestland remaining forestland (FLFL). Emissions include carbon dioxide (CO₂) and non-CO₂ GHGs converted to CO₂ equivalents (CO₂e). Forest fluxes are exchanges with the atmosphere, not counting the lateral transfer of harvested wood to the products sector. The upper line includes the forest carbon sink plus annual emissions from the harvested wood products sector, including firewood burning and annual emissions from wood harvested since 1941, regardless of where the wood was oxidized. [Figure sources: Adapted from ECCC 2016 and Stinson et al., 2011, used with permission.]

Climate change defines complex and uncertain adjustments to net carbon accumulation in forests. Several studies suggest that atmospheric enrichment from CO₂ and nitrogen could increase biomass growth by 0% to 2% annually (Fang et al., 2014; Schimel 2007; Shevliakova et al., 2013). Meanwhile, climate change generally is expected to increase the frequency and severity of natural disturbances in North America in the coming decades, potentially reducing forest carbon stocks considerably (Peterson et al., 2014; U.S. Forest Service 2012). Other climate change impacts—including shifts in growing season length, water availability, and temperature—will interact with atmospheric changes to determine forest growth responses (Gedalof and Berg 2010; McCarthy et al., 2006). Projection experiments that include a trend of increased productivity (+0.4%), coupled with forest age, disturbance, and

management dynamics, indicate some potential for additional carbon uptake over baseline levels described previously (+5.1% from 2015 to 2050; Wear and Coulston 2015). However, increases are small relative to the projected changes for all other driving variables. Forest sink strength is likely to diminish gradually over the next 20 years as forest area gains tail off and forests continue to age. Uncertainty regarding the future carbon balance of North American forests increases with time. There is some potential for enhanced productivity resulting in a larger carbon sink, but disturbance rates and other elements of global change could increase carbon emissions from forests (Kurz et al., 2013; Lemprière et al., 2008). Uncertainties about the impacts of global change remain high. Increased sinks are unlikely to be of sufficient magnitude to offset higher emissions from increased disturbances



and enhanced release of carbon from decomposition (Kurz et al., 2013). However, the forest sink in the eastern temperate zone of North America is expected to be relatively stable despite these pressures (Wear and Coulston 2015).

9.5 Global Perspective

The North American forest carbon sink of 217 Tg C reported in this chapter represents about 20% of the global net forest carbon sink (Pan et al., 2011) on forest area that is 18% of the global total (FAO 2016b). Most of the North American carbon sink is in temperate U.S. forests that are managed relatively intensively for wood products and other services, indicating that managed forests typically are maintained with a lower stand density and lower carbon stocks than mature forests but have potentially higher growth rates. Current carbon stocks of North American forests average 155.4 Mg C per hectare, which is about 69% of the average for global forests (Pan et al., 2011), indicating higher-than-average carbon uptake and substantial capacity to increase average carbon stocks. According to the most comprehensive global estimates (FAO 2016a; Nabuurs et al., 2007), the mitigation potential of North American forests represents about 15% of the global forest mitigation potential for forestry activities according to “bottom-up” studies, sufficient to offset 2% of global CO₂ emissions (Le Quéré et al., 2015). The main mitigation activities for North American forests include reducing deforestation, increasing afforestation, and improving forest management—activities that are most viable in tropical and temperate biomes (FAO 2016a; Nabuurs et al., 2007).

9.6 Societal Drivers and Impacts

Atmospheric CO₂ uptake in U.S. forests has partially offset carbon emissions in other sectors of the U.S. economy. The 2014 net uptake estimate from forestland remaining forestland was 742 Tg CO₂e per year, which offset about 11% of gross U.S. GHG emissions. Assuming no policy intervention, the U.S. Department of Agriculture (USDA) reference scenario developed for the 2016 U.S. Biennial Report (USDA-OCE 2016) projects that annual

carbon uptake will decrease to 320 Tg CO₂e per year in 2050 as a result of forest aging, forest disturbance, and land-use change.

Government policies to boost forest carbon uptake have the potential to slow its projected decline. Available options include altering (e.g., slowing, intensifying, or redirecting) development and increasing afforestation of private land in the eastern United States (12 million ha) and reforestation of public land in the western United States (5 million ha) to achieve no net loss of forest area beginning in 2025. Relative to the reference scenario, this option is projected to increase cumulative carbon uptake by 26% from 2015 to 2060 (USDA-OCE 2016).

One way to estimate the societal impact of policy options to increase forest carbon uptake is to estimate the benefit in terms of avoided damages resulting from a net carbon emissions reduction. This benefit is estimated using social cost of carbon (SCC) estimates, which are dollar estimates of the long-term damage done by a ton of CO₂ emissions in a given year. One report indicates that the SCC would increase from \$42 in 2015 per 0.9 Mg CO₂e emitted to \$80 in 2050, which can be translated to equivalent savings for uptake of CO₂e (using an average annual discount rate of 3%, with values in 2016 U.S. dollars; U.S. Interagency Working Group on Social Cost of Carbon 2013). As an example of the potential benefit of exploring policy options to boost forest carbon uptake, the current value of increased forest carbon uptake under a policy that reduces land development and increases afforestation and reforestation relative to the reference scenario is \$132 billion (Bluffstone et al., 2017).

A policy option that involves afforestation of private forestland to increase forest carbon uptake could be achieved with incentives to private landowners. The USDA has five voluntary incentive programs, which account for more than 95% of USDA conservation spending (USDA-ERS 2014). When estimating benefits of incentive programs to increase forest carbon uptake, problems of “additionality” and “leakage” may lead to overestimating carbon uptake



gains (Lubowski et al., 2006). Estimates of forest carbon uptake by voluntary incentives may not be fully additional because some of this carbon would have been taken up on private forestland without the program. Furthermore, leakage could occur if landowners clear forestland for farming to compensate for land enrolled in the incentive program. Both additionality and leakage need to be accounted for when estimating the benefits of incentive programs to increase carbon uptake on private forestlands.

9.7 Carbon Management

Forest management activities have the potential to sustain and enhance the role of the North American forest sector in mitigating rising GHG concentrations over the next century. Key opportunities include 1) avoided deforestation emissions, 2) carbon uptake with afforestation and management to enhance stock growth, and 3) harvest removals directed toward clean energy options, including using logging residues and waste wood as a substitute for fossil fuels and long-lived wood products to replace building materials such as cement and steel that are more carbon emissions intensive (Birdsey et al., 2006; Lemprière et al., 2013).

Slowing deforestation and targeting clearings toward lands with lower carbon density could reduce carbon emissions substantially (Lemprière et al., 2013). Reducing harvest intensity, lengthening harvest rotations, and increasing stand densities are additional leading options because they generally increase carbon stocks in the absence of severe disturbance (Creutzburg et al., 2017; D'Amato et al., 2011; Harmon and Marks 2002; Perez-Garcia et al., 2007; Taylor et al., 2008). McKinley et al. (2011) reported that a combination of longer harvest intervals, management to increase vegetation growth rates, and establishment of preserves may increase carbon uptake by 30 to 105 Tg C per year in the United States alone. Important to note, however, is that slowing deforestation and harvesting in one region may simply displace such activities (i.e., leakage) if unmatched by a change in the demand for associated land uses and forest products. Moreover,

increased carbon stocks in areas prone to severe disturbance may not act as a lasting sink for atmospheric carbon.

Forestry activities also may be adapted to promote soil carbon maintenance and transfer by minimizing disturbances to soil and stand structure and increasing forest productivity and the inputs to the soil (Canadell and Raupach 2008; Jandl et al., 2007). Other forestry efforts can minimize impacts to belowground carbon stocks associated with some management and harvesting activities (Nave et al., 2010; Noormets et al., 2015). Fuel reduction treatments that aim to lower severe fire risk may constitute a limited future sink for atmospheric carbon if expected future fire emissions could be reduced more than the carbon emissions from prescribed burning and mechanical removal (Hurteau and North 2009). Treatments that utilize wood removals for bioenergy may have additional mitigation benefits depending on the type of woody material used (harvest residues versus whole trees) and the fate of that material in the absence of fuel-reduction treatments (Dale et al., 2017). However, treatment areas tend to be much larger than the area they ultimately protect, so the net benefits over large landscapes may not be realized (Boer et al., 2015; Campbell et al., 2012; Hudiburg et al., 2013; Loehman et al., 2014).

Regarding afforestation, the potential for increasing carbon uptake in the United States alone is high, given that 1) the country's current forestland amounts to about 72% of that in 1630 (Smith et al., 2009) and 2) 60% of the CO₂ emitted from forest harvesting in the United States a century ago has yet to be resequenced (McKinley et al., 2011). U.S. afforestation alone could yield 1 to 225 Tg of additional forest carbon uptake per year in coming decades (McKinley et al., 2011). However, there are major practical limits to widespread implementation since the higher levels of afforestation would require taking land from other uses such as food production (Ray et al., 2009). In Canada, afforestation could add up to 59 Tg C per year (Lemprière et al., 2013). In Mexico, minimal data are available on the carbon



uptake potential of afforestation, or even forest management in general.

Another potential opportunity for reducing carbon emissions is shifting harvested wood from short-lived products toward uses with slower or no carbon release to the atmosphere (Bellassen and Luyssaert 2014; Lemprière et al., 2013; Oliver et al., 2014). An additional possibility is the use of forest biomass as a substitute for fossil fuels for energy production (Miner et al., 2014). Worth noting, however, is that long time frames, accurate counterfactuals, and full life cycle assessments often are needed to estimate the mitigation benefits of these and other carbon management activities, including bioenergy (Hudiburg et al., 2013; McKechnie et al., 2011; Perez-Garcia et al., 2007).

Estimates of the potential for forest management to mitigate rising GHGs vary widely because of uncertainties, mainly in natural disturbances, leakage effects, and carbon markets (Anderegg et al., 2015b; ECCC 2016; Gough et al., 2016; Harmon et al., 2011). Climate change effects are also uncertain and differ by forest type and location, making climate-adaptive forest management increasingly important (Duveneck and Scheller 2015). Assessment of carbon management opportunities may need to include consideration of vulnerability to disturbances. For example, locating carbon uptake activities in low-disturbance environments may be appropriate, along with perhaps focusing carbon emission actions (e.g., harvesting and land clearings) in higher-disturbance environments.

In the future, forest carbon management likely will be a co-benefit of many other forest uses and values. Owners and managers may decide to maintain lower carbon stocks as a side effect of pursuing other values, such as promoting habitat for select wildlife and reducing risk of severe wildfires.

9.8 Synthesis, Knowledge Gaps, and Outlook

9.8.1 Synthesis

Net carbon uptake by North American forests is well documented. Its strength varies regionally, with

about 80% of the North American forest sink for atmospheric carbon occurring within the United States. Attributing North America's forest carbon sink to drivers remains difficult. Forest regrowth following historical clearing plays a role, but studies also suggest sizeable contributions from growth enhancements such as CO₂ fertilization, nitrogen deposition, or climate trends supporting accelerated growth. Resolving each factor's contribution is a major challenge and critical for developing reliable predictions. Several factors driving this sink are expected to decline over coming decades, and an increasing rate of natural disturbance could further diminish current net carbon uptake in the near term, possibly giving way to increased net carbon uptake in the more distant future if forests fully recover from today's disturbance trends.

Intensive forestry in select regions causes large annual reductions in forest carbon stocks that are eventually compensated for by forest regrowth, often over decades, if biomass recovers to preharvest conditions. However, carbon releases from the associated decay of harvested wood products offset a substantial portion (about half) of the net carbon sink in North American forests. Recent trends in natural disturbance rates have diminished the strength of net forest carbon uptake across much of North America. Net loss of forest carbon stocks from land conversions also reduces sink strength across the continent, with carbon losses from forest conversion exceeding carbon gains from afforestation and reforestation.

9.8.2 Gaps

Forests across North America are quite diverse. Although much is known about this diversity, datasets are still needed to characterize forest conditions at the scale of disturbance and management units (e.g., stand scale, ~30 m × 30 m). Such data would provide managers with the information necessary to design and implement effective carbon policy and management aiming to increase carbon uptake or reduce emissions. Maps of site productivity, stand age, and biomass at a stand scale (e.g., 30 m) would be



particularly valuable, offering practical improvements to current assessment capabilities.

Remeasurement data on tree- and stand-scale carbon stocks—including standing dead and downed wood and soil carbon pools and their turnover rates—are needed to record contemporary rates of carbon accumulation, improve understanding of net carbon uptake drivers, and aid assessment frameworks and models required for prediction. Also needed are analyses of expected shifts in forest composition in response to trends in climate; atmospheric composition; disturbances; the establishment and spread of invasive and/or exotic insects, pathogens, and plants; and management to improve projections of future carbon dynamics beyond an assumption of steady forest compositions and static ecotones. Conclusive evaluation of the rate and magnitude of woody encroachment is still lacking. Delivery of forest carbon to wetlands and waterways via erosion and drainage also is poorly quantified, despite its importance for continental-scale carbon budgeting and management.

Basic understanding of carbon flux and stock dynamics following disturbance is still limited, with some studies suggesting a substantial impact to fluxes (Edburg et al., 2011) and other studies reporting a more muted response (Moore et al., 2013; Reed et al., 2014). Predictions of future disturbance trends are hampered by limited understanding of disturbance interactions involving legacies of flammability and host species presence and absence, as well as active management responses such as fuel reduction treatments or preemptive and salvage logging. Also needed is knowledge of how belowground carbon stocks change as lands transition across uses over time (Domke et al., 2016). These gaps challenge assessments of legacy emissions and post-disturbance recovery and hamper attempts to quantify the potential of management activities to promote long-lived forest carbon sinks and reduce carbon emissions.

The use of remote sensing (e.g., Landsat) has led to major advances over the past decade in

monitoring aspects of disturbance and land-use change (Bachelet et al., 2015; Hansen et al., 2013), but major research gaps remain. Disturbance histories at the stand scale and attribution to disturbance type and severity remain poorly characterized, as are rates of forest conversion. Improved estimates of the location, severity, and timing of natural disturbances are needed, particularly in Mexico. Degradation of forest stocks (e.g., from selective logging, low-severity disturbances, and stress) also remain poorly characterized at the scales needed for assessing carbon dynamics and managing forest carbon. Landscape-scale records of management practices such as replanting, selective harvesting, cyclical use, and agroforestry also are needed. Integration of a range of remote-sensing technologies, including light detection and ranging (LIDAR), with field plot data and carbon cycle modeling, promises to substantially improve the ability to measure and monitor forest carbon dynamics at large scales. Addressing these and other gaps ultimately will lead to spatially explicit estimates of carbon stocks and fluxes that comprehensively assess impacts of disturbance, management, and environmental changes on carbon fluxes.

Coupled experiments and models as well as multifactor manipulations are needed to better understand carbon cycling in forest ecosystems and the drivers contributing to carbon dynamics. Full life cycle analyses are required to improve understanding of today's carbon sinks in a longer temporal context, account for the full effects of management and global change drivers, and evaluate the costs and benefits of substituting wood products for other building materials or energy sources. Also needed is better information on the origin and fate of harvested wood products, which should enable more accurate and comprehensive estimation of harvesting impacts.

Collectively, the large uncertainties and substantial variation in model predictions and GHG inventory estimates can be attributed to the gaps identified in this section. Future assessments should attempt to better integrate data sources and products and



move beyond a focus on forest carbon exchange with the atmosphere toward full climate impact assessment such as in Anderson-Teixeira et al. (2012). Considerations are needed of 1) albedo changes from forest change, 2) CH₄ and N₂O fluxes, and 3) dynamics of other radiatively active atmospheric constituents such as aerosols and black carbon.

Also needed are management and planning tools (e.g., see Figure 9.6, this page) designed to help develop and evaluate alternative landscape-scale strategies for managing forests to address a range of ecosystem services including carbon. Platforms, such as the Forest Vegetation Simulator (FVS; www.fs.fed.us/fmsc/fvs/) and i-Tree (www.itreetools.org), enable assessment of impacts from disturbance trends and management scenarios in the context of uncertain global environmental changes to inform policymakers, land managers, industry, and the public. Such platforms can be designed to

consider a wide range of ecosystem values beyond carbon to assess full climate forcing (i.e., albedo impacts), as well as biodiversity, habitat, water quality and quantity, timber production, disturbance avoidance, and other goods and services. Moreover, these platforms can be designed to flexibly handle uncertainty in forest responses to changes in climate and interactive trends in management and natural disturbance regimes.

9.8.3 Outlook

Climate change is influencing forest carbon in diverse ways, supporting enhanced carbon uptake in some regions by lengthening growing seasons and elevating CO₂ supply to photosynthesis. However, climate change also is leading to plant stress that reduces growth, increases the likelihood of mortality, and supports more extensive and severe disturbance-induced releases of carbon. All these drivers are altering the ecology and natural resources of North America's forests. How these processes and

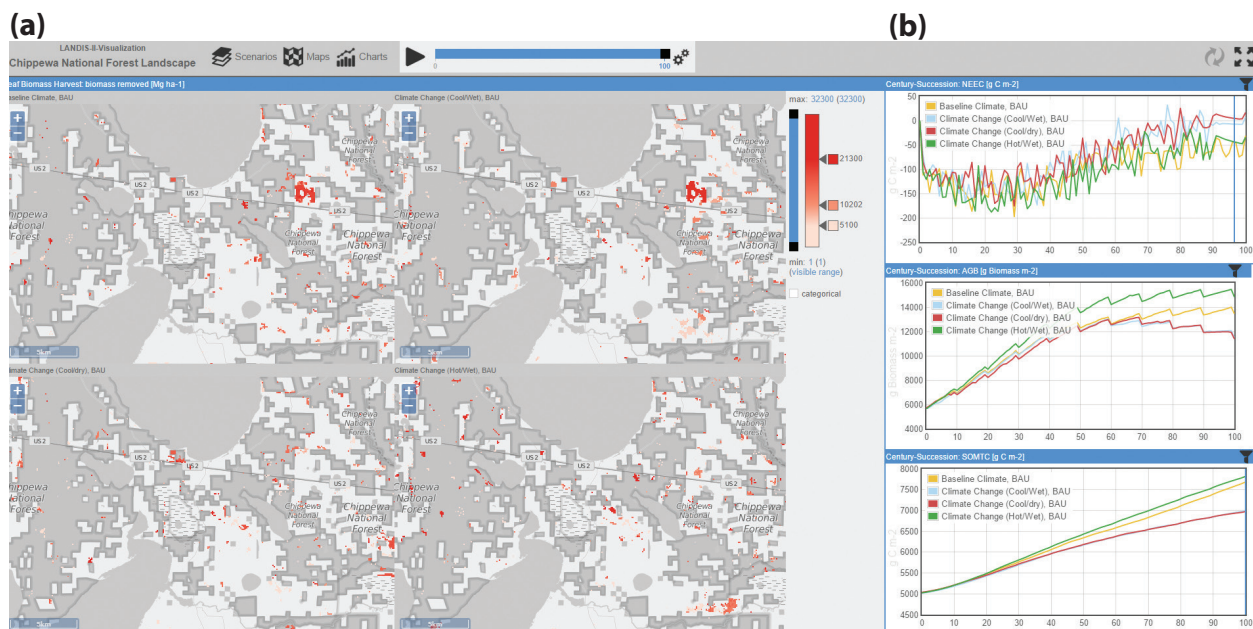


Figure 9.6. LandViz: A Forest Management and Planning Tool. LandViz maps and charts are generated for harvested timber (a) and carbon uptake rates, aboveground biomass, and soil carbon (b) using a forest simulation model (LANDIS-II) under historic climate and three climate change scenarios. LandViz is a visualization tool designed for forest managers to facilitate the integration of climate change results into the forest planning process. [Figure source: LandViz, Gustafson et al., 2016.]



their net effect will unfold over coming decades remains unclear.

Harvesting is the dominant forest management activity affecting carbon dynamics in North American forests; it has a net effect of reducing land carbon stocks and emitting carbon to the atmosphere. Slowing harvesting rates or modifying cutting practices could affect future forest carbon stocks significantly.

Several management activities could increase forest uptake of atmospheric carbon and decrease emissions in the forest sector (Birdsey et al., 2006; McKinley et al., 2011; Post et al., 2012). These activities include delaying or avoiding emissions

from wood products by producing renewable building materials and developing energy sources with lower life cycle emissions than their GHG-intensive alternatives. Management through afforestation also may promote rapid regrowth of carbon stocks within forests (Erb et al., 2013) and even expand forestlands (Birdsey et al., 2006). However, practical limits are likely to severely constrain implementation, along with competition with other management and use objectives (Ray et al., 2009). Although climate mitigation activities, and associated carbon markets, remain highly uncertain, they clearly have the potential to substantially influence the priority placed on forest management to promote forest sector carbon storage.



SUPPORTING EVIDENCE

KEY FINDING 1

Net uptake of 217 teragrams of carbon (Tg C) per year by the forest sector in North America is well documented and has persisted at about this level over the last decade. The strength of net carbon uptake varies regionally, with about 80% of the North American forest carbon sink occurring within the United States (*high confidence, very likely*).

Description of evidence base

Net carbon uptake in North American forests, as documented in national inventory reports from Canada (ECCC 2016), Mexico (INECC/SEMARNAT 2015), and the United States (U.S. EPA 2018), is in broad agreement with results from a wide range of sources (Hayes et al., 2012; King et al., 2015). These sources include atmospheric inversion models (Peylin et al., 2013), syntheses of forest inventory and land-change data (Pan et al., 2011), measurements of forest-atmosphere carbon exchange with eddy covariance (Amiro et al., 2010), and ecosystem process models (Sitch et al., 2015).

Major uncertainties

Regions differ widely in their source and sink patterns and drivers. For example, in the United States, the Northeast has a prevailing legacy of carbon uptake from historical land clearing; in the Southeast, carbon uptake is dominated by regrowth from contemporary harvesting; and the West has increasing carbon releases from the recent rise in environmental stresses (e.g., droughts, insects, and pathogens) and disturbances (Williams et al., 2016). Fluxes also exhibit large spatial variability at landscape scales (Turner et al., 2016; Williams et al., 2014), with neighboring stands ranging from sources to sinks because of a host of factors including time since disturbance, disturbance type and severity, forest type, local climate, site fertility, topographic position, and other edaphic factors.

Assessment of confidence based on evidence and agreement, including short description of nature of evidence and level of agreement

While some uncertainty remains about the spatial patterns and drivers of carbon sources and sinks across the continent, multiple lines of evidence converge to provide high confidence regarding the magnitude of net carbon uptake across North America's forests in recent decades.

Summary sentence or paragraph that integrates the above information

It is highly likely that North American forests represent a net sink of carbon, given the convergence in evidence across multiple inventory, scaling, and modeling approaches in Canada, Mexico, and the United States.

KEY FINDING 2

Forest regrowth following historical clearing plays a substantial role in determining the size of the forest carbon sink, but studies also suggest sizeable contributions from growth enhancements such as carbon dioxide (CO₂) fertilization, nitrogen deposition, or climate trends supporting accelerated growth (*medium confidence*). Resolving each factor's contribution is a major challenge and critical for developing reliable predictions.



Description of evidence base

Although the use of remote sensing (e.g., Landsat) has led to major advances over the past decade in monitoring aspects of disturbance and land-use change (Bachelet et al., 2015; Hansen et al., 2013), critical research gaps remain. Disturbance histories at the stand scale and attribution to disturbance type and severity remain poorly characterized, as are rates of forest conversion.

Major uncertainties

Improved estimates of the location, severity, and timing of natural disturbances are needed, particularly in Mexico. Degradation of forest stocks (e.g., from selective logging, low-severity disturbances, and stress) also remain poorly characterized at the scales needed for assessing carbon dynamics and managing forest carbon. Also needed are landscape-scale records of management practices such as replanting, selective harvesting, cyclical use, and agroforestry. Integration of a range of remote-sensing technologies, including light detection and ranging (LIDAR), with field plot data and carbon cycle modeling, promises to substantially improve the ability to measure and monitor forest carbon dynamics at large scales. Addressing these and other gaps ultimately will lead to spatially explicit estimates of carbon stocks and fluxes that comprehensively assess impacts of disturbance, management, and environmental changes on carbon fluxes.

Assessment of confidence based on evidence and agreement, including short description of nature of evidence and level of agreement

While the evidence base strongly supports the finding of net carbon uptake by North American forests, attribution of this carbon uptake to driving factors remains less well understood. This is in part because each factor's contribution is likely to change across diverse forest settings and conditions.

Summary sentence or paragraph that integrates the above information

Attributing carbon fluxes in North American forests to specific natural and human activities remains a challenge given the diversity of forest types, land-use changes, disturbance dynamics, and human activities that influence these fluxes.

KEY FINDING 3

Annual harvest removals from forestry operations in select regions decrease forest carbon stocks, but this decline in stocks is balanced by post-harvest recovery and regrowth in forestlands that were harvested in prior years. Removal, processing, and use of harvested biomass causes carbon emissions outside of forests, offsetting a substantial portion (about half) of the net carbon sink in North American forests (*high confidence*).

Description of evidence base

Recent trends in natural disturbance rates indicate that the strength of net forest uptake has diminished across much of North America. Net loss of forest carbon stocks from land conversions also reduces sink strength across the continent, with carbon losses from forest conversion exceeding carbon gains from afforestation and reforestation. These findings are supported by 1) national inventory reports of greenhouse gas emissions and removals in the forestland category in Canada (ECCC 2016), Mexico (INECC/SEMARNAT 2015), and the United States (U.S. EPA 2018); 2) atmospheric inversion models (Peylin et al., 2013); 3) syntheses of forest inventory and land-change data (Pan et al., 2011); 4) measurements of forest-atmosphere carbon exchange with eddy covariance (Amiro et al., 2010); and 5) ecosystem process models (Sitch et al., 2015).



Major uncertainties

Intensively managed forests are among the most well understood ecosystems in North America. Decomposition dynamics associated with harvested wood products are less well understood, however, and changes in forest use and climate may alter these dynamics in the future. Furthermore, basic understanding of carbon flux and stock dynamics following disturbance is still limited, with some studies suggesting a substantial impact to fluxes (Edburg et al., 2011) and others reporting a more muted response (Moore et al., 2013; Reed et al., 2014). Predictions of future disturbance trends are hampered by limited understanding of disturbance interactions from legacies of flammability, host species presence and absence, and active management responses such as fuel reduction treatments or preemptive and salvage logging.

Assessment of confidence based on evidence and agreement, including short description of nature of evidence and level of agreement

The carbon balance impacts of harvesting are well observed and well understood thanks to a wide range of observations that are compiled, analyzed, and reported in detailed accounts.

Summary sentence or paragraph that integrates the above information

Intensive forest management in select regions is widely known to cause large annual reductions in forest carbon stocks. Less understood is how forest regrowth (which often takes decades) compensates for these losses.

KEY FINDING 4

Recent trends in some disturbance rates (e.g., wildfires and insects) have diminished the strength of net forest carbon uptake across much of North America. Net loss of forest carbon stocks from land conversions reduced sink strength across the continent by 11 Tg C per year, with carbon losses from forest conversion exceeding carbon gains from afforestation and reforestation (*medium confidence*).

Description of evidence base

Carbon impacts of disturbance vary with several key features, including disturbance type and severity, temporal sequence of events, and biotic and climatic conditions of forest regeneration (Hicke et al., 2012; Williams et al., 2016). The extent, severity, and frequency of natural disturbances have increased in recent decades (Allen et al., 2010; Hicke et al., 2013), likely influenced by recent climate change and human activities.

Major uncertainties

Basic understanding of carbon flux and stock dynamics following disturbance is still limited, with some studies suggesting a substantial impact to fluxes (Edburg et al., 2011) and others reporting a more muted response (Moore et al., 2013; Reed et al., 2014). Predictions of future disturbance trends are hampered by limited understanding of disturbance interactions from legacies of flammability, host species presence and absence, and active management responses such as fuel reduction treatments or preemptive and salvage logging.

Assessment of confidence based on evidence and agreement, including short description of nature of evidence and level of agreement

Patterns and trends of major disturbances and forest conversions are well documented, however, their effects on carbon uptake and release can be diverse, presenting a significant challenge for assessing impacts on the carbon cycle.



Summary sentence or paragraph that integrates the above information

Detection and quantification of natural disturbance and land-use change in forest ecosystems have improved over the last decade. However, basic understanding of carbon dynamics following these events is still limited. Nevertheless, evidence suggests that recent trends in natural disturbance rates have diminished the strength of net forest uptake across much of North America.

KEY FINDING 5

Several factors driving the carbon sink in North American forests are expected to decline over coming decades, and an increasing rate of natural disturbance could further diminish current net carbon uptake (*medium confidence*).

Description of evidence base

Accounting for land-use change, management, disturbance, and forest aging, U.S. forests are projected to continue to uptake carbon but at declining rates, largely because of land-use dynamics and aging forests (USDA-OCE 2016; Wear and Coulston 2015). After 20 years of net gains, forest area is projected to level and then decline gradually after 2030 because of ongoing population growth and declining afforestation on agricultural lands (U.S. Forest Service 2012; Wear and Coulston 2015). In the western United States, aging forests coupled with disturbance dynamics are projected to diminish carbon uptake to negligible levels by midcentury. Younger productive forests in the East are expected to take up atmospheric carbon at a high rate, though harvest-related emissions substantially reduce the net effect on atmospheric carbon.

Major uncertainties

Basic understanding of carbon flux and stock dynamics following disturbance is still limited, with some studies suggesting a substantial impact to fluxes (Edburg et al., 2011) and others reporting a more muted response (Moore et al., 2013; Reed et al., 2014). Predicting disturbance trends into the future is challenging because of limited understanding of disturbance interactions from legacies of flammability, host species presence and absence, and active management responses such as fuel reduction treatments or preemptive and salvage logging. Forest regrowth following historical clearing plays a role, but studies also suggest sizeable contributions from growth enhancements such as CO₂ fertilization, nitrogen deposition, or climate trends supporting accelerated growth. Resolving each factor's contribution is a major challenge and critical for developing reliable predictions.

Assessment of confidence based on evidence and agreement, including short description of nature of evidence and level of agreement

Although projections vary depending on future climate and land-use scenarios, theory, observations, and modeling all support the expectation that today's carbon uptake from aging forests and from forest expansion will begin to decline in coming decades, and that natural disturbances will become more frequent and severe, releasing more forest carbon to the atmosphere.

Summary sentence or paragraph that integrates the above information

Although detection and quantification of natural disturbance and land-use change in forest ecosystems have improved over the last decade, basic understanding of carbon dynamics following these events is still limited. Several factors driving the forest carbon sink are expected to decline over coming decades, and although predicting disturbance trends into the future is challenging, an increasing rate of natural disturbance could further diminish the current estimated net carbon uptake by North American forests.



REFERENCES

- Aber, J., W. McDowell, K. Nadelhoffer, A. Magill, G. Berntson, M. Kamakea, S. McNulty, W. Currie, L. Rustad, and I. Fernandez, 1998: Nitrogen saturation in temperate forest ecosystems: Hypotheses revisited. *BioScience*, **48**(11), 921-934, doi: 10.2307/1313296.
- Allen, C. D., A. K. Macalady, H. Chenchouni, D. Bachelet, N. McDowell, M. Vennetier, T. Kitzberger, A. Rigling, D. D. Breshears, E. H. Hogg, P. Gonzalez, R. Fensham, Z. Zhang, J. Castro, N. Demidova, J. H. Lim, G. Allard, S. W. Running, A. Semerci, and N. Cobb, 2010: A global overview of drought and heat-induced tree mortality reveals emerging climate change risks for forests. *Forest Ecology and Management*, **259**(4), 660-684, doi: 10.1016/j.foreco.2009.09.001.
- Amiro, B. D., A. G. Barr, J. G. Barr, T. A. Black, R. Bracho, M. Brown, J. Chen, K. L. Clark, K. J. Davis, A. R. Desai, S. Dore, V. Engel, J. D. Fuentes, A. H. Goldstein, M. L. Goulden, T. E. Kolb, M. B. Lavigne, B. E. Law, H. A. Margolis, T. Martin, J. H. McCaughey, L. Misson, M. Montes-Helu, A. Noormets, J. T. Randerson, G. Starr, and J. Xiao, 2010: Ecosystem carbon dioxide fluxes after disturbance in forests of North America. *Journal of Geophysical Research*, **115**, doi: 10.1029/2010jg001390.
- Anderegg, W. R., L. Plavcova, L. D. Anderegg, U. G. Hacke, J. A. Berry, and C. B. Field, 2013a: Drought's legacy: Multiyear hydraulic deterioration underlies widespread Aspen forest die-off and portends increased future risk. *Global Change Biology*, **19**(4), 1188-1196, doi: 10.1111/gcb.12100.
- Anderegg, W. R. L., J. M. Kane, and L. D. L. Anderegg, 2013b: Consequences of widespread tree mortality triggered by drought and temperature stress. *Nature Climate Change*, **3**(1), 30-36.
- Anderegg, W. R., C. Schwalm, F. Biondi, J. J. Camarero, G. Koch, M. Litvak, K. Ogle, J. D. Shaw, E. Shevliakova, A. P. Williams, A. Wolf, E. Ziaco, and S. Pacala, 2015a: Pervasive drought legacies in forest ecosystems and their implications for carbon cycle models. *Science*, **349**(6247), 528-532, doi: 10.1126/science.aab1833.
- Anderegg, W. R., J. A. Hicke, R. A. Fisher, C. D. Allen, J. Aukema, B. Bentz, S. Hood, J. W. Lichstein, A. K. Macalady, N. McDowell, Y. Pan, K. Raffa, A. Sala, J. D. Shaw, N. L. Stephenson, C. Tague, and M. Zeppel, 2015b: Tree mortality from drought, insects, and their interactions in a changing climate. *New Phytologist*, **208**(3), 674-683, doi: 10.1111/nph.13477.
- Anderson-Teixeira, K. J., P. K. Snyder, T. E. Twine, S. V. Cuadra, M. H. Costa, and E. H. DeLucia, 2012: Climate-regulation services of natural and agricultural ecoregions of the Americas. *Nature Climate Change*, **2**, 177, doi: 10.1038/nclimate1346.
- Archer, S., 1994: Woody plant encroachment into southwestern grasslands and savannas: Rates, patterns and proximate causes. In: *Ecological Implications of Livestock Herbivory in the West*. [M. Vavra, W. Laycock, and R. Pieper (eds.)]. Society for Range Management, 13-68 pp.
- Asner, G. P., S. Archer, R. F. Hughes, R. J. Ansley, and C. A. Wessman, 2003: Net changes in regional woody vegetation cover and carbon storage in Texas Drylands, 1937-1999. *Global Change Biology*, **9**(3), 316-335, doi: 10.1046/j.1365-2486.2003.00594.x.
- Bachelet, D., K. Ferschweiler, T. J. Sheehan, B. M. Sleeter, and Z. Zhu, 2015: Projected carbon stocks in the conterminous USA with land use and variable fire regimes. *Global Change Biology*, **21**(12), 4548-4560, doi: 10.1111/gcb.13048.
- Beaudoin, A., P. Y. Bernier, L. Guindon, P. Villemaire, X. J. Guo, G. Stinson, T. Bergeron, S. Magnussen, and R. J. Hall, 2014: Mapping attributes of Canada's forests at moderate resolution through *k*NN prediction and MODIS imagery. *Canadian Journal of Forest Research*, **44**, 521-532. doi: 10.1139/cjfr-2013-0401.
- Bellassen, V., and S. Luyssaert, 2014: Carbon sequestration: Managing forests in uncertain times. *Nature*, **506**(7487), 153-155, doi: 10.1038/506153a.
- Birdsey, R., and Y. D. Pan, 2011: Ecology drought and dead trees. *Nature Climate Change*, **1**(9), 444-445, doi: 10.1038/nclimate1298.
- Birdsey, R., K. Pregitzer, and A. Lucier, 2006: Forest carbon management in the United States: 1600-2100. *Journal of Environmental Quality*, **35**(4), 1461-1469, doi: 10.2134/jeq2005.0162.
- Blackard, J. A. M. V. Finco, E. H. Helmer, G. R. Holden, M. L. Hoppus, D. M. Jacobs, A. J. Lister, G. G. Moisen, M. D. Nelson, R. Riemann, B. Ruefenacht, D. Salajanu, D. L. Weyermann, K. C. Winterberger, T. J. Brandeis, R. L. Czaplewski, R. E. McRoberts, P. L. Patterson, R. P. Tymcio, 2008: Mapping U.S. forest biomass using nationwide forest inventory data and moderate resolution information. *Remote Sensing of the Environment*, **112**, 1658-1677. doi: 10.1016/j.rse.2007.08.021.
- Bluffstone, R., J. Coulston, R. G. Haight, J. Kline, S. Polasky, D. N. Wear, and K. Zook, 2017: Estimated values of carbon sequestration resulting from forest management scenarios. In: *The Valuation of Ecosystem Services from Farms and Forests: Informing a Systematic Approach to Quantifying Benefits of Conservation Programs*. [L. Wainger and D. Ervin (eds.)]. Report No. 0114-301. Council on Food, Agricultural and Resource Economics, Washington, DC., U.S.A., 18 pp.
- Boer, M. M., O. F. Price, and R. A. Bradstock, 2015: Wildfires: Weigh policy effectiveness. *Science*, **350**(6263), 920, doi: 10.1126/science.350.6263.920-a.
- Briggs, J. M., A. K. Knapp, and B. L. Brock, 2002: Expansion of woody plants in tallgrass prairie: A fifteen-year study of fire and fire-grazing interactions. *American Midland Naturalist*, **147**(2), 287-294, doi: 10.1674/0003-0031(2002)147[0287:Eowpit]2.0.Co;2.
- Brzostek, E. R., D. Dragoni, H. P. Schmid, A. F. Rahman, D. Sims, C. A. Wayson, D. J. Johnson, and R. P. Phillips, 2014: Chronic water stress reduces tree growth and the carbon sink of deciduous hardwood forests. *Global Change Biology*, **20**(8), 2531-2539, doi: 10.1111/gcb.12528.



- Campbell, J. L., M. E. Harmon, and S. R. Mitchell, 2012: Can fuel-reduction treatments really increase forest carbon storage in the western US by reducing future fire emissions? *Frontiers in Ecology and the Environment*, **10**(2), 83-90, doi: 10.1890/110057.
- Canadell, J. G., and E. D. Schulze, 2014: Global potential of biospheric carbon management for climate mitigation. *Nature Communications*, **5**, 5282, doi: 10.1038/ncomms6282.
- Canadell, J. G., and M. R. Raupach, 2008: Managing forests for climate change mitigation. *Science*, **320**(5882), 1456-1457, doi: 10.1126/science.1155458.
- Caspersen, J. P., S. W. Pacala, J. C. Jenkins, G. C. Hurtt, P. R. Moorcroft, and R. A. Birdsey, 2000: Contributions of land-use history to carbon accumulation in U.S. forests. *Science*, **290**(5494), 1148-1151, doi: 10.1126/science.290.5494.1148.
- CCSP, 2007: *First State of the Carbon Cycle Report (SOCCR): The North American Carbon Budget and Implications for the Global Carbon Cycle. A Report by the U.S. Climate Change Science Program and the Subcommittee on Global Change Research*. [A. W. King, L. Dilling, G. P. Zimmerman, D. M. Fairman, R. A. Houghton, G. Marland, A. Z. Rose, and T. J. Wilbanks (eds.)]. National Oceanic and Atmospheric Administration, National Climatic Data Center, Asheville, NC, USA, 242 pp.
- Chambers, J. Q., J. I. Fisher, H. Zeng, E. L. Chapman, D. B. Baker, and G. C. Hurtt, 2007: Hurricane Katrina's carbon footprint on U.S. Gulf Coast forests. *Science*, **318**(5853), 1107, doi: 10.1126/science.1148913.
- Clark, K. L., N. Skowronski, and J. Hom, 2010: Invasive insects impact forest carbon dynamics. *Global Change Biology*, **16**(1), 88-101, doi: 10.1111/j.1365-2486.2009.01983.x.
- Coulston, J. W., C. W. Woodall, G. M. Domke, and B. F. Walters, 2016: Refined forest land use classification with implications for United States national carbon accounting. *Land Use Policy*, **59**, 536-542, doi: 10.1016/j.landusepol.2016.10.003.
- Coulston, J. W., D. N. Wear, and J. M. Vose, 2015: Complex forest dynamics indicate potential for slowing carbon accumulation in the Southeastern United States. *Scientific Reports*, **5**, 8002, doi: 10.1038/srep08002.
- Creutzburg, M. K., R. M. Scheller, M. S. Lucash, S. D. LeDuc, and M. G. Johnson, 2017: Forest management scenarios in a changing climate: Trade-offs between carbon, timber, and old forest. *Ecological Applications*, **27**(2), 503-518, doi: 10.1002/eap.1460.
- Dale, V. H., K. L. Kline, E. S. Parish, A. L. Cowie, R. Emory, R. W. Malmshiemer, R. Slade, C. T. Smith, T. B. Wigley, N. S. Bentsen, G. Berndes, P. Bernier, M. Brandão, H. L. Chum, R. Diaz-Chavez, G. Egnell, L. Gustavsson, J. Schweinle, I. Stupak, P. Trianosky, A. Walter, C. Whittaker, M. Brown, G. Chescheir, I. Dimitriou, C. Donnison, A. Goss Eng, K. P. Hoyt, J. C. Jenkins, K. Johnson, C. A. Levesque, V. Lockhart, M. C. Negri, J. E. Nettles, and M. Wellisch, 2017: Status and prospects for renewable energy using wood pellets from the southeastern United States. *GCB Bioenergy*, **9**(8), 1296-1305, doi: 10.1111/gcbb.12445.
- D'Amato, A. W., J. B. Bradford, S. Fraver, and B. J. Palik, 2011: Forest management for mitigation and adaptation to climate change: Insights from long-term silviculture experiments. *Forest Ecology and Management*, **262**(5), 803-816, doi: 10.1016/j.foreco.2011.05.014.
- Diffenbaugh, N. S., D. L. Swain, and D. Touma, 2015: Anthropogenic warming has increased drought risk in California. *Proceedings of the National Academy of Sciences USA*, **112**(13), 3931-3936, doi: 10.1073/pnas.1422385112.
- Domke, G. M., C. H. Perry, B. F. Walters, C. W. Woodall, M. B. Russell, and J. E. Smith, 2016: Estimating litter carbon stocks on forest land in the United States. *Science of the Total Environment*, **557-558**, 469-478, doi: 10.1016/j.scitotenv.2016.03.090.
- Drake, J. E., A. Gallet-Budynek, K. S. Hofmockel, E. S. Bernhardt, S. A. Billings, R. B. Jackson, K. S. Johnsen, J. Lichter, H. R. McCarthy, M. L. McCormack, D. J. Moore, R. Oren, S. Palmroth, R. P. Phillips, J. S. Phippen, S. G. Pritchard, K. K. Treseder, W. H. Schlesinger, E. H. Delucia, and A. C. Finzi, 2011: Increases in the flux of carbon belowground stimulate nitrogen uptake and sustain the long-term enhancement of forest productivity under elevated CO₂. *Ecology Letters*, **14**(4), 349-357, doi: 10.1111/j.1461-0248.2011.01593.x.
- Du, E., W. de Vries, J. N. Galloway, X. Hu, and F. Jingyun, 2014: Changes in wet nitrogen deposition in the United States between 1985 and 2012. *Environmental Research Letters*, **9**(9), 095004.
- Duveneck, M. J., and R. M. Scheller, 2015: Climate-suitable planting as a strategy for maintaining forest productivity and functional diversity. *Ecological Applications*, **25**(6), 1653-1668, doi: 10.1890/14-0738.1.
- Dyk, A., D. Leckie, S. Tinis, and S. Ortlepp, 2015: *Canada's National Deforestation Monitoring System: System Description*. Natural Resources Canada, Canadian Forest Service, Pacific Forestry Centre. 30 pp.
- ECCC, 2016: *National Inventory Report: 1990-2014, Greenhouse Gas Sources and Sinks in Canada*. Environment and Climate Change Canada. [http://publications.gc.ca/collections/collection_2016/eccc/En81-4-1-2014-eng.pdf]
- ECCC, 2017: *National Inventory Report: 1990-2015, Greenhouse Gas Sources and Sinks in Canada*. Environment and Climate Change Canada. [<https://www.canada.ca/en/environment-climate-change/services/climate-change/greenhouse-gas-emissions/sources-sinks-executive-summary.html>]
- Edburg, S. L., J. A. Hicke, D. M. Lawrence, and P. E. Thornton, 2011: Simulating coupled carbon and nitrogen dynamics following mountain pine beetle outbreaks in the Western United States. *Journal of Geophysical Research: Biogeosciences*, **116**, doi: 10.1029/2011jg001786.



- Erb, K. H., T. Kastner, S. Luyssaert, R. A. Houghton, T. Kuemmerle, P. Olofsson, and H. Haberl, 2013: Commentary: Bias in the attribution of forest carbon sinks. *Nature Climate Change*, **3**(10), 854-856, doi: 10.1038/nclimate2004.
- Fang, J., T. Kato, Z. Guo, Y. Yang, H. Hu, H. Shen, X. Zhao, A. W. Kishimoto-Mo, Y. Tang, and R. A. Houghton, 2014: Evidence for environmentally enhanced forest growth. *Proceedings of the National Academy of Sciences USA*, **111**(26), 9527-9532, doi: 10.1073/pnas.1402333111.
- FAO, 2010: *Global Forest Resources Assessment 2010*. UN Food and Agriculture Organization. [http://www.fao.org/forestry/fra/fra2010/en/]
- FAO, 2016a: *Forestry for a Low-Carbon Future: Integrating Forests and Wood Products in Climate Change Strategies*. FAO Forestry Paper 177. 180 pp. [http://www.fao.org/forestry/58718/en/]
- FAO, 2016b: *Global Forest Resources Assessment 2015: How Are the World's Forests Changing?* UN Food and Agriculture Organization. [http://www.fao.org/3/a-i4793e.pdf]
- Finzi, A. C., and A. H. Schlesinger, 2002: Species control variation in litter decomposition in a pine forest exposed to elevated CO₂. *Global Change Biology*, **8**(12), 1217-1229, doi: 10.1046/j.1365-2486.2002.00551.x.
- Fisk, J. P., G. C. Hurtt, J. Q. Chambers, H. Zeng, K. A. Dolan, and R. I. Negron-Juarez, 2013: The impacts of tropical cyclones on the net carbon balance of eastern US forests (1851-2000). *Environmental Research Letters*, **8**(4), 045017, doi: 10.1088/1748-9326/8/4/045017.
- Frank, D., M. Reichstein, M. Bahn, K. Thonicke, D. Frank, M. D. Mahecha, P. Smith, M. van der Velde, S. Vicca, F. Babst, C. Beer, N. Buchmann, J. G. Canadell, P. Ciais, W. Cramer, A. Ibrom, F. Miglietta, B. Poulter, A. Rammig, S. I. Seneviratne, A. Walz, M. Wattenbach, M. A. Zavala, and J. Zscheischler, 2015: Effects of climate extremes on the terrestrial carbon cycle: Concepts, processes and potential future impacts. *Global Change Biology*, **21**(8), 2861-2880, doi: 10.1111/gcb.12916.
- French, N. H. F., W. J. de Groot, L. K. Jenkins, B. M. Rogers, E. Alvarado, B. Amiro, B. de Jong, S. Goetz, E. Hoy, E. Hyer, R. Keane, B. E. Law, D. McKenzie, S. G. McNulty, R. Ottmar, D. R. Perez-Salicrup, J. Randerson, K. M. Robertson, and M. Turetsky, 2011: Model comparisons for estimating carbon emissions from North American wildland fire. *Journal of Geophysical Research: Biogeosciences*, **116**, doi: 10.1029/2010jg001469.
- Gedalof, Z., and A. A. Berg, 2010: Tree ring evidence for limited direct CO₂ fertilization of forests over the 20th century. *Global Biogeochemical Cycles*, **24**, doi: 10.1029/2009gb003699.
- Ghimire, B., C. A. Williams, G. J. Collatz, and M. Vanderhoof, 2012: Fire-induced carbon emissions and regrowth uptake in western U.S. Forests: Documenting variation across forest types, fire severity, and climate regions. *Journal of Geophysical Research: Biogeosciences*, **117**(G3), doi: 10.1029/2011jg001935.
- Ghimire, B., C. A. Williams, G. J. Collatz, M. Vanderhoof, J. Rogan, D. Kulakowski, and J. G. Masek, 2015: Large carbon release legacy from bark beetle outbreaks across western United States. *Global Change Biology*, **21**(8), 3087-3101, doi: 10.1111/gcb.12933.
- Goodale, C. L., M. J. Apps, R. A. Birdsey, C. B. Field, L. S. Heath, R. A. Houghton, J. C. Jenkins, G. H. Kohlmaier, W. Kurz, S. Liu, G.-J. Nabuurs, S. Nilsson, and A. Z. Shvidenko, 2002: Forest carbon sinks in the Northern Hemisphere. *Ecological Applications*, **12**(3), 891-899, doi: 10.1890/1051-0761(2002)012[0891:FCSITN]2.0.CO;2.
- Gough, C. M., P. S. Curtis, B. S. Hardiman, C. M. Scheuermann, and B. Bond-Lamberty, 2016: Disturbance, complexity, and succession of net ecosystem production in North America's temperate deciduous forests. *Ecosphere*, **7**(6), doi: 10.1002/ecs2.1375.
- Gustafson, E., M. Lucash, J. Liem, H. Jenny, R. Scheller, K. Barrett, and B. Sturtevant, 2016: *Seeing the Future Impacts of Climate Change and Forest Management: A Landscape Visualization System for Forest Managers*. U.S. Department of Agriculture, Forest Service, Northern Research Station. 18 pp.
- Hansen, M. C., P. V. Potapov, R. Moore, M. Hancher, S. A. Turubanova, A. Tyukavina, D. Thau, S. V. Stehman, S. J. Goetz, T. R. Loveland, A. Kommareddy, A. Egorov, L. Chini, C. O. Justice, and J. R. Townshend, 2013: High-resolution global maps of 21st-century forest cover change. *Science*, **342**(6160), 850-853, doi: 10.1126/science.1244693.
- Harmon, M. E., and B. Marks, 2002: Effects of silvicultural practices on carbon stores in Douglas-fir—Western hemlock forests in the Pacific Northwest, U.S.A.: Results from a simulation model. *Canadian Journal of Forest Research*, **32**(5), 863-877, doi: 10.1139/x01-216.
- Harmon, M. E., B. Bond-Lamberty, J. W. Tang, and R. Vargas, 2011: Heterotrophic respiration in disturbed forests: A review with examples from North America. *Journal of Geophysical Research: Biogeosciences*, **116**, doi: 10.1029/2010jg001495.
- Hayes, D. J., D. P. Turner, G. Stinson, A. D. McGuire, Y. X. Wei, T. O. West, L. S. Heath, B. Dejong, B. G. McConkey, R. A. Birdsey, W. A. Kurz, A. R. Jacobson, D. N. Huntzinger, Y. D. Pan, W. Mac Post, and R. B. Cook, 2012: Reconciling estimates of the contemporary North American carbon balance among terrestrial biosphere models, atmospheric inversions, and a new approach for estimating net ecosystem exchange from inventory-based data. *Global Change Biology*, **18**(4), 1282-1299, doi: 10.1111/j.1365-2486.2011.02627.x.
- Hermosilla, T., M. A. Wulder, J. C. White, N. C. Coops, G. W. Hobart, and L. B. Campbell, 2016: Mass data processing of time series landsat imagery: Pixels to data products for forest monitoring. *International Journal of Digital Earth*, **9**(11), 1035-1054, doi: 10.1080/17538947.2016.1187673.



- Hibbard, K. A., S. Archer, D. S. Schimel, and D. W. Valentine, 2001: Biogeochemical changes accompanying woody plant encroachment in a subtropical savanna. *Ecology*, **82**(7), 1999-2011, doi: 10.2307/2680064.
- Hicke, J. A., A. J. H. Meddens, C. D. Allen, and C. A. Kolden, 2013: Carbon stocks of trees killed by bark beetles and wildfire in the western United States. *Environmental Research Letters*, **8**(3), doi: 10.1088/1748-9326/8/3/035032.
- Hicke, J. A., C. D. Allen, A. R. Desai, M. C. Dietze, R. J. Hall, E. H. Hogg, D. M. Kashian, D. Moore, K. F. Raffa, R. N. Sturrock, and J. Vogelmann, 2012: Effects of biotic disturbances on forest carbon cycling in the United States and Canada. *Global Change Biology*, **18**(1), 7-34, doi: 10.1111/j.1365-2486.2011.02543.x.
- Hogg, E. H., J. P. Brandt, and M. Michaellian, 2008: Impacts of a regional drought on the productivity, dieback, and biomass of western Canadian Aspen forests. *Canadian Journal of Forest Research*, **38**(6), 1373-1384, doi: 10.1139/X08-001.
- Hudiburg, T. W., S. Luysaert, P. E. Thornton, and B. E. Law, 2013: Interactive effects of environmental change and management strategies on regional forest carbon emissions. *Environmental Science and Technology*, **47**(22), 13132-13140, doi: 10.1021/es402903u.
- Hughes, R. F., S. R. Archer, G. P. Asner, C. A. Wessman, C. McMurtry, J. Nelson, and R. J. Ansley, 2006: Changes in above-ground primary production and carbon and nitrogen pools accompanying woody plant encroachment in a temperate savanna. *Global Change Biology*, **12**(9), 1733-1747, doi: 10.1111/J.1365-2486.2006.01210.x.
- Hurteau, M. D., G. W. Koch, and B. A. Hungate, 2008: Carbon protection and fire risk reduction: Toward a full accounting of forest carbon offsets. *Frontiers in Ecology and the Environment*, **6**(9), 493-498, doi: 10.1890/070187.
- Hurteau, M., and M. North, 2009: Fuel treatment effects on tree-based forest carbon storage and emissions under modeled wildfire scenarios. *Frontiers in Ecology and the Environment*, **7**(8), 409-414, doi: 10.1890/080049.
- INECC/SEMARNAT, 2015: *First Biennial Update Report to the United Nations Framework Convention on Climate Change*. [http://unfccc.int/files/national_reports/non-annex_i_parties/biennial_update_reports/application/pdf/executive_summary.pdf]
- IPCC, 2003: *Good Practice Guidance for Land Use, Land-Use Change, and Forestry*. [J. Penman, M. Gytarsky, T. Krug, D. Kruger, R. Pipatti, L. Buendia, K. Miwa, T. Ngara, K. Tanabe, and F. Wagner (eds.)]. IGES, 593 pp.
- IPCC, 2006: *Guidelines for National Greenhouse Gas Inventories: Volume 4 Agriculture, Forestry and Other Land Use*. Prepared by the National Greenhouse Gas Inventories Programme. [H. S. Eggleston, L. Buendia, K. Miwa, T. Ngara, and K. Tanabe (eds.)]. IGES, 593 pp.
- Jackson, R. B., J. L. Banner, E. G. Jobbagy, W. T. Pockman, and D. H. Wall, 2002: Ecosystem carbon loss with woody plant invasion of grasslands. *Nature*, **418**(6898), 623-626, doi: 10.1038/nature00910.
- Jandl, R., M. Lindner, L. Vesterdal, B. Bauwens, R. Baritz, F. Hagedorn, D. W. Johnson, K. Minkinen, and K. A. Byrne, 2007: How strongly can forest management influence soil carbon sequestration? *Geoderma*, **137**(3-4), 253-268, doi: 10.1016/j.geoderma.2006.09.003.
- Johnson, D. W., R. B. Thomas, K. L. Griffin, D. T. Tissue, J. T. Ball, B. R. Strain, and R. F. Walker, 1998: Effects of carbon dioxide and nitrogen on growth and nitrogen uptake in ponderosa and loblolly pine. *Journal of Environmental Quality*, **27**(2), 414, doi: 10.2134/jeq1998.00472425002700020024x.
- Joos, F., I. C. Prentice, and J. I. House, 2002: Growth enhancement due to global atmospheric change as predicted by terrestrial ecosystem models: Consistent with U.S. forest inventory data. *Global Change Biology*, **8**(4), 299-303, doi: 10.1046/j.1354-1013.2002.00505.x.
- Karnosky, D. F., D. R. Zak, K. S. Pregitzer, C. S. Awmack, J. G. Bockheim, R. E. Dickson, G. R. Hendrey, G. E. Host, J. S. King, B. J. Kopper, E. L. Kruger, M. E. Kubiske, R. L. Lindroth, W. J. Mattson, E. P. McDonald, A. Noormets, E. Oksanen, W. F. J. Parsons, K. E. Percy, G. K. Podila, D. E. Riemenschneider, P. Sharma, R. Thakur, A. Sober, J. Sober, W. S. Jones, S. Anttonen, E. Vapaavuori, B. Mankovska, W. Heilman, and J. G. Isebrands, 2003: Tropospheric O₃ moderates responses of temperate hardwood forests to elevated CO₂: A synthesis of molecular to ecosystem results from the Aspen FACE project. *Functional Ecology*, **17**(3), 289-304, doi: 10.1046/j.1365-2435.2003.00733.x.
- Kim, Y., and N. Tanaka, 2003: Effect of forest fire on the fluxes of CO₂, CH₄ and N₂O in boreal forest soils, interior Alaska. *Journal of Geophysical Research: Atmospheres*, **108**(D1), doi: 10.1029/2001jd000663.
- King, A. W., R. J. Andres, K. J. Davis, M. Hafer, D. J. Hayes, D. N. Huntzinger, B. de Jong, W. A. Kurz, A. D. McGuire, R. Vargas, Y. Wei, T. O. West, and C. W. Woodall, 2015: North America's net terrestrial CO₂ exchange with the atmosphere 1990-2009. *Biogeosciences*, **12**(2), 399-414, doi: 10.5194/bg-12-399-2015.
- Köhl, M., R. Lasco, M. Cifuentes, Ö. Jonsson, K. T. Korhonen, P. Mundhenk, J. de Jesus Navar, and G. Stinson, 2015: Changes in forest production, biomass and carbon: Results from the 2015 UN FAO Global Forest Resource Assessment. *Forest Ecology and Management*, **352**, 21-34, doi: 10.1016/j.foreco.2015.05.036.
- Kurz, W. A., and M. J. Apps, 1999: A 70-year retrospective analysis of carbon fluxes in the Canadian forest sector. *Ecological Applications*, **9**(2), 526-547, doi: 10.1890/1051-0761(1999)009[0526:Ayrcoc]2.0.Co;2.



- Kurz, W. A., G. Stinson, G. J. Rampley, C. C. Dymond, and E. T. Neilson, 2008a: Risk of natural disturbances makes future contribution of Canada's forests to the global carbon cycle highly uncertain. *Proceedings of the National Academy of Sciences USA*, **105**(5), 1551-1555, doi: 10.1073/pnas.0708133105.
- Kurz, W. A., C. C. Dymond, G. Stinson, G. J. Rampley, E. T. Neilson, A. L. Carroll, T. Ebata, and L. Safranyik, 2008b: Mountain pine beetle and forest carbon feedback to climate change. *Nature*, **452**(7190), 987-990, doi: 10.1038/nature06777.
- Kurz, W. A., C. H. Shaw, C. Boisvenue, G. Stinson, J. Metsaranta, D. Leckie, A. Dyk, C. Smyth, and E. T. Neilson, 2013: Carbon in Canada's boreal forest — a synthesis. *Environmental Reviews*, **21**(4), 260-292, doi: 10.1139/er-2013-0041.
- Le Quéré, C., R. Moriarty, R. M. Andrew, J. G. Canadell, S. Sitch, J. I. Korsbakken, P. Friedlingstein, G. P. Peters, R. J. Andres, T. A. Boden, R. A. Houghton, J. I. House, R. F. Keeling, P. Tans, A. Arneeth, D. C. E. Bakker, L. Barbero, L. Bopp, J. Chang, F. Chevallier, L. P. Chini, P. Ciais, M. Fader, R. A. Feely, T. Gkritzalis, I. Harris, J. Hauck, T. Ilyina, A. K. Jain, E. Kato, V. Kitidis, K. Klein Goldewijk, C. Koven, P. Landschützer, S. K. Lauvset, N. Lefèvre, A. Lenton, I. D. Lima, N. Metzl, F. Millero, D. R. Munro, A. Murata, J. E. M. S. Nabel, S. Nakaoka, Y. Nojiri, K. O'Brien, A. Olsen, T. Ono, F. F. Pérez, B. Pfeil, D. Pierrot, B. Poulter, G. Rehder, C. Rödenbeck, S. Saito, U. Schuster, J. Schwinger, R. Séférian, T. Steinhoff, B. D. Stocker, A. J. Sutton, T. Takahashi, B. Tilbrook, I. T. van der Laan-Luijckx, G. R. van der Werf, S. van Heuven, D. Vandemark, N. Viovy, A. Wiltshire, S. Zaehle, and N. Zeng, 2015: Global carbon budget 2015. *Earth System Science Data*, **7**(2), 349-396, doi: 10.5194/essd-7-349-2015.
- Lemprière, T. C., P. Y. Bernier, A. L. Carroll, M. D. Flannigan, R. P. Gilson, D. W. McKenney, E. H. Hogg, J. H. Pedlar, and D. Blain, 2008: *The Importance of Forest Sector Adaptation to Climate Change*. Canadian Forest Service, Natural Resources Canada. [<https://cfs.nrcan.gc.ca/publications?id=29154>]
- Lemprière, T. C., W. A. Kurz, E. H. Hogg, C. Schmoll, G. J. Rampley, D. Yemshanov, D. W. McKenney, R. Gilson, A. Beatch, D. Blain, J. S. Bhatti, and E. Krcoar, 2013: Canadian boreal forests and climate change mitigation. *Environmental Reviews*, **21**(4), 293-321, doi: 10.1139/er-2013-0039.
- Lichter, J., S. A. Billings, S. E. Ziegler, D. Gaiadh, R. Ryals, A. C. Finzi, R. B. Jackson, E. A. Stemmler, and W. H. Schlesinger, 2008: Soil carbon sequestration in a pine forest after 9 years of atmospheric CO₂ enrichment. *Global Change Biology*, **14**(12), 2910-2922, doi: 10.1111/j.1365-2486.2008.01701.x.
- Likens, G. E., C. T. Driscoll, and D. C. Buso, 1996: Long-term effects of acid rain: Response and recovery of a forest ecosystem. *Science*, **272**(5259), 244-246, doi: 10.1126/science.272.5259.244.
- Likens, G. E., T. J. Butler, and D. C. Buso, 2001: Long- and short-term changes in sulfate deposition: Effects of the 1990 Clean Air Act Amendments. *Biogeochemistry*, **52**(1), 1-11, doi: 10.1023/a:1026563400336.
- Loehman, R. A., E. Reinhardt, and K. L. Riley, 2014: Wildland fire emissions, carbon, and climate: Seeing the forest and the trees — a cross-scale assessment of wildfire and carbon dynamics in fire-prone, forested ecosystems. *Forest Ecology and Management*, **317**, 9-19, doi: 10.1016/j.foreco.2013.04.014.
- Loudermilk, E. L., R. M. Scheller, P. J. Weisberg, and A. Kretchun, 2016: Bending the carbon curve: Fire management for carbon resilience under climate change. *Landscape Ecology*, 1-12, doi: 10.1007/s10980-016-0447-x.
- Loya, W. M., K. S. Pregitzer, N. J. Karberg, J. S. King, and C. P. Giardina, 2003: Reduction of soil carbon formation by tropospheric ozone under increased carbon dioxide levels. *Nature*, **425**(6959), 705-707, doi: 10.1038/nature02047.
- Lubowski, R. N., A. J. Plantinga, and R. N. Stavins, 2006: Land-use change and carbon sinks: Econometric estimation of the carbon sequestration supply function. *Journal of Environmental Economics and Management*, **51**(2), 135-152, doi: 10.1016/j.jeem.2005.08.001.
- Ma, Z., C. Peng, Q. Zhu, H. Chen, G. Yu, W. Li, X. Zhou, W. Wang, and W. Zhang, 2012: Regional drought-induced reduction in the biomass carbon sink of Canada's boreal forests. *Proceedings of the National Academy of Sciences USA*, **109**(7), 2423-2427, doi: 10.1073/pnas.1111576109.
- Masek, J. G., W. B. Cohen, D. Leckie, M. A. Wulder, R. Vargas, B. de Jong, S. Healey, B. Law, R. Birdsey, R. A. Houghton, D. Mil-drexler, S. Goward, and W. B. Smith, 2011: Recent rates of forest harvest and conversion in North America. *Journal of Geophysical Research: Biogeosciences*, **116**, doi: 10.1029/2010jg001471.
- McCarthy, H. R., R. Oren, A. C. Finzi, and K. H. Johnsen, 2006: Canopy leaf area constrains CO₂-induced enhancement of productivity and partitioning among aboveground carbon pools. *Proceedings of the National Academy of Sciences USA*, **103**(51), 19356-19361, doi: 10.1073/pnas.0609448103.
- McKechnie, J., S. Colombo, J. Chen, W. Mabee, and H. L. MacLean, 2011: Forest bioenergy or forest carbon? Assessing trade-offs in greenhouse gas mitigation with wood-based fuels. *Environmental Science and Technology*, **45**(2), 789-795, doi: 10.1021/es1024004.
- McKinley, D. C., M. G. Ryan, R. A. Birdsey, C. P. Giardina, M. E. Harmon, L. S. Heath, R. A. Houghton, R. B. Jackson, J. F. Morrison, B. C. Murray, D. E. Patakl, and K. E. Skog, 2011: A synthesis of current knowledge on forests and carbon storage in the United States. *Ecological Applications*, **21**(6), 1902-1924, doi: 10.1890/10-0697.1.
- Melillo, J. M., S. Butler, J. Johnson, J. Mohan, P. Steudler, H. Lux, E. Burrows, F. Bowles, R. Smith, L. Scott, C. Vario, T. Hill, A. Burton, Y. M. Zhou, and J. Tang, 2011: Soil warming, carbon-nitrogen interactions, and forest carbon budgets. *Proceedings of the National Academy of Sciences USA*, **108**(23), 9508-9512, doi: 10.1073/pnas.1018189108.



- Melillo, J. M., S. D. Frey, K. M. DeAngelis, W. J. Werner, M. J. Bernard, F. P. Bowles, G. Pold, M. A. Knorr, and A. S. Grandy, 2017: Long-term pattern and magnitude of soil carbon feedback to the climate system in a warming world. *Science*, **358**(6359), 101-105, doi: 10.1126/science.aan2874.
- Michaelian, M., E. H. Hogg, R. J. Hall, and E. Arsenault, 2011: Massive mortality of Aspen following severe drought along the southern edge of the Canadian boreal forest. *Global Change Biology*, **17**(6), 2084-2094, doi: 10.1111/j.1365-2486.2010.02357.x.
- Miner, R. A., R. C. Abt, J. L. Bowyer, M. A. Buford, R. W. Malmshemer, J. O'Laughlin, E. E. Oneil, R. A. Sedjo, and K. E. Skog, 2014: Forest carbon accounting considerations in US bio-energy policy. *Journal of Forestry*, **112**(6), 591-606, doi: 10.5849/jof.14-009.
- Moore, D. J., N. A. Trahan, P. Wilkes, T. Quaipe, B. B. Stephens, K. Elder, A. R. Desai, J. Negron, and R. K. Monson, 2013: Persistent reduced ecosystem respiration after insect disturbance in high elevation forests. *Ecology Letters*, **16**(6), 731-737, doi: 10.1111/ele.12097.
- MREDD+ Alliance, 2013: *Map and Database on the Distribution of Aerial Biomass of Woody Vegetation in Mexico. Version 1.0*. Woods Hole Research Center, U.S. Agency for International Development, Mexican National Forestry Commission, National Commission for the Knowledge and Use of Biodiversity, Proyecto Mexico Norway Project. Mexico. April 2013.
- Nabuurs, G. J., O. Masera, K. Andrasko, P. Benitez-Ponce, R. Boer, M. Dutschke, E. Elsiddig, J. Ford-Robertson, P. Frumhoff, T. Karjalainen, O. Krankina, W. A. Kurz, M. Matsumoto, W. Oyhantcaba, N. H. Ravindranath, M. J. Sanz Sanchez, and X. Zhang, 2007: *Forestry. Climate Change 2007: Mitigation. Contribution of Working Group III to the Fourth Assessment Report of the Intergovernmental Panel on Climate Change*. [B. Metz, O. R. Davidson, P. R. Bosch, R. Dave, and L. A. Meyer (eds.)]. Cambridge University Press, 541-584 pp.
- Nabuurs, G.-J., M. Lindner, P. J. Verkerk, K. Gunia, P. Deda, R. Michalak, and G. Grassi, 2013: First signs of carbon sink saturation in European forest biomass. *Nature Climate Change*, **3**(9), 792-796, doi: 10.1038/nclimate1853.
- NALCMS, 2018: *North American Land Change Monitoring System*. [<http://www.cec.org/tools-and-resources/north-american-environmental-atlas/north-american-land-change-monitoring-system>]
- Nave, L. E., E. D. Vance, C. W. Swanston, and P. S. Curtis, 2010: Harvest impacts on soil carbon storage in temperate forests. *Forest Ecology and Management*, **259**(5), 857-866, doi: 10.1016/j.foreco.2009.12.009.
- Noormets, A., D. Epron, J. C. Domec, S. G. McNulty, T. Fox, G. Sun, and J. S. King, 2015: Effects of forest management on productivity and carbon sequestration: A review and hypothesis. *Forest Ecology and Management*, **355**, 124-140, doi: 10.1016/j.foreco.2015.05.019.
- Norby, R. J., E. H. Delucia, B. Gielen, C. Calfapietra, C. P. Giardina, J. S. King, J. Ledford, H. R. McCarthy, D. J. Moore, R. Ceulemans, P. De Angelis, A. C. Finzi, D. F. Karnosky, M. E. Kubiske, M. Lukac, K. S. Pregitzer, G. E. Scarascia-Mugnozza, W. H. Schlesinger, and R. Oren, 2005: Forest response to elevated CO₂ is conserved across a broad range of productivity. *Proceedings of the National Academy of Sciences USA*, **102**(50), 18052-18056, doi: 10.1073/pnas.0509478102.
- Odum, E. P., 1969: The strategy of ecosystem development. *Science*, **164**(3877), 262-270, doi: 10.1126/science.164.3877.262.
- Ogle, S. M., and J. Zeigler, 2016: *Methodology for Estimating Carbon Stock Changes of Woodlands in the U.S. National Greenhouse Gas Inventory*. Report to U.S. Environmental Protection Agency, Agreement No. EP-W-13-005.
- Oliver, C. D., N. T. Nassar, B. R. Lippke, and J. B. McCarter, 2014: Carbon, fossil fuel, and biodiversity mitigation with wood and forests. *Journal of Sustainable Forestry*, **33**(3), 248-275, doi: 10.1080/10549811.2013.839386.
- Ollinger, S. V., J. D. Aber, P. B. Reich, and R. J. Freuder, 2002: Interactive effects of nitrogen deposition, tropospheric ozone, elevated CO₂ and land use history on the carbon dynamics of northern hardwood forests. *Global Change Biology*, **8**(6), 545-562, doi: 10.1046/j.1365-2486.2002.00482.x.
- Oren, R., D. S. Ellsworth, K. H. Johnsen, N. Phillips, B. E. Ewers, C. Maier, K. V. Schafer, H. McCarthy, G. Hendrey, S. G. McNulty, and G. G. Katul, 2001: Soil fertility limits carbon sequestration by forest ecosystems in a CO₂-enriched atmosphere. *Nature*, **411**(6836), 469-472, doi: 10.1038/35078064.
- Pan, Y. D., R. A. Birdsey, O. L. Phillips, and R. B. Jackson, 2013: The structure, distribution, and biomass of the world's forests. *Annual Review of Ecology, Evolution, and Systematics*, **44**, 593-622, doi: 10.1146/annurev-ecolsys-110512-135914.
- Pan, Y. D., R. Birdsey, J. Hom, and K. McCullough, 2009: Separating effects of changes in atmospheric composition, climate and land-use on carbon sequestration of US Mid-Atlantic temperate forests. *Forest Ecology and Management*, **259**(2), 151-164, doi: 10.1016/j.foreco.2009.09.049.
- Pan, Y., R. A. Birdsey, J. Fang, R. Houghton, P. E. Kauppi, W. A. Kurz, O. L. Phillips, A. Shvidenko, S. L. Lewis, J. G. Canadell, P. Ciais, R. B. Jackson, S. W. Pacala, A. D. McGuire, S. Piao, A. Rautiainen, S. Sitch, and D. Hayes, 2011: A large and persistent carbon sink in the world's forests. *Science*, **333**(6045), 988-993, doi: 10.1126/science.1201609.
- Peng, C. H., Z. H. Ma, X. D. Lei, Q. Zhu, H. Chen, W. F. Wang, S. R. Liu, W. Z. Li, X. Q. Fang, and X. L. Zhou, 2011: A drought-induced pervasive increase in tree mortality across Canada's boreal forests. *Nature Climate Change*, **1**(9), 467-471, doi: 10.1038/nclimate1293.



- Perez-Garcia, J., B. Lippke, J. Comnick, and C. Manriquez, 2007: An assessment of carbon pools, storage, and wood products market substitution using life-cycle analysis results. *Wood and Fiber Science*, **37**, 140-148.
- Peterson, D. L., V. J. M., and T. Patel-Weynand, 2014: Climate change and United States forests. *Advances in Global Change Research*, **57**, doi: 10.1007/978-94-007-7515-2.
- Peylin, P., R. M. Law, K. R. Gurney, F. Chevallier, A. R. Jacobson, T. Maki, Y. Niwa, P. K. Patra, W. Peters, P. J. Rayner, C. Rodenbeck, I. T. van der Laan-Luijkx, and X. Zhang, 2013: Global atmospheric carbon budget: Results from an ensemble of atmospheric CO₂ inversions. *Biogeosciences*, **10**(10), 6699-6720, doi: 10.5194/bg-10-6699-2013.
- Post, W. M., R. C. Izaurralde, T. O. West, M. A. Liebig, and A. W. King, 2012: Management opportunities for enhancing terrestrial carbon dioxide sinks. *Frontiers in Ecology and the Environment*, **10**(10), 554-561, doi: 10.1890/120065.
- Potter, C. S., 2016: Landsat image analysis of tree mortality in the Southern Sierra Nevada region of California during the 2013-2015 drought. *Journal of Earth Science and Climatic Change*, **07**(03), 342, doi: 10.4172/2157-7617.1000342.
- Ray, D. G., R. S. Seymour, N. A. Scott, and W. S. Keeton, 2009: Mitigating climate change with managed forests: Balancing expectations, opportunity, and risk. *Journal of Forestry*, **107**(1), 50-51.
- Reed, D. E., B. E. Ewers, and E. Pendall, 2014: Impact of mountain pine beetle induced mortality on forest carbon and water fluxes. *Environmental Research Letters*, **9**(10), doi: 10.1088/1748-9326/9/10/105004.
- Schimel, D., 2007: Carbon cycle conundrums. *Proceedings of the National Academy of Sciences USA*, **104**(47), 18353-18354, doi: 10.1073/pnas.0709331104.
- Schwalm, C. R., C. A. Williams, K. Schaefer, A. Arneth, D. Bonal, N. Buchmann, J. Q. Chen, B. E. Law, A. Lindroth, S. Luysaert, M. Reichstein, and A. D. Richardson, 2010: Assimilation exceeds respiration sensitivity to drought: A FLUXNET synthesis. *Global Change Biology*, **16**(2), 657-670, doi: 10.1111/j.1365-2486.2009.01991.x.
- Schwalm, C. R., C. A. Williams, K. Schaefer, D. Baldocchi, T. A. Black, A. H. Goldstein, B. E. Law, W. C. Oechel, T. P. U. Kyaw, and R. L. Scott, 2012: Reduction in carbon uptake during turn of the century drought in western North America. *Nature Geoscience*, **5**(8), 551-556, doi: 10.1038/Ngeo1529.
- Shevliakova, E., R. J. Stouffer, S. Malyshev, J. P. Krasting, G. C. Hurtt, and S. W. Pacala, 2013: Historical warming reduced due to enhanced land carbon uptake. *Proceedings of the National Academy of Sciences USA*, **110**(42), 16730-16735, doi: 10.1073/pnas.1314047110.
- Sitch, S., P. Friedlingstein, N. Gruber, S. D. Jones, G. Murray-Tortarolo, A. Ahlstrom, S. C. Doney, H. Graven, C. Heinze, C. Huntingford, S. Levis, P. E. Levy, M. Lomas, B. Poulter, N. Viovy, S. Zaehle, N. Zeng, A. Arneth, G. Bonan, L. Bopp, J. G. Canadell, F. Chevallier, P. Ciais, R. Ellis, M. Gloor, P. Peylin, S. L. Piao, C. Le Quere, B. Smith, Z. Zhu, and R. Myneni, 2015: Recent trends and drivers of regional sources and sinks of carbon dioxide. *Biogeosciences*, **12**(3), 653-679, doi: 10.5194/bg-12-653-2015.
- Skog, K. E., 2008: Sequestration of carbon in harvested wood products for the United States. *Forest Products Journal*, **58**(6), 56-72.
- Skog, K. E., K. Pingoud, and J. E. Smith, 2004: A method countries can use to estimate changes in carbon stored in harvested wood products and the uncertainty of such estimates. *Environmental Management*, **33**, S65-S73, doi: 10.1007/s00267-003-9118-1.
- Smith, W. B., P. D. Miles, C. H. Perry, and S. A. Pugh, 2009: *Forest Resources of the United States, 2007*. U.S. Department of Agriculture, Forest Service, Washington Office, 336 pp.
- Stinson, G., W. A. Kurz, C. E. Smyth, E. T. Neilson, C. C. Dymond, J. M. Metsaranta, C. Boisvenue, G. J. Rampley, Q. Li, T. M. White, and D. Blain, 2011: An inventory-based analysis of Canada's managed forest carbon dynamics, 1990 to 2008. *Global Change Biology*, **17**(6), 2227-2244, doi: 10.1111/j.1365-2486.2010.02369.x.
- Sun, G., P. V. Caldwell, and S. G. McNulty, 2015: Modelling the potential role of forest thinning in maintaining water supplies under a changing climate across the conterminous United States. *Hydrological Processes*, **29**(24), 5016-5030, doi: 10.1002/hyp.10469.
- Taylor, A. R., J. R. Wang, and W. A. Kurz, 2008: Effects of harvesting intensity on carbon stocks in Eastern Canadian red spruce (*Picea rubens*) forests: An exploratory analysis using the CBM-CFS3 simulation model. *Forest Ecology and Management*, **255**(10), 3632-3641, doi: 10.1016/j.foreco.2008.02.052.
- Templer, P. H., R. W. Pinder, and C. L. Goodale, 2012: Effects of nitrogen deposition on greenhouse-gas fluxes for forests and grasslands of North America. *Frontiers in Ecology and the Environment*, **10**(10), 547-553, doi: 10.1890/120055.
- Terrer, C., S. Vicca, B. A. Hungate, R. P. Phillips, and I. C. Prentice, 2016: Mycorrhizal association as a primary control of the CO₂ fertilization effect. *Science*, **353**(6294), 72-74, doi: 10.1126/science.aaf4610.
- Thomas, R. Q., C. D. Canham, K. C. Weathers, and C. L. Goodale, 2010: Increased tree carbon storage in response to nitrogen deposition in the US. *Nature Geoscience*, **3**(1), 13-17, doi: 10.1038/Ngeo721.
- Tian, H. Q., W. Ren, J. Yang, B. Tao, W. J. Cai, S. E. Lohrenz, C. S. Hopkinson, M. L. Liu, Q. C. Yang, C. Q. Lu, B. W. Zhang, K. Banger, S. F. Pan, R. Y. He, and Z. Xue, 2015: Climate extremes dominating seasonal and interannual variations in carbon export from the Mississippi River Basin. *Global Biogeochemical Cycles*, **29**(9), 1333-1347, doi: 10.1002/2014gb005068.



- Turner, D. P., W. D. Ritts, R. E. Kennedy, A. N. Gray, and Z. Q. Yang, 2016: Regional carbon cycle responses to 25 years of variation in climate and disturbance in the US Pacific Northwest. *Regional Environmental Change*, **16**(8), 2345-2355, doi: 10.1007/s10113-016-0956-9.
- Turner, M. G., D. C. Donato, and W. H. Romme, 2013: Consequences of spatial heterogeneity for ecosystem services in changing forest landscapes: Priorities for future research. *Landscape Ecology*, **28**(6), 1081-1097, doi: 10.1007/s10980-012-9741-4.
- U.S. Department of State, 2016: *Second Biennial Report of the United States of America under the United Nations Framework Convention on Climate Change*. U.S. Department of State. [http://unfccc.int/national_reports/biennial_reports_and_iar/submitted_biennial_reports/items/7550.php]
- U.S. EPA, 2018: *Inventory of U.S. Greenhouse Gas Emissions and Sinks: 1990-2016*. EPA 430-P-18-003. U.S. Environmental Protection Agency. [https://www.epa.gov/ghgemissions/inventory-us-greenhouse-gas-emissions-and-sinks-1990-2016]
- U.S. Forest Service, 2018: *Forest Inventory and Analysis*. U.S. Forest Service. [https://www.fia.fs.fed.us/]
- U.S. Forest Service, 2012: *Future of America's Forest and Rangelands: Forest Service 2010 Resources Planning Act Assessment. General Technical Report*. WO-87, 198 pp. U.S. Forest Service. [https://www.fs.fed.us/research/publications/gtr/gtr_wo87.pdf]
- U.S. Interagency Working Group on Social Cost of Carbon, 2013: *Technical Support Document: Technical Update of the Social Cost of Carbon for Regulatory Impact Analysis Under Executive Order 12866*. United States Government. [https://www.epa.gov/sites/production/files/2016-12/documents/sc_co2_tsd_august_2016.pdf]
- UNFCCC, 2003: *Estimation, Reporting, and Accounting of Harvested Wood Product. Technical Report*. FCC/TP/2003/7 27. United Nations Framework Convention on Climate Change. [http://unfccc.int/resource/docs/tp/tp0307.pdf]
- USDA-ERS, 2014: *Conservation Spending Seeks to Improve Environmental Performance in Agriculture*. U.S. Department of Agriculture Economic Research Service. [http://www.ers.usda.gov/topics/natural-resources-environment/conservation-programs/background.aspx]
- USDA-OCE, 2016: *USDA Integrated Projections for Agriculture and Forest Sector Land Use, Land-Use Change, and GHG Emissions and Removals: 2015 to 2060*. U.S. Department of Agriculture Office of the Chief Economist. [https://www.usda.gov/oce/climate_change/mitigation_technologies/Projections2015documentation01192016.docx]
- van Groenigen, K. J., X. Qi, C. W. Osenberg, Y. Luo, and B. A. Hungate, 2014: Faster decomposition under increased atmospheric CO₂ limits soil carbon storage. *Science*, **344**(6183), 508-509, doi: 10.1126/science.1249534.
- van Mantgem, P. J., N. L. Stephenson, J. C. Byrne, L. D. Daniels, J. F. Franklin, P. Z. Fule, M. E. Harmon, A. J. Larson, J. M. Smith, A. H. Taylor, and T. T. Veblen, 2009: Widespread increase of tree mortality rates in the western United States. *Science*, **323**(5913), 521-524, doi: 10.1126/science.1165000.
- Wear, D. N., and J. W. Coulston, 2015: From sink to source: Regional variation in U.S. forest carbon futures. *Scientific Reports*, **5**, 16518, doi: 10.1038/srep16518.
- Weisberg, P. J., E. Lingua, and R. B. Pillai, 2007: Spatial patterns of pinyon-juniper woodland expansion in central Nevada. *Rangeland Ecology and Management*, **60**(2), 115-124, doi: 10.2111/05-224r2.1.
- White, J. C., M. A. Wulder, T. Hermosilla, N. C. Coops, and G. W. Hobart, 2017: A nationwide annual characterization of 25 years of forest disturbance and recovery for Canada using Landsat time series. *Remote Sensing of Environment*, **194**, 303-321, doi: 10.1016/j.rse.2017.03.035.
- Williams, C. A., G. J. Collatz, J. Masek, C. Q. Huang, and S. N. Goward, 2014: Impacts of disturbance history on forest carbon stocks and fluxes: Merging satellite disturbance mapping with forest inventory data in a carbon cycle model framework. *Remote Sensing of Environment*, **151**, 57-71, doi: 10.1016/j.rse.2013.10.034.
- Williams, C. A., H. Gu, R. MacLean, J. G. Masek, and G. J. Collatz, 2016: Disturbance and the carbon balance of US forests: A quantitative review of impacts from harvests, fires, insects, and droughts. *Global and Planetary Change*, **143**, 66-80, doi: 10.1016/j.gloplacha.2016.06.002.
- Wilson, B. T., C. W. Woodall, and D. M. Griffith, 2013: Imputing forest carbon stock estimates from inventory plots to a nationally continuous coverage. *Carbon Balance and Management* **8**(1). doi: 10.1186/1750-0680-8-1.
- Woodall, C. W., J. W. Coulston, G. M. Domke, B. F. Walters, D. N. Wear, J. E. Smith, H.-E. Anderson, B. J. Clough, W. B. Cohen, D. M. Griffith, S. C. Hagan, I. S. Hanou, M. C. Nichols, C. H. Perry, M. B. Russell, J. A. Westfall, and B. T. Wilson, 2015: *The U.S. Forest Carbon Accounting Framework: Stocks and Stock Change, 1990-2016. General Technical Report*. NRS-GTR-154. 49 pp. U.S. Forest Service. [https://www.fs.usda.gov/treearch/pubs/49858]
- Zeng, H., J. Q. Chambers, R. I. Negron-Juarez, G. C. Hurtt, D. B. Baker, and M. D. Powell, 2009: Impacts of tropical cyclones on U.S. Forest tree mortality and carbon flux from 1851 to 2000. *Proceedings of the National Academy of Sciences USA*, **106**(19), 7888-7892, doi: 10.1073/pnas.0808914106.
- Zhang, F., J. M. Chen, Y. Pan, R. A. Birdsey, S. Shen, W. Ju, and L. He, 2012: Attributing carbon changes in conterminous U.S. Forests to disturbance and non-disturbance factors from 1901 to 2010. *Journal of Geophysical Research: Biogeosciences*, **117**(G2), doi: 10.1029/2011jg001930.



10 Grasslands

Lead Author

Elise Pendall, Western Sydney University

Contributing Authors

Dominique Bachelet, Oregon State University; Richard T. Conant, Colorado State University; Bassil El Masri, Murray State University; Lawrence B. Flanagan, University of Lethbridge; Alan K. Knapp, Colorado State University; Jinxun Liu, U.S. Geological Survey; Shuguang Liu, Central South University of Forestry and Technology; Sean M. Schaeffer, University of Tennessee

Acknowledgments

Sasha C. Reed (Science Lead), U.S. Geological Survey; Rachel Melnick (Review Editor), USDA National Institute of Food and Agriculture; Nancy Cavallaro (Federal Liaison), USDA National Institute of Food and Agriculture; Anne Marsh (Federal Liaison), USDA Forest Service

Recommended Citation for Chapter

Pendall, E., D. Bachelet, R. T. Conant, B. El Masri, L. B. Flanagan, A. K. Knapp, J. Liu, S. Liu, and S. M. Schaeffer, 2018: Chapter 10: Grasslands. In *Second State of the Carbon Cycle Report (SOCCR2): A Sustained Assessment Report* [Cavallaro, N., G. Shrestha, R. Birdsey, M. A. Mayes, R. G. Najjar, S. C. Reed, P. Romero-Lankao, and Z. Zhu (eds.)]. U.S. Global Change Research Program, Washington, DC, USA, pp. 399-427, <https://doi.org/10.7930/SOCCR2.2018.Ch10>.



KEY FINDINGS

1. Total grassland carbon stocks in the conterminous United States, estimated to be about 7.4 petagrams of carbon (Pg C) in 2005, are projected to increase to about 8.2 Pg C by 2050. Although U.S. grasslands are expected to remain carbon sinks over this period, the uptake rate is projected to decline by about half. In the U.S. Great Plains, land-use and land-cover changes are expected to cause much of the change in carbon cycling as grasslands are converted to agricultural lands or to woody biomes (*medium confidence*).
2. Increasing temperatures and rising atmospheric carbon dioxide (CO₂) concentrations interact to increase productivity in northern North American grasslands, but this productivity response will be mediated by variable precipitation, soil moisture, and nutrient availability (*high confidence, very likely*).
3. Soil carbon in grasslands is likely to be moderately responsive to changes in climate over the next several decades. Field experiments in grasslands suggest that altered precipitation can increase soil carbon, while warming and elevated CO₂ may have only minimal effects despite altered productivity (*medium confidence, likely*).
4. Carbon stocks and net carbon uptake in grasslands can be maintained with appropriate land management including moderate levels of grazing. Fire suppression can lead to encroachment of woody vegetation and increasing carbon storage in mesic regions, at the expense of grassland vegetation (*high confidence, likely*).

Note: Confidence levels are provided as appropriate for quantitative, but not qualitative, Key Findings and statements.

10.1 Carbon Cycling in Grasslands

Grasslands cover 30% of North America and provide a wealth of essential ecosystem services, such as wildlife habitat, hydrological buffering, soil stabilization, carbon storage, and forage production. Grassland ecosystems are characterized by herbaceous vegetation, including grasses and nongrass species, with a minor component of woody vegetation in most regions. Most grasslands in North America are dominated by perennial vegetation, or species that continue growing for many years, although in parts of California and the Intermountain West, nonnative annual grasses now dominate. Grasses allocate 40% to 80% of net primary production (NPP) to roots (Hui and Jackson 2006), so most carbon storage takes place below ground (Silver et al., 2010; Smith et al., 2008; Soussana et al., 2004). Grasslands across North America occupy over 7 million km² (see Table 10.1, p. 401) and contain 10 to 90 megagrams of carbon (Mg C) per hectare in the top 20 cm of soil (Burke et al., 1989; Potter and Derner 2006; Silver et al., 2010).

Carbon storage, defined as the net uptake of carbon by a given pool or reservoir (IPCC 2013), can be quantified as the change in stocks measured over time, or as annual net ecosystem production (NEP), which can be measured as NPP minus losses from soil organic matter (SOM) decomposition (Chapin et al., 2006). NEP is also estimated from the sum of high-frequency net carbon dioxide (CO₂) exchange (NEE) measurements from eddy covariance “flux tower” methods. By contrast, net ecosystem carbon balance (NECB) accounts for all carbon uptake and loss processes, including harvest, natural disturbance, leaching, and trace gas species in addition to CO₂ (Chapin et al., 2006).

This chapter is relevant to both the Northern and Southern Plains National Climate Assessment regions, as well as the Southwest and Midwest regions. The spatial scope of this chapter encompasses the major North American grassland regions, which can be defined by climatic limitations. Grasslands occur where potential evaporation exceeds



**Table 10.1. Average Modeled Net Ecosystem Production
(In Tg C per Year During 2000 to 2006)**

Country	Approximate Grassland Area (km ²) ^a	Inventory Analysis ^{b, c}	Atmospheric Inversion Models ^{c, d}	Land-Surface Models ^{c, d}
Canada	3,920,000	-3.06	-51.2	-29.3
United States	2,580,000	-13.2	-266.2	-104.8
Mexico	760,000	-9.06	-15.1	+3.6
North America	7,260,000	-25.2	-332.5	-130.5

This table, adapted from Hayes et al. (2012), presents three different approaches for estimating net ecosystem production (NEP): inventory analysis, atmospheric inversion models, and land-surface models.

Notes

- Approximate grassland area is derived from www.statista.com/statistics/201761/projection-for-total-us-grassland-area-from-2010.
- Inventory analysis estimates, in teragrams of carbon (Tg C) per year, are the sum of livestock methane (CH₄) emissions, livestock carbon dioxide (CO₂) emissions, and grassland net ecosystem exchange (NEE) for Canada and the United States. For Mexico, the NEP value for "Others" was used from Table S10 in Hayes et al. (2012).
- A negative flux represents net ecosystem carbon uptake, while a positive flux indicates carbon loss from the ecosystem.
- Atmospheric inversion models and land-surface models are from Table 2 in Hayes et al. (2012) and exclude CH₄ emissions and human settlement emissions.

precipitation, such as in central North America from Canada through Mexico and in mountain rain shadows in the western United States (Sims and Risser 2000). They also occur in more mesic (wet) regions where disturbance, management, or soil conditions prevent woody growth, such as in central Florida (Stephenson 2011). North American grasslands generally increase in productivity and carbon storage as precipitation increases, from west to east (Sims and Risser 2000). This pattern is observed in Canada and to a lesser extent in Mexico. Mixed-grass prairie is extensive in south-central Canada, while more arid desert grassland and shortgrass steppe extend through the southwestern United States into Mexico (Sims and Risser 2000). Grasslands at the more arid extreme are considered more vulnerable to diminished productivity in a future warmer climate (Hufkens et al., 2016), whereas grasslands in more mesic climates may be vulnerable to woody encroachment (Knapp et al., 2008a).

Land management strongly affects productivity and carbon cycling in grasslands (see Figure 10.1, p. 402).

In the conterminous United States, grasslands, shrublands, rangelands, and pastures make up at least 40% of land cover (Reeves and Mitchell 2012; see Figure 10.1). Most areas of highly productive grasslands have been converted to agriculture (see Ch. 5: Agriculture, p. 229, for more details; Bachelet et al., 2017).

10.2 Current Understanding of Grassland Productivity and Carbon Stocks

10.2.1 Grassland Carbon Stocks and Fluxes

Key Finding 1 is based on estimates of carbon stocks and fluxes as determined by upscaling inventories with remote-sensing products and modeling approaches. This section of the chapter describes the current understanding of carbon stocks and fluxes, and later sections evaluate the processes responsible for changes in these pools and fluxes.

Continental Scale

Terrestrial biosphere models are important tools for understanding how the carbon cycle responds

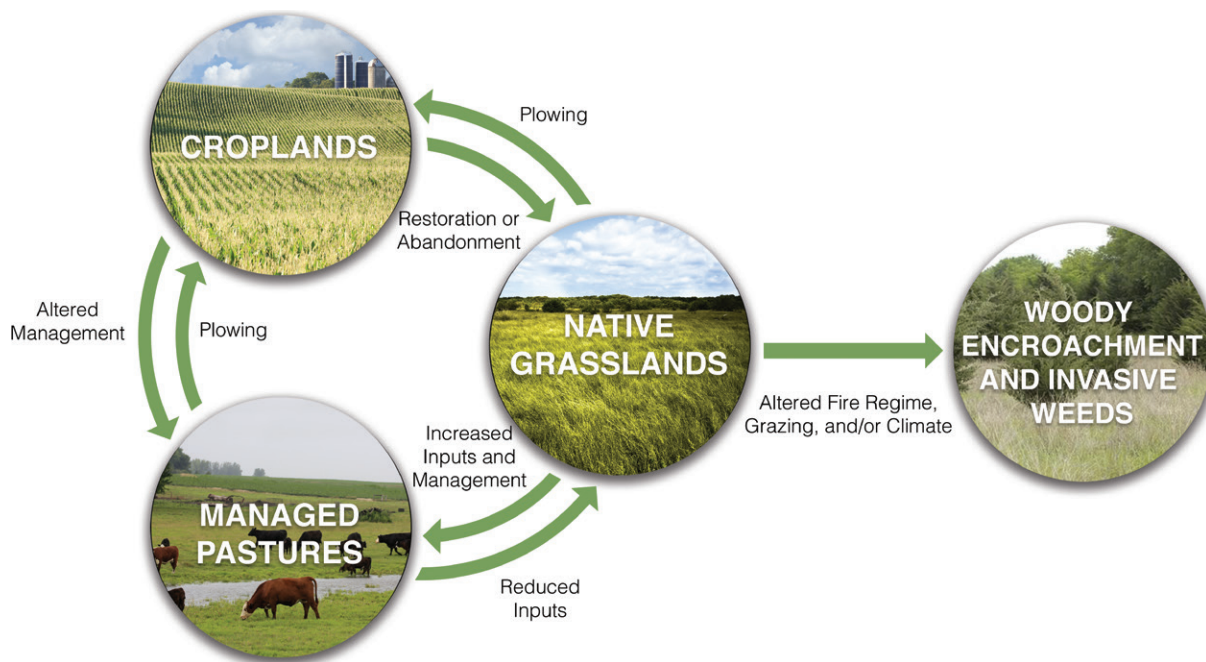


Figure 10.1. Management Activities and Their Effects on Grassland Carbon Cycling. Reduced fire frequency in mesic native grassland has allowed woody vegetation such as *Juniperus virginia* to expand and has been associated with rapid increases in carbon stocks in vegetation and soils (McKinley and Blair 2008). Other observed management impacts include lower carbon density in agricultural lands compared with grasslands (Zhu et al., 2011) and the rapid accumulation of soil carbon in intensively managed pastures in the southeastern United States (Machmuller et al., 2015). In addition, the rate of carbon uptake by croplands in the Great Plains is 30% lower than that of grasslands (Wylie et al., 2016).

to changes in climate, nutrient availability, and land use. Modeled rates of uptake or loss are dependent on a given region's processes and area. A multimodel synthesis study estimated that North American grassland acted as a carbon sink, with an average uptake rate of 38 grams of carbon (g C) per m² per year during the first 5 years of this century (Raczka et al., 2013). A similar synthesis of 17 land-surface models (LSMs) showed that North American grasslands acted as carbon sinks (see Table 10.1, p. 401) from 2000 to 2006 (Hayes et al., 2012). Atmospheric inversion models (AIMs) also predicted a carbon sink for North American grasslands but at a rate roughly twice the magnitude compared to that in land-surface models (see Table 10.1, p. 401; Hayes et al., 2012). At the national level, carbon sinks are proportional to the area in grasslands and reflect different management

and climate conditions. U.S. grasslands contribute the continent's largest sink, followed by those in Canada, with Mexican grasslands approaching carbon-neutral status.

Similar to the modeled estimates, inventory analyses also suggest that Canadian and U.S. grasslands are carbon sinks (see Table 10.1, p. 401; Hayes et al., 2012). The differences in estimated carbon sink magnitude between these approaches could stem from estimating fluxes using changes in stocks (i.e., inventory methods) versus changes in atmospheric CO₂ concentrations (i.e., AIMs) or carbon cycle processes (i.e., LSMs), or from extrapolating fluxes over different land areas. Furthermore, most previous LSMs have not considered effects of land-use change and fire suppression, both which are implicit in AIM analyses. Inventories might miss these



Table 10.2. Carbon Fluxes and Stocks for Grasslands and Shrublands in the Conterminous United States (Summarized from the LandCarbon Project, landcarbon.org/categories)

	Time Period	Biomass ^a	Soil ^b	Other ^c	Total	Area (10 ⁶ km ²)
Annual Flux (Tg C per Year)^d						
	2000–2005	+7.2	–45.5	–16.3	–54.7	2.66
	2005–2050	+5.8	–20.1	–7.6	–21.8	2.51
Total Carbon Stock (Tg C)^d						
	2005	1,362.1	5,090.4	958.6	7,411.1	2.66
	2050	1,090.4	6,021.8	1,072.3	8,184.5	2.51

Notes

- Biomass includes aboveground and belowground live plant parts.
- Soil stocks consider the top 20 cm.
- Other includes leaf litter and woody debris.
- Values, in teragrams of carbon (Tg C), are averages of the A1B, A2, and B1 climate scenarios and estimated using the FORE-casting SCENarios of land-use change (FORE-SCE) model and the Erosion-Deposition-Carbon-Model (EDCM), CENTURY, and PBN carbon models (Liu et al., 2012b, 2014; Zhu et al., 2011). A negative carbon flux represents net ecosystem carbon uptake, while a positive carbon flux indicates carbon loss from the ecosystem.

effects if they consider only areas that remain as grasslands. Recent LSM simulations indicate that fire suppression reduces areal extent of grasslands in the conterminous United States and allows woody biomass to encroach (Bachelet et al., 2017). A recently developed remote-sensing method discovered 300% more burned areas in the Great Plains than did the previous method for the 1984 to 2013 period (Hawbaker 2017). These examples demonstrate that considering disturbance and land-use effects is key to reducing uncertainties in inventories and model projections of carbon cycling. Section 10.5, p. 415, discusses these societal impact questions in more detail.

Conterminous United States

Various efforts on scaling up flux tower observations and biogeochemical modeling mostly confirm that U.S. grasslands typically have been a carbon sink in recent years (Liu et al., 2012b, 2014; Xiao et al., 2014; Zhang et al., 2011; Zhu et al., 2011). By scaling up flux tower observations, Zhang et al. (2011) showed that the Great Plains, which makes up the majority of U.S. grasslands, was a net sink from 2000 to 2008, with an average net uptake of 24 ± 14 g C per m² per year (i.e., annual uptake varied from 0.3 to

47.7 g C per m² per year). The result was consistent with a similar study over North America that showed U.S. grasslands were a net carbon sink from 2001 to 2012 (Xiao et al., 2014). However, a recent biogeochemical modeling study suggested that U.S. grasslands during 2001 to 2005 lost 3 teragrams of carbon (Tg C) per year, amounting to about 120 g C per m² averaged over the conterminous United States (Wang et al., 2015). These contrasting results, along with the differences shown in Table 10.1, p. 401, indicate a discrepancy between modeling estimates and empirical, data-driven values that contribute to uncertainty in grassland carbon cycling rates.

The LandCarbon project (www2.usgs.gov/climate_landuse/land_carbon) provided a national ecosystem carbon sequestration assessment conducted by the U.S. Geological Survey (USGS) in response to requirements of the Energy Independence and Security Act of 2007 (EISA; H.R. 6 — 110th Congress 2007). The objective of the EISA assessment was to evaluate policy-relevant carbon sequestration capacity in terrestrial ecosystems through management or restoration activities. Climate, land-cover change, and fire disturbance were included in the carbon assessment. Grassland and shrubland assessments were combined for this chapter. U.S. national

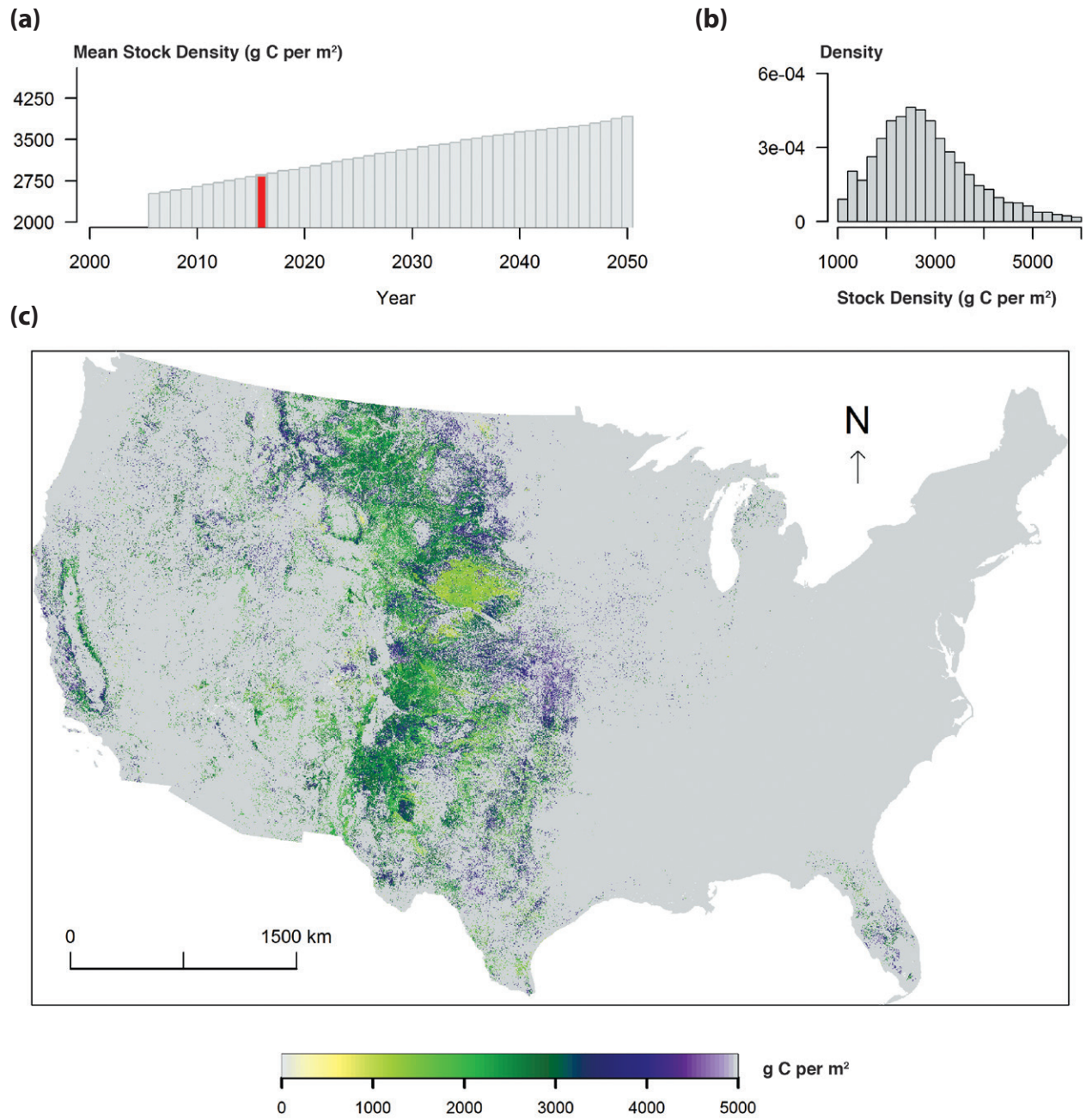


Figure 10.2. Model Simulation of Total Carbon Storage in U.S. Grasslands, 2016. (a) Spatial mean of carbon density in stocks over the 2005–2050 simulation period (red bar, 2016). (b) Number of pixels across the range of carbon density for 2016. (c) Total carbon storage in soils and vegetation for grasslands of the conterminous United States, simulated using the Erosion-Deposition-Carbon-Model (EDCM). Model simulations started in 1992 with initial soil carbon data from the Soil Survey Geographic database (SSURGO) and future climate projection from the Model for Interdisciplinary Research on Climate (MIROC; Liu et al., 2012a; Liu et al., 2014; Zhu et al., 2011). The Moderate Resolution Imaging Spectroradiometer (MODIS) net primary production products from 2001 to 2011 were used to constrain EDCM simulations, and the inverse model parameter values were used for future projections. Key: g C, grams of carbon.



summaries for 2001 to 2005 and 2006 to 2050 are shown in Table 10.2, p. 403, and Figure 10.2, p. 404. These projections represent simulation results using:

- Climate change data from the Model for Interdisciplinary Research on Climate (MIROC) general circulation model under three emissions scenarios (i.e., A1B, A2, and B1; IPCC 2000);
- Land-cover change data from the FOREcasting SCEnarios of land-use change (FORE-SCE) model (Sohl et al., 2007); and
- Three biogeochemistry models: Erosion-Deposition-Carbon Model (EDCM), CENTURY, and PBN (Liu et al., 2012b, 2014; Zhu et al., 2011).

Although the USGS LandCarbon Project currently does not include new representative concentration pathway (RCP) scenarios in its biological carbon sequestration assessment, the project considers climate projections for temperature and precipitation to be quite similar between the IPCC (2000) and RCP scenarios (Knutti and Sedláček 2013).

Figure 10.2 shows the estimated spatial pattern of carbon stocks in vegetation and soil in the top 20-cm layer in 2016 and the temporal change of the mean U.S. grassland carbon stock from 2005 to 2050 under the Intergovernmental Panel on Climate Change (IPCC) scenario A1B (IPCC 2000), estimated using the EDCM model (Liu et al., 2011, 2014; Zhu et al., 2011). More information about the methodology and results from other carbon models and scenarios can be found in a series of reports (Zhu and Reed 2012, 2014; Zhu et al., 2011) and the LandCarbon project (www2.usgs.gov/climate_landuse/land_carbon). The majority of U.S. grassland is distributed in the central Great Plains ecoregion, California, and central Florida, with large spatial variability in carbon stocks. At the U.S. national scale, the mean carbon stock was projected to increase over time (see Figure 10.2, p. 404).

The spatial distribution of the current decadal mean rate of the grassland NECB is shown in Figure 10.3, p. 406. The average annual carbon uptake varied from 15 to 40 g C per m² per year

with a decreasing trend after 2030 under scenario A1B (see Figure 10.3, p. 406). Carbon stocks were projected to continue increasing until mid-century despite declining NECB. The clear spatial pattern of the carbon fluxes from 2007 to 2016 is characterized by 1) carbon-neutral status (e.g., the Nebraska Sandhills in the central United States), 2) carbon losses mostly in north-central United States, and 3) carbon uptake mostly in the midwestern United States and California. The carbon dynamics since 2005 were simulated using the MIROC climate projections. Consequently, the simulated NECB and its spatial pattern might be different from reality, especially in the severely drought impacted areas of California in recent years.

Regional Scale: Great Plains Ecoregion as a Case Study

The Great Plains, comprising 2.17 million km² are dominated by grasslands, interspersed with shrublands, that account for 48% of the total area, while agricultural lands cover 42% of the total area (Zhu et al., 2011; see Figure 10.4, p. 407). Zhang et al. (2011) integrated remotely sensed vegetation greenness and weather datasets from 2000 to 2008 with NEP data from 15 eddy covariance flux tower sites to scale up and calculate a carbon budget for the Great Plains biome. The entire Great Plains was shown to have an average (\pm standard deviation) uptake rate of 24 ± 14 g C per m² per year (i.e., a range of 0.3 to 47.7 g C per m² per year). While the carbon uptake by the Great Plains was lower in the dry years, the entire biome remained a net carbon sink in 8 of the 9 years (Zhang et al., 2011). This study illustrated that, despite significant interannual and spatial variation, mature native grasslands have the potential to sequester significant amounts of carbon for extended periods of time (see Figure 10.4, p. 407). A recent regression tree analysis based on remote-sensing and flux tower data estimated a spatially averaged annual uptake by grasslands of 45 g C per m² per year in the same period (Wylie et al., 2016), confirming previous findings that grasslands are resilient carbon sinks.

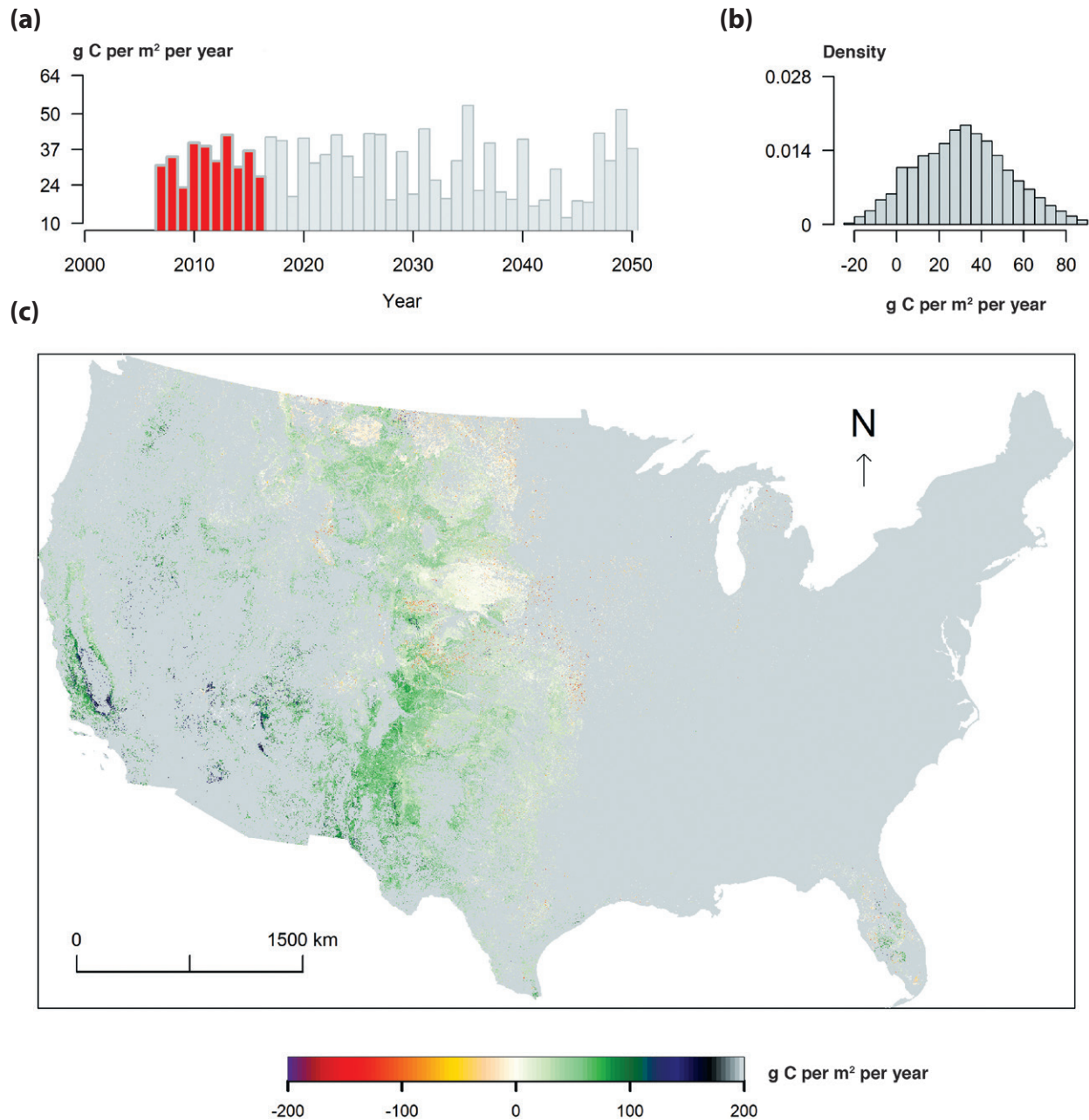


Figure 10.3. Model Simulation of Net Ecosystem Carbon Balance (NECB) for U.S. Grasslands in Response to Intergovernmental Panel on Climate Change Scenario A1B. (a) Spatial mean of NECB fluxes over the 2005–2050 simulation period (red bars, 2007–2016). Carbon increase rates are projected to decrease after 2030. (b) Probability of fluxes for the period 2007–2016. Positive and negative values indicate net input to and net loss from grasslands, respectively. (c) Spatial patterns of the decadal mean fluxes of NECB are shown from 2007 to 2016 (red portion in panel (a)). Effects of climate and land-use change on NECB are combined in this simulation by the Erosion-Deposition-Carbon-Model (EDCM; Liu et al., 2014; Liu et al., 2012b; Zhu et al., 2011). Positive and negative values indicate net input to and net loss from grasslands, respectively. Key: g C, grams of carbon.

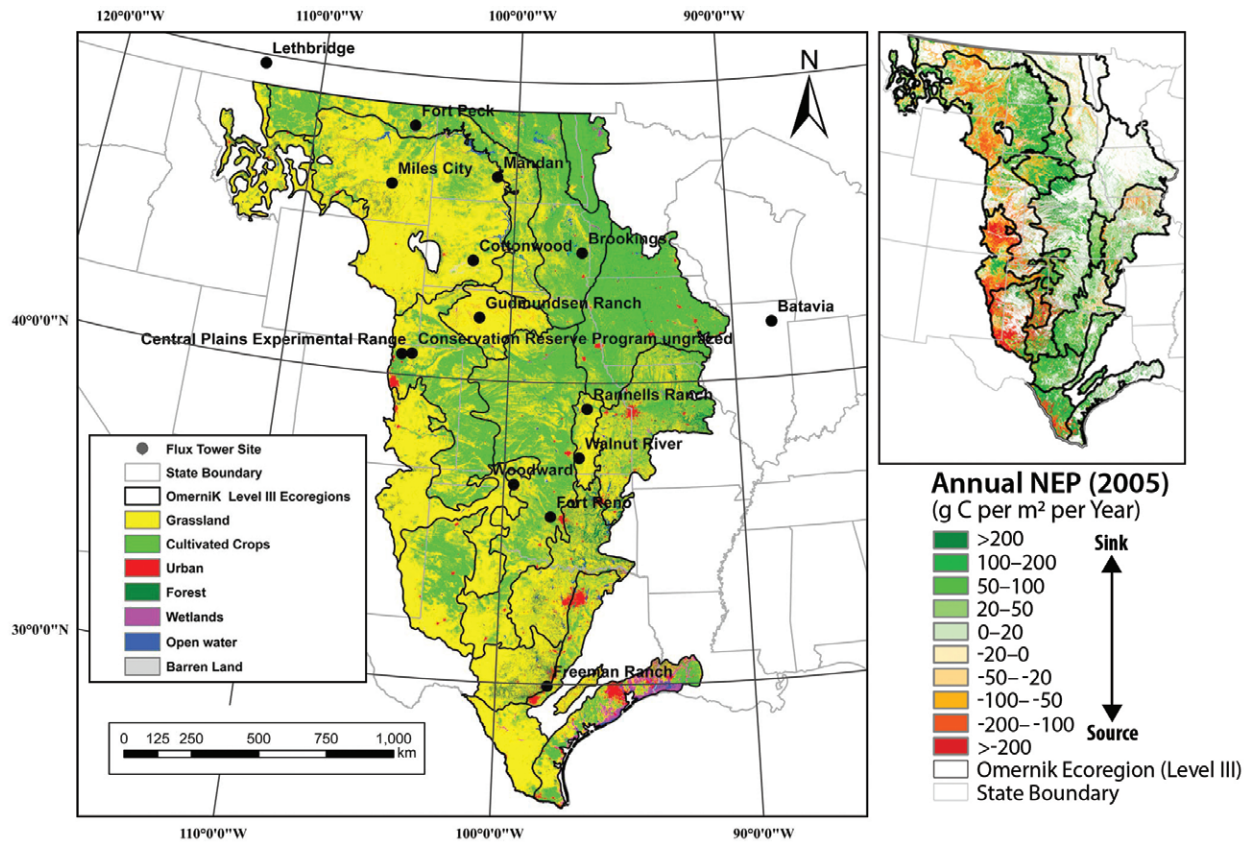


Figure 10.4. The Great Plains Ecoregion: Land Cover, Grassland Flux Towers, and Carbon Flux in 2005. The land-cover map for the Great Plains Ecoregion (Omernik 1987) was derived from the 2001 National Land Cover Database. The net ecosystem production (NEP) map was simulated based on land-cover type (Homer et al., 2004) and flux tower measurements using weather conditions for 2005. No fire disturbance or land-cover change effects were included. Key: g C, grams of carbon. [Figure source: Adapted from Zhang et al., 2011, used with permission.]

10.2.2 Processes Affecting Carbon Stocks and Fluxes in Grasslands

Climate Variability

Key Findings 2 and 3 relate to climate effects on grasslands, which will vary spatially and temporally. Grassland carbon balance is strongly sensitive to precipitation, often resulting in increased carbon losses in dry years or over drought-affected areas, particularly in the southwestern Great Plains (see Figure 10.4, this page; Biederman et al., 2016; Scott et al., 2015; Svejcar et al., 2008; Zhang et al., 2011). These frequent shifts from uptake to emissions in response to reduced precipitation indicate that grasslands are closer to the threshold for net carbon

storage than are forests (Scott et al., 2015). This interannual variation in grassland NEP results from interactions between moisture and temperature controls on leaf area production, photosynthesis, and respiration (Flanagan and Adkinson 2011). If moisture is not limiting, carbon storage can increase significantly in response to warmer conditions and rising atmospheric CO₂ (see Section 10.3.3, p. 410). In part, this increase results from flexible timing of grassland plant growth and photosynthesis (Ryan et al., 2016; Zelikova et al., 2015). For example, drought decreased the growing season length and led to reductions in NPP and carbon sequestration in the Canadian Great Plains (Flanagan and Adkinson 2011).



Land-Use and Land-Cover Changes (Grazing and Species Shifts)

Key Finding 4 relates to management impacts on grassland carbon stocks and fluxes. A recent simulation suggests that Great Plains grassland area declined by 16% from 1992 to 2005 due to land-use change, including fire suppression (Bachelet et al., 2017). However, carbon stocks in remaining grasslands are considered to be stable or increasing (Zhu et al., 2011).

Grazing Effects on Grassland Carbon Cycling.

Grasslands in North America evolved with native herbivores, historically grazed by livestock with varying intensities. Poor grazing management has been associated with reductions in productivity and soil carbon stocks, but improved management approaches, such as appropriate fertilization or reduced grazing intensity, can restore or even increase the original potential for carbon storage (Conant et al., 2001). Grazing intensity affects species composition and soil carbon content. For instance, heavy grazing can reduce aboveground productivity and root biomass, alter microbial community composition, and increase soil decomposition rates (Klumpp et al., 2009). However, intensive, early spring grazing may improve net carbon uptake by stimulating re-growth of plants later in the growing season, contingent on rainfall seasonality (Owensby et al., 2006; Svejcar et al., 2008). Some studies reported no effect of grazing on grassland carbon exchange (Polley et al., 2008; Risch and Frank 2006), and moderately grazed prairies can remain net carbon sinks (Frank 2004). In one recent study, moderate grazing was associated with average net carbon uptake of nearly 300 g per m² per year, but this was reduced to zero with heavy grazing (Morgan et al., 2016). Furthermore, low-precipitation years can reduce productivity in grazed ecosystems (Ingram et al., 2008; Polley et al., 2008), leading to net carbon losses in combination with heavy grazing (Morgan et al., 2016). In intensively managed, fertilized pastures on degraded former croplands in the mesic southeastern United States, soil carbon stocks returned to their pre-agricultural levels within about 6 years, because of

high NPP and rapid belowground carbon cycling (Machmuller et al., 2015). In mesic Texas rangelands, adaptive management, using high stocking rates for short durations across multiple paddocks, increased soil carbon relative to continuous heavy grazing (Teague et al., 2011). These studies suggest that grassland carbon cycling is resilient to appropriately managed grazing (see Figure 10.1, p. 402). However, a global meta-analysis indicates that grazing impacts on carbon storage are contingent on many factors, including precipitation, soil texture, plant species competition, and grazing intensity; for example, grazing stimulated carbon storage in C₄ grasslands by 67% but decreased it in C₃ grasslands by 18% (McSherry and Ritchie 2013).

Species Shifts: Invasive Grasses and Woody

Encroachment. The species composition, productivity, and carbon storage in grasslands are partly controlled by fire regimes, whether managed or unmanaged. Reduced fire frequency is associated with encroachment of woody plants into grassland ecosystems, while expansion of non-native, annual grasses such as cheatgrass can lead to increased fire frequency (see Figure 10.1, p. 402; Jones et al., 2015). Species shifts from perennial to annual vegetation may lead to reductions in productivity and carbon storage (Prater et al., 2006). For example, net carbon losses averaging 150 g per m² per year were observed for cheatgrass, mainly from increased decomposition rates (Verburg et al., 2004). Cheatgrass enhanced greenhouse gas (GHG) emissions, especially nitrous oxide (N₂O), and carbon cycling rates, compared with those for native perennial grasses (Norton et al., 2008). Further expansion of cheatgrass is expected to occur in response to rising temperatures across the western United States (Blumenthal et al., 2016).

Woody plant encroachment, with its increasing abundance of shrubs and trees, is one of the greatest threats to grasslands in North America, particularly with regard to changes in the magnitude and distribution of carbon stored in major terrestrial pools (Archer et al., 2001; Barger et al., 2011; Jackson et al., 2002; Knapp et al., 2008b). Changes in ecosystem carbon storage accompanying increases in



woody plants in grasslands represent a potentially significant but highly uncertain component of the carbon budget for North America (Houghton et al., 1999; Pacala et al., 2007), with positive, neutral, or negative effects documented (Barger et al., 2011). The most recent synthesis of studies quantifying the carbon consequences of woody plant encroachment in grasslands suggests that carbon in aboveground pools decreases in more water limited regions (i.e., mean annual precipitation < 330 mm) but increases in regions with greater precipitation (Barger et al., 2011; Knapp et al., 2008a). In the U.S. Great Plains, fire suppression with its associated woody encroachment from 1971 to 2005 is estimated to have increased total carbon stocks by an extra 5% relative to a nonfire-suppression scenario, with gains in woody biomes more than exceeding losses in grasslands (Bachelet et al., 2017). Changes in soil carbon from woody encroachment were not strongly related to aboveground carbon. However, loss of soil carbon is most likely to occur in humid grasslands, with increases in soil carbon apparent in arid regions (Barger et al., 2011; Jackson et al., 2002). Combining major aboveground and belowground pools, Barger et al. (2011) concluded woody plant encroachment generally would result in a net increase in ecosystem carbon stocks. Although some shrub-dominated ecosystems are more likely to lose carbon during drought periods than nearby grass-dominated systems (Scott et al., 2015), other areas indicate shrubs can maintain net carbon uptake despite drought (Petrie et al., 2015).

Woody plants are still increasing in many grasslands as a result of reduced fire frequency, rising CO₂, and increased precipitation intensity (Kulmatiski and Beard 2013). Because changes in carbon pools occur at very different rates above and below ground, ecosystem carbon changes driven by woody plant encroachment are likely to remain dynamic in the future. Overall, shifts in plant species composition and ecosystem structure represent a significant source of uncertainty in predicting future carbon cycling in grasslands.

10.3 Indicators, Trends, and Feedbacks

10.3.1 Future Projections of Carbon Stocks and Fluxes in Conterminous U.S. Grasslands

In estimating carbon stock and fluxes, several different models were used (see Key Finding 1, p. 400) to assess their projections, The LandCarbon project simulated future carbon stocks (see Figure 10.2, p. 404) and fluxes (see Figure 10.3, p. 406) using projections from MIROC A1B, A2, and B1 climate scenarios; FORE-SCE model; and EDCM (Liu et al., 2012b, 2014). Thus, these simulations combine the effects of land-use change and climate on carbon sequestration by grasslands in the conterminous United States (see Table 10.2, p. 403). While these model predictions are useful as general guidelines, additional empirical and simulation experiments are needed to disaggregate the effects of land-cover change from those of climate change and to examine regional differences in carbon cycling.

10.3.2 Impacts of Land-Use and Land-Cover Change on Future Carbon Cycling

Zhu et al. (2011) demonstrate that land-use and land-cover conversions were major drivers of the predicted changes in carbon storage in Great Plains grasslands. Future land-use change in the region (data provided by the *Intergovernmental Panel on Climate Change's Special Report on Emission Scenarios*; IPCC 2000) is driven by the demand for agricultural commodities, including biofuels, resulting in a 1.4% to 9.2% expansion of agricultural land by 2050, mostly at the expense of grasslands (-2.2% to -9.3%). Areas where woody vegetation expands into grassland because of fire suppression are re-classified as forest. This change tends to result in higher carbon stocks and uptake rates but also can be subject to catastrophic carbon losses in hot and dry fire years following wet years' boosting of fuel loads (Bachelet et al., 2017).

In the Great Plains, carbon stocks for the years 2001 to 2005 are assessed as 7,500 Tg C with 45.8% in agricultural lands, 34.9% in grasslands and



shrublands, 15.5% in the few existing forested areas, and almost 3% in wetlands. By 2050, models estimate those percentages will change to reflect a small increase in agricultural land carbon stocks (47%), a large decrease in grassland carbon stocks (29%), an increase in forestland carbon stocks (20.4%) due to woody encroachment and forest growth, and no change in carbon stocks of wetlands or other lands. Conversion of grasslands to agriculture may lead to a cumulative reduction in stored carbon of 26 to 157 Tg from 2001 to 2050, an amount which could contribute up to 4% loss of mean total carbon sequestration potential (Zhu et al., 2011). Shrub encroachment and afforestation cannot mitigate carbon losses to agricultural expansion. Fires are also a source of carbon loss. Areas burned and carbon emissions from fires vary both spatially and temporally due to climatic, biological, and physical factors. However, fires in grasslands were not projected to change significantly under future climate conditions when models did not include the role of annual invasives or fire suppression. Average fire emissions from grasslands range from 0.18 to 24.72 Tg CO₂ equivalent¹ (CO₂e) per year (Zhu et al., 2011).

10.3.3 Climate Change Impacts on Grassland Productivity

Numerous environmental factors interact to affect grassland production, including warming, rising CO₂, hydrology, and nutrient availability. Grassland productivity is very sensitive to variations in climate, especially precipitation and including both the mean and extremes such as droughts and floods (Huxman et al., 2004; Knapp et al., 2001, 2008b, 2015). Their sensitivity indicates a strong potential for climate change to alter carbon cycling in grasslands (see Key Finding 2, p. 400; Figure 10.5, p. 411). Productivity is predicted to decline in the southwestern United States and northern Mexico as a result of reduced precipitation and to increase in the northern Great Plains as a result of temperature and precipitation

increases that allow an increase in growing season length (Hufkens et al., 2016; Polley et al., 2013; Reeves et al., 2014). However, significant projected increases in productivity did not arise until after 2030 because of scenarios projecting CO₂ fertilization and rising temperatures (Reeves et al., 2014).

North American grassland growth in this century was simulated based on hydrology and repeat-photography observations of vegetation greenness (Hufkens et al., 2016). Despite a projected increase in climate aridity by 2100, increases in fractional plant cover were predicted over almost 90% of the study area, with greater increases in cover and net carbon sequestration in the more northerly areas. The primary mechanism contributing to the projected increase in grassland growth was a shift to earlier leaf emergence in the spring and delayed leaf senescence in the autumn, both of which compensated for drought-induced reduction in plant productivity during the summer (Hufkens et al., 2016).

Predictions from the vegetation-hydrology model are supported by a climate manipulation experiment in Wyoming mixed-grass prairie, where the growing season started earlier in spring because of the warming treatment and ended later in autumn because of increased soil moisture made available by the elevated CO₂ treatment (Reyes-Fox et al., 2014). The lengthening of the growing season was dependent on a mix of C₃ and C₄ species adapted to different climate conditions. In the same experiment, greenness was enhanced (i.e., indicating increased aboveground biomass and cover) with warming and elevated CO₂, but the effects of seasonal and interannual rainfall variability were much stronger (Zelikova et al., 2015). High-precipitation years had two to three times greater vegetation greenness than dry years. Warming in combination with elevated CO₂ increased total plant biomass by an average of 25%, especially below ground (Mueller et al., 2016). Warming and elevated CO₂ also interacted to affect soil moisture and nitrogen availability (Mueller et al., 2016). While elevated CO₂ conditions increased soil moisture (Morgan et al., 2011), warming decreased soil moisture, and soil nitrate tended to follow trends opposite to those for elevated CO₂ (Mueller et al.,

¹ Carbon dioxide equivalent (CO₂e): Amount of CO₂ that would produce the same effect on the radiative balance of Earth's climate system as another greenhouse gas, such as methane (CH₄) or nitrous oxide (N₂O), on a 100-year timescale. For comparison to units of carbon, each kg CO₂e is equivalent to 0.273 kg C (0.273 = 1/3.67). See Box P.2, p. 12, in the Preface for details.

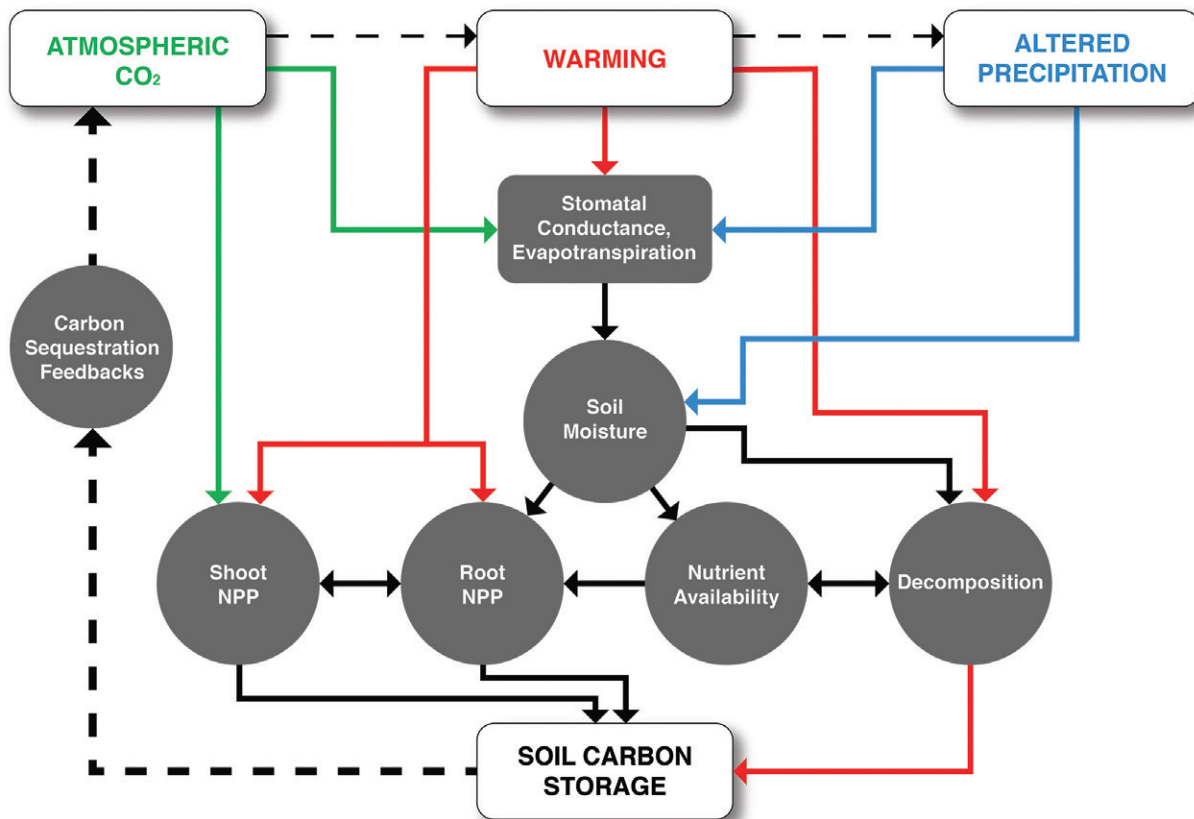


Figure 10.5. Interacting Effects of Rising Atmospheric Carbon Dioxide (CO₂), Warming, and Altered Precipitation on Grasslands. Climate variations can impact grassland plant productivity and soil organic matter (SOM) storage, which in turn are mediated by soil moisture and nutrient availability. Root and shoot net primary production (NPP) are correlated, and both are dependent on soil moisture and nutrient availability. Plant nutrient uptake can decrease soil nutrients, which may be made available during SOM decomposition. [Figure conception derived from numerous studies, including Hufkens et al., 2016; Morgan et al., 2011; Mueller et al., 2016; Reich and Hobbie 2013; Reyes-Fox et al., 2014; and Zelikova et al., 2015.]

2016). A warming experiment in desert grasslands suggested warming could reduce C₃ and C₄ grass carbon fixation rates and aboveground biomass, with no significant effects on shrub photosynthesis or growth (Wertin et al., 2015, 2017). Figure 10.5, this page, illustrates carbon cycle interactions and feedbacks associated with multiple climate change factors. Furthermore, changing seasonality of precipitation events, as well as more extreme weather conditions, are expected to affect carbon cycling increasingly more in the future (Knapp et al., 2008b).

Nutrient limitation may reduce the potential for CO₂ fertilization in grasslands, especially over

decadal timescales (see Figure 10.5, this page). For example, a long-term experiment in a nutrient-poor grassland in Minnesota revealed that elevated CO₂ effects on NPP were dependent on soil nitrogen availability and experiment duration. During the first 3 years of the experiment, elevated CO₂ stimulated aboveground biomass by 11% and was not contingent on nitrogen availability, but over the longer term (4 to 13 years), the biomass response to elevated CO₂ increased by up to 20% with added nitrogen fertilizer (Reich and Hobbie 2013). However, in the coming decades, elevated temperature may enhance nitrogen availability, as shown by Mueller et al. (2016). Moreover, increasing nitrogen



deposition will stimulate NPP, up to a threshold, and GHG emissions also may follow a similar nonlinear response to nutrient loading (Gomez-Casanovas et al., 2016). Interacting effects of multiple global change factors still represent a large source of uncertainty in predicting carbon cycle responses (Norby and Luo 2004).

10.3.4. Trends and Climate Feedbacks from Soil Carbon Cycling

The effect of climate change on the stability of carbon in SOM pools is one of the largest sources of uncertainty in projections of climate-carbon interactions (Heimann and Reichstein 2008) because these pools are large and vulnerable to climate change (Davidson and Janssens 2006; see Key Finding 3, p. 400). In grasslands, decomposition of roots is thought to drive SOM accumulation (Jackson et al., 1996; Jobbagy and Jackson 2000), so processes affecting belowground productivity are likely to affect soil carbon storage (see Figure 10.5, p. 411). The importance of impacts from aboveground inputs compared to those from direct inputs via root production depends on climate, soil type, and plant species (Sanderman and Amundson 2008). Therefore, grassland species composition and productivity, both above and below ground, and their responses to climatic and land-use changes are key determinants of soil carbon storage. SOM decomposition rates vary with temperature and moisture and can be affected by plant-microbe interactions (van Groenigen et al., 2014) via nutrient uptake processes (Nie and Pendall 2016).

Soil Carbon Responses to Altered Precipitation.

Precipitation is the most important climate driver of productivity in grasslands (Knapp and Smith 2001) and is likely to influence carbon storage in soils over longer timescales, via mechanisms related to both plant inputs and decomposition losses (see Figure 10.5, p. 411). A meta-analysis indicated that soil carbon content increased in response to both reductions and additions of moisture in grasslands (Zhou et al., 2016). Experimentally increased precipitation likely enhanced soil carbon pools via the stimulation of biomass inputs, whereas reduced

precipitation may have enhanced the soil carbon pools by reducing SOM decomposition rates as well as by increasing allocation to root biomass production (Zhou et al., 2016).

Soil Carbon Responses to Warming. Earth System Models (ESMs) assume that warming will stimulate SOM decomposition at an exponential rate, leading to potentially strong positive feedbacks to climate change (Figure 10.5; Davidson and Janssens 2006). Experimental evidence of this assumption has been accumulating from numerous individual studies worldwide (Luo 2007). A recent synthesis of warming-experiment results confirms that SOM is vulnerable to warming and indicates that the magnitude of carbon loss depends on initial carbon stocks (Crowther et al., 2016). This study also showed that deserts and arid grasslands, with lower soil carbon pools, are less vulnerable to warming than colder ecosystems. A reduction in decomposition rates with warming-induced soil desiccation could potentially explain these results (Pendall et al., 2013).

Using results from field experiments to inform model parameters is a powerful way to reduce uncertainties, constrain the models, and enhance modeling tools to extrapolate results more broadly. Data from a 9-year warming experiment in tallgrass prairie were assimilated into a biogeochemistry model to demonstrate that soil carbon pools would decrease over the coming century (Shi et al., 2015). This study confirms that carbon in productive grasslands like the tallgrass prairie in Oklahoma can be vulnerable to warming, in part because of the resulting increased decomposition of a large, partially protected soil carbon pool. Key uncertainties were related to the mismatch between the long-term residence time of the large, recalcitrant soil carbon pool and the duration of the experiment (Shi et al., 2015).

Soil Carbon Responses to Rising CO₂ and Interactions with Multiple Drivers. While rising atmospheric CO₂ concentrations can stimulate grassland productivity above and below ground, especially in combination with warming (Mueller et al., 2016), increased productivity has not necessarily translated



into increased soil carbon storage (Luo et al., 2006). A meta-analysis revealed that carbon inputs to grasslands increased by 20% with experimentally increased CO₂, but this increase was accompanied by a 16.5% increase in the decomposition rate constant (van Groenigen et al., 2014). The “priming effect” that stimulates SOM decomposition may be caused by the increased microbial activity caused by increased belowground carbon inputs (Carney et al., 2007) and soil moisture (Pendall et al., 2003), and this effect may be “widespread and persistent” (van Groenigen et al., 2014). A simulation model calibrated to realistic field conditions in semiarid Wyoming grassland predicted that soil carbon would decrease with elevated CO₂ and increase with warming, because of indirect effects mediated by soil moisture (Parton et al., 2007). However, the importance of interactive effects of multiple climate changes in predictions of long-term soil carbon storage still needs to be confirmed with field results.

Few field experiments have been conducted that combine two or more climate drivers over a long enough duration to evaluate soil carbon responses (Luo et al., 2011), making realistic predictions of soil carbon sequestration challenging. A recent meta-analysis failed to uncover significant changes in soil carbon with the combined effects of elevated CO₂ and temperature, although belowground (i.e., root) production was significantly stimulated (Dieleman et al., 2012). While synthesis studies and meta-analyses are useful for discovering general patterns, they cannot distinguish mechanisms underlying these patterns. Major uncertainties in soil carbon storage and ecosystem carbon cycling remain because there are too few long-term, multi-factor climate manipulation experiments to constrain mechanisms, feedbacks, and interactive effects among global change drivers.

10.4 Societal Drivers, Impacts, and Carbon Management

Because grassland vegetation is predominantly herbaceous (i.e., nonwoody), biomass carbon stocks in grassland systems are a small, transient carbon

pool with soil constituting the dominant carbon stock. The main processes governing the carbon balance of grassland soils are the same as for other ecosystems—the photosynthetic uptake and assimilation of CO₂ into organic compounds and the release of gaseous carbon, primarily CO₂ but also methane (CH₄), through respiration and fire (see Key Finding 4, p. 400). In grasslands, carbon assimilation is directed toward production of forage by manipulating species composition and sometimes growing conditions (e.g., soil fertility and irrigation).

10.4.1 Grazing Management

For most grasslands in North America, grazing management is the primary feasible management practice that can be manipulated to alter soil carbon stocks. The capacity to increase grassland system carbon stocks is a function of 1) carbon stock changes that might be realized with a shift from suboptimal to best management practices and 2) the areal extent of grasslands that are not optimally managed (Conant and Paustian 2004). Estimates of the potential to sequester carbon in North American grasslands by improving grazing management practices seem likely to be on the order of tens of teragrams of carbon per year (Follett et al., 2001). Uncertainty across these and similar estimates stems from variation in soil carbon responses to management practices, which vary substantially from place to place. Some uncertainty also arises from limited information about past management and the extent to which those historical practices have depleted soil carbon stocks. Additionally, plot-level research indicates that a wide variety of practices could drive increases in soil carbon stocks (Chambers et al., 2016; Conant et al., 2001; Henderson et al., 2015). What is not clear is whether practices used in field experiments can be replicated reasonably under real-world conditions or the extent to which experiments are indicative of potentially observed real-world carbon stock rate changes (Conant et al., 2017).

Removal of some (30% to 50%) aboveground biomass through grazing can reduce the amount of carbon returned to the soil, potentially leading to reduced soil carbon stocks (Conant et al., 2017).



Similarly, shifts in species composition in response to grazing could lead to reductions in carbon inputs and soil carbon stocks. Some of the carbon lost from grassland soils can be recovered with changes in management practices that increase carbon inputs, stabilize carbon within the system, or reduce carbon losses (Conant et al., 2017; Eagle and Olander 2012). Adaptive and intensive grazing practices can increase soil carbon stocks (Machmuller et al., 2015; Teague et al., 2011). However, the management practices that promote soil carbon sequestration would need to be maintained over decades to avoid subsequent losses of sequestered carbon.

10.4.2 Fire Suppression and Woody Encroachment

Grazing management, fire suppression, and climate interactively control grassland species composition and productivity, and these responses vary regionally. Woody plant cover is increasing in many grasslands because of management activities such as fire suppression and anthropogenic GHG emissions that increase atmospheric CO₂ concentrations (Kulmatiski and Beard 2013). The most recent syntheses suggest that carbon in aboveground pools decreases in regions with more-limited water (mean annual precipitation < 330 mm) but increases in regions with greater precipitation (Barger et al., 2011; Knapp et al., 2008b). For example, fire suppression in Kansas allowed the expansion of *Juniperus virginiana* that was associated with rapid increases in carbon stocks in vegetation and soils (McKinley and Blair 2008). In the more arid Chihuahuan Desert, shrub encroachment related to historical over-grazing led to higher net carbon uptake rates (Petrie et al., 2015) but may lead to additional loss of grass vegetation (Thomey et al., 2014). Soil carbon pools may increase with woody encroachment, depending on other disturbance factors, especially fire (Barger et al., 2011). If management policies continue to allow woody plants to expand into native grasslands, the central United States may become a significant regional carbon sink (McKinley and Blair 2008), given sufficient precipitation.

Regional responses to management and climate change are partly related to distinct evolutionary pressures. The combination of grazing and aridity in the Great Plains grasslands may have favored traits that impart resistance to both those disturbances (Milchunas et al., 1988; Moran et al., 2014; Quiroga et al., 2010). In contrast, desert grasslands evolved the ability to rapidly respond to and effectively use highly variable precipitation (McClaran 1997), though often requiring years to recover from disturbance (Peters et al. 2012) and thus allowing rapid expansion of woody species (McClaran et al., 2010). If the frequency of burning increases in mesic tallgrass prairie, decreased nitrogen may become a limiting factor, eventually diminishing aboveground production (Soong and Cotrufo 2015). Thus, fire regime management can influence carbon storage via its effects on above- and belowground production, as well as inputs of recalcitrant, pyrogenic organic matter to soil.

10.4.3 Land Conversion

Agricultural policies can have a large influence on land-use change. For example, in the U.S. Great Plains during 1973 to 2000, grassland and shrubland area expanded by 2.2% while agricultural area decreased by 1.8%, in part related to farm policy programs such as the Conservation Reserve Program (CRP; landcover.trends.usgs.gov/gp/eco43Report.html). However, the area held in CRP peaked in 2007 at 37 million acres and has since declined (Ahlering et al., 2016). In the coming three decades, agricultural expansion is expected to continue to reduce the extent of grasslands by 2% to 9% by 2050 (see Section 10.3.2, p. 409; Zhu et al., 2011), depending on annual crop prices (Stubbs 2014).

Grasslands generally take up and store more carbon than croplands; for example, in the Great Plains, the average uptake rates were about 45 g C per m² per year for grasslands and 31 g C per m² per year for croplands from 2000 to 2008 (Wylie et al., 2016). Soil carbon losses occur when native grasslands are initially tilled, with the amount determined by the tillage method and the soil's initial carbon content. In a modeling study, this "carbon debt" was repaid



after 2 to 25 years of no-till corn ethanol production, but that process was 50% longer in a full-tillage production scenario (Kim et al., 2009). Moreover, GHG emissions from croplands tend to be higher than those from grasslands, especially when CH₄ and N₂O are considered. Protection of grasslands from conversion to croplands in the northern mixed-grass prairie pothole region of the Dakotas would reduce emissions significantly, but carbon offsets alone cannot compete with high market prices for corn (Ahlering et al., 2016). For more details on the effects of agricultural management on carbon cycling, see Ch. 5: Agriculture, p. 229.

10.5 Synthesis, Knowledge Gaps, and Outlook

10.5.1 Synthesis

Grasslands are globally important carbon sinks that are resilient to climate change and managed grazing because the mixture of native species that occur are adapted to variable climatic conditions and grazing pressure. In drier regions, such as the southwestern United States and Mexico, grasslands may lose carbon in response to droughts or overgrazing. Mesic grasslands in Florida have stored vast amounts of soil carbon, which may be vulnerable to losses from fire and flooding, and CH₄ emissions from these and other poorly drained grasslands can be significant. Changes in the geographic extent of grasslands caused by land-use change, including cropping and grazing management, will affect grassland carbon cycling. The net uptake rate of carbon is higher in grasslands than in agricultural lands, but management that takes carbon storage into consideration may mitigate potential carbon losses. Invasive species also are likely to alter grassland carbon cycling: woody species such as juniper or mesquite may increase net carbon uptake while herbaceous invasive species, such as cheatgrass, may diminish net carbon uptake.

10.5.2 Knowledge Gaps

Grassland productivity and carbon cycling are linked very closely to variations in precipitation and soil moisture availability in space and time. Changes

in climate that lead to altered moisture availability are likely to affect the ability of grasslands to store carbon. Therefore, one of the main sources of uncertainty in predicting grassland carbon cycling is related to predictions of future precipitation, in terms of means, extremes, and seasonal distribution. The forecasted intensification of the global hydrological cycle will manifest in many ways, including increased interannual precipitation variability, more frequent extreme precipitation years (wet and dry), and alterations in annual precipitation amount (IPCC 2013). Recent climatological trends have supported these predictions (Fischer and Knutti 2014; Min et al., 2011). In grasslands, carbon uptake processes have been shown to be quite responsive to precipitation amount and event size and timing (Cherwin and Knapp 2012; Goldstein and Suding 2014; Heisler-White et al., 2008, 2009; Knapp et al., 2008b; Kulmatiski and Beard 2013; Thomey et al., 2011), but both positive and negative effects have been documented. Resolving the effects on carbon cycling from altered precipitation regimes—including seasonality—in future grasslands will reduce uncertainty in responses (Knapp et al., 2008b). Moreover, also unknown are future effects on carbon cycling from interactions between climate change and species composition. Additional simulations with dynamic vegetation models, including management parameters such as fire suppression, will help reduce these uncertainties (Bachelet et al., 2017).

Model intercomparison projects that address large differences in future projections of carbon cycling in grasslands and other ecosystem types also will reduce uncertainties (Medlyn et al., 2015). Methodological differences in estimating regional- to continental-scale carbon stocks and fluxes have resulted in large apparent uncertainties in budgets. For inventory methods, these uncertainties appear to stem from extrapolating carbon stocks and fluxes from point measurements to regional scales based on land-use classifications. For land-surface models, uncertainties can result from different assumptions, drivers, and processes. For atmospheric inverse models, the attribution of specified land areas may not align well with other approaches. For all these



methods, inconsistencies in the depth of soil carbon can lead to large differences in stocks and process rates. Reconciling these divergent results likely will lead to improved understanding of processes and narrow the range of uncertainty in carbon forecasts.

Projections of soil carbon trends in response to future climate and land-use changes remain highly uncertain, particularly in warm, dry areas of Mexico and the U.S. Southwest and at high northern latitudes where data to inform modeling are limited. One uncertainty is related to the depth of soil carbon storage, with most models considering only the top 20 cm. However, validation and calibration datasets are not readily available, so models are rarely updated (e.g., Liu et al., 2003), and there is disagreement about which drivers of soil carbon dynamics should be included in models (Wieder et al., 2015). A recent study that simulated results from several multifactor climate change experiments indicated that productivity and decomposition responded more to increased precipitation and elevated CO₂

in drier sites, including grasslands, than they did in wetter sites (Luo et al., 2008). The four tested ecosystem models all demonstrated significant interactive effects of warming, elevated CO₂, and altered precipitation, although results for different sites varied because model formulations differed (Luo et al., 2008). These disparate findings demonstrate that rigorously evaluating model assumptions against experimental results will improve ESM projections (Medlyn et al., 2015).

10.5.3 Outlook

Grasslands, the most extensive land-use type in the continental United States when combined with rangelands, shrublands, and pastures (Reeves and Mitchell 2012), are expected to maintain net carbon uptake at least until the middle of this century. The most significant threats to this carbon uptake potential likely will be related to land management and land use, along with changes in the precipitation regime associated with ongoing climate change.



SUPPORTING EVIDENCE

KEY FINDING 1

Total grassland carbon stocks in the conterminous United States, estimated to be about 7.4 petagrams of carbon (Pg C) in 2005, are projected to increase to about 8.2 Pg C by 2050. Although U.S. grasslands are expected to remain carbon sinks over this period, the uptake rate is projected to decline by about half. In the U.S. Great Plains, land-use and land-cover changes are expected to cause much of the change in carbon cycling as grasslands are converted to agricultural lands or to woody biomes (*medium confidence*).

Description of evidence base

Total carbon stocks are from Table 10.2, p. 403, based on LandCarbon project estimates (land-carbon.org/categories). Various efforts confirm that the U.S. and North American grasslands in recent years have been a weak carbon sink (i.e., mostly within the range of 10 to 40 g per m² per year; Hayes et al., 2012; Liu et al., 2012b; Raczka et al., 2013; Wylie et al., 2016; Xiao et al., 2014; Zhang et al., 2011). Recent results generated from the assessment of carbon sequestration potentials in the United States conducted by the U.S. Geological Survey (Zhu and Reed 2012, 2014; Zhu et al., 2011) provided more integrated grassland carbon assessment. Land-use change scenarios and spatial dynamics were developed empirically by ecoregions across the United States under the Intergovernmental Panel on Climate Change (IPCC) scenarios A1B, A2, and B1 (Sleeter et al., 2012; Sohl et al., 2007), which are considered to be similar to representative concentration pathway (RCP) scenarios (Knutti and Sedláček 2013). Carbon dynamics in grassland ecosystems were simulated with the General Ensemble Biogeochemical Modeling System (GEMS) using three climate projections: the Second Generation Coupled Global Climate Model (CGCM2), Australia's national Commonwealth Science and Industry Research Organization (CSIRO), and Model for Interdisciplinary Research on Climate (MIROC) for each of the three IPCC scenarios (Liu et al., 2012b, 2014). The data included in this report include simulations from two process-based models: CENTURY (Parton et al., 1987) and the Erosion-Deposition-Carbon-Model (EDCM; Liu et al., 2003), and both were encapsulated in GEMS. The findings are supported by a recent synthesis of eddy covariance data with remote sensing, which shows that grasslands take up somewhat more carbon than crops in the Great Plains, although both were weak carbon sinks from 2000 to 2008 (Wylie et al., 2016).

Major uncertainties

There are significant differences in evaluation of grassland carbon stocks and fluxes (Hayes et al., 2012; Raczka et al., 2013; Zhu and Reed 2014). The primary source of model difference comprises modeling method (i.e., inventory, flux towers, inversion, and process-based modeling) and land-cover characterization and spatial resolution. For example, the LandCarbon study (Zhu and Reed 2012, 2014; Zhu et al., 2011) combined grass and shrub into grassland and considered fire disturbance, while Zhang et al. (2011) used data from 15 flux towers at natural grassland and pastures or hay sites but without considering fires.

Assessment of confidence based on evidence and agreement, including short description of nature of evidence and level of agreement

The magnitudes of the estimates of carbon stocks and fluxes vary depending on the method used, indicating a medium to low level of confidence in the results.

**Summary sentence or paragraph that integrates the above information**

Grasslands appear very likely to be weak carbon sinks and will remain so for at least the coming three decades, but reconciling different methods will reduce uncertainties in the quantities.

KEY FINDING 2

Increasing temperatures and rising atmospheric carbon dioxide (CO₂) concentrations interact to increase productivity in northern North American grasslands, but this productivity response will be mediated by variable precipitation, soil moisture, and nutrient availability (*high confidence, very likely*).

Description of evidence base

Experimental manipulations in the field provide evidence of climate change effects on grassland productivity by up to 33%, but this is contingent on nutrient and moisture availability (e.g., Morgan et al., 2011; Mueller et al., 2016; Reich and Hobbie 2013). Spatially distributed observations of vegetation phenology (i.e., greenness) and carbon fluxes combined with empirical modeling provide evidence of regional differences in grassland responses to future climate change (Hufkens et al., 2016). Simulation models are in general agreement with empirical evidence that carbon stocks will increase in grasslands in the coming three to four decades (Zhu et al., 2011). In grasslands, carbon uptake is responsive to precipitation amount and event size and timing, with both positive and negative effects documented, but droughts are associated with carbon losses across all grasslands (Cherwin and Knapp 2012; Goldstein and Suding 2014; Heisler-White et al., 2008, 2009; Knapp et al., 2008b; Kulmatiski and Beard 2013; Thomey et al., 2011).

Major uncertainties

The largest source of uncertainty is related to future precipitation regimes in the grassland biomes of North America, with both increases and decreases in precipitation predicted (IPCC 2013). The degree to which altered precipitation regimes will affect carbon cycling in future grasslands is uncertain (Knapp et al., 2008b). The relative response of grassland productivity to moisture availability is contingent upon prior conditions, which vary temporally and spatially (Heisler-White et al., 2009). Empirical models represent grassland phenology and productivity well, but they lack explicit physiological processes, leading to uncertainties in mechanisms underlying ecosystem responses to climate change (Hufkens et al., 2016).

Assessment of confidence based on evidence and agreement, including short description of nature of evidence and level of agreement

Confidence is high that grassland production will increase with precipitation as atmospheric CO₂ and temperature increase in the coming three to four decades, based on empirical evidence from field experiments.

Estimated likelihood of impact or consequence, including short description of basis of estimate

If grassland productivity decreases in response to climate change, such as reduced precipitation, forage production for livestock is very likely to be at risk. This has been demonstrated by numerous experiments and models as explained above in the description of evidence base.



Summary sentence or paragraph that integrates the above information

Grassland productivity is highly likely to respond positively to increased precipitation and temperature, especially in the Northern Great Plains. Neutral or negative responses of productivity to warming in the Southern Great Plains, the southwestern United States, and Mexico may be offset by positive responses to elevated CO₂.

KEY FINDING 3

Soil carbon in grasslands is likely to be moderately responsive to changes in climate over the next several decades. Field experiments in grasslands suggest that altered precipitation can increase soil carbon, while warming and elevated CO₂ may have only minimal effects despite altered productivity (*medium confidence, likely*).

Description of evidence base

Meta-analysis of numerous field experiments showed that soil carbon stocks increase when precipitation is increased or decreased in grasslands (Zhou et al., 2016). Meta-analysis also showed that elevated CO₂ increased soil carbon decomposition rate, limiting carbon storage potential (van Groenigen et al., 2014). Field experiments indicate that soil carbon stocks decrease with warming, especially in regions where stocks are high to begin with (Crowther et al., 2016), although warming-induced soil carbon losses from grasslands may be insignificant (Lu et al., 2013). These results are confirmed in some simulation experiments (e.g., Parton et al., 2007; Shi et al., 2015).

Major uncertainties

Major uncertainties in soil carbon storage come from insufficient understanding of physical and biological mechanisms that determine the stability of soil carbon. Physical mechanisms underlying carbon stability in soil, such as protection within aggregates and their sensitivity to climate change, are still poorly described (Heimann and Reichstein 2008). In particular, regulation of soil organic matter decomposition by microbe-plant interactions is poorly understood and not well represented in models (Wieder et al., 2015). Improving mechanistic understanding of soil carbon dynamics, and incorporating key mechanisms into models, will reduce uncertainties in future carbon cycle predictions (Todd-Brown et al., 2013).

Assessment of confidence based on evidence and agreement, including short description of nature of evidence and level of agreement

Mechanistic understanding of soil carbon stability in the face of climate change is still limited, leading to only medium confidence levels regarding the response of soil carbon to climate changes.

Estimated likelihood of impact or consequence, including short description of basis of estimate

Soils in grasslands are not likely to respond strongly to climate change; small carbon losses or gains could occur in the future with warming or elevated CO₂. Larger carbon gains are likely to occur with increased precipitation.

Summary sentence or paragraph that integrates the above information

Mechanisms regulating soil carbon storage in response to climate change can be incorporated into models to improve confidence in model predictions of future carbon cycling.



KEY FINDING 4

Carbon stocks and net carbon uptake in grasslands can be maintained with appropriate land management including moderate levels of grazing. Fire suppression can lead to encroachment of woody vegetation and increasing carbon storage in mesic regions, at the expense of grassland vegetation (*high confidence, likely*).

Description of evidence base

Studies of carbon fluxes using eddy covariance indicate that moderate grazing allows grasslands to continue to be net carbon sinks, but heavy grazing diminishes their capacity to take up carbon (Frank 2004; Morgan et al., 2016; Polley et al., 2008; Risch and Frank 2006). Soil inventory studies indicate that moderate to light grazing does not negatively affect carbon stocks (Conant et al., 2001, 2017), and improving grazing management can augment carbon stocks (Chambers et al., 2016). Carbon cycle responses to woody encroachment are determined from inventories of carbon stocks in vegetation and soils in plots that have been experiencing woody encroachment for different periods of time (Barger et al., 2011; Knapp et al., 2008a).

Major uncertainties

Uncertainties in grazing management impacts on carbon cycling in grasslands stem mainly from the regional variations in soil carbon responses to management, from challenges in designing scientific studies that adequately represent real-world management practices, and from limitations faced when extrapolating plot-level studies to broader areas (Conant et al., 2017). Interactive effects of grazing, climate, soil type and plant community composition on carbon storage are not well constrained (McSherry and Ritchie 2013). The magnitude of carbon accumulation below ground in response to woody encroachment is poorly constrained, but change in carbon pools above ground is well known (Barger et al., 2011; Knapp et al., 2008a). Fire regimes are changing with increasing temperatures and altered vegetation; uncertainties in future fire risk add uncertainty to projections of carbon budgets.

Assessment of confidence based on evidence and agreement, including short description of nature of evidence and level of agreement

There is high confidence with general agreement across several studies that moderate to light grazing will not have a negative impact on carbon cycling.

Estimated likelihood of impact or consequence, including short description of basis of estimate

Woody encroachment likely will lead to increased carbon storage in mesic grasslands.

Summary sentence or paragraph that integrates the above information

Carbon likely will continue to accumulate for the next several decades in grasslands if they are appropriately managed.

SUPPORTING EVIDENCE FOR TABLES

Table 10.1, p. 401, is based on Hayes et al. (2012). The areas for grasslands by countries and the continent are from the models and inventory analyses used in their study (see Table S10 in Hayes et al., 2012). The area for “Others” is smaller for the models than the inventory analysis mainly because the latter includes urban areas. Inventory estimates are the sum of livestock methane



(CH₄) emissions + livestock carbon dioxide (CO₂) emissions + grassland net ecosystem exchange (NEE) for Canada and the United States. Taiga was excluded from Canada grassland NEE and livestock emissions. For Mexico, the number for “Others” was used because extracting grassland NEE was not possible. Atmospheric inversion models (AIMs) and land-surface models (LSMs) are from Table 2 in Hayes et al. (2012) and do not include CH₄ emissions or human settlement emissions. Thus, the AIM values of NEE for “Others” should be representative of grassland and pastureland NEE. Area estimate for grasslands: www.statista.com/statistics/201761/projection-for-total-us-grassland-area-from-2010.

Table 10.2, p. 403. Carbon fluxes and stocks for grasslands and shrublands in the conterminous United States summarized from the LandCarbon project (landcarbon.org/categories). Values are averages of the A1B, A2, and B1 climate scenarios and estimated using the FOREcasting SCEnarios of land-use change (FORE-SCE) model and the Erosion-Deposition-Carbon-Model (EDCM), CENTURY, and PBN carbon models (Liu et al., 2012b, 2014; Zhu et al., 2011). Climate projections based on emissions scenarios used by the LandCarbon Project are considered to be similar to representative concentration pathway (RCP) scenarios (Knutti and Sedláček 2013). Negative fluxes indicate carbon losses from the ecosystem; positive fluxes indicate carbon gains by the ecosystem. The total flux is considered to be the net ecosystem carbon balance (NECB). Land-cover classification could be a source of differences. Flux towers mostly measure actual grassland and rangeland, whereas the General Ensemble Biogeochemical Modeling System (GEMS) includes both grassland and shrubland. The conterminous United States has about 1 million km² of grassland and 1.3 million km² of shrubland (from Liu et al. land-cover data). The area difference is notable. Land conversion to and from agriculture and permanent grassland loss to urban land all contribute to the total carbon number.



REFERENCES

- Ahlering, M., J. Fargione, and W. Parton, 2016: Potential carbon dioxide emission reductions from avoided grassland conversion in the northern great plains. *Ecosphere*, **7**(12), doi: 10.1002/ecs2.1625.
- Archer, S. R., T. Boutton, and K. Hibbard, 2001: Trees in grasslands: Biogeochemical consequences of woody plant expansion. In: *Global Biogeochemical Cycles in the Climate System*, [E. D. Schulze (ed.)]. Academic Press, pp. 115-138.
- Bachelet, D., K. Ferschweiler, T. Sheehan, B. Baker, B. Sleeter, and Z. Zhu, 2017: Human footprint affects U.S. carbon balance more than climate change. *Reference Module in Earth Systems and Environmental Sciences*, doi: 10.1016/B978-0-12-409548-9.09770-0.
- Barger, N. N., S. R. Archer, J. L. Campbell, C. Y. Huang, J. A. Morton, and A. K. Knapp, 2011: Woody plant proliferation in North American drylands: A synthesis of impacts on ecosystem carbon balance. *Journal of Geophysical Research: Biogeosciences*, **116**, 17, doi: 10.1029/2010jg001506.
- Biederman, J. A., R. L. Scott, M. L. Goulden, R. Vargas, M. E. Litvak, T. E. Kolb, E. A. Yopez, W. C. Oechel, P. D. Blanken, T. W. Bell, J. Garatuza-Payan, G. E. Maurer, S. Dore, and S. P. Burns, 2016: Terrestrial carbon balance in a drier world: The effects of water availability in southwestern North America. *Global Change Biology*, **22**(5), 1867-1879, doi: 10.1111/gcb.13222.
- Blumenthal, D. M., J. A. Kray, W. Ortmans, L. H. Ziska, and E. Pendall, 2016: Cheatgrass is favored by warming but not CO₂ enrichment in a semi-arid grassland. *Global Change Biology*, **22**(9), 3026-3038, doi: 10.1111/gcb.13278.
- Burke, I. C., C. M. Yonker, W. J. Parton, C. V. Cole, D. S. Schimel, and K. Flach, 1989: Texture, climate, and cultivation effects on soil organic matter content in U.S. grassland soils. *Soil Science Society of America Journal*, **53**(3), 800, doi: 10.2136/sssaj1989.03615995005300030029x.
- Carney, K. M., B. A. Hungate, B. G. Drake, and J. P. Megonigal, 2007: Altered soil microbial community at elevated CO₂ leads to loss of soil carbon. *Proceedings of the National Academy of Sciences USA*, **104**(12), 4990-4995, doi: 10.1073/pnas.0610045104.
- Chambers, A., R. Lal, and K. Paustian, 2016: Soil carbon sequestration potential of U.S. croplands and grasslands: Implementing the 4 per thousand initiative. *Journal of Soil and Water Conservation*, **71**(3), 68A-74A, doi: 10.2489/jswc.71.3.68A.
- Chapin, F. S., G. M. Woodwell, J. T. Randerson, E. B. Rastetter, G. M. Lovett, D. D. Baldocchi, D. A. Clark, M. E. Harmon, D. S. Schimel, R. Valentini, C. Wirth, J. D. Aber, J. J. Cole, M. L. Goulden, J. W. Harden, M. Heimann, R. W. Howarth, P. A. Matson, A. D. McGuire, J. M. Melillo, H. A. Mooney, J. C. Neff, R. A. Houghton, M. L. Pace, M. G. Ryan, S. W. Running, O. E. Sala, W. H. Schlesinger, and E. D. Schulze, 2006: Reconciling carbon-cycle concepts, terminology, and methods. *Ecosystems*, **9**(7), 1041-1050, doi: 10.1007/s10021-005-0105-7.
- Cherwin, K., and A. Knapp, 2012: Unexpected patterns of sensitivity to drought in three semi-arid grasslands. *Oecologia*, **169**(3), 845-852, doi: 10.1007/s00442-011-2235-2.
- Conant, R. T., and K. Paustian, 2004: Grassland management activity data: Current sources and future needs. *Environmental Management*, **33**(4), 467-473, doi: 10.1007/s00267-003-9104-7.
- Conant, R. T., K. Paustian, and E. T. Elliott, 2001: Grassland management and conversion into grassland: Effects on soil carbon. *Ecological Applications*, **11**(2), 343-355, doi: 10.1890/1051-0761(2001)011[0343:Gmacy]2.0.Co;2.
- Conant, R. T., C. E. Cerri, B. B. Osborne, and K. Paustian, 2017: Grassland management impacts on soil carbon stocks: A new synthesis. *Ecological Applications*, **27**(2), 662-668, doi: 10.1002/eap.1473.
- Crowther, T. W., K. E. Todd-Brown, C. W. Rowe, W. R. Wieder, J. C. Carey, M. B. Machmuller, B. L. Snoek, S. Fang, G. Zhou, S. D. Allison, J. M. Blair, S. D. Bridgman, A. J. Burton, Y. Carrillo, P. B. Reich, J. S. Clark, A. T. Classen, F. A. Dijkstra, B. Elberling, B. A. Emmett, M. Estiarte, S. D. Frey, J. Guo, J. Harte, L. Jiang, B. R. Johnson, G. Kroel-Dulay, K. S. Larsen, H. Laudon, J. M. Lavallee, Y. Luo, M. Lupascu, L. N. Ma, S. Marhan, A. Michelsen, J. Mohan, S. Niu, E. Pendall, J. Penuelas, L. Pfeifer-Meister, C. Poll, S. Reinsch, L. L. Reynolds, I. K. Schmidt, S. Sistla, N. W. Sokol, P. H. Templer, K. K. Treseder, J. M. Welker, and M. A. Bradford, 2016: Quantifying global soil carbon losses in response to warming. *Nature*, **540**(7631), 104-108, doi: 10.1038/nature20150.
- Davidson, E. A., and I. A. Janssens, 2006: Temperature sensitivity of soil carbon decomposition and feedbacks to climate change. *Nature*, **440**(7081), 165-173, doi: 10.1038/nature04514.
- Dieleman, W. I., S. Vicca, F. A. Dijkstra, F. Hagedorn, M. J. Hoven, K. S. Larsen, J. A. Morgan, A. Volder, C. Beier, J. S. Dukes, J. King, S. Leuzinger, S. Linder, Y. Luo, R. Oren, P. De Angelis, D. Tingey, M. R. Hoosbeek, and I. A. Janssens, 2012: Simple additive effects are rare: A quantitative review of plant biomass and soil process responses to combined manipulations of CO₂ and temperature. *Global Change Biology*, **18**(9), 2681-2693, doi: 10.1111/j.1365-2486.2012.02745.x.
- Eagle, A. J., and L. P. Olander, 2012: Greenhouse gas mitigation with agricultural land management activities in the United States—a side-by-side comparison of biophysical potential. *Advances in Agronomy*, **115**, 79-179, doi: 10.1016/b978-0-12-394276-0.00003-2.
- Fischer, E. M., and R. Knutti, 2014: Detection of spatially aggregated changes in temperature and precipitation extremes. *Geophysical Research Letters*, **41**(2), 547-554, doi: 10.1002/2013gl058499.
- Flanagan, L. B., and A. C. Adkinson, 2011: Interacting controls on productivity in a northern Great Plains grassland and implications for response to ENSO events. *Global Change Biology*, **17**(11), 3293-3311, doi: 10.1111/j.1365-2486.2011.02461.x.



- Follett, R. F., J. M. Kimble, and R. Lal, 2001: *The Potential of U.S. Grazing Lands to Sequester Soil Carbon*. [R. F. Follett, J. M. Kimble, and R. Lal (eds.)]. CRC Press, 401-430 pp.
- Frank, A. B., 2004: Six years of CO₂ flux measurements for a moderately grazed mixed-grass prairie. *Environmental Management*, **33**, S426-S431, doi: 10.1007/s00267-003-9150-1.
- Goldstein, L. J., and K. N. Suding, 2014: Intra-annual rainfall regime shifts competitive interactions between coastal sage scrub and invasive grasses. *Ecology*, **95**(2), 425-435, doi: 10.1890/12-0651.1.
- Gomez-Casanovas, N., T. W. Hudiburg, C. J. Bernacchi, W. J. Parton, and E. H. Delucia, 2016: Nitrogen deposition and greenhouse gas emissions from grasslands: Uncertainties and future directions. *Global Change Biology*, **22**, 1348-1360, doi: 10.1111/gcb.13187.
- H.R. 6 — 110th Congress, 2007: *Energy Independence and Security Act of 2007*. [<https://www.congress.gov/bill/110th-congress/house-bill/6>]
- Hawbaker, T. J., 2017: Mapping burned areas using dense time-series of Landsat data. *Remote Sensing of Environment*, **198**, 504-522, doi:10.1016/j.rse.2017.06.027.
- Hayes, D. J., D. P. Turner, G. Stinson, A. D. McGuire, Y. X. Wei, T. O. West, L. S. Heath, B. Dejong, B. G. McConkey, R. A. Birdsey, W. A. Kurz, A. R. Jacobson, D. N. Huntzinger, Y. D. Pan, W. Mac Post, and R. B. Cook, 2012: Reconciling estimates of the contemporary North American carbon balance among terrestrial biosphere models, atmospheric inversions, and a new approach for estimating net ecosystem exchange from inventory-based data. *Global Change Biology*, **18**(4), 1282-1299, doi: 10.1111/j.1365-2486.2011.02627.x.
- Heimann, M., and M. Reichstein, 2008: Terrestrial ecosystem carbon dynamics and climate feedbacks. *Nature*, **451**(7176), 289-292, doi: 10.1038/nature06591.
- Heisler-White, J. L., A. K. Knapp, and E. F. Kelly, 2008: Increasing precipitation event size increases aboveground net primary production in a semi-arid grassland. *Oecologia*, **158**, 129-140.
- Heisler-White, J. L., J. M. Blair, E. F. Kelly, K. Harmoney, and A. K. Knapp, 2009: Contingent productivity responses to more extreme rainfall regimes across a grassland biome. *Global Change Biology*, **15**(12), 2894-2904, doi: 10.1111/j.1365-2486.2009.01961.x.
- Henderson, B. B., P. J. Gerber, T. E. Hilinski, A. Falcucci, D. S. Ojima, M. Salvatore, and R. T. Conant, 2015: Greenhouse gas mitigation potential of the world's grazing lands: Modeling soil carbon and nitrogen fluxes of mitigation practices. *Agriculture, Ecosystems and Environment*, **207**, 91-100, doi: 10.1016/j.agee.2015.03.029.
- Homer, C., C. Q. Huang, L. M. Yang, B. Wylie, and M. Coan, 2004: Development of a 2001 national land-cover database for the United States. *Photogrammetric Engineering and Remote Sensing*, **70**(7), 829-840.
- Houghton, R. A., J. L. Hackler, and K. T. Lawrence, 1999: The U.S. carbon budget: Contributions from land-use change. *Science*, **285**(5427), 574-578, doi: 10.1126/science.285.5427.574.
- Hufkens, K., T. F. Keenan, L. B. Flanagan, R. L. Scott, C. J. Bernacchi, E. Joo, N. A. Brunsell, J. Verfaillie, and A. D. Richardson, 2016: Productivity of North American grasslands is increased under future climate scenarios despite rising aridity. *Nature Climate Change*, **6**(7), 710-714, doi: 10.1038/nclimate2942.
- Hui, D., and R. B. Jackson, 2006: Geographical and interannual variability in biomass partitioning in grassland ecosystems: A synthesis of field data. *New Phytologist*, **169**(1), 85-93, doi: 10.1111/j.1469-8137.2005.01569.x.
- Huxman, T. E., M. D. Smith, P. A. Fay, A. K. Knapp, M. R. Shaw, M. E. Loik, S. D. Smith, D. T. Tissue, J. C. Zak, J. F. Weltzin, W. T. Pockman, O. E. Sala, B. M. Haddad, J. Harte, G. W. Koch, S. Schwinning, E. E. Small, and D. G. Williams, 2004: Convergence across biomes to a common rain-use efficiency. *Nature*, **429**(6992), 651-654, doi: 10.1038/nature02561.
- Ingram, L. J., P. D. Stahl, G. E. Schuman, J. S. Buyer, G. F. Vance, G. K. Ganjegunte, J. M. Welker, and J. D. Derner, 2008: Grazing impacts on soil carbon and microbial communities in a mixed-grass ecosystem. *Soil Science Society of America Journal*, **72**(4), 939-948, doi: 10.2136/sssaj2007.0038.
- IPCC, 2000: *IPCC Special Report: Emissions Scenarios. Summary for Policymakers*. Intergovernmental Panel on Climate Change. [<https://www.ipcc.ch/pdf/special-reports/spm/sres-en.pdf>]
- IPCC, 2013: *Climate Change 2013: The Physical Science Basis. Contribution of Working Group I to the Fifth Assessment Report of the Intergovernmental Panel on Climate Change*. [T. F. Stocker, D. Qin, G. K. Plattner, M. Tignor, S. K. Allen, J. Boschung, A. Nauels, Y. Xia, V. Bex and P. M. Midgley (eds.)]. Cambridge University Press, Cambridge, UK, and New York, NY, USA, 1535 pp.
- Jackson, R. B., J. L. Banner, E. G. Jobbagy, W. T. Pockman, and D. H. Wall, 2002: Ecosystem carbon loss with woody plant invasion of grasslands. *Nature*, **418**(6898), 623-626, doi: 10.1038/nature00910.
- Jackson, R. B., J. Canadell, J. R. Ehleringer, H. A. Mooney, O. E. Sala, and E. D. Schulze, 1996: A global analysis of root distributions for terrestrial biomes. *Oecologia*, **108**(3), 389-411, doi: 10.1007/Bf00333714.
- Jobbagy, E. G., and R. B. Jackson, 2000: The vertical distribution of soil organic carbon and its relation to climate and vegetation. *Ecological Applications*, **10**(2), 423-436, doi: 10.2307/2641104.
- Jones, R., J. C. Chambers, D. W. Johnson, R. R. Blank, and D. I. Board, 2015: Effect of repeated burning on plant and soil carbon and nitrogen in cheatgrass (*Bromus tectorum*) dominated ecosystems. *Plant and Soil*, **386**(1-2), 47-64, doi: 10.1007/s11104-014-2242-2.



- Kim, H., S. Kim, and B. E. Dale, 2009: Biofuels, land use change, and greenhouse gas emissions: Some unexplored variables. *Environmental Science and Technology*, **43**(3), 961-967, doi: 10.1021/es802681k.
- Klump, K., S. Fontaine, E. Attard, X. Le Roux, G. Gleixner, and J. F. Soussana, 2009: Grazing triggers soil carbon loss by altering plant roots and their control on soil microbial community. *Journal of Ecology*, **97**(5), 876-885, doi: 10.1111/j.1365-2745.2009.01549.x.
- Knapp, A. K., and M. D. Smith, 2001: Variation among biomes in temporal dynamics of aboveground primary production. *Science*, **291**(5503), 481-484, doi: 10.1126/science.291.5503.481.
- Knapp, A. K., J. M. Briggs, and J. K. Koelliker, 2001: Frequency and extent of water limitation to primary production in a mesic temperate grassland. *Ecosystems*, **4**(1), 19-28, doi: 10.1007/s100210000057.
- Knapp, A. K., C. J. Carroll, E. M. Denton, K. J. La Pierre, S. L. Collins, and M. D. Smith, 2015: Differential sensitivity to regional-scale drought in six central U.S. grasslands. *Oecologia*, **177**(4), 949-957, doi: 10.1007/s00442-015-3233-6.
- Knapp, A. K., J. M. Briggs, S. L. Collins, S. R. Archer, M. S. Bret-Harte, B. E. Ewers, D. P. Peters, D. R. Young, G. R. Shaver, E. Pendall, and M. B. Cleary, 2008a: Shrub encroachment in North American grasslands: Shifts in growth form dominance rapidly alters control of ecosystem carbon inputs. *Global Change Biology*, **14**(3), 615-623, doi: 10.1111/j.1365-2486.2007.01512.x.
- Knapp, A. K., C. Beier, D. D. Briske, A. T. Classen, Y. Luo, M. Reichstein, M. D. Smith, S. D. Smith, J. E. Bell, P. A. Fay, J. L. Heisler, S. W. Leavitt, R. Sherry, B. Smith, and E. Weng, 2008b: Consequences of more extreme precipitation regimes for terrestrial ecosystems. *BioScience*, **58**(9), 811-821, doi: 10.1641/b580908.
- Knutti, R., and J. Sedláček, 2013: Robustness and uncertainties in the new CMIP5 climate model projections. *Nature Climate Change*, **3**, 369-373.
- Kulmatiski, A., and K. H. Beard, 2013: Woody plant encroachment facilitated by increased precipitation intensity. *Nature Climate Change*, **3**(9), 833-837, doi: 10.1038/Nclimate1904.
- Liu, S., N. Bliss, E. T. Sundquist, and T. G. Huntington, 2003: Modeling carbon dynamics in vegetation and soil under the impact of soil erosion and deposition. *Global Biogeochemical Cycles*, **17**, doi: 10.1029/2002GB002010.
- Liu, S., Y. Wu, C. Young, D. Dahal, J. L. Werner, and J. Liu, 2012a: Projected Future Carbon Storage and Greenhouse-Gas Fluxes of Terrestrial Ecosystems in the Western United States. U.S. Geological Survey.
- Liu, S., J. Liu, Y. Wu, C. J. Young, J. M. Werner, D. Dahal, J. Oeding, and G. L. Schmidt, 2014: Baseline and projected future carbon storage, carbon sequestration, and greenhouse-gas fluxes in terrestrial ecosystems of the Eastern United States. In: *Baseline and Projected Future Carbon Storage and Greenhouse Gas Fluxes in Ecosystems of the Eastern United States*, U.S. Geological Survey Professional Paper 1804. [Z. Zhu and B. C. Reed (eds.)]. pp. 115-156.
- Liu, S., J. Liu, C. Young, J. Werner, Y. Wu, Z. Li, D. Dahal, J. Oeding, G. Schmidt, T. Sohl, T. Hawbaker, and B. Sleeter, 2011: *Baseline and Projected Future Carbon Storage and Greenhouse-Gas Fluxes in Ecosystems of the Western United States*, U.S. Geological Survey Professional Paper 1797. [Z. Zhu and B. Reed (eds.)]. U.S. Geological Survey, 20 pp. [https://pubs.usgs.gov/pp/1797/]
- Liu, S., J. Liu, C. Young, J. Werner, Y. Wu, Z. Li, D. Dahal, J. Oeding, G. Schmidt, T. Sohl, T. Hawbaker, and B. Sleeter, 2012b: Baseline carbon storage, carbon sequestration, and greenhouse gas fluxes in terrestrial ecosystems of the western United States. In: *Baseline and Projected Future Carbon Storage and Greenhouse-Gas Fluxes in Ecosystems of the Western United States*, U.S. Geological Survey Professional Paper 1797. [Z. Zhu and B. Reed (eds.)]. US Geological Survey, 20p. pp.
- Lu, M., X. H. Zhou, Q. Yang, H. Li, Y. Q. Luo, C. M. Fang, J. K. Chen, X. Yang, and B. Li, 2013: Responses of ecosystem carbon cycle to experimental warming: A meta-analysis. *Ecology*, **94**(3), 726-738.
- Luo, Y., 2007: Terrestrial carbon-cycle feedback to climate warming. *Annual Review of Ecology, Evolution and Systematics*, **38**, 683-712.
- Luo, Y., D. Hui, and D. Zhang, 2006: Elevated CO₂ stimulates net accumulations of carbon and nitrogen in land ecosystems: A meta-analysis. *Ecology*, **87**(1), 53-63, doi: 10.1890/04-1724.
- Luo, Y., D. Gerten, G. Le Maire, W. J. Parton, E. Weng, X. Zhou, C. Keough, C. Beier, P. Ciais, W. Cramer, J. S. Dukes, B. Emmett, P. J. Hanson, A. Knapp, S. Linder, D. Nepstad, and L. Rustad, 2008: Modeled interactive effects of precipitation, temperature, and CO₂ on ecosystem carbon and water dynamics in different climatic zones. *Global Change Biology*, **14**(9), 1986-1999, doi: 10.1111/j.1365-2486.2008.01629.x.
- Luo, Y., J. Melillo, S. L. Niu, C. Beier, J. S. Clark, A. T. Classen, E. Davidson, J. S. Dukes, R. D. Evans, C. B. Field, C. I. Czimczik, M. Keller, B. A. Kimball, L. M. Kueppers, R. J. Norby, S. L. Pelini, E. Pendall, E. Rastetter, J. Six, M. Smith, M. G. Tjoelker, and M. S. Torn, 2011: Coordinated approaches to quantify long-term ecosystem dynamics in response to global change. *Global Change Biology*, **17**(2), 843-854, doi: 10.1111/j.1365-2486.2010.02265.x.
- Machmuller, M. B., M. G. Kramer, T. K. Cyle, N. Hill, D. Hancock, and A. Thompson, 2015: Emerging land use practices rapidly increase soil organic matter. *Nature Communications*, **6**, 6995, doi: 10.1038/ncomms7995.
- McClaran, M. P., 1997: Desert grasslands and grasses. In: *The Desert Grassland*. [M. P. McClaran and T. R. V. Devender (eds.)]. University of Arizona Press.
- McClaran, M. P., D. M. Browning, and C. Huang, 2010: Temporal dynamics and spatial variability in desert grassland vegetation. In: *Repeat Photography: Methods and Applications in the Natural Sciences*. [R. H. Webb, D. E. Boyer, and R. M. Turner (eds.)]. Island Press.



- McKinley, D. C., and J. M. Blair, 2008: Woody plant encroachment by *Juniperus virginiana* in a mesic native grassland promotes rapid carbon and nitrogen accrual. *Ecosystems*, **11**(3), 454-468, doi: 10.1007/s10021-008-9133-4.
- McSherry, M. E., and M. E. Ritchie, 2013: Effects of grazing on grassland soil carbon: A global review. *Global Change Biology*, **19**, 1347-1357, doi: 10.1111/gcb.12144.
- Medlyn, B. E., S. Zaehle, M. G. De Kauwe, A. P. Walker, M. C. Dietze, P. J. Hanson, T. Hickler, A. K. Jain, Y. Q. Luo, W. Parton, I. C. Prentice, P. E. Thornton, S. S. Wang, Y. P. Wang, E. S. Weng, C. M. Iversen, H. R. McCarthy, J. M. Warren, R. Oren, and R. J. Norby, 2015: Using ecosystem experiments to improve vegetation models. *Nature Climate Change*, **5**(6), 528-534, doi: 10.1038/nclimate2621.
- Milchunas, D. G., O. E. Sala, and W. K. Lauenroth, 1988: A generalized model of the effects of grazing by large herbivores on grassland community structure. *The American Naturalist*, **132**, 87-106.
- Min, S. K., X. Zhang, F. W. Zwiers, and G. C. Hegerl, 2011: Human contribution to more-intense precipitation extremes. *Nature*, **470**(7334), 378-381, doi: 10.1038/nature09763.
- Moran, M. S., G. E. Ponce-Campos, A. Huete, M. P. McClaran, Y. Zhang, E. P. Hamerlynck, D. J. Augustine, S. A. Gunter, S. G. Kitchen, D. P. Peters, P. J. Starks, and M. Hernandez, 2014: Functional response of U.S. grasslands to the early 21st-century drought. *Ecology*, **95**, 2121-2133.
- Morgan, J. A., W. Parton, J. D. Derner, T. G. Gilmanov, and D. P. Smith, 2016: Importance of early season conditions and grazing on carbon dioxide fluxes in Colorado shortgrass steppe. *Rangeland Ecology and Management*, **69**(5), 342-350, doi: 10.1016/j.rama.2016.05.002.
- Morgan, J. A., D. R. LeCain, E. Pendall, D. M. Blumenthal, B. A. Kimball, Y. Carrillo, D. G. Williams, J. Heisler-White, F. A. Dijkstra, and M. West, 2011: C₄ grasses prosper as carbon dioxide eliminates desiccation in warmed semi-arid grassland. *Nature*, **476**(7359), 202-205, doi: 10.1038/nature10274.
- Mueller, K. E., D. M. Blumenthal, E. Pendall, Y. Carrillo, F. A. Dijkstra, D. G. Williams, R. F. Follett, and J. A. Morgan, 2016: Impacts of warming and elevated CO₂ on a semi-arid grassland are non-additive, shift with precipitation, and reverse over time. *Ecology Letters*, **19**(8), 956-966, doi: 10.1111/ele.12634.
- Nie, M., and E. Pendall, 2016: Do rhizosphere priming effects enhance plant nitrogen uptake under elevated CO₂? *Agriculture, Ecosystems and Environment*, **224**, 50-55, doi: 10.1016/j.agee.2016.03.032.
- Norby, R. J., and Y. Q. Luo, 2004: Evaluating ecosystem responses to rising atmospheric CO₂ and global warming in a multi-factor world. *New Phytologist*, **162**, 281-293, doi: 10.1111/j.1469-8137.2004.01047.x.
- Norton, U., A. R. Mosier, J. A. Morgan, J. D. Derner, L. J. Ingram, and P. D. Stahl, 2008: Moisture pulses, trace gas emissions and soil C and N in cheatgrass and native grass-dominated sagebrush-steppe in Wyoming, USA. *Soil Biology and Biochemistry*, **40**(6), 1421-1431, doi: 10.1016/j.soilbio.2007.12.021.
- Omernik, J., 1987: Map supplements: Ecoregions of the conterminous United States. *Annals of the Association of American Geographers*, **77**, 118-125.
- Owensby, C. E., J. M. Ham, and L. M. Auen, 2006: Fluxes of CO₂ from grazed and ungrazed tallgrass prairie. *Rangeland Ecology and Management*, **59**(2), 111-127, doi: 10.2111/05-116r2.1.
- Pacala, S., R. A. Birdsey, S. D. Bridgman, R. T. Conant, K. Davis, B. Hales, R. A. Houghton, J. C. Jenkins, M. Johnston, G. Marland, and K. Paustian, 2007: The North American carbon budget past and present. In: *First State of the Carbon Cycle Report (SOCCR): The North American Carbon Budget and Implications for the Global Carbon Cycle. A Report by the U.S. Climate Change Science Program and the Subcommittee on Global Change Research*. [A. King, W. L. Dilling, G. P. Zimmerman, D. M. Fairman, R. A. Houghton, G. Marland, A. Z. Rose, and T. J. Wilbanks (eds.)]. National Oceanic and Atmospheric Administration, National Climatic Data Center, Asheville, NC, USA, 29-36 pp.
- Parton, W. J., D. S. Schimel, C. V. Cole, and D. S. Ojima, 1987: Analysis of factors controlling soil organic matter levels in great plains grasslands. *Soil Science Society of America Journal*, **51**, 1173-1179.
- Parton, W. J., J. A. Morgan, G. Wang, and S. Del Grosso, 2007: Projected ecosystem impact of the prairie heating and CO₂ enrichment experiment. *New Phytologist*, **174**(4), 823-834, doi: 10.1111/j.1469-8137.2007.02052.x.
- Pendall, E., J. L. Heisler-White, D. G. Williams, F. A. Dijkstra, Y. Carrillo, J. A. Morgan, and D. R. LeCain, 2013: Warming reduces carbon losses from grassland exposed to elevated atmospheric carbon dioxide. *PLOS One*, **8**(8), e71921, doi: 10.1371/journal.pone.0071921.
- Pendall, E., S. Del Grosso, J. Y. King, D. R. LeCain, D. G. Milchunas, J. A. Morgan, A. R. Mosier, D. S. Ojima, W. A. Parton, P. P. Tans, and J. W. C. White, 2003: Elevated atmospheric CO₂ effects and soil water feedbacks on soil respiration components in a Colorado grassland. *Global Biogeochemical Cycles*, **17**(2), doi: 10.1029/2001gb001821.
- Peters, D. P., J. Yao, O. E. Sala, and J. P. Anderson, 2012: Directional climate change and potential reversal of desertification in arid and semiarid ecosystems. *Global Change Biology*, **18**, 151-163.
- Petrie, M. D., S. L. Collins, A. M. Swann, P. L. Ford, and M. E. Litvak, 2015: Grassland to shrubland state transitions enhance carbon sequestration in the northern Chihuahuan Desert. *Global Change Biology*, **21**(3), 1226-1235, doi: 10.1111/gcb.12743.



- Polley, H. W., A. B. Frank, J. Sanabria, and R. L. Phillips, 2008: Interannual variability in carbon dioxide fluxes and flux-climate relationships on grazed and ungrazed northern mixed-grass prairie. *Global Change Biology*, **14**(7), 1620-1632, doi: 10.1111/j.1365-2486.2008.01599.x.
- Polley, H. W., D. D. Briske, J. A. Morgan, K. Wolter, D. W. Bailey, and J. R. Brown, 2013: Climate change and North American rangelands: Trends, projections, and implications. *Rangeland Ecology and Management*, **66**(5), 493-511, doi: 10.2111/Rem-D-12-00068.1.
- Potter, K. N., and J. D. Derner, 2006: Soil carbon pools in central Texas: Prairies, restored grasslands, and croplands. *Journal of Soil and Water Conservation*, **61**(3), 124-128.
- Prater, M. R., D. Obrist, J. A. Arnone, and E. H. DeLucia, 2006: Net carbon exchange and evapotranspiration in postfire and intact sagebrush communities in the Great Basin. *Oecologia*, **146**, 595-607, doi: 10.1007/s00442-005-0231-0.
- Quiroga, R. E., R. A. Golluscio, L. J. Blanco, and R. J. Fernandez, 2010: Aridity and grazing as convergent selective forces: An experiment with an Arid Chaco bunchgrass. *Ecological Applications*, **20**, 1876-1889.
- Raczka, B. M., K. J. Davis, D. Huntzinger, R. P. Neilson, B. Poulter, A. D. Richardson, J. F. Xiao, I. Baker, P. Ciais, T. F. Keenan, B. Law, W. M. Post, D. Ricciuto, K. Schaefer, H. Q. Tian, E. Tomelleri, H. Verbeeck, and N. Viovy, 2013: Evaluation of continental carbon cycle simulations with North American flux tower observations. *Ecological Monographs*, **83**(4), 531-556, doi: 10.1890/12-0893.1.
- Reeves, M. C., and J. Mitchell, 2012: *A Synoptic View of U.S. Rangelands: A Technical Document Supporting the Forest Service 2010 RPA Assessment*. U.S. Forest Service General Technical Report RMRS-GTR-288, 128 pp. [http://www.fs.fed.us/rm/pubs/rmrs_gtr288.pdf]
- Reeves, M. C., A. L. Moreno, K. E. Bagne, and S. W. Running, 2014: Estimating climate change effects on net primary production of rangelands in the United States. *Climatic Change*, **126**(3-4), 429-442, doi: 10.1007/s10584-014-1235-8.
- Reich, P. B., and S. E. Hobbie, 2013: Decade-long soil nitrogen constraint on the CO₂ fertilization of plant biomass. *Nature Climate Change*, **3**(3), 278-282, doi: 10.1038/Nclimate1694.
- Reyes-Fox, M., H. Steltzer, M. J. Trlica, G. S. McMaster, A. A. Andales, D. R. LeCain, and J. A. Morgan, 2014: Elevated CO₂ further lengthens growing season under warming conditions. *Nature*, **510**(7504), 259-262, doi: 10.1038/nature13207.
- Risch, A. C., and D. A. Frank, 2006: Carbon dioxide fluxes in a spatially and temporally heterogeneous temperate grassland. *Oecologia*, **147**(2), 291-302, doi: 10.1007/s00442-005-0261-7.
- Ryan, E. M., K. Ogle, D. Peltier, A. P. Walker, M. G. De Kauwe, B. E. Medlyn, D. G. Williams, W. Parton, S. Asao, B. Guenet, A. Harper, X. Lu, K. A. Luus, S. Zaehle, S. Shu, C. Werner, J. Xia, and E. Pendall, 2016: Gross primary production responses to warming, elevated CO₂, and irrigation: Quantifying the drivers of ecosystem physiology in a semiarid grassland. *Global Change Biology*, doi: 10.1111/gcb.13602.
- Sanderman, J., and R. Amundson, 2008: A comparative study of dissolved organic carbon transport and stabilization in California forest and grassland soils. *Biogeochemistry*, **89**(3), 309-327, doi: 10.1007/s10533-008-9221-8.
- Scott, R. L., J. A. Biederman, E. P. Hamerlynck, and G. A. Barron-Gafford, 2015: The carbon balance pivot point of southwestern U.S. semiarid ecosystems: Insights from the 21st century drought. *Journal of Geophysical Research: Biogeosciences*, **120**(12), 2612-2624, doi: 10.1002/2015jg003181.
- Shi, Z., X. Xu, O. Hararuk, L. F. Jiang, J. Y. Xia, J. Y. Liang, D. J. Li, and Y. Q. Luo, 2015: Experimental warming altered rates of carbon processes, allocation, and carbon storage in a tallgrass prairie. *Ecosphere*, **6**(11), doi: 10.1890/Es14-00335.1.
- Silver, W. L., R. Ryals, and V. Eviner, 2010: Soil carbon pools in California's annual grassland ecosystems. *Rangeland Ecology and Management*, **63**(1), 128-136, doi: 10.2111/Rem-D-09-00106.1.
- Sims, P. L., and P. G. Risser, 2000: Grasslands. In: *North American Terrestrial Vegetation*. [M. G. Barbour and Billings (eds.)]. Cambridge University Press, pp. 323-356.
- Sleeter, B. M., T. L. Sohl, M. A. Bouchard, R. R. Reker, C. E. Soulard, W. Acevedo, G. E. Griffith, R. R. Sleeter, R. F. Auch, K. L. Saylor, S. Prislely, and Z. L. Zhu, 2012: Scenarios of land use and land cover change in the conterminous United States: Utilizing the special report on emission scenarios at ecoregional scales. *Global Environmental Change-Human and Policy Dimensions*, **22**(4), 896-914, doi: 10.1016/j.gloenvcha.2012.03.008.
- Smith, P., C. M. Fang, J. J. C. Dawson, and J. B. Moncrieff, 2008: Impact of global warming on soil organic carbon. *Advances in Agronomy*, **97**, 1-43, doi: 10.1016/S0065-2113(07)00001-6.
- Sohl, T. L., K. L. Saylor, M. A. Drummond, and T. R. Loveland, 2007: The FORE-SCE model: A practical approach for projecting land cover change using scenario-based modeling. *Journal of Land Use Science*, **2**(2), 103-126, doi: 10.1080/17474230701218202.
- Soong, J. L., and M. F. Cotrufo, 2015: Annual burning of a tallgrass prairie inhibits C and N cycling in soil, increasing recalcitrant pyrogenic organic matter storage while reducing N availability. *Global Change Biology*, **21**(6), 2321-2333, doi: 10.1111/gcb.12832.
- Soussana, J.-F., P. Loiseau, N. Vuichard, E. Ceschia, J. Balesdent, T. Chevallier, and D. Arrouays, 2004: Carbon cycling and sequestration opportunities in temperate grasslands. *Soil Use and Management*, **20**, 219-230, doi: 10.1079/SUM2003234.



- Stephenson, K. E., 2011: Distribution of Grasslands in 19th Century Florida. *American Midland Naturalist*, **165**, 50-59, doi: 10.1674/0003-0031-165.1.50.
- Stubbs, M., 2014: *Conservation Reserve Program (CRP): Status and Issues*. Congressional Research Service 7-5700. R42783. [<http://nationalaglawcenter.org/wp-content/uploads/assets/crs/R42783.pdf>]
- Svejar, T., R. Angell, J. A. Bradford, W. Dugas, W. Emmerich, A. B. Frank, T. Gilmanov, M. Haferkamp, D. A. Johnson, H. Mayeux, P. Mielnick, J. Morgan, N. Z. Saliendra, G. E. Schuman, P. L. Sims, and K. Snyder, 2008: Carbon fluxes on North American rangelands. *Rangeland Ecology and Management*, **61**(5), 465-474, doi: 10.2111/07-108.1.
- Teague, W. R., S. L. Dowhower, S. A. Baker, N. Haile, P. B. DeLaune, and D. M. Conover, 2011: Grazing management impacts on vegetation, soil biota and soil chemical, physical and hydrological properties in tall grass prairie. *Agriculture, Ecosystems and Environment*, **141**(3-4), 310-322, doi: 10.1016/j.agee.2011.03.009.
- Thomey, M. L., P. L. Ford, M. C. Reeves, D. M. Finch, M. E. Litvak, and S. L. Collins, 2014: Climate change impacts on future carbon stores and management of warm deserts of the United States. *Rangelands*, **36**(1), 16-24, doi: 10.2111/rangelands-d-13-00045.1.
- Thomey, M. L., S. L. Collins, R. Vargas, J. E. Johnson, R. F. Brown, D. O. Natvig, and M. T. Friggens, 2011: Effect of precipitation variability on net primary production and soil respiration in a chihuahuan desert grassland. *Global Change Biology*, **17**(4), 1505-1515, doi: 10.1111/j.1365-2486.2010.02363.x.
- Todd-Brown, K. E. O., J. T. Randerson, W. M. Post, F. M. Hoffman, C. Tarnocai, E. A. G. Schuur, and S. D. Allison, 2013: Causes of variation in soil carbon simulations from CMIP5 Earth system models and comparison with observations. *Biogeosciences*, **10**(3), 1717-1736, doi: 10.5194/bg-10-1717-2013.
- van Groenigen, K. J., X. Qi, C. W. Osenberg, Y. Luo, and B. A. Hungate, 2014: Faster decomposition under increased atmospheric CO₂ limits soil carbon storage. *Science*, **344**(6183), 508-509, doi: 10.1126/science.1249534.
- Verburg, P. S. J., J. A. Arnone, D. Obrist, D. E. Schorran, R. D. Evans, D. Leroux-Swarthout, D. W. Johnson, Y. Q. Luo, and J. S. Coleman, 2004: Net ecosystem carbon exchange in two experimental grassland ecosystems. *Global Change Biology*, **10**(4), 498-508, doi: 10.1111/j.1529-8817.2003.00744.x.
- Wang, Y. P., J. Jiang, B. Chen-Charpentier, F. B. Augusto, A. Hastings, F. Hoffman, M. Rasmussen, M. J. Smith, K. Todd-Brown, Y. Wang, X. Xu, and Y. Q. Luo, 2015: Responses of two nonlinear microbial models to warming or increased carbon input. *Biogeosciences Discussions*, **12**(17), 14647-14692, doi: 10.5194/bgd-12-14647-2015.
- Wertin, T. M., J. Belnap, and S. C. Reed, 2017: Experimental warming in a dryland community reduced plant photosynthesis and soil CO₂ efflux although the relationship between the fluxes remained unchanged. *Functional Ecology*, **31**(2), 297-305, doi: 10.1111/1365-2435.12708.
- Wertin, T. M., S. C. Reed, and J. Belnap, 2015: C3 and C4 plant responses to increased temperatures and altered monsoonal precipitation in a cool desert on the Colorado Plateau, USA. *Oecologia*, **177**(4), 997-1013, doi: 10.1007/s00442-015-3235-4.
- Wieder, W. R., S. D. Allison, E. A. Davidson, K. Georgiou, O. Hararuk, Y. J. He, F. Hopkins, Y. Q. Luo, M. J. Smith, B. Sulman, K. Todd-Brown, Y. P. Wang, J. Y. Xia, and X. F. Xu, 2015: Explicitly representing soil microbial processes in Earth system models. *Global Biogeochemical Cycles*, **29**(10), 1782-1800, doi: 10.1002/2015gb005188.
- Wylie, B., D. Howard, D. Dahal, T. Gilmanov, L. Ji, L. Zhang, and K. Smith, 2016: Grassland and cropland net ecosystem production of the U.S. Great Plains: Regression tree model development and comparative analysis. *Remote Sensing*, **8**(11), 944, doi: 10.3390/rs8110944.
- Xiao, J. F., S. V. Ollinger, S. Frohling, G. C. Hurtt, D. Y. Hollinger, K. J. Davis, Y. D. Pan, X. Y. Zhang, F. Deng, J. Q. Chen, D. D. Baldocchi, B. E. Law, M. A. Arain, A. R. Desai, A. D. Richardson, G. Sun, B. Amiro, H. Margolis, L. H. Gu, R. L. Scott, P. D. Blanken, and A. E. Suyker, 2014: Data-driven diagnostics of terrestrial carbon dynamics over North America. *Agricultural and Forest Meteorology*, **197**, 142-157, doi: 10.1016/j.agrformet.2014.06.013.
- Zelikova, T. J., D. G. Williams, R. Hoenigman, D. M. Blumenthal, J. A. Morgan, and E. Pendall, 2015: Seasonality of soil moisture mediates responses of ecosystem phenology to elevated CO₂ and warming in a semi-arid grassland. *Journal of Ecology*, **103**(5), 1119-1130, doi: 10.1111/1365-2745.12440.
- Zhang, L., B. K. Wylie, L. Ji, T. G. Gilmanov, L. L. Tieszen, and D. M. Howard, 2011: Upscaling carbon fluxes over the Great Plains grasslands: Sinks and sources. *Journal of Geophysical Research*, **116**(G3), doi: 10.1029/2010jg001504.
- Zhou, X. H., L. Y. Zhou, Y. Y. Nie, Y. L. Fu, Z. G. Du, J. J. Shao, Z. M. Zheng, and X. H. Wang, 2016: Similar responses of soil carbon storage to drought and irrigation in terrestrial ecosystems but with contrasting mechanisms: A meta-analysis. *Agriculture, Ecosystems and Environment*, **228**, 70-81, doi: 10.1016/j.agee.2016.04.030.
- Zhu, Z., and B. Reed, 2012: *Baseline and Projected Future Carbon Storage and Greenhouse-Gas Fluxes in Ecosystems of the Western United States*. U.S. Geological Survey Professional Paper 1797. 192 pp. [<http://pubs.usgs.gov/pp/1797/>]
- Zhu, Z., and B. Reed, 2014: *Baseline and Projected Future Carbon Storage and Greenhouse-Gas Fluxes in Ecosystems of the Eastern United States*. U.S. Geological Survey Professional Paper 1804.
- Zhu, Z., M. Bouchard, D. Butman, T. Hawbaker, Z. Li, J. Liu, S. Liu, C. McDonald, R. Reker, K. Saylor, B. Sleetor, T. Sohl, S. Stackpoole, and A. Wein, 2011: *Baseline and Projected Future Carbon Storage and Greenhouse-Gas Fluxes in the Great Plains Region of the United States*. U.S. Geological Survey Professional Paper 1787, [Z. Zhu (ed.)]. 28 pp.



11 Arctic and Boreal Carbon

Lead Authors

Edward A. G. Schuur, Northern Arizona University; A. David McGuire, U.S. Geological Survey and University of Alaska, Fairbanks; Vladimir Romanovsky, University of Alaska, Fairbanks

Contributing Authors

Christina Schädel, Northern Arizona University; Michelle Mack, Northern Arizona University

Acknowledgments

Sasha C. Reed (Science Lead), U.S. Geological Survey; Marc G. Kramer (Review Editor), Washington State University, Vancouver; Zhiliang Zhu (Federal Liaison), U.S. Geological Survey; Eric Kasischke (former Federal Liaison), NASA; Jared DeForest (former Federal Liaison), DOE Office of Science

Recommended Citation for Chapter

Schuur, E. A. G., A. D. McGuire, V. Romanovsky, C. Schädel, and M. Mack, 2018: Chapter 11: Arctic and boreal carbon. In *Second State of the Carbon Cycle Report (SOCCR2): A Sustained Assessment Report* [Cavallaro, N., G. Shrestha, R. Birdsey, M. A. Mayes, R. G. Najjar, S. C. Reed, P. Romero-Lankao, and Z. Zhu (eds.)]. U.S. Global Change Research Program, Washington, DC, USA, pp. 428-468, <https://doi.org/10.7930/SOCCR2.2018.Ch11>.



KEY FINDINGS

1. Factors that control terrestrial carbon storage are changing. Surface air temperature change is amplified in high-latitude regions, as seen in the Arctic where temperature rise is about 2.5 times faster than that for the whole Earth. Permafrost temperatures have been increasing over the last 40 years. Disturbance by fire (particularly fire frequency and extreme fire years) is higher now than in the middle of the last century (*very high confidence*).
2. Soils in the northern circumpolar permafrost zone store 1,460 to 1,600 petagrams of organic carbon (Pg C), almost twice the amount contained in the atmosphere and about an order of magnitude more carbon than contained in plant biomass (55 Pg C), woody debris (16 Pg C), and litter (29 Pg C) in the boreal and tundra biomes combined. This large permafrost zone soil carbon pool has accumulated over hundreds to thousands of years. There are additional reservoirs in subsea permafrost and regions of deep sediments that are not added to this estimate because of data scarcity (*very high confidence*).
3. Following the current trajectory of global and Arctic warming, 5% to 15% of the soil organic carbon stored in the northern circumpolar permafrost zone (mean 10% value equal to 146 to 160 Pg C) is considered vulnerable to release to the atmosphere by the year 2100. The potential carbon loss is likely to be up to an order of magnitude larger than the potential increase in carbon stored in plant biomass regionally under the same changing conditions (*high confidence, very likely*).
4. Some Earth System Models project that high-latitude carbon releases will be offset largely by increased plant uptake. However, these findings are not always supported by empirical measurements or other assessments, suggesting that structural features of many models are still limited in representing Arctic and boreal zone processes (*very high confidence, very likely*).

Note: Confidence levels are provided as appropriate for quantitative, but not qualitative, Key Findings and statements.

11.1 Introduction

11.1.1 Drivers of Carbon Cycle Change

This assessment focuses on Arctic and boreal carbon pools and fluxes, particularly those included within the northern circumpolar permafrost (perennially frozen ground) zone, which includes tundra and a large fraction of the boreal biome. Current knowledge of the state of organic carbon in soils and vegetation is evaluated herein, along with the potential for these pools to change over time in response to disturbance regimes and changing climate. Changes in temperature and precipitation act as gradual “press” (i.e., continuous) disturbances that directly affect carbon stocks and fluxes by modifying the biological processes of photosynthesis and respiration (LTER 2007). Climate changes also can modify the occurrence and magnitude of biological disturbances such as insect outbreaks as well as abrupt physical disturbances such as fire,

extreme drought, and soil subsidence and erosion resulting from ice-rich permafrost thaw. These “pulse” (i.e., discrete) disturbances often are part of the ongoing successional cycle in Arctic and boreal ecosystems, but changing rates of occurrence alter the landscape distribution of successional ecosystem states, in turn, affecting landscape carbon storage. This overview introduces recent and expected trends in these drivers; their combined impact on carbon pools and fluxes is detailed later in the chapter.

Continuous Press Disturbances: Temperature, Precipitation

The most pronounced change in high-latitude climate during the last 40 to 50 years is the increase in mean annual surface air temperatures (see Figure 11.1, p. 430). Global temperature change is amplified in high-latitude regions, as seen in the Arctic where temperature rise is about 2.5 times faster than that

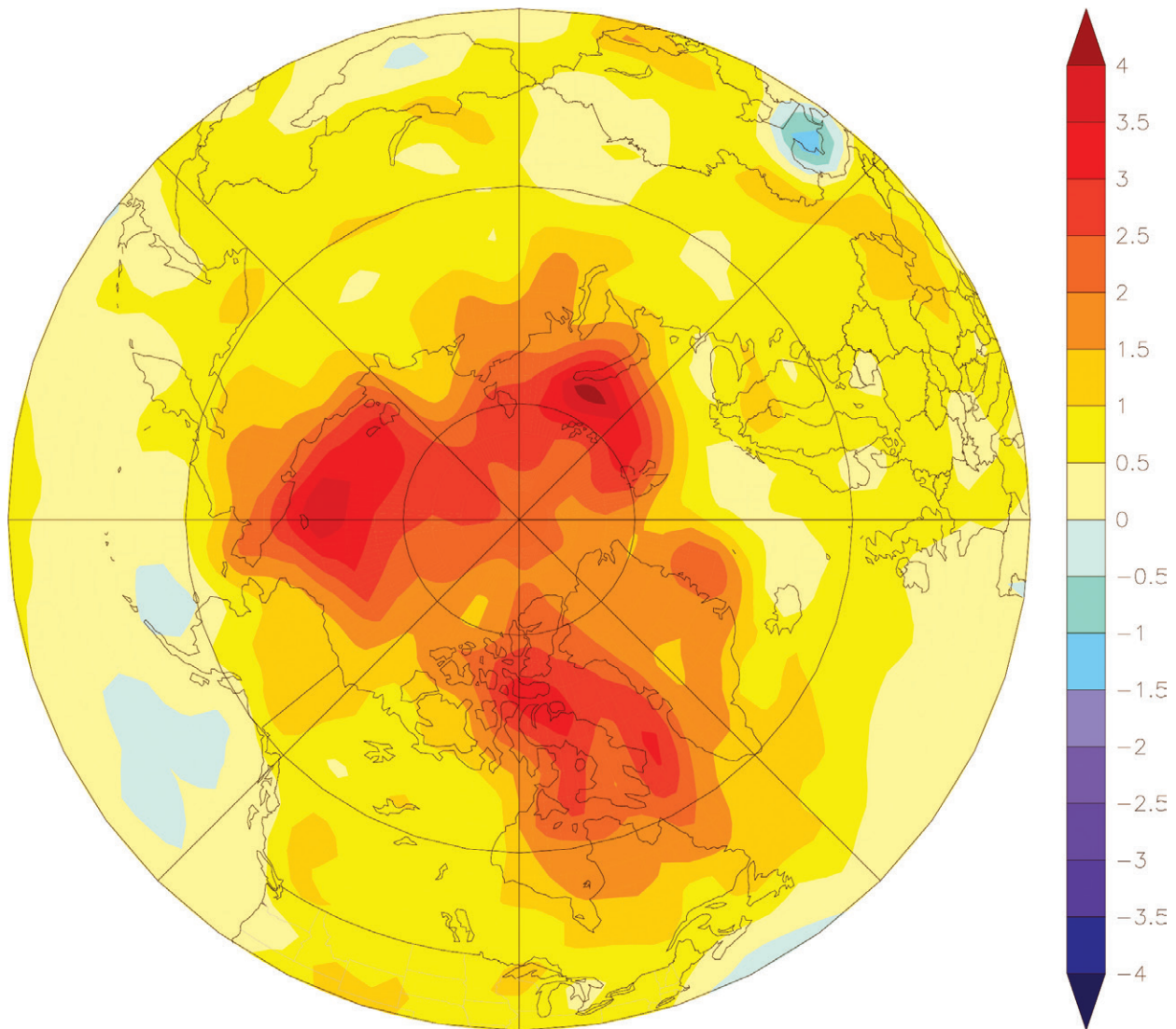


Figure 11.1. Difference in Mean Annual Arctic Surface Air Temperatures (in °C) Between the Period 2001 to 2015 and the Baseline Period 1971 to 2000. Data are from the Goddard Institute for Space Studies Surface Temperature Analysis (GISTEMP) within the National Aeronautics and Space Administration (data.giss.nasa.gov/gistemp). [Figure source: Reprinted from Overland et al., 2014, used with permission under a Creative Commons license (CC-BY-NC-ND 3.0).]

for the whole Earth (IPCC 2013). Air temperature increased in the Arctic by 1 to 2°C over the last 20 to 30 years (Overland et al., 2014). This increase was even more substantial (>3°C) in some regions of the Arctic Ocean and over the central and eastern parts of the Canadian Arctic Archipelago. Warming is most noticeable during the winter, but summer

temperatures also are on the rise, and this differential is expected to continue in the future. The average air temperatures in the cold season (November through April) in Alaska, northern Canada, and in a large portion of Siberia have increased by 2 to 4°C between 1961 and 2014. In contrast, the temperature increase in the warm half of the year (May through October)



was between 1 and 2°C for the same regions and time interval (data.giss.nasa.gov/gistemp/maps).

The degree of projected future warming—dependent on the scenario of changes in greenhouse gas (GHG) emissions through time—ranges widely for different Earth System Models (ESMs). By 2050, the differences in these projections as a result of various Representative Concentration Pathway (RCP) forcing scenarios (e.g., RCP4.5 and RCP8.5) are not large. Averaged across 36 ESMs, the projected mean annual air temperature increases for 60°N to 90°N by 2050 is about 3.7°C compared to the 1981 to 2005 period (2°C increase in the summer and 5.3°C increase in the winter (Overland et al., 2014)). However, projections for 2100 differ significantly for RCP4.5 and RCP8.5. For 2100, the same models project a 4.3°C increase in mean annual temperature for RCP4.5 and an 8.7°C increase for RCP8.5. The summers are predicted to be warmer by 2.3°C for RCP4.5 and by 5.1°C for RCP8.5; winter temperatures are projected to rise by 6 and 12.5°C, respectively. Projected changes in precipitation are less consistent and vary significantly from region to region and over different time intervals. However, most models project increasing precipitation in the Arctic, especially in the winter. The percentage increases are largest in the cold season and, as a result of the RCP8.5 scenario, over the Arctic Ocean (IPCC 2013).

Permafrost is technically defined as subsurface Earth materials (e.g., rock, soil, and ice) remaining <0°C for at least 2 consecutive years. Observed changes in climate triggered a substantial increase in permafrost temperatures during the last 40 years (Romanovsky et al., 2010, 2016; Smith et al., 2010). Based on data from a selection of sites with both long-term records and good geographical coverage, annual mean permafrost temperatures generally have been increasing (Noetzi et al., 2016; Romanovsky et al., 2016; see Figure 11.2, p. 432). The greatest temperature increase is found in colder permafrost (approximately –15 to –2°C) in the Arctic where current permafrost temperatures are more than 2 to 2.5°C higher than they were 30 years ago. In areas with warmer permafrost (approximately –2 to

0°C)—such as the southern and central Mackenzie Valley, interior Alaska, Siberia’s discontinuous permafrost zone, and the Nordic region—the absolute temperature change in permafrost has been much smaller, with increases generally less than 1°C since the 1980s.

Permafrost change in these warmer regions typically involves near-surface degradation, as measured by the thickness of the seasonally thawed layer at the soil surface, which thaws in summer and refreezes in winter. This parameter is defined as the active layer thickness (ALT), the maximum thaw depth at the end of the summer. ALT responds more to short-term variation in climate as compared to the deeper ground temperature. Ground-based records of ALT, therefore, exhibit greater interannual variability, primarily in response to variation in summer temperature (Smith et al., 2009). Although decadal trends in ALT vary by region (Shiklomanov et al., 2012), most regions where long-term ground-based ALT observations are available show an increase in ALT during the last 5 to 10 years (Romanovsky et al., 2016). These measured ALT increases actually may underestimate surface permafrost degradation because the ground surface can settle with permafrost thaw, obscuring actual changes in the permafrost surface using this metric (Shiklomanov et al., 2013). Recently, several direct and indirect remote-sensing methods were proposed for regional ALT estimations over large geographical areas using both airborne and spaceborne sensors (Gogineni et al., 2014; Liu et al., 2012; Pastick et al., 2013). However, these methods are still in development and thus are not yet used in an operational mode. The increase in ground surface temperatures over the last 30 years triggered long-term permafrost thaw in natural conditions at many locations not only within the discontinuous permafrost zone, but also in the cold continuous permafrost (Drozdov et al., 2012; James et al., 2013; Liljedahl et al., 2016; Malkova et al., 2014; Melnikov et al., 2015).

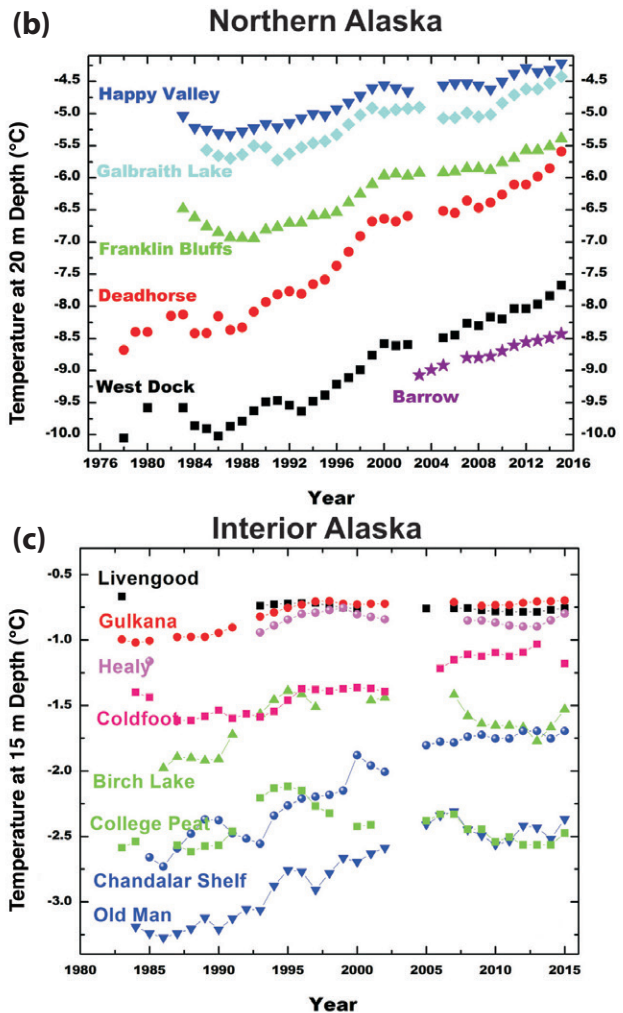
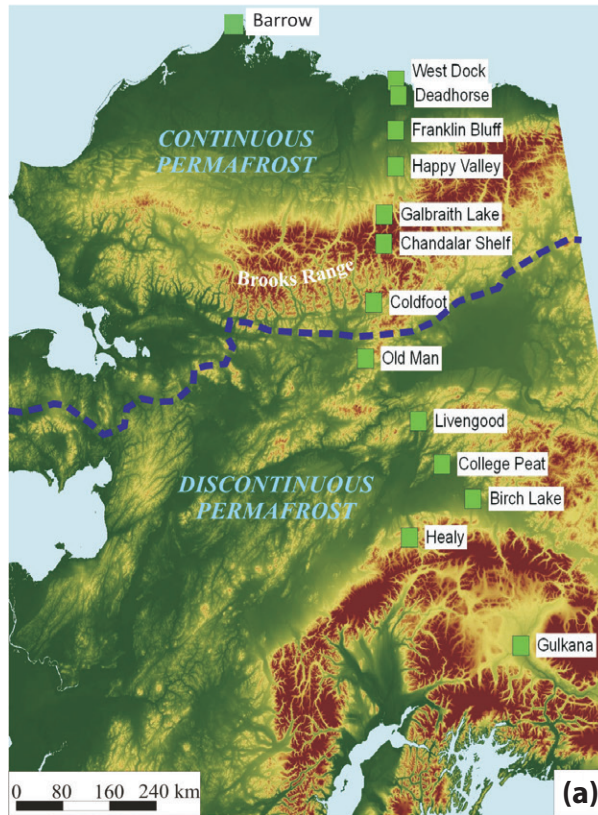


Figure 11.2. Deep Permafrost Temperature Across a Latitudinal Transect in Alaska. (a) Location of the measurement stations. Changes for northern Alaska (b) and interior Alaska (c). Rising permafrost temperatures are greatest for cold permafrost. [Figure source: Adapted and updated with new time-series data from the National Oceanic and Atmospheric Administration’s 2012 Arctic Report Card (NOAA 2012).]

**Episodic Pulse Disturbances:
Wildfire, Abrupt Thaw**

Beyond documented change in climate that has affected permafrost directly as a press disturbance, recent observations suggest that climate-sensitive pulse disturbance events, such as wildfire and abrupt permafrost thaw, are increasing in frequency, intensity, and extent across many high-latitude regions. Shifts in pulse disturbances are propelled by gradual climate warming (Jorgenson 2013); extreme weather events (Balsler et al., 2014); insect and

disease outbreaks (Kurz et al., 2008); and interactions among disturbances, such as those between abrupt thaw and wildfire (Hu et al., 2010; Jones et al., 2015; Lara et al., 2016) or human activities (Jorgenson et al., 2006).

Of all pulse disturbance types, wildfire affects the most land area annually and is currently the best characterized at the regional to continental scale. Fire activity is intimately coupled to climatic variation in regions where fuel buildup is not limiting to burning (van Leeuwen et al., 2014). Recent climate

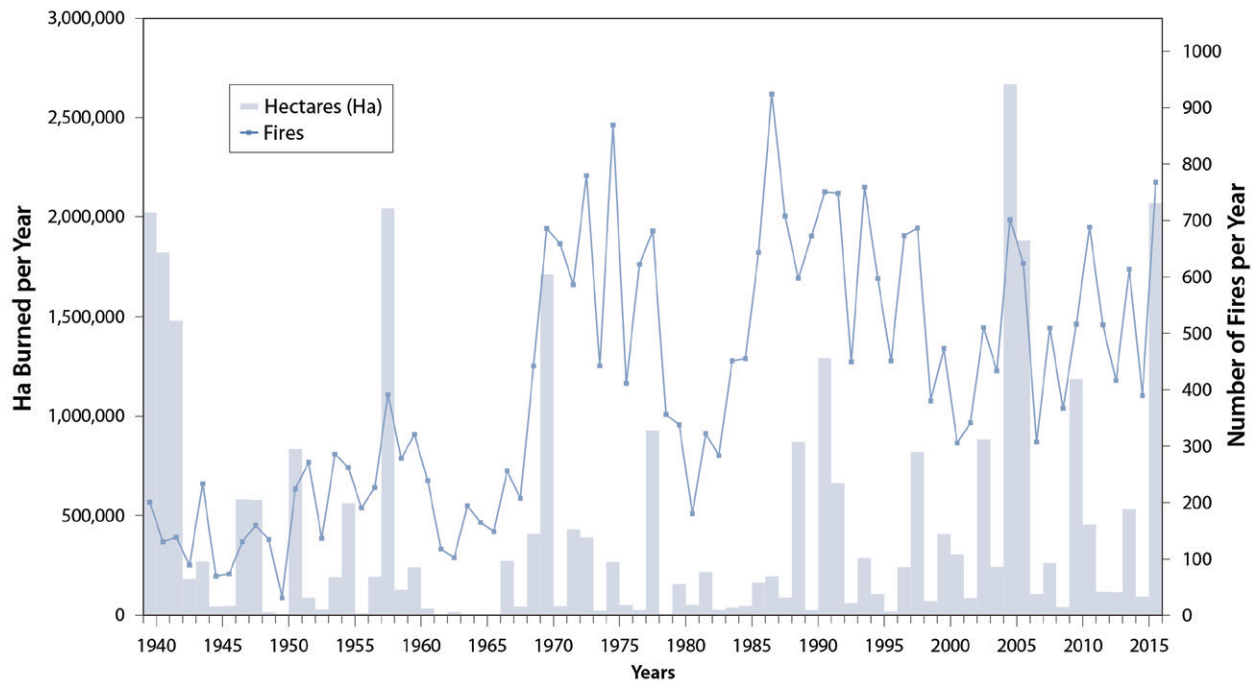


Figure 11.3. Wildfire Occurrence in Alaska from 1939 to 2015. Bars on the left y-axis show area burned in hectares per year. Right y-axis and points connected by a line show the number of fires per year. [Figure source: Redrawn from Alaska Interagency Coordination Center, used with permission.]

warming has been linked to increased wildfire activity in the boreal forest regions of Alaska (see Figure 11.3, this page; Kelly et al., 2013) and western Canada (Flannigan et al., 2009; Kasischke and Turetsky 2006), where fire has been part of historic disturbance regimes (Johnson 1992). Based on satellite imagery, an estimated 8 million hectares (ha) of boreal area was burned globally per year from 1997 to 2011 (Giglio et al., 2013; van der Werf et al., 2010). Roughly 50% of this burned area is forested; the rest is classified as low-density forest savanna, shrubland, or, in the case of boreal Eurasia, cropland. Eurasian boreal forests account for 69% of global boreal forest area and approximately 70% of the boreal area burned (Giglio et al., 2013). However, extreme fire years in northern Canada during 2014 and Alaska during 2015 doubled the long-term (1997 to 2011) average area burned annually in this region, surpassing Eurasia to contribute 60% of the global boreal area burned (Giglio et al., 2013; Mu et al., 2011; Randerson et al., 2012; van der Werf

et al., 2010). These extreme North American fire years were balanced by lower-than-average area burned in Eurasian forests, resulting in a 5% overall increase in global boreal area burned. Decadal trends (Flannigan et al., 2009; Kasischke and Turetsky 2006) and paleoecological reconstructions (Kelly et al., 2013) support the idea that area burned, fire frequency, and extreme fire years are higher now than in the first half of the last century, or even the last 10,000 years.

Fire also appears to be expanding as a novel disturbance into tundra and forest-tundra boundary regions previously protected by cool, moist climate (Hu et al., 2010, 2015; Jones et al., 2009). The annual area burned in Arctic tundra is generally small compared to that in the forested boreal biome. However, the expansion of fire into tundra that has not experienced large-scale disturbance for centuries causes large reductions in soil carbon stocks (Mack et al., 2011), shifts in vegetation composition and



productivity (Bret-Harte et al., 2013), and can lead to widespread permafrost degradation (Jones et al., 2015). In Alaska—the only region where estimates of burned area exist for both boreal forest and tundra vegetation types—tundra burning averaged approximately 0.3 million ha per year during the last half century (French et al., 2015), accounting for 12% of the average annual area burned throughout the state. Change in the rate of tundra burning projected for this century is highly uncertain (Rupp et al., 2016), but these regions appear to be particularly vulnerable to climatically induced shifts in fire activity. Modeled estimates range from a reduction in activity based on a regional process-model study of Alaska (Rupp et al., 2016) to a fourfold increase across the circumboreal region estimated using a statistical approach (Young et al., 2016).

Variability in northern fire regimes ultimately is a product of both climate and ecological controls over fuel characteristics and accumulation. Fire regime affects vegetation composition and productivity, creating the potential for fire-vegetation feedbacks to emerge that either increase or decrease fire activity at the regional scale. Although interannual variability in the fire regime is high across Alaska and western Canada, fire frequency and area burned have increased in recent years (Rupp et al., 2016). This trend is projected to continue for the rest of the century across most of this region for many climate scenarios, with the boreal region projected to have the greatest increase in total area burned (Balshi et al., 2009; Rupp et al., 2016). As fire activity increases, however, flammable vegetation, such as the black spruce forest that dominates boreal Alaska, is projected to decline as it is replaced by low-flammability deciduous forest. This shift in fuel flammability and accumulation rate could create regional-scale feedbacks that reduce the spread of fire on the landscape, even as the frequency of fire weather increases (Johnstone et al., 2011). In western Canada, by contrast, black spruce could be replaced by the even more flammable jack pine, creating regional-scale feedbacks that increase the spread of fire on the landscape (Johnson 1992). In tundra regions, graminoid (herbaceous, grass-like)

tundra is projected to decrease in future climate scenarios, while flammable shrub tundra generally is projected to increase (Rupp et al., 2016). Similarly, tree migration into tundra could further increase fuel loading and flammability, creating novel fire regimes in these highly sensitive areas. Each of these scenarios has important implications for carbon release during fire.

11.1.2 Geographical Coverage

Most permafrost is located in the Northern Hemisphere, where the permafrost zone occupies 24% of the exposed land surface (22.8×10^6 km²; Brown et al., 1998, revised February 2001; Zhang et al., 2000; see Figure 11.4, p. 435). Within the Northern Hemisphere, 47% of the permafrost zone is classified as continuous permafrost, where >90% of the land surface is underlain by frozen ground. Another 19% is classified as discontinuous permafrost, where 50% to 90% of the land surface is underlain by frozen ground. The remaining 34% of the total permafrost zone is split between sporadic and isolated permafrost, where 10% to 50% and <10% of the land surface is underlain by frozen ground, respectively. Soils in this region cover 17.8×10^6 km²; this subset of the entire permafrost zone excludes exposed bedrock, glaciers, ice sheets, and water bodies, which, with the exception of water bodies, contain little to no organic carbon stocks (Hugelius et al., 2014). Alaska, Canada, and Greenland comprise 39% of the soil area, and Eurasia (including Russia, Mongolia, and Scandinavia) comprises 61%. The northern circumpolar permafrost zone is used for soil carbon accounting and is largely comparable to most tundra and a large fraction of the boreal biome in the Northern Hemisphere but does not overlap with them completely (see Figure 11.4). Biome regions are used for vegetation carbon accounting and cover 5×10^6 km² (tundra) and 12×10^6 km² (boreal forest), respectively (Jobbágy and Jackson 2000; Margolis et al., 2015; Neigh et al., 2013; Reynolds et al., 2012). The Tibetan plateau is outside of the geographical scope of this chapter described above. Permafrost underlays 1.35×10^6 km², 67% of the total plateau

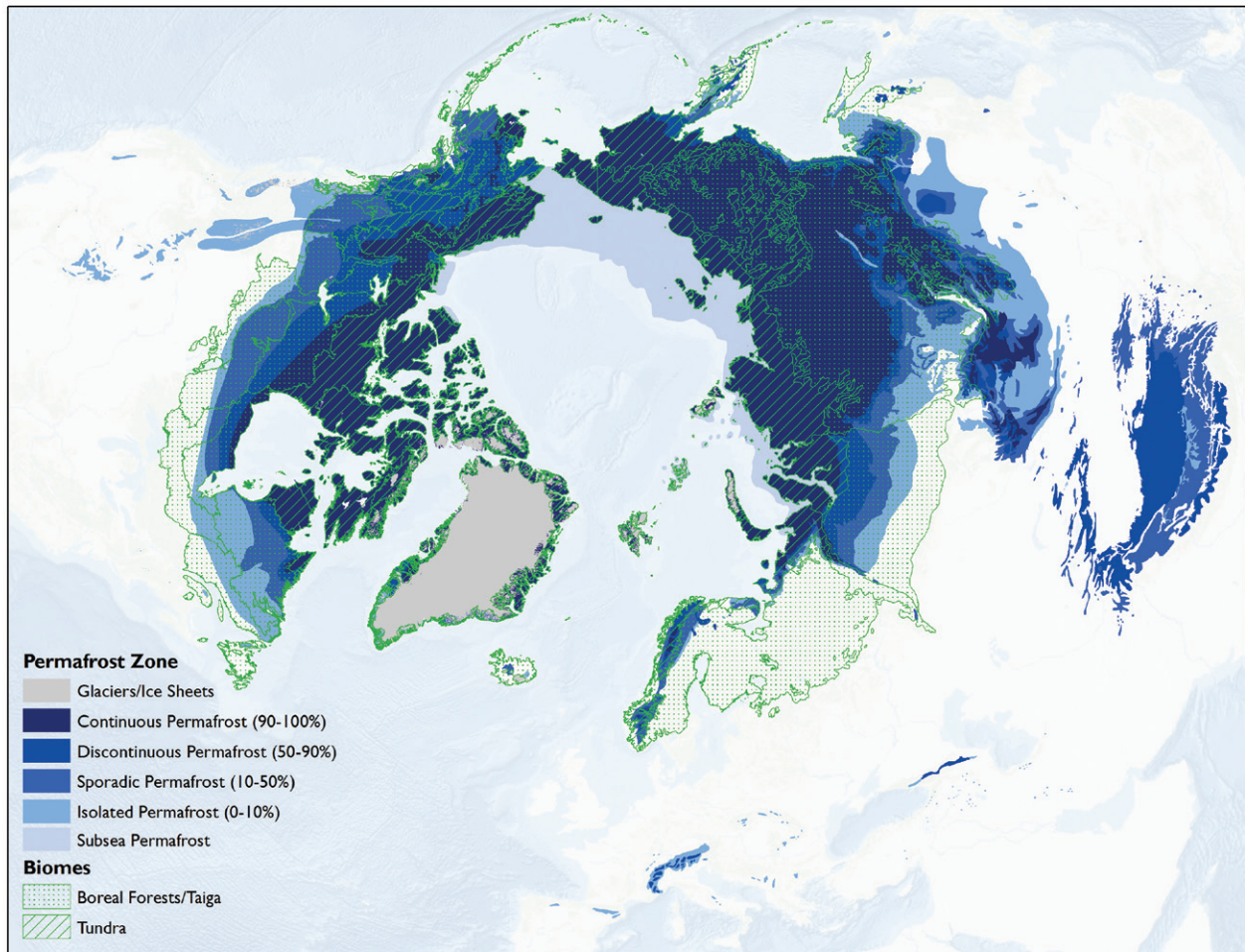


Figure 11.4. Permafrost Zones and Biome Area for Tundra and Boreal Regions. Blue areas are permafrost zones, with the legend showing percent of ground underlain by permafrost. Green dots and hashed lines define biome areas and their intersections with permafrost across some, but not all, of the region. Tundra and boreal regions outlined here are larger in area than regions quantified for carbon in this chapter, which focuses specifically on Arctic tundra and boreal forest. [Figure source: Christopher DeRolph, Oak Ridge National Laboratory. Data sources: Derived from the International Permafrost Association; Brown et al., 1997, 1998—revised February 2001; Olson et al., 2001; and World Wildlife Fund 2012.]

area, but is not classified within the tundra or boreal biome. Due to its permafrost, the soil carbon inventory is briefly discussed in this chapter in the context of the circumpolar permafrost zone soil carbon inventory.

11.1.3 Temporal Coverage

The Arctic is remote and understudied compared with more populated areas of Earth. As a result, state-of-the-art quantification of carbon pools still is

being conducted for current conditions rather than as repeat measurements through time. However, a few sites have been recording time-series measurements of carbon fluxes over a few decades, although with severely restricted spatial coverage considering the large geographical scale of this domain (e.g., see Belshe et al., 2013). Observation-based changes in carbon cycling extend back to the 1970s, and this chapter focuses on historical model simulations that estimate the 50-year period from 1960 to 2009.



Forward projections typically span the time frame until 2100 using future climate projections based on emissions scenarios from the Intergovernmental Panel on Climate Change (IPCC).

11.2 Historical Context of Vegetation and Soil Carbon Pools

A unique feature of carbon pools in the northern permafrost zone compared with those in other biomes is the predominance of carbon stored in soils as a proportion of the total ecosystem carbon stock (Chapin et al., 2011). This feature partly arises from the harsh environmental conditions and short growing season that limit plant biomass. Boreal forest often is characterized by low tree density (i.e., stems per hectare) and small tree size, while tundra comprises low-statured vegetation including dwarf shrubs and graminoids with an understory of mosses (Dixon et al., 1994). Despite low plant biomass and low primary production (i.e., the amount of new carbon that plants transfer into the ecosystem annually), ecosystem carbon storage can be largely due to the tremendous quantity of carbon stored as soil organic matter. This organic matter is the remains of plants, animals, and microbes that have lived and died in these ecosystems over hundreds to thousands of years. Soil carbon accumulates in all systems (see Ch. 12: Soils, p. 469), and the overall mechanisms of soil carbon preservation are the same at high latitudes (Post et al., 1982). What makes soil carbon density particularly high in these biomes is the combination of frozen soils (either seasonally in the surface soil active layer or perennially in the permafrost) and waterlogging that restricts the resupply of oxygen below ground (Gorham 1991; Jones et al., 2017; Treat et al., 2016). Cold and water-saturated conditions reduce organic matter decomposition rates, leading to substantial soil carbon accumulation even though annual inputs of new carbon by plants is relatively low (see Figure 11.5, this page; Hobbie et al., 2000). In fact, water-saturated soils are a common feature of high-latitude ecosystems, even beyond those defined as wetlands. This saturation results from restriction of the downward movement of surface water by permafrost, creating a perched water table within the soil profile of mesic and drier

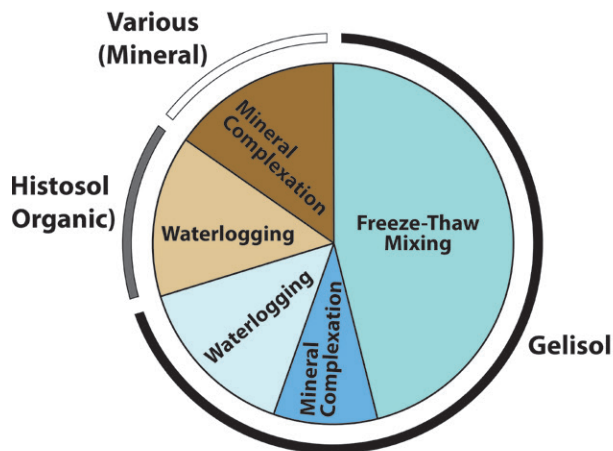


Figure 11.5. Mechanisms of Soil Carbon Stabilization Associated with Different Soil Orders in the Northern Circumpolar Permafrost Zone. Gelisol soils have a seasonally frozen active layer at the soil surface and perennially frozen (permafrost) layer at depth. Histosol and other soil orders in the permafrost zone have seasonally frozen soil at the surface. Of the Gelisol soils, freeze-thaw mixing is indicative of the Turbel suborder and waterlogging of the Histel suborder; Orthels do not have characteristics of the first two suborders. Mineral complexation and other mechanisms preserving carbon are features of all soils but are labeled here as soil orders and suborders not strongly characterized by freeze-thaw processes or waterlogging. Pie area represents proportional storage of carbon (soil depth of 0 to 3 m) in the permafrost zone. [Data source: Hugelius et al., 2014; see also Table 11.1, p. 439.]

upland ecosystems as well as lowland ecosystems. Waterlogged and frozen conditions slow both microbial decomposition and combustion by fire, which are primary mechanisms returning carbon from the soil back to the atmosphere. Both of these environmental conditions that slow decomposition increase in magnitude, intensity, and effect moving down into the soil profile. In addition, soil waterlogging also helps to control whether carbon returns to the atmosphere as carbon dioxide (CO₂) or methane (CH₄), both of which are important GHGs exchanged between high-latitude terrestrial ecosystems and the atmosphere.

Several features of soil development in the permafrost zone have the effect of transporting carbon from the surface (where it enters the ecosystem

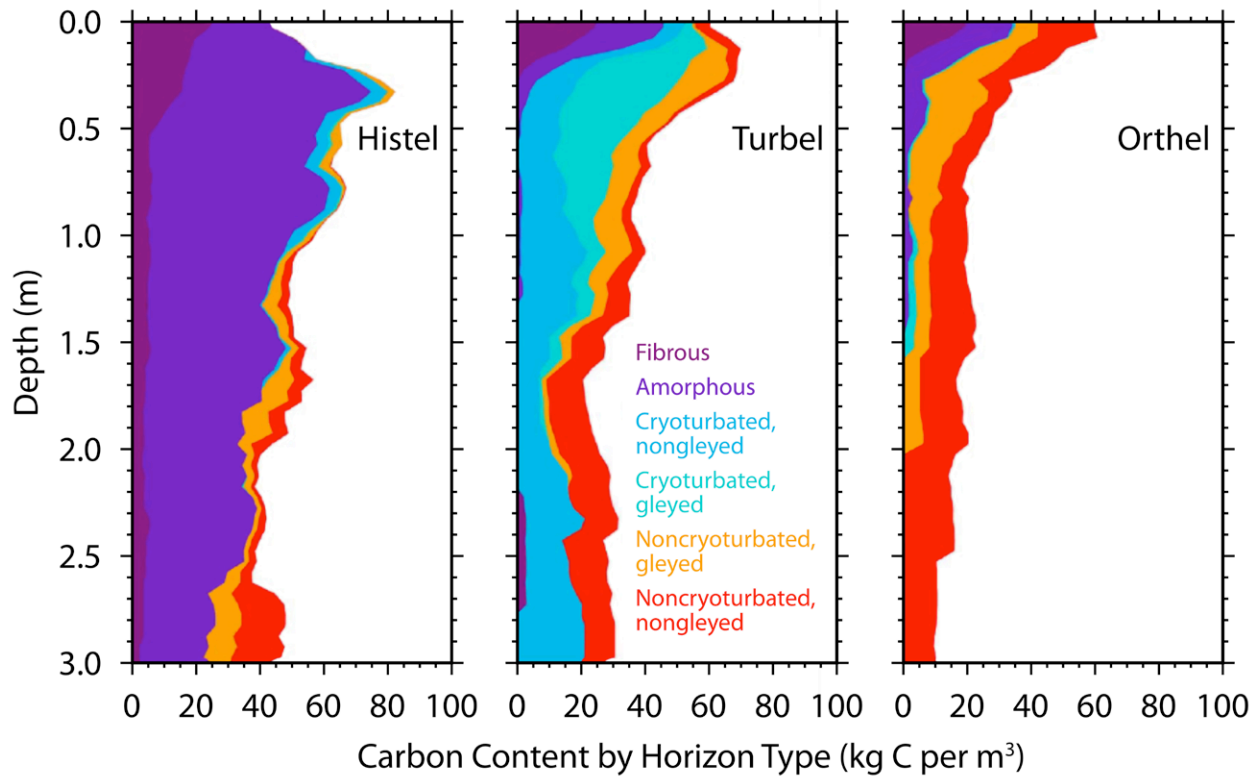


Figure 11.6. Soil Carbon Distribution in Major Suborders of the Gelisol Soil Order. Carbon in suborders Histel, Turbel, and Orthel of Gelisol (permafrost-affected soils) is shown distributed by depth and horizon type. Purple colors indicate organic horizons (>20% carbon) with less (fibrous) or more (amorphous) decomposition. Cryoturbation (freeze-thaw mixing) brings relatively carbon-rich material from the surface deeper into the soil profile. Soil horizons at depth can show evidence of periodically waterlogged (oxygen-limited) conditions (gleyed), or not (nongleyed). [Figure source: Redrawn from Harden et al., 2012, used with permission.]

through plant tissue turnover and mortality) to depth (see Figure 11.6, this page; Schuur et al., 2008). Freeze-thaw mixing (cryoturbation) occurs in permafrost soils. Cold air temperatures in the fall begin freezing soils from the surface downward, while the permafrost at depth simultaneously refreezes soils at the base of the active layer upward. This process exerts pressure on the middle soil layer that can push soil upward to release pressure through cracks to the surface. As a result, surface carbon is mixed at high concentrations deeper into the soil profile than it otherwise would have been, effectively increasing the limiting factors of temperature and waterlogging on decomposition. Another landscape-level feature of soil development that leads to relatively high carbon at depth is the

upward accumulation of soil and permafrost that occurs in high latitudes, particularly regions not covered by ice during the last glacial period, which peaked roughly 20,000 years ago (Schirmer et al., 2002). Ice sheets covered large areas of Canada, Eurasia, and Greenland, but in Alaska, Siberia, and Beringia (i.e., the land connection between the two continents that was exposed by lower sea levels), a large swath of land remained free of ice because of dry conditions and low precipitation. These unglaciated areas received deposits of silt material generated at the margins of ice sheets and glaciers and transported by wind and water. Sediment accumulated in some areas at rates of centimeters per year, which effectively increased soil surface elevation. Permafrost depth in these soils



is controlled, in part, by the insulating effect of the overlying soil, and, with increased soil elevation, the permafrost table also moved upward, which trapped plant roots and other organic matter at depth into permafrost (Zimov et al., 2006). Additionally, these soils accumulated carbon over tens to hundreds of thousands of years, whereas ecosystems covered by ice sheets in the Last Glacial Maximum only started accumulating their current soil carbon stocks since the transition to the Holocene (Harden et al., 1992). Length of time for carbon accumulation, however, is not as important as some of the direct limits to microbial decomposition, in terms of overall soil carbon stocks. For example, large areas such as the Hudson Bay Lowlands and the Western Siberian peatlands accumulated high carbon stocks since the retreat of ice sheets in the last 10,000 years because of persistent waterlogged conditions (Smith et al., 2004; Loisel et al., 2014). Lastly, the direct human footprint on carbon pools and fluxes in this region is small relative to other biomes. More than 80% of tundra and boreal biomes fall into the land-use categories of “remote forest,” “wild forest,” “sparse trees,” and “barren” (Ellis and Ramankutty 2008). Forest harvest is the primary land-use activity affecting ecosystem carbon, with fire management also playing a role, but both occur on a relatively small proportion of the overall region. More broadly, impacts to the region’s carbon cycle more likely occur indirectly through 1) changes in climate, such as temperature, precipitation, and growing season length; 2) changes in pulse disturbances, such as wildfires, abrupt thaw, and insects; and 3) rising atmospheric CO₂, which has the potential to alter ecosystems everywhere.

11.3 Current Understanding of Carbon Pools and Fluxes

11.3.1 Soil Carbon Pools

The total pool of organic carbon stored in permafrost zone soils comprises carbon frozen at depth in peatlands (>20% carbon) and carbon mixed with mineral soils (<20% carbon). Each type dominates different locations in the Northern Hemisphere, depending on physiographic and environmental characteristics (Gorham 1991; Jobbágy and Jackson 2000; Mishra and Riley 2012; Post et al., 1982;

Tarnocai et al., 2009). Recent work has shown permafrost soil carbon pools to be much larger at depth than previously recognized because of cryogenic (freeze-thaw) mixing (Bockheim and Hinkel 2007; Ping et al., 2008) and sediment deposition (Schirrmeister et al., 2002, 2011; Zimov et al., 2006). In particular, the 1.2×10^6 km² “yedoma” region (i.e., areas of Siberia and Alaska that remained ice-free during the last Ice Age) contains accumulated silt (loess) soils many meters thick. Even though carbon concentrations of these mineral soils are not remarkably high (0.2% to 2% carbon), the depths of these sediments give rise to large carbon inventories.

The current best estimate of total soil organic carbon (terrestrial) in the northern circumpolar permafrost zone is 1,460 to 1,600 petagrams (Pg; 1 Pg = 1 billion metric tons; Hugelius et al., 2014; Schuur et al., 2015; Strauss et al., 2017). This inventory includes all soil orders within the permafrost zone and thus also counts carbon in nonpermafrost soil orders, active-layer carbon that thaws seasonally, and peatlands. All permafrost zone soils estimated to 3 m in depth contain 1035 ± 150 Pg of carbon (C; see Table 11.1, p. 439, and Figure 11.7a, p. 440). Based on somewhat earlier estimates for the 1-m inventory, two-thirds of the soil carbon pool is in Eurasia, with the remaining one-third in North America, including Greenland (Tarnocai et al., 2009).

New synthesis reports account for 327 to 466 Pg C in deep loess (wind- and water-borne) sediment accumulations below 3 m in Siberia and Alaska (Strauss et al., 2013, 2017; Walter Anthony et al., 2014; Zimov et al., 2006; see Figure 11.7b, p. 440). This yedoma region contains both intact yedoma deposits that have remained primarily frozen since the last glacial period and deposits where abrupt thaw led to ground subsidence (thermokarst) and lake formation. These thermokarst lake deposits later refroze into permafrost when the lakes drained. The carbon density of intact yedoma is now thought to be lower than previously estimated because of revisions in soil bulk density estimates to account for excess pore ice (Schirrmeister et al., 2011).

**Table 11.1. Soil Carbon Pools to 3 m in Depth for the Northern Circumpolar Permafrost Zone**

Soil Orders	Soil Suborders	Soil Carbon Pool (Pg C, 0 to 3 m in depth)	Area ($\times 10^6$ km ²)
Gelisol	Turbels	476	6.2
	Orthels	98	2.5
	Histels	153	1.4
Histosol, Organic		149	0.9
Non-Gelisol, Mineral		158	6.8
Total Circumpolar		1,035^a	17.8

Soil suborders are shown for Gelisol (permafrost soil order) only, but soil carbon (petagrams of carbon [Pg C]) in this zone also is contained in Histosol (peat soil) and non-Gelisol soil orders (various). Data are from Hugelius et al. (2014).

Notes

a) Total is different from the sum due to rounding.

In contrast, thermokarst lake deposits previously believed to have depleted soil carbon stocks are now thought to have accumulated net soil carbon (Walter Anthony et al., 2014). The discovery of increased net soil carbon as a result of the thermokarst lake cycle compensated in part for the downward revision of the carbon pool contained in intact yedoma (Strauss et al., 2013; Walter Anthony et al., 2014). The range here represents different methodologies for scaling carbon pools and also accounts for carbon remaining in thawed sediments below currently existing lakes (high estimate only).

River deltas are now thought to contain 96 ± 55 Pg C, a quantity much less than originally estimated for these deep deposits (Hugelius et al., 2014; Strauss et al., 2017; Tarnocai et al., 2009). However, other deep sediment deposits located over 5×10^6 km² outside the yedoma and delta areas are not included in the total soil carbon stock reported here. Simple calculations based on extremely limited data suggest that these regions may roughly contain an additional 350 to 465 Pg C, but more sampling and data synthesis are needed to verify or revise estimates of these potential deep permafrost carbon deposits (Schuur et al., 2015; see Figure 11.7b, p. 440).

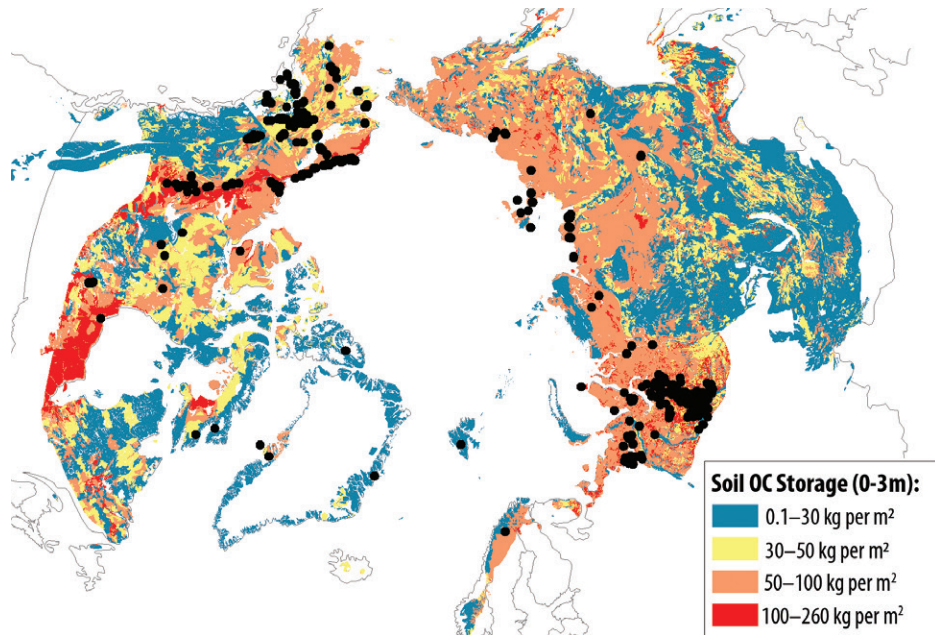
Two additional pools of permafrost carbon are not included in the permafrost carbon pool summarized

previously. The first are new estimates for the permafrost region of the Tibetan plateau that are built on earlier work (Wang et al., 2008), which now place 15.3 Pg C in the top 3 m of soil (Ding et al., 2016). This new carbon inventory extended deep carbon measurements substantially and used improved upscaling techniques, resulting in a somewhat smaller inventory for Tibetan permafrost than had been reported previously (Mu et al., 2015). An additional 20.4 Pg C are contained in 1-m inventories of permafrost soils in northern China estimated by earlier first-order inventories (Luo et al., 2000) for a total of 35.7 Pg C for this region as a whole.

The second uncounted pool is a reservoir of organic carbon in permafrost stored on the continental shelf under the Arctic Ocean (Brown et al., 1998—revised February 2001; Rogers and Morack 1980). This undersea permafrost carbon initially formed on land as the continental shelf was exposed when sea level was approximately 120 m lower during the last glacial period (Walter et al., 2007). Subsequent inundation of this area at the Pleistocene-Holocene transition started thawing this loess permafrost (Rachold et al., 2007). No reliable published estimates exist for the total organic carbon in this subsea pool (setting aside inorganic CH₄ clathrates), but yedoma deposits are thought to have covered much



(a)



(b)

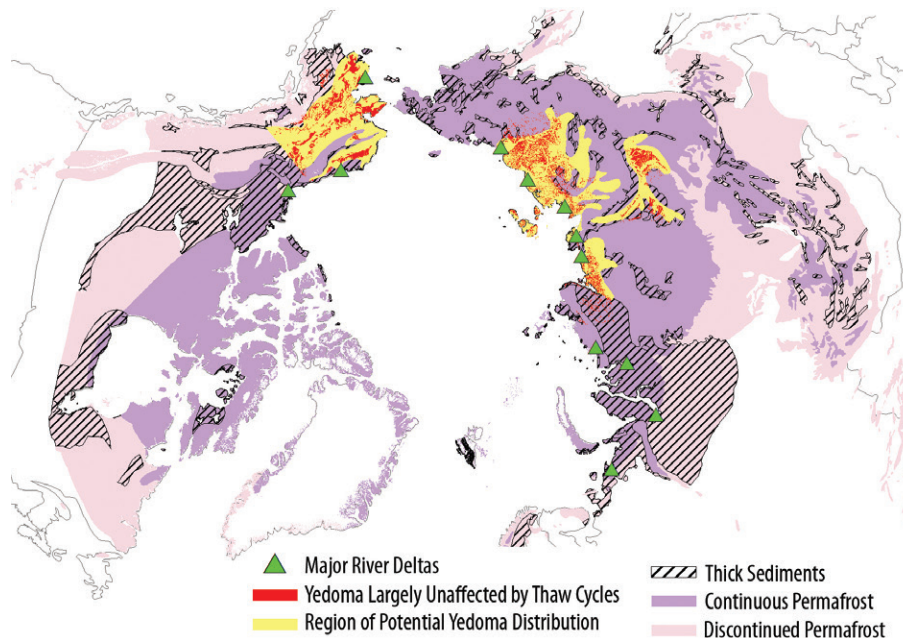


Figure 11.7. Soil Organic (SOC) Carbon Maps. (a) The SOC pool in kg of carbon per m² contained in the interval of 0 to 3 m in depth of the northern circumpolar permafrost zone. Black dots show field site locations for carbon inventory measurements of 0 to 3 m. (b) Deep permafrost carbon pools (>3 m), including the location of major permafrost-affected river deltas (green triangles); extent of the yedoma region previously used to estimate the carbon content of these deposits (yellow); current extent of yedoma-region soils largely unaffected by thaw-lake cycles that alter original carbon content (red); and extent of thick sediments overlying bedrock (black hashed). Yedoma regions generally are also thick sediments. The base map layer shows permafrost distribution with continuous regions to the north having permafrost everywhere (>90%, purple shading) and discontinuous regions further south having permafrost in some, but not all, locations (<90%, pink shading). [Figure source: Reprinted from Schuur et al., 2015, copyright Macmillan Publishers Ltd, used with permission.]



of the shallow shelf during its exposure. Although there are no shelf carbon inventories comparable to those for land, the shallow shelf area exposed as dry land in the area around Alaska and Siberia during the last Ice Age (currently 125 m deep in the ocean) is almost 3×10^6 km², or about 2.5 times the size of the current terrestrial yedoma region (Brosius et al., 2012; Strauss et al., 2013). At the same time, submergence over thousands of years helped thaw permafrost, exposing organic carbon to decomposition, potentially under anaerobic conditions. These processes and conditions would have converted a portion of the carbon pool to CO₂ and CH₄, leaving an unknown quantity of organic carbon remaining in both the sediment and the permafrost that persists under the ocean.

Soils in the top 3 m of the rest of Earth's biomes (excluding Arctic and boreal biomes) contain 2,050 Pg organic carbon (Jobbágy and Jackson 2000). The soil carbon quantified here from the northern circumpolar permafrost zone adds another 50% to this 3-m inventory, even though it occupies only 15% of the total global soil area (Schoor et al., 2015). Making this comparison with deposits deeper than 3 m (such as those in yedoma) is difficult because deeper deposits are not always as systematically quantified in soil carbon inventories outside the permafrost zone. Assuming that permafrost has preserved deep carbon stocks at higher levels than elsewhere on Earth, the proportion of total soil carbon contained in the northern circumpolar permafrost region could be even larger.

11.3.2 Vegetation Carbon Pools

Most carbon stored in the vegetation of northern high latitudes is in boreal forests, which account for one-third of global forests (Pan et al., 2011). Nonsoil carbon pools of the boreal forest consist of deadwood, litter, and above- and belowground live biomass (Pan et al., 2011). The boreal zone, generally defined by latitudes between 45°N and 70°N (Margolis et al., 2015; McGuire et al., 2009; Neigh et al., 2013), is characterized by tundra at the northern boundary and temperate forest, steppe, or prairie at the southern boundary (see Figure 11.4,

p. 435). Spruce, pine, and fir are typical coniferous tree species within the boreal zone mixed with deciduous species of larch, birch, alder, and aspen (Neigh et al., 2013). The North American boreal zone spans a total area of 3.73×10^6 km², which is one-third of the entire circumpolar boreal zone (11.35×10^6 km² to 11.93×10^6 km²; see Table 11.2, p. 442; Neigh et al., 2013; Pan et al., 2011). Biomass estimates for boreal forests mostly exclude root biomass because it is not measured in many inventories. This chapter uses a ratio of 0.27 for root-to-total phytomass (Saugier et al., 2001) and calculates total carbon pools for the boreal zone (see Table 11.2). Numbers are presented for Alaska, eastern and western Canada, and the circumpolar North using the aboveground biomass values reported in Margolis et al. (2015) and Neigh et al. (2013), which combine satellite light detection and ranging (LIDAR), airborne LIDAR, and ground plot estimates.

Half the carbon in Alaska and Canada's boreal zone is stored in coniferous forests; this is also true for the entire circumpolar region (7.66 Pg C in North America; see Table 11.2, p. 442). The second largest forest type is "mixed wood" (i.e., coniferous and deciduous trees) followed by "hardwood" (i.e., deciduous trees), which together account for 35% to 42% of the total boreal vegetation carbon stocks. A small portion of vegetation carbon in the boreal zone is found in the biomass of wetlands (5% to 12%) and in burned areas (about 1%). A separate synthesis reported 14.0 Pg C for all living biomass (both above and below ground) in Canada, covering 2.29×10^6 km²; Pan et al., 2011). Estimates for that synthesis were based on forest inventory data; growth and yield data; and data on natural disturbances, forest management, and land-use change. Because forest inventory data were used, areas covering 1.18×10^6 km² of unmanaged boreal forest in Canada and 0.51×10^6 km² of unmanaged forest in Alaska were excluded, but, in general, the stock-based carbon numbers are similar to the remotely sensed estimates for Canada and the circumpolar North. Discrepancies in carbon pools could arise from different measurement approaches and the known limitations of satellite-based LIDAR measurements in steep topography (Margolis et al., 2015).

**Table 11.2. Vegetation Carbon Pools for North America and Global Northern High-Latitude Regions**

Vegetation Type	Region/Ecosystem	Vegetation Carbon Pool (Pg C)	Area ($\times 10^6$ km ²)
Boreal Forest	Alaska		
	Wetlands	0.09	0.06
	Hardwood	0.3	0.05
	Conifer	0.79	0.21
	Mixed Wood	0.24	0.05
	Burned	0.02	0.01
	Total Alaska	1.51	0.37
	Canada		
	Wetlands	1.61	0.78
	Hardwood	1.84	0.27
	Conifer	6.87	1.7
	Mixed Wood	3.05	0.53
	Burned	0.14	0.04
	Total Canada	13.56	3.36
	Circumboreal		
	Wetlands	2.21	1.25
	Hardwood	2.44	0.37
	Conifer	27.6	7.28
Mixed Wood	19.26	2.84	
Burned	0.48	0.18	
Total Circumboreal	52.05	11.93	
Tundra	<i>Alaska</i>	0.35	0.48
	<i>Canada</i>	1.01	2.34
	Total Circumpolar^a	3.17	4.98

Boreal forest vegetation carbon includes carbon in above- (Neigh et al., 2013) and belowground live biomass. Belowground numbers were calculated based on root-to-total biomass ratios (after Saugier et al., 2001). Ratios are 0.27 for boreal forests and 0.62 for tundra biomass. Tundra area data exclude ice caps and large water bodies (Raynolds et al., 2012). Estimates for deadwood carbon and litter carbon pools are reported in the main chapter text. Totals are reported from the original publication (Neigh et al., 2013) and, in some cases, may not match the component sums exactly due to rounding differences.

Notes

a) Total circumpolar also includes estimates for Eurasia (data not shown). Eurasia quantities are equivalent to the total minus the estimates for Alaska and Canada.

The Arctic tundra vegetation zone is north of the boreal tree line, extending all the way above 80°N latitude in the Canadian High Arctic and is described in detail in the circumpolar Arctic vegetation map (see Figure 11.4, p. 435; Walker et al., 2009).

Recent estimates quantified a total vegetated area of 4.98×10^6 km² in the circumpolar tundra zone, of which a little less than half is in Canada and about 10% in Alaska (see Table 11.2, this page; Raynolds et al., 2012). Tundra vegetation mostly consists of



shrubland, peaty graminoid tundra, mountain complexes, barrens, graminoid tundra, prostrate shrubs, and wetlands (Walker et al., 2009). Using a relationship of aboveground biomass and the normalized difference vegetation index (NDVI), the North American tundra zone is estimated to contain 1.03 Pg C in aboveground plant biomass (0.27 Pg C in Alaska and 0.76 Pg C in Canada; Reynolds et al., 2012). Assuming that 62% of the total tundra biomass is below ground (Saugier et al., 2001) and half the biomass is carbon (Epstein et al., 2012), there is a total carbon stock of 1.36 Pg C contained in North American tundra vegetation (see Table 11.2, p. 442). For the entire circumpolar region, this amount is equal to 3.17 Pg C. There is an offset in land area between the soil carbon and vegetation carbon estimates of 0.89×10^6 km², which is likely either non-Arctic (sub-Arctic or alpine) tundra or sparse conifer forest (taiga). Using tundra carbon pools as a low-end estimate, there could be another 0.57 Pg C in vegetation biomass contained on these lands but not reported in Table 11.2.

Earlier estimates for vegetation carbon in northern high latitudes reported 5 Pg C in Alaska, 12 Pg C in Canada, and 60 to 70 Pg C for the circumpolar North (McGuire et al., 2009). Although previous carbon estimates for Canada and the circumpolar North are relatively similar to the new remotely sensed and inventoried estimates reported here, the 5 Pg C estimate for Alaska is higher. Combining the latest boreal and tundra vegetation estimates, North American high-latitude areas, which are 30% of the entire circumpolar region, contain 16.43 Pg C in vegetation (15.07 Pg C boreal; 1.36 Pg C tundra).

Deadwood and litter are two nonsoil carbon pools poorly constrained by data at regional and continental scales. The deadwood pool has been estimated (in 2007) at 16.1 Pg C for a region of the boreal forest covering 11.35×10^6 km², again excluding 1.18×10^6 km² of unmanaged boreal forest in Canada and 0.51×10^6 km² of unmanaged forest in Alaska (Pan et al., 2011). This same boreal region was estimated to contain a litter carbon pool of 27.0 Pg C, which together with deadwood represents at least 83% of the carbon contained in the living above- and below-ground biomass. An older modeling study estimated

tundra litter to contribute 2 Pg C at the circumpolar scale (Potter and Klooster 1997).

11.4 Indicators, Trends, and Feedbacks

11.4.1 Drivers of Carbon Pool Change

Changes in soil and vegetation carbon pools are a result of changing carbon fluxes over time. In the absence of pulse disturbances, CO₂ exchange between ecosystems and the atmosphere is the major pathway of carbon input and output (Chapin et al., 2006). Carbon dioxide enters ecosystems via plant photosynthesis and is returned to the atmosphere through respiration of plants and all heterotrophic organisms that depend directly or indirectly on energy contained in plant biomass. Over the past few centuries to millennia, tundra and boreal ecosystems acted as net carbon sinks at the regional scale, as the amount of carbon released by respiration was smaller than that absorbed by photosynthesis. Vegetation biomass is likely to have reached peak amounts over decades to perhaps a century or more. In contrast, soils act as a long-term (i.e., century to millennia) carbon sink as carbon continues to accumulate as dead organic matter (Harden et al., 1992). Carbon accumulation resulting from the net difference between photosynthesis and respiration also is punctuated by periods of abrupt loss catalyzed by ecological disturbances. In the tundra and boreal biomes, large-scale pulse disturbances include fire, insect outbreaks, and abrupt permafrost thaw and soil subsidence (known as thermokarst). Periods of disturbances generally favor carbon losses either abiotically (e.g., fire emissions) or biotically (e.g., stimulating respiration). These losses often occur as a pulse loss, whereas carbon gains through vegetation growth and succession and new soil carbon accumulation occur over decadal to century timescales. Other smaller but important carbon fluxes in high-latitude ecosystems include CH₄ flux and the lateral export of dissolved inorganic carbon (DIC), dissolved organic carbon (DOC), and particulate organic carbon (POC) in water (McGuire et al., 2009). Methane flux by weight is usually an



order of magnitude smaller than CO₂ flux but has a higher global warming potential (GWP). Dissolved carbon losses are a persistent feature of undisturbed and disturbed ecosystems and also are typically an order of magnitude smaller than CO₂ exchanges. An exception is POC, which usually is similar in magnitude to other dissolved losses and relatively small in many circumstances. However, it is the one flux that can approach the magnitude of CO₂ exchanges, at least for short periods, when erosion is a consequence of another disturbance such as abrupt permafrost thaw or fire.

11.4.2 Carbon Fluxes in Recent Decades

Stock Changes

Changes in vegetation and soil carbon stocks over time provide an estimate of landscape carbon budgets. For boreal and Arctic ecosystems, the challenge is that study sites are remote and often not spatially representative. Inventories of aboveground plant biomass in forests are probably the best measured of all ecosystem carbon pools, along with harvested wood products (i.e., managed forests) and then deadwood. Rather than estimated through time, belowground biomass, litter, and soil stocks usually are estimated from single time-point measurements and extrapolated using simple scaling assumptions. The most recent regional estimates for Eurasian and Canadian boreal forests put total carbon flux (total of all pools described above) at 493 ± 76 teragrams (Tg) C per year from 1990 to 1999 and at 499 ± 83 Tg C per year from 2000 to 2007 (Pan et al., 2011). These estimates do not include forestland in interior Alaska (0.51×10^6 km²) or unmanaged forests in northern Canada (1.18×10^6 km²), essentially assuming those lands to be at steady state in regard to carbon pools.

Carbon Dioxide

Recent syntheses have outlined changes in tundra carbon flux over time. A broad survey of data from a number of dry to wet tundra types found that in most studies since 1995, tundra acts as a carbon sink during summer, when photosynthetic uptake exceeds respiration losses during this approximately

100-day season (McGuire et al., 2012). Summer carbon sequestration is offset partially by carbon losses in fall, winter, and spring when microbes are still metabolically active and releasing CO₂, while plants are largely dormant and carbon assimilation has slowed or ceased. While absolute levels of CO₂ flux are low during the nonsummer season, the long period of more than 250 days is enough to offset, in some cases, the net carbon that accumulated during summer. A critical issue for determining net change in ecosystem carbon storage is the relative scarcity of nonsummer flux measurements in comparison to summer flux measurements. For example, the recent regional carbon balance estimate for the North American subregion had 80 study-years of summer measurements and only 9 study-years of nonsummer measurements available for upscaling (McGuire et al., 2012). This order of magnitude difference across seasons was similar across the other upscaled tundra subregions.

A first-order upscaling synthesis that used plot-scale measurements scaled by regional land area showed that North American tundra was a source of carbon on the order of 124 Tg C per year during the 1990s and a sink of 13 Tg C per year during the 2000s (McGuire et al., 2012). This increase in uptake relative to losses was similar to that in the Eurasian tundra that was reported as a 19 Tg C per year source in the 1990s and a sink of 185 Tg C per year in the 2000s. This study reported a global carbon exchange in the tundra region of 13 Tg C per year (i.e., a small sink but near neutral exchange) over both decades using a scaling region of 9.2×10^6 km², which includes the tundra biome plus a portion of the boreal forest biome for comparison to large-scale atmospheric inversion models. A follow-up synthesis study focused on a subset of the same tundra sites and also included new sites with nonsummer data to bolster undersampled seasons (Belshe et al., 2013). Although this analysis supported the previous finding that the summer-season carbon sink increased in the 2000s compared with the 1990s, it suggested that the mean tundra flux remained a carbon source annually across both decades when additional nonsummer flux data were included. In this analysis,



the source potential appears to decline over time, although this decline is statistically nonsignificant. Separately analyzing the record for the nonsummer data-intensive period (2004 to 2010) showed a trend of increasing nonsummer carbon flux and an overall increase in tundra carbon source during that period. Because changes in measurement technology parallel trends in time, data also were analyzed relative to the mean annual temperatures of the study sites. The trend of tundra consistently acting as an annual carbon source was significant across the range of tundra sites, with the net loss ranging from 23 to 56 grams (g) C per m² per year. This relationship also predicts a 2 g C per °C increase in loss rates across the range of mean annual temperatures. These figures, when scaled to a region consistent with the previous study (10.5 × 10⁶ km²; Callaghan et al., 2004; McGuire et al., 1997, 2012), predict that the tundra is acting as current source of 462 Tg C per year that could increase by almost 35% to 620 Tg C per year, given the “business-as-usual” warming projected for the Arctic (i.e., an increase of 7.5°C).

Recent measurements of atmospheric GHG concentrations over Alaska have been used to estimate carbon source and sink status of those Arctic and boreal ecosystems for 2012 to 2014 (Commane et al., 2017). During this period, tundra regions of Alaska were a consistent net CO₂ source to the atmosphere, whereas boreal forests were either neutral or a net CO₂ sink. The larger interannual variability of boreal forests was due both to changes in the balance of photosynthesis and respiration and to the amount of combustion emissions by wildfire. The Alaska study region as a whole was estimated to be a net carbon source of 25 ± 14 Tg C per year averaged over the land area of both biomes for the entire study period. If this Alaskan region (1.6 × 10⁶ km²) was representative of the entire northern circumpolar permafrost zone soil area (17.8 × 10⁶ km²), this amount would be equivalent to a region-wide net source of 0.3 Pg C per year.

Methane

Uncertainty in the scaling of “bottom-up” field-based flux observations of CH₄ emissions across

the northern permafrost region (32 to 112 Tg CH₄ per year; McGuire et al., 2009) is much larger than uncertainty from “top-down” atmospheric analyses based on the spatial and temporal variability of CH₄ concentration measurements (15 to 50 Tg CH₄ per year; McGuire et al., 2009; Crill and Thornton 2018). Flux estimates include those from terrestrial ecosystems (e.g., wetlands), lakes, and coastal waters underlain by permafrost. Observational studies reviewed by McGuire et al. (2012) indicate that during the 1990s and 2000s, the tundra emitted 14.7 Tg CH₄ per year (with an uncertainty range of 0 to 29.3 Tg CH₄ per year). Kirschke et al. (2013) suggest a Eurasian boreal wetland source of 14 Tg CH₄ per year (uncertainty = 9 to 23) from field flux measurements and 9 Tg CH₄ per year (uncertainty = 4 to 13) from atmospheric measurements, which also estimate an upland soil sink of 3 Tg CH₄ per year (uncertainty = 1 to 5). For North American high-latitude wetlands, estimated emissions are 9 Tg CH₄ per year (uncertainty = 6 to 17) from atmospheric measurements and 16 Tg CH₄ per year (uncertainty = 9 to 28) from field flux measurements, along with a soil sink of 2 Tg CH₄ per year (uncertainty = 1 to 2) estimated from atmospheric measurements. The most recent assessment reports that the field flux uncertainty in CH₄ emissions from tundra terrestrial ecosystems and lakes in the Arctic was between 10 and 43 Tg CH₄ per year during the 1990s and 2000s (AMAP 2015). This estimate indicates that bottom-up uncertainties have not been reduced by more recent assessments. Estimates of CH₄ fluxes from lakes likely are confounded with those from wetlands in spatial scaling procedures. A recent synthesis that focused just on lakes in the northern permafrost region indicates that CH₄ emissions from lakes range from 6 to 25 Tg CH₄ per year (Walter Anthony et al., 2016; Wik et al., 2016). Also, there are large uncertainties about the magnitude of CH₄ emitted from submarine permafrost in coastal waters of the Arctic Ocean and its marginal seas (Berchet et al., 2016; Shakhova et al., 2010, 2014). The degree to which the source of CH₄ emissions in coastal waters results from biogenic methanogenesis, fossil sources, or the dissociation of gas hydrates



is not clear. The amount of CH₄ emitted from fossil sources is an issue for both land and ocean environments in the permafrost region. Emissions include CH₄ from natural sources such as geological seeps and human activities, including oil and gas exploration and transport (Ruppel and Kessler 2017; Kohnert et al., 2017). Top-down estimates of CH₄ emissions from the permafrost region are useful because they integrate the various sources of CH₄ to the atmosphere. However, these top-down flux estimates also have substantial uncertainties because they are derived from models, which still need to be better reconciled with field flux measurements.

Recent developments include increased use of atmospheric measurements from aircraft, which have the great advantage of avoiding biases induced by logistical constraints on ground-based study site selections or “hotspot”-focused studies that ignore potentially vast areas of CH₄ uptake (e.g., 3.2 ± 1.4 mg CH₄ per m² per day in dry tundra and 1.2 ± 0.6 mg CH₄ per m² per day in moist tundra in northeast Greenland; Juncher Jørgensen et al., 2015). Aircraft atmospheric measurements also inherently include previously neglected freshwater systems estimated to contribute as much as 13 Tg CH₄ per year north of 54°N (Bastviken et al., 2011). A recent study used aircraft concentration data and inverse modeling to derive regional fluxes averaged over all of Alaska amounting to 2.1 ± 0.5 Tg CH₄ from May to September 2012 (Chang et al., 2014). This quantity includes all biogenic, anthropogenic, and geological sources such as seeps, which alone contribute an estimated 1.5 to 2 Tg CH₄ per year (Walter Anthony et al., 2012), based on extrapolating ground-based measurements.

Spatial analyses of CH₄ emissions in the northern permafrost region indicate that “wetter” wetlands are primarily sensitive to variation in soil temperature, whereas “drier” wetlands are primarily sensitive to changes in water-table position (Olefeldt et al., 2013). Similar analyses for lakes indicate that in systems with suitable organic substrate, CH₄ emissions are sensitive to water temperature, particularly in the continuous permafrost zone (Wik et al., 2016). In

addition, some studies have proposed that seasonality of CH₄ emissions is potentially sensitive to ongoing climate change, with emissions possibly persisting further into fall as soils remain unfrozen for longer periods (Mastepanov et al., 2008; Miller et al., 2016; Zona et al., 2016) or elevating in spring as CH₄ is released from trapped pockets in the frozen soil (Raz-Yaseef et al., 2016). These sensitivities suggest that observed changes in temperature of the northern permafrost region should have resulted in increased CH₄ emissions (Walter Anthony et al., 2016), and modeling studies that have incorporated these sensitivities conclude this as well (Riley et al., 2011; Xu et al., 2016). However, while temperature has increased substantially in the northern permafrost region in recent decades, there is no indication from analyses of atmospheric data that CH₄ emissions in the region have increased (Bergamaschi et al., 2013; Bruhwiler et al., 2014; Dlugokencky et al., 2009; Sweeney et al., 2016). The lack of significant long-term trends suggests more complex biogeochemical processes may be counteracting the observed short-term temperature sensitivity (Sweeney et al., 2016). Alternatively, separating biogenic changes in northern ecosystems from fossil-fuel derived emissions from lower latitudes may be difficult using surface atmospheric concentration measurements alone (Parazoo et al., 2016).

Lateral Hydrologic Losses

Carbon can move laterally into inland waters from terrestrial upland and wetland ecosystems in Arctic and boreal biomes. In inland waters, carbon derived from living and dead organic matter is transported largely to the ocean as DOC, DIC, and POC (see Ch. 14: Inland Waters, p. 568). The annual export of carbon from rivers to the Arctic Ocean is estimated to be 43 Tg C as DIC, 33 Tg C as DOC, and 6 Tg C as POC, for a total of 82 Tg C per year (McGuire et al., 2009). A recent assessment for Alaska estimates that the riverine flux of DIC, DOC, and POC to the ocean is 18 to 25 Tg C per year (Stackpoole et al., 2016), representing 22% to 30% of the total riverine flux of carbon to the Arctic Ocean estimated by McGuire et al. (2009). Although this percentage of



the total appears large for Alaska relative to its small geographic discharge area, it may indicate that earlier estimates were too low (McGuire et al., 2009).

Coastal erosion in the Arctic is an important source of POC to the Arctic Ocean, and this flux is likely to increase with warming because of enhanced erosion associated with the loss of a protective sea ice buffer, increasing storm activity, and thawing of coastal permafrost (e.g., Jorgenson and Brown 2005; Rachold et al., 2000, 2004). Based on recent estimates (Rachold et al., 2004), POC transport across the Arctic land-ocean interface through coastal erosion is about 6 to 7 Tg C per year (McGuire et al., 2009).

Fire

Fire has the largest footprint of any pulse disturbance in the northern circumpolar permafrost zone; thus, increases in the size, frequency, and severity of regional fire regimes will have important impacts on current and future carbon stocks and fluxes (Balshi et al., 2009; Bond-Lamberty et al., 2007; Kasischke et al., 1995). At the ecosystem scale, fire catalyzes abrupt changes in stocks by transferring carbon from plants and soils to the atmosphere. In contrast to temperate and tropical wildfires, soil organic matter is the dominant source of carbon emissions from boreal and tundra wildfires, and fire-driven changes in soil structure can alter controls over ecosystem carbon dynamics such as ALT, hydrology, and vegetation age and composition. At the landscape scale, increasing fire activity will alter the age structure of forests and tundra, decreasing landscape carbon stocks and increasing or, perhaps less frequently, decreasing carbon sequestration (Yue et al., 2016).

Estimates of carbon emissions from global boreal forest fires averaged 155 Tg C per year (with a range of 78 to 334 Tg C per year) from 1997 to 2013 (Giglio et al., 2013; van der Werf et al., 2010). North American boreal forests contributed 7% to 79% of these emissions and averaged 30%, which is similar to their proportional area (see Table 11.2, p. 442). However, recent extreme fire years (2014 in northern Canada and 2015 in Alaska) doubled emissions from this region to about 100 Tg C per year, similar

to average emissions from the much larger Eurasian boreal region. Extreme fire years are common in both regions. For example, within the last 19 years, North American boreal forests had 6 years where emissions were double the long-term average of 56 Tg C per year, and boreal Eurasian forests had 3 years with emissions double the long-term average of 106 Tg C per year. In contrast to the boreal forest, global carbon emissions from tundra wildfires are poorly constrained, but, on a per-unit-burned-area basis, tundra emissions can be similar in magnitude to boreal forest emissions because of the deep burning of organic soils (Mack et al., 2011). This finding suggests that increased tundra burning will have a similar per-unit-area impact to increased boreal forest burning.

Regional patterns of changing fire severity are less understood than changes in area. Increases in fire frequency are important because they reduce carbon recovery time post-fire and make forests more vulnerable to high-intensity fires (Hoy et al., 2016) or shifts in vegetation dominance (Brown and Johnstone 2012). In permafrost-affected soils, a large quantity of organic carbon resides in a thick soil organic layer that can be hundreds to thousands of years old; this carbon is a legacy of past fire cycles (Harden et al., 2000). Combustion of the soil organic layer dominates carbon emissions during fires (Boby et al., 2010; Kasischke et al., 1995; Mack et al., 2011), and more severe fires result in deeper burning (Turetsky et al., 2011a). Because soil carbon accumulation rates vary across the landscape (Hobbie et al., 2000), deeper burning may not always combust legacy carbon (Mack et al., 2011), but when it does, this burning could rapidly shift ecosystems across a carbon cycling threshold, from net accumulation of carbon from the atmosphere over multiple fire cycles to net loss (Turetsky et al., 2011b).

Fires that burn deeply into the soil organic layer can persistently alter both physical and biological controls over carbon cycling, including permafrost stability, hydrology, and vegetation. Reduction or loss of the soil organic layer decreases ground insulation (Jiang et al., 2015; Jorgenson 2013; Jorgenson et al.,



2013; Shur and Jorgenson 2007), warming permafrost soils and exposing organic matter that has been frozen for hundreds to thousands of years to microbial decomposition, mineralization, and atmospheric release of GHGs (Schuur et al., 2008). Permafrost degradation also can increase or decrease soil drainage, leading to abrupt changes in soil moisture regimes that affect both decomposition and production (Jorgenson 2013; Jorgenson et al., 2013; Schuur et al., 2009). These changes sometimes lead to abrupt permafrost thaw and thermal erosion events that drive further change in ecosystem processes. In addition, loss of the soil organic layer exposes mineral soil seedbeds (Johnstone et al., 2009), leading to recruitment of deciduous tree and shrub species that do not establish on organic soil (Kasischke and Johnstone 2005). This recruitment has been shown to shift post-fire vegetation to alternate successional trajectories (Johnstone et al., 2010). Model projections suggest that the Alaskan boreal forest could cross a tipping point, where recent increases in fire activity have made deciduous stands as abundant as spruce stands on the landscape (Mann et al., 2012). In Arctic *Larix* forests of northeastern Siberia, increased fire severity can lead to increased tree density in forested areas and forest expansion into tundra (Alexander et al., 2012). Additionally, burned graminoid tundra has been observed to increase in post-fire greenness (Hu et al., 2015), an occurrence that has been linked to increased tall deciduous shrub dominance (Racine et al., 2004; Rocha et al., 2012). Plant-soil-microbial feedbacks within new vegetation types determine long-term trajectories of nutrient dynamics (Melvin et al., 2015) that, in turn, constrain ecosystem carbon storage (Alexander and Mack 2016; Johnstone et al., 2010) and resultant climate feedbacks via carbon and energy (Randerson et al., 2006; Rocha et al., 2012).

11.4.3 Future Vulnerabilities

Carbon in Arctic and boreal ecosystems is expected to be subject both to press disturbances such as increasing temperatures, changing precipitation regimes, and rising CO₂ and to pulse disturbances including wildfire, insect outbreaks, and abrupt permafrost thaw. Rates of both disturbance types may

change over time depending on future human activities and the resulting ecosystem- and landscape-level feedbacks. No single future assessment technique includes all these mechanisms comprehensively. This section provides estimates of carbon pool change using three different assessment techniques: 1) semiquantitative assessment that relied on expert knowledge of the system; 2) dynamical models that relied on environmental input data and knowledge of underlying mechanistic relationships of ecosystem dynamics; and 3) upscaling of laboratory measurements of potential soil carbon change.

Expert Assessment

To provide an integrated assessment of the effect of environmental changes in combination with heterogeneity in permafrost decomposability across the region, experts were asked to provide quantitative estimates of permafrost carbon change in response to four scenarios of warming (Schuur et al., 2013). For the highest warming scenario (RCP8.5), experts hypothesized that carbon release from permafrost zone soils could be 19 to 45 Pg C by 2040, 162 to 288 Pg C by 2100, and 381 to 616 Pg C by 2300 in CO₂ equivalent¹ using a 100-year CH₄ GWP. The values become 50% larger using a 20-year CH₄ GWP, with one-third to one-half of expected climate forcing coming from CH₄, even though it accounted for only 2.3% of the expected carbon release. Experts projected that two-thirds of this release could be avoided under the lowest warming scenario (RCP2.6; Schuur et al., 2013). According to the experts, changes in tundra and boreal vegetation biomass were smaller, totaling an increase of about 15 Pg C by 2100 under the highest warming scenario (RCP8.5; Abbott et al., 2016). In contrast to soil, assessment of biomass change was more divergent among experts, with one-third of respondents predicting either no change, or even

¹ Carbon dioxide equivalent (CO₂e): Amount of CO₂ that would produce the same effect on the radiative balance of Earth's climate system as another greenhouse gas, such as methane (CH₄) or nitrous oxide (N₂O), on a 100-year timescale. For comparison to units of carbon, each kg CO₂e is equivalent to 0.273 kg C (0.273 = 1/3.67). See Box P.2, p. 12, in the Preface for more details.



a decrease, in biomass over all time intervals and warming scenarios that were considered.

Model Projections

A number of ecosystem models and ESMs have incorporated a first approximation of global permafrost carbon dynamics. Recent key improvements include the physical representation of permafrost soil thermodynamics and the role of environmental controls (particularly the soil freeze-thaw state) in organic carbon decomposition (Koven et al., 2011, 2013; Lawrence et al., 2008). These improved models specifically address processes known to be important in permafrost ecosystems but were missing from earlier model representations. They have been key to forecasting the potential release of permafrost carbon with warming and the impact this release would have on the rate of climate change. Model scenarios show potential carbon release from the permafrost zone ranging from 37 to 174 Pg C by 2100 under the current climate warming trajectory (RCP8.5), with an average across models of 92 ± 17 Pg C (mean \pm standard error [SE]); Burke et al., 2012, 2013; Koven et al., 2011; MacDougall et al., 2012; Schaefer et al., 2011; Schaphoff et al., 2013; Schneider von Deimling et al., 2012; Zhuang et al., 2006). This range is generally consistent with several newer, data-driven modeling approaches that estimated soil carbon releases by 2100 (for RCP8.5) to be 57 Pg C (Koven et al., 2015) and 87 Pg C (Schneider von Deimling et al., 2015), as well as an updated estimate of 102 Pg C from one of the previous models (MacDougall and Knutti, 2016). Furthermore, thawing permafrost carbon is forecasted to affect global climate for centuries. Models that projected emissions further out into the future beyond 2100 estimated additional carbon releases beyond those reported above. More than half of eventual total permafrost carbon emissions projected by the models, on average, would occur after 2100. While carbon releases over these time frames are understandably uncertain, they illustrate the momentum of a warming climate that thaws near-surface permafrost, causing a cascading release of GHGs, as microbes slowly decompose

newly thawed permafrost carbon. The latest model simulations performed either with structural enhancements to better represent permafrost carbon dynamics (Burke et al., 2017) or with common environmental input data (McGuire et al., 2016) show similar soil carbon losses. However, they also indicate the potential for stimulated plant growth (e.g., with increased nutrients, temperature and growing season length, and CO₂ fertilization) to offset some or all of these losses by sequestering new carbon into plant biomass and increasing inputs into the surface soil (McGuire 2018).

Within the wide uncertainty of forecasts, some broader patterns are just beginning to emerge. Models vary widely when predicting the current pool of permafrost carbon, which is the fuel for future carbon emissions in a warmer world. The model average size of the permafrost carbon pool was estimated at 771 ± 100 Pg C (mean \pm SE), about half as much as the measurement-based estimate (Schuur et al., 2015). The difference in the two estimates potentially is related, in part, to the fact that most models represented carbon to a depth of only 3 m. A smaller modeled carbon pool, in principle, could constrain forecasted carbon emissions. Normalizing the emissions estimates from the dynamic models by their initial permafrost carbon pool size, $15 \pm 3\%$ (mean \pm SE) of the initial pool is expected to be lost as GHG emissions by 2100 (Schaefer et al., 2014). However, within these complex models, sensitivity to modeled Arctic climate change and the responses of soil temperature, moisture, and carbon dynamics are important controls over emissions predictions, not just pool size alone (Koven et al., 2013; Lawrence et al., 2012; Slater and Lawrence 2013).

These dynamic models also simultaneously assess the countering influence of plant carbon uptake that may partially offset permafrost carbon release. Warmer temperatures, longer growing seasons, elevated CO₂, and increased nutrients released from decomposing organic carbon all may stimulate plant growth (Shaver et al., 2000). New carbon can be stored in larger plant biomass or deposited into surface soils (Sistla et al., 2013). An intercomparison



of biogeochemical models applied to the permafrost region indicates much larger plant production responses to climate change in the last few decades than observation-based trends in plant productivity (McGuire et al., 2016), suggesting that future plant production responses to changing climate may also be less than models predict. A previous generation of ESMs that did not include permafrost carbon mechanisms but did simulate changes in plant carbon uptake estimated that the vegetation carbon pool could increase by 17 ± 8 Pg C by 2100, with increased plant growth also contributing to new soil carbon accumulation of similar magnitude (Qian et al., 2010). The models reviewed here with permafrost carbon mechanisms also include many of the same mechanisms that stimulate plant growth as the previous generation of models and generally indicate that increased plant carbon uptake will more than offset soil carbon emissions from the permafrost region for several decades as the climate becomes warmer (Koven et al., 2011; MacDougall et al., 2012; Schaefer et al., 2011). Over longer timescales and with continued warming, however, microbial release of carbon overwhelms the capacity for plant carbon uptake, leading to net carbon emissions from permafrost ecosystems to the atmosphere. Modeled carbon emissions projected under various warming scenarios translate into a range of 0.13 to 0.27°C additional global warming by 2100 and up to 0.42°C by 2300, but currently remain one of the least constrained biospheric feedbacks to climate (IPCC 2013).

In many of the model projections previously discussed, CH₄ release is not explicitly represented because fluxes are small. However, the higher GWP of CH₄ makes these emissions relatively more important than on a mass basis alone. Observed short-term temperature sensitivity of CH₄ from the Arctic possibly will have little impact on the global atmospheric CH₄ budget in the long term if future trajectories evolve with the same temperature sensitivity (Sweeney et al., 2016). Global models that include the short-term sensitivities of CH₄ to warming show increased CH₄ emissions with future warming in the northern permafrost region (Gao

et al., 2013; Riley et al., 2011). Yet, these models conclude that if these increased emissions were to occur, they would have little influence on the climate system because of their relatively small magnitude. However, most models do not include abrupt thaw processes (i.e., thawing of ice-rich permafrost) that can result in lake expansion, wetland formation, and massive erosion and exposure to decomposition of previously frozen carbon-rich permafrost. A substantial area of the northern permafrost region is susceptible to abrupt thaw (Olefeldt et al., 2016), which could result in more substantial CH₄ emissions in the future than are currently projected by models. Although the current generation of comprehensive ESMs largely do not include abrupt thaw processes, progress is being made to include surface subsidence that occurs as a result of ground ice loss (Lee et al., 2014). A recent study suggests that the largest CH₄ emission rates will occur around the middle of this century when simulated thermokarst lake extent is at its maximum and when abrupt thaw under thermokarst lakes is taken into account (Schneider von Deimling et al., 2015). Furthermore, the simulated CH₄ fluxes can cause up to 40% of total permafrost-affected radiative forcing in this century. Similarly, no global models currently consider the effects of warming on CH₄ emissions from coastal systems in the Arctic. Models clearly need to include an expanded suite of processes, such as those described previously, that can affect CH₄ dynamics (Xu et al., 2016). These more comprehensive CH₄ models must be effectively benchmarked in a retrospective context (McGuire et al., 2016) before the research community can reduce uncertainty over changes in CH₄ dynamics of the northern permafrost region in response to future warming.

Laboratory-Based Empirical Upscaling

In addition to the amount of carbon stored in permafrost, the decomposability of organic matter determines how much carbon is released to the atmosphere. A recent synthesis using permafrost soil from various circumpolar locations assessed the decomposability of permafrost carbon using long-term (longer than 1 year) aerobic incubation



studies (Schädel et al., 2014). A small fraction of organic matter in thawed permafrost can decompose in weeks to months (Bracho et al., 2016; Dutta et al., 2006; Knoblauch et al., 2013; Lee et al., 2012), but the larger fraction decomposes over decades and even centuries (Schädel et al., 2014). Decade-long potential carbon release as CO₂ was estimated to range from 1% to 76% across a variety of soil types with strong landscape-scale variation. This landscape variation in decomposability was linked to the carbon-to-nitrogen ratio of the bulk organic matter, with higher ratio soils having a greater potential to release carbon during laboratory incubation. The carbon-to-nitrogen ratio is initiated by 1) the type of vegetation carbon that is input to the permafrost soil pool over years, centuries, and even longer; 2) subsequent microbial activity acting on those inputs; and 3) pedogenic processes that help control soil organic matter formation and decay. Upscaling these incubation results using a data-driven modeling approach estimated that soil carbon releases by 2100 (for RCP8.5) will be 57 PgC (Koven et al., 2015).

In a future climate, microbial decomposition of organic matter will happen under a wide variety of environmental conditions that control the amount and form of GHG release. Although temperature control over decomposition is implicit when considering permafrost thaw, northern high latitudes also are characterized by widespread lakes, wetlands, and waterlogged soils. Oxygen-rich conditions are found in drier upland soils where microbial decomposition produces mainly CO₂; oxygen-poor conditions occur in lowlands when ice-rich permafrost thaws, runoff is prevented by the underlying permafrost, and both CO₂ and CH₄ are produced by microbial decomposition. A recent meta-analysis compared GHG release from aerobic and anaerobic laboratory incubation conditions (Schädel et al., 2016). The study quantified that drier, aerobic soil conditions result in three times higher carbon release into the atmosphere compared to the same soil decomposing in wetter, anaerobic soil conditions. Most of the carbon released to the atmosphere was in the form

of CO₂. Under anaerobic conditions, a small amount of carbon also was released as CH₄ (about 5% of total carbon release). Even though CH₄ is the more potent GHG, the much faster decomposition under aerobic conditions dominates the overall carbon release from permafrost. These results show that CO₂ released from drier and oxygen-rich environments will be as or more important than CO₂ and CH₄ released from oxygen-poor environments on a per-unit soil carbon basis. The ultimate effect of these ecosystem types on climate would be scaled, of course, by the landscape coverage of these drier and wetter environments. In addition, these results present laboratory potentials for GHG release from permafrost; there are variety of factors excluded from this technique, such as increased plant biomass input to the soils, changing plant communities, and the priming of old carbon decomposition from new plant litter inputs.

11.5 Societal Drivers, Impacts, and Carbon Management

Forestry is the most widespread human management activity that affects the carbon cycle in the most productive and accessible portion of the boreal forest. This section focuses on a case study of how wildfire management in Alaska has the potential to affect the fire cycle and, consequently, carbon pools via pathways described earlier in the chapter. In Alaska, all lands are classified into fire management planning options depending on the proximity to and density of human infrastructure. The range of management options include “Limited” (i.e., the least amount of management where fire activity is largely observed but not suppressed), “Modified,” “Full,” and “Critical” (i.e., assigned to lands immediately surrounding human settlements and key infrastructure and resources). Each option represents an increasing amount of human intervention to suppress wildfire activity. This case study describes a modeling experiment conducted to determine the impact of changing fire management planning options from the current designation of Limited or Modified to Full protection for all military lands in the greater Fairbanks, Alaska, area. This change

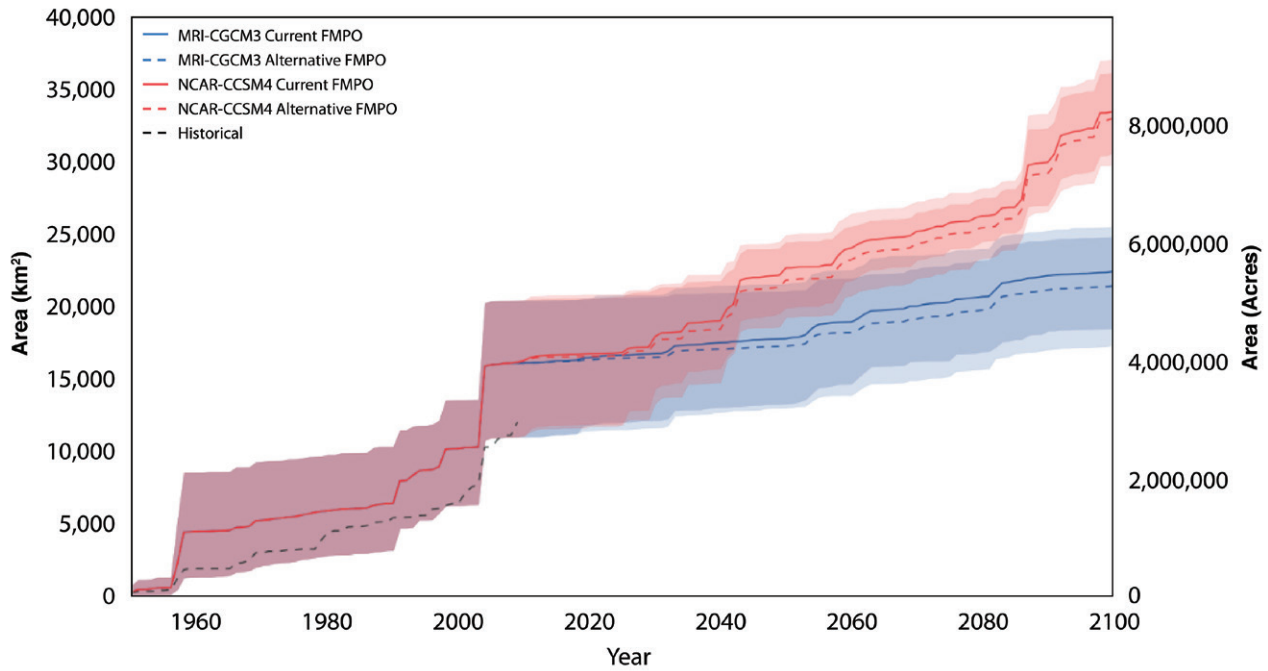


Figure 11.8. Effects of Two Climate Scenarios and Two Management Scenarios for a Subregion of Alaska. Cumulative area burned is modeled for the historical (1950 to 2009) and projected (2010 to 2100) periods for the Upper Tanana Hydrological Basin in interior Alaska near Fairbanks. Model results are presented for scenarios of fire management plan options (FMPO) driven by two Earth System Models: Meteorological Research Institute Coupled Global Climate Model version 3 (MRI-CGCM3) and National Center for Atmospheric Research Community Climate System Model version 4 (NCAR-CCSM4) using the Representative Concentration Pathway (RCP) 8.5 “business-as-usual” emissions scenario. Data presented are means, and shading indicates results from 200 model replicates; black dashed line is the actual fire record through 2010. [Figure source: Redrawn from Breen et al., 2016; Schuur et al., 2016, used with permission.]

in fire management led to a small increase in the projected number of fires per decade because more flammable vegetation (e.g., late successional conifer forests) would be preserved, but, importantly, there was a projected decrease in the cumulative area burned through 2100 compared to the status quo (see Figure 11.8, this page). Depending on the particular climate projection, active fire management (Full) decreased the projected cumulative area burned by 1.5% to 4.4% by 2100 (Breen et al., 2016). Differences in projected climate by 2100 arising from different climate model formulations have a strong impact on cumulative area burned, but fire management does have a small effect no matter the actual climate realized at the end of the century.

In the absence of changing fire severity, the effect on carbon emissions would be exactly proportional to the difference in area burned. However, the somewhat small difference in cumulative area burned, and the proportional resulting effect on the carbon cycle, would need to be considered in context with the additional resources required to change the fire management planning option from the lower to higher level.

11.6 Summary and Outlook

Observation and modeling results synthesized in this chapter suggest that significant changes in the carbon stocks of Arctic and boreal regions may occur with impacts on the atmospheric GHG



budget. These projections primarily are due to the large pools of soil carbon preserved in cold and waterlogged environments vulnerable to a changing climate. This region, which previously has sequestered large amounts of carbon for centuries to millennia, is expected to transform into a one that acts as a net carbon source to the atmosphere over the next decades to centuries in a warming climate. Indeed, Arctic and boreal systems possibly have gone through this transition already.

Carbon offsets by vegetation remain a key part of the net response of this region to warming. Rising Arctic temperatures appear to have increased plant biomass, an effect observed in the tundra over the last three decades using satellite remote-sensing tools (Frost and Epstein 2014; Jia et al., 2003; Ju and Masek 2016) and field observations (Elmendorf et al., 2012; Salmon et al., 2016). A greener Arctic has important implications for regional and global climate because of anticipated increases in atmospheric CO₂ uptake, changes in surface energy, and altered nutrient and water cycling. Despite this long-term trend toward a greener Arctic, a distinct reversal of this trend has been observed for tundra from 2011 to 2014 (Epstein et al., 2015; Phoenix and Bjerke 2016), and the long-term trend is in contrast to boreal regions that show decreased NDVI (browning; Beck and Goetz 2011). Models, in contrast, tend to show consistent increases in plant growth, both in retrospective analyses (McGuire

et al., 2016) and in future forecasts. Documenting changes in biomass with repeat LIDAR measurements is an approach for producing future datasets that help validate or refute model projections of enhanced carbon uptake.

Emerging research on disturbance of permafrost soils by abrupt thaw is another knowledge gap where new information on modeling and landscape mapping is helping to describe patterns and processes (Olefeldt et al., 2016). Abrupt permafrost thaw can trigger destabilization of permafrost and soils at rates much higher than predicted from changes in temperature alone. However, this disturbance occurs at specific points covering only a fraction of the landscape compared to that affected by the influence of temperature increases occurring regionally (Kokelj et al., 2017). New research is critical for highlighting the importance of this subgrid pulse disturbance at the landscape scale and for providing the process-level detail needed but currently lacking in regional- and global-scale models.

Lastly, apparent offsets in carbon flux estimates made by top-down atmospheric measurements and from bottom-up scaling of ecosystem measurements always will be hampered in this region because of the relative scarcity of study locations. New research and satellite capabilities currently focused on high-latitude ecosystems are helping to increase data coverage in this remote and understudied region and will set important baselines against which to measure future change.



SUPPORTING EVIDENCE

KEY FINDING 1

Factors that control terrestrial carbon storage are changing. Surface air temperature change is amplified in high-latitude regions, as seen in the Arctic where temperature rise is about 2.5 times faster than that for the whole Earth. Permafrost temperatures have been increasing over the last 40 years. Disturbance by fire (particularly fire frequency and extreme fire years) is higher now than in the middle of the last century (*very high confidence*).

Description of evidence base

Key Finding 1 is supported by observational evidence from ground-based and remote-sensing measurements. Documented changes in surface air temperatures (data.giss.nasa.gov/gistemp/maps) at a rate higher than the global average are consistent with model projections (Overland et al., 2014) and theory (Pithan and Mauritsen 2014). Permafrost temperatures documented in borehole networks (Biskaborn et al., 2015) are increasing, with the largest absolute temperature increases in cold permafrost regions (Noetzli et al., 2016; Romanovsky et al., 2016). Decadal trends (Flannigan et al., 2009; Kasischke and Turetsky 2006) and paleoecological reconstructions (Kelly et al., 2013) show that area burned, fire frequency, and extreme fire years are higher now than in the first half of the last century and likely will last even longer.

Major uncertainties

Data are not collected uniformly across regions and often are limited by site access. High-latitude observation stations are limited as well. Boreholes often are not located at sites where abrupt permafrost change is evident (Biskaborn et al., 2015). Area burned and other metrics of fire severity can be quantified by remote sensing, but some metrics rely on more limited ground-truth information. Direct measurements of permafrost temperature and fire extend back only 50 to 60 years, but these factors can respond to drivers (e.g., past temperature fluctuations and fire cycles) over even longer time intervals.

Assessment of confidence based on evidence and agreement, including short description of nature of evidence and level of agreement

There is high confidence that drivers of carbon pool change are increasing in strength. In addition, there is very high confidence that surface air temperature change is amplified in high-latitude regions, as seen in the Arctic, where temperature rise is about 2.5 times faster than that for the entire planet. There is high confidence that permafrost temperatures have been rising and that fire disturbance is increasing, although the data records for the latter are shorter compared to temperature records.

Summary sentence or paragraph that integrates the above information

For Key Finding 1, there is very high confidence that drivers of carbon pool changes are increasing in strength. Key Finding 1 is supported by a large amount of observational evidence documented in the peer-reviewed literature. Similar statements previously have been made in assessments of Arctic climate change, including IPCC (2013) and Melillo et al. (2014). Key uncertainties are the length of the data records and the limited ground-based information for variables such as fire severity.



KEY FINDING 2

Soils in the northern circumpolar permafrost zone store 1,460 to 1,600 petagrams of organic carbon (Pg C), almost twice the amount contained in the atmosphere and about an order of magnitude more carbon than contained in plant biomass (55 Pg C), woody debris (16 Pg C), and litter (29 Pg C) in the boreal and tundra biomes combined. This large permafrost zone soil carbon pool has accumulated over hundreds to thousands of years. There are additional reservoirs in subsea permafrost and regions of deep sediments that are not added to this estimate because of data scarcity (*very high confidence*).

Description of evidence base

Key Finding 2 is supported by observational evidence from ground-based measurements of ecosystem carbon pools. Large surface soil carbon pools (to 1 m in depth) have been reported in the literature for decades (e.g., Gorham 1991), with new information on deeper permafrost carbon pools accumulating over the last decade (Hugelius et al., 2014; Schuur et al., 2015; Tarnocai et al., 2009; Zimov et al., 2006). Biomass pools have been synthesized from forest inventory data (Pan et al., 2011), and more recently using remote sensing (Neigh et al., 2013; Reynolds et al., 2012).

Major uncertainties

Soils data are not collected uniformly across regions and often are limited by site access (Johnson et al., 2011). Deep-soil inventories (>1 m in depth) are much more limited than surface soil information (Hugelius et al., 2014). Biomass inventories often exclude unmanaged forests, which are prevalent in this region (Pan et al., 2011). Aboveground plant biomass is best quantified, whereas root biomass most often is estimated (Saugier et al., 2001). Coarse wood and litter also are poorly known carbon pools, and, in some cases, large-scale estimates for these pools are model derived.

Assessment of confidence based on evidence and agreement, including short description of nature of evidence and level of agreement

There is very high confidence that permafrost soil carbon stocks are large and protected currently by waterlogged and frozen soil conditions across much of the region. There is also very high confidence that soil carbon stocks are more than 10 times larger than stocks of carbon in plant biomass, woody debris, and litter pools.

Summary sentence or paragraph that integrates the above information

In Key Finding 2, there is very high confidence that permafrost soil carbon stocks are large and protected currently by waterlogged and frozen soil conditions across much of the region. There is also very high confidence that soil carbon stocks are more than 10 times larger than stocks of carbon in plant biomass, woody debris, and litter pools. This Key Finding is supported by a large amount of observational evidence documented in the peer-reviewed literature. The key uncertainty is the scarcity of measurements for deep permafrost soil carbon relative to those for surface soils, biomass inventories in unmanaged forests, and belowground biomass.

KEY FINDING 3

Following the current trajectory of global and Arctic warming, 5% to 15% of the soil organic carbon stored in the northern circumpolar permafrost zone (mean 10% value equal to 146 to 160 Pg C) is considered vulnerable to release to the atmosphere by the year 2100. The potential carbon loss is likely to be up to an order of magnitude larger than the potential increase in carbon stored in plant biomass regionally under the same changing conditions (*high confidence, very likely*).

**Description of evidence base**

Key Finding 3 is supported by observational and modeling evidence from a range of literature sources and synthesized by Schuur et al. (2015). Observational data include soil incubation studies (Schädel et al., 2014, 2016) and synthesis of field observations (Belshe et al., 2013). Modeling evidence includes Burke et al. (2012), Burke et al. (2013), Koven et al. (2011), MacDougall et al. (2012), Schaefer et al. (2011), Schaphoff et al. (2013), Schneider von Deimling et al. (2012), and Zhuang et al. (2006).

Major uncertainties

This estimate is based largely on estimates of top-down permafrost thaw as a result of a warming climate and does not include abrupt permafrost thaw processes that can expose permafrost soils to higher temperature more rapidly than predicted by top-down thaw alone. Increasing evidence suggests that abrupt thaw processes are likely to be widespread across Arctic and boreal regions (Olefeldt et al., 2016). Waterlogging (oxygen limitation) is common in surface and subsurface soils because of limited infiltration as a result of permafrost. Oxygen limitation slows the decomposition of organic matter, but both wetter or drier soil conditions can result from degrading permafrost at the site scale. Whether high-latitude terrestrial ecosystems will be wetter or drier in the future at the landscape scale is unclear.

Assessment of confidence based on evidence and agreement, including short description of nature of evidence and level of agreement

There is high confidence that permafrost soil carbon stocks are vulnerable to loss with changing climate conditions. This is also true of changing plant biomass but with more uncertainty about the relative magnitude of change.

Estimated likelihood of impact or consequence, including short description of basis of estimate

Thawing permafrost has significant impacts on the global carbon cycle, serving as a source of carbon dioxide (CO₂) and methane (CH₄) emissions. The level of emissions projected here very likely will accelerate the rate of global climate change. Future emissions from the permafrost zone are expected to be a fraction of those from fossil fuels, but they may be similar to current estimates of land-use change emissions.

Summary sentence or paragraph that integrates the above information

For Key Finding 3, there is high confidence that permafrost soil carbon stocks are vulnerable to loss with changing climate conditions. Thawing permafrost has a significant impact on the global carbon cycle, serving as a source of CO₂ and CH₄ emissions. Permafrost-zone emissions levels are expected to be a fraction of those from fossil fuels, but they may be similar to current estimates of land-use change emissions. Key Finding 3 is supported by observational and modeling evidence documented in the peer-reviewed literature. Primary key uncertainties include the influence of abrupt thaw processes that can expose permafrost soil carbon much more rapidly than top-down thawing, which is the process represented by model projections. Also unclear is the degree to which soil waterlogging will increase or decrease as permafrost degrades, which influences the relative release of CO₂ and CH₄.



KEY FINDING 4

Some Earth System Models project that high-latitude carbon releases will be offset largely by increased plant uptake. However, these findings are not always supported by empirical measurements or other assessments, suggesting that structural features of many models are still limited in representing Arctic and boreal zone processes (*very high confidence, very likely*).

Description of evidence base

Key Finding 4 is supported by observational and modeling evidence from a range of literature sources. Modeling results are based on a permafrost carbon model intercomparison project that summarizes the results for 1960 to 2009 for 15 Earth System Models (McGuire et al., 2016) and on an earlier model intercomparison of dynamic global vegetation models for high latitudes (Qian et al., 2010). Observational data include tundra and boreal normalized difference vegetation index (NDVI) trend studies (Beck and Goetz 2011; Epstein et al., 2015) and expert assessment (Abbott et al., 2016).

Major uncertainties

NDVI trends represent changes in canopy and thus are not directly measuring carbon pools; observational datasets at regional to continental scales in the Arctic are scarce, making model evaluation difficult.

Assessment of confidence based on evidence and agreement, including short description of nature of evidence and level of agreement

There is high confidence that model projections are not always in agreement with observational constraints about plant carbon uptake offset.

Estimated likelihood of impact or consequence, including short description of basis of estimate

Thawing permafrost has significant impacts to the global carbon cycle, serving as a source of CO₂ and CH₄ emissions. Plant uptake may offset some of these releases, but the mismatch between models and observations may cause significant over- or underestimates of this offset, as well as shift the timing of significant net carbon change for this region.

Summary sentence or paragraph that integrates the above information

For Key Finding 4, there is high confidence that model projections are not always in agreement with observational constraints about plant carbon uptake offset. Thawing permafrost has significant impacts to the global carbon cycle, serving as a source of CO₂ and CH₄ emissions. Plant uptake may offset some of that release, but the mismatch between models and observations may cause significant over- or underestimates of this offset, as well as shift the timing of significant net carbon change for this region. Key Finding 4 is supported by observational and modeling evidence documented in the peer-reviewed literature. Primary key uncertainties include the response of plant growth to multiple global change factors, including primarily CO₂ fertilization but also rising temperatures, changes in precipitation and growing season length, and changes in species distribution. Other uncertainties include deposition and storage of new carbon into surface soils.



REFERENCES

- Abbott, B. W., J. B. Jones, E. A. G. Schuur, F. S. I. Chapin, W. B. Bowden, M. S. Bret-Harte, H. E. Epstein, M. D. Flannigan, T. K. Harms, T. N. Hollingsworth, M. C. Mack, A. D. McGuire, S. Natali, M., A. V. Rocha, S. E. Tank, M. Turetsky, R., J. E. Vonk, K. P. Wickland, G. R. Aiken, H. D. Alexander, R. M. W. Amon, B. W. Bensoter, Y. Bergeron, K. Bishop, O. Blarquez, B. Bond-Lamberty, A. L. Breen, I. Buffam, Y. Cai, C. Carcaillet, S. K. Carey, J. M. Chen, H. Y. H. Chen, T. R. Christensen, L. W. Cooper, J. H. C. Cornelissen, W. J. de Groot, T. H. DeLuca, E. Dorrepaal, N. Fetcher, J. C. Finlay, B. C. Forbes, N. H. F. French, S. Gauthier, M. P. Girardin, S. J. Goetz, J. G. Goldammer, L. Gouch, P. Grogan, L. Guo, P. E. Higuera, L. Hinzman, F. S. Hu, G. Hugelius, E. E. Jafarov, R. Jandt, J. F. Johnstone, J. Karlsson, E. S. Kasischke, G. Kattner, R. Kelly, F. Keuper, G. W. Kling, P. Kortelainen, J. Kouki, P. Kuhry, H. Laudon, I. Laurion, R. W. Macdonald, P. J. Mann, P. J. Martikainen, J. W. McClelland, U. Molau, S. F. Oberbauer, D. Olefeldt, D. Paré, M.-A. Parisien, S. Payette, C. Peng, O. S. Pokrovsky, E. B. Rastetter, P. A. Raymond, M. K. Reynolds, G. Rein, J. F. Reynolds, M. Robard, B. M. Rogers, C. Schädel, K. Schaefer, I. K. Schmidt, A. Shvidenko, J. Sky, R. G. M. Spencer, G. Starr, R. G. Striegl, R. Teisserenc, L. J. Tranvik, T. Virtanen, J. M. Welker, and S. Zimov, 2016: Biomass offsets little or none of permafrost carbon release from soils, streams, and wildfire: An expert assessment. *Environmental Research Letters*, **11**(3), 034014.
- Alexander, H. D., and M. C. Mack, 2016: A canopy shift in interior Alaskan boreal forests: Consequences for above- and belowground carbon and nitrogen pools during post-fire succession. *Ecosystems*, **19**(1), 98-114, doi: 10.1007/s10021-015-9920-7.
- Alexander, H. D., M. C. Mack, S. Goetz, M. M. Loranty, P. S. A. Beck, K. Earl, S. Zimov, S. Davydov, and C. C. Thompson, 2012: Carbon accumulation patterns during post-fire succession in Cajander larch (*Larix cajanderi*) forests of Siberia. *Ecosystems*, **15**(7), 1065-1082, doi: 10.1007/s10021-012-9567-6.
- AMAP, 2015: AMAP assessment 2015: Methane as an Arctic climate forcer. Arctic Monitoring and Assessment Programme, 139 pp. [<https://www.amap.no/documents/doc/amap-assessment-2015-methane-as-an-arctic-climate-forcer/1285>]
- Balser, A. W., J. B. Jones, and R. Gens, 2014: Timing of retrogressive thaw slump initiation in the Noatak Basin, northwest Alaska, USA. *Journal of Geophysical Research: Earth Surface*, **119**(5), 1106-1120.
- Balshi, M. S., A. D. McGuire, P. Duffy, M. Flannigan, D. W. Kicklighter, and J. Melillo, 2009: Vulnerability of carbon storage in North American boreal forests to wildfires during the 21st century. *Global Change Biology*, **15**(6), 1491-1510, doi: 10.1111/j.1365-2486.2009.01877.x.
- Bastviken, D., L. J. Tranvik, J. A. Downing, P. M. Crill, and A. Enrich-Prast, 2011: Freshwater methane emissions offset the continental carbon sink. *Science*, **331**(6013), 50-50, doi: 10.1126/science.1196808.
- Beck, P. S. A., and S. J. Goetz, 2011: Satellite observations of high northern latitude vegetation productivity changes between 1982 and 2008: Ecological variability and regional differences. *Environmental Research Letters*, **6**(4), 049501.
- Belshe, E. F., E. A. G. Schuur, and B. M. Bolker, 2013: Tundra ecosystems observed to be CO₂ sources due to differential amplification of the carbon cycle. *Ecology Letters*, **16**(10), 1307-1315, doi: 10.1111/ele.12164.
- Berchet, A., P. Bousquet, I. Pison, R. Locatelli, F. Chevallier, J. D. Paris, E. J. Dlugokencky, T. Laurila, J. Hatakka, Y. Viisanen, D. E. J. Worthy, E. Nisbet, R. Fisher, J. France, D. Lowry, V. Ivakhov, and O. Hermansen, 2016: Atmospheric constraints on the methane emissions from the East Siberian Shelf. *Atmospheric Chemistry and Physics*, **16**(6), 4147-4157, doi: 10.5194/acp-16-4147-2016.
- Bergamaschi, P., S. Houweling, A. Segers, M. Krol, C. Frankenberg, R. A. Scheepmaker, E. Dlugokencky, S. C. Wofsy, E. A. Kort, C. Sweeney, T. Schuck, C. Brenninkmeijer, H. Chen, V. Beck, and C. Gerbig, 2013: Atmospheric CH₄ in the first decade of the 21st century: Inverse modeling analysis using SCIAMACHY satellite retrievals and NOAA surface measurements. *Journal of Geophysical Research: Atmospheres*, **118**(13), 7350-7369, doi: 10.1002/jgrd.50480.
- Biskaborn, B. K., J. P. Lanckman, H. Lantuit, K. Elger, D. A. Streletskiy, W. L. Cable, and V. E. Romanovsky, 2015: The new database of the Global Terrestrial Network for Permafrost (GTN-P). *Earth System Science Data*, **7**(2), 245-259, doi: 10.5194/essd-7-245-2015.
- Boby, L. A., E. A. G. Schuur, M. C. Mack, D. Verbyla, and J. F. Johnstone, 2010: Quantifying fire severity, carbon, and nitrogen emissions in Alaska's boreal forest. *Ecological Applications*, **20**(6), 1633-1647, doi: 10.1890/08-2295.1.
- Bockheim, J. G., and K. M. Hinkel, 2007: The importance of "deep" organic carbon in permafrost-affected soils of Arctic Alaska. *Soil Science Society of America Journal*, **71**(6), 1889-1892, doi: 10.2136/sssaj2007.0070N.
- Bond-Lamberty, B., S. D. Peckham, D. E. Ahl, and S. T. Gower, 2007: Fire as the dominant driver of central Canadian boreal forest carbon balance. *Nature*, **450**(7166), 89-92, doi: 10.1038/nature06272.
- Bracho, R., S. Natali, E. Pegoraro, K. G. Crummer, C. Schädel, G. Celis, L. Hale, L. Wu, H. Yin, J. M. Tiedje, K. T. Konstantinidis, Y. Luo, J. Zhou, and E. A. G. Schuur, 2016: Temperature sensitivity of organic matter decomposition of permafrost-region soils during laboratory incubations. *Soil Biology and Biochemistry*, **97**, 1-14, doi: 10.1016/j.soilbio.2016.02.008.
- Breen, A. L., A. Bennett, T. Kurkowski, M. Lindgren, J. Schroder, A. D. McGuire, and T. S. Rupp, 2016: Projecting vegetation and wildfire response to changing climate and fire management in interior Alaska. Alaska Fire Science Consortium Research Summary. 7 pp.



- Bret-Harte, M. S., M. C. Mack, G. R. Shaver, D. C. Huebner, M. Johnston, C. A. Mojica, C. Pizano, and J. A. Reiskind, 2013: The response of Arctic vegetation and soils following an unusually severe tundra fire. *Philosophical Transactions of the Royal Society B: Biological Sciences*, **368**(1624), doi: 10.1098/rstb.2012.0490.
- Brosius, L. S., K. M. Walter Anthony, G. Grosse, J. P. Chanton, L. M. Farquharson, P. P. Overduin, and H. Meyer, 2012: Using the deuterium isotope composition of permafrost meltwater to constrain thermokarst lake contributions to atmospheric CH₄ during the last deglaciation. *Journal of Geophysical Research: Biogeosciences*, **117**(G1), G01022, doi: 10.1029/2011jg001810.
- Brown, C. D., and J. F. Johnstone, 2012: Once burned, twice shy: Repeat fires reduce seed availability and alter substrate constraints on *Picea mariana* regeneration. *Forest Ecology and Management*, **266**, 34-41, doi: 10.1016/j.foreco.2011.11.006.
- Brown, J., O. J. J. Ferrians, J. A. Heginbottom, and E. S. Melnikov, 1997: Circum-Arctic map of permafrost and ground-ice conditions. Circum-Pacific Map 45. U.S. Geological Survey, doi: 10.3133/cp45. [<http://pubs.er.usgs.gov/publication/cp45>]
- Brown, J., O. J. J. Ferrians, J. A. Heginbottom, and E. S. Melnikov, 1998—revised February 2001: Circum-Arctic map of permafrost and ground-ice conditions. Circum-Pacific Map Series CP-45, scale 1:10,000,000, 1 sheet, National Snow and Ice Data Center/World Data Center for Glaciology. [https://nsidc.org/data/docs/fgdc/ggd318_map]
- Bruhwieler, L., E. Dlugokencky, K. Masarie, M. Ishizawa, A. Andrews, J. Miller, C. Sweeney, P. Tans, and D. Worthy, 2014: CarbonTracker-CH₄: An assimilation system for estimating emissions of atmospheric methane. *Atmospheric Chemistry and Physics*, **14**(16), 8269-8293, doi: 10.5194/acp-14-8269-2014.
- Burke, E. J., I. P. Hartley, and C. D. Jones, 2012: Uncertainties in the global temperature change caused by carbon release from permafrost thawing. *Cryosphere*, **6**(5), 1063-1076, doi: 10.5194/tc-6-1063-2012.
- Burke, E. J., C. D. Jones, and C. D. Koven, 2013: Estimating the permafrost-carbon climate response in the CMIP5 climate models using a simplified approach. *Journal of Climate*, **26**(14), 4897-4909, doi: 10.1175/jcli-d-12-00550.1.
- Burke, E. J., A. Ekici, Y. Huang, S. E. Chadburn, C. Huntingford, P. Ciais, P. Friedlingstein, S. Peng, and G. Krinner, 2017: Quantifying uncertainties of permafrost carbon-climate feedbacks. *Biogeosciences*, **14**(12), 3051-3066, doi: 10.5194/bg-14-3051-2017.
- Callaghan, T. V., L. O. Bjorn, Y. Chernov, T. Chapin, T. R. Christensen, B. Huntley, R. A. Ims, M. Johansson, D. Jolly, S. Jonasson, N. Matveyeva, N. Panikov, W. Oechel, and G. Shaver, 2004: Effects on the function of Arctic ecosystems in the short- and long-term perspectives. *AMBIO*, **33**(7), 448-458, doi: 10.1639/0044-7447(2004)033[0448:eotfoa]2.0.co;2.
- Chang, R. Y., C. E. Miller, S. J. Dinardo, A. Karion, C. Sweeney, B. C. Daube, J. M. Henderson, M. E. Mountain, J. Eluszkiewicz, J. B. Miller, L. M. Bruhwiler, and S. C. Wofsy, 2014: Methane emissions from Alaska in 2012 from CARVE airborne observations. *Proceedings of the National Academy of Sciences USA*, **111**(47), 16694-16699, doi: 10.1073/pnas.1412953111.
- Chapin, F. S., G. M. Woodwell, J. T. Randerson, E. B. Rastetter, G. M. Lovett, D. D. Baldocchi, D. A. Clark, M. E. Harmon, D. S. Schimel, R. Valentini, C. Wirth, J. D. Aber, J. J. Cole, M. L. Goulden, J. W. Harden, M. Heimann, R. W. Howarth, P. A. Matson, A. D. McGuire, J. M. Melillo, H. A. Mooney, J. C. Neff, R. A. Houghton, M. L. Pace, M. G. Ryan, S. W. Running, O. E. Sala, W. H. Schlesinger, and E. D. Schulze, 2006: Reconciling carbon-cycle concepts, terminology, and methods. *Ecosystems*, **9**(7), 1041-1050, doi: 10.1007/s10021-005-0105-7.
- Chapin, F. S., P. A. Matson, and P. M. Vitousek, 2011: *Principles of Terrestrial Ecosystem Ecology*. Springer-Verlag, 529 pp.
- Commane, R., J. Lindaas, J. Benmergui, K. A. Luus, R. Y. Chang, B. C. Daube, E. S. Euskirchen, J. M. Henderson, A. Karion, J. B. Miller, S. M. Miller, N. C. Parazoo, J. T. Randerson, C. Sweeney, P. Tans, K. Thoning, S. Veraverbeke, C. E. Miller, and S. C. Wofsy, 2017: Carbon dioxide sources from Alaska driven by increasing early winter respiration from Arctic tundra. *Proceedings of the National Academy of Sciences USA*, **114**(21), 5361-5366, doi: 10.1073/pnas.1618567114.
- Crill, P. M., and B. F. Thornton, 2018: Whither methane in the IPCC process? *Nature Climate Change*, **8**(3), 257-257, doi: 10.1038/s41558-017-0035-3.
- Ding, J., F. Li, G. Yang, L. Chen, B. Zhang, L. Liu, K. Fang, S. Qin, Y. Chen, Y. Peng, C. Ji, H. He, P. Smith, and Y. Yang, 2016: The permafrost carbon inventory on the Tibetan plateau: A new evaluation using deep sediment cores. *Global Change Biology*, **22**(8), 2688-2701, doi: 10.1111/gcb.13257.
- Dixon, R. K., A. M. Solomon, S. Brown, R. A. Houghton, M. C. Trexler, and J. Wisniewski, 1994: Carbon pools and flux of global forest ecosystems. *Science*, **263**(5144), 185-190, doi: 10.1126/science.263.5144.185.
- Dlugokencky, E. J., L. Bruhwiler, J. W. C. White, L. K. Emmons, P. C. Novelli, S. A. Montzka, K. A. Masarie, P. M. Lang, A. M. Crotwell, J. B. Miller, and L. V. Gatti, 2009: Observational constraints on recent increases in the atmospheric CH₄ burden. *Geophysical Research Letters*, **36**(18), doi: 10.1029/2009GL039780.
- Drozhdov, D. S., G. V. Malkova, N. G. Ukraintseva, and Y. V. Korostelev, 2012: Permafrost monitoring of southern tundra landscapes in the Russian European north and west Siberia. In: *Proceedings of the Tenth International Conference on Permafrost. Vol. 2: Translations of Russian Contributions*, Salekhard, Russia, The Northern Publisher, 65-70.
- Dutta, K., E. A. G. Schuur, J. C. Neff, and S. A. Zimov, 2006: Potential carbon release from permafrost soils of northeastern Siberia. *Global Change Biology*, **12**(12), 2336-2351, doi: 10.1111/j.1365-2486.2006.01259.x.



- Ellis, E. C., and N. Ramankutty, 2008: Putting people in the map: Anthropogenic biomes of the world. *Frontiers in Ecology and the Environment*, **6**(8), 439-447, doi: 10.1890/070062.
- Elmendorf, S. C., G. H. R. Henry, R. D. Hollister, R. G. Bjork, N. Boulanger-Lapointe, E. J. Cooper, J. H. C. Cornelissen, T. A. Day, E. Dorrepaal, T. G. Elumeeva, M. Gill, W. A. Gould, J. Harte, D. S. Hik, A. Hofgaard, D. R. Johnson, J. F. Johnstone, I. S. Jonsdottir, J. C. Jorgenson, K. Klanderud, J. A. Klein, S. Koh, G. Kudo, M. Lara, E. Levesque, B. Magnusson, J. L. May, J. A. Mercado-Diaz, A. Michelsen, U. Molau, I. H. Myers-Smith, S. F. Oberbauer, V. G. Onipchenko, C. Rixen, N. Martin Schmidt, G. R. Shaver, M. J. Spasojevic, o. E. orhallsdottir, A. Tolvanen, T. Troxler, C. E. Tweedie, S. Villareal, C.-H. Wahren, X. Walker, P. J. Webber, J. M. Welker, and S. Wipf, 2012: Plot-scale evidence of tundra vegetation change and links to recent summer warming. *Nature Climate Change*, **2**(6), 453-457, doi: 10.1038/nclimate1465.
- Epstein, H. E., M. K. Reynolds, D. A. Walker, U. S. Bhatt, C. J. Tucker, and J. E. Pinzon, 2012: Dynamics of aboveground phytomass of the circumpolar Arctic tundra during the past three decades. *Environmental Research Letters*, **7**(1), 015506, doi: 10.1088/1748-9326/7/1/015506.
- Epstein, H. E., U. S. Bhatt, M. K. Reynolds, D. A. Walker, P. A. Bieniek, C. J. Tucker, J. E. Pinzon, I. H. Myers-Smith, B. C. Forbes, M. Macias-Fauria, N. T. Boelman, and S. K. Sweet, 2015: Tundra greenness. *Arctic Report Card: Update for 2015*. [M. O. Jeffries, J. Richter-Menge, and J. E. Overland, (eds.)]. [<https://www.arctic.noaa.gov/Report-Card/Report-Card-2015/ArtMID/5037/ArticleID/221/Tundra-Greenness>]
- Flannigan, M., B. Stocks, M. Turetsky, and M. Wotton, 2009: Impacts of climate change on fire activity and fire management in the circumboreal forest. *Global Change Biology*, **15**(3), 549-560, doi: 10.1111/j.1365-2486.2008.01660.x.
- French, N. H., L. K. Jenkins, T. V. Loboda, M. Flannigan, R. Jandt, L. L. Bourgeau-Chavez, and M. Whitley, 2015: Fire in Arctic tundra of Alaska: Past fire activity, future fire potential, and significance for land management and ecology. *International Journal of Wildland Fire*, **24**(8), 1045-1061.
- Frost, G. V., and H. E. Epstein, 2014: Tall shrub and tree expansion in Siberian tundra ecotones since the 1960s. *Global Change Biology*, **20**(4), 1264-1277, doi: 10.1111/gcb.12406.
- Gao, X., C. A. Schlosser, A. Sokolov, K. W. Anthony, Q. Zhuang, and D. Kicklighter, 2013: Permafrost degradation and methane: Low risk of biogeochemical climate-warming feedback. *Environmental Research Letters*, **8**(3), doi: 10.1088/1748-9326/8/3/035014.
- Giglio, L., J. T. Randerson, and G. R. van der Werf, 2013: Analysis of daily, monthly, and annual burned area using the fourth-generation Global Fire Emissions Database (GFED4). *Journal of Geophysical Research: Biogeosciences*, **118**(1), 317-328, doi: 10.1002/jgrg.20042.
- Gogineni, P., V. E. Romanovsky, J. Cherry, C. Duguay, S. Goetz, M. T. Jorgenson, and M. Moghaddam, 2014: *Opportunities to Use Remote Sensing in Understanding Permafrost and Related Ecological Characteristics: Report of a Workshop*. The National Academies Press. 1-84 pp. doi: 10.17226/18711.
- Gorham, E., 1991: Northern peatlands: Role in the carbon-cycle and probable responses to climatic warming. *Ecological Applications*, **1**(2), 182-195, doi: 10.2307/1941811.
- Harden, J. W., R. K. Mark, E. T. Sundquist, and R. F. Stallard, 1992: Dynamics of soil carbon during deglaciation of the Laurentide Ice Sheet. *Science*, **258**(5090), 1921-1924, doi: 10.1126/science.258.5090.1921.
- Harden, J. W., S. E. Trumbore, B. J. Stocks, A. Hirsch, S. T. Gower, K. P. O'Neill, and E. S. Kasichke, 2000: The role of fire in the boreal carbon budget. *Global Change Biology*, **6**, 174-184, doi: 10.1046/j.1365-2486.2000.06019.x.
- Harden, J. W., C. D. Koven, C.-L. Ping, G. Hugelius, A. David McGuire, P. Camill, T. Jorgenson, P. Kuhry, G. J. Michaelson, J. A. O'Donnell, E. A. G. Schuur, C. Tarnocai, K. Johnson, and G. Grosse, 2012: Field information links permafrost carbon to physical vulnerabilities of thawing. *Geophysical Research Letters*, **39**(15), doi: 10.1029/2012gl051958.
- Hobbie, S. E., J. P. Schimel, S. E. Trumbore, and J. R. Randerson, 2000: Controls over carbon storage and turnover in high-latitude soils. *Global Change Biology*, **6**, 196-210, doi: 10.1046/j.1365-2486.2000.06021.x.
- Hoy, E. E., M. R. Turetsky, and E. S. Kasichke, 2016: More frequent burning increases vulnerability of Alaskan boreal black spruce forests. *Environmental Research Letters*, **11**(9), 095001, doi: 10.1088/1748-9326/11/9/095001.
- Hu, F. S., P. E. Higuera, J. E. Walsh, W. L. Chapman, P. A. Duffy, L. B. Brubaker, and M. L. Chipman, 2010: Tundra burning in Alaska: Linkages to climatic change and sea ice retreat. *Journal of Geophysical Research: Biogeosciences*, **115**(G4), doi: 10.1029/2009JG001270.
- Hu, F. S., P. E. Higuera, P. Duffy, M. L. Chipman, A. V. Rocha, A. M. Young, R. Kelly, and M. C. Dietze, 2015: Arctic tundra fires: Natural variability and responses to climate change. *Frontiers in Ecology and the Environment*, **13**(7), 369-377, doi: 10.1890/150063.
- Hugelius, G., J. Strauss, S. Zubrzycki, J. W. Harden, E. A. G. Schuur, C. L. Ping, L. Schirrmeyer, G. Grosse, G. J. Michaelson, C. D. Koven, J. A. O'Donnell, B. Elberling, U. Mishra, P. Camill, Z. Yu, J. Palmtag, and P. Kuhry, 2014: Estimated stocks of circumpolar permafrost carbon with quantified uncertainty ranges and identified data gaps. *Biogeosciences*, **11**(23), 6573-6593, doi: 10.5194/bg-11-6573-2014.



- IPCC, 2013: *The Physical Science Basis. Contribution of Working Group I to the Fifth Assessment Report of the Intergovernmental Panel On Climate Change*. [T. Stocker, D. Qin, G.-K. Plattner, M. Tignor, S. Allen, J. Boschung, A. Nauels, Y. Xia, V. Bex, and P. Midgley (eds.).] Cambridge University Press, Cambridge, UK, and New York, NY, USA, 1535 pp.
- James, M., A. G. Lewkowicz, S. L. Smith, and C. M. Miceli, 2013: Multi-decadal degradation and persistence of permafrost in the Alaska Highway corridor, northwest Canada. *Environmental Research Letters*, **8**(4), 045013, doi: 10.1088/1748-9326/8/4/045013.
- Jia, G. J., H. E. Epstein, and D. A. Walker, 2003: Greening of Arctic Alaska, 1981–2001. *Geophysical Research Letters*, **30**(20), doi: 10.1029/2003GL018268.
- Jiang, Y., A. V. Rocha, J. A. O'Donnell, J. A. Drysdale, E. B. Rastetter, G. R. Shaver, and Q. Zhuang, 2015: Contrasting soil thermal responses to fire in Alaskan tundra and boreal forest. *Journal of Geophysical Research: Earth Surface*, **120**(2), 363–378, doi: 10.1002/2014JF003180.
- Jobbágy, E. G., and R. B. Jackson, 2000: The vertical distribution of soil organic carbon and its relation to climate and vegetation. *Ecological Applications*, **10**(2), 423–436, doi: 10.1890/1051-0761(2000)010[0423:TVDOS0]2.0.CO;2.
- Johnson, E. A., 1992: *Fire and Vegetation Dynamics. Studies from the North American Boreal Forest*. Cambridge University Press.
- Johnson, K. D., J. Harden, A. D. McGuire, N. B. Bliss, J. G. Bockheim, M. Clark, T. Nettleton-Hollingsworth, M. T. Jorgenson, E. S. Kane, M. Mack, J. O'Donnell, C.-L. Ping, E. A. G. Schuur, M. R. Turetsky, and D. W. Valentine, 2011: Soil carbon distribution in Alaska in relation to soil-forming factors. *Geoderma*, **167–168**, 71–84, doi: 10.1016/j.geoderma.2011.10.006.
- Johnstone, J., L. Boby, E. Tissier, M. Mack, D. Verbyla, and X. Walker, 2009: Postfire seed rain of black spruce, a semiserotinous conifer, in forests of interior Alaska. *Canadian Journal of Forest Research*, **39**(8), 1575–1588, doi: 10.1139/X09-068.
- Johnstone, J. F., T. S. Rupp, M. Olson, and D. Verbyla, 2011: Modeling impacts of fire severity on successional trajectories and future fire behavior in Alaskan boreal forests. *Landscape Ecology*, **26**(4), 487–500, doi: 10.1007/s10980-011-9574-6.
- Johnstone, J. F., F. S. Chapin, T. N. Hollingsworth, M. C. Mack, V. Romanovsky, and M. Turetsky, 2010: Fire, climate change, and forest resilience in interior Alaska. *Canadian Journal of Forest Research*, **40**(7), 1302–1312, doi: 10.1139/X10-061.
- Jones, B., C. Kolden, R. Jandt, J. Abatzoglou, F. Urban, and C. Arp, 2009: Fire behavior, weather, and burn severity of the 2007 Anaktuvuk River tundra fire, North Slope, Alaska. *Arctic, Antarctic, and Alpine Research*, **41**(3), 309–316, doi: 10.1657/1938-4246-41.3.309.
- Jones, B. M., G. Grosse, C. D. Arp, E. Miller, L. Liu, D. J. Hayes, and C. F. Larsen, 2015: Recent Arctic tundra fire initiates widespread thermokarst development. *Scientific Reports*, **5**, 15865, doi: 10.1038/srep15865.
- Jones, M. C., J. Harden, J. O'Donnell, K. Manies, T. Jorgenson, C. Treat, and S. Ewing, 2017: Rapid carbon loss and slow recovery following permafrost thaw in boreal peatlands. *Global Change Biology*, **23**(3), 1109–1127, doi: 10.1111/gcb.13403.
- Jorgenson, M. T., 2013: *Landscape-Level Ecological Mapping of Northern Alaska and Field Site Photography*. Arctic Landscape Conservation Cooperative, US Fish and Wildlife Service. 48 pp. [http://arcticlcc.org/assets/products/ALCC2011-06/reports/NorthernAK_Landscape_Mapping_Field_Photos_Final_RPT.pdf]
- Jorgenson, M. T., and J. Brown, 2005: Classification of the Alaskan Beaufort Sea coast and estimation of carbon and sediment inputs from coastal erosion. *Geo-Marine Letters*, **25**(2), 69–80, doi: 10.1007/s00367-004-0188-8.
- Jorgenson, M. T., Y. L. Shur, and E. R. Pullman, 2006: Abrupt increase in permafrost degradation in Arctic Alaska. *Geophysical Research Letters*, **33**(2), L02503, doi: 10.1029/2005gl024960.
- Jorgenson, M. T., J. W. Harden, M. Kanevskiy, J. A. O'Donnell, K. P. Wickland, S. A. Ewing, K. L. Manies, Q. Zhuang, Y. Shur, R. Striegl, and J. Koch, 2013: Reorganization of vegetation, hydrology and soil carbon after permafrost degradation across heterogeneous boreal landscapes. *Environmental Research Letters*, **8**(3), 035017, doi: 10.1088/1748-9326/8/3/035017.
- Ju, J., and J. G. Masek, 2016: The vegetation greenness trend in Canada and US Alaska from 1984–2012 Landsat data. *Remote Sensing of Environment*, **176**, 1–16, doi: 10.1016/j.rse.2016.01.001.
- Juncher Jørgensen, C., K. M. Lund Johansen, A. Westergaard-Nielsen, and B. Elberling, 2015: Net regional methane sink in high Arctic soils of northeast Greenland. *Nature Geoscience*, **8**(1), 20–23, doi: 10.1038/ngeo2305.
- Kasischke, E. S., and J. F. Johnstone, 2005: Variation in postfire organic layer thickness in a black spruce forest complex in interior Alaska and its effects on soil temperature and moisture. *Canadian Journal of Forest Research*, **35**(9), 2164–2177, doi: 10.1139/x05-159.
- Kasischke, E. S., and M. R. Turetsky, 2006: Recent changes in the fire regime across the North American boreal region—spatial and temporal patterns of burning across Canada and Alaska. *Geophysical Research Letters*, **33**(9), doi: 10.1029/2006GL025677.
- Kasischke, E. S., N. L. Christensen, and B. J. Stocks, 1995: Fire, global warming, and the carbon balance of boreal forests. *Ecological Applications*, **5**(2), 437–451, doi: 10.2307/1942034.
- Kelly, R., M. L. Chipman, P. E. Higuera, I. Stefanova, L. B. Brubaker, and F. S. Hu, 2013: Recent burning of boreal forests exceeds fire regime limits of the past 10,000 years. *Proceedings of the National Academy of Sciences USA*, **110**(32), 13055–13060, doi: 10.1073/pnas.1305069110.



- Kirschke, S., P. Bousquet, P. Ciais, M. Saunois, J. G. Canadell, E. J. Dlugokencky, P. Bergamaschi, D. Bergmann, D. R. Blake, L. Bruhwiler, P. Cameron-Smith, S. Castaldi, F. Chevallier, L. Feng, A. Fraser, M. Heimann, E. L. Hodson, S. Houweling, B. Josse, P. J. Fraser, P. B. Krummel, J.-F. Lamarque, R. L. Langenfelds, C. Le Quere, V. Naik, S. O'Doherty, P. I. Palmer, I. Pison, D. Plummer, B. Poulter, R. G. Prinn, M. Rigby, B. Ringeval, M. Santini, M. Schmidt, D. T. Shindell, I. J. Simpson, R. Spahni, L. P. Steele, S. A. Strode, K. Sudo, S. Szopa, G. R. van der Werf, A. Voulgarakis, M. van Weele, R. F. Weiss, J. E. Williams, and G. Zeng, 2013: Three decades of global methane sources and sinks. *Nature Geoscience*, **6**(10), 813-823, doi: 10.1038/ngeo1955.
- Knoblauch, C., C. Beer, A. Sosnin, D. Wagner, and E.-M. Pfeiffer, 2013: Predicting long-term carbon mineralization and trace gas production from thawing permafrost of northeast Siberia. *Global Change Biology*, **19**(4), 1160-1172, doi: 10.1111/gcb.12116.
- Kohnert, K., A. Serafimovich, S. Metzger, J. Hartmann, and T. Sachs, 2017: Strong geologic methane emissions from discontinuous terrestrial permafrost in the Mackenzie Delta, Canada. *Science Report*, **7**(1), 5828, doi: 10.1038/s41598-017-05783-2.
- Kokelj, S. V., T. C. Lantz, J. Tunnicliffe, R. Segal, and D. Lacelle, 2017: Climate-driven thaw of permafrost preserved glacial landscapes, northwestern Canada. *Geology*, **45**(4), 371-374, doi: 10.1130/g38626.1.
- Koven, C. D., W. J. Riley, and A. Stern, 2013: Analysis of permafrost thermal dynamics and response to climate change in the CMIP5 Earth system models. *Journal of Climate*, **26**(6), 1877-1900, doi: 10.1175/jcli-d-12-00228.1.
- Koven, C. D., B. Ringeval, P. Friedlingstein, P. Ciais, P. Cadule, D. Khvorostyanov, G. Krinner, and C. Tarnocai, 2011: Permafrost carbon-climate feedbacks accelerate global warming. *Proceedings of the National Academy of Sciences USA*, **108**(36), 14769-14774, doi: 10.1073/pnas.1103910108.
- Koven, C. D., E. A. G. Schuur, C. Schädel, T. J. Bohn, E. J. Burke, G. Chen, X. Chen, P. Ciais, G. Grosse, J. W. Harden, D. J. Hayes, G. Hugelius, E. E. Jafarov, G. Krinner, P. Kuhry, D. M. Lawrence, A. H. MacDougall, S. S. Marchenko, A. D. McGuire, S. M. Natali, D. J. Nicolsky, D. Olefeldt, S. Peng, V. E. Romanovsky, K. M. Schaefer, J. Strauss, C. C. Treat, and M. Turetsky, 2015: A simplified, data-constrained approach to estimate the permafrost carbon-climate feedback. *Philosophical Transactions of the Royal Society A: Mathematical, Physical and Engineering Sciences*, **373**(2054), doi: 10.1098/rsta.2014.0423.
- Kurz, W. A., G. Stinson, G. J. Rampley, C. C. Dymond, and E. T. Neilson, 2008: Risk of natural disturbances makes future contribution of Canada's forests to the global carbon cycle highly uncertain. *Proceedings of the National Academy of Sciences USA*, **105**(5), 1551-1555, doi: 10.1073/pnas.0708133105.
- Lara, M. J., H. Genet, A. D. McGuire, E. S. Euskirchen, Y. Zhang, D. R. Brown, M. T. Jorgenson, V. Romanovsky, A. Breen, and W. R. Bolton, 2016: Thermokarst rates intensify due to climate change and forest fragmentation in an Alaskan boreal forest lowland. *Global Change Biology*, **22**(2), 816-829, doi: 10.1111/gcb.13124.
- Lawrence, D. M., A. G. Slater, and S. C. Swenson, 2012: Simulation of present-day and future permafrost and seasonally frozen ground conditions in CCSM4. *Journal of Climate*, **25**(7), 2207-2225, doi: 10.1175/jcli-d-11-00334.1.
- Lawrence, D. M., A. G. Slater, V. E. Romanovsky, and D. J. Nicolsky, 2008: Sensitivity of a model projection of near-surface permafrost degradation to soil column depth and representation of soil organic matter. *Journal of Geophysical Research: Earth Surface*, **113**(F2), F02011, doi: 10.1029/2007JF000883.
- Lee, H., S. C. Swenson, A. G. Slater, and D. M. Lawrence, 2014: Effects of excess ground ice on projections of permafrost in a warming climate. *Environmental Research Letters*, **9**(12), 124006, doi: 10.1088/1748-9326/9/12/124006.
- Lee, H., E. A. G. Schuur, K. S. Inglett, M. Lavoie, and J. P. Chanton, 2012: The rate of permafrost carbon release under aerobic and anaerobic conditions and its potential effects on climate. *Global Change Biology*, **18**(2), 515-527, doi: 10.1111/j.1365-2486.2011.02519.x.
- Liljedahl, A. K., J. Boike, R. P. Daanen, A. N. Fedorov, G. V. Frost, G. Grosse, L. D. Hinzman, Y. Iijima, J. C. Jorgenson, N. Matveyeva, M. Necsoiu, M. K. Reynolds, V. E. Romanovsky, J. Schulla, K. D. Tape, D. A. Walker, C. J. Wilson, H. Yabuki, and D. Zona, 2016: Pan-Arctic ice-wedge degradation in warming permafrost and its influence on tundra hydrology. *Nature Geoscience*, **9**(4), 312-318, doi: 10.1038/ngeo2674.
- Liu, L., K. Schaefer, T. Zhang, and J. Wahr, 2012: Estimating 1992-2000 average active layer thickness on the Alaskan north slope from remotely sensed surface subsidence. *Journal of Geophysical Research: Earth Surface*, **117**(F1), doi: 10.1029/2011JF002041.
- Loisel, J., Z. Yu, D. W. Beilman, P. Camill, J. Alm, M. J. Amesbury, D. Anderson, S. Andersson, C. Bochicchio, K. Barber, L. R. Belyea, J. Bunbury, F. M. Chambers, D. J. Charman, F. De Vleeschouwer, B. Fialkiewicz-Koziele, S. A. Finkelstein, M. Galka, M. Garneau, D. Hammarlund, W. Hinchcliffe, J. Holmquist, P. Hughes, M. C. Jones, E. S. Klein, U. Kokfelt, A. Korhola, P. Kuhry, A. Lamarre, M. Lamentowicz, D. Large, M. Lavoie, G. MacDonald, G. Magnan, M. Mäkilä, G. Mallon, P. Mathijssen, D. Mauquoy, J. McCarroll, T. R. Moore, J. Nichols, B. O'Reilly, P. Oksanen, M. Packalen, D. Peteet, P. J. H. Richard, S. Robinson, T. Ronkainen, M. Rundgren, A. B. K. Sannel, C. Tarnocai, T. Thom, E.-S. Tuittila, M. Turetsky, M. Välranta, M. van der Linden, B. van Geel, S. van Bellen, D. Vitt, Y. Zhao, and W. Zhou, 2014: A database and synthesis of northern peatland soil properties and Holocene carbon and nitrogen accumulation. *The Holocene*, **24**(9), 1028-1042, doi: 10.1177/0959683614538073.
- LTER, 2007: *The Decadal Plan for LTER—Integrative Science for Society and the Environment: A Plan for Science, Education, and Cyber-infrastructure in the U.S. Long-Term Ecological Research Network*. Publication Series No. 24, U.S. Long Term Ecological Research Network Office. [https://lternet.edu/wp-content/themes/ndic/library/pdf/reports/TheDecadalPlanReformattedForBook_with_citation.pdf]



- Luo, G. B., G. L. Zhang, and Z. T. Gong, 2000: A real evaluation of organic carbon pools in cryic soils of China. In: *Global Climate Change and Cold Regions Ecosystems*. [R. Lal, J. M. Kimble, and B. A. Stewart (eds.)]. Lewis Publisher, pp. 211-222.
- MacDougall, A. H., C. A. Avis, and A. J. Weaver, 2012: Significant contribution to climate warming from the permafrost carbon feedback. *Nature Geoscience*, **5**(10), 719-721, doi: 10.1038/ngeo1573.
- MacDougall, A. H., and R. Knutti, 2016: Projecting the release of carbon from permafrost soils using a perturbed parameter ensemble modelling approach. *Biogeosciences*, **13**(7), 2123-2136, doi: 10.5194/bg-13-2123-2016.
- Mack, M. C., M. S. Bret-Harte, T. N. Hollingsworth, R. R. Jandt, E. A. G. Schuur, G. R. Shaver, and D. L. Verbyla, 2011: Carbon loss from an unprecedented Arctic tundra wildfire. *Nature*, **475**(7357), 489-492, doi: 10.1038/nature10283.
- Malkova, G. D., M. O. Leibman, D. S. Drozdov, V. I. Khomutova, A. A. Guubarkov, and A. B. Sherstyukov, 2014: Impact of climate change on natural terrestrial systems. In: *The Second Assessment Report of Roshydromet on Climate Change and Their Consequences on the Territory of the Russian Federation*. [M. Roshydromet (ed.)]. pp 410-458. [http://downloads.igce.ru/publications/OD_2_2014/v2014/htm/]
- Mann, D. H., T. Scott Rupp, M. A. Olson, and P. A. Duffy, 2012: Is Alaska's boreal forest now crossing a major ecological threshold? *Arctic, Antarctic, and Alpine Research*, **44**(3), 319-331, doi: 10.1657/1938-4246-44.3.319.
- Margolis, H. A., R. F. Nelson, P. M. Montesano, A. Beaudoin, G. Sun, H.-E. Andersen, and M. A. Wulder, 2015: Combining satellite LIDAR, airborne LIDAR, and ground plots to estimate the amount and distribution of aboveground biomass in the boreal forest of North America. *Canadian Journal of Forest Research*, **45**(7), 838-855, doi: 10.1139/cjfr-2015-0006.
- Mastepanov, M., C. Sigsgaard, E. J. Dlugokencky, S. Houweling, L. Strom, M. P. Tamstorf, and T. R. Christensen, 2008: Large tundra methane burst during onset of freezing. *Nature*, **456**(7222), 628-630, doi: 10.1038/nature07464.
- McGuire, A. D., J. M. Melillo, D. W. Kicklighter, Y. Pan, X. Xiao, J. Helfrich, B. Moore, C. J. Vorosmarty, and A. L. Schloss, 1997: Equilibrium responses of global net primary production and carbon storage to doubled atmospheric carbon dioxide: Sensitivity to changes in vegetation nitrogen concentration. *Global Biogeochemical Cycles*, **11**(2), 173-189, doi: 10.1029/97GB00059.
- McGuire, A. D., L. G. Anderson, T. R. Christensen, S. Dallimore, L. D. Guo, D. J. Hayes, M. Heimann, T. D. Lorenson, R. W. Macdonald, and N. Roulet, 2009: Sensitivity of the carbon cycle in the Arctic to climate change. *Ecological Monographs*, **79**(4), 523-555, doi: 10.1890/08-2025.1.
- McGuire, A. D., T. R. Christensen, D. Hayes, A. Heroult, E. Euskirchen, J. S. Kimball, C. Koven, P. Laflour, P. A. Miller, W. Oechel, P. Peylin, M. Williams, and Y. Yi, 2012: An assessment of the carbon balance of Arctic tundra: Comparisons among observations, process models, and atmospheric inversions. *Biogeosciences*, **9**(8), 3185-3204, doi: 10.5194/bg-9-3185-2012.
- McGuire, A. D., C. Koven, D. M. Lawrence, J. S. Clein, J. Xia, C. Beer, E. Burke, G. Chen, X. Chen, C. Delire, E. Jafarov, A. H. MacDougall, S. Marchenko, D. Nicolsky, S. Peng, A. Rinke, K. Saito, W. Zhang, R. Alkama, T. J. Bohn, P. Ciais, B. Decharme, A. Ekici, I. Gouttevin, T. Hajima, D. J. Hayes, D. Ji, G. Krinner, D. P. Lettenmaier, Y. Luo, P. A. Miller, J. C. Moore, V. Romanovsky, C. Schädel, K. Schaefer, E. A. G. Schuur, B. Smith, T. Sueyoshi, and Q. Zhuang, 2016: Variability in the sensitivity among model simulations of permafrost and carbon dynamics in the permafrost region between 1960 and 2009. *Global Biogeochemical Cycles*, **30**(7), 1015-1037, doi: 10.1002/2016gb005405.
- McGuire, A. D., D. M. Lawrence, C. Koven, J. S. Clein, E. Burke, G. Chen, E. Jafarov, A. H. MacDougall, S. Marchenko, D. Nicolsky, S. Peng, A. Rinke, P. Ciais, I. Gouttevin, D. J. Hayes, D. Ji, G. Krinner, J. C. Moore, V. Romanovsky, C. Schadel, K. Schaefer, E. A. G. Schuur, and Q. Zhuang, 2018: Dependence of the evolution of carbon dynamics in the northern permafrost region on the trajectory of climate change. *Proceedings of the National Academy of Sciences USA*, **115**(15), 3882-3887, doi: 10.1073/pnas.1719903115.
- Melillo, J. M., T.C. Richmond, and E. G.W. Yohe (eds.), 2014: *Climate Change Impacts in the United States: The Third National Climate Assessment*. U.S. Global Change Research Program, 841, [<http://nca2014.globalchange.gov>]
- Melnikov, V. P., D. S. Drozdov, and V. V. Pendin, 2015: Arctic permafrost: Dynamics, risks, problems and solutions. In: *Moscow, XXII International Science-Practical Conference: New Ideas In Earth Science*, 123-138.
- Melvin, A. M., M. C. Mack, J. F. Johnstone, A. David McGuire, H. Genet, and E. A. G. Schuur, 2015: Differences in ecosystem carbon distribution and nutrient cycling linked to forest tree species composition in a mid-successional boreal forest. *Ecosystems*, **18**(8), 1472-1488, doi: 10.1007/s10021-015-9912-7.
- Miller, S. M., C. E. Miller, R. Commane, R. Y. W. Chang, S. J. Dinardo, J. M. Henderson, A. Karion, J. Lindaas, J. R. Melton, J. B. Miller, C. Sweeney, S. C. Wofsy, and A. M. Michalak, 2016: A multiyear estimate of methane fluxes in Alaska from CARVE atmospheric observations. *Global Biogeochemical Cycles*, **30**(10), 1441-1453, doi: 10.1002/2016GB005419.
- Mishra, U., and W. J. Riley, 2012: Alaskan soil carbon stocks: Spatial variability and dependence on environmental factors. *Biogeosciences*, **9**(9), 3637-3645, doi: 10.5194/bg-9-3637-2012.
- Mu, C., T. Zhang, Q. Wu, X. Peng, B. Cao, X. Zhang, B. Cao, and G. Cheng, 2015: Editorial: Organic carbon pools in permafrost regions on the Qinghai-Xizang (Tibetan) Plateau. *Cryosphere*, **9**(2), 479-486, doi: 10.5194/tc-9-479-2015.



- Mu, M., J. T. Randerson, G. R. van der Werf, L. Giglio, P. Kasibhatla, D. Morton, G. J. Collatz, R. S. DeFries, E. J. Hyer, E. M. Prins, D. W. T. Griffith, D. Wunch, G. C. Toon, V. Sherlock, and P. O. Wennberg, 2011: Daily and 3-hourly variability in global fire emissions and consequences for atmospheric model predictions of carbon monoxide. *Journal of Geophysical Research: Atmospheres*, **116**(D24), doi: 10.1029/2011JD016245.
- Neigh, C. S. R., R. F. Nelson, K. J. Ranson, H. A. Margolis, P. M. Montesano, G. Sun, V. Kharuk, E. Næsset, M. A. Wulder, and H.-E. Andersen, 2013: Taking stock of circumboreal forest carbon with ground measurements, airborne and spaceborne LIDAR. *Remote Sensing of Environment*, **137**, 274-287, doi: 10.1016/j.rse.2013.06.019.
- Noetzli, J., H. H. Christiansen, M. Guglielmin, V. E. Romanovsky, N. I. Shiklomanov, S. L. Smith, and L. Zhao, 2016: Global climates: Cryosphere, permafrost thermal state. In: *State of the Climate in 2015*. Bulletin of the American Meteorological Society, pp. S20-S22.
- NOAA, 2012: *Arctic Report Card: Update for 2012*. [M. O. Jeffries, J. Richter-Menge, and J. E. Overland (eds.)].
- Olefeldt, D., M. R. Turetsky, P. M. Crill, and A. D. McGuire, 2013: Environmental and physical controls on northern terrestrial methane emissions across permafrost zones. *Global Change Biology*, **19**(2), 589-603, doi: 10.1111/gcb.12071.
- Olefeldt, D., S. Goswami, G. Grosse, D. Hayes, G. Hugelius, P. Kuhry, A. D. McGuire, V. E. Romanovsky, A. B. K. Sannel, E. A. G. Schuur, and M. R. Turetsky, 2016: Circumpolar distribution and carbon storage of thermokarst landscapes. *Nature Communications*, **7**, 13043, doi: 10.1038/ncomms13043.
- Olson, D. M., E. Dinerstein, E. D. Wikramanayake, N. D. Burgess, G. V. N. Powell, E. C. Underwood, J. A. D'Amico, I. Itoua, H. E. Strand, J. C. Morrison, C. J. Loucks, T. F. Allnutt, T. H. Ricketts, Y. Kura, J. F. Lamoreux, W. W. Wettengel, P. Hedao, and K. R. Kassem, 2001: Terrestrial ecoregions of the world: A new map of life on Earth. *BioScience*, **51**(11), 933, doi: 10.1641/0006-3568(2001)051[0933:teotwa]2.0.co;2.
- Overland, J. E., M. Wang, J. E. Walsh, and J. C. Stroeve, 2014: Future Arctic climate changes: Adaptation and mitigation time scales. *Earth's Future*, **2**(2), 68-74, doi: 10.1002/2013EF000162.
- Pan, Y., R. A. Birdsey, J. Fang, R. Houghton, P. E. Kauppi, W. A. Kurz, O. L. Phillips, A. Shvidenko, S. L. Lewis, J. G. Canadell, P. Ciaia, R. B. Jackson, S. W. Pacala, A. D. McGuire, S. Piao, A. Rautiainen, S. Sitch, and D. Hayes, 2011: A large and persistent carbon sink in the world's forests. *Science*, **333**(6045), 988-993, doi: 10.1126/science.1201609.
- Parazoo, N. C., R. Commane, S. C. Wofsy, C. D. Koven, C. Sweeney, D. M. Lawrence, J. Lindaas, R. Y.-W. Chang, and C. E. Miller, 2016: Detecting regional patterns of changing CO₂ flux in Alaska. *Proceedings of the National Academy of Sciences USA*, **113**(28), 7733-7738, doi: 10.1073/pnas.1601085113.
- Pastick, N. J., M. T. Jorgenson, B. K. Wylie, B. J. Minsley, L. Ji, M. A. Walvoord, B. D. Smith, J. D. Abraham, and J. R. Rose, 2013: Extending airborne electromagnetic surveys for regional active layer and permafrost mapping with remote sensing and ancillary data, Yukon Flats Ecoregion, central Alaska. *Permafrost and Periglacial Processes*, **24**(3), 184-199, doi: 10.1002/ppp.1775.
- Phoenix, G. K., and J. W. Bjerke, 2016: Arctic browning: Extreme events and trends reversing Arctic greening. *Global Change Biology*, **22**(9), 2960-2962, doi: 10.1111/gcb.13261.
- Ping, C. L., G. J. Michaelson, J. M. Kimble, V. E. Romanovsky, Y. L. Shur, D. K. Swanson, and D. A. Walker, 2008: Cryogenesis and soil formation along a bioclimate gradient in Arctic North America. *Journal of Geophysical Research: Biogeosciences*, **113**(G3), doi: 10.1029/2008jg000744.
- Pithan, F., and T. Mauritsen, 2014: Arctic amplification dominated by temperature feedbacks in contemporary climate models. *Nature Geoscience*, **7**(3), 181-184, doi: 10.1038/ngeo2071.
- Post, W. M., W. R. Emanuel, P. J. Zinke, and A. G. Stangenberger, 1982: Soil carbon pools and world life zones. *Nature*, **298**, 156-159, doi: 10.1038/298156a0.
- Potter, C. S., and S. A. Klooster, 1997: Global model estimates of carbon and nitrogen storage in litter and soil pools: Response to changes in vegetation quality and biomass allocation. *Tellus B: Chemical and Physical Meteorology*, **49**(1), 1-17, doi: 10.3402/tellusb.v49i1.15947.
- Qian, H., R. Joseph, and N. Zeng, 2010: Enhanced terrestrial carbon uptake in the northern high latitudes in the 21st century from the coupled carbon cycle climate model intercomparison project model projections. *Global Change Biology*, **16**(2), 641-656, doi: 10.1111/j.1365-2486.2009.01989.x.
- Rachold, V., M. N. Grigoriev, F. E. Are, S. Solomon, E. Reimnitz, H. Kassens, and M. Antonow, 2000: Coastal erosion vs riverine sediment discharge in the Arctic Shelf seas. *International Journal of Earth Sciences*, **89**(3), 450-460, doi: 10.1007/s005310000113.
- Rachold, V., H. Eicken, V. V. Gordeev, M. N. Grigoriev, H. W. Hubberten, A. P. Lisitzin, V. P. Shevchenko, and L. Schirrmeister, 2004: Modern terrigenous organic carbon input to the Arctic Ocean. In: *The Organic Carbon Cycle in the Arctic Ocean*. [R. Stein and R. W. MacDonald (eds.)]. Springer Berlin Heidelberg, 33-55 pp.
- Rachold, V., D. Y. Bolshiyaynov, M. N. Grigoriev, H.-W. Hubberten, R. Junker, V. V. Kunitsky, F. Merker, P. Overduin, and W. Schneider, 2007: Nearshore Arctic subsea permafrost in transition. *Eos, Transactions American Geophysical Union*, **88**(13), 149-150, doi: 10.1029/2007EO130001.
- Racine, C. H., R. Jandt, C. P. Meyer, and J. Dennis, 2004: Tundra fire and vegetation change along a hillslope on the Seward Peninsula, Alaska, USA. *Arctic, Antarctic, and Alpine Research*, **36**(1), 1-10, doi: 10.1657/1523-0430(2004)036[0001:tfavca]2.0.co;2.



- Randerson, J. T., Y. Chen, G. R. van der Werf, B. M. Rogers, and D. C. Morton, 2012: Global burned area and biomass burning emissions from small fires. *Journal of Geophysical Research: Biogeosciences*, **117**(G4), doi: 10.1029/2012JG002128.
- Randerson, J. T., H. Liu, M. G. Flanner, S. D. Chambers, Y. Jin, P. G. Hess, G. Pfister, M. C. Mack, K. K. Treseder, L. R. Welp, F. S. Chapin, J. W. Harden, M. L. Goulden, E. Lyons, J. C. Neff, E. A. G. Schuur, and C. S. Zender, 2006: The impact of boreal forest fire on climate warming. *Science*, **314**(5802), 1130-1132, doi: 10.1126/science.1132075.
- Raynolds, M. K., D. A. Walker, H. E. Epstein, J. E. Pinzon, and C. J. Tucker, 2012: A new estimate of tundra-biome phytomass from trans-Arctic field data and AVHRR NDVI. *Remote Sensing Letters*, **3**(5), 403-411, doi: 10.1080/01431161.2011.609188.
- Raz-Yaseef, N., M. S. Torn, Y. Wu, D. P. Billesbach, A. K. Liljedahl, T. J. Kneafsey, V. E. Romanovsky, D. R. Cook, and S. D. Wullschleger, 2016: Large CO₂ and CH₄ emissions from polygonal tundra during spring thaw in northern Alaska. *Geophysical Research Letters*, **44**(1), 504-513, doi: 10.1002/2016GL071220.
- Riley, W. J., Z. M. Subin, D. M. Lawrence, S. C. Swenson, M. S. Torn, L. Meng, N. M. Mahowald, and P. Hess, 2011: Barriers to predicting changes in global terrestrial methane fluxes: Analyses using CLM4Me, a methane biogeochemistry model integrated in CESM. *Biogeosciences*, **8**(7), 1925-1953, doi: 10.5194/bg-8-1925-2011.
- Rocha, A. V., M. M. Lorant, P. E. Higuera, M. C. Mack, F. S. Hu, B. M. Jones, A. L. Breen, E. B. Rastetter, S. J. Goetz, and G. R. Shaver, 2012: The footprint of Alaskan tundra fires during the past half-century: Implications for surface properties and radiative forcing. *Environmental Research Letters*, **7**(4), 044039, doi: 10.1088/1748-9326/7/4/044039.
- Rogers, J. C., and J. L. Morack, 1980: Geophysical evidence of shallow nearshore permafrost, Prudhoe Bay, Alaska. *Journal of Geophysical Research: Solid Earth*, **85**(B9), 4845-4853, doi: 10.1029/JB085iB09p04845.
- Romanovsky, V. E., S. L. Smith, and H. H. Christiansen, 2010: Permafrost thermal state in the polar Northern Hemisphere during the international polar year 2007–2009: A synthesis. *Permafrost and Periglacial Processes*, **21**(2), 106-116, doi: 10.1002/ppp.689.
- Romanovsky, V. E., S. L. Smith, K. Isaksen, N. I. Shiklomanov, D. A. Streletskiy, A. L. Kholodov, H. H. Christiansen, D. S. Drozdov, G. V. Malkova, and S. S. Marchenko, 2016: The Arctic: Terrestrial permafrost. In: *State of the Climate in 2015*, Bulletin of the American Meteorological Society, S149-S152 pp.
- Rupp, T. S., P. Duffy, M. Leonawicz, M. Lindgren, A. Breen, T. Kurkowski, A. Floyd, A. Bennett, and L. Krutikov, 2016: Climate scenarios, land cover, and wildland fire. In: *Baseline and Projected Future Carbon Storage and Greenhouse-Gas Fluxes in Ecosystems of Alaska*, pp. 17-52. [Z. Zhu and A. D. McGuire (eds.)].
- Ruppel, C. D., and J. D. Kessler, 2017: The interaction of climate change and methane hydrates. *Reviews of Geophysics*, doi: 10.1002/2016RG000534.
- Salmon, V. G., P. Soucy, M. Mauritz, G. Celis, S. M. Natali, M. C. Mack, and E. A. G. Schuur, 2016: Nitrogen availability increases in a tundra ecosystem during five years of experimental permafrost thaw. *Global Change Biology*, **22**(5), 1927-1941, doi: 10.1111/gcb.13204.
- Saugier, B., J. Roy, and H. A. Mooney, 2001: Estimations of global terrestrial productivity: Converging toward a single number? *Terrestrial global productivity*, Academic Press, pp. 543-557. [http://www.sciencedirect.com/science/article/pii/B9780125052900500247]
- Schädel, C., E. A. G. Schuur, R. Bracho, B. Elberling, C. Knoblauch, H. Lee, Y. Luo, G. R. Shaver, and M. R. Turetsky, 2014: Circumpolar assessment of permafrost C quality and its vulnerability over time using long-term incubation data. *Global Change Biology*, **20**(2), 641-652, doi: 10.1111/gcb.12417.
- Schädel, C., M. K. F. Bader, E. A. G. Schuur, C. Biasi, R. Bracho, P. Capek, S. De Baets, K. Diakova, J. Ernakovich, C. Estop-Aragones, D. E. Graham, I. P. Hartley, C. M. Iversen, E. Kane, C. Knoblauch, M. Lupascu, P. J. Martikainen, S. M. Natali, R. J. Norby, J. A. O'Donnell, T. R. Chowdhury, H. Santruckova, G. Shaver, V. L. Sloan, C. C. Treat, M. R. Turetsky, M. P. Waldrop, and K. P. Wickland, 2016: Potential carbon emissions dominated by carbon dioxide from thawed permafrost soils. *Nature Climate Change*, **6**(10), 950-953, doi: 10.1038/nclimate3054.
- Schaefer, K., T. Zhang, L. Bruhwiler, and A. P. Barrett, 2011: Amount and timing of permafrost carbon release in response to climate warming. *Tellus B: Chemical and Physical Meteorology*, **63**(2), 165-180, doi: 10.1111/j.1600-0889.2011.00527.x.
- Schaefer, K., H. Lantuit, V. E. Romanovsky, E. A. G. Schuur, and R. Witt, 2014: The impact of the permafrost carbon feedback on global climate. *Environmental Research Letters*, **9**(8), 085003, doi: 10.1088/1748-9326/9/8/085003.
- Schaphoff, S., U. Heyder, S. Ostberg, D. Gerten, J. Heinke, and W. Lucht, 2013: Contribution of permafrost soils to the global carbon budget. *Environmental Research Letters*, **8**(1), 014026, doi: 10.1088/1748-9326/8/1/014026.
- Schirrmeister, L., C. Siegert, V. V. Kunitzky, P. M. Grootes, and H. Erlenkeuser, 2002: Late quaternary ice-rich permafrost sequences as a paleoenvironmental archive for the Laptev Sea region in northern Siberia. *International Journal of Earth Sciences*, **91**(1), 154-167, doi: 10.1007/s005310100205.
- Schirrmeister, L., G. Grosse, S. Wetterich, P. P. Overduin, J. Strauss, E. A. G. Schuur, and H.-W. Hubberten, 2011: Fossil organic matter characteristics in permafrost deposits of the northeast Siberian Arctic. *Journal of Geophysical Research: Biogeosciences*, **116**(G2), G00M02, doi: 10.1029/2011jg001647.



- Schneider von Deimling, T., M. Meinshausen, A. Levermann, V. Huber, K. Frieler, D. M. Lawrence, and V. Brovkin, 2012: Estimating the near-surface permafrost-carbon feedback on global warming. *Biogeosciences*, **9**(2), 649-665, doi: 10.5194/bg-9-649-2012.
- Schneider von Deimling, T., G. Grosse, J. Strauss, L. Schirrmeister, A. Morgenstern, S. Schaphoff, M. Meinshausen, and J. Boike, 2015: Observation-based modelling of permafrost carbon fluxes with accounting for deep carbon deposits and thermokarst activity. *Biogeosciences*, **12**(11), 3469-3488, doi: 10.5194/bg-12-3469-2015.
- Schuur, E., A. D. McGuire, J. Johnstone, M. Mack, S. Rupp, E. Euskirchen, A. Melvin, H. Genet, A. Breen, X. Walker, M. Jean, and M. Frey, 2016: *Identifying Indicators of State Change and Forecasting Future Vulnerability in Alaskan Boreal Ecosystems*. Department of Defense Strategic Environmental Research and Development Program. SERDP Project RC-2109, 144 pp.
- Schuur, E. A. G., A. D. McGuire, C. Schädel, G. Grosse, J. W. Harden, D. J. Hayes, G. Hugelius, C. D. Koven, P. Kuhry, D. M. Lawrence, S. M. Natali, D. Olefeldt, V. E. Romanovsky, K. Schaefer, M. R. Turetsky, C. C. Treat, and J. E. Vonk, 2015: Climate change and the permafrost carbon feedback. *Nature*, **520**(7546), 171-179, doi: 10.1038/nature14338.
- Schuur, E. A. G., B. W. Abbott, W. B. Bowden, V. Brovkin, P. Camill, J. G. Canadell, J. P. Chanton, F. S. Chapin, III, T. R. Christensen, P. Ciais, B. T. Crosby, C. I. Czimczik, G. Grosse, J. Harden, D. J. Hayes, G. Hugelius, J. D. Jastrow, J. B. Jones, T. Kleinen, C. D. Koven, G. Krinner, P. Kuhry, D. M. Lawrence, A. D. McGuire, S. M. Natali, J. A. O'Donnell, C. L. Ping, W. J. Riley, A. Rinke, V. E. Romanovsky, A. B. K. Sannel, C. Schädel, K. Schaefer, J. Sky, Z. M. Subin, C. Tarnocai, M. R. Turetsky, M. P. Waldrop, K. M. Walter Anthony, K. P. Wickland, C. J. Wilson, and S. A. Zimov, 2013: Expert assessment of vulnerability of permafrost carbon to climate change. *Climatic Change*, **119**(2), 359-374, doi: 10.1007/s10584-013-0730-7.
- Schuur, E. A. G., J. G. Vogel, K. G. Crummer, H. Lee, J. O. Sickman, and T. E. Osterkamp, 2009: The effect of permafrost thaw on old carbon release and net carbon exchange from tundra. *Nature*, **459**(7246), 556-559, doi: 10.1038/nature08031.
- Schuur, E. A. G., J. Bockheim, J. G. Canadell, E. Euskirchen, C. B. Field, S. V. Goryachkin, S. Hagemann, P. Kuhry, P. M. Lafleur, H. Lee, G. Mazhitova, F. E. Nelson, A. Rinke, V. E. Romanovsky, N. Shiklomanov, C. Tarnocai, S. Venevsky, J. G. Vogel, and S. A. Zimov, 2008: Vulnerability of permafrost carbon to climate change: Implications for the global carbon cycle. *BioScience*, **58**(8), 701-714, doi: 10.1641/b580807.
- Shakhova, N., I. Semiletov, I. Leifer, A. Salyuk, P. Rekant, and D. Kosmach, 2010: Geochemical and geophysical evidence of methane release over the east Siberian Arctic Shelf. *Journal of Geophysical Research: Oceans*, **115**, C08007, doi: 10.1029/2009jc005602.
- Shakhova, N., I. Semiletov, I. Leifer, V. Sergienko, A. Salyuk, D. Kosmach, D. Chernykh, C. Stubbs, D. Nicolsky, V. Tumskey, and O. Gustafsson, 2014: Ebullition and storm-induced methane release from the east Siberian Arctic Shelf. *Nature Geoscience*, **7**(1), 64-70, doi: 10.1038/ngeo2007.
- Shaver, G. R., J. Canadell, F. S. Chapin, J. Gurevitch, J. Harte, G. Henry, P. Ineson, S. Jonasson, J. Melillo, L. Pitelka, and L. Rustad, 2000: Global warming and terrestrial ecosystems: A conceptual framework for analysis. *BioScience*, **50**(10), 871-882, doi: 10.1641/0006-3568(2000)050[0871:GWATEA]2.0.CO;2.
- Shiklomanov, N. I., D. A. Streletskiy, and F. E. Nelson, 2012: Northern Hemisphere component of the global Circumpolar Active Layer Monitoring (CALM) program. *10th International Conference on Permafrost*, 377-382.
- Shiklomanov, N. I., D. A. Streletskiy, J. D. Little, and F. E. Nelson, 2013: Isotropic thaw subsidence in undisturbed permafrost landscapes. *Geophysical Research Letters*, **40**(24), 6356-6361, doi: 10.1002/2013GL058295.
- Shur, Y. L., and M. T. Jorgenson, 2007: Patterns of permafrost formation and degradation in relation to climate and ecosystems. *Permafrost and Periglacial Processes*, **18**(1), 7-19, doi: 10.1002/ppp.582.
- Sistla, S. A., J. C. Moore, R. T. Simpson, L. Gough, G. R. Shaver, and J. P. Schimel, 2013: Long-term warming restructures Arctic tundra without changing net soil carbon storage. *Nature*, **497**(7451), 615-618, doi: 10.1038/nature12129.
- Slater, A. G., and D. M. Lawrence, 2013: Diagnosing present and future permafrost from climate models. *Journal of Climate*, **26**(15), 5608-5623, doi: 10.1175/jcli-d-12-00341.1.
- Smith, L. C., G. M. MacDonald, A. A. Velichko, D. W. Beilman, O. K. Borisova, K. E. Frey, K. V. Kremenetski, and Y. Sheng, 2004: Siberian peatlands a net carbon sink and global methane source since the early Holocene. *Science*, **303**(5656), 353-356, doi: 10.1126/science.1090553.
- Smith, S. L., S. A. Wolfe, D. W. Riseborough, and F. M. Nixon, 2009: Active-layer characteristics and summer climatic indices, Mackenzie Valley, Northwest Territories, Canada. *Permafrost and Periglacial Processes*, **20**(2), 201-220, doi: 10.1002/ppp.651.
- Smith, S. L., V. E. Romanovsky, A. G. Lewkowicz, C. R. Burn, M. Allard, G. D. Clow, K. Yoshikawa, and J. Throop, 2010: Thermal state of permafrost in North America: A contribution to the international polar year. *Permafrost and Periglacial Processes*, **21**(2), 117-135, doi: 10.1002/ppp.690.
- Stackpole, S., D. Butman, D. Clow, K. Verdin, B. V. Gaglioti, and R. Striegl, 2016: Chapter 8. Carbon burial, transport, and emission from inland aquatic ecosystems in Alaska. *Baseline and Projected Future Carbon Storage and Greenhouse-Gas Fluxes in Ecosystems of Alaska*. Z. Zhu and A. D. McGuire, Eds., 196 pp. [https://pubs.er.usgs.gov/publication/pp1826]
- Strauss, J., L. Schirrmeister, G. Grosse, S. Wetterich, M. Ulrich, U. Herzschuh, and H.-W. Hubberten, 2013: The deep permafrost carbon pool of the Yedoma region in Siberia and Alaska. *Geophysical Research Letters*, **40**, 6165-6170, doi: 10.1002/2013gl058088.



- Strauss, J., L. Schirrmeyer, G. Grosse, D. Fortier, G. Hugelius, C. Knoblauch, V. Romanovsky, C. Schädel, T. Schneider von Deimling, E. A. G. Schuur, D. Shmelev, M. Ulrich, and A. Veremeeva, 2017: Deep Yedoma permafrost: A synthesis of depositional characteristics and carbon vulnerability. *Earth-Science Reviews*, **172**, 75-86, doi: 10.1016/j.earscirev.2017.07.007.
- Sweeney, C., E. Dlugokencky, C. E. Miller, S. Wofsy, A. Karion, S. Dinardo, R. Y. W. Chang, J. B. Miller, L. Bruhwiler, A. M. Crotwell, T. Newberger, K. McKain, R. S. Stone, S. E. Wolter, P. E. Lang, and P. Tans, 2016: No significant increase in long-term CH₄ emissions on North Slope of Alaska despite significant increase in air temperature. *Geophysical Research Letters*, **43**(12), 6604-6611, doi: 10.1002/2016GL069292.
- Tarnocai, C., J. G. Canadell, E. A. G. Schuur, P. Kuhry, G. Mazhitova, and S. Zimov, 2009: Soil organic carbon pools in the northern circumpolar permafrost region. *Global Biogeochemical Cycles*, **23**, Gb2023, doi: 10.1029/2008gb003327.
- Treat, C. C., M. C. Jones, P. Camill, A. Gallego-Sala, M. Garneau, J. W. Harden, G. Hugelius, E. S. Klein, U. Kokfelt, P. Kuhry, J. Loisel, P. J. H. Mathijssen, J. A. O'Donnell, P. O. Oksanen, T. M. Ronkainen, A. B. K. Sannel, J. Talbot, C. Tarnocai, and M. Väliranta, 2016: Effects of permafrost aggradation on peat properties as determined from a pan-Arctic synthesis of plant macrofossils. *Journal of Geophysical Research: Biogeosciences*, **121**(1), 78-94, doi: 10.1002/2015jg003061.
- Turetsky, M. R., E. S. Kane, J. W. Harden, R. D. Ottmar, K. L. Manies, E. Hoy, and E. S. Kasischke, 2011a: Recent acceleration of biomass burning and carbon losses in Alaskan forests and peatlands. *Nature Geoscience*, **4**(1), 27-31, doi: 10.1038/ngeo1027.
- Turetsky, M. R., W. F. Donahue, and B. W. Benscoter, 2011b: Experimental drying intensifies burning and carbon losses in a northern peatland. *Nature Communications*, **2**, 514, doi: 10.1038/ncomms1523.
- van der Werf, G. R., J. T. Randerson, L. Giglio, G. J. Collatz, M. Mu, P. S. Kasibhatla, D. C. Morton, R. S. DeFries, Y. Jin, and T. T. van Leeuwen, 2010: Global fire emissions and the contribution of deforestation, savanna, forest, agricultural, and peat fires (1997–2009). *Atmospheric Chemistry and Physics*, **10**(23), 11707-11735, doi: 10.5194/acp-10-11707-2010.
- van Leeuwen, T. T., G. R. van der Werf, A. A. Hoffmann, R. G. Detmers, G. Rucker, N. H. F. French, S. Archibald, J. A. Carvalho Jr, G. D. Cook, W. J. de Groot, C. Hély, E. S. Kasischke, S. Kloster, J. L. McCarty, M. L. Pettinari, P. Savadogo, E. C. Alvarado, L. Boschetti, S. Manuri, C. P. Meyer, F. Siegert, L. A. Trollope, and W. S. W. Trollope, 2014: Biomass burning fuel consumption rates: A field measurement database. *Biogeosciences*, **11**(24), 7305-7329, doi: 10.5194/bg-11-7305-2014.
- Walker, D. A., M. K. Reynolds, F. J. A. Daniëls, E. Einarsson, A. Elvebakk, W. A. Gould, A. E. Katenin, S. S. Kholod, C. J. Markon, E. S. Melnikov, N. G. Moskalenko, S. S. Talbot, and B. A. Yurtsev, 2009: The Circumpolar Arctic vegetation map. *Journal of Vegetation Science*, **16**(3), 267-282, doi: 10.1111/j.1654-1103.2005.tb02365.x.
- Walter Anthony, K., R. Daanen, P. Anthony, T. Schneider von Deimling, C.-L. Ping, J. P. Chanton, and G. Grosse, 2016: Methane emissions proportional to permafrost carbon thawed in Arctic lakes since the 1950s. *Nature Geoscience*, **9**, 679-682, doi: 10.1038/ngeo2795.
- Walter Anthony, K. M., P. Anthony, G. Grosse, and J. Chanton, 2012: Geologic methane seeps along boundaries of Arctic permafrost thaw and melting glaciers. *Nature Geoscience*, **5**(6), 419-426, doi: 10.1038/ngeo1480.
- Walter Anthony, K. M., S. A. Zimov, G. Grosse, M. C. Jones, P. M. Anthony, F. S. C. Iii, J. C. Finlay, M. C. Mack, S. Davydov, P. Frenzel, and S. Frolking, 2014: A shift of thermokarst lakes from carbon sources to sinks during the Holocene epoch. *Nature*, **511**(7510), 452-456, doi: 10.1038/nature13560.
- Walter, K. M., M. E. Edwards, G. Grosse, S. A. Zimov, and F. S. Chapin, 2007: Thermokarst lakes as a source of atmospheric CH₄ during the last deglaciation. *Science*, **318**(5850), 633-636, doi: 10.1126/science.1142924.
- Wang, G., Y. Li, Y. Wang, and Q. Wu, 2008: Effects of permafrost thawing on vegetation and soil carbon pool losses on the Qinghai-Tibet Plateau, China. *Geoderma*, **143**(1–2), 143-152, doi: 10.1016/j.geoderma.2007.10.023.
- Wik, M., R. K. Varner, K. W. Anthony, S. MacIntyre, and D. Bastviken, 2016: Climate-sensitive northern lakes and ponds are critical components of methane release. *Nature Geoscience*, **9**, 99-105, doi: 10.1038/ngeo2578.
- World Wildlife Fund, 2012: Terrestrial ecoregions of the world. [<https://www.worldwildlife.org/publications/terrestrial-ecoregions-of-the-world>]
- Xu, X., W. J. Riley, C. D. Koven, D. P. Billesbach, R. Y. W. Chang, R. Commane, E. S. Euskirchen, S. Hartery, Y. Harazono, H. Iwata, K. C. McDonald, C. E. Miller, W. C. Oechel, B. Poulter, N. Raz-Yaseef, C. Sweeney, M. Torn, S. C. Wofsy, Z. Zhang, and D. Zona, 2016: A multi-scale comparison of modeled and observed seasonal methane emissions in northern wetlands. *Biogeosciences*, **13**(17), 5043-5056, doi: 10.5194/bg-13-5043-2016.
- Young, A. M., P. E. Higuera, P. A. Duffy, and F. S. Hu, 2016: Climatic thresholds shape northern high-latitude fire regimes and imply vulnerability to future climate change. *Ecography*.
- Yue, C., P. Ciais, D. Zhu, T. Wang, S. S. Peng, and S. L. Piao, 2016: How have past fire disturbances contributed to the current carbon balance of boreal ecosystems? *Biogeosciences*, **13**(3), 675-690, doi: 10.5194/bg-13-675-2016.



Zhang, T., J. A. Heginbottom, R. G. Barry, and J. Brown, 2000: Further statistics on the distribution of permafrost and ground ice in the Northern Hemisphere. *Polar Geography*, **24**(2), 126-131, doi: 10.1080/10889370009377692.

Zhuang, Q., J. M. Melillo, M. C. Sarofim, D. W. Kicklighter, A. D. McGuire, B. S. Felzer, A. Sokolov, R. G. Prinn, P. A. Steudler, and S. Hu, 2006: CO₂ and CH₄ exchanges between land ecosystems and the atmosphere in northern high latitudes over the 21st century. *Geophysical Research Letters*, **33**(17), doi: 10.1029/2006gl026972.

Zimov, S. A., E. A. G. Schuur, and F. S. Chapin, 2006: Permafrost and the global carbon budget. *Science*, **312**(5780), 1612-1613, doi: 10.1126/science.1128908.

Zona, D., B. Gioli, R. Commane, J. Lindaas, S. C. Wofsy, C. E. Miller, S. J. Dinardo, S. Dengel, C. Sweeney, A. Karion, R. Y.-W. Chang, J. M. Henderson, P. C. Murphy, J. P. Goodrich, V. Moreaux, A. Liljedahl, J. D. Watts, J. S. Kimball, D. A. Lipson, and W. C. Oechel, 2016: Cold season emissions dominate the Arctic tundra methane budget. *Proceedings of the National Academy of Sciences USA*, **113**(1), 40-45, doi: 10.1073/pnas.1516017113.



12 Soils

Lead Authors

Kate Lajtha, Oregon State University; Vanessa L. Bailey, Pacific Northwest National Laboratory

Contributing Authors

Karis McFarlane, Lawrence Livermore National Laboratory; Keith Paustian, Colorado State University; Dominique Bachelet, Oregon State University; Rose Abramoff, Lawrence Berkeley National Laboratory; Denis Angers, Agriculture and Agri-Food Canada; Sharon A. Billings, University of Kansas; Darrel Cerkowski, Agriculture and Agri-Food Canada; Yannis G. Djalynas, University of Cyprus (formerly at Georgia Institute of Technology); Adrien Finzi, Boston University; Nancy H. F. French, Michigan Technological University; Serita Frey, University of New Hampshire; Noel P. Gurwick, U.S. Agency for International Development; Jennifer Harden, U.S. Geological Survey and Stanford University; Jane M. F. Johnson, USDA Agricultural Research Service; Kristofer Johnson, USDA Forest Service; Johannes Lehmann, Cornell University; Shuguang Liu, Central South University of Forestry and Technology; Brian McConkey, Agriculture and Agri-Food Canada; Umakant Mishra, Argonne National Laboratory; Scott Ollinger, University of New Hampshire; David Paré, Natural Resources Canada, Canadian Forest Service; Fernando Paz Pellat, Colegio de Postgraduados Montecillo; Daniel deB. Richter, Duke University; Sean M. Schaeffer, University of Tennessee; Joshua Schimel, University of California, Santa Barbara; Cindy Shaw, Natural Resources Canada, Canadian Forest Service; Jim Tang, Marine Biological Laboratory; Katherine Todd-Brown, Pacific Northwest National Laboratory; Carl Trettin, USDA Forest Service; Mark Waldrop, U.S. Geological Survey; Thea Whitman, University of Wisconsin, Madison; Kimberly Wickland, U.S. Geological Survey

Acknowledgments

Melanie A. Mayes (Science Lead), Oak Ridge National Laboratory; Francesca Cotrufo (Review Editor), Colorado State University; Nancy Cavallaro (Federal Liaison), USDA National Institute of Food and Agriculture

Recommended Citation for Chapter

Lajtha, K., V. L. Bailey, K. McFarlane, K. Paustian, D. Bachelet, R. Abramoff, D. Angers, S. A. Billings, D. Cerkowski, Y. G. Djalynas, A. Finzi, N. H. F. French, S. Frey, N. P. Gurwick, J. Harden, J. M. F. Johnson, K. Johnson, J. Lehmann, S. Liu, B. McConkey, U. Mishra, S. Ollinger, D. Paré, F. Paz Pellat, D. deB. Richter, S. M. Schaeffer, J. Schimel, C. Shaw, J. Tang, K. Todd-Brown, C. Trettin, M. Waldrop, T. Whitman, and K. Wickland, 2018: Chapter 12: Soils. In *Second State of the Carbon Cycle Report (SOCCR2): A Sustained Assessment Report* [Cavallaro, N., G. Shrestha, R. Birdsey, M. A. Mayes, R. G. Najjar, S. C. Reed, P. Romero-Lankao, and Z. Zhu (eds.)]. U.S. Global Change Research Program, Washington, DC, USA, pp. 469-506, <https://doi.org/10.7930/SOCCR2.2018.Ch12>.



KEY FINDINGS

1. Estimates for soil carbon stocks in the conterminous United States plus Alaska range from 142 to 154 petagrams of carbon (Pg C) to 1 m in depth. Estimates for Canada average about 262 Pg C, but sampling is less extensive. Soil carbon for Mexico is calculated as 18 Pg C (1 m in depth), but there is some uncertainty in this value (*medium confidence*).
2. Most Earth System Models (ESMs) are highly variable in projecting the direction and magnitude of soil carbon change under future scenarios. Predictions of global soil carbon change through this century range from a loss of 72 Pg C to a gain of 253 Pg C with a multimodel mean gain of 65 Pg C. ESMs projecting large gains do so largely by projecting increases in high-latitude soil organic carbon (SOC) that are inconsistent with empirical studies that indicate significant losses of soil carbon with predicted climate change (*high confidence*).
3. Soil carbon stocks are sensitive to agricultural and forestry practices and loss of carbon-rich soils such as wetlands. Soils in North America have lost, on average, 20% to 75% of their original top soil carbon (0 to 30 cm) with historical conversion to agriculture, with a mean estimate for Canada of $24\% \pm 6\%$. Current agricultural management practices can increase soil organic matter in many systems through reduced summer fallow, cover cropping, effective fertilization to increase plant production, and reduced tillage. Forest soil carbon loss with harvest is small under standard management practices and mostly reversible at the century scale. Afforestation of land in agriculture, industry, or wild grasslands in the United States and Canadian border provinces could increase SOC by $21\% \pm 9\%$ (*high confidence*).
4. Large uncertainties remain regarding soil carbon budgets, particularly the impact of lateral movement and transport of carbon (via erosion and management) across the landscape and into waterways. By 2015, cumulative regeneration of soil carbon at eroded agricultural sites and the preservation of buried, eroded soil carbon may have represented an offset of $37 \pm 10\%$ of carbon returned to the atmosphere by human-caused land-use change (*medium confidence*).
5. Evidence is strong for direct effects of increased temperature on loss of soil carbon, but warming and atmospheric carbon dioxide increases also may enhance plant production in many ecosystems, resulting in greater carbon inputs to soil. Globally, projected warming could cause the release of 55 ± 50 Pg C over the next 35 years from a soil pool of $1,400 \pm 150$ Pg C. In particular, an estimated 5% to 15% of the peatland carbon pool could become a significant carbon flux to the atmosphere under future anthropogenic disturbances (e.g., harvest, development, and peatland drainage) and change in disturbance regimes (e.g., wildfires and permafrost thaw) (*medium confidence*).

Note: Confidence levels are provided as appropriate for quantitative, but not qualitative, Key Findings and statements.

12.1 Introduction

Globally, soils contain more than three times as much carbon as the atmosphere and four and a half times more carbon than the world's biota (Lal 2004); therefore, even small changes in soil carbon stocks could lead to large changes in the atmospheric concentration of carbon dioxide (CO₂). Despite their importance, however, stocks of soil organic carbon (SOC), which is the carbon component of soil organic matter (SOM), have been depleted through changes in land use and

land cover and unsustainable land management practices associated with agriculture, grazing, and forest management. To better manage and sustain SOC stocks, a focused understanding of microbial and biogeochemical processes that interact in soils, regardless of land cover, to control soil carbon stabilization and destabilization is needed. Soil organic matter (the organic component of soil, consisting of organic residues at various stages of decomposition, soil organisms, and substances synthesized by soil organisms) also is considered a central indicator of



soil health because it regulates multiple ecosystem services that humanity derives from soils, including moderation of climate. SOM stores nutrients, increases water-holding capacity to promote plant growth, limits leaching of nutrients, and adds structure that improves drainage and reduces erosion (Oldfield et al., 2015).

The current best estimates for global SOC stocks are $1,400 \pm 150$ petagrams of carbon (Pg C) to 1 m in depth and $2,060 \pm 220$ Pg C to 2 m in depth (Batjes 2016). These values are derived from the Harmonized World Soil Database with corrections for underrepresented regions, including the Northern Circumpolar Region, using measured soil profiles and geospatial modeling. The resulting values are consistent with other global SOC pool estimates (Govers et al., 2013; Köchy et al., 2015). An estimated 90 to 100 Pg C is released by soils to the atmosphere as soil respiration each year, an efflux that represents both heterotrophic (approximately 51 Pg C) and autotrophic (approximately 40 Pg C) respiration (Bond-Lamberty and Thomson 2010; Hashimoto et al., 2015), roughly balanced by carbon incorporated into SOC from plant residues. This flux value can be compared to estimates from the most recent Intergovernmental Panel on Climate Change (IPCC) report that estimated the gross efflux from surface ocean water to the atmosphere as 78.4 Pg C per year (with a net sink of 2.3 ± 0.7 Pg C per year), carbon emissions from fossil fuel combustion and cement production as 7.8 ± 0.6 Pg C per year, and outgassing from freshwater as 1.0 Pg C per year (Ciais et al., 2013). Soil carbon storage and flux at a given location are controlled by variations in 1) soil-forming factors (Jenny 1941; McBratney et al., 2003; Mishra et al., 2010), 2) anthropogenic activities (Lal 2004), and 3) climatic forcings (Heimann and Reichstein 2008; Richter and Houghton 2011). Future change in the frequency of climatic extremes (Seneviratne et al., 2012) and land use and land management (Nave et al., 2013; Ogle et al., 2010; Wills et al., 2014) may alter SOC stocks and fluxes that affect land feedbacks to climate change, changing the magnitude of, or even

reversing (i.e., change from sink to source), the land carbon sink (Friedlingstein et al., 2014).

Soils of North America store 366 to 509 Pg of organic carbon to 1 m in depth based on continental-scale analyses (Batjes 2016; Liu et al., 2013). Breakdown of SOC stocks by country are discussed in more detail later in this chapter. At the continental scale, nearly 75% of SOC stocks down to 1 m are found in the top 30 cm (Liu et al., 2013), which also is the portion of the soil profile most vulnerable to changes induced by land-use and land-cover changes, disturbance and extreme events, management practices, and climate change. Several knowledge gaps exist in the current ability to measure SOC stocks and fluxes across North America. Researchers employ diverse analytical methods to measure carbon concentration and take measurements at different depths; furthermore, many measurements lack bulk density estimates that are needed to calculate stock estimates. Most SOC stock estimates lack systematic uncertainty (i.e., error propagation) estimates. Consequently, this chapter shows many values of stocks and fluxes without companion uncertainty values. Therefore, significant risks exist for biased conclusions due to inadequate and uneven distributions of SOC profile observations, especially in permafrost regions (Mishra et al., 2013), for depths >1 m and in bulk density estimates for organic soils (Köchy et al., 2015). Recent updates to soil databases have improved coverage, but distributions of available samples across geographic regions are uneven and thus not sufficient to fully characterize SOC dependence on climate, edaphic factors, and land-cover types (Hengl et al., 2014; Mishra and Riley 2012). However, recent efforts, notably the U.S. Department of Agriculture's (USDA) Rapid Carbon Assessment (RaCA), will yield a much more consistent estimate of current soil carbon stocks (see Section 12.4.1, p. 479). Similarly, RaCA recently initiated a field-based soil carbon inventory for Mexico, and comprehensive stock estimates for different regions and land uses are forthcoming (see Section 12.4.2, p. 481).



Since cultivation of land began nearly 12,000 years ago, humans have been altering soil carbon stocks. Just since 1850, human degradation of soil worldwide may have resulted in a loss of 44 to 537 Pg SOC, largely through land-use change and conversion to agriculture (Lal 2001; Paustian et al., 1997). Globally, agricultural soils have lost 20% to 75%, or 30 to 40 megagrams of carbon (Mg C) per hectare (ha), of their antecedent SOC pool (Lal et al., 2015). In contrast, afforestation (the establishment of forest cover on land that previously did not have tree cover) and land restoration have the potential to recover depleted SOC stocks from the atmosphere (Lal 2004). For example, newly afforested lands cover 4 billion ha globally and have a carbon sequestration potential of 1.2 to 1.4 Mg C per year (Lal et al., 2015). Meta-analysis of afforestation effects on soil carbon storage in the United States and Canadian border provinces found that land conversion to forest from agriculture, industry, or wild grassland increased SOC by $21\% \pm 9\%$ (Nave et al., 2013). The researchers found that the largest increase was in lands previously used for industrial purposes such as mining (173%), for areas with woody encroachment into unmanaged grassland (31%; see Ch. 10: Grasslands, p. 399), and for agricultural areas in the Northern Plains (32%; see Ch. 5: Agriculture, p. 229). Such SOC increases via afforestation and reforestation contribute to the net carbon sequestration by U.S. forests, currently estimated at 313 ± 40 teragrams of carbon (Tg C) per year (Lu et al., 2015).

12.2 Carbon Cycling Processes in Soils

Progress has been made over the last 10 years in understanding specific processes that determine the magnitude and direction of SOC stabilization and destabilization (see Figure 12.1, p. 473). This new information will not only help explain spatial patterns of SOC in North America, but also will help improve modeling of the large soil carbon pool in Earth System Models (ESMs). Outlined here are the processes that govern overall carbon stocks and fluxes through soils, from inputs through microbial transformations in the bulk soil and rhizosphere,

and the protection mechanisms that govern the overall longevity of carbon in soils.

12.2.1 Precipitation

Overriding many soil carbon processes is the complicated role of precipitation and moisture on soil carbon stocks. Precipitation effects on SOC are complicated by the various and often opposing effects of precipitation on the various processes that control carbon stabilization and destabilization. On one hand, where moisture is limiting, increased soil moisture stimulates soil microbial activity, thus increasing soil respiration and destabilization of soil carbon. On the other hand, precipitation has strong effects on both vegetation type and plant production, and thus increases in precipitation in moisture-limited systems generally lead to increases in soil carbon through indirect effects on enhanced plant production, particularly increased root production (Jobbágy and Jackson 2000). In a global analysis (Jobbágy and Jackson 2000) total soil carbon content increased with precipitation and clay content and decreased with temperature. These results match numerous regional studies showing that precipitation in temperate ecosystems has a strong and positive relationship with SOC, likely through effects on total plant biomass, especially belowground biomass (Burke et al., 1989; Liu et al., 2012). Taken together these results suggest a greater response of plant production compared to decomposition from increased precipitation.

Several analyses have noted a wide divergence in estimates of soil carbon stocks from terrestrial biosphere models (Tian et al., 2015; Todd-Brown et al., 2013). Todd-Brown et al. (2013) noted that the parameterization of soil heterotrophic respiration was a significant cause of the discrepancy in model predictions, while Tian et al. (2015) suggested that mechanisms such as changes in the proportion of labile to passive soil carbon pools, as well as sensitivities of respiration to climate, are significant sources of uncertainty in the modeling estimates of soil carbon. Thus, more accurate biome-specific analyses of the effects of precipitation on soil respiration,

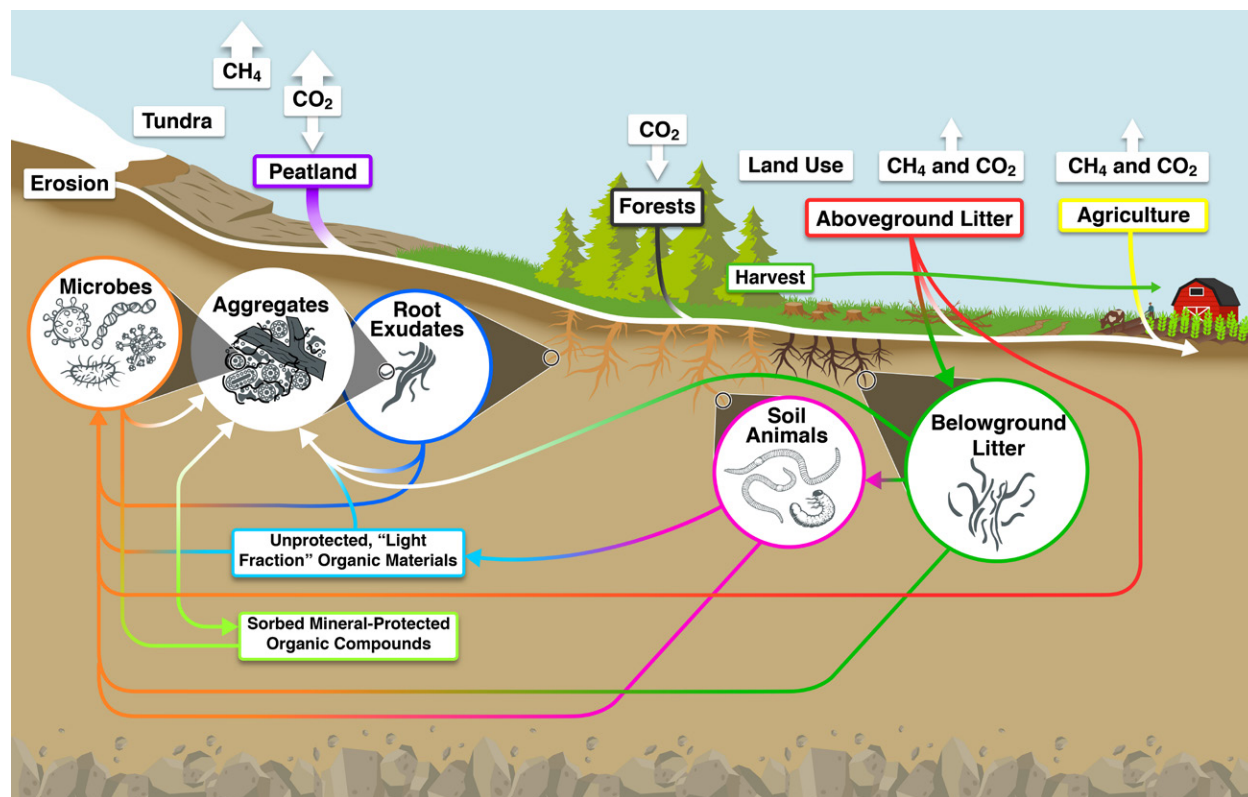


Figure 12.1. Processes Involved in Controlling Fluxes and Stabilization of Soil Carbon. A variety of soil animals and microbes can process plant litter that contributes to a pool of unprotected particulate organic matter (OM) with a relatively short turnover time. Alternatively, soil microbes also can process this litter into more stabilized forms such as aggregates or mineral-protected OM with relatively long turnover times. In this carbon pool, belowground litter appears to be preferentially stabilized, partly because of its proximity to both microbes and minerals. Root exudates may contribute to microbial carbon pools or to priming (i.e., the loss of mineral-protected soil carbon). Respiratory losses—occurring at all stages of biotic processing—can be affected by microbial carbon use efficiency and by conditions in the natural environment or those arising from land use. Not only can land use significantly affect both the quality and quantity of plant residues delivered to soils and their processing, it also can affect erosional losses and deposition. Climate change, especially in northern latitudes, may cause significant losses of soil carbon. (Key: CO₂, carbon dioxide; CH₄, methane.)

litter and root production, and vegetation type will be needed to improve soil carbon models.

12.2.2 Plant Litter Inputs

Many factors, including climate regime, atmospheric CO₂, land management, soil mineralogy and fertility, and nitrogen deposition strongly influence the structure of the plant community and thus the amount and quality of organic inputs (e.g., litter, wood, and root debris) to the surface of soils (Jandl et al., 2007; McLauchlan 2007; Smith et al., 2007). For example, elevated nitrogen deposition and high

soil fertility generally increase plant shoot:root ratios and also decrease concentrations of plant protective compounds such as lignin (Haynes and Gower 1995; Luo and Polle 2009; Pitre et al., 2007). Chemical composition of litter, variably measured as carbon:nitrogen, lignin:nitrogen, or by the presence of complex aromatic compounds, has been shown to influence litter decomposition (Papa et al., 2013; Trofymow et al., 1995; Wardle et al., 2002), with high lignin or aromatic content observed to limit decomposition rates. However, the linkages among litter quantity, litter composition, and SOC stocks



are much less clear than would be expected due to other contributing factors. For example, several long-term litter manipulation experiments have shown that increased litter inputs do not always result in increased SOC storage (Lajtha et al., 2014a, 2014b; Mayzelle et al., 2014). Fresh carbon inputs can alter the decomposition of existing SOM because microbes, which play a major role as decomposers in soil ecosystems, will use the new inputs as fuel to decompose existing SOM (Bernal et al., 2016; Crow et al., 2009; Georgiou et al., 2015), resulting in a net decrease in SOC. Site-specific differences in soil mineralogy and microbial physiology also can influence the magnitude of response in SOC concentrations to changes in litter inputs (Geyer et al., 2016; see Section 12.2.3, this page). These kinds of interactions with soil minerals and microbes help to explain why chemical factors, such as lignin content, that are known to control litter decomposition do not always appear to be primary controls on SOC stabilization or destabilization (Rasse et al., 2006; Sulman et al., 2014). There also is evidence that root litter may be preferentially stabilized over shoot-derived litter (Iversen et al., 2008; Kong and Six 2010; Rasse et al., 2005; Russell et al., 2004). Thus, further research is needed to determine how changes in net primary production (NPP), vegetation, and litter quality due to rising atmospheric CO₂ concentrations will affect SOC stabilization in the future.

12.2.3 Soil Microbes

Soil microbes, including bacteria, fungi, and archaea, ultimately process all carbon inputs; consequently, microbes are referred to as “the eye of the needle through which all organic materials must pass” (Jenkinson 1977). The organic products and by-products of microbial decomposition, including microbial necromass, can accumulate in soils as SOM, and the chemistry of SOM is distinct from its source material including litter, roots, insect and animal necromass, and wood. The transformation from litter inputs through microbes and into SOM produces inorganic, carbon-containing gases such as CO₂ and methane (CH₄) through microbial

respiration. Because of its important role in carbon transformation, the soil microbial community is key to understanding SOC stocks (Bernal et al., 2016; Guenet et al., 2012), even though the microbial biomass is typically only 1% to 2% of total SOM mass (Xu et al., 2013). Understanding microbial response to microclimate is key to understanding the carbon balance of soils under climate change, because soil balance under changing temperature and moisture is dependent on microbial community and physiological responses to changing temperature and moisture (e.g., Billings and Ballantyne 2013; Yan et al., 2016).

In addition to their direct role mineralizing SOM into inorganic gases, microbes contribute to physical mechanisms of SOC stabilization, indirectly affecting the rate and nature of SOC inputs from plants. A key mechanism of SOC stabilization is protection within soil aggregates (Six et al., 2002), and fungal mycelia and bacterial extracellular polysaccharides are important in forming and stabilizing these aggregates (Aspiras et al., 1971). SOC also is protected by chemical interactions with minerals, particularly silt and clay (Six et al., 2002), and microbes living on minerals may facilitate these interactions by depositing microbially derived carbon directly onto mineral surfaces (Uroz et al., 2015). Microbes can affect plant carbon inputs by regulating plant nutrient supply (Bever et al., 2010; van der Heijden et al., 2006), which affects plant community composition and the timing, mass, and properties of plant inputs of litter and exudates. Thus, although they compose a small fraction of SOC stocks, microbes play a central role in the SOC cycle, affecting inputs, storage, and outputs in diverse ways.

12.2.4 Macrofauna (Food Web)

Soil is home to millions of different organisms, from microorganisms to soil animals (fauna) such as microscopic roundworms (nematodes), tardigrades, rotifers, collembolans, mites, isopods, ants, spiders, and earthworms (Orgiazzi et al., 2015). These fauna exist in food webs containing multiple trophic levels—herbivores that feed directly on the roots of living plants, consumers that feed on living microorganisms associated with dead organic



materials, predators that prey on other soil fauna, and plant or animal parasites and pathogens (Coleman and Wall 2015). Through soil bioturbation and feeding on plant roots, organic matter, and their associated microorganisms, soil animals are intimately involved in every step of SOM turnover and soil formation. Sometimes referred to as “ecosystem engineers,” soil animals play a disproportionate role in the carbon cycle relative to their abundance and biomass. Carbon stocks of the soil fauna range from 0.3 to 50 kilograms of carbon per hectare, with desert soils containing the smallest faunal biomass and temperate grassland and tropical rainforest soils the greatest (Fierer et al., 2009). However, across biomes, the biomass of soil fauna typically represents less than 3% of the total biomass of living soil organisms, with soil microorganisms making up the majority. Despite their low biomass relative to soil microbes, soil fauna contribute significantly to carbon cycling through their regulation of microbial activity and through their physical mixing of organic materials and soil. The presence of soil fauna stimulates decomposition, respiration rates (i.e., CO₂ flux), and losses of dissolved organic carbon through leaching (de Vries et al., 2013). The positive impact of soil fauna on carbon cycling is attributed to organic matter fragmentation, which increases 1) the surface area available for microbial colonization; 2) the partial digestion of organic materials, enhancing their decomposability; 3) the direct contact of soil microbes with organic matter; and 4) the direct consumption of soil microbes—all impacts which stimulate microbial activity and the release of carbon and nutrients (Coleman and Wall 2015). However, one study found that the activity of earthworms increases carbon stabilization onto minerals to a greater degree than the increase in carbon mineralization, leading to net soil carbon increase (Zhang et al., 2013). Current ecosystem-scale models and ESMs typically overlook the significant effects of soil fauna on the carbon cycle, but guidelines for development of next-generation models call for explicitly incorporating soil food web properties and the responses of

soil fauna to land use and climate change (de Vries et al., 2013).

12.2.5 Rhizosphere Interactions

The rhizosphere is defined as an area of soil where microbial activity is stimulated by the presence of roots. A substantial portion of plant biomass is located below ground in the form of roots. Estimates of belowground NPP based on root:shoot ratios assign 30% to 60% of total plant biomass to roots, depending on the biome (Bolinder et al., 2007; Rytter 2001). Regularly shedding sloughed cells and mucilage, roots exude a variety of simple carbon compounds into the soil immediately surrounding them (Hirsch et al., 2013). These root “exudates” comprise primarily organic acids, sugars, and amino acids (Hirsch et al., 2013; Jones 1998). These exudates can interact with minerals by sorption or can liberate organic compounds and nutrients for plant or microbial uptake (Dessureault-Rompere et al., 2007; Keiluweit et al., 2015). In general, the mass of soil in the rhizosphere makes up a smaller fraction (<40%) of total soil than does root-free soil, but it disproportionately affects carbon cycling. For example, microbial biomass, extracellular enzyme activity, decomposition, and mineralization rates are consistently higher in rhizosphere soil compared with those in bulk soil. Fungal hyphae can extend >40 cm away from roots (Finlay and Read 1986), extending the influence of root carbon past the rhizosphere (Zak et al., 1993). Dead root biomass is a substrate source for saprotrophic microbes and detritivores, while living roots are a source of carbon to mycorrhizal fungi.

Mycorrhizal material, shown to be a dominant pathway through which carbon enters the SOM pool, exceeds the input via leaf litter and fine-root turnover (Godbold et al., 2006). Mycorrhizae also may stimulate the decomposition of soil carbon to mine nutrients, paradoxically causing destabilization of soil carbon pools. The effects of mycorrhizae on soil carbon balance are thus complicated by the balance between carbon stabilization effects and soil carbon priming effects (Brzostek et al., 2015). However, recent research (Averill and Hawkes 2016;



Averill et al., 2014) demonstrated that ecosystems dominated by plants with symbiotic ectomycorrhizal fungi store more carbon in soils than ecosystems dominated by arbuscular mycorrhizae-associated plants.

12.2.6 Nitrogen Effects on SOM Dynamics

There are substantial interactions between biogeochemical cycles of carbon and nitrogen. Human activities (e.g., fertilizer production, fossil fuel combustion, and industry) have substantially increased nitrogen supply to ecosystems (Vitousek et al., 1997). Global annual nitrogen deposition has increased tenfold over the past 150 years (Lamarque et al., 2005; Yue et al., 2016), although nitrogen deposition has decreased significantly across North America over the last decade due to pollution control. Historic nitrogen loading increased NPP (Elser et al., 2007; LeBauer and Treseder 2008; Xia and Wan 2008), which in turn increased carbon inputs to the forest floor and overall production of plant biomass (Hyvonen et al., 2007; Vitousek et al., 1997). Across biomes, total soil carbon tends to increase with experimental nitrogen addition (Yue et al., 2016), yet this may result less from increases in inputs and more from altering the extent or rates of decomposition (Frey et al., 2014; Liu and Greaver 2010). Microbial decomposition of soil carbon is generally retarded by nitrogen deposition (Hagedorn et al., 2003), but carbon allocation to roots also decreases with nitrogen deposition, limiting new carbon inputs to soil. However, a recent meta-analysis suggested that the reduction in soil carbon respiration, and thus increase in soil carbon stocks resulting from nitrogen deposition, might be equal in magnitude to the amount of additional carbon sequestered by aboveground vegetation (Janssens et al., 2010). Literature surveys suggest that the soil carbon response to anthropogenic nitrogen will fall in the range of 0 to 23 grams of carbon per gram of nitrogen added (Reay et al., 2008), but the uncertainty around this value is very high.

12.2.7 Protection Mechanisms

The extent of carbon protection (i.e., resistance to microbial decomposition) in soil historically has

been attributed to litter chemistry, and this remains an element of carbon persistence (Clemente et al., 2011) in organic soils or organic soil horizons that accumulate on the surface of the mineral soil in forests. In recent decades, studies have shown that the controls on carbon stability in mineral soils are more likely dominated by physical and biological factors in the soil environment (Jastrow et al., 2006; Lehmann and Kleber 2015; Lin and Simpson 2016). Physical protection by spatial isolation (i.e., aggregate formation; McCarthy et al., 2008) and chemical associations with soil minerals (i.e., sorption) are both key drivers of carbon persistence in soils. Protection of carbon within soil aggregates (i.e., physical associations between soil minerals and organic compounds) can lead to long-term carbon storage in soils (Jastrow et al., 1996; Six et al., 2004). Compromising the physical structure of aggregates such as by tillage can result in substantial carbon losses because SOC becomes more available physically to decomposition (Navarro-Garcia et al., 2012). Alternatively, carbon may be protected via sorption to soil minerals in which reactive surfaces, including phyllosilicates, oxides, and other minerals, bind carbon molecules via chemical bridges and bonds. The types of compounds sorbed range from discrete chemical compounds (Solomon et al., 2012) to fragments of partially decayed microbial biomass (Courtier-Murias et al., 2013). Mineral-associated carbon stocks can have half-lives ranging from 30 to 4,500 years (Hall et al., 2015a, 2015b; Heckman et al., 2014), yet they can be rendered vulnerable as local environmental conditions change in ways that alter the chemical binding strength, such as changes in precipitation, infiltration, or temperature. In addition, larger-scale processes can serve to protect soil carbon, such as freezing, waterlogging, cryoturbation, or erosion deposition (Kaiser et al., 2007; Grosse et al., 2011; Berhe et al., 2007; Kroetsch et al., 2011).

12.2.8 Losses

Gas Fluxes

Gases including CO₂ and CH₄ are released from soils as a result of SOM and litter decomposition by soil microbes. Respiration of live roots and their



associated mycorrhizal symbionts also release CO₂ into the subsurface (Bond-Lamberty et al., 2004; Hanson et al., 2000; Subke et al., 2006; Tang et al., 2005). Globally, approximately 90 to 100 Pg C per year was released to the atmosphere from microbial soil respiration, and the projected rate increase is about 0.1 Pg C per year under a warming climate (Bond-Lamberty and Thomson 2010; Hashimoto et al., 2015). Soil respiration is affected by soil temperature, soil moisture, and organic carbon availability (Davidson and Janssens 2006). Typically, warming increases microbial respiration, while increases in moisture variably affect microbial respiration with maximum CO₂ emissions observed under partially saturated conditions. As soils saturate, methanogenesis is likely to emerge as the dominant carbon emission. Other global change factors such as elevated atmospheric CO₂ and naturally and anthropogenically altered soil nitrogen status also interactively affect soil respiration in direct and indirect ways (Billings and Ziegler 2008; Zhou et al., 2016). Also observed are vast differences in the amount of gas evolution as a function of landscape heterogeneity, underlying geology and soil type, and vegetative cover, as well as daily and seasonal temporal changes. Consequently, ESMs have not fully used soil respiration data for validation and calibration (Phillips et al., 2016).

Compared with CO₂, CH₄ has 28 times higher global warming potential over a 100-year time horizon (Saunio et al., 2016). Worldwide biogenic (i.e., associated with plants, animals, and microbes) sources of CH₄ emissions, including those from natural ecosystems, agriculture, biomass burning, and landfill waste, are estimated to be 0.33 Pg C per year or 12.4 Pg CO₂ equivalent¹ (CO₂e) per year, including anthropogenic biogenic sources of 7.4 Pg CO₂e per year (Tian et al., 2016). The U.S. inventory of greenhouse gases (GHGs) estimated anthropogenic total CH₄ emissions of 0.87 Pg CO₂e per year in 2015 if the 100-year global warming potential of

28 is used to calculate the CO₂ equivalent for CH₄, including anthropogenic biogenic sources of 0.42 Pg CO₂e per year, mostly from agriculture, landfill, and waste management (U.S. EPA 2017). Methane in North American soils is produced primarily under anaerobic conditions by methanogenic microbes, mostly in freshwater wetlands and rice paddies. However, CH₄ emissions are the net balance of both CH₄ production and oxidation (i.e., CH₄ destruction) by methanotrophic microbes (Tate 2015). The oxidation (i.e., consumption) of CH₄ in wetlands is important and may reduce potential CH₄ emissions by over 50% (Segarra et al., 2015).

Erosion

Soil erosion mobilizes about 75 Pg of soil each year by water and wind, with most erosion stemming from agricultural lands (Berhe et al., 2007). This accelerated movement of soil has major effects on the carbon cycle, most obviously because erosion physically removes SOC from soil profiles, exposing some fraction to oxidation during transit or upon deposition (Lal 2003). However, the degree to which soil erosion contributes to atmospheric CO₂ depends on several additional factors. Erosion can alter SOC mineralization and stabilization at both eroding and depositional sites, for example by burying and partially preserving SOC at the depositional site (Billings et al., 2010; Dialynas et al., 2016). Oxidation of eroded SOC is, therefore, only one component of net SOC change (Van Oost et al., 2012). Stallard (1998) first introduced the concept of new SOC production at an eroding site, a process which can balance the oxidation of eroded SOC (Berhe et al., 2007; Billings et al., 2010; Dialynas et al., 2016; Fang et al., 2006; Harden et al., 1999; Jenerette and Lal 2007; Liu et al., 2003; Quine and Van Oost 2007; Rosenbloom et al., 2006; Smith et al., 2001; Van Oost et al., 2007). Global estimates of the carbon sink strength of erosion and deposition vary widely. Several studies suggest that soil net erosion and deposition may result in a small net carbon sink, perhaps up to about 0.1 Pg C per year (Van Oost et al., 2007), although Berhe et al. (2007) suggest a modern erosion-induced carbon sink strength of about 0.7 to 1 Pg C per year. Wang et al. (2017) estimate a cumulative offset of atmospheric carbon of 78 ± 22 Pg C

¹ Carbon dioxide equivalent (CO₂e): Amount of CO₂ that would produce the same effect on the radiative balance of Earth's climate system as another greenhouse gas, such as methane (CH₄) or nitrous oxide (N₂O), on a 100-year timescale. For comparison to units of carbon, each kg CO₂e is equivalent to 0.273 kg C (0.273 = 1/3.67). See Preface, p. 5, for details.



due to agriculturally enhanced erosion during the period 6000 BC to AD 2015, which represents approximately $37 \pm 10\%$ of carbon emissions linked to contemporary anthropogenic land-cover change. Carbon burial rates have increased by a factor of 4.6 since AD 1850, consistent with erosion-induced carbon fluxes occurring disproportionately in recent centuries. Extrapolating globally, Billings et al. (2010) suggest an upper limit of a maximum net global sink of 3.1 Pg C per year (if all eroded carbon were protected from oxidation) and a net source of 1.1 Pg C per year if all eroded carbon were oxidized.

Estimating the rates of the erosion-induced redistribution of soil carbon has many uncertainties (Berhe et al., 2007; Regnier et al., 2013). These uncertainties derive from 1) the dynamics of eroded and deposited SOM (Hu and Kuhn 2014); 2) the texture and mineralogy of the soil being eroded; 3) the geomorphological nature and potential for decomposition in depositional environments; 4) the history and future of land uses, especially in intensively managed landscapes such as harvested forests and agriculture (Papanicolaou et al., 2015); and 5) changes to climate and hydrological cycles, including the timing and frequency of extreme events. Additional watershed-based studies, experimental studies, and modeling can address these uncertainties.

12.3 Modeling SOC Dynamics

At the global scale, the response of SOC to the influences of land use, disturbances, and climate change is projected using ESMs, which include simplified versions of soil carbon cycling models (Harmon et al., 2011; Tian et al., 2015). These early soil carbon models (e.g., CENTURY, Bolker et al., 1998; RothC, Gottschalk et al., 2012) largely assume exchanges of carbon between soil carbon pools are first-order exchanges defined by pool turnover times (Todd-Brown et al., 2013), and such assumptions (and model frameworks) continue into contemporary large-scale ESMs such as the Community Land Model (Huang et al., 2018) or the E3SM Land Model (Tang and Riley 2016). However, different models use different strategies to simplify and represent the complex cycling processes that were discussed in Section 12.2, p. 472; thus, model simulation

results tend to diverge. For example, model outputs can vary widely in their projections of global carbon stocks and microbial respiration (Tian et al., 2015) based on nonmodeled outputs such as deep carbon storage and wetland carbon storage. The addition of land use to some models has indicated that soils previously projected to be sinks for CO₂ may actually be sources (Eglin et al., 2010). Because SOC stocks are so large compared to other global compartments (e.g., vegetation and atmosphere), the wide variations in projections of SOC stocks contribute a great deal of uncertainty to future carbon cycle projections (Todd-Brown et al., 2013). Wider adoption of global data products including the Harmonized World Soil Database and SoilsGrid (FAO/IIASA/ISRIC/ISSCAS/JRC 2012; Hengl et al., 2014) may facilitate the development of new tools to better integrate both local SOC observations (Dietze et al., 2014; Xia et al., 2013; Xu et al., 2006) and global data products into future models (Hararuk et al., 2014).

At a finer scale, the recognition that small-scale processes, including microbial respiration, nutrient limitation, and soil microclimate (Luo et al., 2016; Tian et al., 2015), affect overall soil carbon fluxes has prompted the emergence of microbially explicit and process-rich models for soil carbon cycling (Manzoni and Porporato 2009; Sulman et al., 2014; Tang and Riley 2014; Wieder et al., 2013). Models that include the size of the microbial biomass, microbial dormancy, and enzyme functions (Wang et al., 2014) are beginning to represent previously ignored processes such as priming (accelerated decomposition of stable carbon), mineral association, and temperature sensitivities, as well as their feedbacks to the Earth's physical system in the form of altered GHG emissions. The most recent soil-specific models, such as the Millennial Model (Abramoff et al., 2018), further classify SOC into measurable physicochemical categories (e.g., mineral-associated carbon, carbon physically entrapped in aggregates, dissolved carbon, and fragments of plant detritus) and include explicit processes regulating the transfers of carbon between pools, in contrast to the earlier models based on empirical turnover times (Abramoff et al., 2018).

These modeling types reflect very different scales, with ESMs simulating kilometer-scale landscapes and the more process-rich models simulating regional processes at finer scales such as centimeters to meters. Bridging these scales requires further empirical understanding and new mathematical frameworks (e.g., Wang et al., 2017). As models continue to advance, other challenges include determining which new models and approaches can be parameterized with empirical data and used for larger-scale decision making.

12.4 North American and Regional Context

12.4.1 United States

Scientists have used several approaches to estimate U.S. SOC stocks. These stocks may be aggregated in

specific land areas such as geopolitical boundaries (i.e., states) or Land Resource Regions, or they may be grouped by soil-order or land-cover classes (Guo et al., 2006; Wills et al., 2014). Most efforts have developed estimates for the conterminous United States (CONUS), but results vary based on methods and assumptions. Guo et al. (2006) estimated SOC stocks for CONUS as between 30 and 150 Pg (0 to 2 m in depth) by soil order using the State Soil Geographic database (STATSGO; USDA Soil Conservation Service 1993) and another 23 to 94 Pg C stock as inorganic carbon within the top 2 m of surface. Compared with CONUS, fewer studies have estimated soil carbon stocks for Alaska. Mishra and Riley (2012) estimated stocks in Alaska as 77 Pg C, an update from the value of 48 Pg estimated by Bliss and Maursetter (2010). The U.S. Geological

Table 12.1. Estimates of Soil Carbon Storage in the Conterminous United States in Different Land-Use Classes^{a-d}

Land Cover	Soil Organic Carbon (from RaCA ^e)	Soil Organic Carbon (Bliss et al., 2014)	Soil Organic Carbon (Sundquist et al., 2009)	Soil Organic Carbon (Other Estimates)
Forests and Woodlands	20	13.1	25.1	28 ^f
Agriculture	13	13.4	27.4 ^d	
Shrublands		5.6	9.7	
Urban		3.3		1.9 ^g
Wetlands	14	8.9		13.5 ^h – 11.5 ⁱ
Rangelands (+ Pasture)	19	12.3	11.2 ^d	
Totals	65	57.2^j	73.4	

Notes

- Storage measured in soil down to 1 m in depth.
- All values are in petagrams of carbon (Pg C).
- No total is given for “Other Estimates” values because the values do not represent all land-use classes and some land-use classes likely overlap (e.g., urban is partially accounted for in agriculture [see d] and developed; range estimates likely include some agricultural land).
- “Agriculture” is listed in Sundquist et al. (2009) as “agriculture and developed”; “rangelands and pasture” is listed as “other” and includes all grasslands.
- RaCA, U.S. Department of Agriculture’s Rapid Carbon Assessment.
- Domke et al. (2017).
- Pouyat et al. (2006).
- From the *Second State of the Carbon Cycle Report (SOCCR2)*, Ch. 13: Terrestrial Wetlands, p. 507.
- Nahlik and Fennessy (2016).
- Total soil profile of carbon is 73 Pg.

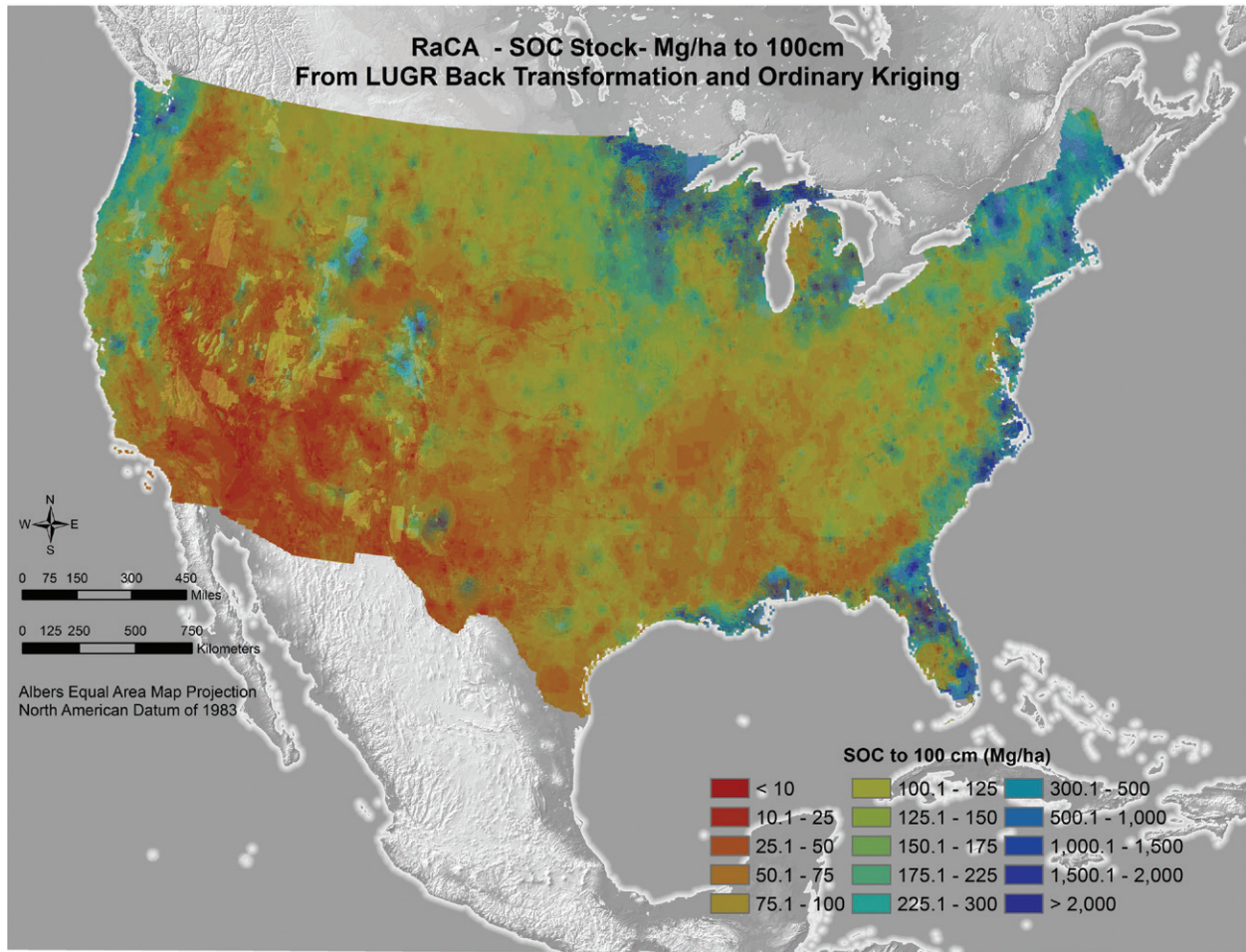


Figure 12.2. Rapid Carbon Assessment (RaCA) of Soil Organic Carbon (SOC) Stock Values. Data are in mega-grams (Mg) of carbon per hectare (ha) to 100 cm. Soil group strata and land use and land cover (LULC) strata were linked together into a LULC-Soil Group Combination, designated as “LUGR.” Prepared using the geometric mean of pedon stocks according to RaCA methodology. [Figure source: Reprinted from U.S. Department of Agriculture Natural Resources Conservation Service, Soil Survey Staff, RaCA project. Prepared by Skye Wills, 2016]

Survey (USGS) calculated CONUS SOC storage as 77.4 Pg C from the Soil Survey Geographic (SSURGO) database, developed by the USDA Natural Resources Conservation Service (NRCS). This information is supplemented with data from the Digital General Soil Map of the United States (STATSGO2; catalog.data.gov/dataset/u-s-general-soil-map-statsgo2-for-the-united-states-of-america; Sundquist et al., 2009; see Table 12.1, p. 479).

The NRCS’s recent RaCA project captures information on the carbon content of soils across CONUS at a relatively uniform point in time (Soil Survey

and Loecke 2016). A secondary goal was to capture SOC stocks in different kinds of soils and land uses. For this assessment, RaCA collected 144,833 samples from the upper 1 m of 32,084 soil profiles at 6,017 randomly selected locations across the United States. Independently developed soil groups for each RaCA region were combined with land-use, land-cover information, yielding an estimate of the total carbon stock across CONUS of 65 Pg C (see Figure 12.2, this page). Different estimates of soil carbon pools are expected to differ; individual soil and land-cover classes have different levels of uncertainties surrounding their carbon pool estimates, and errors



can include land-classification differences and different ways of aggregating sparse data. For example, Domke et al. (2017) used the USDA Forest Service's Forest Inventory and Analysis (or FIA) data to project SOC density in CONUS forest types and parts of Alaska and compared regional projections to those from RaCA. These modeled SOC density projections were substantially smaller than those of RaCA for most NRCS Land Resource Regions, at times by more than a factor of three.

Carbon storage in interior CONUS wetlands are assessed (see Ch. 13: Terrestrial Wetlands, p. 507) using a combination of NRCS SSURGO data and the U.S. Fish and Wildlife Service's (USFWS) National Wetland Inventory. These estimates of the upper 1 m indicate that terrestrial wetlands store about 13.6 Pg C, a value very similar to that of Nahlik and Fennessy (2016), who reported a value of 11.5 Pg. Storage of carbon in CONUS saline wetlands is significantly lower. Estimates of tidal wetland soil stocks along the freshwater-to-saline transition area plus the seagrass soil stocks are 0.8 Pg C for "blue carbon" ecosystems (see Ch. 15: Tidal Wetlands and Estuaries, p. 596). Given that more than half the historical U.S. wetland area has been lost due to anthropogenic activities, further loss of wetland soils represents a key vulnerability that could result in a net transfer of carbon from the soil to the atmosphere.

12.4.2 Mexico

The most recent estimate of soil carbon stocks in Mexico is reported to a depth of only 30 cm. According to Jobbágy and Jackson (2000), the top 20 cm of soil typically represents 40% of total soil carbon stocks averaged across vegetation communities in Mexico. At 9.13 Pg C in the top 30 cm, this reported SOC stock is 73% of the country's total terrestrial stock (CONAFOR 2010), but a conservative estimate of SOC stocks to 1 m in depth might be 18 Pg C, assuming that the top 30 cm represents about half the total soil carbon stocks. However, this estimate remains highly uncertain as acquisition of field data to fill data gaps (e.g., bulk density measurements) and spatial extrapolation methods continue to evolve (de Jong et al., 2010). For example, simply using different versions of land-cover maps for spatially extrapolating mean SOC values results in significant differences for semitropical low forests and mangroves (Paz Pellat et al., 2016). Despite these issues, almost half (48%) of Mexico's SOC appears to be contained in forests, especially the dry deciduous, semi-evergreen, and oak forests (see Tables 12.2, this page, and 12.3, p. 482). Furthermore, grazing lands accounted for 23% of the total SOC stock, mostly due to their extensive area. Finally, despite the relatively low soil carbon density of shrublands, they were extensive enough to account for 7% of the total SOC stock (Paz Pellat et al., 2016).

Table 12.2. Soil Organic Carbon Distribution in Mexico by FAO FRA^a Classes^b

FAO FRA Classes ^a	Area in Millions of Hectares	Petagrams of Carbon
Forestlands	65	4.3
Other Forestlands	20	0.6
Other Lands	108	4.1
Planted Forest	0.33	< 0.01
Totals	194	9.1

Notes

a) Global Forest Resources Assessment (FRA) of the United Nations Food and Agriculture Organization (FAO).

b) From Paz Pellat et al. (2016).



Table 12.3. Soil Organic Carbon Distribution in Mexico for Vegetation Types with Top Five Highest Total Soil Carbon Estimates^a

Vegetation Types (Top Five)	Area in Millions of Hectares	Teragrams of Carbon	Percent of Total
Grazing Lands	50	2,115	23
Deciduous Dry Forest	14	690	8
Desert Microphyll Shrub	22	600	7
Medium Semi-Evergreen Forest	5	570	6
Oak Forest	11	564	6

Notes

a) From the National Institute for Statistics and Geography of Mexico for 2007 (from Paz Pellat et al., 2016).

At the national scale, CO₂ fluxes from mineral soils to the atmosphere were estimated as 30.2 Tg CO₂ per year, mostly from deforestation of secondary oak, pine-oak, and tropical dry forests (de Jong et al., 2010). About 10% of Mexico's land is strongly affected by soil erosion, with about 36% remaining stable (Bolaños-González et al., 2016).

Temperate forests in Mexico are potential areas of carbon sequestration because about 10% of total GHG emissions in Mexico are attributed to land-use change from opening new areas to cultivation and logging. Tropical forests in Mexico also experience much of the same pressures of land-use change, but they occur over stronger gradients of precipitation. Land-use change from forest to pasture appears to interact strongly with precipitation. For example, dry tropical forest conversion to pasture may increase SOC (3.7% at 788 mm per year), yet this same land-use change appears to decrease SOC as precipitation increases (−0.2% at 2,508 mm per year; −2.2% at 4,725 mm per year; Campo et al., 2016). Mangroves in Mexico have the highest density of soil carbon (364 Mg C per hectare), located throughout Mexico's extensive coastline and riverine systems. A variety of disturbances affect mangroves and, as in many parts of the world, include erosion, increasing sea level change, and salt intrusion (Gilman et al., 2008). Due to the difficulty in sampling these soils, few estimates are available, especially if attempting to quantify this stock to the

bottom of the organic layer. Nevertheless, the Gulf of Mexico region generally has the highest carbon stocks (1,300 Mg C per hectare) of SOC compared with those of the other regions in Mexico (100 to 1,100 Mg per hectare; Herrera Silveira et al., 2016).

12.4.3 Canada

Canada has a total land area of 998.5 megahectares (Mha) that contains 72.2 gigatons of carbon (Gt C) to a depth of 30 cm (Tarnocai 1997). The total of 55.2 Mha of land currently used for agriculture contain about 4.14 Gt C to a depth of 30 cm and 5.5 Gt to 1 m. As about 80% of agricultural land is located in the Canadian Prairies, most (approximately 88%) SOC is also found in Prairie soils, which are mostly carbon-rich Chernozemic soils developed under grassland. Tarnocai (1997) estimated a total of 262.3 Pg C in soils within the tundra, forest, and agricultural regions of Canada. Over half the carbon (147.1 Pg C; Tarnocai 2006) is in organic (peat) soils, some of which are affected by permafrost. Total soil carbon estimates for Canada likely will increase as knowledge of deep carbon stocks in permafrost soils increases (Hugelius et al., 2014). For example, Kurz et al. (2013) estimated that soils in Canada's boreal forest region alone contain 208 Pg C, which is about 80% of the Tarnocai (1997) estimate of the total carbon stocks in Canada. Of this 208 Pg, the majority (137 Pg) of the boreal soil carbon stocks are in the deep organic soils of the country's extensive peatlands, and the remainder (71 Pg) are in upland



Table 12.4. Estimates of Soil Carbon Storage in Canada^{a-b}

Land Cover	Soil Organic Carbon
Organic (Peat) Soils	147.1 ^c , 137 ^e
Agriculture	5.5 ^d
Boreal Forest Region	208 ^{e,f}
Upland Forest Soils	71 ^e
Total	262.3^{c,g}

Notes

- a) Storage measured in soil down to 1 m in depth.
- b) Values in petagrams.
- c) Tarnocai (2006).
- d) Tarnocai (1997).
- e) Kurz et al. (2013).
- f) Note that this overlaps with estimates of organic peat soil carbon.
- g) Columns do not add up due to overlap in categories.

forest soils that often have thick organic soil horizons (42 to 55 Mg C per hectare; estimated from Letang and de Groot 2012) that overlay the mineral soil (Kurz et al., 2013; see Table 12.4, this page).

Canadian forest soil carbon research over the last decade has focused on understanding the dynamics of SOC as influenced by 1) mosses (Bona et al., 2013, 2016); 2) forest composition and soil taxonomy (Laganiere et al., 2015; Shaw et al., 2008, 2015); 3) invasive earthworms (Cameron et al., 2015); 4) response to temperature changes (Laganiere et al., 2015; Smyth et al., 2011); 5) response to wildfire, specifically in peatlands (Granath et al., 2016; Kettridge et al., 2015); and 6) recovery patterns (Ward et al., 2014). Under development is a national peatland carbon modeling system (Webster et al., 2016) that will fill information gaps previously identified, including a peatland-type map; landscape-scale modeling of forested, treed, and nontreed peatland types; water table fluctuation in response to climate change; and CH₄ fluxes (Shaw et al., 2016). Eventually, responses to permafrost thaw, wildfire, and anthropogenic disturbances will be included (Shaw et al., 2016; Webster et al., 2016).

Several new spatial products and databases have improved the understanding of relationships among vegetation types (Beaudoin et al., 2014; Thompson et al., 2016) and changes in disturbance-type patterns (Hermosilla et al., 2016), improving accuracy and enhancing the ability to scale up and integrate results from fine-scale to landscape-scale studies reporting national GHG emissions.

The 55.7 Mha of land that currently are used for agriculture in Canada are estimated to contain about 4.3 Pg C to a depth of 30 cm and 6.6 Pg C to 1 m using the Canadian Soil Information Service (CanSIS) National Soil Database. As of 2013, Canadian agricultural land removed 11 Tg CO₂ per year, an amount which represents about 2% of the total national GHG emissions (ECCC 2015). This is due largely to a reduction in the use of summer fallow lands and increased adoption of no-till practices in the Canadian Prairies. However, this value has declined from the reported 13 Tg in 2005 because changes in SOC stocks and fluxes tend to reach equilibrium at some point after a change in conditions.

12.4.4 Arctic and Boreal Ecosystems

Arctic and boreal ecosystems cover about 22% of the global land surface (Chapin et al., 2000) and contain 1,035 ± 150 Pg C in the upper 3 m of surface soil (Hugelius et al., 2014), amounts which equal about 33% of the total global surface SOC pool (Jobbágy and Jackson 2000; Schuur et al., 2015). The presence of permafrost and waterlogged soils in boreal and Arctic soils has allowed the accumulation of large quantities of carbon in this biome (McGuire et al., 2009; see Ch. 11: Arctic and Boreal Carbon, p. 428, for more details). Deep soils (>3 m in depth) contain significant stocks estimated between 210 ± 70 Pg C and 456 ± 45 Pg C, particularly in carbon-rich Pleistocene-age sediments called “yedoma” found in unglaciated parts of Alaska and Siberia, as well as in their alluvial deposits (Hugelius et al., 2014).

The changing disturbance regime can strongly affect soil carbon storage and flux. Permafrost thaw (Schuur et al., 2015) is tied to changes in the timing, frequency, and severity of wildfires



(Chapin et al., 2010; Kasischke et al., 2010), plant community composition (Mann et al., 2012), and alterations in the hydrological cycle (Jorgenson et al., 2001, 2010; Roach et al., 2013). Thaw will affect both storage and fluxes of carbon as the climate continues to warm. An estimated 5% to 15% of the terrestrial permafrost carbon pool is thought to be vulnerable to decomposition and release to the atmosphere, based on a synthesis of experimental studies, ecosystem models, and expert assessments (Schuur et al., 2015). Carbon loss from peatlands has shown large responses to water table fluctuations (Waddington et al., 2015), wildfire events (Turetsky et al., 2011), and permafrost thaw (Jones et al., 2017; Wissler et al., 2011). Key uncertainties as to the future of carbon storage in Arctic and boreal regions include the extent to which plant community productivity will respond to elevated CO₂ (McGuire et al., 2009), whether landscapes will become wetter or drier in the future (Schuur et al., 2015), the magnitude of winter fluxes (Commane et al., 2017), and the extent of the permafrost carbon feedback (Schaefer et al., 2011; Schuur et al., 2015).

12.5 Societal Drivers, Impacts, and Carbon Management

12.5.1 Agriculture

Because more than 50% of the Earth's vegetated surface is dedicated to agriculture (e.g., cropland and grazing land), understanding the role of agricultural management on SOC stocks is critical (see Ch. 2: The North American Carbon Budget, p. 71). Virtually all management choices (e.g., crop type, rotation, tillage, fertilization, irrigation, and residue management) will affect carbon inputs (e.g., crop residues and manure) and the decay rate or erosional loss of SOM (Paustian et al., 1997; Smith 2008). In most cases, SOC changes occur slowly and short-term (annual) changes are difficult to measure, but studies from long-term experiments, together with improved predictive models, provide a basis for guiding management and policies to improve SOC stocks (NAS 2010; Ogle et al., 2014; Paustian et al., 2016).

Causes of SOC loss include 1) reduced biomass carbon inputs; 2) enhanced erosion and leaching; and 3) increased decomposition rates due to tillage disturbance (Paustian et al., 2016). A meta-analysis for Canadian soils reported that, when native soil was converted to agricultural land, there was an average loss of 24% ± 6% of soil carbon (VandenBygaart et al., 2003). Globally, agricultural soils have lost, on average, 20% to 45% of their original top soil carbon (0 to 30 cm) but with much higher losses in cultivated organic soils and where extensive erosion has occurred (Don et al., 2011; Ogle et al., 2005). Following restoration of perennial forest and grassland vegetation on annual cropland (e.g., for soil restoration or retiring marginal lands from production), much of the lost soil carbon stocks eventually can be recovered. Conversion of annual cropland to perennial grassland in temperate environments increased soil carbon stocks, on average, by 13% to 16%, with greater relative increases occurring in more mesic climates (Ogle et al., 2005).

In recent decades, SOC stocks in agricultural soils in the United States and Canada have stabilized and in some cases begun to increase (Follett et al., 2011; U.S. EPA 2015) as new conversion of land to agricultural use has largely halted and adoption of soil conservation practices and crop yields have increased (Chambers et al., 2016; Johnson et al., 2006). Effects of agriculture on soil carbon stocks, along with effects of conservation measures, are reviewed and quantified in Angers and Eriksen-Hamel (2008), Hutchinson et al. (2007), Luo et al. (2010), Palm et al. (2014), Paustian et al. (2016), Powlson et al. (2014), and many others. Improved residue management, added forage in crop rotations or adoption of agroforestry, double-cropping, conservation reserve planting, increased use of perennials in rotation, and use of practices that increase plant growth such as effective fertilization are successful in increasing soil carbon (Hutchinson et al., 2007; Luo et al., 2010; Palm et al., 2014), especially if more than one practice is used. In Canada, the wide adoption of reduced tillage and summer fallow over many regions has resulted in soil carbon increases and reduced erosion



(Agriculture and Agri-Food Canada 2016; Soil Conservation Council of Canada 2016).

An analysis of no-till only versus conventional till by Palm et al. (2014) found that carbon gains occurred in only half the paired comparisons and that increased residue retention had a greater effect on soil carbon than reduced tillage. Powlson et al. (2014) argue that adoption of no-till agriculture can improve crop production and reduce erosion in many cases, but it may not have significant effects on carbon sequestration. However, a meta-analysis by Kopittke et al. (2017) saw an overall small positive (+9%) effect of conversion to no-till from conventional till methods. Most analyses of tillage effects do not account for SOC erosion. Montgomery (2007) calculated a mean erosion rate difference between conventional agriculture and no-till agriculture of about 1 mm per year. Although this eroded soil causes a net movement of carbon from the site with associated negative effects on soil fertility and health, this movement might not represent a net loss of soil carbon globally and could represent a net sink, because the eroded carbon can be buried and therefore protected. Meanwhile, carbon accumulation can continue in the site from which the erosion originally occurred via the usual processes of additions and transformations of plant residues (Wang et al., 2017).

Estimates of the current SOC balance for U.S. agricultural lands suggest a small net sink on long-term cropland (6.4 Tg C per year) and on land recently converted to grassland (2.4 Tg C per year), while small net losses of SOC were estimated for long-term grassland (3.3 Tg C per year) and land recently converted to cropland (4.4 Tg C per year; U.S. EPA 2015). A similar picture appears for Canadian agricultural soils with an estimated net sink of about 3 Tg C per year (ECCC 2015). A full soil carbon inventory for Mexican agricultural soils is still in progress; however, with ongoing forest conversion to agricultural uses (see Section 12.4.2, p. 481), there likely is a substantial loss of SOC due to agricultural activities.

Other chapters present more information on management of agricultural soils and its effects on

carbon (see Ch. 5: Agriculture, p. 229; Ch. 7: Tribal Lands, p. 303; and Ch. 10: Grasslands, p. 399).

12.5.2 Forestry

A wide variety of forest management practices affect around 204 Mha of timberlands in CONUS (see Ch. 9: Forests, p. 365). Those practices typically involve a combination of harvesting, stand regeneration, and stand tending. The intensity of those practices and their resulting effects on soils depend on landowner management objectives.

To date, most research on forest harvest effects on soil carbon has suggested that mild to moderate intensity harvesting does not cause measurable changes in upland soils (Johnson and Curtis 2001), but that intensive harvesting and plantation management may cause reductions in mineral soil carbon (Buchholz et al., 2014; Johnson and Curtis 2001), especially if imposed on old-growth natural stands. A meta-analysis of studies measuring effects of forest harvest on soil carbon stocks by Nave et al. (2010) found that while forest floor carbon generally was reduced after harvest, mineral soil carbon was less affected, although certain soil orders were more susceptible to mineral soil carbon loss than others. Forest soil carbon stores have the ability to recover to preharvest stages, although recovery might take decades (Nave et al., 2010) to a century or more (Diochon et al., 2009); thus, rotation length plays a significant role in the degree of harvest impacts on soil carbon. Several chronosequence studies have observed reductions in mineral-bound carbon pools in successional stands decades after harvesting (Diochon et al., 2009; Lacroix et al., 2016; Petrenko and Friedland 2015). Because this timing of carbon loss corresponds to periods of high nutrient demands during biomass re-accumulation, the cause could be mining of SOM by plants and mycorrhizal fungi to alleviate nutrient limitation. Dean et al. (2017) argue from a modeling standpoint that there are more significant losses of soil carbon with forest harvest of primary forests when calculated over centuries, but this model result is not supported by empirical studies.

Afforestation and agroforestry (the practice of integrating woody vegetation with crop and/or



animal production systems) have been cited as having potential for increasing soil carbon sequestration (IPCC 2000; Upson et al., 2016). Several meta-analyses conducted on afforestation effects on former croplands have produced a general consensus that soil carbon gains may take more than 30 years to be measurable (Barcena et al., 2014; Li et al., 2012; Nave et al., 2013) but can increase carbon stocks by 19% to 53% (Guo and Gifford 2002; Nave et al., 2013). However, while tree establishment in both grasslands and croplands showed greatly increased aboveground biomass carbon storage, meta-analysis of studies found that tree establishment on pastureland led to losses or no changes in soil carbon (Shi et al., 2013).

12.6 Synthesis and Outlook

Soil carbon is vulnerable to both pervasive warming and moisture disturbances, as well as to land-use decisions, all of which can strongly affect soil carbon contents. In northern latitudes, which are particularly vulnerable to soil carbon loss, some of the fastest warming trends (Cohen et al., 2014) and largest carbon stocks (Ping et al., 2008) occur. A significant portion of northern soil carbon is stored as organic peat horizons, which play a pivotal role in insulating permafrost from temperature changes but are particularly sensitive to changes in soil moisture (Johnson et al., 2013). Thus, the feedbacks among warming, moisture, and wildfire have important consequences to the carbon cycle at a global scale (Olefeldt et al., 2016). Meanwhile, localized “hotspots” for soil carbon storage, while also vulnerable to warming and soil moisture, can be sensitive to management practices as well and, therefore, can offer potential mitigation opportunities to avoid carbon emissions. For example, maintaining high water tables in carbon-rich peatlands potentially avoids carbon emissions that otherwise would accompany drainage.

Management options for actively sequestering carbon into soil are important opportunities for climate mitigation, but several issues arise before there is confidence in the outcome for a given soil under a given management setting. Topographical and mineralogical characteristics and disturbance histories (e.g., fire-return interval and land-use change history)

likely influence the net balance between input and loss and yet are highly variable across North America. Strategic experimental designs with consistent oversight and methodologies could constrain the uncertainties and understanding of the processes that control carbon storage. Building spatially and temporally explicit databases could improve process-based models to provide better estimates for soil carbon trajectories and thereby empower land managers to chart the trajectory of soil carbon.

Increasingly, the development of policies to 1) promote improved soil health (Kibblewhite et al., 2008; Vrebos et al., 2017), 2) encourage soil carbon sequestration for GHG mitigation (Chambers et al., 2016; Follett et al., 2011), and 3) satisfy consumer demands for more sustainable products (Lavallee and Plouffe 2004) will demand strong scientific support for improved understanding of SOC dynamics, new technologies to increase SOC stocks, and decision-support tools to effectively assess options and monitor progress. Along with new research on more conventional practices to build soil carbon (e.g., improved rotations, reduced tillage, and cover crops), scientists are investigating newer practices and technologies to increase SOC stocks, including 1) applying biochar (Woolf et al., 2010) and compost (Ryals et al., 2015), 2) using deep tillage to increase the total depth and storage of SOC-rich soil (Alcantara et al., 2016), 3) deploying new crop varieties with increased allocation of carbon below ground and deeper into the soil profile (Paustian et al., 2016), and 4) planting perennial plants in place of annual crops (Cox et al., 2006). New research and best practices in forestry such as selective harvesting and residue management (Peckham and Gower 2011), tailored for particular soils (Hazlett et al., 2014), also have the potential to increase carbon retention in forest soils. As new knowledge is generated about the applicability of various practices in different environments, incorporating this new information into improved decision-support tools (see Ch. 18: Carbon Cycle Science in Support of Decision Making, p. 728) will guide land managers, industry, policymakers, and other stakeholders in building healthier soils that are rich in organic matter.



SUPPORTING EVIDENCE

KEY FINDING 1

Estimates for soil carbon stocks in the conterminous United States plus Alaska range from 142 to 154 petagrams of carbon (Pg C) to 1 m in depth. Estimates for Canada average about 262 Pg C, but sampling is less extensive. Soil carbon for Mexico is calculated as 18 Pg C (1 m in depth), but there is some uncertainty in this value (*medium confidence*).

Description of evidence base

The value range of soil carbon to a depth of 1 m for the United States is based on several compilations: Alaska is estimated in Mishra and Riley (2012) as 77 Pg C, an increase from the value reported by Bliss and Maursetter (2010) of 48 Pg. The sampling for the Mishra and Riley (2012) estimate is quite extensive, and land types for areal weighting are well known and documented. Modern estimates for the conterminous United States (CONUS) span the range from the U.S. Geological Survey (USGS) estimate of Sundquist et al. (2009) at 77 Pg C and the Rapid Carbon Assessment (RaCA, initiated by the Soil Science Division of the U.S. Department of Agriculture's National Resources Conservation Service in 2010) estimate (Soil Survey and Loecke 2016) at 65 Pg C (see Table 12.1, p. 479). The RaCA estimate is based on 144,833 soil samples and extrapolation using detailed soil maps. The soil carbon value of 9 Pg C for Mexico is based on Paz Pellat et al. (2016), but that estimate is based on sampling to a depth of only 30 cm. Based on conversion factors in Jobbágy and Jackson (2000), a conservative extrapolation to 1 m yields a value of 18 Pg C. The estimates for Canada are from Tarnocai (1997, 2006). This assessment recognizes that 1 m is a very arbitrary depth to consider; Batjes (1996) reported a 60% increase in the global soil organic carbon (SOC) budget when the second meter of soil was included.

Major uncertainties

There is medium high confidence in the estimates from CONUS due to new extensive and intensive sampling, although estimates for specific land-use classes still vary with different estimates. Confidence is relatively high for estimates in the agricultural areas of Canada but lower for forested areas. In Canada, uncertainty for the large peatlands areas in the boreal and Arctic regions is high due to low-sampling intensity and low-resolution mapping of peatland types. Uncertainty for estimates from Mexico are likely high due to low sampling coverage, and available data are only to a depth of 30 cm.

Assessment of confidence based on evidence and agreement, including short description of nature of evidence and level of agreement

Soil carbon was extensively sampled in three independent studies for CONUS, so the confidence for the range of values reported here is very high. Due to the complex nature of estimating soil carbon in boreal and peat regions, the uncertainty is greater surrounding values for Canada. There is low confidence in values reported for Mexico as sampling is not as extensive and the depth of sampling is not as great.

Summary sentence or paragraph that integrates the above information

The estimates of total soil carbon stores are reasonably accurate for CONUS and Canada but are less accurate for Mexico.



KEY FINDING 2

Most Earth System Models (ESMs) are highly variable in projecting the direction and magnitude of soil carbon change under future scenarios. Predictions of global soil carbon change through this century range from a loss of 72 Pg C to a gain of 253 Pg C with a multimodel mean gain of 65 Pg C. ESMs projecting large gains do so largely by projecting increases in high-latitude soil organic carbon (SOC) that are inconsistent with empirical studies that indicate significant losses of soil carbon with predicted climate change (*high confidence*).

Description of evidence base

A description of the scientific concerns with current ESMs is presented in He et al. (2016). They analyzed ^{14}C data from 157 globally distributed soil profiles sampled to a depth of 1 m to demonstrate that ESMs currently overestimate the soil carbon sink potential. Todd-Brown et al. (2014) also pointed out major sources of error in current ESMs and suggested that most ESMs poorly represented permafrost dynamics and omitted potential constraints on SOC storage, such as priming effects, nutrient availability, mineral surface stabilization, and aggregate formation. For example, many ESMs simulated large changes in high-latitude SOC that ranged from losses of 37 Pg C to gains of 146 Pg C. The poor performance of current ESMs can result from biases in model structure, parameterization, initial values of carbon pools, and other variables (Luo et al., 2016).

There is currently a great deal of controversy over how to improve the representation of soil carbon in models (Chen et al., 2015); several authors suggest that microbial dynamics, including the priming effect, need better representation (Georgiou et al., 2015; Sulman et al., 2014; Wieder et al., 2014), as does soil carbon response to nitrogen enrichment (Janssens and Luysaert 2009; Riggs and Hobbie 2016). However, there is no evidence that suggests how much detail is needed to adequately represent future soil carbon dynamics and soil carbon pools.

Deep carbon (>1 m in depth) generally has been found to be more stable and resistant to management or climate change than carbon in surface soils (Rumpel and Kögel-Knabner 2010; Schrumpf et al., 2013), but, given that subsurface horizons contain more than half the soil carbon (Jobbágy and Jackson 2000), small changes could significantly affect carbon budgets. Although less well studied, deep carbon has been shown to be sensitive to management practices (Alcantara et al., 2016; Ward et al., 2016).

Microbial dynamics, including the priming effect, are key controls on soil carbon turnover (Bernal et al., 2016; Guenet et al., 2012). Carbon-use efficiency of different substrates by microbes might be a key factor in soil carbon stabilization (Cotrufo et al., 2013).

Major uncertainties

How much detailed information on microbial physiology, coupled carbon-nitrogen cycles, or other processes is needed to improve soil carbon models is not well known.

Assessment of confidence based on evidence and agreement, including short description of nature of evidence and level of agreement

Models can be tested against empirical data, and they do not perform very well; thus, determining the accuracy of future projections is difficult.



Summary sentence or paragraph that integrates the above information

The poor performance of current ESMs can result from biases in model structure, parameterization, initial values of carbon pools, and other variables. Most ESMs poorly represent permafrost dynamics and omit potential constraints on SOC storage, such as priming effects, nutrient availability, mineral surface stabilization, and aggregate formation.

KEY FINDING 3

Soil carbon stocks are sensitive to agricultural and forestry practices and loss of carbon-rich soils such as wetlands. Soils in North America have lost, on average, 20% to 75% of their original top soil carbon (0 to 30 cm) with historical conversion to agriculture, with a mean estimate for Canada of $24\% \pm 6\%$. Current agricultural management practices can increase soil organic matter in many systems through reduced summer fallow, cover cropping, effective fertilization to increase plant production, and reduced tillage. Forest soil carbon loss with harvest is small under standard management practices and mostly reversible at the century scale. Afforestation of land in agriculture, industry, or wild grasslands in the United States and Canadian border provinces could increase SOC by $21\% \pm 9\%$ (*high confidence*).

Description of evidence base

Converting native forests or pastures to cropland can reduce soil carbon by 42% to 59%, respectively (Guo and Gifford 2002). A meta-analysis for Canadian soils reported that, when native soil was converted to agricultural land, there was an average 24% loss of soil carbon (VandenBygaart et al., 2003). Estimates for Mexico also suggest that loss of soil carbon due to management remains significant (Huber-Sannwald et al., 2006).

Agricultural effects on soil carbon stocks, including effects of conservation measures, are reviewed and quantified in Angers and Eriksen-Hamel (2008), Hutchinson et al. (2007), Luo et al. (2010), Palm et al. (2014), Paustian et al. (2016), Powlson et al. (2014), and many others. Specific conservation measures for improved soil carbon retention have been shown to be effective in both Canada and the United States. In Canada, conservation measures, including reduced summer fallow and reduced tillage, have been widely adopted over many regions and have resulted in soil carbon increases and reduced erosion (Soil Conservation Council of Canada 2016). Agriculture and Agri-Food Canada (2016; AAFC) has 30 years of data showing that, in the Canadian Prairies, reduced tillage combined with reduced summer fallow have led to significant SOC increases. Improved residue management, including adding forage in crop rotations or adopting agroforestry, and practices that increase plant growth such as effective fertilization are effective in increasing soil carbon (Hutchinson et al., 2007; Palm et al., 2014). A meta-analysis by Angers and Eriksen-Hamel (2008) suggested that, although significant increases in surface soil carbon with reduced tillage are commonly observed, the slight decreases in soil below the plow layer also are common, thus making overall increases in total soil carbon profiles averaged across studies small but significant. In a more recent meta-analysis by Luo et al. (2010), increased soil carbon with reduced tillage was seen only for double-cropping systems, a finding which agrees with the AAFC result that reduced summer fallow and reduced tillage together caused significant increases in soil carbon.

Palm et al. (2014) point out serious methodological flaws with many tillage comparisons that include sampling by depth not equivalent soil mass, flaws which cause significant overestimates



of soil carbon in no-till soils with higher bulk densities. In their 2014 meta-analysis, about half the paired comparisons showed small increases in soil carbon from reduced till but half did not, suggesting that increased residue retention is more significant than reducing tillage. A similar meta-analysis by Kopittke et al. (2017) that also corrected for changes in bulk density found an overall small positive (+9%) effect of conversion to no-till practices from conventional till. Powlson et al. (2014) point out that the gains in surface soil carbon with adoption of no-till methods can improve crop production and reduce erosion in many cases, but the reverse can be true in cool, wet climates or the wet tropics.

Several meta-analyses of afforestation effects on former croplands have been conducted, and there is general consensus that soil carbon gains may take more than 30 years to be seen (Barcena et al., 2014; Li et al., 2012; Nave et al., 2013) and can increase carbon stocks by 19% to 53% (Guo and Gifford 2002; Nave et al., 2013).

Data on forest harvest effects are from a comprehensive meta-analysis by Nave et al. (2010), who report variable and low changes in mineral soil carbon stocks with forest harvest but significant decreases in forest floor carbon. Several chronosequences support this meta-analysis. Dean et al. (2017) argue from a modeling standpoint that there are significant long-term losses of soil carbon with forest harvest of primary forests; however, much of this argument is based on assumptions about the relationship between plant inputs and soil carbon sequestration that are not necessarily supported by empirical studies.

Wetland estimates are based on information in this report's (SOCCR2) two wetland chapters. All chapters showed findings of strong evidence that loss of wetlands is a significant factor for total soil carbon loss, given the very high carbon density of wetland soils.

Wear and Coulston (2015), using data from the National Greenhouse Gas Inventory (NGHGI), report annual forest carbon accumulation, including both sequestration and land-use transfers in the United States as 223 teragrams of carbon (Tg C) per year, roughly 0.5% of the stored forest carbon. This likely translates into increased soil carbon storage, although this distinction was not made in the analysis. Similar estimates have not been made for Canada or Mexico.

Major uncertainties

The certainty for forest harvest effects on soil carbon appears to be very robust and based on many studies across North America, although a recent modeling study suggests that these other studies, carried out over decades, miss a multicentury-scale slow loss of soil carbon with forest harvest. However, there are no data to support that model result. Uncertainty arises because there are few empirical studies that compare soil carbon stocks in true primary forests to forests that have undergone centuries-long harvest cycles.

Uncertainties for agricultural effects have to do with site-specific variation in management implementation and lack of knowledge of deep soil carbon dynamics. However, convergence of the different meta-analyses on similar figures and research in this field is quite extensive (Li et al., 2012).

The wetland estimate also is quite robust given the high sampling density of the National Wetland Condition Assessment (NWCA) of the National Aquatic Resource Surveys. The NGHGI estimate of forest cover increase is quite robust given the quality of input data.



Assessment of confidence based on evidence and agreement, including short description of nature of evidence and level of agreement

The meta-analyses of Nave et al. (2010, 2013) suggest very good agreement over forestry effects on soil carbon, although Dean et al. (2017) suggest that, over centuries, logging has had more significant effects on soil carbon. Given that the Dean et al. (2017) study is based on modeling with assumptions that are not supported in this analysis, such as that SOC is strongly related to biomass inputs, SOCCR2 is placing greater confidence in the Nave analyses (Nave et al., 2010, 2013).

The analysis by Paustian et al. (2016) suggests that there is some disagreement over agricultural management effects on SOC and that these effects are specific to local site and climatic conditions. The Li et al. (2012) meta-analysis suggests that afforestation of former croplands globally results in net SOC increases but that local results are so variable that local projection is difficult and results depend on soil type, management, and the type of tree species.

The wetland estimate is quite robust given the high sampling density of the NWCA.

Estimated likelihood of impact or consequence, including short description of basis of estimate

Conversion to agriculture is a significant source of greenhouse gases to the atmosphere and loss of soil carbon. However, across North America, mitigation strategies such as conversion to no-till or reduced-till methods, adoption of crop rotations that provide greater carbon inputs, increased residue retention, and the use of cover crops during fallow periods are reducing the impact of agriculture (Paustian et al., 2016). Similar results are seen in Canada (Soil Conservation Council of Canada 2016). Erosion of soil carbon from agricultural lands is still a significant concern (Montgomery 2007). Afforestation has caused increases in soil carbon across CONUS.

Summary sentence or paragraph that integrates the above information

Studies have shown that conversion of native land to agriculture significantly reduced soil carbon, although improved management of agricultural land has the potential to have significant positive effects on soil carbon reserves. While modeling exercises suggest that logging and management of primary forest cause a significant SOC loss, robust meta-analyses suggest that this loss is quite minimal with effective forestry management.

KEY FINDING 4

Large uncertainties remain regarding soil carbon budgets, particularly the impact of lateral movement and transport of carbon (via erosion and management) across the landscape and into waterways. By 2015, cumulative regeneration of soil carbon at eroded agricultural sites and the preservation of buried, eroded soil carbon may have represented an offset of $37 \pm 10\%$ of carbon returned to the atmosphere by human-caused land-use change (*medium confidence*).

Description of evidence base

Best estimates of the effects of erosion are summarized in Billings et al. (2010), Van Oost et al. (2007), and Wang et al. (2017). Erosion can significantly affect productivity in agricultural regions, and some authors have argued that loss of eroded carbon represents a true loss to the atmosphere (Lal and Pimentel 2008). However, work based on multiple eroding profiles indicates that approximately 26% of eroded SOC can be replaced at the eroding site, representing a



small but significant carbon sink (Van Oost et al., 2007). Harden et al. (1999) suggest that U.S. cropping patterns before 1950 likely resulted in about a 20% to 30% reduction of original SOC but that on-site recovery of soil organic matter (SOM) levels occurred after the 1950s. In Canada, VandenBygaart et al. (2012) also note a net carbon sink for eroded agricultural soils. Van Oost et al. (2007) suggest that replacement of eroded SOC, along with damped SOC mineralization upon burial, may combine to generate a small net carbon sink up to about 0.1 Pg C per year. Wang et al. (2017) calculate that cumulative, agriculturally accelerated erosion prompted SOC replacement and buried SOC preservation, representing an offset of $70 \pm 16\%$ of carbon emissions by anthropogenic land-cover change up to AD 1600; after this period, the cumulative value represented a smaller offset ($37 \pm 10\%$ in 2015).

Major uncertainties

The fate of eroded agricultural soil can only be modeled, not directly measured, and the production of new soil carbon after exposure of new mineral surfaces also cannot be directly measured.

Assessment of confidence based on evidence and agreement, including short description of nature of evidence and level of agreement

Erosion of soil is known to occur, but the fate of the eroded SOC is less clear. Currently, findings conclude that the eroded SOM appears to represent a small sink of carbon but that not all material is accounted for, and the geographic extent of full carbon budget studies is quite limited. Although subsurface soil carbon appears to be relatively stable, the responses to future changes in management and climate are not well understood.

Estimated likelihood of impact or consequence, including short description of basis of estimate

In the United States, conservation measures introduced after the Dust Bowl of the 1930s suggest that the potential for massive erosional losses of soil carbon are unlikely, but similar measures are not used in Mexico. In Canada, conservation measures including zero-till have been widely adopted over many regions and have resulted in soil carbon increases and reduced erosion (Soil Conservation Council of Canada 2016). Estimates for Mexico suggest that loss of soil carbon due to management practices remains significant (Huber-Sannwald et al., 2006).

Summary sentence or paragraph that integrates the above information

Large uncertainties remain in specific key areas, including the impact of lateral movement and transport of carbon through erosion and management.

KEY FINDING 5

Evidence is strong for direct effects of increased temperature on loss of soil carbon, but warming and atmospheric carbon dioxide increases also may enhance plant production in many ecosystems, resulting in greater carbon inputs to soil. Globally, projected warming could cause the release of 55 ± 50 Pg C over the next 35 years from a soil pool of $1,400 \pm 150$ Pg C. In particular, an estimated 5% to 15% of the peatland carbon pool could become a significant carbon flux to the atmosphere under future anthropogenic disturbances (e.g., harvest, development, and peatland drainage) and change in disturbance regimes (e.g., wildfires and permafrost thaw) (*medium confidence*).



Description of evidence base

Although many laboratory experiments have shown that soils respond to increased temperature with increased respiration, there are many potential causes for this increase, including increased belowground inputs (Giardina et al., 2014) or increased plant production (Phillips et al., 2016). A global meta-analysis has shown that soil respiration increases with temperature (Bond-Lamberty and Thomson 2010), but how much of this is due to turnover of new, labile plant inputs is unclear (reviewed in Bradford et al., 2016). Empirical relationships developed by Crowther et al. (2016) suggest that global soil carbon stocks in the upper soil horizons will fall by 30 ± 30 Pg C under a temperature increase of 1°C , and 55 ± 50 Pg C with expected warming in the next 35 years, depending on the rate at which the effects of warming are realized.

Many studies have suggested that peatlands and boreal ecosystems are particularly vulnerable to warming (Bridgman et al., 2008; Dise 2009; Hicks Pries et al., 2015; Koven et al., 2015) because of factors such as permafrost thawing and drying effects on decomposition (Ise et al., 2008), increased fire from drying (Turetsky et al., 2014), and poleward expansion of low-carbon ecosystems (Koven 2013). Thawing of sporadic and discontinuous permafrost may release up to 24 Pg C currently stored in boreal peatlands over decades to centuries (Jones et al., 2017). Wildfire combustion of organic soils across permafrost-dominated landscapes can produce carbon losses ranging from 2.95 ± 0.12 to 6.15 ± 0.41 kilograms of carbon per m^2 , depending on the season (Turetsky et al. 2011).

Major uncertainties

Most laboratory experiments demonstrate that warming causes the loss of soil carbon, but how soils in natural ecosystems will respond to global warming is less predictable, given the different possible trajectories of plant production responses in different ecosystems and the possibility of increased plant production matching elevated soil respiration (Xu et al., 2016). Acclimation of soil microbes to warming could modulate the response of soils (Luo et al., 2001), although a meta-analysis (Wang et al., 2014) suggests that heterotrophic activity will not significantly acclimate to warming.

Assessment of confidence based on evidence and agreement, including short description of nature of evidence and level of agreement

At current rates of carbon dioxide and temperature increase, peatlands are highly likely to release a significant amount of stored soil carbon. Less certain is whether soils in other ecosystems, especially those subject to drought, will respond similarly to elevated temperature.

Summary sentence or paragraph that integrates the above information

The release of carbon from peatland soils could represent a major positive feedback loop to continued disturbance regimes related to climate change and human activities.



REFERENCES

- Abramoff, R., X. Xu, M. Hartman, S. O'Brien, W. Feng, E. Davidson, A. Finzi, D. Moorhead, J. Schimel, M. Torn, and M. A. Mayes, 2018: The millennial model: In search of measurable pools and transformations for modeling soil carbon in the new century. *Biogeochemistry*, **137**(1), 51-71, doi: 10.1007/s10533-017-0409-7.
- Agriculture and Agri-Food Canada, 2016: *Soil Organic Matter Indicator*. Agriculture and Agri-Food Canada; Government of Canada. [<http://www.agr.gc.ca/eng/science-and-innovation/agricultural-practices/soil-and-land/soil-organic-matter-indicator/?id=1462905651688>]
- Alcantara, V., A. Don, R. Well, and R. Nieder, 2016: Deep ploughing increases agricultural soil organic matter stocks. *Global Change Biology*, **22**(8), 2939-2956, doi: 10.1111/gcb.13289.
- Angers, D. A., and N. S. Eriksen-Hamel, 2008: Full-inversion tillage and organic carbon distribution in soil profiles: A meta-analysis. *Soil Science Society of America Journal*, **72**(5), 1370, doi: 10.2136/sssaj2007.0342.
- Aspiras, R. B., O. N. Allen, R. F. Harris, and G. Chesters, 1971: The role of microorganisms in the stabilization of soil aggregates. *Soil Biology and Biochemistry*, **3**(4), 347-353, doi: 10.1016/0038-0717(71)90045-9.
- Averill, C., and C. V. Hawkes, 2016: Ectomycorrhizal fungi slow soil carbon cycling. *Ecology Letters*, **19**(8), 937-947, doi: 10.1111/ele.12631.
- Averill, C., B. L. Turner, and A. C. Finzi, 2014: Mycorrhiza-mediated competition between plants and decomposers drives soil carbon storage. *Nature*, **505**(7484), 543-545, doi: 10.1038/nature12901.
- Barcena, T. G., L. P. Kjaer, L. Vesterdal, H. M. Stefansdottir, P. Gundersen, and B. D. Sigurdsson, 2014: Soil carbon stock change following afforestation in northern Europe: A meta-analysis. *Global Change Biology*, **20**(8), 2393-2405, doi: 10.1111/gcb.12576.
- Batjes, N. H., 1996: Total carbon and nitrogen in the soils of the world. *European Journal of Soil Science*, **47**(2), 151-163, doi: 10.1111/j.1365-2389.1996.tb01386.x.
- Batjes, N. H., 2016: Harmonized soil property values for broad-scale modelling (WISE30sec) with estimates of global soil carbon stocks. *Geoderma*, **269**, 61-68, doi: 10.1016/j.geoderma.2016.01.034.
- Beaudoin, A., P. Y. Bernier, L. Guindon, P. Villemaire, X. J. Guo, G. Stinson, T. Bergeron, S. Magnussen, and R. J. Hall, 2014: Mapping attributes of Canada's forests at moderate resolution through kNN and MODIS imagery. *Canadian Journal of Forest Research*, **44**(5), 521-532, doi: 10.1139/cjfr-2013-0401.
- Berhe, A. A., J. Harte, J. W. Harden, and M. S. Torn, 2007: The significance of the erosion-induced terrestrial carbon sink. *BioScience*, **57**(4), 337, doi: 10.1641/b570408.
- Bernal, B., D. C. McKinley, B. A. Hungate, P. M. White, T. J. Mozdzer, and J. P. Megonigal, 2016: Limits to soil carbon stability; Deep, ancient soil carbon decomposition stimulated by new labile organic inputs. *Soil Biology and Biochemistry*, **98**, 85-94, doi: 10.1016/j.soilbio.2016.04.007.
- Bever, J. D., I. A. Dickie, E. Facelli, J. M. Facelli, J. Klironomos, M. Moora, M. C. Rillig, W. D. Stock, M. Tibbett, and M. Zobel, 2010: Rooting theories of plant community ecology in microbial interactions. *Trends in Ecology and Evolution*, **25**(8), 468-478, doi: 10.1016/j.tree.2010.05.004.
- Billings, S. A., and F. Ballantyne, 2013: How interactions between microbial resource demands, soil organic matter stoichiometry, and substrate reactivity determine the direction and magnitude of soil respiratory responses to warming. *Global Change Biology*, **19**(1), 90-102, doi: 10.1111/gcb.12029.
- Billings, S. A., and S. E. Ziegler, 2008: Altered patterns of soil carbon substrate usage and heterotrophic respiration in a pine forest with elevated CO₂ and N fertilization. *Global Change Biology*, **14**(5), 1025-1036, doi: 10.1111/j.1365-2486.2008.01562.x.
- Billings, S. A., R. W. Buddemeier, D. deB. Richter, K. Van Oost, and G. Bohling, 2010: A simple method for estimating the influence of eroding soil profiles on atmospheric CO₂. *Global Biogeochemical Cycles*, **24**(2), GB2001, doi: 10.1029/2009gb003560.
- Bliss, N. B., and J. Maursetter, 2010: Soil organic carbon stocks in Alaska estimated with spatial and pedon data. *Soil Science Society of America Journal*, **74**(2), 565, doi: 10.2136/sssaj2008.0404.
- Bliss, N. B., S. W. Waltman, L. T. West, A. Neale, and M. Mehafey, 2014: Distribution of soil organic carbon in the conterminous United States. In: *Soil Carbon. Progress in Soil Science*. [A. Hartemink and K. McSweeney (eds.)]. Springer, Cham, pp. 85-93.
- Bolaños González, M. A., F. Paz Pellat, C. O. Cruz Gaistardo, J. A. Argumedo Espinoza, V. M. Romero Benítez, and J. C. de la Cruz Cabrera, 2016: Mapa de erosión de los suelos de México y posibles implicaciones en el almacenamiento de carbono orgánico del suelo. *Terra Latinoam*, **34**(3), 271-288.
- Bolinder, M. A., H. H. Janzen, E. G. Gregorich, D. A. Angers, and A. J. VandenBygaart, 2007: An approach for estimating net primary productivity and annual carbon inputs to soil for common agricultural crops in Canada. *Agriculture, Ecosystems and Environment*, **118**(1-4), 29-42, doi: 10.1016/j.agee.2006.05.013.
- Bolker, B. M., S. W. Pacala, and W. J. Parton, 1998: Linear analysis of soil decomposition: Insights from the CENTURY model. *Ecological Applications*, **8**(2), 425-439, doi: 10.1890/1051-0761(1998)008[0425:LAOSDI]2.0.CO;2.
- Bona, K. A., C. H. Shaw, J. W. Fyles, and W. A. Kurz, 2016: Modeling moss-derived carbon in upland black spruce forests. *Canadian Journal of Forest Research*, **46**(4), 520-534, doi: 10.1139/cjfr-2015-0512.



- Bona, K. A., J. W. Fyles, C. Shaw, and W. A. Kurz, 2013: Are mosses required to accurately predict upland black spruce forest soil carbon in national-scale forest C accounting models? *Ecosystems*, **16**(6), 1071-1086, doi: 10.1007/s10021-013-9668-x.
- Bond-Lamberty, B., and A. Thomson, 2010: Temperature-associated increases in the global soil respiration record. *Nature*, **464**(7288), 579-582, doi: 10.1038/nature08930.
- Bond-Lamberty, B., C. Wang, and S. T. Gower, 2004: A global relationship between the heterotrophic and autotrophic components of soil respiration? *Global Change Biology*, **10**(10), 1756-1766, doi: 10.1111/j.1365-2486.2004.00816.x.
- Bradford, M. A., W. R. Wieder, G. B. Bonan, N. Fierer, P. A. Raymond, and T. W. Crowther, 2016: Managing uncertainty in soil carbon feedbacks to climate change. *Nature Climate Change*, **6**(8), 751-758, doi: 10.1038/Nclimate3071.
- Bridgman, S. D., J. Pastor, B. Dewey, J. F. Weltzin, and K. Updegraff, 2008: Rapid carbon response of peatlands to climate change. *Ecology*, **89**(11), 3041-3048, doi: 10.1890/08-0279.1.
- Brzostek, E. R., D. Dragoni, Z. A. Brown, and R. P. Phillips, 2015: Mycorrhizal type determines the magnitude and direction of root-induced changes in decomposition in a temperate forest. *New Phytologist*, **206**(4), 1274-1282, doi: 10.1111/nph.13303.
- Buchholz, T., A. J. Friedland, C. E. Hornig, W. S. Keeton, G. Zanchi, and J. Nunery, 2014: Mineral soil carbon fluxes in forests and implications for carbon balance assessments. *GCB Bioenergy*, **6**(4), 305-311, doi: 10.1111/gcbb.12044.
- Burke, I. C., C. M. Yonker, W. J. Parton, C. V. Cole, D. S. Schimel, and K. Flach, 1989: Texture, climate, and cultivation effects on soil organic matter content in U.S. grassland soils. *Soil Science Society of America Journal*, **53**(3), 800-805, doi: 10.2136/sssaj1989.03615995005300030029x.
- Cameron, E. K., C. H. Shaw, E. M. Bayne, W. A. Kurz, and S. J. Kull, 2015: Modelling interacting effects of invasive earthworms and wildfire on forest floor carbon storage in the boreal forest. *Soil Biology and Biochemistry*, **88**, 189-196, doi: 10.1016/j.soilbio.2015.05.020.
- Campo, J. F., O. A. García, S. Navarrete, and C. Siebe, 2016: Almacenes y dinámica del carbono orgánico en ecosistemas forestales tropicales de México. *Terra Latinoamericana*, **34**(1), 31-38.
- Chambers, A., R. Lal, and K. Paustian, 2016: Soil carbon sequestration potential of US croplands and grasslands: Implementing the 4 per thousand initiative. *Journal of Soil and Water Conservation*, **71**(3), 68A-74A, doi: 10.2489/jswc.71.3.68A.
- Chapin, F. S., A. D. McGuire, J. Randerson, R. Pielke, D. Baldocchi, S. E. Hobbie, N. Roulet, W. Eugster, E. Kasischke, E. B. Rastetter, S. A. Zimov, and S. W. Running, 2000: Arctic and boreal ecosystems of western North America as components of the climate system. *Global Change Biology*, **6**(S1), 211-223, doi: 10.1046/j.1365-2486.2000.06022.x.
- Chapin, F. S., A. D. McGuire, R. W. Ruess, T. N. Hollingsworth, M. C. Mack, J. F. Johnstone, E. S. Kasischke, E. S. Euskirchen, J. B. Jones, M. T. Jorgenson, K. Kielland, G. P. Kofinas, M. R. Turetsky, J. Yarie, A. H. Lloyd, and D. L. Taylor, 2010: Resilience of Alaska's boreal forest to climatic change. *Canadian Journal of Forest Research*, **40**(7), 1360-1370, doi: 10.1139/x10-074.
- Chen, L., P. Smith, and Y. Yang, 2015: How has soil carbon stock changed over recent decades? *Global Change Biology*, **21**(9), 3197-3199, doi: 10.1111/gcb.12992.
- Ciais, P., C. Sabine, G. Bala, L. Bopp, V. Brovkin, J. Canadell, A. Chhabra, R. DeFries, J. Galloway, M. Heimann, C. Jones, C. Le Quéré, R. B. Myneni, S. Piao, and P. Thornton, 2013: Carbon and other biogeochemical cycles. In: *Climate Change 2013: The Physical Science Basis. Contribution of Working Group I to the Fifth Assessment Report of the Intergovernmental Panel on Climate Change*. [T. F. Stocker, D. Qin, G. K. Plattner, M. Tignor, S. K. Allen, J. Boschung, A. Nauels, Y. Xia, V. Bex and P. M. Midgley (eds.)]. Cambridge University Press, Cambridge, UK, and New York, NY, USA, pp. 465-570.
- Clemente, J. S., A. J. Simpson, and M. J. Simpson, 2011: Association of specific organic matter compounds in size fractions of soils under different environmental controls. *Organic Geochemistry*, **42**(10), 1169-1180, doi: 10.1016/j.orggeochem.2011.08.010.
- Cohen, J., J. A. Screen, J. C. Furtado, M. Barlow, D. Whittleston, D. Coumou, J. Francis, K. Dethloff, D. Entekhabi, J. Overland, and J. Jones, 2014: Recent Arctic amplification and extreme mid-latitude weather. *Nature Geoscience*, **7**(9), 627-637, doi: 10.1038/Ngeo2234.
- Coleman, D. C., and D. H. Wall, 2015: Soil fauna. In: *Occurrence, Biodiversity, and Roles in Ecosystem Function, Soil Microbiology, Ecology and Biochemistry*, 4th ed. [E. A. Paul (ed.)]. Academic Press, pp. 111-149.
- Commane, R., J. Lindaas, J. Benmergui, K. A. Luus, R. Y. Chang, B. C. Daube, E. S. Euskirchen, J. M. Henderson, A. Karion, J. B. Miller, S. M. Miller, N. C. Parazoo, J. T. Randerson, C. Sweeney, P. Tans, K. Thoning, S. Veraverbeke, C. E. Miller, and S. C. Wofsy, 2017: Carbon dioxide sources from Alaska driven by increasing early winter respiration from Arctic tundra. *Proceedings of the National Academy of Sciences USA*, **114**(21), 5361-5366, doi: 10.1073/pnas.1618567114.
- CONAFOR, 2010: *Evaluación de los Recursos Forestales Mundiales 2010 Informe Nacional*. Rome, Italy.
- Cotrufo, M. F., M. D. Wallenstein, C. M. Boot, K. Deneff, and E. Paul, 2013: The Microbial Efficiency-Matrix Stabilization (MEMS) framework integrates plant litter decomposition with soil organic matter stabilization: Do labile plant inputs form stable soil organic matter? *Global Change Biology*, **19**(4), 988-995, doi: 10.1111/gcb.12113.
- Courtier-Murias, D., A. J. Simpson, C. Marzadori, G. Baldoni, C. Ciavatta, J. M. Fernandez, E. G. Lopez-De-Sa, and C. Plaza, 2013: Unraveling the long-term stabilization mechanisms of organic materials in soils by physical fractionation and NMR spectroscopy. *Agriculture, Ecosystems and Environment*, **171**, 9-18, doi: 10.1016/j.agee.2013.03.010.



- Cox, T. S., J. D. Glover, D. L. Van Tassel, C. M. Cox, and L. R. DeHaan, 2006: Prospects for developing perennial grain crops. *BioScience*, **56**(8), 649, doi: 10.1641/0006-3568(2006)56[649:pdfp-gc]2.0.co;2.
- Crow, S. E., K. Lajtha, R. D. Bowden, Y. Yano, J. B. Brant, B. A. Caldwell, and E. W. Sulzman, 2009: Increased coniferous needle inputs accelerate decomposition of soil carbon in an old-growth forest. *Forest Ecology and Management*, **258**(10), 2224-2232, doi: 10.1016/j.foreco.2009.01.014.
- Crowther, T. W., K. E. Todd-Brown, C. W. Rowe, W. R. Wieder, J. C. Carey, M. B. Machmuller, B. L. Snoek, S. Fang, G. Zhou, S. D. Allison, J. M. Blair, S. D. Bridgman, A. J. Burton, Y. Carrillo, P. B. Reich, J. S. Clark, A. T. Classen, F. A. Dijkstra, B. Elberling, B. A. Emmett, M. Estiarte, S. D. Frey, J. Guo, J. Harte, L. Jiang, B. R. Johnson, G. Kroel-Dulay, K. S. Larsen, H. Laudon, J. M. Lavallee, Y. Luo, M. Lupascu, L. N. Ma, S. Marhan, A. Michelsen, J. Mohan, S. Niu, E. Pendall, J. Penuelas, L. Pfeifer-Meister, C. Poll, S. Reinsch, L. L. Reynolds, I. K. Schmidt, S. Sistla, N. W. Sokol, P. H. Templer, K. K. Treseder, J. M. Welker, and M. A. Bradford, 2016: Quantifying global soil carbon losses in response to warming. *Nature*, **540**(7631), 104-108, doi: 10.1038/nature20150.
- Davidson, E. A., and I. A. Janssens, 2006: Temperature sensitivity of soil carbon decomposition and feedbacks to climate change. *Nature*, **440**(7081), 165-173, doi: 10.1038/nature04514.
- de Jong, B., C. Anaya, O. Maser, M. Olguín, F. Paz Pellat, J. Etchevers, R. D. Martínez, G. Guerrero, and C. Balbontin, 2010: Greenhouse gas emissions between 1993 and 2002 from land-use change and forestry in Mexico. *Forest Ecology and Management*, **260**(10), 1689-1701, doi: 10.1016/j.foreco.2010.08.011.
- de Vries, F. T., E. Thebault, M. Liiri, K. Birkhofer, M. A. Tsiafouli, L. Bjornlund, H. Bracht Jorgensen, M. V. Brady, S. Christensen, P. C. de Ruiter, T. d'Hertefeldt, J. Frouz, K. Hedlund, L. Hemerik, W. H. Hol, S. Hotes, S. R. Mortimer, H. Setälä, S. P. Sgardelis, K. Uteseny, W. H. van der Putten, V. Wolters, and R. D. Bardgett, 2013: Soil food web properties explain ecosystem services across European land use systems. *Proceedings of the National Academy of Sciences USA*, **110**(35), 14296-14301, doi: 10.1073/pnas.1305198110.
- Dean, C., J. B. Kirkpatrick, and A. J. Friedland, 2017: Conventional intensive logging promotes loss of organic carbon from the mineral soil. *Global Change Biology*, **23**(1), 1-11, doi: 10.1111/gcb.13387.
- Dessureault-Romppe, J., B. Nowack, R. Schulin, and J. Luster, 2007: Spatial and temporal variation in organic acid anion exudation and nutrient anion uptake in the rhizosphere of *Lupinus albus* L. *Plant and Soil*, **301**(1-2), 123-134, doi: 10.1007/s11104-007-9427-x.
- Dialynas, Y. G., S. Bastola, R. L. Bras, S. A. Billings, D. Markewitz, and D. d. Richter, 2016: Topographic variability and the influence of soil erosion on the carbon cycle. *Global Biogeochemical Cycles*, **30**(5), 644-660, doi: 10.1002/2015gb005302.
- Dietze, M. C., S. P. Serbin, C. Davidson, A. R. Desai, X. H. Feng, R. Kelly, R. Kooper, D. LeBauer, J. Mantooth, K. McHenry, and D. Wang, 2014: A quantitative assessment of a terrestrial biosphere model's data needs across North American biomes. *Journal of Geophysical Research: Biogeosciences*, **119**(3), 286-300, doi: 10.1002/2013jg002392.
- Diochon, A., L. Kellman, and H. Beltrami, 2009: Looking deeper: An investigation of soil carbon losses following harvesting from a managed northeastern red spruce (*Picea rubens* Sarg.) forest chronosequence. *Forest Ecology and Management*, **257**(2), 413-420, doi: 10.1016/j.foreco.2008.09.015.
- Dise, N. B., 2009: Environmental science. Peatland response to global change. *Science*, **326**(5954), 810-811, doi: 10.1126/science.1174268.
- Domke, G. M., C. H. Perry, B. F. Walters, L. E. Nave, C. W. Woodall, and C. W. Swanston, 2017: Toward inventory-based estimates of soil organic carbon in forests of the United States. *Ecological Applications*, **27**(4), 1223-1235, doi: 10.1002/eap.1516.
- Don, A., J. Schumacher, and A. Freibauer, 2011: Impact of tropical land-use change on soil organic carbon stocks – a meta-analysis. *Global Change Biology*, **17**(4), 1658-1670, doi: 10.1111/j.1365-2486.2010.02336.x.
- ECCE 2015: *National Inventory Report, 1990–2013: Greenhouse Gas Sources and Sinks in Canada*. Environment and Climate Change Canada. [<http://www.ec.gc.ca/ges-ghg/default.asp?lang=En&nav=83A34A7A-1>]
- Eglin, T., P. Ciais, S. L. Piao, P. Barre, V. Bellassen, P. Cadule, C. Chenu, T. Gasser, C. Koven, M. Reichstein, and P. Smith, 2010: Historical and future perspectives of global soil carbon response to climate and land-use changes. *Tellus B: Chemical and Physical Meteorology*, **62**(5), 700-718, doi: 10.1111/j.1600-0889.2010.00499.x.
- Elser, J. J., M. E. Bracken, E. E. Cleland, D. S. Gruner, W. S. Harpole, H. Hillebrand, J. T. Ngai, E. W. Seabloom, J. B. Shurin, and J. E. Smith, 2007: Global analysis of nitrogen and phosphorus limitation of primary producers in freshwater, marine and terrestrial ecosystems. *Ecology Letters*, **10**(12), 1135-1142, doi: 10.1111/j.1461-0248.2007.01113.x.
- Fang, H. J., S. L. Cheng, X. P. Zhang, A. Z. Liang, X. M. Yang, and C. F. Drury, 2006: Impact of soil redistribution in a sloping landscape on carbon sequestration in northeast China. *Land Degradation and Development*, **17**(1), 89-96, doi: 10.1002/ldr.697.
- FAO/IIASA/ISRIC/ISSCAS/JRC, 2012. *Harmonized World Soil Database (Version 1.2)*. Food and Agriculture Organization of the United Nations, Rome, Italy, and International Institute for Applied Systems Analysis, Laxenburg, Austria.
- Fierer, N., M. S. Strickland, D. Liptzin, M. A. Bradford, and C. C. Cleveland, 2009: Global patterns in belowground communities. *Ecology Letters*, **12**(11), 1238-1249, doi: 10.1111/j.1461-0248.2009.01360.x.



- Finlay, R. D., and D. J. Read, 1986: The structure and function of the vegetative mycelium of ectomycorrhizal plants. II. The uptake and distribution of phosphorus by mycelial strands interconnecting host plants. *New Phytologist*, **103**(1), 157-165, doi: 10.1111/j.1469-8137.1986.tb00604.x.
- Follett, R. F., S. Mooney, J. A. Morgan, K. Paustian, L. H. Allen Jr, S. Archibeque, S. J. Del Grosso, J. D. Derner, F. Dijkstra, A. J. Franzluebbers, L. Kurkalova, B. McCarl, S. Ogle, W. Parton, J. Petersen, G. P. Robertson, M. Schoeneberger, T. West, and J. Williams, 2011. Carbon Sequestration and Greenhouse Gas Fluxes in Agriculture: Challenges and Opportunities. Council for Agricultural Science and Technology, Issue Paper, 112 pp.
- Frey, S. D., S. Ollinger, K. Nadelhoffer, R. Bowden, E. Brzostek, A. Burton, B. A. Caldwell, S. Crow, C. L. Goodale, A. S. Grandy, A. Finzi, M. G. Kramer, K. Lajtha, J. LeMoine, M. Martin, W. H. McDowell, R. Minocha, J. J. Sadowsky, P. H. Templer, and K. Wickings, 2014: Chronic nitrogen additions suppress decomposition and sequester soil carbon in temperate forests. *Biogeochemistry*, **121**(2), 305-316, doi: 10.1007/s10533-014-0004-0.
- Friedlingstein, P., M. Meinshausen, V. K. Arora, C. D. Jones, A. Anav, S. K. Liddicoat, and R. Knutti, 2014: Uncertainties in CMIP5 climate projections due to carbon cycle feedbacks. *Journal of Climate*, **27**(2), 511-526, doi: 10.1175/jcli-d-12-00579.1.
- Georgiou, K., C. D. Koven, W. J. Riley, and M. S. Torn, 2015: Toward improved model structures for analyzing priming: Potential pitfalls of using bulk turnover time. *Global Change Biology*, **21**(12), 4298-4302, doi: 10.1111/gcb.13039.
- Geyer, K. M., E. Kyker-Snowman, A. S. Grandy, and S. D. Frey, 2016: Microbial carbon use efficiency: Accounting for population, community, and ecosystem-scale controls over the fate of metabolized organic matter. *Biogeochemistry*, **127**(2-3), 173-188, doi: 10.1007/s10533-016-0191-y.
- Giardina, C. P., C. M. Litton, S. E. Crow, and G. P. Asner, 2014: Warming-related increases in soil CO₂ efflux are explained by increased below-ground carbon flux. *Nature Climate Change*, **4**(9), 822-827, doi: 10.1038/nclimate2322.
- Gilman, E. L., J. Ellison, N. C. Duke, and C. Field, 2008: Threats to mangroves from climate change and adaptation options: A review. *Aquatic Botany*, **89**(2), 237-250, doi: 10.1016/j.aquabot.2007.12.009.
- Godbold, D. L., M. R. Hoosbeek, M. Lukac, M. F. Cotrufo, I. A. Janssens, R. Ceulemans, A. Polle, E. J. Velthorst, G. Scarascia-Mugnozza, P. De Angelis, F. Miglietta, and A. Peressotti, 2006: Mycorrhizal hyphal turnover as a dominant process for carbon input into soil organic matter. *Plant and Soil*, **281**(1-2), 15-24, doi: 10.1007/s11104-005-3701-6.
- Gottschalk, P., J. U. Smith, M. Wattenbach, J. Bellarby, E. Stehfest, N. Arnell, T. J. Osborn, C. Jones, and P. Smith, 2012: How will organic carbon stocks in mineral soils evolve under future climate? Global projections using RothC for a range of climate change scenarios. *Biogeosciences*, **9**(8), 3151-3171, doi: 10.5194/bg-9-3151-2012.
- Govers, G. R., K. Merckx, K. Van Oost, and B. van Wesemael, 2013: *Managing Soil Organic Carbon for Global Benefits: A STAP Technical Report*. Global Environmental Facility, Washington, DC.
- Granath, G., P. A. Moore, M. C. Lukenbach, and J. M. Waddington, 2016: Mitigating wildfire carbon loss in managed northern peatlands through restoration. *Scientific Reports*, **6**, 28498, doi: 10.1038/srep28498.
- Grosse, G., J. Harden, M. Turetsky, A. D. McGuire, P. Camill, C. Tarnocai, S. Frolking, E. A. G. Schuur, T. Jorgenson, S. Marchenko, V. Romanovsky, K. P. Wickland, N. French, M. Waldrop, L. Bourgeau-Chavez, and R. G. Striegl, 2011: Vulnerability of high-latitude soil organic carbon in North America to disturbance. *Journal of Geophysical Research*, **116**, doi: 10.1029/2010jg001507.
- Guenet, B., S. Juarez, G. Bardoux, L. Abbadie, and C. Chenu, 2012: Evidence that stable C is as vulnerable to priming effect as is more labile C in soil. *Soil Biology and Biochemistry*, **52**, 43-48, doi: 10.1016/j.soilbio.2012.04.001.
- Guo, L. B., and R. M. Gifford, 2002: Soil carbon stocks and land use change: A meta analysis. *Global Change Biology*, **8**(4), 345-360, doi: 10.1046/j.1354-1013.2002.00486.x.
- Guo, Y., R. Amundson, P. Gong, and Q. Yu, 2006: Quantity and spatial variability of soil carbon in the conterminous United States. *Soil Science Society of America Journal*, **70**(2), 590-600, doi: 10.2136/sssaj2005.0162.
- Hagedorn, F., D. Spinnler, and R. Siegwolf, 2003: Increased N deposition retards mineralization of old soil organic matter. *Soil Biology and Biochemistry*, **35**(12), 1683-1692, doi: 10.1016/j.soilbio.2003.08.015.
- Hall, S. J., G. McNicol, T. Natake, and W. L. Silver, 2015a: Large fluxes and rapid turnover of mineral-associated carbon across topographic gradients in a humid tropical forest: Insights from paired ¹⁴C analysis. *Biogeosciences*, **12**(8), 2471-2487, doi: 10.5194/bg-12-2471-2015.
- Hall, S. J., W. L. Silver, V. I. Timokhin, and K. E. Hammel, 2015b: Lignin decomposition is sustained under fluctuating redox conditions in humid tropical forest soils. *Global Change Biology*, doi: 10.1111/gcb.12908.
- Hanson, P. J., N. T. Edwards, C. T. Garten, and J. A. Andrews, 2000: Separating root and soil microbial contributions to soil respiration: A review of methods and observations. *Biogeochemistry*, **48**(1), 115-146, doi: 10.1023/a:1006244819642.



- Hararuk, O., J. Y. Xia, and Y. Q. Luo, 2014: Evaluation and improvement of a global land model against soil carbon data using a Bayesian Markov chain Monte Carlo method. *Journal of Geophysical Research: Biogeosciences*, **119**(3), 403-417, doi: 10.1002/2013jg002535.
- Harden, J. W., J. M. Sharpe, W. J. Parton, D. S. Ojima, T. L. Fries, T. G. Huntington, and S. M. Dabney, 1999: Dynamic replacement and loss of soil carbon on eroding cropland. *Global Biogeochemical Cycles*, **13**(4), 885-901, doi: 10.1029/1999gb900061.
- Harmon, M. E., B. Bond-Lamberty, J. W. Tang, and R. Vargas, 2011: Heterotrophic respiration in disturbed forests: A review with examples from North America. *Journal of Geophysical Research: Biogeosciences*, **116**, doi: 10.1029/2010jg001495.
- Hashimoto, S., N. Carvalhais, A. Ito, M. Migliavacca, K. Nishina, and M. Reichstein, 2015: Global spatiotemporal distribution of soil respiration modeled using a global database. *Biogeosciences*, **12**(13), 4121-4132, doi: 10.5194/bg-12-4121-2015.
- Haynes, B. E., and S. T. Gower, 1995: Belowground carbon allocation in unfertilized and fertilized red pine plantations in northern Wisconsin. *Tree Physiology*, **15**(5), 317-325, doi: 10.1093/tree-phys/15.5.317.
- Hazlett, P. W., D. M. Morris, and R. L. Fleming, 2014: Effects of biomass removals on site carbon and nutrients and jack pine growth in boreal forests. *Soil Science Society of America Journal*, **78**, S183-S195, doi: 10.2136/sssaj2013.08.0372nafsc.
- He, Y., S. E. Trumbore, M. S. Torn, J. W. Harden, L. J. Vaughn, S. D. Allison, and J. T. Randerson, 2016: Radiocarbon constraints imply reduced carbon uptake by soils during the 21st century. *Science*, **353**(6306), 1419-1424, doi: 10.1126/science.aad4273.
- Heckman, K., H. Throckmorton, C. Clingensmith, F. J. G. Vila, W. R. Horwath, H. Knicker, and C. Rasmussen, 2014: Factors affecting the molecular structure and mean residence time of occluded organics in a lithosequence of soils under ponderosa pine. *Soil Biology and Biochemistry*, **77**, 1-11, doi: 10.1016/j.soilbio.2014.05.028.
- Heimann, M., and M. Reichstein, 2008: Terrestrial ecosystem carbon dynamics and climate feedbacks. *Nature*, **451**(7176), 289-292, doi: 10.1038/nature06591.
- Hengl, T., J. M. de Jesus, R. A. MacMillan, N. H. Batjes, G. B. Heuvelink, E. Ribeiro, A. Samuel-Rosa, B. Kempen, J. G. Leenaars, M. G. Walsh, and M. R. Gonzalez, 2014: SoilGrids1km – Global soil information based on automated mapping. *PLOS One*, **9**(8), e105992, doi: 10.1371/journal.pone.0105992.
- Hermosilla, T., M. A. Wulder, J. C. White, N. C. Coops, G. W. Hobart, and L. B. Campbell, 2016: Mass data processing of time series Landsat imagery: Pixels to data products for forest monitoring. *International Journal of Digital Earth*, **9**(11), 1035-1054, doi: 10.1080/17538947.2016.1187673.
- Herrera Silveira, J. A., A. C. Rico, E. Pech, M. Pech, J. R. Ramírez, and C. T. Hernández, 2016: Dinámica del carbono (almacenes y flujos) en manglares de México. *Terra Latinoam*, **34**(1), 61-72.
- Hicks Pries, C. E., E. A. G. Schuur, S. M. Natali, and K. G. Crummer, 2015: Old soil carbon losses increase with ecosystem respiration in experimentally thawed tundra. *Nature Climate Change*, **6**, 214-218, doi: 10.1038/nclimate2830.
- Hirsch, P. R., A. J. Miller, and P. G. Dennis, 2013: Do root exudates exert more influence on rhizosphere bacterial community structure than other rhizodeposits? In: *Molecular Microbial Ecology of the Rhizosphere*. [F. J. de Bruijn (ed.)]. John Wiley & Sons, Inc., Hoboken, NJ, 229-242 pp.
- Hu, Y., and N. J. Kuhn, 2014: Aggregates reduce transport distance of soil organic carbon: Are our balances correct? *Biogeosciences Discussions*, **11**(6), 8829-8859, doi: 10.5194/bgd-11-8829-2014.
- Huang, Y., X. Lu, Z. Shi, D. Lawrence, C. D. Koven, J. Xia, Z. Du, E. Kluzek, and Y. Luo, 2018: Matrix approach to land carbon cycle modeling: A case study with the Community Land Model. *Global Change Biology*, **24**(3), 1394-1404, doi: 10.1111/gcb.13948.
- Huber-Sannwald, E., F. T. Maestre, J. E. Herrick, and J. F. Reynolds, 2006: Ecohydrological. Feedbacks and linkages associated with land degradation: A case study from Mexico. *Hydrological Processes*, **20**(15), 3395-3411, doi: 10.1002/hyp.6337.
- Hugelius, G., J. Strauss, S. Zubrzycki, J. W. Harden, E. A. G. Schuur, C. L. Ping, L. Schirrmeyer, G. Grosse, G. J. Michaelson, C. D. Koven, J. A. O'Donnell, B. Elberling, U. Mishra, P. Camill, Z. Yu, J. Palmtag, and P. Kuhry, 2014: Estimated stocks of circumpolar permafrost carbon with quantified uncertainty ranges and identified data gaps. *Biogeosciences*, **11**(23), 6573-6593, doi: 10.5194/bg-11-6573-2014.
- Hutchinson, J. J., C. A. Campbell, and R. L. Desjardins, 2007: Perspectives on carbon sequestration in agriculture. *Agricultural and Forest Meteorology*, **142**(2-4), 288-302, doi: 10.1016/j.agrformet.2006.03.030.
- Hyvonen, R., G. I. Agren, S. Linder, T. Persson, M. F. Cotrufo, A. Ekblad, M. Freeman, A. Grelle, I. A. Janssens, P. G. Jarvis, S. Kellomaki, A. Lindroth, D. Loustau, T. Lundmark, R. J. Norby, R. Oren, K. Pilegaard, M. G. Ryan, B. D. Sigurdsson, M. Stromgren, M. van Oijen, and G. Wallin, 2007: The likely impact of elevated CO₂, nitrogen deposition, increased temperature and management on carbon sequestration in temperate and boreal forest ecosystems: A literature review. *New Phytologist*, **173**(3), 463-480, doi: 10.1111/j.1469-8137.2007.01967.x.
- IPCC, 2000: *Land Use, Land-Use Change and Forestry*. [R. T. Watson, I. R. Noble, B. Bolin, N. H. Ravindranath, D. J. Verardo, and D. J. Dokken (eds.)]. Cambridge University Press, Cambridge, UK.
- Ise, T., A. L. Dunn, S. C. Wofsy, and P. R. Moorcroft, 2008: High sensitivity of peat decomposition to climate change through water-table feedback. *Nature Geoscience*, **1**(11), 763-766, doi: 10.1038/ngeo331.



- Iversen, C. M., J. Ledford, and R. J. Norby, 2008: CO₂ enrichment increases carbon and nitrogen input from fine roots in a deciduous forest. *New Phytologist*, **179**(3), 837-847, doi: 10.1111/j.1469-8137.2008.02516.x.
- Jandl, R., M. Lindner, L. Vesterdal, B. Bauwens, R. Baritz, F. Hagedorn, D. W. Johnson, K. Minkinen, and K. A. Byrne, 2007: How strongly can forest management influence soil carbon sequestration? *Geoderma*, **137**(3-4), 253-268, doi: 10.1016/j.geoderma.2006.09.003.
- Janssens, I. A., and S. Luysaert, 2009: Carbon cycle: Nitrogen's carbon bonus. *Nature Geoscience*, **2**(5), 318-319, doi: 10.1038/ngeo505.
- Janssens, I. A., W. Dieleman, S. Luysaert, J. A. Subke, M. Reichstein, R. Ceulemans, P. Ciais, A. J. Dolman, J. Grace, G. Matteucci, D. Papale, S. L. Piao, E. D. Schulze, J. Tang, and B. E. Law, 2010: Reduction of forest soil respiration in response to nitrogen deposition. *Nature Geoscience*, **3**(5), 315-322, doi: 10.1038/ngeo844.
- Jastrow, J. D., J. E. Amonette, and V. L. Bailey, 2006: Mechanisms controlling soil carbon turnover and their potential application for enhancing carbon sequestration. *Climatic Change*, **80**(1-2), 5-23, doi: 10.1007/s10584-006-9178-3.
- Jastrow, J. D., R. M. Miller, and T. W. Boutton, 1996: Carbon dynamics of aggregate-associated organic matter estimated by carbon-13 natural abundance. *Soil Science Society of America Journal*, **60**(3), 801, doi: 10.2136/sssaj1996.03615995006000030017x.
- Jenerette, G. D., and R. Lal, 2007: Modeled carbon sequestration variation in a linked erosion-deposition system. *Ecological Modelling*, **200**(1-2), 207-216, doi: 10.1016/j.ecolmodel.2006.07.027.
- Jenkinson, D. S., 1977: Studies on the decomposition of plant material in soil. V. The effects of plant cover and soil type on the loss of carbon from ¹⁴C labelled ryegrass decomposing under field conditions. *Journal of Soil Science*, **28**(3), 424-434, doi: 10.1111/j.1365-2389.1977.tb02250.x.
- Jenny, H., 1941: *Factors of Soil Formation: A System of Quantitative Pedology*. McGraw Hill, 261 pp.
- Jobbágy, E. G., and R. B. Jackson, 2000: The vertical distribution of soil organic carbon and its relation to climate and vegetation. *Ecological Applications*, **10**(2), 423-436, doi: 10.1890/1051-0761(2000)010[0423:tvdoso]2.0.co;2.
- Johnson, D. W., and P. S. Curtis, 2001: Effects of forest management on soil C and N storage: Meta analysis. *Forest Ecology and Management*, **140**(2-3), 227-238, doi: 10.1016/S0378-1127(00)00282-6.
- Johnson, J. M. F., R. R. Allmaras, and D. C. Reicosky, 2006: Estimating source carbon from crop residues, roots and rhizodeposits using the national grain-yield database. *Agronomy Journal*, **98**(3), 622-636, doi: 10.2134/agronj2005.0179.
- Johnson, K. D., J. W. Harden, A. D. McGuire, M. Clark, F. M. Yuan, and A. O. Finley, 2013: Permafrost and organic layer interactions over a climate gradient in a discontinuous permafrost zone. *Environmental Research Letters*, **8**(3), doi: 10.1088/1748-9326/8/3/035028.
- Jones, D. L., 1998: Organic acids in the rhizosphere — a critical review. *Plant and Soil*, **205**(1), 25-44, doi: 10.1023/a:1004356007312.
- Jones, M. C., J. Harden, J. O'Donnell, K. Manies, T. Jorgenson, C. Treat, and S. Ewing, 2017: Rapid carbon loss and slow recovery following permafrost thaw in boreal peatlands. *Global Change Biology*, **23**(3), 1109-1127, doi: 10.1111/gcb.13403.
- Jorgenson, M. T., C. H. Racine, J. C. Walters, and T. E. Osterkamp, 2001: Permafrost degradation and ecological changes associated with a warming climate in central Alaska. *Climatic Change*, **48**(4), 551-579, doi: 10.1023/a:1005667424292.
- Jorgenson, M. T., V. Romanovsky, J. Harden, Y. Shur, J. O'Donnell, E. A. G. Schuur, M. Kanevskiy, and S. Marchenko, 2010: Resilience and vulnerability of permafrost to climate change. *Canadian Journal of Forest Research*, **40**(7), 1219-1236, doi: 10.1139/x10-060.
- Kaiser, C., H. Meyer, C. Biasi, O. Rusalimova, P. Barsukov, and A. Richter, 2007: Conservation of soil organic matter through cryoturbation in Arctic soils in Siberia. *Journal of Geophysical Research*, **112**(G2), doi: 10.1029/2006jg000258.
- Kasischke, E. S., D. L. Verbyla, T. S. Rupp, A. D. McGuire, K. A. Murphy, R. Jandt, J. L. Barnes, E. E. Hoy, P. A. Duffy, M. Calef, and M. R. Turetsky, 2010: Alaska's changing fire regime — implications for the vulnerability of its boreal forests. *Canadian Journal of Forest Research*, **40**(7), 1313-1324, doi: 10.1139/x10-098.
- Keiluweit, M., J. J. Bougoure, P. S. Nico, J. Pett-Ridge, P. K. Weber, and M. Kleber, 2015: Mineral protection of soil carbon counteracted by root exudates. *Nature Climate Change*, **5**(6), 588-595, doi: 10.1038/nclimate2580.
- Kettridge, N., M. R. Turetsky, J. H. Sherwood, D. K. Thompson, C. A. Miller, B. W. Benscoter, M. D. Flannigan, B. M. Wotton, and J. M. Waddington, 2015: Moderate drop in water table increases peatland vulnerability to post-fire regime shift. *Scientific Reports*, **5**, 8063, doi: 10.1038/srep08063.
- Kibblewhite, M. G., K. Ritz, and M. J. Swift, 2008: Soil health in agricultural systems. *Philosophical Transactions of the Royal Society B: Biological Sciences*, **363**(1492), 685-701, doi: 10.1098/rstb.2007.2178.
- Köchy, M., R. Hiederer, and A. Freibauer, 2015: Global distribution of soil organic carbon – Part 1: Masses and frequency distributions of SOC stocks for the tropics, permafrost regions, wetlands, and the world. *Soil*, **1**(1), 351-365, doi: 10.5194/soil-1-351-2015.



- Kong, A. Y. Y., and J. Six, 2010: Tracing root vs. residue carbon into soils from conventional and alternative cropping systems. *Soil Science Society of America Journal*, **74**(4), 1201, doi: 10.2136/sssaj2009.0346.
- Kopittke, P. M., R. C. Dalal, D. Finn, and N. W. Menzies, 2017: Global changes in soil stocks of carbon, nitrogen, phosphorus, and sulphur as influenced by long-term agricultural production. *Global Change Biology*, **23**(6), 2509-2519, doi: 10.1111/gcb.13513.
- Koven, C. D., 2013: Boreal carbon loss due to poleward shift in low-carbon ecosystems. *Nature Geoscience*, **6**(6), 452-456, doi: 10.1038/ngeo1801.
- Koven, C. D., D. M. Lawrence, and W. J. Riley, 2015: Permafrost carbon-climate feedback is sensitive to deep soil carbon decomposability but not deep soil nitrogen dynamics. *Proceedings of the National Academy of Sciences USA*, **112**(12), 3752-3757, doi: 10.1073/pnas.1415123112.
- Kroetsch, D. J., X. Geng, S. X. Chang, and D. D. Saurette, 2011: Organic soils of Canada: Part 1. Wetland organic soils. *Canadian Journal of Soil Science*, **91**(5), 807-822, doi: 10.4141/cjss10043.
- Kurz, W. A., C. H. Shaw, C. Boisvenue, G. Stinson, J. Metsaranta, D. Leckie, A. Dyk, C. Smyth, and E. T. Neilson, 2013: Carbon in Canada's boreal forest — A synthesis. *Environmental Reviews*, **21**(4), 260-292, doi: 10.1139/er-2013-0041.
- Lacroix, E. M., C. L. Petrenko, and A. J. Friedland, 2016: Evidence for losses from strongly bound SOM pools after clear cutting in a northern hardwood forest. *Soil Science*, **181**(5), 202-207, doi: 10.1097/ss.000000000000147.
- Laganiere, J., X. Cavad, B. W. Brassard, D. Pare, Y. Bergeron, and H. Y. H. Chen, 2015: The influence of boreal tree species mixtures on ecosystem carbon storage and fluxes. *Forest Ecology and Management*, **354**, 119-129, doi: 10.1016/j.foreco.2015.06.029.
- Lajtha, K., R. D. Bowden, and K. Nadelhoffer, 2014a: Litter and root manipulations provide insights into soil organic matter dynamics and stability. *Soil Science Society of America Journal*, **78**(S1), S261, doi: 10.2136/sssaj2013.08.0370nafsc.
- Lajtha, K., K. L. Townsend, M. G. Kramer, C. Swanston, R. D. Bowden, and K. Nadelhoffer, 2014b: Changes to particulate versus mineral-associated soil carbon after 50 years of litter manipulation in forest and prairie experimental ecosystems. *Biogeochemistry*, **119**(1-3), 341-360, doi: 10.1007/s10533-014-9970-5.
- Lal, R., 2001: World cropland soils as a source or sink for atmospheric carbon. *Advances in Agronomy*, **71**, 145-191, doi: 10.1016/S0065-2113(01)71014-0.
- Lal, R., 2003: Soil erosion and the global carbon budget. *Environmental International*, **29**(4), 437-450, doi: 10.1016/S0160-4120(02)00192-7.
- Lal, R., 2004: Soil carbon sequestration to mitigate climate change. *Geoderma*, **123**(1-2), 1-22, doi: 10.1016/j.geoderma.2004.01.032.
- Lal, R., and D. Pimentel, 2008: Soil erosion: A carbon sink or source? *Science*, **319**(5866), 1040-1042; author reply 1040-1042, doi: 10.1126/science.319.5866.1040.
- Lal, R., W. Negassa, and K. Lorenz, 2015: Carbon sequestration in soil. *Current Opinion in Environmental Sustainability*, **15**, 79-86, doi: 10.1016/j.cosust.2015.09.002.
- Lamarque, J. F., J. T. Kiehl, G. P. Brasseur, T. Butler, P. Cameron-Smith, W. D. Collins, W. J. Collins, C. Granier, D. Hauglustaine, P. G. Hess, E. A. Holland, L. Horowitz, M. G. Lawrence, D. McKenna, P. Merilees, M. J. Prather, P. J. Rasch, D. Rotman, D. Shindell, and P. Thornton, 2005: Assessing future nitrogen deposition and carbon cycle feedback using a multimodel approach: Analysis of nitrogen deposition. *Journal of Geophysical Research: Atmospheres*, **110**(D19), doi: 10.1029/2005jd005825.
- Lavallee, S., and S. Plouffe, 2004: The ecolabel and sustainable development. *International Journal of Life Cycle Assessment*, **9**(6), 349-354, doi: 10.1065/lca2004.09.180.2.
- LeBauer, D. S., and K. K. Treseder, 2008: Nitrogen limitation of net primary productivity in terrestrial ecosystems is globally distributed. *Ecology*, **89**(2), 371-379, doi: 10.1890/06-2057.1.
- Lehmann, J., and M. Kleber, 2015: The contentious nature of soil organic matter. *Nature*, **528**(7580), 60-68, doi: 10.1038/nature16069.
- Letang, D. L., and W. J. de Groot, 2012: Forest floor depths and fuel loads in upland Canadian forests. *Canadian Journal of Forest Research*, **42**, 1551-1565, doi: 10.1139/x2012-093.
- Li, D., S. Niu, and Y. Luo, 2012: Global patterns of the dynamics of soil carbon and nitrogen stocks following afforestation: A meta-analysis. *New Phytologist*, **195**(1), 172-181, doi: 10.1111/j.1469-8137.2012.04150.x.
- Lin, L. H., and M. J. Simpson, 2016: Enhanced extractability of cutin- and suberin-derived organic matter with demineralization implies physical protection over chemical recalcitrance in soil. *Organic Geochemistry*, **97**, 111-121, doi: 10.1016/j.orggeochem.2016.04.012.
- Liu, L., and T. L. Greaver, 2010: A global perspective on below-ground carbon dynamics under nitrogen enrichment. *Ecology Letters*, **13**(7), 819-828, doi: 10.1111/j.1461-0248.2010.01482.x.
- Liu, S., N. Bliss, E. Sundquist, and T. G. Huntington, 2003: Modeling carbon dynamics in vegetation and soil under the impact of soil erosion and deposition. *Global Biogeochemical Cycles*, **17**(2), doi: 10.1029/2002gb002010.
- Liu, S., Y. Wei, W. M. Post, R. B. Cook, K. Schaefer, and M. M. Thornton, 2013: The unified North American soil map and its implications on the soil organic carbon stock in North America. *Biogeochemistry*, **10**(5), 2915-2930, doi: 10.5194/bg-10-2915-2013.



- Liu, W., S. Chen, X. Qin, F. Baumann, T. Scholten, Z. Zhou, W. Sun, T. Zhang, J. Ren, and D. Qin, 2012: Storage, patterns, and control of soil organic carbon and nitrogen in the northeastern margin of the Qinghai–Tibetan Plateau. *Environmental Research Letters*, **7**(3), 035401.
- Lu, X. L., D. W. Kicklighter, J. M. Melillo, J. M. Reilly, and L. Y. Xu, 2015: Land carbon sequestration within the conterminous United States: Regional- and state-level analyses. *Journal of Geophysical Research: Biogeosciences*, **120**(2), 379–398, doi: 10.1002/2014jg002818.
- Luo, Y., A. Ahlström, S. D. Allison, N. H. Batjes, V. Brovkin, N. Carvalhais, A. Chappell, P. Ciais, E. A. Davidson, A. Finzi, K. Georgiou, B. Guenet, O. Hararuk, J. W. Harden, Y. He, F. Hopkins, L. Jiang, C. Koven, R. B. Jackson, C. D. Jones, M. J. Lara, J. Liang, A. D. McGuire, W. Parton, C. Peng, J. T. Randerson, A. Salazar, C. A. Sierra, M. J. Smith, H. Tian, K. E. O. Todd-Brown, M. Torn, K. J. van Groenigen, Y. P. Wang, T. O. West, Y. Wei, W. R. Wieder, J. Xia, X. Xu, X. Xu, and T. Zhou, 2016: Toward more realistic projections of soil carbon dynamics by Earth system models. *Global Biogeochemical Cycles*, **30**(1), 40–56, doi: 10.1002/2015gb005239.
- Luo, Y., S. Wan, D. Hui, and L. L. Wallace, 2001: Acclimatization of soil respiration to warming in a tall grass prairie. *Nature*, **413**(6856), 622–625, doi: 10.1038/35098065.
- Luo, Z., E. Wang, and O. J. Sun, 2010: Can no-tillage stimulate carbon sequestration in agricultural soils? A meta-analysis of paired experiments. *Agriculture, Ecosystems and Environment*, **139**(1–2), 224–231, doi: 10.1016/j.agee.2010.08.006.
- Luo, Z.-B., and A. Polle, 2009: Wood composition and energy content in a poplar short rotation plantation on fertilized agricultural land in a future CO₂ atmosphere. *Global Change Biology*, **15**(1), 38–47, doi: 10.1111/j.1365-2486.2008.01768.x.
- Mann, D. H., T. Scott Rupp, M. A. Olson, and P. A. Duffy, 2012: Is Alaska's boreal forest now crossing a major ecological threshold? *Arctic, Antarctic, and Alpine Research*, **44**(3), 319–331, doi: 10.1657/1938-4246-44.3.319.
- Manzoni, S., and A. Porporato, 2009: Soil carbon and nitrogen mineralization: Theory and models across scales. *Soil Biology and Biochemistry*, **41**(7), 1355–1379, doi: 10.1016/j.soilbio.2009.02.031.
- Mayzelle, M. M., M. L. Krusor, K. Lajtha, R. D. Bowden, and J. Six, 2014: Effects of detrital inputs and roots on carbon saturation deficit of a temperate forest soil. *Soil Science Society of America Journal*, **78**(S1), S76, doi: 10.2136/sssaj2013.09.0415nafsc.
- McBratney, A. B., M. L. Mendonça Santos, and B. Minasny, 2003: On digital soil mapping. *Geoderma*, **117**(1–2), 3–52, doi: 10.1016/s0016-7061(03)00223-4.
- McCarthy, J. F., J. Ilavsky, J. D. Jastrow, L. M. Mayer, E. Perfect, and J. Zhuang, 2008: Protection of organic carbon in soil microaggregates via restructuring of aggregate porosity and filling of pores with accumulating organic matter. *Geochimica et Cosmochimica Acta*, **72**(19), 4725–4744, doi: 10.1016/j.gca.2008.06.015.
- McGuire, A. D., L. G. Anderson, T. R. Christensen, S. Dallimore, L. Guo, D. J. Hayes, M. Heimann, T. D. Lorenson, R. W. Macdonald, and N. Roulet, 2009: Sensitivity of the carbon cycle in the Arctic to climate change. *Ecological Monographs*, **79**(4), 523–555, doi: 10.1890/08-2025.1.
- McLauchlan, K., 2007: The nature and longevity of agricultural impacts on soil carbon and nutrients: A review. *Ecosystems*, **9**(8), 1364–1382, doi: 10.1007/s10021-005-0135-1.
- Mishra, U., and W. J. Riley, 2012: Alaskan soil carbon stocks: Spatial variability and dependence on environmental factors. *Biogeosciences*, **9**(9), 3637–3645, doi: 10.5194/bg-9-3637-2012.
- Mishra, U., J. D. Jastrow, R. Matamala, G. Hugelius, C. D. Koven, J. W. Harden, C. L. Ping, G. J. Michaelson, Z. Fan, R. M. Miller, A. D. McGuire, C. Tarnocai, P. Kuhry, W. J. Riley, K. Schaefer, E. A. G. Schuur, M. T. Jorgenson, and L. D. Hinzman, 2013: Empirical estimates to reduce modeling uncertainties of soil organic carbon in permafrost regions: A review of recent progress and remaining challenges. *Environmental Research Letters*, **8**(3), 035020, doi: 10.1088/1748-9326/8/3/035020.
- Mishra, U., R. Lal, D. S. Liu, and M. Van Meirvenne, 2010: Predicting the spatial variation of the soil organic carbon pool at a regional scale. *Soil Science Society of America Journal*, **74**(3), 906–914, doi: 10.2136/sssaj2009.0158.
- Montgomery, D. R., 2007: Soil erosion and agricultural sustainability. *Proceedings of the National Academy of Sciences USA*, **104**(33), 13268–13272, doi: 10.1073/pnas.0611508104.
- Nahlik, A. M., and M. S. Fennessy, 2016: Carbon storage in US wetlands. *Nature Communications*, **7**, 13835, doi: 10.1038/ncomms13835.
- NAS, 2010: *Verifying Greenhouse Gas Emissions: Methods to Support International Climate Agreements*. The National Academies Press. [https://www.nap.edu/catalog/12883/verifying-greenhouse-gas-emissions-methods-to-support-international-climate-agreements]
- Navarro-Garcia, F., M. A. Casermeiro, and J. P. Schimel, 2012: When structure means conservation: Effect of aggregate structure in controlling microbial responses to rewetting events. *Soil Biology and Biochemistry*, **44**(1), 1–8, doi: 10.1016/j.soilbio.2011.09.019.
- Nave, L. E., C. W. Swanston, U. Mishra, and K. J. Nadelhoffer, 2013: Afforestation effects on soil carbon storage in the United States: A synthesis. *Soil Science Society of America Journal*, **77**(3), 1035, doi: 10.2136/sssaj2012.0236.
- Nave, L. E., E. D. Vance, C. W. Swanston, and P. S. Curtis, 2010: Harvest impacts on soil carbon storage in temperate forests. *Forest Ecology and Management*, **259**(5), 857–866, doi: 10.1016/j.foreco.2009.12.009.
- Ogle, S. M., F. J. Breidt, and K. Paustian, 2005: Agricultural management impacts on soil organic carbon storage under moist and dry climatic conditions of temperate and tropical regions. *Biogeochemistry*, **72**(1), 87–121, doi: 10.1007/s10533-004-0360-2.



- Ogle, S. M., F. J. Breidt, M. Easter, S. Williams, K. Killian, and K. Paustian, 2010: Scale and uncertainty in modeled soil organic carbon stock changes for US croplands using a process-based model. *Global Change Biology*, **16**(2), 810-822, doi: 10.1111/j.1365-2486.2009.01951.x.
- Ogle, S. M., L. Olander, L. Wollenberg, T. Rosenstock, F. Tubiello, K. Paustian, L. Buendia, A. Nihart, and P. Smith, 2014: Reducing greenhouse gas emissions and adapting agricultural management for climate change in developing countries: Providing the basis for action. *Global Change Biology*, **20**(1), 1-6, doi: 10.1111/gcb.12361.
- Oldfield, E. E., S. A. Wood, C. A. Palm, and M. A. Bradford, 2015: How much SOM is needed for sustainable agriculture? *Frontiers in Ecology and the Environment*, **13**(10), 527, doi: 10.1890/1540-9295-13.10.527.
- Olefeldt, D., S. Goswami, G. Grosse, D. Hayes, G. Hugelius, P. Kuhry, A. D. McGuire, V. E. Romanovsky, A. B. Sannel, E. A. Schuur, and M. R. Turetsky, 2016: Circumpolar distribution and carbon storage of thermokarst landscapes. *Nature Communications*, **7**, 13043, doi: 10.1038/ncomms13043.
- Orgiazzi, A., M. B. Dunbar, P. Panagos, G. A. de Groot, and P. Lemanceau, 2015: Soil biodiversity and DNA barcodes: Opportunities and challenges. *Soil Biology and Biochemistry*, **80**, 244-250, doi: 10.1016/j.soilbio.2014.10.014.
- Palm, C., H. Blanco-Canqui, F. DeClerck, L. Gatere, and P. Grace, 2014: Conservation agriculture and ecosystem services: An overview. *Agriculture, Ecosystems and Environment*, **187**, 87-105, doi: 10.1016/j.agee.2013.10.010.
- Papa, G., B. Scaglia, A. Schievano, and F. Adani, 2013: Nanoscale structure of organic matter could explain litter decomposition. *Biogeochemistry*, **117**(2-3), 313-324, doi: 10.1007/s10533-013-9863-z.
- Papanicolaou, A. N., K. M. Wacha, B. K. Abban, C. G. Wilson, J. L. Hatfield, C. O. Stanier, and T. R. Filley, 2015: From soils to landscapes: A landscape-oriented approach to simulate soil organic carbon dynamics in intensively managed landscapes. *Journal of Geophysical Research: Biogeosciences*, **120**(11), 2375-2401, doi: 10.1002/2015jg003078.
- Paustian, K., J. Lehmann, S. Ogle, D. Reay, G. P. Robertson, and P. Smith, 2016: Climate-smart soils. *Nature*, **532**(7597), 49-57, doi: 10.1038/nature17174.
- Paustian, K., O. Andr n, H. H. Janzen, R. Lal, P. Smith, G. Tian, H. Tiessen, M. Noordwijk, and P. L. Woomer, 1997: Agricultural soils as a sink to mitigate CO₂ emissions. *Soil Use and Management*, **13**(s4), 230-244, doi: 10.1111/j.1475-2743.1997.tb00594.x.
- Paz Pellat, F., J. Argumedo Espinoza, C. O. Cruz Gaistardo, J. D. Etchevers, B., and B. de Jong, 2016: Distribuci n especial y temporal del carbono org nico del suelo en los ecosistemas terrestres. *Terra Latinoam*, **34**(3), 289-310.
- Peckham, S. D., and S. T. Gower, 2011: Simulated long-term effects of harvest and biomass residue removal on soil carbon and nitrogen content and productivity for two Upper Great Lakes forest ecosystems. *Global Change Biology Bioenergy*, **3**(2), 135-147, doi: 10.1111/j.1757-1707.2010.01067.x.
- Petrenko, C. L., and A. J. Friedland, 2015: Mineral soil carbon pool responses to forest clearing in northeastern hardwood forests. *GCB Bioenergy*, **7**(6), 1283-1293, doi: 10.1111/gcbb.12221.
- Phillips, C. L., B. Bond-Lamberty, A. R. Desai, M. Lavoie, D. Risk, J. Tang, K. Todd-Brown, and R. Vargas, 2016: The value of soil respiration measurements for interpreting and modeling terrestrial carbon cycling. *Plant and Soil*, **413**(1-2), 1-25, doi: 10.1007/s11104-016-3084-x.
- Ping, C. L., G. J. Michaelson, M. T. Jorgenson, J. M. Kimble, H. Epstein, V. E. Romanovsky, and D. A. Walker, 2008: High stocks of soil organic carbon in the North American Arctic region. *Nature Geoscience*, **1**(9), 615-619, doi: 10.1038/ngeo284.
- Pitre, F. E., J. E. K. Cooke, and J. J. Mackay, 2007: Short-term effects of nitrogen availability on wood formation and fibre properties in hybrid poplar. *Trees-Structure and Function*, **21**(2), 249-259, doi: 10.1007/s00468-007-0123-5.
- Pouyat, R. V., I. D. Yesilonis, and D. J. Nowak, 2006: Carbon storage by urban soils in the United States. *Journal of Environmental Quality*, **35**(4), 1566-1575, doi: 10.2134/jeq2005.0215.
- Powelson, D. S., C. M. Stirling, M. L. Jat, B. G. Gerard, C. A. Palm, P. A. Sanchez, and K. G. Cassman, 2014: Limited potential of no-till agriculture for climate change mitigation. *Nature Climate Change*, **4**(8), 678-683, doi: 10.1038/nclimate2292.
- Quine, T. A., and K. van Oost, 2007: Quantifying carbon sequestration as a result of soil erosion and deposition: Retrospective assessment using caesium-137 and carbon inventories. *Global Change Biology*, **13**(12), 2610-2625, doi: 10.1111/j.1365-2486.2007.01457.x.
- Rasse, D. P., C. Rumpel, and M.-F. Dignac, 2005: Is soil carbon mostly root carbon? Mechanisms for a specific stabilisation. *Plant and Soil*, **269**(1-2), 341-356, doi: 10.1007/s11104-004-0907-y.
- Rasse, D. P., M. F. Dignac, H. Bahri, C. Rumpel, A. Mariotti, and C. Chenu, 2006: Lignin turnover in an agricultural field: From plant residues to soil-protected fractions. *European Journal of Soil Science*, **57**(4), 530-538, doi: 10.1111/j.1365-2389.2006.00806.x.
- Reay, D. S., F. Dentener, P. Smith, J. Grace, and R. A. Feely, 2008: Global nitrogen deposition and carbon sinks. *Nature Geoscience*, **1**(7), 430-437, doi: 10.1038/ngeo230.
- Regnier, P., P. Friedlingstein, P. Ciais, F. T. Mackenzie, N. Gruber, I. A. Janssens, G. G. Laruelle, R. Lauerwald, S. Luysaert, A. J. Andersson, S. Arndt, C. Arnosti, A. V. Borges, A. W. Dale, A. Gallego-Sala, Y. Godderis, N. Goossens, J. Hartmann, C. Heinze, T. Ilyina, F. Joos, D. E. LaRowe, J. Leifeld, F. J. R. Meysman, G. Munhoven, P. A. Raymond, R. Spahni, P. Suntharalingam, and M. Thullner, 2013: Anthropogenic perturbation of the carbon fluxes from land to ocean. *Nature Geoscience*, **6**(8), 597-607, doi: 10.1038/Ngeo1830.



- Richter, D. D., and R. A. Houghton, 2011: Gross CO₂ fluxes from land-use change: Implications for reducing global emissions and increasing sinks. *Carbon Management*, **2**(1), 41-47, doi: 10.4155/Cmt.10.43.
- Riggs, C. E., and S. E. Hobbie, 2016: Mechanisms driving the soil organic matter decomposition response to nitrogen enrichment in grassland soils. *Soil Biology and Biochemistry*, **99**, 54-65, doi: 10.1016/j.soilbio.2016.04.023.
- Roach, J. K., B. Griffith, and D. Verbyla, 2013: Landscape influences on climate-related lake shrinkage at high latitudes. *Global Change Biology*, **19**(7), 2276-2284, doi: 10.1111/gcb.12196.
- Rosenbloom, N. A., J. W. Harden, J. C. Neff, and D. S. Schimel, 2006: Geomorphic control of landscape carbon accumulation. *Journal of Geophysical Research*, **111**(G1), doi: 10.1029/2005jg000077.
- Rumpel, C., and I. Kögel-Knabner, 2010: Deep soil organic matter—a key but poorly understood component of terrestrial C cycle. *Plant and Soil*, **338**(1-2), 143-158, doi: 10.1007/s11104-010-0391-5.
- Russell, A. E., C. A. Cambardella, J. J. Ewel, and T. B. Parkin, 2004: Species, rotation, and life-form diversity effects on soil carbon in experimental tropical ecosystems. *Ecological Applications*, **14**(1), 47-60, doi: 10.1890/02-5299.
- Ryals, R., M. D. Hartman, W. J. Parton, M. S. DeLonge, and W. L. Silver, 2015: Long-term climate change mitigation potential with organic matter management on grasslands. *Ecological Applications*, **25**(2), 531-545, doi: 10.1890/13-2126.1.
- Rytter, R.-M., 2001: Biomass production and allocation, including fine-root turnover, and annual N uptake in lysimeter-grown basket willows. *Forest Ecology and Management*, **140**(2-3), 177-192, doi: 10.1016/S0378-1127(00)00319-4.
- Saunois, M., P. Bousquet, B. Poulter, A. Peregon, P. Ciais, J. G. Canadell, E. J. Dlugokencky, G. Etiope, D. Bastviken, S. Houweling, G. Janssens-Maenhout, F. N. Tubiello, S. Castaldi, R. B. Jackson, M. Alexe, V. K. Arora, D. J. Beerling, P. Bergamaschi, D. R. Blake, G. Brailsford, V. Brovkin, L. Bruhwiler, C. Crevoisier, P. Crill, K. Covey, C. Curry, C. Frankenberg, N. Gedney, L. Hoglund-Isaksson, M. Ishizawa, A. Ito, F. Joos, H. S. Kim, T. Kleinen, P. Krummel, J. F. Lamarque, R. Langenfelds, R. Locatelli, T. Machida, S. Maksyutov, K. C. McDonald, J. Marshall, J. R. Melton, I. Morino, V. Naik, S. O'Doherty, F. J. W. Parmentier, P. K. Patra, C. H. Peng, S. S. Peng, G. P. Peters, I. Pison, C. Prigent, R. Prinn, M. Ramonet, W. J. Riley, M. Saito, M. Santini, R. Schroeder, I. J. Simpson, R. Spahni, P. Steele, A. Takizawa, B. F. Thornton, H. Q. Tian, Y. Tohjima, N. Viovy, A. Voulgarakis, M. van Weele, G. R. van der Werf, R. Weiss, C. Wiedinmyer, D. J. Wilton, A. Wiltshire, D. Worthy, D. Wunch, X. Y. Xu, Y. Yoshida, B. Zhang, Z. Zhang, and Q. Zhu, 2016: The global methane budget 2000-2012. *Earth System Science Data*, **8**(2), 697-751, doi: 10.5194/essd-8-697-2016.
- Schaefer, K., T. Zhang, L. Bruhwiler, and A. P. Barrett, 2011: Amount and timing of permafrost carbon release in response to climate warming. *Tellus B: Chemical and Physical Meteorology*, **63**(2), 165-180, doi: 10.1111/j.1600-0889.2011.00527.x.
- Schrumpf, M., K. Kaiser, G. Guggenberger, T. Persson, I. Kogel-Knabner, and E. D. Schulze, 2013: Storage and stability of organic carbon in soils as related to depth, occlusion within aggregates, and attachment to minerals. *Biogeosciences*, **10**(3), 1675-1691, doi: 10.5194/bg-10-1675-2013.
- Schuur, E. A., A. D. McGuire, C. Schadel, G. Grosse, J. W. Harden, D. J. Hayes, G. Hugelius, C. D. Koven, P. Kuhry, D. M. Lawrence, S. M. Natali, D. Olefeldt, V. E. Romanovsky, K. Schaefer, M. R. Turetsky, C. C. Treat, and J. E. Vonk, 2015: Climate change and the permafrost carbon feedback. *Nature*, **520**(7546), 171-179, doi: 10.1038/nature14338.
- Segarra, K. E., F. Schubotz, V. Samarkin, M. Y. Yoshinaga, K. U. Hinrichs, and S. B. Joye, 2015: High rates of anaerobic methane oxidation in freshwater wetlands reduce potential atmospheric methane emissions. *Nature Communications*, **6**, 7477, doi: 10.1038/ncomms8477.
- Seneviratne, S. I., N. Nicholls, D. Easterling, C. M. Goodess, S. Kanae, J. Kossin, Y. Luo, J. Marengo, K. McInnes, M. Rahimi, M. Reichstein, A. Sorteberg, C. Vera, and X. Zhang, 2012: Changes in climate extremes and their impacts on the natural physical environment. *Managing the Risks of Extreme Events and Disasters to Advance Climate Change Adaptation: A Special Report of Working Groups I and II of the Intergovernmental Panel On Climate Change*. [C. B. Field, V. Barros, T. F. Stocker, D. Qin, D. J. Dokken, K. L. Ebi, M. D. Mastrandrea, K. J. Mach, G.-K. Plattner, S. K. Allen, M. Tignor, and P. M. Midgley (eds.)]. Cambridge University Press, UK, pp. 109-230.
- Shaw, C. H., E. Banfield, and W. A. Kurz, 2008: Stratifying soils into pedogenically similar categories for modeling forest soil carbon. *Canadian Journal of Soil Science*, **88**(4), 501-516, doi: 10.4141/cjss07099.
- Shaw, C. H., K. A. Bona, D. A. Thompson, D. D. Dimitrov, J. S. Bhatti, A. B. Hilger, K. L. Webster, and W. A. Kurz, 2016: *Canadian Model for Peatlands Version 1.0: A Model Design Document. Information report NOR-X-425*. Natural Resources Canada, Canadian Forest Service, Edmonton, AB, Canada, 20 pp. [https://cfs.nrcan.gc.ca/publications?id=37017]
- Shaw, C. H., K. A. Bona, W. A. Kurz, and J. W. Fyles, 2015: The importance of tree species and soil taxonomy to modeling forest soil carbon stocks in Canada. *Geoderma Regional*, **4**, 114-125, doi: 10.1016/j.geodrs.2015.01.001.
- Shi, S. W., W. Zhang, P. Zhang, Y. Q. Yu, and F. Ding, 2013: A synthesis of change in deep soil organic carbon stores with afforestation of agricultural soils. *Forest Ecology and Management*, **296**, 53-63, doi: 10.1016/j.foreco.2013.01.026.



- Six, J., H. Bossuyt, S. Degryze, and K. Denef, 2004: A history of research on the link between (micro)aggregates, soil biota, and soil organic matter dynamics. *Soil and Tillage Research*, **79**(1), 7-31, doi: 10.1016/j.still.2004.03.008.
- Six, J., R. T. Conant, E. A. Paul, and K. Paustian, 2002: Stabilization mechanisms of soil organic matter: Implications for C-saturation of soils. *Plant and Soil*, **241**(2), 155-176, doi: 10.1023/a:1016125726789.
- Smith, P., 2008: Land use change and soil organic carbon dynamics. *Nutrient Cycling in Agroecosystems*, **81**(2), 169-178, doi: 10.1007/s10705-007-9138-y.
- Smith, P., S. J. Chapman, W. A. Scott, H. I. J. Black, M. Wattenbach, R. Milne, C. D. Campbell, A. Lilly, N. Ostle, P. E. Levy, D. G. Lumsdon, P. Millard, W. Towers, S. Zaehle, and J. U. Smith, 2007: Climate change cannot be entirely responsible for soil carbon loss observed in England and Wales, 1978–2003. *Global Change Biology*, **13**(12), 2605-2609, doi: 10.1111/j.1365-2486.2007.01458.x.
- Smith, S. V., W. H. Renwick, R. W. Buddemeier, and C. J. Crossland, 2001: Budgets of soil erosion and deposition for sediments and sedimentary organic carbon across the conterminous United States. *Global Biogeochemical Cycles*, **15**(3), 697-707, doi: 10.1029/2000gb001341.
- Smyth, C. E., W. A. Kurz, and J. A. Trofymow, 2011: Including the effects of water stress on decomposition in the carbon budget model of the Canadian forest sector CBM-CFS3. *Ecological Modelling*, **222**(5), 1080-1091, doi: 10.1016/j.ecolmodel.2010.12.005.
- Soil Conservation Council of Canada, 2016: *Reduced Tillage Helps Reduce Carbon Dioxide Levels*. [http://www.Soilcc.ca/ggmp_feature_articles/2004/2004-02.php]
- Soil Survey, and T. Loecke, 2016: *Rapid Carbon Assessment: Methodology, Sampling, and Summary*. [S. Wills (ed.)]. U.S. Department of Agriculture, Natural Resources Conservation Service.
- Solomon, D., J. Lehmann, J. Harden, J. Wang, J. Kinyangi, K. Heymann, C. Karunakaran, Y. S. Lu, S. Wirick, and C. Jacobsen, 2012: Micro- and nano-environments of carbon sequestration: Multi-element STXM-NEXAFS spectromicroscopy assessment of microbial carbon and mineral associations. *Chemical Geology*, **329**, 53-73, doi: 10.1016/j.chemgeo.2012.02.002.
- Stallard, R. F., 1998: Terrestrial sedimentation and the carbon cycle: Coupling weathering and erosion to carbon burial. *Global Biogeochemical Cycles*, **12**(2), 231-257, doi: 10.1029/98gb00741.
- Subke, J.-A., I. Inglima, and M. Francesca Cotrufo, 2006: Trends and methodological impacts in soil CO₂ efflux partitioning: A meta-analytical review. *Global Change Biology*, **12**(6), 921-943, doi: 10.1111/j.1365-2486.2006.01117.x.
- Sulman, B. N., R. P. Phillips, A. C. Oishi, E. Shevliakova, and S. W. Pacala, 2014: Microbe-driven turnover offsets mineral-mediated storage of soil carbon under elevated CO₂. *Nature Climate Change*, **4**(12), 1099-1102, doi: 10.1038/Nclimate2436.
- Sundquist, E. T., K. V. Ackerman, N. B. Bliss, J. M. Kellndorfer, M. C. Reeves, and M. G. Rollins, 2009: *Rapid Assessment of U.S. Forest and Soil Organic Carbon Storage and Forest Biomass Carbon Sequestration Capacity: U.S. Geological Survey Open-File Report 2009–1283*. 15 pp. [http://pubs.usgs.gov/of/2009/1283/]
- Tang, J. W., L. Misson, A. Gershenson, W. X. Cheng, and A. H. Goldstein, 2005: Continuous measurements of soil respiration with and without roots in a ponderosa pine plantation in the Sierra Nevada mountains. *Agricultural and Forest Meteorology*, **132**(3-4), 212-227, doi: 10.1016/j.agrformet.2005.07.011.
- Tang, J., and W. J. Riley, 2014: Weaker soil carbon–climate feedbacks resulting from microbial and abiotic interactions. *Nature Climate Change*, **5**(1), 56-60, doi: 10.1038/nclimate2438.
- Tang, J., and W. J. Riley, 2016: Large uncertainty in ecosystem carbon dynamics resulting from ambiguous numerical coupling of carbon and nitrogen biogeochemistry: A demonstration with the ACME land model. *Biogeosciences Discussion*, 1-27, doi: 10.5194/bg-2016-233.
- Tarnocai, C. 2006: The effect of climate change on carbon in Canadian peatlands. *Global and Planetary Change*, **53**, 222–232. doi: 10.1016/j.gloplacha.2006.03.012.
- Tarnocai, C., 1997: The amount of organic carbon in various soil orders and ecological provinces in Canada. In: *Soil Processes and the Carbon Cycle*. [R. Lal, J. M. Kimble, R. F. Follett, and B. A. Stewart (eds.)]. Lewis Publishers, CRC Press.
- Tate, K. R., 2015: Soil methane oxidation and land-use change — from process to mitigation. *Soil Biology and Biochemistry*, **80**, 260-272, doi: 10.1016/j.soilbio.2014.10.010.
- Thompson, D. K., B. N. Simpson, and A. Beaudoin, 2016: Using forest structure to predict the distribution of treed boreal peatlands in Canada. *Forest Ecology and Management*, **372**, 19-27, doi: 10.1016/j.foreco.2016.03.056.
- Tian, H. Q., C. Q. Lu, P. Ciais, A. M. Michalak, J. G. Canadell, E. Saikawa, D. N. Huntzinger, K. R. Gurney, S. Sitch, B. W. Zhang, J. Yang, P. Bousquet, L. Bruhwiler, G. S. Chen, E. Dlugokencky, P. Friedlingstein, J. Melillo, S. F. Pan, B. Poulter, R. Prinn, M. Saunois, C. R. Schwalm, and S. C. Wofsy, 2016: The terrestrial biosphere as a net source of greenhouse gases to the atmosphere. *Nature*, **531**(7593), 225-228, doi: 10.1038/nature16946.
- Tian, H., C. Lu, J. Yang, K. Banger, D. N. Huntzinger, C. R. Schwalm, A. M. Michalak, R. Cook, P. Ciais, D. Hayes, M. Huang, A. Ito, A. K. Jain, H. Lei, J. Mao, S. Pan, W. M. Post, S. Peng, B. Poulter, W. Ren, D. Ricciuto, K. Schaefer, X. Shi, B. Tao, W. Wang, Y. Wei, Q. Yang, B. Zhang, and N. Zeng, 2015: Global patterns and controls of soil organic carbon dynamics as simulated by multiple terrestrial biosphere models: Current status and future directions. *Global Biogeochemical Cycles*, **29**(6), 775-792, doi: 10.1002/2014GB005021.



- Todd-Brown, K. E. O., J. T. Randerson, F. Hopkins, V. Arora, T. Hajima, C. Jones, E. Shevliakova, J. Tjiputra, E. Volodin, T. Wu, Q. Zhang, and S. D. Allison, 2014: Changes in soil organic carbon storage predicted by Earth system models during the 21st century. *Biogeosciences*, **11**(8), 2341-2356, doi: 10.5194/bg-11-2341-2014.
- Todd-Brown, K. E. O., J. T. Randerson, W. M. Post, F. M. Hoffman, C. Tarnocai, E. A. G. Schuur, and S. D. Allison, 2013: Causes of variation in soil carbon simulations from CMIP5 Earth system models and comparison with observations. *Biogeosciences*, **10**(3), 1717-1736, doi: 10.5194/bg-10-1717-2013.
- Trofymow, J. A., C. M. Preston, and C. E. Prescott, 1995: Litter quality and its potential effect on decay rates of materials from Canadian forests. *Water Air and Soil Pollution*, **82**(1-2), 215-226, doi: 10.1007/Bf01182835.
- Turetsky, M. R., B. Benscoter, S. Page, G. Rein, G. R. van der Werf, and A. Watts, 2014: Global vulnerability of peatlands to fire and carbon loss. *Nature Geoscience*, **8**(1), 11-14, doi: 10.1038/ngeo2325.
- Turetsky, M. R., E. S. Kane, J. W. Harden, R. D. Ottmar, K. L. Manies, E. Hoy, and E. S. Kasischke, 2011: Recent acceleration of biomass burning and carbon losses in Alaskan forests and peatlands. *Nature Geoscience*, **4**(1), 27-31, doi: 10.1038/Ngeo1027.
- U.S. EPA, 2015: *Inventory of U.S. Greenhouse Gas Emissions and Sinks: 1990-2013*. United States Environmental Protection Agency, EPA 430-R-15-004, Washington, DC: US-EPA. [<https://www.epa.gov/ghgemissions/inventory-us-greenhouse-gas-emissions-and-sinks-1990-2013>]
- U.S. EPA, 2017: *Inventory of U.S. Greenhouse Gas Emissions Sinks 1990-2015*. United States Environmental Protection Agency, EPA 430-P-17-001. [<https://www.epa.gov/ghgemissions/inventory-us-greenhouse-gas-emissions-and-sinks-1990-2015>]
- Upson, M. A., P. J. Burgess, and J. I. L. Morison, 2016: Soil carbon changes after establishing woodland and agroforestry trees in a grazed pasture. *Geoderma*, **283**, 10-20, doi: 10.1016/j.geoderma.2016.07.002.
- Uroz, S., L. C. Kelly, M. P. Turpault, C. Lepleux, and P. Frey-Klett, 2015: The mineralosphere concept: Mineralogical control of the distribution and function of mineral-associated bacterial communities. *Trends in Microbiology*, **23**(12), 751-762, doi: 10.1016/j.tim.2015.10.004.
- USDA Soil Conservation Service, 1993: *State Soil Geographic Data Base (STATSGO) for the Conterminous United States*, Misc. Publ. 1492. U.S. Government Printing Office, Washington, DC.
- van der Heijden, M. G., R. Streitwolf-Engel, R. Riedl, S. Siegrist, A. Neudecker, K. Ineichen, T. Boller, A. Wiemken, and I. R. Sanders, 2006: The mycorrhizal contribution to plant productivity, plant nutrition and soil structure in experimental grassland. *New Phytologist*, **172**(4), 739-752, doi: 10.1111/j.1469-8137.2006.01862.x.
- Van Oost, K., G. Verstraeten, S. Doetterl, B. Notebaert, F. Wiaux, N. Broothaerts, and J. Six, 2012: Legacy of human-induced C erosion and burial on soil-atmosphere C exchange. *Proceedings of the National Academy of Sciences USA*, **109**(47), 19492-19497, doi: 10.1073/pnas.1211162109.
- Van Oost, K., T. A. Quine, G. Govers, S. De Gryze, J. Six, J. W. Harden, J. C. Ritchie, G. W. McCarty, G. Heckrath, C. Kosmas, J. V. Giraldez, J. R. da Silva, and R. Merckx, 2007: The impact of agricultural soil erosion on the global carbon cycle. *Science*, **318**(5850), 626-629, doi: 10.1126/science.1145724.
- VandenBygaert, A. J., D. Kroetsch, E. G. Gregorich, and D. Lobb, 2012: Soil C erosion and burial in cropland. *Global Change Biology*, **18**(4), 1441-1452, doi: 10.1111/j.1365-2486.2011.02604.x.
- VandenBygaert, A. J., E. G. Gregorich, and D. A. Angers, 2003: Influence of agricultural management on soil organic carbon: A compendium and assessment of Canadian studies. *Canadian Journal of Soil Science*, **83**(4), 363-380, doi: 10.4141/s03-009.
- Vitousek, P. M., J. D. Aber, R. W. Howarth, G. E. Likens, P. A. Matson, D. W. Schindler, W. H. Schlesinger, and D. G. Tilman, 1997: Human alteration of the global nitrogen cycle: Sources and consequences. *Ecological Applications*, **7**(3), 737-750, doi: 10.1890/1051-0761(1997)007[0737:haotgn]2.0.co;2.
- Vrebos, D., F. Bampa, R. Creamer, C. Gardi, B. Ghaley, A. Jones, M. Rutgers, T. Sandén, J. Staes, and P. Meire, 2017: The impact of policy instruments on soil multifunctionality in the European Union. *Sustainability*, **9**(3), 407, doi: 10.3390/su9030407.
- Waddington, J. M., P. J. Morris, N. Kettridge, G. Granath, D. K. Thompson, and P. A. Moore, 2015: Hydrological feedbacks in northern peatlands. *Ecology*, **8**(1), 113-127, doi: 10.1002/eco.1493.
- Wang, Y. P., B. C. Chen, W. R. Wieder, M. Leite, B. E. Medlyn, M. Rasmussen, M. J. Smith, F. B. Augusto, F. Hoffman, and Y. Q. Luo, 2014: Oscillatory behavior of two nonlinear microbial models of soil carbon decomposition. *Biogeosciences*, **11**(7), 1817-1831, doi: 10.5194/bg-11-1817-2014.
- Wang, Z. G., T. Hoffmann, J. Six, J. O. Kaplan, G. Govers, S. Doetterl, and K. Van Oost, 2017: Human-induced erosion has offset one-third of carbon emissions from land cover change. *Nature Climate Change*, **7**(5), 345, doi: 10.1038/Nclimate3263.
- Ward, C., D. Pothier, and D. Paré, 2014: Do boreal forests need fire disturbance to maintain productivity? *Ecosystems*, **17**(6), 1053-1067, doi: 10.1007/s10021-014-9782-4.
- Ward, S. E., S. M. Smart, H. Quirk, J. R. Tallwin, S. R. Mortimer, R. S. Shiel, A. Wilby, and R. D. Bardgett, 2016: Legacy effects of grassland management on soil carbon to depth. *Global Change Biology*, **22**(8), 2929-2938, doi: 10.1111/gcb.13246.



- Wardle, D. A., K. I. Bonner, and G. M. Barker, 2002: Linkages between plant litter decomposition, litter quality, and vegetation responses to herbivores. *Functional Ecology*, **16**(5), 585-595, doi: 10.1046/j.1365-2435.2002.00659.x.
- Wear, D. N., and J. W. Coulston, 2015: From sink to source: Regional variation in U.S. forest carbon futures. *Scientific Reports*, **5**, 16518, doi: 10.1038/srep16518.
- Webster, K. A., C. Akumu, J. Bhatti, K. Bona, D. Dimitrov, A. Hilger, W. A. Kurz, C. Shaw, C. Theriault, D. Thompson, and S. Wilson, 2016: *Development of a Forested Peatland Carbon Dynamics Module for the Carbon Budget Model of the Canadian Forest Sector Workshop Report*, GLC-X-14. [https://cfs.nrcan.gc.ca/publications?id=36777]
- Wieder, W. R., A. S. Grandy, C. M. Kallenbach, and G. B. Bonan, 2014: Integrating microbial physiology and physio-chemical principles in soils with the Microbial-Mineral Carbon Stabilization (MIMICS) model. *Biogeosciences*, **11**(14), 3899-3917, doi: 10.5194/bg-11-3899-2014.
- Wieder, W. R., G. B. Bonan, and S. D. Allison, 2013: Global soil carbon projections are improved by modelling microbial processes. *Nature Climate Change*, **3**(10), 909-912, doi: 10.1038/nclimate1951.
- Wills, S., T. Loecke, C. Sequeira, G. Teachman, S. Grunwald, and L. West, 2014: Overview of the U.S. Rapid Carbon Assessment project: Sampling design, initial summary and uncertainty estimates. In: Soil Carbon [A.E. Hartemink and K. McSweeney (eds.)]. Springer International Publishing, Cham, Switzerland, pp. 95-104, doi:10.1007/978-3-319-04084-4_10.
- Wisser, D., S. Marchenko, J. Talbot, C. Treat, and S. Frolking, 2011: Soil temperature response to 21st century global warming: The role of and some implications for peat carbon in thawing permafrost soils in North America. *Earth System Dynamics*, **2**(1), 121-138, doi: 10.5194/esd-2-121-2011.
- Woolf, D., J. E. Amonette, F. A. Street-Perrott, J. Lehmann, and S. Joseph, 2010: Sustainable biochar to mitigate global climate change. *Nature Communications*, **1**, 56, doi: 10.1038/ncomms1053.
- Xia, J., and S. Wan, 2008: Global response patterns of terrestrial plant species to nitrogen addition. *New Phytologist*, **179**(2), 428-439, doi: 10.1111/j.1469-8137.2008.02488.x.
- Xia, J., Y. Luo, Y. P. Wang, and O. Hararuk, 2013: Traceable components of terrestrial carbon storage capacity in biogeochemical models. *Global Change Biology*, **19**(7), 2104-2116, doi: 10.1111/gcb.12172.
- Xu, T., L. White, D. F. Hui, and Y. Q. Luo, 2006: Probabilistic inversion of a terrestrial ecosystem model: Analysis of uncertainty in parameter estimation and model prediction. *Global Biogeochemical Cycles*, **20**(2), doi: 10.1029/2005gb002468.
- Xu, X. F., P. E. Thornton, and W. M. Post, 2013: A global analysis of soil microbial biomass carbon, nitrogen and phosphorus in terrestrial ecosystems. *Global Ecology and Biogeography*, **22**(6), 737-749, doi: 10.1111/geb.12029.
- Xu, X., Z. Shi, X. Chen, Y. Lin, S. Niu, L. Jiang, R. Luo, and Y. Luo, 2016: Unchanged carbon balance driven by equivalent responses of production and respiration to climate change in a mixed-grass prairie. *Global Change Biology*, **22**(5), 1857-1866, doi: 10.1111/gcb.13192.
- Yan, Z. F., C. X. Liu, K. E. Todd-Brown, Y. Y. Liu, B. Bond-Lamberty, and V. L. Bailey, 2016: Pore-scale investigation on the response of heterotrophic respiration to moisture conditions in heterogeneous soils. *Biogeochemistry*, **131**(1-2), 121-134, doi: 10.1007/s10533-016-0270-0.
- Yue, K., Y. Peng, C. Peng, W. Yang, X. Peng, and F. Wu, 2016: Stimulation of terrestrial ecosystem carbon storage by nitrogen addition: A meta-analysis. *Scientific Reports*, **6**, 19895, doi: 10.1038/srep19895.
- Zak, D. R., K. S. Pregitzer, P. S. Curtis, J. A. Teeri, R. Fogel, and D. L. Randlett, 1993: Elevated atmospheric CO₂ and feedback between carbon and nitrogen cycles. *Plant and Soil*, **151**(1), 105-117, doi: 10.1007/Bf00010791.
- Zhang, W., P. F. Hendrix, L. E. Dame, R. A. Burke, J. Wu, D. A. Neher, J. Li, Y. Shao, and S. Fu, 2013: Earthworms facilitate carbon sequestration through unequal amplification of carbon stabilization compared with mineralization. *Nature Communications*, **4**, 2576, doi: 10.1038/ncomms3576.
- Zhou, L., X. Zhou, J. Shao, Y. Nie, Y. He, L. Jiang, Z. Wu, and S. Hosseini Bai, 2016: Interactive effects of global change factors on soil respiration and its components: A meta-analysis. *Global Change Biology*, **22**(9), 3157-3169, doi: 10.1111/gcb.13253.



13 Terrestrial Wetlands

Lead Authors

Randall Kolka, USDA Forest Service; Carl Trettin, USDA Forest Service

Contributing Authors

Wenwu Tang, University of North Carolina, Charlotte; Ken Krauss, U.S. Geological Survey; Sheel Bansal, U.S. Geological Survey; Judith Drexler, U.S. Geological Survey; Kimberly Wickland, U.S. Geological Survey; Rodney Chimner, Michigan Technological University; Diana Hogan, U.S. Geological Survey; Emily J. Pindilli, U.S. Geological Survey; Brian Benschoter, Florida Atlantic University; Brian Tangen, U.S. Geological Survey; Evan Kane, Michigan Technological University; Scott Bridgham, University of Oregon; Curtis Richardson, Duke University

Acknowledgments

Raymond G. Najjar (Science Lead), The Pennsylvania State University; Gil Bohrer (Review Editor), Ohio State University; Zhiliang Zhu (Federal Liaison), U.S. Geological Survey; Eric Kasischke (former Federal Liaison), NASA

Recommended Citation for Chapter

Kolka, R., C. Trettin, W. Tang, K. Krauss, S. Bansal, J. Drexler, K. Wickland, R. Chimner, D. Hogan, E. J. Pindilli, B. Benschoter, B. Tangen, E. Kane, S. Bridgham, and C. Richardson, 2018: Chapter 13: Terrestrial wetlands. In *Second State of the Carbon Cycle Report (SOCCR2): A Sustained Assessment Report* [Cavallaro, N., G. Shrestha, R. Birdsey, M. A. Mayes, R. G. Najjar, S. C. Reed, P. Romero-Lankao, and Z. Zhu (eds.)]. U.S. Global Change Research Program, Washington, DC, USA, pp. 507-567, <https://doi.org/10.7930/SOCCR2.2018.Ch13>.



KEY FINDINGS

1. The assessment of terrestrial wetland carbon stocks has improved greatly since the *First State of the Carbon Cycle Report* (CCSP 2007) because of recent national inventories and the development of a U.S. soils database. Terrestrial wetlands in North America encompass an estimated 2.2 million km², which constitutes about 37% of the global wetland area, with a soil and vegetation carbon pool of about 161 petagrams of carbon that represents approximately 36% of global wetland carbon stock. Forested wetlands compose 55% of the total terrestrial wetland area, with the vast majority occurring in Canada. Organic soil wetlands or peatlands contain 58% of the total terrestrial wetland area and 80% of the carbon (*high confidence, likely*).
2. North American terrestrial wetlands currently are a carbon dioxide sink of about 123 teragrams of carbon (Tg C) per year, with approximately 53% occurring in forested systems. However, North American terrestrial wetlands are a natural source of methane (CH₄), with mineral soil wetlands emitting 56% of the estimated total of 45 Tg C as CH₄ (CH₄ –C) per year (*medium confidence, likely*).
3. The current rate of terrestrial wetland loss is much less than historical rates (about 0.06% of the wetland area from 2004 to 2009), with restoration and creation nearly offsetting losses of natural wetlands. Although area losses are nearly offset, there is considerable uncertainty about the functional equivalence of disturbed, created, and restored wetlands when comparing them to undisturbed natural wetlands. Correspondingly, there remains considerable uncertainty about the effects of disturbance regimes on carbon stocks and greenhouse gas (GHG) fluxes. For this reason, studies and monitoring systems are needed that compare carbon pools, rates of carbon accumulation, and GHG fluxes across disturbance gradients, including restored and created wetlands. Those studies will produce data that are needed for model applications (*high confidence, likely*).

Note: Confidence levels are provided as appropriate for quantitative, but not qualitative, Key Findings and statements.

13.1 Introduction

The objective of this chapter is to characterize the distribution of carbon stocks and fluxes in terrestrial wetlands within North America. The approach was to synthesize available literature from field measurements with analyses of resource inventory data to estimate wetland area, carbon stocks, and net ecosystem exchange (NEE) of carbon and methane (CH₄) fluxes of terrestrial wetlands (see Appendices 13A, p. 547, and 13B, p. 557, for details¹). Then, the findings employed from large-scale simulation studies provided additional context, with consideration given to the effects of disturbance regimes, restoration and creation of terrestrial wetlands, and the

application of modeling tools to assess the carbon cycle of terrestrial wetlands.

13.1.1 Terrestrial Wetland Definition

This chapter focuses on carbon cycling in nontidal freshwater wetlands (referred to hereafter as “terrestrial wetlands”). Although there are various definitions of terrestrial wetlands (Cowardin et al., 1979; IUSS Working Group WRB 2006), all recognize a high water table level as the driver of biological and chemical processes characteristic of wetlands. The United States defines wetlands as soils that are inundated or saturated by surface or groundwater at a frequency and duration sufficient to support, and that do support under normal circumstances, a prevalence of vegetation typically adapted for life in saturated conditions (U.S. EPA 2015). The distribution of U.S. wetlands is considered on the basis of vegetation and hydrogeomorphical setting

¹ The assessment described in this chapter required additional background and parallel analyses of recently published and accessible databases. These analyses pertain only to Ch. 13 and are presented in Appendices 13A and 13B, beginning on p. 547.



using remote-sensing data (Federal Geographic Data Committee 2013). Soils are also indicative of wetland conditions; two major soil types useful for assessing carbon stocks and fluxes recognized here are mineral soils and organic soils. Wetland ecosystems with organic soils, also known as peatlands, are classified as Histosols by the U.S. Department of Agriculture (USDA) Natural Resources Conservation Service (NRCS) Soil Survey (Soil Survey Staff 2010). The Histosol order represents soils with a thick (>40-cm) accumulation of organic matter on top of mineral sediments or rock. Most Histosols are formed under wet conditions (e.g., peat soils), but some of these soils form under aerated conditions. Not considered a wetland, aerated Histosols are distinctly recognized (e.g., suborder Folists) and thus are not considered here. However, all peatlands are formed under wet conditions (Joosten and Clarke 2002), and they are classified as wetlands in Canada (Zoltai and Vitt 1995) and throughout North America (Gorham et al., 2012). The amount and distribution of accumulated soil organic matter reflect the balance between inputs from vegetative production and losses from decomposition or overland transport (e.g., erosion or drainage). While the depth for defining organic soils (Histosols) or peatlands ranges from 10 to 50 cm among different countries, the USDA Soil Survey uses the top 40 cm in the upper 80 cm of soil, which is the definition used here (Soil Survey Staff 2010). Mineral soil wetlands vary widely in the composition and depth of the surface organic layer, varying from a few centimeters to nearly 40 cm in histic-mineral soil wetlands (“histic” refers to soils with a 20- to 40-cm organic horizon, differentiating them from Histosols).

13.1.2 Relationship to Other Chapters and SOCCR1

For this chapter, assessments were made of terrestrial wetlands that occur in boreal, temperate, and tropical climatic zones in Canada, the United States, Mexico, and Puerto Rico. Tidally influenced saltwater and freshwater wetlands are assessed in Ch. 15: Tidal Wetlands and Estuaries, p. 596. Terrestrial wetlands, including peatlands, occurring in

the Arctic permafrost zone are assessed in Ch. 11: Arctic and Boreal Carbon, p. 428. Some types of wetlands are transition zones to inland waters (e.g., riparian wetlands). This report considers that inland waters (see Ch. 14: Inland Waters, p. 568) begin at the shoreline of lake, reservoir, and fluvial systems. Both Ch. 9: Forests, p. 365, and this chapter use the definition of forests from the USDA Forest Service’s Forest Inventory and Analysis (FIA). As a result, there is overlapping data between Ch. 9 and this chapter. Also, Ch. 10: Grasslands, p. 399, describes wetlands in those domains and thus has some overlapping data with this chapter. Similarly, there are overlapping data with Ch. 12: Soils, p. 469, where organic and mineral soil wetlands are assessed. Since Ch. 5: Agriculture, p. 229, includes no jurisdictional wetlands, it does not have overlapping data.

In the *First State of the Carbon Cycle Report* (SOCCR1; CCSP 2007), the Wetlands chapter (Chapter 13; Bridgham et al., 2007) was inclusive of all terrestrial and tidal wetlands, from tropical to Arctic ecosystems. In the *Second State of the Carbon Cycle Report* (SOCCR2), wetlands are assessed in several chapters as described above.

This chapter adds new information on carbon pools and fluxes from terrestrial wetlands that occur in boreal, temperate, and tropical climate zones within North America. It breaks down carbon pools and fluxes between mineral soil wetlands and peatland ecosystems. It also differentiates carbon pools and fluxes between forested and nonforested wetlands (not done in SOCCR1) because of the influence of trees on ecosystem carbon dynamics (see Figure 13.1, p. 510). The term “flux” is used for carbon dioxide (CO₂) and CH₄ as the net balance between uptake and release of these gases relative to the atmosphere. Finally, this chapter reviews dissolved organic carbon (DOC) fluxes from terrestrial wetlands as well as restored wetlands, but it does not consider constructed wetlands or detention ponds, which typically are engineered systems.



Figure 13.1. Forested Peatland in Northern Minnesota. This bog is part of the U.S. Department of Agriculture (USDA) Forest Services's Marcell Experimental Forest. [Figure source: USDA Forest Service.]

13.2 Current and Historical Context

13.2.1 Wetland Regulations

During the settlement of North America, wetlands were viewed as unproductive areas that were impediments to transportation and development, as well as a breeding ground for disease. That sentiment lasted for over 150 years, during which draining of wetlands for agriculture, forestry, and urban development was routine to make these ecosystems productive for commercial use. Once drained, wetlands generally have very productive soils because of their high organic matter and associated nutrients. Not until the mid-1900s did the effects of wetland drainage on both inherent wetland values and larger landscape impacts begin to be identified. Wetlands are now known to provide critical habitats for many rare species, serve as filters for pollutants and sediment, store water to prevent flooding, and sequester and store carbon, but those ecosystem services were not broadly recognized until relatively recently.

Currently, vegetation removal, surface hardening (e.g., pavement and soil compaction), and drainage are identified as the most common physical stressors on U.S. wetlands (U.S. EPA 2016). To address the threats and subsequent losses of wetlands,

wetland policies have been developed to avert further wetland conversion, degradation, or loss. The United States has an overarching policy of “no net loss” of wetlands adopted in 1989. This policy has dramatically slowed U.S. wetland losses and led to the development of wetland banking programs whereby losses due to development are offset by wetlands restored or created elsewhere. In Canada, the main causes for wetland losses are from land conversion to urban or agriculture, water-level control including flooding from hydroelectric development, and climate change (Federal Provincial and Territorial Governments of Canada 2010). In 1991, the Canadian government enacted the Federal Policy on Wetland Conservation (Canadian Wildlife Service 1991). Similarly, the Natural Protected Areas Commission of Mexico announced a national wetland policy in 2014 designed to protect wetlands and avert losses. Recent research in Mexico indicates that drainage for agriculture and conversion to aquaculture are two major threats to wetlands (De Gortari-Ludlow et al., 2015).

These national-level policies are not the only regulations in place designed to protect wetlands. The United States and Canada have wetland-focused state and provincial regulations, as well as other federal regulations that, while not focused on wetlands, do protect wetland habitat. Migratory bird agreements among the United States, Mexico, and Canada often have wetland protection implications. In 1986, the United States and Canada adopted the North American Waterfowl Management Plan and were later joined by Mexico in 1994 (North American Waterfowl Management Plan Committee 2012). This plan establishes strategies to protect wetland habitat for the primary purpose of sustaining migratory bird populations with the associated benefit of protecting carbon pools.

Competing land uses and economic development will continue to threaten wetlands in North America. Multiple policies have been designed to protect against, and mitigate for, wetland loss. However, while losses are greatly stemmed, the United States continues to experience net losses of wetlands in



terms of absolute acreage in spite of the no net-loss policy. Canada and Mexico currently have no nationwide wetlands inventory, limiting the ability to estimate wetland conversion or function, including carbon fluxes and pools. It is important to remember that no net-loss policies do not protect against reduced functionality in restored versus natural wetlands.

13.2.2 Change in Wetland Area

As a result of socioeconomic drivers, there have been massive disturbances and conversions of wetlands over the past 150 or more years in North America. The latest assessment of the status and trends of wetlands in the conterminous United States (CONUS) estimates that there are 445,000 km² of wetlands, which includes 395,197 km² of terrestrial wetlands (USFWS 2011). In colonial America, there were an estimated 894,000 km²; between 1870 and 1980, the United States experienced a 53% loss of wetland area (Dahl 1990). From 2004 to 2009, increased wetland restoration on agricultural lands occurred; however, wetland losses continued to outpace gains, leading to a total wetland area decline of 0.06% (USFWS 2011). The current rate of loss is 23 times less than that of the historical trend (e.g., 1870 to 1980), an indication of changing attitudes toward wetlands and the effectiveness of policies to protect them (USFWS 2011).

Although Canada does not have a national wetlands inventory, estimated losses are approximately 14% of the country's original 1,470,000 km² of wetlands (Environment Canada 1991). Similarly, an estimated 62% of wetland area has been lost from Mexico's original 112,166 km² of wetlands (Casasola 2008; Landgrave and Moreno-Casasola 2012). Mexico's small area of peatlands covers about 20,000 km² generally found in high-elevation ecosystems and near-coastal freshwater marshes (Instituto Nacional de Estadística y Geografía 2010). The country has another 15,000 km² of mineral soil wetlands.

In CONUS, about 468,000 km² of wetlands have been lost, 96% of which have been mineral soil wetlands and 4% peatlands (Bridgham et al., 2007).

Similarly, in Canada, of the 212,000 km² of wetlands lost, 94% have been mineral soil wetlands and 6% peatlands (Bridgham et al., 2007). However, Canadian peatlands are now being lost in large numbers due to urban development, hydroelectric development, and energy production (Chimner et al., 2016), including in the oil sands region where nearly 300 km² have been destroyed by mining (Rooney et al., 2012). In the United States, forested wetlands are undergoing the most rapid losses among terrestrial wetland types. From 2004 to 2009, 1.2% of forested wetlands were lost (2,562 km²) per year, compared to gains of 1,084 km² per year for emergent wetlands and 729 km² per year for shrub wetlands (Dahl 2011).

The change in wetland area is quite high in the U.S. Midwest where Iowa, Missouri, Illinois, Ohio, and Indiana have experienced a greater than 85% loss of their wetlands. California has lost 96% of its original wetlands (Dahl 2011; Garone 2011). Other notable ecosystem examples include bottomland hardwood forests of the Lower Mississippi River Alluvial Plain (i.e., southern Illinois to the Gulf of Mexico); these forests, once comprising an area of approximately 85,000 km², were reduced to about 20,000 km² by 1990, primarily through agricultural conversion and alterations to the hydrological system for flood protection (Stanturf et al., 2000). Major federal flood-control projects that began following a significant flood in 1927 contributed to more than 30% of wetland losses and subsequent agricultural conversions in the Mississippi River Valley (King et al., 2006; Stavins and Jaffe 1990). Similarly, the Prairie Pothole Region (see Section 13.3.3, p. 520) of the United States and Canada included 200,000 km² of wetland area prior to European settlement but has since decreased to 70,000 km² of intact (i.e., not drained) wetland area (Dahl 2014; Euliss et al., 2006). In contrast, Alaska is reported to have had negligible wetland loss (Bridgham et al., 2007), although the state does not have a completed assessment under the U.S. Fish and Wildlife Service (USFWS) National Wetlands Inventory.



Areal extent alone does not indicate the ecosystem function and services that wetlands deliver. In 2011, the U.S. Environmental Protection Agency (EPA) released the first national assessment of the condition of U.S. wetlands. Findings indicated that 48% of wetlands were in good condition, 20% were in fair condition, and 32% were in poor condition (U.S. EPA 2016). While wetlands may remain intact, their alterations by humans are still affecting the ability of wetlands to function similarly to an unaltered state. Carbon sequestration is one of those important functions affected by wetland condition. Connecting wetland condition to carbon stocks and fluxes will be an important next step for assessing impacts on the carbon cycle.

13.2.3 Overview of Disturbance Effects on Carbon Stocks and Fluxes

Wetlands have been sequestering carbon from the atmosphere for thousands of years. Following the end of the last glacial period about 12,000 years ago, wetlands developed over much of the northern part of North America. Low areas or areas with less permeable soils tended to pond water and create the anoxic environment critical for peatland and mineral soil wetland formation. In undisturbed wetlands, carbon pools are relatively stable over short time intervals, but carbon fluxes may be quite variable due to complex interactions of climate, vegetation, soils, and hydrology. For example, annual CO₂ fluxes ranged from a sink of 2 to 112 grams of carbon (g C) per m² per year, and CH₄ fluxes ranged from a source of 2.8 to 4.4 g C per m² per year during a 6-year study in a peatland in southern Ontario (Roulet et al., 2007). Carbon dioxide fluxes generally decrease (i.e., sinks or lesser sources) and CH₄ fluxes generally increase (i.e., sources or lesser sinks) as water tables get nearer to the surface (Olson et al., 2013). During droughts or high-water events, CO₂ and CH₄ fluxes can vary greatly, even in undisturbed wetlands. Changes in carbon fluxes resulting from disturbance lead to changes in carbon pools. Drainage is the main human-caused disturbance that has led to a variety of local- to landscape-level impacts. Wetland drainage causes an abrupt change from anaerobic conditions during flooding to aerobic

conditions subsequent to drainage, resulting in rapid acceleration of decomposition through microbial oxidation of organic matter (Drexler et al., 2009). As a result, wetland drainage generally leads to lower carbon stocks, lower CH₄ fluxes, and a long-term increase in CO₂ fluxes (Bridgham et al., 2006). In peatlands, drainage also can result in significant land-surface subsidence (Drexler et al., 2009). Other human-caused disturbances include filling of wetlands for development, construction of dams that permanently flood wetlands, stream channelization and road construction that can disconnect wetlands from their water source, removal of vegetation (including forest harvesting), and agricultural conversion of surrounding uplands.

13.3 Current Understanding of Wetland Stocks and Fluxes

The occurrence of the water table within the upper soil layers during the growing season differentiates wetlands from upland ecosystems, influencing the biological communities that must adapt to withstand prolonged periods of soil saturation and biogeochemical processes that are a function of the anoxic soil conditions. While net primary production (NPP) of wetlands is comparable to upland ecosystems (Ahl et al., 2004), the rate of organic matter decomposition is generally less due to the anaerobic soil conditions. As a result, wetland soils typically contain considerably more carbon per unit volume than do upland soils. In areas with prolonged periods of soil saturation and high rates of organic matter production, organic matter may accumulate on top of the mineral substrate, forming organic soils or peatlands with thicknesses ranging from 40 cm to many meters.

The anaerobic conditions of wetland soils also influence greenhouse gas (GHG) fluxes. Unlike upland soils that generally are a sink for atmospheric CH₄, wetland soils typically are a net source of CH₄ to the atmosphere. Methane flux from wetlands is regulated largely by oxygen availability and associated water table position, soil temperature, and vegetation type (Bansal et al., 2016; Green and Baird 2012; Hanson et al., 2016). Hence, fluxes can



be highly variable, even within a wetland, as subtle differences in surface topography, temperature gradients, and vegetation affect fluxes (Bridgham et al., 2006). Accordingly, carbon fluxes and storage in wetlands are likely to change dramatically as a result of climate and land-use changes, which alter water-table dynamics, temperatures, and vegetation communities, ultimately affecting the ecosystem carbon balance. Drainage is the common modification to wetlands for agriculture and silviculture and causes most of the wetland loss noted above. The organic matter decomposition rates of those drained wetlands can be very high, and, for peatlands, the effect may persist for many decades. The soil carbon content of converted wetlands may be greater than the surrounding upland, while the fluxes of GHGs, especially CO₂, are likely larger.

This chapter assessed the state of the wetland carbon cycle, considering organic and mineral soils separately because the soil carbon density, or the amount of carbon per unit volume, varies between the two soil types, and they generally reflect different hydrological settings and vegetation communities. Correspondingly, differentiating between forested and nonforested organic and mineral soil wetlands provides a basis to consider the influence of vegetation on the carbon cycle. The approach for quantifying the wetland carbon pools was based primarily on analyses of recently developed geospatial data, providing a more robust basis for the assessment, as contrasted with summarization based on studies reported in the literature. The general framework, using CONUS as an example, consisted of identifying the distribution of forested and nonforested terrestrial wetlands using the USFWS National Wetlands Inventory. The soil carbon stocks were then determined by summarizing USDA's NRCS Soil Survey databases. Forest vegetation carbon stocks were estimated based on the U.S. Forest Service FIA database (U.S. Forest Service 2003), and nonforest vegetation carbon content was estimated using a mean carbon density based on reported values in the literature. Variations to that framework were necessitated by available databases. For example, in Alaska, where the National

Wetlands Inventory has not been completed, a remote sensing-based approach to wetland identification was used (Clewley et al., 2015). Similarly, because Canada does not have a comprehensive national soil inventory, independent assessments of Canadian peatlands and soil landscapes were used. Details about the databases used to calculate the wetland area and associated carbon stocks are provided in Appendix 13A, p. 547.

There are approximately 2.2 million km² of terrestrial wetlands in North America (see Table 13.1, p. 514); the majority of those wetlands (81%) occurs in Canada and Alaska. This estimate is approximately 176,000 km² less than the one used in SOCCR1 (CCSP 2007). The difference in nonpermafrost peatlands and freshwater mineral soil wetlands among the two reports is due primarily to a smaller and more accurate and current assessment of wetland area in Alaska (Clewley et al., 2015), which reduced the total wetlands in the state by approximately 360,000 km²; Canadian wetlands increased by approximately 198,000 km² due primarily to a larger estimate of mineral soil wetlands. The uncertainty in wetland area is greatest at the higher latitudes, hence the reliance on remote-sensing methods for spatial extent estimates, which are expected to improve further as data and processing tools advance. The report on Alaskan wetlands by Clewley et al. (2015) is an example of achieving an accuracy of approximately 94% in discriminating wetlands from uplands. There remains uncertainty in the reported area of Canadian peatlands, which ranges from the 755,000 km² reported by Kroetsch et al. (2011) to the 1.1 million km² reported in SOCCR1 (Bridgham et al., 2007). In contrast to reported inventories and assessments used in SOCCR1, Zhang et al. (2017a) used six models to estimate wetland area for North America (including coastal wetlands), with the modeled estimates ranging from about 1.1 to 3.3 million km², effectively placing the estimated total in Table 13.1 in the middle of that range. Correspondingly, there are large ranges in estimated global wetland area. Based on modeled and observational estimates (Bridgham et al., 2006; Melton et al., 2013; Zhang et al., 2017a), North



Table 13.1. Area, Carbon Pool, Net Ecosystem Exchange of Carbon, and Methane Emissions from Wetlands in North America^{a-c}

Wetland Type	Area ^d (km ²)	Carbon Pool ^e (Pg C)	NEE ^f	CH ₄ Emissions	
			Net Balance (Tg C per Year) ^g	CH ₄ -C (Tg C per Year) ^g	CH ₄ (Tg per Year)
Canada					
Peatland					
Nonforested	415,450	37.8	-6.9 ± 3.5	9.4 ± 2.4	12.6
Forested	703,785	76.7	-33.6 ± 5.9	6.3 ± 7.4	8.4
Mineral					
Nonforested	103,932	9.5	-10.6 ± 7.2	2.7 ± 0.7	3.6
Forested	268,337	5.1	-12.9 ± 6.8	7.2 ± 4.3	9.6
Total	1,491,504	129.0	-64.0 ± 12.0	25.6 ± 8.9	34.2
Conterminous United States					
Peatland					
Nonforested	42,903	3.9	-5.8 ± 3.6	1.0 ± 0.3	1.3
Forested	40,823	4.4	-4.9 ± 3.8	0.4 ± 0.4	0.5
Mineral Soil					
Nonforested	138,381	1.9	-14.1 ± 9.5	3.6 ± 1.0	4.8
Forested	173,091	3.3	-11.6 ± 8.2	4.7 ± 2.8	6.2
Total	395,197	13.5	-36.5 ± 13.6	9.6 ± 3.0	12.8
Alaska					
Peatland					
Nonforested	73,836	5.5	-4.2 ± 4.7	1.7 ± 0.4	2.2
Forested	5,747	0.4	-0.3 ± 0.4	0.1 ± 0.1	0.2
Mineral Soil					
Nonforested	192,013	9.3	-10.9 ± 12.3	5.0 ± 1.4	6.7
Forested	40,162	2.0	-2.3 ± 2.6	1.1 ± 0.6	1.4
Total	311,758	17.3	-17.6 ± 13.5	7.9 ± 1.6	10.5
Puerto Rico					
Peatland					
Nonforested	8	0.001	-0.003 ± 0.003	3.38E-04 ^h ± 2.88E-04	0.0
Forested	1	0.000	0.000 ± 0.000	2.68E-05 ± 2.28E-05	0.0
Mineral Soil					
Nonforested	252	0.006	-0.030 ± 0.110	1.36E-02 ± 0.488E-02	0.0
Forested	50	0.001	-0.006 ± 0.022	2.70E-03 ± 0.966E-03	0.0
Total	311	0.008	-0.039 ± 0.110	1.67E-02 ± 0.500E-02	2.22E-02
Mexico					
Peatland					
Nonforested	17,191	0.43	-5.33 ± 5.25	0.69 ± 0.59	0.9
Forested	3,394	0.24	-1.05 ± 1.04	0.14 ± 0.12	0.2

Continued on next page



(Continued)

Table 13.1. Area, Carbon Pool, Net Ecosystem Exchange of Carbon, and Methane Emissions from Wetlands in North America ^{a-c}					
Wetland Type	Area ^d (km ²)	Carbon Pool ^e (Pg C)	NEE ^f	CH ₄ Emissions	
			Net Balance (Tg C per Year) ^g	CH ₄ -C (Tg C per Year) ^g	CH ₄ (Tg per Year)
Mexico (continued)					
Mineral Soil					
Nonforested	10,320	0.35	-1.25 ± 4.51	0.56 ± 0.20	0.7
Forested	5,288	0.16	-0.64 ± 2.31	0.29 ± 0.10	0.4
Total	36,193	1.17	-8.27 ± 7.37	1.67 ± 0.640	2.22
North America					
Peatland					
Nonforested	549,388	47.7	-22.2 ± 17.1	12.8 ± 3.7	17.0
Forested	753,749	81.8	-39.9 ± 11.0	6.9 ± 8.0	9.2
Mineral Soil					
Nonforested	444,898	21.1	-36.9 ± 33.6	11.9 ± 3.3	15.9
Forested	486,928	10.4	-27.4 ± 19.9	13.3 ± 7.8	17.7
Total	2,234,963	161.0	-126.4 ± 23.8	44.8 ± 9.5	59.8

Notes

- a) Positive emissions indicate net gains to the atmosphere, and negative emissions indicate net gains or sequestration into the ecosystem.
- b) Citations and assumptions in calculations are in the text of this chapter and in Appendices 13A, p. 547, and 13B, p. 557.
- c) Key: C, carbon; NEE, net ecosystem exchange; CH₄, methane; Pg C, petagrams of carbon; Tg C, teragrams of carbon.
- d) Includes freshwater and nontidal terrestrial wetlands. Accuracy of wetland area estimates: Canada: >66% (Tarnocai 2009), conterminous United States: >90% (Nichols 1994), Alaska: 95% (Clewley et al., 2015), Puerto Rico: >90% (Nichols 1994), Mexico: <75% (this report); see Appendix 13A, p. 547, for more information.
- e) Includes soil and plant carbon; soil carbon accounts for approximately 93% of the total pool.
- f) Includes net exchange of CO₂ from the wetland; it does not include lateral fluxes or CH₄ fluxes.
- g) The values here are mean values plus or minus 2 times the standard errors to approximate the minimum and maximum values of a 95% confidence interval.
- h) E = 10x.

America contains 20% to 47% of the global wetland area, depending on the basis.

The dominant carbon flux from terrestrial wetlands is characterized as NEE of CO₂, which is a measure of the difference in CO₂ uptake and CO₂ release; NEE is positive when the net flux is from the wetland to the atmosphere. In addition to NEE of CO₂, this chapter also reports CH₄ fluxes from the wetlands. Estimates of these fluxes are based on studies reported in SOCCR1 (CCSP 2007) and

subsequent literature that used field-based measurements to estimate NEE and CH₄ fluxes (either chamber based or eddy covariance). This chapter categorizes the studies by soil, vegetation type, and region and utilizes a mean flux as the basis for the flux density (flux per unit area) used in the reported regions (see Appendix 13B, p. 557, for flux density factors used in the analyses). Though NEE and CH₄ fluxes are the primary fluxes considered, the wetland net ecosystem carbon balance (Chapin et al., 2006), which is the overall net change in wetland carbon

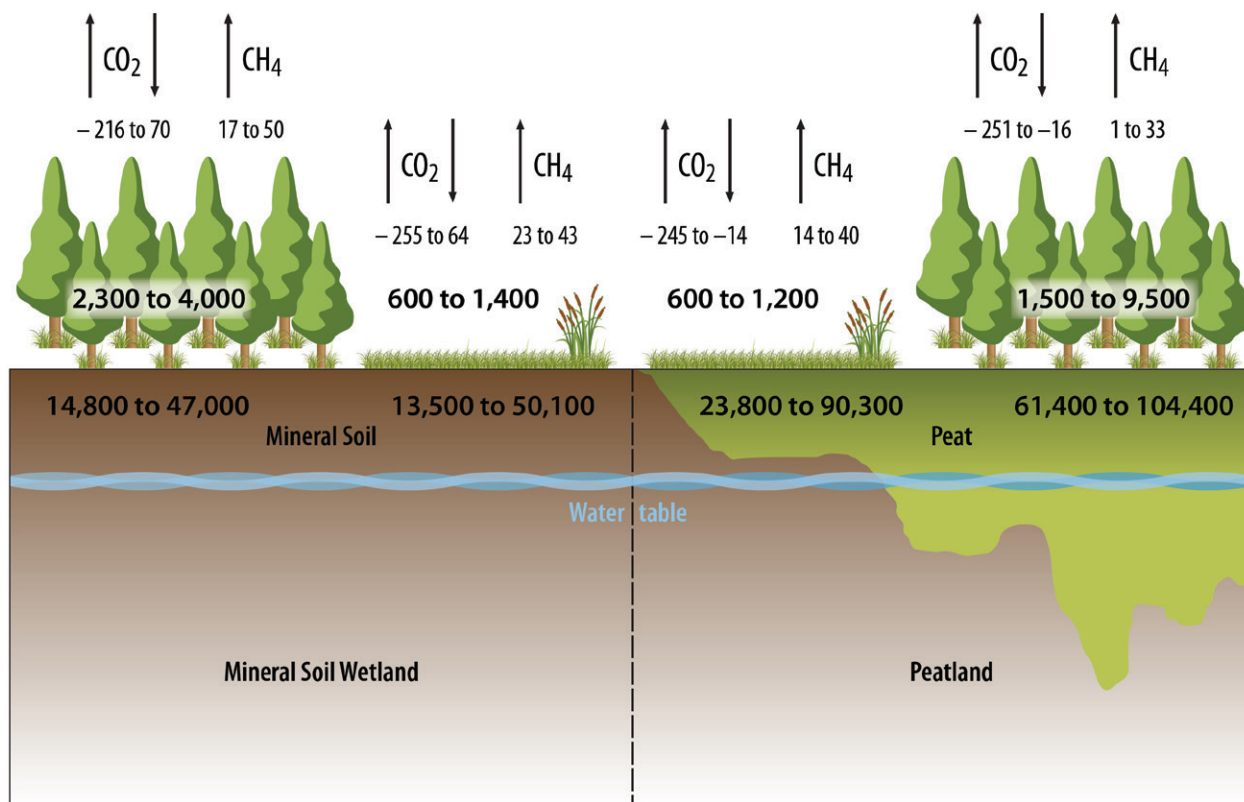


Figure 13.2. Carbon Pools and Fluxes in Forested and Nonforested Mineral Soil Wetlands and Peatlands in North America. The soil and vegetation carbon pools are represented by the range of carbon densities (minimum to maximum) among Canada, Mexico, and the United States. Annual carbon dioxide (CO₂) and methane (CH₄) fluxes (arrows) are represented by a 95% confidence interval; a negative flux indicates a transfer of carbon from the atmosphere to the ecosystem. Stocks and fluxes are in grams of carbon (g C) per m². [Data sources: Table 13.1, p. 514, and Appendices 13A and 13B, p. 547 and p. 557, respectively.]

over a specified time, is also influenced by other fluxes. These additional fluxes include carbon monoxide and volatile organic carbon to the atmosphere (e.g., from fires), lateral fluxes of DOC (see Section 13.3.3, p. 520), dissolved inorganic carbon (DIC), and particulate carbon (Chapin et al., 2006).

Peatlands tend to store more soil carbon than mineral soil wetlands, and forested wetlands store more carbon in the vegetation than nonforested wetlands (see Figure 13.2, this page). Across all studies used in this chapter's analysis, fluxes of CO₂ are overlapping across all wetland types but both forested and nonforested mineral soil wetlands tend to be larger sources (or lesser sinks) of CO₂ (see Figure 13.2). Similarly, CH₄ fluxes overlap across all wetland

types, yet all wetland types tend to be sources of CH₄ (see Figure 13.2, this page).

13.3.1 Peatlands—Carbon Stocks and Fluxes

Peatlands include those ecosystems with organic soils generally classified as either fens or bogs, both of which are defined by water source and pH. Fens tend to be fed by groundwater and precipitation and have circumneutral pH values with vegetation generally dominated by sedges (*Carex* spp.) and brown mosses. In contrast, bogs are predominantly precipitation fed and have much lower pH and *Sphagnum* mosses. Other types of peatlands include riparian systems such as bottomland hardwood ecosystems



in the Mississippi River Valley, pocosins, Atlantic white cedar swamps, Carolina bays in the southeastern United States, and high-elevation peatlands in the Rocky Mountains from Canada to Mexico and throughout the Sierra Nevada of California. The total area of peatland in North America is about 1.3 million km² (see Table 13.1, p. 514).

Peatlands contain about 80% of the wetland carbon stock in North America and account for 48% of the net annual carbon uptake and 44% of the annual CH₄ flux. Approximately 58% of peatlands in North America are forested. The peatland carbon pool in Canada is currently estimated at 114 petagrams of carbon (Pg C), about 67% of which occurs in forests. This pool represents 88% of the total peatland carbon stock for North America (see Table 13.1, p. 514). Canadian peatlands have an estimated annual uptake of 41 teragrams of carbon (Tg C) and an estimated release of 16 Tg CH₄-C per year, 61% from non-forested peatlands. Alaska contains 42% of the U.S. peatland carbon stock and accounts for approximately 39% of the carbon uptake. Forests compose 49% of the peatland carbon stock in CONUS and 7% in Alaska. Methane from U.S. peatlands is 7% of the North American annual peatland flux; CONUS contributes 43% of the U.S. CH₄ flux. This difference in stocks and fluxes between the two countries having the majority of North American peatlands is attributable to the much larger peatland area in Canada. Mexico contains the largest area of tropical peatlands (~20,600 km²), which constitutes approximately 57% of the total wetland area of the country (see Table 13.1, p. 514). Those peatlands contribute 2% of the North American peatland CH₄ flux as a result of the high flux rates in the tropics. Additionally, small areas of tropical peatlands occur in Puerto Rico (9 km²). The estimated CH₄ emission is quite variable for each country or state, with the 95% confidence interval varying from 26% to 118% and 85% to 269% of the mean for temperate and tropical wetlands (see Table 13.1, p. 514), which is a reflection of the high degree of variability in the reported measurement data. The CH₄ fluxes applied for forested and nonforested peatlands (8.9 and 22.7 g C per m² per year, respectively) are less than

the 26 g C per m² per year average for bogs and fens reported by Turetsky et al. (2014).

There is wide variation in intrinsic peat properties that influences the carbon stored in peat and how fast it accumulates after disturbances or with succession. Peat properties related to carbon storage are directly linked to the source material that changes with peatland type (Kracht and Gleixner 2000; Schellekens et al., 2012). For example, “peat moss,” or *Sphagnum*-derived peat, is different in soil carbon density than peat derived from woody plants (“silvic peat”). Also, peat decomposition rates tend to increase with decreases in water tables (Ise et al., 2008). As such, care is needed in making broad assessments of peat accumulation in forested versus open peatlands, especially since dominant cover types can change (e.g., from silvic peat to *Sphagnum* peat) over time, and water tables can be influenced by short- and long-term precipitation patterns (e.g., droughts) and anthropogenic disturbances (e.g., draining). These factors all contribute to the large amount of variation in peatland carbon cycling and rates of peat accumulation. Peat carbon accumulation rates since the last glaciation range from 7 to 300 g C per m² per year (Kolka et al., 2011) in North America, with an average of 23 g C per m² per year during the Holocene (Loisel et al., 2014), but values commonly range from 20 to 30 g C per m² per year (Manies et al., 2016). In terms of peat accumulation, long-term rates range from 0.2 to 10 mm per year but typically range from 0.4 to 2.0 mm per year across all North American peatland types (Kolka et al., 2011). Peatland carbon pools are dependent on the depth of peat, ranging from 20,000 g C per m² in shallow peatlands to more than 300,000 g C per m² in peatlands >5 m deep (Kolka et al., 2011).

Generally, any factor that lowers the water table relative to the peat surface will result in increased CO₂ production, increased decomposition, and decreased CH₄ production (Waddington et al., 2015). There are also generalizations that can be made across peatland types, although variation in CO₂ and CH₄ production is high (e.g., McLaughlin and Webster



2014). Fen ecosystems are generally characterized by having relatively low CH_4 : CO_2 fluxes compared with systems having very little water movement such as bogs, though fluxes vary greatly, both seasonally and latitudinally. In northern peatlands, CH_4 fluxes are generally highest when water tables are near the peat surface and seasonal temperatures are high (Turetsky et al., 2014). Pocosin ecosystem soils are in contact with groundwater except during seasonal droughts, thus their gaseous fluxes can be variable but generally produce less CH_4 than northern peatlands (Bridgham and Richardson 1992). The reduced gaseous fluxes of pocosins may be related to the high polyphenol content of their peats that resists decomposition even during moderate drought (Wang et al., 2015). The composition of the organic matter in peatlands also affects fluxes of CH_4 and CO_2 , with low-quality peat maintaining low rates of decomposition, even when aerated (see Figure 13.3, this page). Those effects are evident both within and between climatic zones.

Gaps in research and monitoring activities to better understand how peatland carbon storage may change in an altered future climate are related mainly to disturbance events that dramatically alter the mechanisms of peat carbon accumulation and stability. Disturbance events of concern are those that alter wetland hydrology, which has a direct feedback to primary production and decomposition. While there is well-developed literature demonstrating that lower water tables coincident with changing precipitation patterns or altered drainage often result in a decline in the carbon sink strength of northern peatlands (Waddington et al., 2015), altered hydrology also has been shown to increase the vulnerability of northern latitude peatlands to wildfire (Benscoter et al., 2011; Turetsky et al., 2011a; Waddington et al., 2012), hence further increasing the vulnerability of peatland carbon pools to decomposition. Research has demonstrated that the extent of fires in boreal North America has steadily increased over the past five decades (Kasischke and Turetsky 2006), often with substantial peat combustion (Turetsky et al., 2011b). For example, a single fire event in northern peatlands can consume 3.3 to



Figure 13.3. Organic Soil Peat Core. Composed primarily from partially decomposed organic matter, this peat sample is from Drosera Fen in Yosemite National Park. [Figure source: Judith Drexler, U.S. Geological Survey.]

3.6 kg C per m^2 (Reddy et al., 2015; Turetsky et al., 2011b), recovery from which would require about 140 years. Disturbance-mediated changes in vegetation community composition also have implications for gas production because different plant species functionally alter rates of CO_2 and CH_4 fluxes from peat, or they affect the ability of peat to resist decomposition (Armstrong et al., 2015; Turetsky et al., 2014). Taken together, the effects of altered hydrology (whether induced by management or as a climatic response) on fire regime and productivity and changes in plant species composition represent key uncertainties in the current understanding of peatland carbon storage in an altered future climate.

13.3.2 Mineral Soil Wetlands—Carbon Stock and Fluxes

The total area of mineral soil wetlands in North America is about 0.9 million km^2 (see Table 13.1, p. 514). The United States contains 52% of the mineral soil wetland carbon stock in North America. Mineral soil wetlands in CONUS have an estimated carbon stock of 5.2 Pg C, with a net annual sequestration of 25.7 Tg C as CO_2 (Tg CO_2 -C) and an estimated emission of 8.3 Tg CH_4 -C per year (see Table 13.1). Alaska has a larger stock (11.3 Pg C), annual sequestration as CO_2 (13.2 Tg C), and CH_4



release (6.1 Tg CH₄-C). Canadian mineral soil wetlands have a carbon stock of 14.6 Pg C, with an annual CO₂ uptake of 23.5 Tg C and an estimated release of 9.9 Tg CH₄-C per year (see Table 13.1). Mexico has much smaller mineral soil wetland stock (0.5 Pg C), CO₂ sequestration, and CH₄ emissions. The estimates of the exchange of CO₂-C and CH₄-C are quite variable, with the 95% confidence interval ranging from 18% to 360% of the reported mean. Mineral soil wetland carbon stocks in North America are nearly equally divided between nonforested and forested wetlands, 48% and 52%, respectively. Methane releases from the wetlands are greatest for mineral soil wetlands in Canada, followed by CONUS and Alaska (see Table 13.1, p. 514); these estimates also are variable, having a 95% confidence interval ranging from 28% to 61% of the reported mean.

Different national agencies classify mineral soil wetlands differently, using various terms such as marshes, swamps, riverine wetlands, palustrine wetlands, prairie potholes, playas, and Carolina bays, as well as many other local and regional terms. Geography and geomorphology are distinguishing factors in some classifications and influence carbon dynamics. Although there is value in broad classifications, such as forested versus nonforested as in Table 13.1, it is important to recognize that boreal, temperate, and tropical regions in North America span from just over 14°N latitude along the Mexican border with Guatemala to boreal regions of Alaska and Canada positioned to 60° to 70°N latitude. Variation in the carbon pool within these mineral soil wetland types and regions correlates strongly with latitude. Modeled NPP of wetlands across all types, including organic soil wetlands, ranged from 461 to 618 g C per m² per year for tropical and lower-latitude temperate regions to as little as 172 to 183 g C per m² per year in boreal regions (Cao et al., 1996). Summarizing carbon dynamics in tropical wetlands, Sjögersten et al. (2014) reported an average NPP of 880 g C per m² per year for tropical mineral soil wetlands. The proportion of carbon being returned to the atmosphere as CH₄ also decreased with increasing latitude, with CH₄ fluxes varying slightly with respect to whether wetlands

were forested or nonforested along this latitudinal gradient (see Table 13.1, p. 514). The data reported by Cao et al. (1996) do not differentiate organic soil wetlands from mineral soil wetlands, but reductions in NPP and CH₄ fluxes for mineral soil wetlands are included and would track with these overall patterns.

Mineral soil wetland carbon pools include those with soil organic layers that are less than 40 cm thick. The Intergovernmental Panel on Climate Change (IPCC) considers a soil depth down to 30 cm as the lower limit for reporting of mineral soil wetland carbon pools (IPCC 2013). To a depth of 30 cm, carbon pools range from 2,200 g C per m² in dry tropical mineral soil wetlands to greater than 10,000 g C per m² in boreal and moist temperate wetlands (Batjes 2011; Wickland et al., 2014). U.S. soil surveys consider soil properties in the upper 200 cm, but values in the top 150 cm are reported in this chapter to provide a uniform basis of comparison that includes both the surface soil layers and the subsoil.

Seasonal and diurnal fluxes of GHGs from boreal and temperate mineral soil wetlands have a wide range. For example, from temperate forested wetlands, CO₂ fluxes ranged from -0.444 to 3.303 g C per m² per day and CH₄ fluxes ranged from -0.014 to 0.0199 g C per m² per day (Alford et al., 1997; Harriss and Sebacher 1981; Harriss et al., 1982, 1988; Kelley et al., 1995; Krauss and Whitbeck 2012; Miller and Ghiorso 1999; Mulholland 1981; Pulliam 1993; Wilson et al., 1989; Yu et al., 2008). The fluxes depend on the wetland type, soil temperature, and soil water regime. These factors are affected not only by latitude, but also by land-use change, leading to much assessment difficulty and uncertainty. North American wetlands release approximately 44 Tg CH₄-C per year, but the uncertainty surrounding this value is considerable (see Table 13.1, p. 514). For nonforested mineral soil wetlands of North America, NEE of carbon as CO₂, ranged from an average of -264 to 527 g C per m² per year. Methane was emitted from these same wetlands at rates of 0.8 to 127 g C per m² per year. Such broad ranges of CO₂ and CH₄ fluxes reflect



sensitivity to biotic and abiotic factors, which drive high uncertainty in estimating the net carbon balance and changes in carbon sinks at large scales and time periods.

Understanding the carbon balance across gradients of hydrology and vegetation within a mineral soil wetland is crucial to determining landscape-scale fluxes, especially for systems associated with fluvial networks. For instance, in a short-hydroperiod floodplain wetland in Virginia, GHG fluxes varied dramatically depending on the floodplain geomorphic unit (i.e., levee, backswamp, and toe slope) and in relation to longitudinal position (i.e., upstream versus downstream; Batson et al., 2015). The focus is often on the *in situ* capacity of forested mineral soil wetlands in controlling the carbon balance. However, many forested mineral soil wetlands are positioned for *allochthonous* inputs, (i.e., organic and inorganic carbon [including dissolved CO₂] that moves across terrestrial landscapes to aquatic environments). Such inputs, along with erosion, may influence the carbon balance significantly through external drivers (Ensign et al., 2013; Noe et al., 2016). Data on these inputs are few, as research has focused intently over the past several decades on carbon balance from organic soil wetlands (e.g., fens, bogs, and coastal marshes).

Prairie "potholes" represent one type of mineral soil wetland that has been studied intensively. The Prairie Pothole Region (PPR) is home to the largest inland mineral soil wetland ecosystem in North America. Covering about 777,000 km² of north-central United States and south-central Canada, the PPR is characterized by millions of closed depressional, mineral soil wetlands or potholes encompassing approximately 70,000 km² of undrained wetlands (Dahl 2014; Euliss et al., 2006). The distinguishing feature of prairie potholes is their lack of a discernable surface drainage network. These wetlands have the potential to represent a considerable contribution to the North American GHG balance, both as carbon storage and sequestration sites and as sources of GHGs (Badiou et al., 2011; Bansal et al., 2016; Tangen et al., 2015). PPR

wetlands, also characterized by periods of inundation ranging from ephemeral to permanent, exist along a water-salinity gradient from fresh to hypersaline and occur primarily within a matrix of croplands and grasslands (Euliss et al., 2004; Goldhaber et al., 2014; Niemuth et al., 2010; Winter and Rosenberry 1998). Many PPR wetlands contain sulfate concentrations comparable to coastal systems, resulting in inhibition of CH₄ production (Goldhaber et al., 2014). Consequently, the biotic and abiotic factors that regulate the carbon dynamics and GHG balance of these systems are highly variable, both temporally and spatially.

Previous work recognizing PPR wetlands as significant carbon storage sites (Euliss et al., 2006) and identifying mineral soil wetlands as a major data gap (Bridgham et al., 2006, 2007) spurred considerable research in recent years pertaining to the overall GHG balance of these wetlands. Soil carbon stores are reduced by 12% to 26% when wetlands are converted from native grasslands to agricultural uses, presumably due to wetland drainage and soil disturbance (Gleason et al., 2008, 2009; Tangen et al., 2015). Peak CH₄ fluxes can exceed 0.75 g C per m² per day, and maximum cumulative seasonal CH₄ fluxes have been shown to be among the greatest reported for North American wetlands (Bansal et al., 2016; Bridgham et al., 2006; Tangen et al., 2015). In terms of the overall radiative balance of PPR mineral soil wetlands, CO₂ contributes the most (about 90%) to net GHG flux, followed by CH₄ (about 9%) and N₂O (about 1%; Gleason et al., 2009).

13.3.3 Lateral Carbon Fluxes from Terrestrial Wetlands

The lateral flux of carbon may occur in the form of DIC, DOC, dissolved CH₄, and particulates. The DOC flux is generally the largest of these fluxes from wetlands and is particularly important because it can be a source of carbon to both surface and groundwater. The rates of DOC production and loss are variable across time, space, and wetland types and appear to be climate dependent (Drösler et al., 2014). The transport of DOC to surface waters is fairly well studied for peatlands (Hope et al., 1994).



The IPCC Wetlands Supplement (2013) chapter on drained inland organic soils reviewed the literature and estimated DOC flux from natural systems across biomes. As part of that supplement, Drösler et al. (2014) found 1) boreal peatland flux to surface waters to be 8.4 g C per m² per year (95% confidence interval ranging from 6.0 to 11.1 g C per m² per year), 2) temperate peatland flux to surface waters to be 21.2 g C per m² per year (17.3 to 26.2 g C per m² per year), and 3) tropical DOC fluxes to surface waters to be 56.9 g C per m² per year (49.2 to 63.8 g C per m² per year). Higher temperatures lead both to more production and decomposition and to higher DOC fluxes.

However, mineral soil wetlands are not well studied, possibly because many mineral soil wetlands have no surface stream drainage outlet. Studies conducted in the temperate northeastern United States summarized data for 30 forested watersheds with no wetlands present and found DOC fluxes to range from 0.5 to 4.9 g C per m² per year (mean = 2.4 g C per m² per year; Raymond and Saiers 2010), considerably lower than the aforementioned mean of 21.2 g C per m² per year found for peatlands. At least for the temperate zone, these fluxes can be considered as the lower bound of mineral soil wetland fluxes. Aitkenhead and McDowell (2000) reviewed the literature and compared riverine DOC fluxes across a wide range of climate and vegetation biomes but did not differentiate DOC contributions between peatland and mineral soil wetlands. Here, the studies in known mountainous and peatland watersheds were removed, with the caveat that they are stream and river fluxes, not wetland fluxes. This chapter estimated the mean DOC flux for streams and rivers that have considerable mineral soil wetlands in their watersheds. The mean DOC flux for mineral soil wetlands in 1) tropical systems is estimated as 9.9 g C per m² per year (n = 2; Day et al., 1977; Malcolm and Durum 1976); 2) in temperate systems, as 5.4 g C per m² per year (n = 6; Clair et al., 1994); and 3) in boreal systems, as 2.1 g C per m² per year (n = 16; Clair and Ehrman 1996; Mulholland and Watts 1982).

Interestingly, this chapter's estimates of mineral soil wetland DOC fluxes as a percentage of organic soil DOC fluxes are relatively consistent across the three biomes (25%, 25%, and 17%, respectively, for boreal, temperate, and tropical ecosystems). DOC fluxes from North American terrestrial wetlands can be estimated using the wetland areas in Table 13.1, p. 514, and characterizing Alaska and Canada as boreal, CONUS as temperate, and Puerto Rico and Mexico as tropical. Boreal DOC fluxes are 11.4 Tg (10.1 Tg from organic wetland soils and 1.3 Tg from mineral wetland soils). Temperate DOC fluxes are 3.5 Tg (1.8 Tg from organic wetland soils and 1.7 Tg from mineral wetland soils). Tropical DOC fluxes are 1.4 Tg (1.2 Tg from organic wetland soils and 0.2 Tg from mineral wetland soils). Together, these fluxes total 16.3 Tg DOC for North America. Although there is low confidence in the amount of lateral DOC fluxes, especially those related to mineral soil wetlands, these fluxes are lower but of similar magnitude as the NEE and about 37% of the CH₄ fluxes from terrestrial wetlands (see Table 13.1).

13.3.4 Carbon Stock and Balance

The estimated North American terrestrial wetland carbon pool of 161 Pg C is less than the 214 Pg C reported in SOCCR1 for permafrost peatlands, nonpermafrost peatlands, and freshwater mineral soil wetlands (CCSP 2007). This difference is attributable to the inclusion of permafrost wetlands in the SOCCR1 report (CCSP 2007) and differences in nonpermafrost wetland area. The estimate here (129 Pg) for the amount of carbon stored in North American peatlands is less than that (163 Pg) reported by Gorham et al. (2012), again, likely a result of the Arctic permafrost area.

The development of a carbon balance sheet for the terrestrial wetlands of North America provides a useful perspective for considering the relative contributions of the various pathways, the relative differences in fluxes, and uncertainties. The wetland carbon balance sheet can be simplified by considering NEE as the net change in the CO₂-carbon exchange between the wetland and the atmosphere (negative values indicate net transfer to



the ecosystem). Net gains to the wetland, assuming a negative NEE, are effectively allocated among vegetation and soils. The principal losses of carbon from the wetlands that are not included in NEE are CH₄ fluxes (see Sections 13.3.1, p. 516, and 13.3.2, p. 518), DOC (see Section 13.3.3, p. 520), hydrological fluxes of DIC and suspended particulates, and losses due to episodic disturbance regimes (e.g., fire). Unfortunately, there is very little information about the loss of carbon as DIC or particulates for terrestrial wetlands. Thus, for current purposes, they are not considered further. Accordingly, the net ecosystem carbon balance for terrestrial wetlands in North America is -65.3 Tg C (-126.4 Tg C input, see Table 13.1, + 44.8 Tg CH₄-C flux, see Table 13.1, + 16.3 Tg DOC loss, see Section 13.3.3), indicating that the wetlands are a net carbon sink. However, the estimated annual accumulation in carbon among the soil and vegetation pools, 47.9 and 43.6 Tg C per year, respectively, yields an imbalance of +30 Tg C, indicating that the estimated NEE is too low or that one or more of the components are overestimated.

There is considerable variability in estimates of wetland carbon fluxes, whether it is from field measurements or large-scale simulations. Accordingly, comparison among reports provides useful perspectives. The North American terrestrial wetland CH₄ flux, based on measurements and extrapolated to the wetland area, is estimated at 45 Tg C per year, which is considerably higher than the estimated amount in SOCCR1 (6.1 Tg C per year). SOCCR1 also used measurements as the basis (CCSP 2007); however, the SOCCR2 estimate is nearer the range of several recent modeling studies. Using an ensemble of models to simulate CH₄ emissions in North America, Poulter et al. (2017) reported annual emissions of 31.8 to 33.5 Tg C for 2007 to 2012. Similarly, using six different datasets, Zhang et al. (2017a) reported an average CH₄ emission rate of 22.6 Tg C per year for the region from 2000 to 2006. This amount is similar to the average annual emission estimated for 1979 to 2008 of 17.8 Tg C per year by Tian et al. (2010). The annual global CH₄ flux from wetlands is estimated between 124 and 139 Tg C per year (Saunois et al., 2016; Bloom et al., 2017; Poulter

et al., 2017; Zhang et al., 2017a, b); accordingly, the contribution of North America to the global CH₄ budget is likely within the range of 20% to 30%. While there are not any large-scale NEE assessments, synthesizing measurement data for terrestrial wetlands, Lu et al. (2017) report an average annual accumulation rate of 93 g C per m², which is considerably higher than the average rate of 53 g C per m² reported here.

Assessing the pools associated with the carbon balance sheet provides additional perspective. Both organic and mineral soils accumulate carbon. Estimates here of carbon accumulation in the soil are 25 and 17 g C per m² per year for peat and mineral soils, respectively; those aggregated rates are based on the mean accumulation rates, reported by Bridgham et al. (2006), weighed by the wetland area. Accordingly, peat and mineral soils gain approximately 32.2 and 15.9 Tg C per year, respectively. Although there is a wide range in vegetation productivity, an estimated 43.6 Tg C is sequestered in biomass annually. The estimate assumes that accumulation in plant biomass is balanced with decomposition in nonforested wetlands and that forested wetlands have a net accumulation of 30 to 50 g C per m² per year (Bridgham et al., 2006; Stinson et al., 2011). The resulting summation of carbon sequestration by the soil and vegetation components (92 Tg C) is greater than the allocation to CH₄ fluxes or DOC.

13.4 Wetland Management, Restoration, and Creation

Generally, terrestrial wetlands are managed for one or more of the ecosystem services they provide. In many cases, wetlands are managed as set-aside areas used as natural filters for water quality, areas for rare species, and land for hunting and trapping due to their faunal diversity. For example, several international conservation organizations consider the PPR of the midwestern United States and Canada as the most important waterfowl habitat in North America. Management decisions and development that change the hydrology, soils, or vegetation will



affect carbon dynamics, often leading to enhanced decomposition, decreased CH₄ flux, and reduced carbon sequestration, particularly when wetlands are drained. In contrast, restoration of drained wetlands (or avoided loss of wetlands through easements) increases carbon sequestration and CH₄ production. Policies using wetlands as carbon banks and using the carbon gained through wetland restoration to trade in carbon markets are becoming increasingly common globally.

13.4.1 Effects of Wetland Management, Restoration, and Creation on Carbon

This section considers wetland management that does not convert wetlands to another land use. Wetland management occurs on a gradient from very intensive management to preservation. As they have been for thousands of years, wetlands managed for preservation or their intrinsic ecosystem services generally are carbon sinks, although there are some indications that rising temperatures from climate change may be changing wetlands from sinks to sources. For example, an undisturbed bog in Canada was a carbon source for 3 years of a 6-year study (Roulet et al., 2007). Even if wetland sinks are smaller than they once were, management or restoration practices could have dramatic feedbacks to atmospheric concentrations of CO₂ and CH₄. In a management example, there are approximately 658 km² of terrestrial wetlands under “moist-soil” management in the U.S. National Wildlife Refuge System, where lands are flooded for wintering and migrating waterfowl. Research has demonstrated that seasonal drainage in moist soil regimes leads to major losses of soil carbon (Drexler et al., 2013). The practice of deeply flooding marshes is not as common in the national wildlife refuges as seasonal drainage, but deep flooding may be an option for increasing carbon sequestration rates (Bryant and Chabreck 1998).

The effect of altered hydrology does not necessarily cause a loss of ecosystem carbon from managed wetlands. Studies of carbon pool response to managed peatlands in Finland have shown that increased forest productivity may offset losses due to water

management resulting in a net increase of carbon, but this response is site dependent (Minkinen et al., 2008). Similarly, forest harvesting only had a transient effect on the soil carbon pool of a mineral soil wetland (Trettin et al., 2011). In contrast, peat utilization, as in peat mining for fuel or horticultural purposes, is the extreme where the peat itself is removed from the wetland. Although peat mining is not common in North America, Canada is the third largest producer of horticultural peat in the world, with much of the peat originating from the peatlands in the St. Lawrence Lowlands on the Canadian side of the Great Lakes (Van Seters and Price 2001). For production agriculture where wetlands remain wetlands, water levels are typically controlled to maximize production, usually at the expense of carbon pools. Prairie potholes and other hydrologically isolated wetlands are often nested within agricultural lands but remain undrained. These cropped, undrained wetlands can be major sources of GHGs due to increased nutrient loading and associated nitrous oxide (N₂O) fluxes. In addition, temporarily ponded wetlands that dry down during the growing season can be tilled and farmed, increasing decomposition rates. Approximately 6,500 km² of U.S. peatlands are being used for crop production (ICF International 2013). The converted peatlands are usually highly productive for agriculture, but they also have high potential as GHG mitigation sites if the land is restored to vegetated wetlands (Richardson et al., 2014; Wang et al., 2015). Specific GHG mitigation benefits accrue from 1) decreases in CO₂ fluxes related to the oxidation of soil carbon while in crop production, 2) decreases in the use of nitrogen fertilizers, 3) decreases in lime application amendments, and 4) increases in carbon sequestered in soils and perennial vegetation (ICF International 2013). Crops such as sugarcane lead to large losses of carbon through enhanced decomposition (Baker et al., 2007). Paddy rice production systems are well-known sources of CH₄ (Lindau et al., 1993) and N₂O. Other crops such as sugar beet, radish, cranberry, blueberry, lettuce, celery, carrot, potato, onion, and mint are grown in wetlands, but little data exist on their influence on ecosystem carbon balance.



Similarly, aquaculture has altered wetlands in North America, but, again, little data exist on the impact on carbon storage or fluxes. Although forest harvesting causes short-term changes in carbon sequestration during the period of stand regeneration, it generally has little impact on long-term wetland soil carbon balance (Roulet 2000; Trettin et al., 2011).

Wetland restoration usually includes the re-establishment of hydrological regimes to support hydrophytic vegetation. Wetland restoration and creation of new wetlands (where none existed previously) and small ponds have counteracted much of the wetland losses in CONUS (Dahl 2011). For instance, from 1998 to 2004 and 2004 to 2009, areas reclassified as wetlands in the United States increased by 17%, meaning that 802 km² of new wetlands were created, but this figure does not indicate how many additional square kilometers of the restored wetlands were still classified as wetlands. In addition, creation of small ponds has increased over the last few decades, with 838 km² per year created from 2004 to 2009 (Dahl 2011).

Wetland restoration can lead to the opposite effects of drainage, with increases in carbon pools and in CH₄ fluxes and lower CO₂ fluxes (Wickland et al., 2014). Research has found that restoring wetlands by rewetting them increases soil carbon storage (Lucchese et al., 2010). IPCC guidelines for mineral soil wetlands state that cultivation leads to losses of up to 71% of the soil organic carbon in the top 30 cm of soil over 20 years and that restoration increases depleted soil carbon pools by 80% over 20 years, and by 100% after 40 years (Wickland et al., 2014). Rewetting also may increase CH₄ fluxes, not only above the previously drained levels, but also above reference levels temporally (Badiou et al., 2011). However, some studies have found that restoration did not increase CH₄ fluxes (Richards and Craft 2015). In the long term, restoring degraded wetlands appears to be a positive for GHG mitigation.

Creating new wetlands and small ponds also can affect both long-term soil carbon storage and gaseous fluxes. Created wetlands tend to have carbon

accumulation rates higher than those of natural wetlands (Bridgham et al., 2006). In addition, created wetlands often have similar or lower CH₄ fluxes (Mitsch and Hernandez 2013; Winton and Richardson 2015). However, assessments have found that small ponds are large sources of CH₄ (Holgerson and Raymond 2016). Similar to created wetlands and some riparian zones, small ponds may sequester carbon at high rates due to high sediment deposition rates from the surrounding land.

Many restored wetlands do not provide the level of ecosystem services they did before their degradation, usually a result of inadequate hydrology restoration. One survey found that only 21% of wetland restoration sites have ecologically equivalent natural functions (Turner et al., 2001). Post-restoration monitoring is critical to determining restoration success and providing opportunities to modify restoration techniques if necessary. Assessment of success usually occurs over relatively short periods (1 to 3 years) and with relatively simple protocols because of time, resource, and technical constraints. Determining success over the short term is difficult because wetland processes, such as soil formation or forest recovery, occur over decades. Also, most current assessment techniques are fairly simple and may not adequately characterize the condition of a wetland, especially if critical functions such as hydrology or processes such as carbon and nutrient cycling are not fully understood. Moreover, inadequate study of many wetland types challenges efforts to understand both the processes that lead to carbon accumulation and fluxes and the impact of wetland restoration on carbon. Furthermore, due to the developmental trajectory of restored wetlands, their capacity to store carbon may change through time, with considerable storage initially and then much less storage thereafter once vegetation has fully colonized and root systems have developed (Anderson et al., 2016).

13.4.2 Processes and Policies that Affect Wetland Management, Restoration, and Creation

Recognition of the values that wetlands provide has led to changes in federal policies aimed at protecting, restoring, and creating wetlands over the past



four decades. Four significant policies are 1) Section 404 of the Clean Water Act (1972); 2) the Highly Erodible Land Conservation and Wetland Conservation Compliance provisions of the 1985 Food Security Act and subsequent amendments, commonly known as the “Swampbuster program”; 3) President George H. W. Bush’s “no net-loss” policy (1989); and 4) the U.S. Army Corps of Engineers and EPA compensatory mitigation rule (USACE 2008). Initially passed as part of the Federal Water Pollution Control Act of 1972, the Clean Water Act focused on nonagricultural wetland conversions (U.S. EPA 2015). In its initial form, the Swampbuster program discouraged farmers from converting wetlands by withholding federal farm program benefits if conversion occurred on nonexempt wetlands. Farm Bill 1990 amendments created the Wetland Reserve Program, which was later consolidated with other easement programs into the Agricultural Conservation Easement Program (ACEP). Rather than withholding incentives, the USDA NRCS incentivizes farmers to restore, protect, and enhance wetlands by purchasing wetland reserve easements via ACEP (USDA 2014). The Agricultural Act of 2014 (i.e., Public Law 113-79, commonly referred to as the 2014 Farm Bill) provided NRCS with the authority to enroll wetlands in 1) permanent easements, with 100% of the easement value and 75% to 100% of restoration costs covered, 2) 30-year easements funded at 50% to 75% of the easement value with 50% to 75% of the restoration costs covered, and 3) term easements with stipulations dependent on state laws.

The no net-loss policy, which sought to replace lost wetland habitat with new habitat by restoring and creating wetlands, is now the cornerstone of U.S. wetland conservation (Mitsch and Gosselink 2015). As a result, numerous federal and state agencies, non-governmental organizations, and private landowners are engaged in wetland restoration and creation across the United States with a keen focus on establishing the proper hydrological conditions needed to support flora and fauna specific to a certain wetland type. Such activities often result in preserving or expanding the carbon pool of wetlands, but little

attention has been given to ensuring the long-term sustainability of such newly formed carbon sinks. Wetland restoration is still a relatively new field, and management approaches for maintaining the sustainability of carbon sinks are still being developed, tested, and refined.

The Federal Policy on Wetland Conservation in Canada (Canadian Wildlife Service 1991) also encourages no net-loss of wetlands. The regulation is focused largely on activities undertaken by the Canadian government on its federal land. Although the policy discourages wetland destruction or degradation, the Canadian government does not require compensatory mitigation. Though currently limited, the Natural Protected Areas Commission of Mexico has a national wetland policy to protect wetlands and avert losses.

13.5 Terrestrial Wetland Trends and Feedbacks

An important concern globally is how wetlands will respond to a changing climate. Climate change has the potential to affect carbon cycling of natural, degraded, created, and restored wetlands. However, there is considerable uncertainty regarding the likely responses, including how warming and variations in precipitation regimes will influence the balance between plant productivity and organic matter decomposition. An example pattern might be warming followed by drier conditions leading to wetland carbon losses, as has occurred in simulated peatland droughts (Fenner and Freeman 2011). Altered precipitation regimes also may shift the hydrological balance in the absence of warming. Even on an annual timescale, individual wetlands can alternate between a carbon sink in wet years to a carbon source in dry years, illustrating the sensitivity of wetlands to biotic and abiotic conditions. However, the direct correspondence of increased peat oxidation with a lowered water table is not universal. Instead, Makiranta et al. (2008) showed soil temperature controlled more of the variability in peatland soil respiration than did the water-table position. Similarly, CH₄ fluxes in high-latitude wetland ecosystems with high



water tables were more sensitive to soil temperature than were those ecosystems with lower water tables, which were more sensitive to water-table position (Olefeldt et al., 2013). Accordingly, changes in carbon pools and fluxes in response to changes in temperature and precipitation regimes will vary greatly based on wetland type and interactions with hydrology because carbon cycling may be different under warmer and wetter conditions than under warmer and drier conditions. For example, CH₄ fluxes from PPR wetlands were four times higher under warmer and wetter conditions than the fluxes were under warmer and drier conditions (Bansal et al., 2016). Northern seasonally frozen peatlands already are undergoing rapid changes, and increased carbon fluxes are likely to continue over the coming decades to centuries as conditions continue to warm (Schoor et al., 2015). Another general pattern is that drier conditions will facilitate and exacerbate fires, especially in peatlands, resulting in large fluxes from the oxidized peat (Turetsky et al., 2011b; see also Ch. 11: Arctic and Boreal Carbon, p. 428).

The response of mineral soil wetlands to changes in temperature and precipitation regimes is uncertain, largely because of the wide range in properties and geomorphic setting. Histic-mineral soil wetlands (“histic” refers to soils with a 20- to 40-cm organic horizon) may be expected to respond similarly to peatlands. For other types, such as mineral soil wetlands in floodplains where the surface organic layer is thin due to high turnover rate, the changes in that layer associated with climate change are likely small. Changes in the hydrological regime also are expected to alter the carbon balance. Increased periods of a high water table or flooding may be expected to reduce productivity (Trettin et al., 2006) and increase CH₄ fluxes (Sharitz and Pennings 2006). The effect of climate change on organic matter decomposition and carbon export from the wetland is an important uncertainty and feedback to adjoining aquatic ecosystems. The uncertainty in mineral soil wetland response is high, largely because there are far fewer studies on mineral soil wetlands than on peatlands.

Rising atmospheric CO₂ is considered likely to increase GHG fluxes from wetlands due to increased CH₄ fluxes offsetting gains from increased plant carbon sequestration (Bridgman et al., 2007; Hyvonen et al., 2007). Hyvonen et al. (2007) suggest that soil carbon in the temperate and boreal zones will increase because of increased litter input, but the magnitude of the response will depend on available nitrogen and land management. Little is known about interactions between changes in water regime and plant productivity. In upper Michigan, lowered water tables led to increased productivity in vascular plants (e.g., shrubs and sedges) and *Polytrichum*; higher water tables led to higher *Sphagnum* production (Potvin et al., 2015). Demonstrating the importance of field experimentation, Dijkstra et al. (2012) measured increases in CH₄ in both mineral soil wetlands and peatlands following manipulation of the water regime. Understanding these interactions with CH₄ fluxes is fundamental to considering the feedback associated with rising atmospheric CO₂ (Petrescu et al., 2015; Zhang et al., 2017b).

13.6 Global, North American, and Regional Context

13.6.1 Global and Continental Perspectives

Observational studies suggest that wetlands cover an estimated 8.2 million km² globally (Lehner and Döll 2004). However, based on recent studies that use both observations and models, the mean global area may be 12.3 million km² (Melton et al., 2013). The largest concentrations of wetlands generally are found between 50° and 70°N latitude, with substantial concentrations also found between 0° to 10°S latitude (Lehner and Döll 2004). North of 70°N latitude, continuous permafrost ecosystems also contain considerable soil carbon (see Ch. 11: Arctic and Boreal Carbon, p. 428). Wetlands are estimated to cover approximately 2.2 million km² in North America (see Table 13.1, p. 514), or about 9% of the continental land area. Although approximate global and regional extents of wetlands are generally known, there are significant challenges that hinder estimating wetland coverage with a high degree of



confidence. These challenges include, but are not limited to, lack of detailed inventories, nonuniform definitions of wetlands, limitations of remotely sensed data and models, and continuing drainage and conversion of wetlands worldwide.

Positioning the North American wetland carbon stock in a global context is difficult due to the broad range (300 to 530 Pg C) reported (Mitra et al., 2005). Accordingly, the North American wetlands (161 Pg C) compose a significant but uncertain proportion (30% to 54%) of the global wetland carbon stock.

Natural wetlands are the largest natural source of CH₄ fluxes to the atmosphere (Kirschke et al., 2013) and thus are an important consideration of large-scale modeling assessments. Saunio et al. (2016) conducted a comprehensive assessment of the global atmospheric CH₄ budget using “top-down” and “bottom-up” approaches, which respectively are based on inversions of atmospheric CH₄ data and process-based wetland biogeochemical models. Twenty top-down and 11 bottom-up estimates were provided for North American wetland fluxes averaged from 2003 to 2012. The multimodel mean (± 1 standard deviation) was 16 ± 4 Tg CH₄-C emitted per year for the top-down estimates, and 35 ± 11 Tg CH₄-C per year for the bottom-up estimates. Boreal North America (i.e., Alaska and Canada) account for most of the difference between these two estimates, with the bottom-up approaches exceeding the top-down approaches by 19 Tg CH₄-C per year. Estimating the CH₄ flux from North American wetlands between 1979 and 2008, Tian et al. (2010) estimated an average of 17.8 Tg CH₄-C per year. Those simulation approaches are less than the estimate of North American wetland fluxes reported in this chapter, 44.8 Tg CH₄-C per year (see Table 13.1, p. 514). Both approaches have relatively large uncertainty levels associated with the CH₄ flux. Extrapolation of measurement data across the wetland area presumes a uniform response that belies the considerable differences among wetlands across the landscape. The large-scale model assessments suffer from the same issue of not having the capacity to consider variation

among wetlands, but they have the ability to accommodate some aspects of spatial variability. The relative correspondence of the wetland CH₄ flux attests to the merits of both the large-scale process-based models and the need for additional empirical studies, particularly on mineral soil wetlands, to provide a broad base for model validation.

13.6.2 Regional Perspectives— United States, Canada, and Mexico

Within North America, Canada has the greatest wetland coverage, with estimates ranging from 1.27 to 1.60 million km², followed by Alaska with an estimated 0.18 to 0.71 million km² of wetlands (Lehner and Döll 2004; Zhu and McGuire 2016). Estimates of terrestrial wetlands for CONUS from the USFWS National Wetlands Inventory (0.39 million km²) and Mexico (~0.05 million km²) are smaller than the total wetland area suggested by Lehner and Döll (2004), 0.45 and 0.16 million km², respectively. The reported soil carbon stock for CONUS terrestrial wetlands (12.6 Pg C) approximates the estimate (10.6 Pg C) provided through the U.S. EPA’s National Wetland Condition Assessment (NWCA; Nahlik and Fennessy 2016). The relatively small difference in soil carbon stock is attributable to less wetland area as reported in the NWCA (a difference of about 11,000 km²) and a shallower reporting depth (120 cm). Wetlands in Canada are dominated by peatlands, which harbor large carbon stocks estimated at 115 Pg C for this assessment (see Table 13.1, p. 514) and 150 Pg C by Tarnocai et al. (2005). The greatest concentration of wetlands is in the provinces of Manitoba and Ontario, which contain about 41% of Canada’s wetlands (Mitsch and Hernandez 2013).

The recent cartographic assessment of Mexico’s wetlands provides important new information about the distribution of wetlands and context for assessing their loss (Landgrave and Moreno-Casasola 2012). Inland marshes are found in deltaic regions of the southeastern states of Veracruz, Tabasco, and Campeche, where the floodplains have deep organic soils (Smardon 2006). Marshes also are found in mountain ranges of central Mexico and in localized



Table 13.2. Estimates of Wetland Area, Total Carbon Storage, Carbon Dioxide and Methane Fluxes, and Net Carbon Flux by Major U.S. Region^{a-b}

Region	Wetland Area (km ²)	Total Carbon Storage ^c (Pg C)	CO ₂ Exchange ^d (Pg CO ₂ per Year)	CH ₄ Exchange ^e (Pg CO ₂ e per Year)	Net Carbon Flux ^f (Pg C per Year)
Eastern United States ^g	271,482	3.8, 4.2	-0.18, -0.048	0.186, 0.187	-0.049, -0.013
Great Plains ^h	30,380	0.22	NR ⁱ	0.082	-0.02
Western United States ^j	10,114	0.06, 0.07	-0.005, 0.0002	0.002	-0.0015, 0
Boreal Alaska – North ^k	112,007	2.4	NR	0.020	-0.002
Boreal Alaska – South ^k	18,627	0.9	NR	0.006	0.001

Notes

- a) From U.S. Geological Survey's LandCarbon Program. Cells with two numbers represent the reported minimum and maximum. Carbon amounts are in petagrams (Pg).
- b) See references for uncertainty analyses for the respective regions.
- c) Total carbon storage for the eastern United States, Great Plains, and western United States is for 2005 and is the sum of biomass (live and dead) and the upper 20 cm of soil; for Alaska, total carbon storage is the average stock from 2000 to 2009 and is the sum of biomass (live above ground, live below ground, and dead), moss, litter, surface organic soil layers, and the upper 1 m of mineral soil.
- d) Carbon dioxide (CO₂) flux for the eastern United States, Great Plains, and western United States is for 2001 to 2005; for Alaska, it is for 2000 to 2009.
- e) Methane (CH₄) flux for the eastern United States, Great Plains, and western United States is for 2001 to 2005 and is presented in CO₂ equivalent (CO₂e) using a global warming potential (GWP) of 21; for Alaska, the flux is for 2000 to 2009 and is presented in CO₂e using a GWP of 25. Note that CO₂e is the amount of CO₂ that would produce the same effect on the radiative balance of Earth's climate system as another greenhouse gas, such as CH₄ or nitrous oxide, on a 100-year timescale. For comparison to units of carbon, each kg CO₂e is equivalent to 0.273 kg C (0.273 = 1/3.67). See Box P.2, Global Carbon Cycle, Global Warming Potential, and Carbon Dioxide Equivalent, p. 12, in the Preface for more details.
- f) Net carbon fluxes for the eastern United States, Great Plains, and western United States are for 2001 to 2005; for Alaska, they are for 2000 to 2009.
- g) Zhu and Reed (2014).
- h) Zhu and McGuire (2011).
- i) Not reported.
- j) Zhu and Reed (2012).
- k) Zhu and McGuire (2016).

areas in the Sonoran and Chihuahuan deserts where springs feed shallow swamps (Mitsch and Hernandez 2013). However, little is known about their carbon stock or CO₂ and CH₄ fluxes.

The U.S. Geological Survey's LandCarbon Program developed ecoregion estimates of current and future projections of carbon storage, net CO₂ exchange and CH₄ fluxes, and net carbon balance of U.S. wetlands (Zhu and McGuire 2010), providing context for the current assessment. Wetland area, carbon stocks, and fluxes were estimated using process-based models and land-use

and land-cover maps. These estimates, originally reported by level II ecoregion in a series of reports, are summarized by region in Table 13.2, this page. The LandCarbon assessment provides a basis for regional comparisons using a common methodology. However, the reported pools and fluxes are substantially different than those included in Table 13.1, p. 514, which uses the National Wetlands Inventory as the basis for wetland area, summarizes geospatial databases for the pools, and synthesizes observational studies as the basis for the pools and fluxes.



13.7 Synthesis, Knowledge Gaps, and Outlook

13.7.1 Summary of Terrestrial Wetlands Carbon Cycling

North American wetlands constitute a significant proportion (37%) of the global wetland area. The uncertainty in wetland area for North America is relatively low because wetlands in CONUS and Alaska, Mexico, and Canada have relatively recent inventories and assessments. However, more information about soil carbon and vegetation biomass within the wetlands is needed to assess carbon pools and fluxes and reduce uncertainties in the estimates. Wetland soil type varies significantly with latitude, with Alaska and Canada having the majority of the peatland area. Mineral soil wetlands are predominant (79%) in CONUS and contain 38% of its wetland carbon stock. An important consideration regarding the estimate of carbon pools in peatlands, which consist of 58% of the North American wetland area, is that total depth of peat is seldomly reported, while the average depth commonly exceeds the typical assessment depths of 1 to 2 m. Peatlands contain approximately 80% of the North American carbon, a proportion that is likely to increase substantially if the entire peat depth were considered. Nonforested vegetation communities compose 44% of the wetland area in North America, contain approximately 43% of the carbon pool, and accumulate 47% of the net carbon gain.

Historically, the wetland loss in North America has been significant, particularly in CONUS. However, to assess contemporary losses, periodic inventories at the national scale are needed. Currently, only the United States has regular updates to its wetlands inventory. Restoration and creation of new wetlands are major offsets to loss of natural U.S. wetlands. Whether these new wetlands have the same carbon dynamics as natural wetlands is a major uncertainty that will become more important as restored wetlands become a larger proportion of the total wetland area. A global meta-analysis comparing 621 restored and created wetlands to 556 reference wetlands indicated that functions related

to biogeochemical cycling (mainly to carbon storage) were 23% lower in the restored and created wetlands (Moreno-Mateos et al., 2012). Successful functioning of those wetlands will be critical to mitigate the long-term losses of carbon from degraded wetlands.

13.7.2 Knowledge Gaps and Associated Uncertainties in the Wetland Carbon Cycle

The following are some major gaps in current knowledge about the North American wetland carbon cycle.

1. Future wetland response to climate change is uncertain. Because temperatures are predicted to increase at greater rates at higher latitudes, northern temperate wetlands, especially peatlands, are expected to be the most affected. More uncertainty exists in the predictions of precipitation, changes in which could either mitigate or exacerbate carbon sequestration rates in terrestrial wetlands. Although contemporary measurements and modeling offer perspective, additional manipulative experiments—such as the U.S. Department of Energy’s Spruce and Peatland Responses Under Changing Environments (SPRUCE) experiment in northern Minnesota (Hanson et al., 2017) and USDA’s former PEATcosm experiment in the Upper Peninsula of Michigan (Potvin et al., 2015)—are critical to test how wetlands will respond to changes in temperature and hydrological regime in the field. Work in mineral soil wetlands is particularly needed because of the paucity of studies and the functional linkages with aquatic systems.
2. Greater understanding is needed of the factors controlling carbon cycling in wetlands. Additional measurements of GHG fluxes and processes regulating the fluxes and carbon storage using improved inventories and methods at multiple spatial scales are required to 1) understand the interactions of soil, vegetation, and climatic factors; 2) provide a basis for quantifying fluxes to reduce significant uncertainties; and 3) evaluate biogeochemical and inverse-atmospheric models.



Particularly needed are studies that assess convergence across diverse spatial and temporal scales or lead to a process-based understanding of why convergence does not occur.

3. Dissolved carbon export, including both DIC and DOC, is a major uncertainty in the wetland carbon cycle. Dissolved carbon affects water quality and is an important food source for aquatic systems and estuaries, and dissolved gases may contribute to atmospheric loading. Understanding the mechanisms controlling dissolved carbon production and transformation is a major gap requiring field and watershed-scale assessments.
4. A better understanding is needed of the relationship between the sustainability of stored carbon and the particular chemistry of the carbon compounds that make up the carbon sink. Preliminary research shows that polyphenol content may serve to preserve peats under moderate drought conditions (Wang et al., 2015), but little is known about either the exact types of polyphenols or the plant communities that have the highest sustainability under projected climate and environmental conditions.
5. Data on restored and managed wetlands are sparse and insufficient to support assessment and modeling needs. Measurements to document the carbon balance in these wetlands are needed. Also necessary are standardized measurements and methods for collecting basic data in the field at the same depth and for analyzing parameters such as bulk density and percent of organic carbon. Monitoring of wetland restoration needs to extend through the entire trajectory of the project to gain a functional understanding of the differences in gaseous fluxes and carbon accumulation between natural and restored wetlands.

13.7.3 Tools for Assessing the Wetland Carbon Cycle

Due to the extremely wide variation in wetlands across North America, as well as the certainty that there will never be enough measurements to adequately quantify the wetland carbon stocks and

fluxes, models present the means to represent the biophysical processes inherent to wetlands at variable spatial scales. Those tools provide needed capabilities to inform conservation, management, and mitigation strategies to sustain ecosystem services inherently linked to the wetland and global carbon cycle. Models also are useful for addressing the uncertainties within the carbon cycle and, in turn, for focusing field monitoring and experiments to fill critical information gaps. Mechanistic models provide the capabilities for simulating the processes that regulate carbon dynamics in wetlands reflecting the myriad soil, vegetation, and climatic conditions and management influences. Because of the water table's regulatory function in the wetland carbon cycle, an accurate representation of wetland hydrology is critical to model performance. There are fewer models for wetlands compared to those for uplands. Among biogeochemical models that are widely applicable to terrestrial wetlands and have the broadest capabilities with respect to soil and vegetation types are the Forest DNDC (or DeNitrification DeComposition) model, which was identified by USDA in the development of its carbon accounting framework (Ogle et al., 2014), and the DayCent model (Parton et al., 1998), which is widely used in grassland and agroecosystem simulations. Scaling wetland hydrology within a biogeochemical model is difficult; hence, coupling a biogeochemical model with a hydrological model can provide an effective basis for considering the inherent spatial variability among uplands and wetlands (Dai et al., 2012a). Simulating CH₄ fluxes is particularly difficult because of various interactions among controls of CH₄ production and transport from wetlands, including ebullition, that vary over very short distances such as 10 m or less (Bridgman et al., 2013). Correspondingly, uncertainties associated with plant carbon allocation and organic matter quality and decomposition impair the ability of field-scale biogeochemical models to predict CH₄ flux from the soil surface. These considerations are particularly important for small-scale models that are evaluated with field data.

Another major challenge to modeling carbon dynamics in wetlands is the inherent heterogeneity



of conditions within a wetland and the spatial heterogeneity of wetlands across the landscape. Accordingly, new approaches for accommodating high-resolution geospatial data with robust biogeochemical models are needed to provide capabilities to simulate wetland carbon dynamics at large scales. Such capabilities, in turn, would provide a basis for linking wetland biogeochemical models with atmospheric models (Gockede et al., 2010), thereby improving the basis for simulating the effects of climate change on wetland carbon. Large-scale bottom-up and top-down models are

providing those capabilities to address CH₄ fluxes at the regional and global scales (Melton et al., 2013; Saunio et al., 2016; Bloom et al. 2017; Zhang et al., 2017a). However, estimates among the CH₄ models can vary considerably (Miller et al., 2016). Correspondingly, there is a real need for tools to assess wetland NEE; unfortunately, the large-scale models for assessing wetland NEE are not available or widely reported. Accordingly, ecosystem models must be upscaled to develop the components to simulate wetland NEE.



SUPPORTING EVIDENCE

KEY FINDING 1

The assessment of terrestrial wetland carbon stocks has improved greatly since the *First State of the Carbon Cycle Report* (CCSP 2007) because of recent national inventories and the development of a U.S. soils database. Terrestrial wetlands in North America encompass an estimated 2.2 million km², which constitutes about 37% of the global wetland area, with a soil and vegetation carbon pool of about 161 petagrams of carbon that represents approximately 36% of global wetland carbon stock. Forested wetlands compose 55% of the total terrestrial wetland area, with the vast majority occurring in Canada. Organic soil wetlands or peatlands contain 58% of the total terrestrial wetland area and 80% of the carbon (*high confidence, likely*).

Description of evidence base

Key Finding 1 is supported by an extensive analysis of the most current wetland soil and vegetation information available across the conterminous United States (CONUS), Alaska, Hawai'i, Puerto Rico, Canada, and Mexico, updating previous estimates made in SOCCR1 (see SOCCR2 Appendices 13A, p. 547 and 13B, p. 557).

Major uncertainties

Uncertainties are high where wetlands are present but not extensively mapped, such as in Alaska.

Assessment of confidence based on evidence and agreement, including short description of nature of evidence and level of agreement

Over much of the area under consideration, confidence is high that this assessment has accurately mapped carbon pools in mineral soil wetlands and peatlands.

Estimated likelihood of impact or consequence, including short description of basis of estimate

Understanding current carbon pools is critical in predicting how changes in, for example, climate, land use, and restoration will affect the carbon stored in terrestrial wetlands.

Summary sentence or paragraph that integrates the above information

Terrestrial wetlands are the largest reservoir of carbon in North America. Understanding the processes that lead to carbon storage and fluxes is important to predict how future changes will influence this large carbon pool and subsequent feedbacks to the atmosphere.

KEY FINDING 2

North American terrestrial wetlands currently are a carbon dioxide sink of about 123 teragrams of carbon (Tg C) per year, with approximately 53% occurring in forested systems. However, North American terrestrial wetlands are a natural source of methane (CH₄), with mineral soil wetlands emitting 56% of the estimated total of 45 Tg as CH₄ (CH₄-C) per year (*medium confidence, likely*).

Description of evidence base

Key Finding 2 and this chapter's narrative are based on the most recently reported wetland inventories integrated with reported values of soil carbon density (mass per unit area) and gaseous



fluxes of carbon dioxide (CO₂) and CH₄. Accordingly, the projections are dependent on estimates of wetland area and the pool and flux values assigned to the wetland types (see Appendices 13A, p. 547, and 13B, p. 557).

Major uncertainties

Similar to Key Finding 1, one major uncertainty is the mapped area, especially in areas with considerable wetlands that have not been adequately mapped. A second important uncertainty are the flux rates, which are applied globally to wetland types but are highly variable in time and space. Moreover, in many cases, few data exist.

Assessment of confidence based on evidence and agreement, including short description of nature of evidence and level of agreement

Confidence is medium, given both the incompleteness in mapping and variability in flux rates.

Estimated likelihood of impact or consequence, including short description of basis of estimate

Greenhouse gas fluxes from terrestrial wetlands in North America contribute to the global CO₂ and CH₄ cycles and associated climate forcing.

Summary sentence or paragraph that integrates the above information

Understanding both terrestrial wetland carbon pools (Key Finding 1) and net fluxes to the atmosphere (Key Finding 2) is critical because these wetlands are stable long-term carbon sinks and also an important source of CH₄.

KEY FINDING 3

The current rate of terrestrial wetland loss is much less than historical rates (about 0.06% of the wetland area from 2004 to 2009) with restoration and creation nearly offsetting losses of natural wetlands. Although area losses are nearly offset, there is considerable uncertainty about the functional equivalence of disturbed, created, and restored wetlands when comparing them to undisturbed natural wetlands. Correspondingly, there remains considerable uncertainty about the effects of disturbance regimes on carbon stocks and greenhouse gas (GHG) fluxes. For this reason, studies and monitoring systems are needed that compare carbon pools, rates of carbon accumulation, and GHG fluxes across disturbance gradients, including restored and created wetlands. Those studies will produce data that are needed for model applications (*high confidence, likely*).

Description of evidence base

The evidence for Key Finding 3 is from updated published literature for the United States and Mexico (Casasola 2008; Landgrave and Moreno-Casasola 2012; USFWS 2011) and the same data reported in SOCCR1 (CCSP 2007) for Canada. The amount of wetlands being restored is also a function of recent literature estimates (e.g., Dahl 2011). Disturbance also needs to be considered in the context of changes to carbon cycling processes.

Major uncertainties

Where wetlands are mapped well, the area of wetland loss is very certain. Some areas not mapped well, such as remote locations in Alaska, generally are not under threat from development, but changes in climatic conditions threatened the boreal region more than temperate and tropical



regions. However, the opposite is true for areas under development in Mexico. The amount of area being restored is also not tracked very well, especially when restoration fails. Crossing the gradient from disturbed to restored and/or created wetlands, there exists considerable uncertainty about the level of functions that those wetlands provide.

Assessment of confidence based on evidence and agreement, including short description of nature of evidence and level of agreement

There is high confidence that systems for reporting wetland losses and gains are accurate in the United States, but periodic inventories in other countries are lacking. Also, tracking the amount of wetlands that have been disturbed in some way is very difficult.

Estimated likelihood of impact or consequence, including short description of basis of estimate

Although the area of restored or created wetlands is small relative to the total wetland area of North America, the impact is likely important because understanding even small changes in wetland area is critical to scaling up carbon pools and fluxes.

Summary sentence or paragraph that integrates the above information

Although there are very reliable data that track wetland change across CONUS, no such data are available for Canada because regular wetland assessments for that country are lacking. In addition, field-based wetland mapping is generally poor in Alaska and Mexico, and restored and disturbed wetland areas also are difficult to track.



REFERENCES

- Ahl, D. E., S. T. Gower, D. S. Mackay, S. N. Burrows, J. M. Norman, and G. R. Diak, 2004: Heterogeneity of light use efficiency in a northern Wisconsin forest: Implications for modeling net primary production with remote sensing. *Remote Sensing and the Environment*, **93**, 168-178.
- Aitkenhead, J. A., and W. H. McDowell, 2000: Soil C:N ratio as a predictor of annual riverine DOC flux at local and global scales. *Global Biogeochemical Cycles*, **14**(1), 127-138, doi: 10.1029/1999GB900083.
- Alford, D. P., R. D. Delaune, and C. W. Lindau, 1997: Methane flux from Mississippi River Deltaic Plain wetlands. *Biogeochemistry*, **37**(3), 227-236, doi: 10.1023/a:1005762023795.
- Anderson, F. E., B. Bergamaschi, C. Sturtevant, S. Knox, L. Hastings, L. Windham-Myers, M. Detto, E. L. Hestir, J. Drexler, R. L. Miller, J. H. Matthes, J. Verfaillie, D. Baldocchi, R. L. Snyder, and R. Fujii, 2016: Variation of energy and carbon fluxes from a restored temperate freshwater wetland and implications for carbon market verification protocols. *Journal of Geophysical Research: Biogeosciences*, **121**(3), 777-795, doi: 10.1002/2015jg003083.
- Armstrong, A., S. Waldron, N. J. Ostle, H. Richardson, and J. Whitaker, 2015: Biotic and abiotic factors interact to regulate northern peatland carbon cycling. *Ecosystems*, **18**(8), 1395-1409, doi: 10.1007/s10021-015-9907-4.
- Badiou, P., R. McDougal, D. Pennock, and B. Clark, 2011: Greenhouse gas emissions and carbon sequestration potential in restored wetlands of the Canadian prairie pothole region. *Wetlands Ecology and Management*, **19**(3), 237-256, doi: 10.1007/s11273-011-9214-6.
- Baker, J. M., T. E. Ochsner, R. T. Venterea, and T. J. Griffis, 2007: Tillage and soil carbon sequestration—what do we really know? *Agriculture, Ecosystems and Environment*, **118**(1-4), 1-5, doi: 10.1016/j.agee.2006.05.014.
- Bansal, S., B. Tangen, and R. Finocchiaro, 2016: Temperature and hydrology affect methane emissions from prairie pothole wetlands. *Wetlands*, **36**(S2), 371-381, doi: 10.1007/s13157-016-0826-8.
- Bartlett, K. B., and R. C. Harriss, 1993: Review and assessment of methane emissions from wetlands. *Chemosphere*, **26**(1-4), 261-320, doi: 10.1016/0045-6535(93)90427-7.
- Bartlett, K. B., R. C. Harriss, and D. I. Sebacher, 1985: Methane flux from coastal salt marshes. *Journal of Geophysical Research: Atmospheres*, **90**(D3), 5710-5720, doi: 10.1029/JD090iD03p05710.
- Bartlett, K. B., D. S. Bartlett, R. C. Harriss, and D. I. Sebacher, 1987: Methane emissions along a salt marsh salinity gradient. *Biogeochemistry*, **4**(3), 183-202, doi: 10.1007/bf02187365.
- Bartlett, D. S., K. B. Bartlett, J. M. Hartman, R. C. Hanks, D. C. Sebacher, R. Pelletier-Travis, D. D. Dow, and D. P. Brannon, 1989: Methane flux from the Florida Everglades: Patterns of variability in a regional wetland ecosystem. *Global Biogeochemical Cycles*, **3**(4), 363-374.
- Batjes, N. H., 2011: Soil organic carbon stocks under native vegetation - revised estimates for use with the simple assessment option of the carbon benefits project system. *Agriculture, Ecosystems and Environment*, **142**(3-4), 365-373, doi: 10.1016/j.agee.2011.06.007.
- Batson, J., G. B. Noe, C. R. Hupp, K. W. Krauss, N. B. Rybicki, and E. R. Schenk, 2015: Soil greenhouse gas emissions and carbon budgeting in a short-hydroperiod floodplain wetland. *Journal of Geophysical Research: Biogeosciences*, **120**(1), 77-95, doi: 10.1002/2014jg002817.
- Benscoter, B. W., D. K. Thompson, J. M. Waddington, M. D. Flannigan, B. M. Wotton, W. J. de Groot, and M. R. Turetsky, 2011: Interactive effects of vegetation, soil moisture and bulk density on depth of burning of thick organic soils. *International Journal of Wildland Fire*, **20**(3), 418, doi: 10.1071/wf08183.
- Blodau, C., and T. R. Moore, 2003: Micro-scale CO₂ and CH₄ dynamics in a peat soil during a water fluctuation and sulfate pulse. *Soil Biology and Biochemistry*, **35**(4), 535-547, doi: 10.1016/s0038-0717(03)00008-7.
- Bloom, A. A., K. W. Bowman, M. Lee, A. J. Turner, R. Schroeder, J. R. Worden, R. Weidner, K. C. McDonald, and D. J. Jacob, 2017: A global wetland emissions and uncertainty dataset for atmospheric chemical transport models (WetCHARTs version 1.0). *Geoscientific Model Development*, **10**, 2141-2156, doi: 10.5194/gmd-10-2141-2017.
- Bonneville, M.-C., I. B. Strachan, E. R. Humphreys, and N. T. Roulet, 2008: Net ecosystem CO₂ exchange in a temperate cattail marsh in relation to biophysical properties. *Agricultural and Forest Meteorology*, **148**(1), 69-81, doi: 10.1016/j.agrformet.2007.09.004.
- Bortolotti, L. E., V. L. St. Louis, R. D. Vinebrooke, and A. P. Wolfe, 2015: Net ecosystem production and carbon greenhouse gas fluxes in three prairie wetlands. *Ecosystems*, **19**(3), 411-425, doi: 10.1007/s10021-015-9942-1.
- Bridgman, S. D., and C. J. Richardson, 1992: Mechanisms controlling soil respiration (CO₂ and CH₄) in southern peatlands. *Soil Biology and Biochemistry*, **24**(11), 1089-1099, doi: 10.1016/0038-0717(92)90058-6.
- Bridgman, S. D., H. Cadillo-Quiroz, J. K. Keller, and Q. Zhuang, 2013: Methane emissions from wetlands: Biogeochemical, microbial, and modeling perspectives from local to global scales. *Global Change Biology*, **19**(5), 1325-1346, doi: 10.1111/gcb.12131.
- Bridgman, S. D., C. A. Johnston, J. Pastor and K. Updegraff, 1995: Potential feedbacks of northern wetlands on climate change. *BioScience*, **45**, 262-274.



- Bridgman, S. D., J. P. Megonigal, J. K. Keller, N. B. Bliss, and C. Trettin, 2006: The carbon balance of North American wetlands. *Wetlands*, **26**(4), 889-916; doi: 10.1672/0277-5212(2006)26[889:tcbona]2.0.co;2.
- Bridgman, S. D., J.P. Megonigal, J.K. Keller, N.B. Bliss, and C. Trettin, 2007: Wetlands. In: *First State of the Carbon Cycle Report (SOCCR): The North American Carbon Budget and Implications for the Global Carbon Cycle. A Report by the U.S. Climate Change Science Program and the Subcommittee on Global Change Research*. [A. King, W. L. Dilling, G. P. Zimmerman, D. M. Fairman, R. A. Houghton, G. Marland, A. Z. Rose, and T. J. Wilbanks (eds.)]. National Oceanic and Atmospheric Administration, National Climatic Data Center, Asheville, NC, USA, 139-148 pp.
- Bryant, J. C., and R. H. Chabreck, 1998: Effects of impoundment on vertical accretion of coastal marsh. *Estuaries*, **21**(3), 416, doi: 10.2307/1352840.
- Buttler, A., H. Diné, and P. E. M. Lévesque, 1994: Effects of physical, chemical and botanical characteristics of peat on carbon gas fluxes. *Soil Science*, **158**(5), 365-374.
- Canadian Wildlife Service, 1991: *The Federal Policy on Wetland Conservation*. Minister of Environment, Minister of Supply and Services Canada. [<http://nawcc.wetlandnetwork.ca/Federal%20Policy%20on%20Wetland%20Conservation.pdf>]
- Cao, M., S. Marshall, and K. Gregson, 1996: Global carbon exchange and methane emissions from natural wetlands: Application of a process-based model. *Journal of Geophysical Research: Atmospheres*, **101**(D9), 14399-14414, doi: 10.1029/96jd00219.
- Carroll, P. and P. Crill, 1997: Carbon balance of a temperate poor fen. *Global Biogeochemical Sciences*, **11**, 349-356.
- Casasola, P. M., 2008: Los humedales en Mexico: Tendencias y oportunidades. *Cuadernos de Biodiversidad*, **28**, 10-18, doi: 10.14198/cdbio.2008.28.02.
- CCSP, 2007: *First State of the Carbon Cycle Report (SOCCR): The North American Carbon Budget and Implications for the Global Carbon Cycle. A Report by the U.S. Climate Change Science Program and the Subcommittee on Global Change Research*. [A. W. King, L. Dilling, G. P. Zimmerman, D. M. Fairman, R. A. Houghton, G. Marland, A. Z. Rose, and T. J. Wilbanks (eds.)]. National Oceanic and Atmospheric Administration, National Climatic Data Center, Asheville, NC, USA, 242 pp.
- Chapin, F. S., G. M. Woodwell, J. T. Randerson, E. B. Rastetter, G. M. Lovett, D. D. Baldocchi, D. A. Clark, M. E. Harmon, D. S. Schimel, R. Valentini, C. Wirth, J. D. Aber, J. J. Cole, M. L. Goulden, J. W. Harden, M. Heimann, R. W. Howarth, P. A. Matson, A. D. McGuire, J. M. Melillo, H. A. Mooney, J. C. Neff, R. A. Houghton, M. L. Pace, M. G. Ryan, S. W. Running, O. E. Sala, W. H. Schlesinger, and E. D. Schulze, 2006: Reconciling carbon-cycle concepts, terminology, and methods. *Ecosystems*, **9**(7), 1041-1050, doi: 10.1007/s10021-005-0105-7.
- Chimner, R.A. and D.J. Cooper, 2003: Influence of water table levels on CO₂ emissions in a Colorado subalpine fen: An *in situ* microcosm study. *Soil Biology and Biochemistry*, **35**(3), 345-351, doi: 10.1016/S0038-0717(02)00284-5.
- Chimner, R. A., D. J. Cooper, F. C. Wurster, and L. Rochefort, 2016: An overview of peatland restoration in North America: Where are we after 25 years? *Restoration Ecology*, doi: 10.1111/rec.12434.
- Chu, H., J. F. Gottgens, J. Chen, G. Sun, A. R. Desai, Z. Ouyang, C. Shao, and K. Czajkowski, 2015: Climatic variability, hydrologic anomaly, and methane emission can turn productive freshwater marshes into net carbon sources. *Global Change Biology*, **21**(3), 1165-1181, doi: 10.1111/gcb.12760.
- Ciais, P., A. J. Dolman, A. Bombelli, R. Duren, A. Peregon, P. J. Rayner, C. Miller, N. Gobron, G. Kinderman, G. Marland, N. Gruber, F. Chevallier, R. J. Andres, G. Balsamo, L. Bopp, F.-M. Breon, G. Broquet, R. Dargaville, T. J. Battin, A. Borges, H. Bovensmann, M. Buchwitz, J. Butler, J. G. Canadell, R. B. Cook, R. DeFries, R. Engelen, K. R. Gurney, C. Heinze, M. Heimann, A. Held, M. Henry, B. Law, S. Luyssaert, J. Miller, T. Moriyama, C. Moulin, R. B. Myneni, C. Nussli, M. Obersteiner, D. Ojima, Y. Pan, J.-D. Paris, S.L. Piao, B. Poulter, S. Plummer, S. Quegan, P. Raymond, M. Reichstein, L. Rivier, C. Sabine, D. Schimel, O. Tarasova, R. Valentini, R. Wang, G. van der Werf, D. Wickland, M. Williams and C. Zehner, 2014: Current systematic carbon-cycle observations and the need for implementing a policy-relevant carbon observing system. *Biogeosciences*, **11**(13), 3547-3602, doi: 10.5194/bg-11-3547-2014.
- Clair, T. A., and J. M. Ehrman, 1996: Variations in discharge and dissolved organic carbon and nitrogen export from terrestrial basins with changes in climate: A neural network approach. *Limnology and Oceanography*, **41**(5), 921-927, doi: 10.4319/lo.1996.41.5.0921.
- Clair, T. A., T. L. Pollock, and J. M. Ehrman, 1994: Exports of carbon and nitrogen from river basins in Canada's Atlantic provinces. *Global Biogeochemical Cycles*, **8**(4), 441-450, doi: 10.1029/94GB02311.
- Clewley, D., J. Whitcomb, M. Moghaddam, K. McDonald, B. Chapman, and P. Bunting, 2015: Evaluation of ALOS PALSAR data for high-resolution mapping of vegetated wetlands in Alaska. *Remote Sensing*, **7**(6), 7272-7297, doi: 10.3390/rs70607272.
- Coles, J.R.P. and J. B. Yavitt, 2004: Linking belowground carbon allocation to anaerobic CH₄ and CO₂ production in a forested peatland, New York State. *Geomicrobiology Journal*, **21**(7), 445-455, doi: 10.1080/01490450490505419.
- Cowardin, L. M., V. Carter, F. C. Golet, and E. T. LaRoe, 1979: *Classification of Wetlands and Deepwater Habitats of the United States*. Report FWS/OBS-79/31, USFWS, 131 pp.



- Crill, P. M., K. B. Bartlett, R. C. Harriss, E. Gorham, E. S. Verry, D. I. Sebacher, L. Madzar, and W. Sanner, 1988: Methane flux from Minnesota peatlands. *Global Biogeochemical Cycles*, **2**(4), 371-384, doi: 10.1029/GB002i004p00371.
- Dahl, T. E., 1990: *Wetlands Losses in the United States: 1780's to 1980's*. U.S. Fish and Wildlife Service, Washington, D.C., 13 pp. [<https://www.fws.gov/wetlands/Documents/Wetlands-Losses-in-the-United-States-1780s-to-1980s.pdf>]
- Dahl, T. E., 2011: *Status and Trends of Wetlands in the Conterminous United States 2004 to 2009*. US Department of the Interior, U.S. Fish and Wildlife Service, Fisheries and Habitat Conservation. [<https://www.fws.gov/wetlands/Documents/Status-and-Trends-of-Wetlands-in-the-Conterminous-United-States-2004-to-2009.pdf>]
- Dahl, T. E., 2014: *Status and Trends of Prairie Wetlands in the United States 1997 to 2009*. U.S. Department of the Interior; Fish and Wildlife Service, Ecological Services, 67 pp. [<https://www.fws.gov/wetlands/Documents/Status-and-Trends-of-Prairie-Wetlands-in-the-United-States-1997-to-2009.pdf>]
- Dai, Z. H., C. C. Trettin, C. S. Li, H. Li, G. Sun, and D. M. Amatya, 2012: Effect of assessment scale on spatial and temporal variations in CH₄, CO₂, and N₂O fluxes in a forested wetland. *Water Air and Soil Pollution*, **223**(1), 253-265, doi: 10.1007/s11270-011-0855-0.
- Day, J. W., T. J. Butler, and W. H. Conner, 1977: Productivity and nutrient export studies in a cypress swamp and lake system in Louisiana. In: *Estuarine Processes. Vol. 2*. [M. Wiley, (ed.)]. Academic, San Diego, CA, 255-269 pp.
- De Gortari-Ludlow, N., G. Espinosa-Reyes, J. Flores-Rivas, J. Salgado-Ortiz, and L. Chapa-Vargas, 2015: Threats, conservation actions, and research within 78 Mexican non-coastal protected wetlands. *Journal for Nature Conservation*, **23**, 73-79, doi: 10.1016/j.jnc.2014.06.005.
- Desai, A. R., K. Xu, H. Tian, P. Weishampel, J. Thom, D. Baumann, A. E. Andrews, B. D. Cook, J. Y. King, and R. Kolka, 2015: Landscape-level terrestrial methane flux observed from a very tall tower. *Agricultural and Forest Meteorology*, **201**, 61-75, doi: 10.1016/j.agrformet.2014.10.017.
- Dijkstra, F. A., S. A. Prior, G. B. Runion, H. A. Torbert, H. Q. Tian, C. Q. Lu, and R. T. Venterea, 2012: Effects of elevated carbon dioxide and increased temperature on methane and nitrous oxide fluxes: Evidence from field experiments. *Frontiers in Ecology and the Environment*, **10**(10), 520-527, doi: 10.1890/120059.
- Ding, W.-X., and Z.-C. Cai, 2007: Methane emission from natural wetlands in China: Summary of years 1995-2004 studies. *Pedosphere*, **17**(4), 475-486, doi: 10.1016/s1002-0160(07)60057-5.
- Dise, N. B., 1992: Winter fluxes of methane from Minnesota peatlands. *Biogeochemistry*, **17**(2), doi: 10.1007/bf00002641.
- Dise, N. B., 1993: Methane emission from Minnesota peatlands: Spatial and seasonal variability. *Global Biogeochemical Cycles*, **7**(1), 123-142, doi: 10.1029/92GB02299.
- Dise, N. B., and E. S. Verry, 2001: Suppression of peatland methane emission by cumulative sulfate deposition in simulated acid rain. *Biogeochemistry*, **53**(2), 143-160, doi: 10.1023/a:1010774610050.
- Drexler, J. Z., C. S. Fontaine, and S. J. Deverel, 2009: The legacy of wetland drainage on the remaining peat in the Sacramento-San Joaquin Delta, California, USA. *Wetlands*, **29**(1), 372-386, doi: 10.1672/08-97.1.
- Drexler, J. Z., K. W. Krauss, M. C. Sasser, C. C. Fuller, C. M. Swarzenski, A. Powell, K. M. Swanson, and J. Orlando, 2013: A long-term comparison of carbon sequestration rates in impounded and naturally tidal freshwater marshes along the lower Waccamaw River, South Carolina. *Wetlands*, **33**(5), 965-974, doi: 10.1007/s13157-013-0456-3.
- Drösler, M., L.V. Verchot, A. Freibauer, and G. Pan, 2013: Chapter 2: Drained inland organic soils. In: *Supplement to the 2006 IPCC Guidelines for National Greenhouse Gas Inventories: Wetlands*. [T. Hiraishi, T. Krug, K. Tanabe, N. Srivastava, J. Baasansuren, M. Fukuda, and T.G. Troxler (eds.)]. Intergovernmental Panel on Climate Change, Switzerland. [<http://www.ipcc-nggip.iges.or.jp/public/wetlands/>]
- Ensign, S. H., C. R. Hupp, G. B. Noe, K. W. Krauss, and C. L. Stagg, 2013: Sediment accretion in tidal freshwater forests and oligohaline marshes of the Waccamaw and Savannah rivers, USA. *Estuaries and Coasts*, **37**(5), 1107-1119, doi: 10.1007/s12237-013-9744-7.
- Environment Canada, 1991: *The Federal Policy on Wetland Conservation*. Government of Canada, Canadian Wildlife Service, 13 pp. [<http://publications.gc.ca/site/eng/100725/publication.html>]
- Euliss, N. H., J. W. LaBaugh, L. H. Fredrickson, D. M. Mushet, M. K. Laubhan, G. A. Swanson, T. C. Winter, D. O. Rosenberry, and R. D. Nelson, 2004: The wetland continuum: A conceptual framework for interpreting biological studies. *Wetlands*, **24**(2), 448-458, doi: 10.1672/0277-5212(2004)024[0448:twcacf]2.0.co;2.
- Euliss, N. H., Jr., R. A. Gleason, A. Olness, R. L. McDougal, H. R. Murkin, R. D. Robarts, R. A. Bourbonniere, and B. G. Warner, 2006: North American prairie wetlands are important non-forested land-based carbon storage sites. *Science of the Total Environment*, **361**(1-3), 179-188, doi: 10.1016/j.scitotenv.2005.06.007.
- Federal Geographic Data Committee, 2013: *Classification of Wetlands and Deepwater Habitats of the United States*. 2nd ed. FGDC-STD-004-2013.
- Federal Provincial and Territorial Governments of Canada, 2010: *Canadian Biodiversity: Ecosystem Status and Trends 2010*. Canadian Councils of Resource Ministers, 142 pp. [<http://www.biodivcanada.ca/default.asp?lang=En&n=F07D520A-1>]



- Fenner, N., and C. Freeman, 2011: Drought-induced carbon loss in peatlands. *Nature Geoscience*, **4**(12), 895-900, doi: 10.1038/Ngeo1323.
- Freeman, C., M. A. Lock, and B. Reynolds, 1993: Fluxes of CO₂, CH₄ and N₂O from a Welsh peatland following simulation of water table draw-down: Potential feedback to climatic change. *Biogeochemistry*, **19**(1), doi: 10.1007/bf00000574.
- Frolking, S. and P. Crill. 1994: Climate control on temporal variability of methane flux from a poor fen in southeastern New Hampshire: Measurement and modeling. *Global Biogeochemical Cycles*, **8**, 385-397.
- Garone, P., 2011: *The Fall and Rise of Wetlands of California's Great Central Valley*. University of California Press, 448 pp.
- Glaser, P.H., J.C. Volin, T.J. Givinish, B.C.S. Hansen, and C.A. Stricker, 2012: Carbon and sediment accumulation in the Everglades (USA) during the past 4000 years: Rates, drivers, and sources of error. *Journal of Geophysical Research*, **117**, G03026, doi: 10.1029/2011JG001821.
- Gleason, R., M. Laubhan, and N. Euliss, Jr., 2008: *Ecosystem Services Derived from Wetland Conservation Practices in the United States Prairie Pothole Region with an Emphasis on the United States Department of Agriculture Conservation Reserve and Wetlands Reserve Programs*. U.S. Geological Survey professional paper 1745. [https://pubs.usgs.gov/pp/1745/]
- Gleason, R. A., B. A. Tangen, B. A. Browne, and N. H. Euliss Jr, 2009: Greenhouse gas flux from cropland and restored wetlands in the prairie pothole region. *Soil Biology and Biochemistry*, **41**(12), 2501-2507, doi: 10.1016/j.soilbio.2009.09.008.
- Gockede, M., A. M. Michalak, D. Vickers, D. P. Turner, and B. E. Law, 2010: Atmospheric inverse modeling to constrain regional-scale CO₂ budgets at high spatial and temporal resolution. *Journal of Geophysical Research: Atmospheres*, **115**, doi: 10.1029/2009jd012257.
- Goldhaber, M. B., C. T. Mills, J. M. Morrison, C. A. Stricker, D. M. Mushet, and J. W. LaBaugh, 2014: Hydrogeochemistry of prairie pothole region wetlands: Role of long-term critical zone processes. *Chemical Geology*, **387**, 170-183, doi: 10.1016/j.chemgeo.2014.08.023.
- Golovatskaya, E. A., and E. A. Dyukarev, 2008: Carbon budget of oligotrophic mire sites in the Southern Taiga of Western Siberia. *Plant and Soil*, **315**(1-2), 19-34, doi: 10.1007/s11104-008-9842-7.
- Gorham, E., 1991: Northern peatlands: Role in the carbon cycle and probable responses to climatic warming. *Ecological Applications*, **1**(2), 182-195, doi: 10.2307/1941811.
- Gorham, E., C. Lehman, A. Dyke, D. Clymo, and J. Janssens, 2012: Long-term carbon sequestration in North American peatlands. *Quaternary Science Reviews*, **58**, 77-82, doi: 10.1016/j.quascirev.2012.09.018.
- Green, S. M., and A. J. Baird, 2012: A mesocosm study of the role of the sedge *Eriophorum angustifolium* in the efflux of methane—including that due to episodic ebullition—from peatlands. *Plant and Soil*, **351**(1-2), 207-218, doi: 10.1007/s11104-011-0945-1.
- Hanson, P. J., A. L. Gill, X. Xu, J. R. Phillips, D. J. Weston, R. K. Kolka, J. S. Riggs, and L. A. Hook, 2016: Intermediate-scale community-level flux of CO₂ and CH₄ in a Minnesota peatland: Putting the SPRUCE project in a global context. *Biogeochemistry*, **129**(3), 255-272, doi: 10.1007/s10533-016-0230-8.
- Hanson, P. J., J. S. Riggs, W. R. Nettles, J. R. Phillips, M. B. Krassovski, L. A. Hook, L. H. Gu, A. D. Richardson, D. M. Aubrecht, D. M. Ricciuto, J. M. Warren, and C. Barbier, 2017: Attaining whole-ecosystem warming using air and deep-soil heating methods with an elevated CO₂ atmosphere. *Biogeosciences*, **14**(4), 861-883, doi: 10.5194/bg-14-861-2017.
- Happell, J. D., J. P. Chanton, and W. S. Showers, 1994: The influence of methane oxidation on the stable isotopic composition of methane emitted from Florida swamp forests. *Geochimica et Cosmochimica Acta*, **58**(20), 4377-4388, doi: 10.1016/0016-7037(94)90341-7.
- Harriss, R. C., and D. I. Sebacher, 1981: Methane flux in forested freshwater swamps of the Southeastern United States. *Geophysical Research Letters*, **8**(9), 1002-1004, doi: 10.1029/GL008i009p01002.
- Harriss, R. C., D. I. Sebacher, and F. P. Day, 1982: Methane flux in the Great Dismal Swamp. *Nature*, **297**(5868), 673-674, doi: 10.1038/297673a0.
- Harriss, R. C., E. Gorham, D. I. Sebacher, K. B. Bartlett, and P. A. Flebbe, 1985: Methane flux from northern peatlands. *Nature*, **315**(6021), 652-654, doi: 10.1038/315652a0.
- Harriss, R. C., D. I. Sebacher, K. B. Bartlett, D. S. Bartlett, and P. M. Crill, 1988: Sources of atmospheric methane in the south Florida environment. *Global Biogeochemical Cycles*, **2**(3), 231-243, doi: 10.1029/GB002i003p00231.
- He, Y., H. Genet, A.D. McGuire, Q. Zhuang, B. K. Wylie, and Y. Zhang, 2016: Terrestrial carbon modeling: Baselines and projections in lowland ecosystems of Alaska. In: *Baseline and Projected Future Carbon Storage and Greenhouse-Gas Fluxes in Ecosystems of Alaska: U.S. Geological Survey Professional Paper 1826*. [Zhu, Zhiliang, and McGuire, A.D., eds.]. 196 p., https://pubs.er.usgs.gov/publication/pp1826.
- Helbig, M., W.L. Quinton, O. Sonnentag, 2017: Warm spring conditions increase annual methane emissions from a boreal peat landscape with sporadic permafrost. *Environmental Research Letters*, **12**, 115009, doi: 10.1088/1748-9326/aa8c85.
- Herbst, M., T. Friberg, R. Ringgaard, and H. Soegaard, 2011: Interpreting the variations in atmospheric methane fluxes observed above a restored wetland. *Agricultural and Forest Meteorology*, **151**(7), 841-853, doi: 10.1016/j.agrformet.2011.02.002.



- Holgerson, M. A., and P. A. Raymond, 2016: Large contribution to inland water CO₂ and CH₄ emissions from very small ponds. *Nature Geoscience*, **9**(3), 222-226, doi: 10.1038/ngeo2654.
- Holm, G. O., B. C. Perez, D. E. McWhorter, K. W. Krauss, D. J. Johnson, R. C. Raynie, and C. J. Killebrew, 2016: Ecosystem level methane fluxes from tidal freshwater and brackish marshes of the Mississippi River Delta: Implications for coastal wetland carbon projects. *Wetlands*, **36**(3), 401-413, doi: 10.1007/s13157-016-0746-7.
- Hommeltenberg, J., M.-M., M. Drösler, K. Heidbach, P. Werle, H. Schmid, 2014: Ecosystem scale methane fluxes in a natural temperate bog-pine forest in southern Germany. *Agricultural and Forest Meteorology*, **198**, 273-284, doi: 10.1016/j.agrformet.2014.08.017.
- Hope, D., M. F. Billett, and M. S. Cresser, 1994: A review of the export of carbon in river water: Fluxes and processes. *Environmental Pollution*, **84**(3), 301-324, doi: 10.1016/0269-7491(94)90142-2.
- Huang, Y. A. O., W. Sun, W. E. N. Zhang, Y. Yu, Y. Su, and C. Song, 2010: Marshland conversion to cropland in northeast China from 1950 to 2000 reduced the greenhouse effect. *Global Change Biology*, **16**(2), 680-695, doi: 10.1111/j.1365-2486.2009.01976.x.
- Hyvonen, R., G. I. Agren, S. Linder, T. Persson, M. F. Cotrufo, A. Ekblad, M. Freeman, A. Grelle, I. A. Janssens, P. G. Jarvis, S. Kellomaki, A. Lindroth, D. Loustau, T. Lundmark, R. J. Norby, R. Oren, K. Pilegaard, M. G. Ryan, B. D. Sigurdsson, M. Stromgren, M. van Oijen, and G. Wallin, 2007: The likely impact of elevated CO₂, nitrogen deposition, increased temperature and management on carbon sequestration in temperate and boreal forest ecosystems: A literature review. *New Phytologist*, **173**(3), 463-480, doi: 10.1111/j.1469-8137.2007.01967.x.
- ICF International, 2013: *Greenhouse Gas Mitigation Options and Costs for Agricultural Land and Animal Production Within the United States*. U.S. Department of Agriculture. [https://www.usda.gov/oce/climate_change/mitigation_technologies/GHGMitigation-Production_Cost.htm]
- Instituto Nacional de Estadística y Geografía, 2010: *Humedales potenciales*. [<http://www.inegi.org.mx/geo/contenidos/reclnat/humedales/metodologia.aspx>]
- IPCC, 2013: *Supplement to the 2006 IPCC Guidelines for National Greenhouse Gas Inventories: Wetlands*. [T. Hiraishi, T. Krug, K. Tanabe, N. Srivastava, J. Baasansuren, M. Fukuda, and T.G. Troxler (eds.)]. Intergovernmental Panel on Climate Change, Switzerland. [<http://www.ipcc-nggip.iges.or.jp/public/wetlands/>]
- Ise, T., A.L. Dunn, S.C. Wofsy, and P.R. Moorcroft, 2008: High sensitivity of peat decomposition to climate change through water table feedback. *Nature Geoscience*, **1**: 763-766.
- IUSS Working Group WRB, 2006: *World Reference Base for Soil Resources 2006*. World Soil Resources Reports no. 103 FAO. [<http://www.fao.org/3/a-a0510e.pdf>]
- Jimenez, K. L., G. Starr, C. L. Staudhammer, J. L. Schedlbauer, H. W. Loescher, S. L. Malone, and S. F. Oberbauer, 2012: Carbon dioxide exchange rates from short- and long-hydroperiod Everglades freshwater marsh. *Journal of Geophysical Research: Biogeosciences*, **117**(G4), doi: 10.1029/2012JG002117.
- Joosten, H., and D. Clarke, 2002: *Wise Use of Mires and Peatlands - Background and Principles Including a Framework for Decision-Making*. International Mire Conservation Group and the International Peat Society. Saarijärvi, Finland, 304 pp. [http://www.imcg.net/media/download_gallery/books/wump_wise_use_of_mires_and_peatlands_book.pdf]
- Juutinen, Alm, Martikainen, and Silvola, 2001: Effects of spring flood and water level draw-down on methane dynamics in the littoral zone of boreal lakes. *Freshwater Biology*, **46**(7), 855-869, doi: 10.1046/j.1365-2427.2001.00721.x.
- Kasischke, E. S., and M. R. Turetsky, 2006: Recent changes in the fire regime across the North American boreal region—spatial and temporal patterns of burning across Canada and Alaska. *Geophysical Research Letters*, **33**(9), L09703, doi: 10.1029/2006gl025677.
- Kayranli, B., M. Scholz, A. Mustafa, and A. Hedmark, 2010: Carbon storage and fluxes within freshwater wetlands: A critical review. *Society of Wetland Scientists*, **30**, 111-124, doi: 10.1007/s13157-009-0003-4.
- Kelley, C. A., C. S. Martens, and W. Ussler, 1995: Methane dynamics across a tidally flooded riverbank margin. *Limnology and Oceanography*, **40**(6), 1112-1129, doi: 10.4319/lo.1995.40.6.1112.
- Kim, J., S. B. Verma, and D. P. Billesbach, 1999: Seasonal variation in methane emission from a temperate phragmites-dominated marsh: Effect of growth stage and plant-mediated transport. *Global Change Biology*, **5**(4), 433-440, doi: 10.1046/j.1365-2486.1999.00237.x.
- King, S. L., D. J. Twedt, and R. R. Wilson, 2006: The role of the wetland reserve program in conservation efforts in the Mississippi River Alluvial Valley. *Wildlife Society Bulletin (1973-2006)*, **34**(4), 914-920.
- Kirschke, S., P. Bousquet, P. Ciais, M. Saunio, J. G. Canadell, E. J. Dlugokencky, P. Bergamaschi, D. Bergmann, D. R. Blake, L. Bruhwiler, P. Cameron-Smith, S. Castaldi, F. Chevallier, L. Feng, A. Fraser, M. Heimann, E. L. Hodson, S. Houweling, B. Josse, P. J. Fraser, P. B. Krummel, J.-F. Lamarque, R. L. Langenfelds, C. Le Quééré, V. Naik, S. O'Doherty, P. I. Palmer, I. Pison, D. Plummer, B. Poulter, R. G. Prinn, M. Rigby, B. Ringeval, M. Santini, M. Schmidt, D. T. Shindell, I. J. Simpson, R. Spahni, L. P. Steele, S. A. Strode, K. Sudo, S. Szopa, G. R. van der Werf, A. Voulgarakis, M. van Weele, R. F. Weiss, J. E. Williams, and G. Zeng, 2013: Three decades of global methane sources and sinks. *Nature Geoscience*, **6**(10), 813-823, doi: 10.1038/ngeo1955.



- Knox, S. H., C. Sturtevant, J.H. Matthes, L. Koteen, J. Verfaillie, and D. Baldocchi, 2015: Agricultural peatland restoration: Effects of land-use change on greenhouse gas (CO₂ and CH₄) fluxes in the Sacramento-San Joaquin Delta. *Global Change Biology*, **21**, 750-765.
- Koehler, A.-K., M. Sottocornola, and G. Kiely, 2011: How strong is the current carbon sequestration of an Atlantic blanket bog? *Global Change Biology*, **17**(1), 309-319, doi:10.1111/j.1365-2486.2010.02180.x
- Kolka, R. K., M. C. Rabenhorst, and D. Swanson, 2011: Histosols. In: *Handbook of Soil Sciences Properties and Processes*. 2nd ed. [P. M. Huang, Y. Li, and M. E. Sumner (eds.)]. CRC Press, 33.38-33.29 pp.
- Kracht, O., and G. Gleixner, 2000: Isotope analysis of pyrolysis products from sphagnum peat and dissolved organic matter from bog water. *Organic Geochemistry*, **31**(7-8), 645-654, doi: 10.1016/S0146-6380(00)00041-3.
- Krauss, K. W., and J. L. Whitbeck, 2012: Soil greenhouse gas fluxes during wetland forest retreat along the Lower Savannah River, Georgia (USA). *Wetlands*, **32**(1), 73-81, doi: 10.1007/s13157-011-0246-8.
- Krauss, K. W., G. O. Holm, B. C. Perez, D. E. McWhorter, N. Cormier, R. F. Moss, D. J. Johnson, S. C. Neubauer, and R. C. Raynie, 2016: Component greenhouse gas fluxes and radiative balance from two deltaic marshes in Louisiana: Pairing chamber techniques and eddy covariance. *Journal of Geophysical Research: Biogeosciences*, **121**(6), 1503-1521, doi: 10.1002/2015JG003224.
- Kroetsch, D. G., X. Geng, S.X. Chang, and D.S. Saurette. 2011: Organic soils of Canada: Part 1. Wetland organic soils. *Canadian Journal of Soil Science*, **91**, 807-822.
- Kudray, G.M. and M.R. Gale, 2000: Evaluation of National Wetland Inventory maps in a heavily forested region in the upper Great Lakes. *Wetlands*, **20**(4) 581-587.
- Lai, C. Y., X.E. Yang, Y.N. Tang, B.E. Rittmann, H.P. Zhao, 2014: Nitrate shaped the selenate-reducing microbial community in a hydrogen-based biofilm reactor. *Environmental Science Technology*, **48**, 3395-3402.
- Lai, D.Y.F, T.R. Moore, N.T. Roulet, 2014: Spatial and temporal variations of methane flux measured by autochambers in a temperate ombrotrophic peatland. *Journal of Geophysical Research Biogeosciences*, **119**, 864-880, doi: 10.1002/2013JG02410.
- Landgrave, R., and P. Moreno-Casasola, 2012: Evaluación cuantitativa de la pérdida de humedales en México. *Investigación Ambiental*, **4**(1), 19-35.
- Lansdown, J. M., P. D. Quay, and S. L. King, 1992: CH₄ production via CO₂ reduction in a temperate bog: A source of 13C-depleted CH₄. *Geochimica et Cosmochimica Acta*, **56**(9), 3493-3503, doi: 10.1016/0016-7037(92)90393-w.
- Lehner, B., and P. Döll, 2004: Development and validation of a global database of lakes, reservoirs and wetlands. *Journal of Hydrology*, **296**(1-4), 1-22, doi: 10.1016/j.jhydrol.2004.03.028.
- Li, X., and W.J. Mitsch, 2016: Methane emissions from created and restored freshwater and brackish marshes in southwest Florida, USA. *Ecological Engineering*, **91**, 529-536, doi: 10.1016/j.ecoleng.2016.01.001.
- Lindau, C. W., P. K. Bollich, R. D. Delaune, A. R. Mosier, and K. F. Bronson, 1993: Methane mitigation in flooded Louisiana rice fields. *Biology and Fertility of Soils*, **15**(3), 174-178, doi: 10.1007/Bf00361607.
- Loisel, J., Z. Yu, D.W. Beilman, P. Camill, J. Alm, M.J. Amesbury, D. Anderson, S. Anderson, C. Bochicchio, K. Barber, L.R. Belyea, J. Bunbury, F.M. Chambers, D.J. Charman, F. D. Vleeschouwer, B. Fialkiewicz-Koziel, S.A. Finkelstein, M. Galka, M. Garneau, D. Hammarlund, W. Hinchcliffe, J. Holmquist, P. Hughes, M.C. Jones, E.S. Klein, U. Kokfelt, A. Korhola, P. Kuhry, A. Lamarre, M. Lamentowicz, D. Larg, M. Lavoie, G. MacDonald, G. Magnan, M. Makila, G. Mallon, p. Mathijssen, D. Mauquoy, J. McCarroll, T.R. Moore, J. Nichols, B. O'Reilly, P. Oksanen, M. Packalen, D. Peteet, P. J.H. Richard, S. Robinson, T. Ronkainen, M. Rundgren, A.B.K. Sannel, C. Tarnocai, T. Thom, E.-S. Tuittila, M. Turetsky, M. Valiranta, M. van der Linden, B. van Geel, S. van Bellen, D. Vitt, Y. Zhao, and W. Zhou, 2014: A database and synthesis of northern peatland soil properties and Holocene carbon and nitrogen accumulation. *The Holocene*, **24**(9), 1028-1042, doi: 10.117/0959683614538073.
- Lu, W., J. Xiao, F. Liu, Y. Zhang, C. Liu, and G. Lin, 2017: Contrasting ecosystem CO₂ fluxes of inland and coastal wetlands: A meta-analysis of eddy covariance data. *Global Change Biology*, **23**, 1180-1198, doi: 10.1111/gcb.13424.
- Lucchese, M., J. M. Waddington, M. Poulin, R. Pouliot, L. Rochefort, and M. Strack, 2010: Organic matter accumulation in a restored peatland: Evaluating restoration success. *Ecological Engineering*, **36**(4), 482-488, doi: 10.1016/j.ecoleng.2009.11.017.
- Lund, M., P.M. Lafleur, N.T. Roulet, A. Lindroth, T.R. Christensen, M. Aurela, B.H. Chojnicki, L.B. Flanagan, E.R. Humphreys, T. Laurila, W.C. Oechel, J. Olejnik, J. Rinne, P. Schubert, and M.B. Nilsson, 2010: Variability in exchange of CO₂ across 12 northern peatland and tundra sites. *Global Change Biology*, **16**, 2436-2448.
- Makiranta, P., K. Minkinen, J. Hytonen, and J. Laine, 2008: Factors causing temporal and spatial variation in heterotrophic and rhizospheric components of soil respiration in afforested organic soil croplands in Finland. *Soil Biology and Biochemistry*, **40**(7), 1592-1600, doi: 10.1016/j.soilbio.2008.01.009.
- Malcolm, R. L., and W. H. Durum, 1976: Organic carbon and nitrogen concentrations and annual organic carbon load of selected rivers of the United States. *Water Supply Paper*. 1817F. [http://pubs.er.usgs.gov/publication/wsp1817F]



- Malone, S. L., C. L. Staudhammer, S. F. Oberbauer, P. Olivas, M. G. Ryan, J. L. Schedlbauer, H. W. Loescher, and G. Starr, 2014: El Niño Southern Oscillation (ENSO) enhances CO₂ exchange rates in freshwater marsh ecosystems in the Florida Everglades. *PLoS One*, **9**(12), e115058, doi: 10.1371/journal.pone.0115058.
- Manies, K. L., J. W. Harden, C. C. Fuller, and M. R. Turetsky, 2016: Decadal and long-term boreal soil carbon and nitrogen sequestration rates across a variety of ecosystems. *Biogeosciences*, **13**, 4315-4327, doi: 10.5194/bg-13-4315-2016.
- Marek M.V., Janouš D., Taufarová K., Havránková K., Pavelka M., Kaplan V., and Marková I., 2011: Carbon exchange between ecosystems and atmosphere in the Czech Republic is affected by climate factors. *Environmental Pollution*, **159**, 1035-1039.
- McLaughlin, J., and K. Webster, 2014: Effects of climate change on peatlands in the far north of Ontario, Canada: A synthesis. *Arctic, Antarctic, and Alpine Research*, **46**(1), 84-102, doi: 10.1657/1938-4246-46.1.84.
- Melton, J. R., R. Wania, E. L. Hodson, B. Poulter, B. Ringeval, R. Spahni, T. Bohn, C. A. Avis, D. J. Beerling, G. Chen, A. V. Eliseev, S. N. Denisov, P. O. Hopcroft, D. P. Lettenmaier, W. J. Riley, J. S. Singarayer, Z. M. Subin, H. Tian, S. Zürcher, V. Brovkin, P. M. van Bodegom, T. Kleinen, Z. C. Yu, and J. O. Kaplan, 2013: Present state of global wetland extent and wetland methane modelling: Conclusions from a model inter-comparison project (WET-CHIMP). *Biogeosciences*, **10**(2), 753-788, doi: 10.5194/bg-10-753-2013.
- Miller, D. N., and W. C. Ghiorso, 1999: Seasonal patterns and controls on methane and carbon dioxide fluxes in forested swamp pools. *Geomicrobiology Journal*, **16**(4), 325-331, doi: 10.1080/014904599270578.
- Miller, S. M., R. Commane, J. R. Melton, A. E. Andrews, J. Benmergui, E. J. Dlugokencky, G. Janssens-Maenhout, A. M. Michalak, C. Sweeney, and D. E. J. Worthy, 2016: Evaluation of wetland methane emissions across North America using atmospheric data and inverse modeling. *Biogeosciences*, **13**, 1329-1339, doi: 10.5194/bg-13-1329-2016.
- Minkinen, K., K. Byrne, and C. C. Trettin, 2008: Climate impacts to peatland forestry. In: *Peatlands and Climate Change*. [M. Strack (ed.)]. International Peat Society, 98-122 pp. [<http://www.peat-society.org/peatlands-and-peat/peatlands-and-climate-change>]
- Mitra, S., R. Wassmann, and P. L. Vlek, 2005: An appraisal of global wetland area and its organic carbon stock. *Current Science*, **88**(1), 25-35.
- Mitsch, W., and J. Gosselink, 2015: *Wetlands*. 5th edition. Wiley.
- Mitsch, W. J., and X. Wu, 1995: Wetlands and Global Change. In: *Advances in Soil Science, Soil Management and Greenhouse Effect*. [R. Lal, J. Kimble, E. Levine, and B. A. Stewart (eds.)]. CRC Lewis Publishers, Boca Raton, Florida.
- Mitsch, W. J., and M. E. Hernandez, 2013: Landscape and climate change threats to wetlands of North and Central America. *Aquatic Sciences*, **75**(1), 133-149, doi: 10.1007/s00027-012-0262-7.
- Moore, T. R., and N. T. Roulet, 1995: Methane emissions from Canadian peatlands. In: *Soils and Global Change*. [R. Lal, J. Kimble, E. Levine, and B. A. Stewart, (eds.)]. Lewis Publishers, Boca Raton, FL, USA, 153-164 pp.
- Moreno-Mateos, D., M. E. Power, F. A. Comin, and R. Yockteng, 2012: Structural and functional loss in restored wetland ecosystems. *PLoS Biology*, **10**(1), e1001247, doi: 10.1371/journal.pbio.1001247.
- Morrissey, L. A. and W. R. Sweeney, 2006: *An Assessment of NWI Maps: Implications for Wetland Protection*. American Water Resources Association 2006 Spring Specialty Conference, GIS and Water Resources IV, May 8-10, 2006, Houston, Texas.
- Morse, J. L., M. Ardón, and E. S. Bernhardt, 2012: Greenhouse gas fluxes in southeastern U.S. Coastal plain wetlands under contrasting land uses. *Ecological Applications*, **22**(1), 264-280, doi: 10.1890/11-0527.1.
- Mulholland, P. J., 1981: Organic-carbon flow in a swamp-stream ecosystem. *Ecological Monographs*, **51**(3), 307-322, doi: 10.2307/2937276.
- Mulholland, P. J., and J. A. Watts, 1982: Transport of organic carbon to the oceans by rivers of North America: A synthesis of existing data. *Tellus*, **34**(2), 176-186, doi: 10.1111/j.2153-3490.1982.tb01805.x.
- Nahlik, A. M., and W. J. Mitsch, 2010: Methane emissions from created riverine wetlands. *Wetlands*, **30**(4), 783-793, doi: 10.1007/s13157-010-0038-6.
- Nahlik, A. M., and M. S. Fennessy, 2016: Carbon storage in US wetlands. *Nature Communications*, **7**, 13835, doi: 10.1038/ncomms13835.
- Naiman, R. J., T. Manning, and C. A. Johnston, 1991: Beaver population fluctuations and tropospheric methane emissions in boreal wetlands. *Biogeochemistry*, **12**(1), 1-15.
- National Wetlands Working Group, 1987: *The Canadian Wetland Classification System, Provisional Edition*. Ecological Land Classification Series, No. 21. Canadian Wildlife Service, Environment Canada. Ottawa, Ontario. 18 p.
- Neff, J.C., W.D. Bowman, E.A. Holland, M.C. Fisk, S.K. Schmidt, 1994: Fluxes of nitrous oxide and methane from nitrogen-amended soils in a Colorado alpine ecosystem. *Biogeochemistry*, **27**, 23-33.
- Neubauer, S. C., W. D. Miller, and I. C. Anderson, 2000: Carbon cycling in a tidal freshwater marsh ecosystem: A carbon gas flux study. *Marine Ecology Progress Series*, **199**, 13-30.



- Nichols, C., 1994: *Map Accuracy of National Wetlands Inventory Maps for Areas Subject to Maine Land Use Regulation Commission Jurisdictions*. U.S. Fish and Wildlife Service: Hadley, ME, USA. Ecological Services Report R5-94/6.
- Niemuth, N. D., B. Wangler, and R. E. Reynolds, 2010: Spatial and temporal variation in wet area of wetlands in the prairie pothole region of North Dakota and South Dakota. *Wetlands*, **30**(6), 1053-1064, doi: 10.1007/s13157-010-0111-1.
- Noe, G. B., C. R. Hupp, C. E. Bernhardt, and K. W. Krauss, 2016: Contemporary deposition and long-term accumulation of sediment and nutrients by tidal freshwater forested wetlands impacted by sea level rise. *Estuaries and Coasts*, **39**(4), 1006-1019, doi: 10.1007/s12237-016-0066-4.
- North American Waterfowl Management Plan Committee, 2012: *North American Waterfowl Management Plan 2012: People Conserving Waterfowl and Wetlands*. [<https://www.fws.gov/migratory-birds/pdf/management/NAWMP/2012NAWMP.pdf>]
- Nykänen, H., J. Alm, K. Lang, J. Silvola, and P. Martikainen, 1995: Emissions of CH₄, N₂O and CO₂ from a virgin fen and a fen drained for grassland in Finland. *Journal of Biogeography: Terrestrial Ecosystem Interactions with Global Change* **22**(2-3), 351-357.
- Ogle, S. M., P. Hunt, and C. Trettin, 2014: Quantifying greenhouse gas sources and sinks in managed wetland systems. In: *Quantifying Greenhouse Gas Fluxes in Agriculture and Forestry: Methods for Entity-Scale Inventory. Technical Bulletin Number 1939*. [M. Eve, D. Pape, M. Flugge, R. Steele, D. Man, M. Riley-Gilbert, and S. Biggar, (eds.)]. Office of the Chief Economist, U.S. Department of Agriculture, 606 pp.
- Olefeldt, D., M. R. Turetsky, P. M. Crill, and A. D. McGuire, 2013: Environmental and physical controls on northern terrestrial methane emissions across permafrost zones. *Global Change Biology*, **19**(2), 589-603, doi: 10.1111/gcb.12071.
- Olson, D. M., T. J. Griffis, A. Noormets, R. Kolka, and J. Chen, 2013: Interannual, seasonal, and retrospective analysis of the methane and carbon dioxide budgets of a temperate peatland. *Journal of Geophysical Research: Biogeosciences*, **118**(1), 226-238, doi: 10.1002/jgrg.20031.
- Ortiz-Llorente, M. J., and M. Alvarez-Cobelas, 2012: Comparison of biogenic methane emissions from unmanaged estuaries, lakes, oceans, rivers and wetlands. *Atmospheric Environment*, **59**, 328-337, doi: 10.1016/j.atmosenv.2012.05.031.
- Parton, W. J., M. D. Hartman, D. S. Ojima, and D. S. Schimel, 1998: DAYCENT: Its land surface submodel—Description and testing. *Global Planetary Change* **19**, 35-48.
- Peichl, M., M. Öquist, M. O. Löfvenius, U. Ilstedt, J. Sagerfors, A. Grelle, A. Lindroth, M. B. Nilsson, 2014: A 12-year record reveals pre-growing season temperature and water table level threshold effects on the net carbon dioxide exchange in a boreal fen. *Environmental Research Letters*, **9**, 055006, doi: 10.1088/1748-9326/9/5/055006.
- Pennock, D., T. Yates, A. Bedard-Haughn, K. Phipps, R. Farrell, and R. McDougal, 2010: Landscape controls on N₂O and CH₄ emissions from freshwater mineral soil wetlands of the Canadian Prairie Pothole region. *Geoderma*, **155**(3-4), 308-319, doi: 10.1016/j.geoderma.2009.12.015.
- Petrescu, A. M. R., A. Lohila, J. P. Touvinen, D. D. Baldocchi, A. R. Desai, N. T. Roulet, T. Vesala, A. J. Dolman, W. C. Oechel, B. Marcolla, T. Friborg, J. Rinne, J. H. Matthes, L. Merbold, A. Meijide, G. Kiely, M. Sottocornola, T. Sachs, D. Zona, A. Varlagin, D. Y. F. Lai, E. Veenendaal, F.-J. W. Parmentier, U. Skiba, M. Lund, A. Hensen, J. van Huissteden, L. B. Flanagan, N. J. Shurpali, T. Grunwald, E. R. Humphreys, M. Jackowicz-Korczynski, M. A. Aurela, T. Laurila, C. Gruning, C. A. R. Corradi, A. P. Schrier-Uijl, T. R. Christensen, M. P. Tamstorf, M. Mastepanov, P. J. Martikainen, S. B. Verma, C. Bernhofer, and A. Cescatti, 2015: The uncertain climate footprint of wetlands under human pressure. *Proceedings of the National Academy of Sciences USA*, **112** (15), 4594-4599, doi: 10.1073/pnas.1416267112.
- Potvin, L. R., E. S. Kane, R. A. Chimner, R. K. Kolka, and E. A. Lilleskov, 2015: Effects of water table position and plant functional group on plant community, aboveground production, and peat properties in a peatland mesocosm experiment (PEATcosm). *Plant and Soil*, **387**(1-2), 277-294, doi: 10.1007/s11104-014-2301-8.
- Poulter, B., P. Bousquet, J. G. Canadell, P. Ciais, A. Peregon, M. Saunio, V. K. Arora, D. J. Beerling, V. Brovkin, C. D. Jones, F. Joos, N. Gedney, A. Ito, T. Kleinen, C. D. Koven, K. McDonald, J. R. Melton, C. Peng, S. Peng, C. Prigent, R. Schroeder, W. J. Riley, M. Saito, R. Spahni, H. Tian, L. Taylor, N. Viovy, D. Wilton, A. Wiltshire, X. Xu, B. Zhang, Z. Zhang, and Q. Zhu, 2017: Global wetland contribution to 2000-2012 atmospheric methane growth rate dynamics. *Environmental Research Letters*, **12**, 094013, doi: 10.1088/1748-9326/aa8391.
- Pulliam, W. M., 1993: Carbon-dioxide and methane exports from a southeastern floodplain swamp. *Ecological Monographs*, **63**(1), 29-53, doi: 10.2307/2937122.
- Rask, H., J. Schoenau, and D. Anderson, 2002: Factors influencing methane flux from a boreal forest wetland in Saskatchewan, Canada. *Soil Biology and Biochemistry*, **34**(4), 435-443, doi: 10.1016/s0038-0717(01)00197-3.
- Raymond, P. A., and J. E. Saiers, 2010: Event controlled DOC export from forested watersheds. *Biogeochemistry*, **100**(1-3), 197-209, doi: 10.1007/s10533-010-9416-7.
- Reddy, A. D., T. J. Hawbaker, F. Wurster, Z. Zhu, S. Ward, D. Newcomb, and R. Murray, 2015: Quantifying soil carbon loss and uncertainty from a peatland wildfire using multi-temporal LIDAR. *Remote Sensing of Environment*, **170**, 306-316, doi: 10.1016/j.rse.2015.09.017.
- Richards, B., and C. B. Craft, 2015: Greenhouse gas fluxes from restored agricultural wetlands and natural wetlands, Northwestern Indiana. In: *The Role of Natural and Constructed Wetlands in Nutrient Cycling and Retention on the Landscape*, Springer International Publishing, 17-32 pp.



- Richardson, C. J., N. Flanagan, H. Wang, and M. Ho, 2014: *Impacts of Peatland Ditching and Draining on Water Quality and Carbon Sequestration Benefits of Peatland Restoration*. Eastern North Carolina/Southeastern Virginia Strategic Habitat Conservation Team, U.S. Fish and Wildlife Service, Region 4 and The Nature Conservancy North Carolina Chapter. [<https://catalog.data.gov/dataset/nc-impacts-of-peatland-ditching-and-draining-on-water-quality-and-carbon-sequestration-ben>]
- Rooney, R.C., S.E. Bayley, and D.W. Shindler, 2012: Oil sands mining and reclamation cause massive loss of peatland and carbon storage. *Proceedings of the National Academy Sciences USA*, **109**: 4933-4937.
- Roulet, N. T., 2000: Peatlands, carbon storage, greenhouse gases, and the Kyoto protocol: Prospects and significance for Canada. *Wetlands*, **20**(4), 605-615, doi: 10.1672/0277-5212(2000)020[0605:Pcsgga]2.0.Co;2.
- Roulet, N. T., P. M. Lafleur, P. J. H. Richard, T. R. Moore, E. R. Humphreys, and J. Bubier, 2007: Contemporary carbon balance and late Holocene carbon accumulation in a northern peatland. *Global Change Biology*, **13**(2), 397-411, doi: 10.1111/j.1365-2486.2006.01292.x.
- Saunois, M., P. Bousquet, B. Poulter, A. Peregon, P. Ciais, J. G. Canadell, E. J. Dlugokencky, G. Etiope, D. Bastviken, S. Houweling, G. Janssens-Maenhout, F. N. Tubiello, S. Castaldi, R. B. Jackson, M. Alexe, V. K. Arora, D. J. Beerling, P. Bergamaschi, D. R. Blake, G. Brailsford, V. Brovkin, L. Bruhwiler, C. Crevoisier, P. Crill, K. Covey, C. Curry, C. Frankenberg, N. Gedney, L. Hoglund-Isaksson, M. Ishizawa, A. Ito, F. Joos, H. S. Kim, T. Kleinen, P. Krummel, J. F. Lamarque, R. Langenfelds, R. Locatelli, T. Machida, S. Maksyutov, K. C. McDonald, J. Marshall, J. R. Melton, I. Morino, V. Naik, S. O'Doherty, F. J. W. Parmentier, P. K. Patra, C. H. Peng, S. S. Peng, G. P. Peters, I. Pison, C. Prigent, R. Prinn, M. Ramonet, W. J. Riley, M. Saito, M. Santini, R. Schroeder, I. J. Simpson, R. Spahni, P. Steele, A. Takizawa, B. F. Thornton, H. Q. Tian, Y. Tohjima, N. Viovy, A. Voulgarakis, M. van Weele, G. R. van der Werf, R. Weiss, C. Wiedinmyer, D. J. Wilton, A. Wiltshire, D. Worthy, D. Wunch, X. Y. Xu, Y. Yoshida, B. Zhang, Z. Zhang, and Q. Zhu, 2016: The global methane budget 2000-2012. *Earth System Science Data*, **8**(2), 697-751, doi: 10.5194/essd-8-697-2016.
- Schedlbauer, J. L., S. F. Oberbauer, G. Starr, and K. L. Jimenez, 2010: Seasonal differences in the CO₂ exchange of a short-hydroperiod Florida Everglades marsh. *Agricultural and Forest Meteorology*, **150**(7-8), 994-1006, doi: 10.1016/j.agrformet.2010.03.005.
- Schellekens, J., P. Buurman, and T. W. Kuyper, 2012: Source and transformations of lignin in carex-dominated peat. *Soil Biology and Biochemistry*, **53**, 32-42, doi: 10.1016/j.soilbio.2012.04.030.
- Schipper, L., and K. Reddy, 1994: *Methane Production and Emissions from Four Reclaimed and Pristine Wetlands of Southeastern United States*. Vol. 58, 1270-275 pp.
- Schuur, E. A., A. D. McGuire, C. Schadel, G. Grosse, J. W. Harden, D. J. Hayes, G. Hugelius, C. D. Koven, P. Kuhry, D. M. Lawrence, S. M. Natali, D. Olefeldt, V. E. Romanovsky, K. Schaefer, M. R. Turetsky, C. C. Treat, and J. E. Vonk, 2015: Climate change and the permafrost carbon feedback. *Nature*, **520**(7546), 171-179, doi: 10.1038/nature14338.
- Sebacher, D. I., R. C. Harriss, K. B. Bartlett, S. M. Sebacher, and S. S. Grice, 1986: Atmospheric methane sources: Alaskan tundra bogs, an alpine fen, and a subarctic boreal marsh. *Tellus B: Chemical and Physical Meteorology*, **38**(1), 1-10, doi: 10.3402/tellusb.v38i1.15059.
- Segarra, K. E. A., V. Samarkin, E. King, C. Meile, and S. B. Joye, 2013: Seasonal variations of methane fluxes from an unvegetated tidal freshwater mudflat (Hammersmith Creek, GA). *Biogeochemistry*, **115**(1-3), 349-361, doi: 10.1007/s10533-013-9840-6.
- Shannon, R., and J. White, 1994: A three-year study of controls on methane emissions from two Michigan peatlands. *Biogeochemistry*, **27**(1), doi: 10.1007/bf00002570.
- Sharitz, R. R., and S. C. Pennings, 2006: Development of wetland plant communities. In: *Ecology of Freshwater and Estuarine Wetlands*, [D. P. Batzer and R. R. Sharitz (eds.)]. University of California Press, 177-241 pp.
- Shurpali, N. J., and S. B. Verma, 1998: Micrometeorological measurements of methane flux in a Minnesota peatland during two growing seasons. *Biogeochemistry*, **40**(1), 1-15.
- Sjögersten, S., C. R. Black, S. Evers, J. Hoyos-Santillan, E. L. Wright, and B. L. Turner, 2014: Tropical wetlands: A missing link in the global carbon cycle? *Global Biogeochem Cycles*, **28**(12), 1371-1386, doi: 10.1002/2014GB004844.
- Sjögersten, S., S. Caul, T. J. Daniell, A. P. S. Jurd, O. S. O'Sullivan, C. S. Stapleton, and J. J. Titman, 2016: Organic matter chemistry controls greenhouse gas emissions from permafrost peatlands. *Soil Biology and Biochemistry*, **98**, 42-53, doi: 10.1016/j.soilbio.2016.03.016.
- Smardon, R. C., 2006: Heritage values and functions of wetlands in southern Mexico. *Landscape and Urban Planning*, **74**(3-4), 296-312, doi: 10.1016/j.landurbplan.2004.09.009.
- Smith, L. K., and W. M. Lewis, 1992: Seasonality of methane emissions from five lakes and associated wetlands of the Colorado Rockies. *Global Biogeochemical Cycles*, **6**(4), 323-338, doi: 10.1029/92GB02016.
- Soil Survey Staff, 2010: *Key to Soil Taxonomy*. 11th ed. U.S. Department of Agriculture Natural Resource Conservation Service, 338 pp. [https://www.nrcs.usda.gov/Internet/FSE_DOCUMENTS/nrcs142p2_050915.pdf]



- Song, C., B. Yan, Y. Wang, Y. Wang, Y. Lou, and Z. Zhao, 2003: Fluxes of carbon dioxide and methane from swamp and impact factors in Sanjiang Plain, China. *Chinese Science Bulletin*, **48**(24), 2749-2753, doi: 10.1007/bf02901769.
- Song, C., X.U. Xiaofeng, H. Tian, Y. Wang, 2009: Ecosystem-atmosphere exchange of CH₄ and N₂O and ecosystem respiration in wetlands in the Sanjiang Plain, Northeastern China. *Global Change Biology*, **59**, 692-705.
- Stanturf, J. A., E. S. Gardiner, P. B. Hamel, M. S. Devall, T. D. Leininger, and M. E. Warren, 2000: Restoring bottomland hardwood ecosystems in the lower Mississippi Alluvial Valley. *Journal of Forestry*, **98**(8), 10-16.
- Stavins, R. N., and A. B. Jaffe, 1990: Unintended impacts of public investments on private decisions: The depletion of forested wetlands. *American Economic Review*, **80**(3), 337-352.
- Stinson, G., W.A. Kurz, C.E. Smyth, E.T. Neilson, C.C. Dymond, J.M. Metsaranta, C. Boisvenue, G.J. Rampley, Q. Li, T.M. White, and D. Blain, 2011: An inventory-based analyses of Canada's managed forest carbon dynamics, 1990-2008. *Global Change Biology*, **17**, 2227-2244.
- Strachan, I. B., K. A. Nugent, S. Crombie, and M.-C. Bonneville, 2015: Carbon dioxide and methane exchange at a cool-temperate freshwater marsh. *Environmental Research Letters*, **10**(6), 065006, doi: 10.1088/1748-9326/10/6/065006.
- Strack, M., and J. M. Waddington, 2007: Response of peatland carbon dioxide and methane fluxes to a water table drawdown experiment. *Global Biogeochemical Cycles*, **21**(1), doi: 10.1029/2006GB002715.
- Strack, M., J. M. Waddington, and E. S. Tuittila, 2004: Effect of water table drawdown on northern peatland methane dynamics: Implications for climate change. *Global Biogeochemical Cycles*, **18**(4), doi: 10.1029/2003GB002209.
- Sulman, B., A. R. Desai, B. D. Cook, N. Saliendra, and D. S. Mackay, 2009: Contrasting carbon dioxide fluxes between a drying shrub wetland in Northern Wisconsin, USA, and nearby forests. *Biogeosciences*, **6**, 1115-1126, doi:10.5194/bg-6-1115-2009.
- Sulman, B. N., A. R. Desai, N. M. Schroeder, D. Ricciuto, A. Barr, A. D. Richardson, L. B. Flanagan, P. M. Lafleur, H. Tian, and G. Chen, 2012: Impact of hydrological variations on modeling of peatland CO₂ fluxes: Results from the North American Carbon Program site synthesis. *Journal of Geophysical Research: Biosciences*, **117**, G01031, doi:10.1029/2011JG001862.
- Svensson, B. H., and T. Rosswall, 1984: *In situ* methane production from acid peat in plant communities with different moisture regimes in a subarctic mire. *Oikos*, **43**(3), 341, doi: 10.2307/3544151.
- Swartwout, D.J., W.P. MacConnell, and J.T. Finn, 1981: An evaluation of the National Wetlands Inventory in Massachusetts. In: *The In-Place Resource Inventories Workshop*. Orono, ME, USA.
- Syed, K. H., L. B. Flanagan, P. Carlson, A. Glenn, and K. E. V. Gaalen, 2006: Environmental control of net ecosystem CO₂ exchange in a treed, moderately rich fen in northern Alberta. *Agricultural and Forest Meteorology*, **140**(1-4), 97-114, doi:10.1016/j.agrformet.2006.03.022.
- Tangen, B. A., R. G. Finocchiaro, and R. A. Gleason, 2015: Effects of land use on greenhouse gas fluxes and soil properties of wetland catchments in the prairie pothole region of North America. *Science of the Total Environment*, **533**, 391-409, doi: 10.1016/j.scitotenv.2015.06.148.
- Tarnocai, C., 2006: The effect of climate change on carbon in Canadian peatlands. *Global and Planetary Change*, **53**(4), 222-232, doi: 10.1016/j.gloplacha.2006.03.012.
- Tarnocai, C., 2009: The impact of climate change on Canadian peatlands. *Canadian Water Resources Journal*, **34**(4), 453-466.
- Tarnocai, C., I. M. Kettles, and B. P. Lacelle, 2005: *Peatlands of Canada*. R. B. Agriculture and Agri-Food Canada.
- Tarnocai, C., I.M. Kettles, and B.P. Lacelle, 2011: *Peatlands of Canada*. Geological Survey of Canada, Open File 6561.
- Tian, H., X. Xu, M. Liu, W. Ren, C. Zhang, G. Chen, and C. Lu, 2010: Spatial and temporal patterns of CH₄ and N₂O fluxes in terrestrial ecosystems of North America during 1979-2008: Application of a global biogeochemistry model. *Biogeosciences*, **7**, 2673-2694, doi: 10.5194/bg-7-2673-2010.
- Tolonen, K., and J. Turunen, 1996: Accumulation rates of carbon in mires in Finland and implications for climate change. *The Holocene*, **6**(2), 171-178, doi: 10.1177/095968369600600204.
- Trettin, C. C., R. Laiho, K. Minkkinen, and J. Laine, 2006: Influence of climate change factors on carbon dynamics in northern forested peatlands. *Canadian Journal of Soil Science*, **86**(2), 269-280, doi: 10.4141/s05-089.
- Trettin, C. C., M. F. Jurgensen, M. R. Gale, and J. W. McLaughlin, 2011: Recovery of carbon and nutrient pools in a northern forested wetland 11 years after harvesting and site preparation. *Forest Ecology and Management*, **262**(9), 1826-1833, doi: 10.1016/j.foreco.2011.07.031.
- Turetsky, M. R., W. F. Donahue, and B. W. Benscotter, 2011a: Experimental drying intensifies burning and carbon losses in a northern peatland. *Nature Communications*, **2**, 514, doi: 10.1038/ncomms1523.
- Turetsky, M. R., E. S. Kane, J. W. Harden, R. D. Ottmar, K. L. Manies, E. Hoy, and E. S. Kasichke, 2011b: Recent acceleration of biomass burning and carbon losses in Alaskan forests and peatlands. *Nature Geoscience*, **4**(1), 27-31, doi: 10.1038/ngeo1027.



- Turetsky, M. R., R. K. Wieder, D. H. Vitt, R. J. Evans, and K. D. Scott, 2007: The disappearance of relict permafrost in boreal North America: Effects on peatland carbon storage and fluxes. *Global Change Biology*, **13**(9), 1922-1934, doi: 10.1111/j.1365-2486.2007.01381.x.
- Turetsky, M. R., A. Kotowska, J. Bubier, N. B. Dise, P. Crill, E. R. Hornibrook, K. Minkinen, T. R. Moore, I. H. Myers-Smith, H. Nykanen, D. Olefeldt, J. Rinne, S. Saarnio, N. Shurpali, E. S. Tuittila, J. M. Waddington, J. R. White, K. P. Wickland, and M. Wilming, 2014: A synthesis of methane emissions from 71 northern, temperate, and subtropical wetlands. *Global Change Biology*, **20**(7), 2183-2197, doi: 10.1111/gcb.12580.
- Turner, R. E., A. M. Redmond, and J. B. Zedler, 2001: Count it by acre or function—mitigation adds up to net loss of wetlands. *National Wetlands Newsletter*, **23**(6). [<https://www.eli.org>]
- Updegraff, K., S. D. Bridgman, J. Pastor, P. Weishampel, and C. Harth, 2001: Response of CO₂ and CH₄ emissions from peatlands to warming and water table manipulation. *Ecological Applications*, **11**(2), 311-326, doi: 10.1890/1051-0761(2001)011[0311:roca-ce]2.0.co;2.
- U.S. EPA, 2015: Section 404 and swampbuster. In: *Wetlands on Agricultural Lands*. [<https://www.epa.gov/cwa-404/section-404-and-swampbuster-wetlands-agricultural-lands>]
- U.S. EPA, 2016: National Wetland Condition Assessment 2011: A Collaborative Survey of the Nation's Wetlands. EPA Report EPA-843-R-15-005. [<https://www.epa.gov/national-aquatic-resource-surveys/nwca>]
- USACE, 2008: *Compensatory Mitigation for Losses of Aquatic Resources*. U.S. Corps of Engineers and U.S. Environmental Protection Agency. Federal Register, **73**(70), 19594-19705 pp. [<http://www.gpo.gov/fdsys/pkg/FR-2008-04-10/pdf/E8-6918.pdf>]
- USDA, 2014: ACEP—Agricultural Conservation Easement Program: Natural Resource Conservation Service. U.S. Department of Agriculture. [<https://www.nrcs.usda.gov/wps/portal/nrcs/main/national/programs/easements/acep/>]
- USDA Forest Service Forest Inventory and Analysis Database, 2003. [<https://data.fs.usda.gov/geodata/rastergateway/biomass/>]
- USFWS, 2011: *Status and Trends of Wetlands in the Conterminous United States 2004 to 2009, Report to Congress*. [<https://www.fws.gov/wetlands/status-and-trends/>]
- Van Seters, T. E., and J. S. Price, 2001: The impact of peat harvesting and natural regeneration on the water balance of an abandoned cutover bog, Quebec. *Hydrological Processes*, **15**(2), 233-248, doi: 10.1002/hyp.145.
- Villa, J. A., W. J. Mitsch, K. Song, and S. Miao, 2014: Contribution of different wetland plant species to the DOC exported from a mesocosm experiment in the Florida Everglades. *Ecological Engineering*, **71**, 118-125, doi: 10.1016/j.ecoleng.2014.07.011.
- Villa, J. A. and W. J. Mitsch, 2014: Methane emissions from five wetland plant communities with different hydroperiods in the Big Cypress Swamp region of Florida Everglades. *Ecology and Hydrobiology*, **14**, 253-266.
- Waddington, J. M., T. J. Griffis, and W. R. Rouse, 1998: Northern Canadian wetlands: Net ecosystem CO₂ exchange and climatic change. *Climatic Change*, **40**(2), 267-275, doi: 10.1023/a:1005468920206.
- Waddington, J. M., P. J. Morris, N. Kettridge, G. Granath, D. K. Thompson, and P. A. Moore, 2015: Hydrological feedbacks in northern peatlands. *Ecology and Hydrobiology*, **8**(1), 113-127, doi: 10.1002/eco.1493.
- Waddington, J. M., D. K. Thompson, M. Wotton, W. L. Quinton, M. D. Flannigan, B. W. Benschoter, S. A. Baisley, and M. R. Turetsky, 2012: Examining the utility of the Canadian forest fire weather index system in boreal peatlands. *Canadian Journal of Forest Research*, **42**(1), 47-58, doi: 10.1139/x11-162.
- Wang, H. J., C. J. Richardson, and M. C. Ho, 2015: Dual controls on carbon loss during drought in peatlands. *Nature Climate Change*, **5**(6), 584-587, doi: 10.1038/nclimate2643.
- Wang, J.M., J.G. Murphy, J. A. Geddes, C.L. Winsborough, N. Basiliko, and S.C. Thomas, 2013: Methane fluxes measured by eddy covariance and static chamber techniques at a temperate forest in central Ontario, Canada. *Biogeosciences*, **10**, 4371-4382, doi: 10.5194/bg-10-4371-2013.
- Ward, S. E., R. D. Bardgett, N. P. McNamara, J. K. Adamson, and N. J. Ostle, 2007: Long-term consequences of grazing and burning on northern peatland carbon dynamics. *Ecosystems*, **10**(7), 1069-1083, doi: 10.1007/s10021-007-9080-5.
- Warner, B.G., 2005: *Canadian Peatlands*. Neue Serie **35**, 353-372. [https://www.zobodat.at/pdf/STAPFIA_0085_0353-0372.pdf]
- Werner, C., K. Davis, P. Bakwin, C. Yi, D. Hurst, and L. Lock, 2003: Regional-scale measurements of CH₄ exchange from a tall tower over a mixed temperate/boreal lowland and wetland forest. *Global Change Biology*, **9**(9), 1251-1261, doi: 10.1046/j.1365-2486.2003.00670.x.
- West, A. E., P. D. Brooks, M. C. Fisk, L. K. Smith, E. A. Holland, I. C. H. Jaeger, S. Babcock, R. S. Lai, and S. K. Schmidt, 1999: Landscape patterns of CH₄ fluxes in an Alpine tundra ecosystem. *Biogeochemistry*, **45**(3), 243-264, doi: 10.1023/a:1006130911046.
- Wickland, K. P., R. G. Striegl, S. K. Schmidt, and M. A. Mast, 1999: Methane flux in subalpine wetland and unsaturated soils in the southern Rocky Mountains. *Global Biogeochemical Cycles*, **13**(1), 101-113, doi: 10.1029/1998GB900003.



- Wickland, K. P., A. V. Krusche, R. K. Kolka, A. W. Kishimoto-Mo, R. A. Chimner, Y. Serengil, S. Ogle, and N. Srivastava, 2014: Inland wetland mineral soils. In: *Supplement to the 2006 Intergovernmental Panel on Climate Change Guidelines for National Greenhouse Gas Inventories: Wetlands*. [Hiraishi, T., Krug, T., Tanabe, K., Srivastava, N., Baasansuren, J., Fukuda, M. and Troxler, T.G. (eds.)]. Switzerland. 354 pp. [<http://www.ipcc-nggip.iges.or.jp/public/wetlands/>]
- Wieder, R. K., J. Yavitt, and G. Lang, 1990: Methane production and sulfate reduction in two Appalachian peatlands. *Biogeochemistry*, **10**(2), doi: 10.1007/bf00002225.
- Wilson, J. O., P. M. Crill, K. B. Bartlett, D. I. Sebacher, R. C. Harriss, and R. L. Sass, 1989: Seasonal variation of methane emissions from a temperate swamp. *Biogeochemistry*, **8**(1), 55-71, doi: 10.1007/bf02180167.
- Winter, T. C., and D. O. Rosenberry, 1998: Hydrology of prairie pothole wetlands during drought and deluge: A 17-year study of the Cottonwood Lake wetland complex in North Dakota in the perspective of longer term measured and proxy hydrological records. *Climatic Change*, **40**(2), 189-209, doi: 10.1023/a:1005448416571.
- Winton, R. S., and C. J. Richardson, 2015: The effects of organic matter amendments on greenhouse gas emissions from a mitigation wetland in Virginia's coastal plain. *Wetlands*, **35**(5), 969-979, doi: 10.1007/s13157-015-0674-y.
- Yang, L., F. Lu, X. Wang, X. Duan, W. Song, B. Sun, S. Chen, Q. Zhang, P. Hou, F. Zheng, Y. Zhang, X. Zhou, Y. Zhou, and Z. Ouyang, 2012: Surface methane emissions from different land use types during various water levels in three major drawdown areas of the Three Gorges Reservoir. *Journal of Geophysical Research: Atmospheres*, **117**(D10), doi: 10.1029/2011jd017362.
- Yavitt, J.B., 1997: Methane and carbon dioxide dynamics in *Typha latifolia* (L.) wetlands in central New York state. *Wetlands*, **17**, 394-406.
- Yavitt, J. B., G. E. Lang, and A. J. Sexstone, 1990: Methane fluxes in wetland and forest soils, beaver ponds, and low-order streams of a temperate forest ecosystem. *Journal of Geophysical Research*, **95**(D13), 22463, doi: 10.1029/JD095iD13p22463.
- Yavitt, J. B., J. A. Simmons, and T. J. Fahey, 1993: Methane fluxes in a northern hardwood forest ecosystem in relation to acid precipitation. *Chemosphere*, **26**(1-4), 721-730, doi: 10.1016/0045-6535(93)90456-f.
- Yavitt, J. B., C. J. Williams, and R. K. Wieder, 1997: Production of methane and carbon dioxide in peatland ecosystems across North America: Effects of temperature, aeration, and organic chemistry of peat. *Geomicrobiology Journal*, **14**(4), 299-316, doi: 10.1080/01490459709378054.
- Yu, K., S. P. Faulkner, and M. J. Baldwin, 2008: Effect of hydrological conditions on nitrous oxide, methane, and carbon dioxide dynamics in a bottomland hardwood forest and its implication for soil carbon sequestration. *Global Change Biology*, **14**(4), 798-812, doi: 10.1111/j.1365-2486.2008.01545.x.
- Yu, K. H., Z.K. Jin, K. Su, X.D. Dong, W. Zhang, H.U. Du, , Y. Chen, and W.D. Zhang, 2013: The Cambrian sedimentary characteristics and their implications for oil and gas exploration in north margin of Middle-Upper Yangtze Plate. *Science China: Earth Sciences*, **56**, 1014-1028, doi: 10.1007/s11430-013-4611-8.
- Yu, Z., J. Loisel, D. P. Brosseau, D. W. Beilman, and S. J. Hunt, 2010: Global peatland dynamics since the Last Glacial Maximum. *Geophysical Research Letters*, **37**, L13402, doi: 10.1029/2010GL043584.
- Zhang, B., H. Tian, C. Lu, G. Chen, S. Pan, C. Anderson, and B. Poulter, 2017a: Methane emissions from global wetlands: An assessment of the uncertainty associated with various wetland extent data sets. *Atmospheric Environment*, **165**, 310-321, doi: 10.1016/j.atmosenv.2017.01.001.
- Zhang, Z., N.E. Zimmermann, A. Stenke, X. Li, E.L. Hodson, G. Zhu, C. Huang, and B. Poulter, 2017b: Emerging role of wetland methane emissions in driving 21st century climate change. *Proceedings of the National Academy of Sciences USA*, **114** (36), 9647-9652, doi: 10.1073/pnas.1618765114.
- Zhu, Z., and A. D. McGuire, 2010: *A Method for Assessing Carbon Stocks, Carbon Sequestration, and Greenhouse-Gas Fluxes in Ecosystems of the United States Under Present Conditions and Future Scenarios*. U.S. Geological Survey Scientific Investigations Report 2010-5233. [Z. Zhu, (ed.)], 188 pp. [<https://pubs.usgs.gov/sir/2010/5233/>]
- Zhu, Z., and A. D. McGuire, 2011: *Baseline and Projected Future Carbon Storage and Greenhouse-Gas Fluxes in the Great Plains Region of the United States*. U.S. Geological Survey Professional Paper 1787. [Z. Zhu, (ed.)], 28 pp. [<https://pubs.usgs.gov/pp/1787/>]
- Zhu, Z., and B. Reed, 2012: *Baseline and Projected Future Carbon Storage and Greenhouse-Gas Fluxes in Ecosystems of the Western United States*. U.S. Geological Survey Professional Paper 1797. 192 pp. [<http://pubs.usgs.gov/pp/1797/>]
- Zhu, Z., and B. C. Reed, 2014: *Baseline and Projected Future Carbon Storage and Greenhouse-Gas Fluxes in Ecosystems of the Eastern United States*. U.S. Geological Survey Professional Paper 1804. 214 pp. [<https://pubs.usgs.gov/pp/1804/>]
- Zhu, Z., and A. D. McGuire, 2016: *Baseline and Projected Future Carbon Storage and Greenhouse-Gas Fluxes in Ecosystems of Alaska*. U.S. Geological Survey Professional Paper 1826. [Z. Zhu and A. D. McGuire, (eds.)], 196 pp. [<https://pubs.er.usgs.gov/publication/pp1826>]
- Zoltai, S. C., and D. H. Vitt, 1995: Canadian wetlands: Environmental gradients and classification. *Vegetatio*, **118**(1-2), 131-137, doi: 10.1007/bf00045195.



Appendix 13A

Terrestrial Wetland Area and Carbon Pools

Prepared by Carl Trettin,¹ Wenwu Tang,² and Steven Campbell³

¹USDA Forest Service; ²University of North Carolina, Charlotte; ³USDA Natural Resources Conservation Service

13A.1 Introduction

This appendix provides the methodologies and data used to estimate the area and carbon pools of terrestrial wetlands in North America. Since the *First State of the Carbon Cycle Report* (SOCCR1; CCSP 2007), several developed geospatial databases have provided the opportunity to improve the estimation of carbon pools beyond what is feasible using area density factors. The development of the Gridded Soil Survey Geographic (gSSURGO) database by the U.S. Department of Agriculture's (USDA) Natural Resources Conservation Service (NRCS) was a particularly important advancement, availing gridded soil survey information for the United States and Puerto Rico. Similarly, the USDA Forest Service's Forest Inventory and Analysis (FIA) database uses forest biomass data for the United States, thereby facilitating its incorporation into carbon pool assessments. Sections 13A.2–13A.6 detail the

data and methods used to obtain the reported wetland area and carbon pools.

13A.2 Conterminous United States

13A.2.1 Approach

The U.S. Fish and Wildlife Service's (USFWS) National Wetlands Inventory (NWI) was used as the basis for identifying terrestrial (i.e., nontidal) freshwater wetlands within the conterminous United States (CONUS) and for distinguishing between forested and nonforested wetlands. Subsequently, geospatial databases were used to calculate the carbon pools in soils and forests. Specifically, the gSSURGO database was used to calculate soil carbon, and the FIA database was used to calculate forest carbon based on the reported biomass. A carbon pool density factor was used for the nonforest vegetation biomass because an appropriate geospatial database was not available.

13A.2.2 Data

The datasets used for analyses of the wetland area and carbon pool computations are summarized in Table 13A.1, this page.

Table 13A.1. Source Datasets

Dataset	Year	Publisher	Download Link
Gridded Soil Survey Geographic (gSSURGO)	2016	U.S. Department of Agriculture (USDA) Natural Resources Conservation Service (NRCS)	gdg.sc.egov.usda.gov
National Wetlands Inventory (NWI)	2015	U.S. Fish and Wildlife Service	www.fws.gov/wetlands/Data/State-Downloads.html
Forest Inventory Analysis (FIA) Forest Biomass	2003	USDA Forest Service FIA	data.fs.usda.gov/geodata/rastergateway/biomass/index.php
Value-Added Look Up Table Database	2016	USDA NRCS	gdg.sc.egov.usda.gov
Cartographic Boundary	2015	U.S. Census Bureau	www.census.gov/geo/maps-data/data/cbf/cbf_state.html

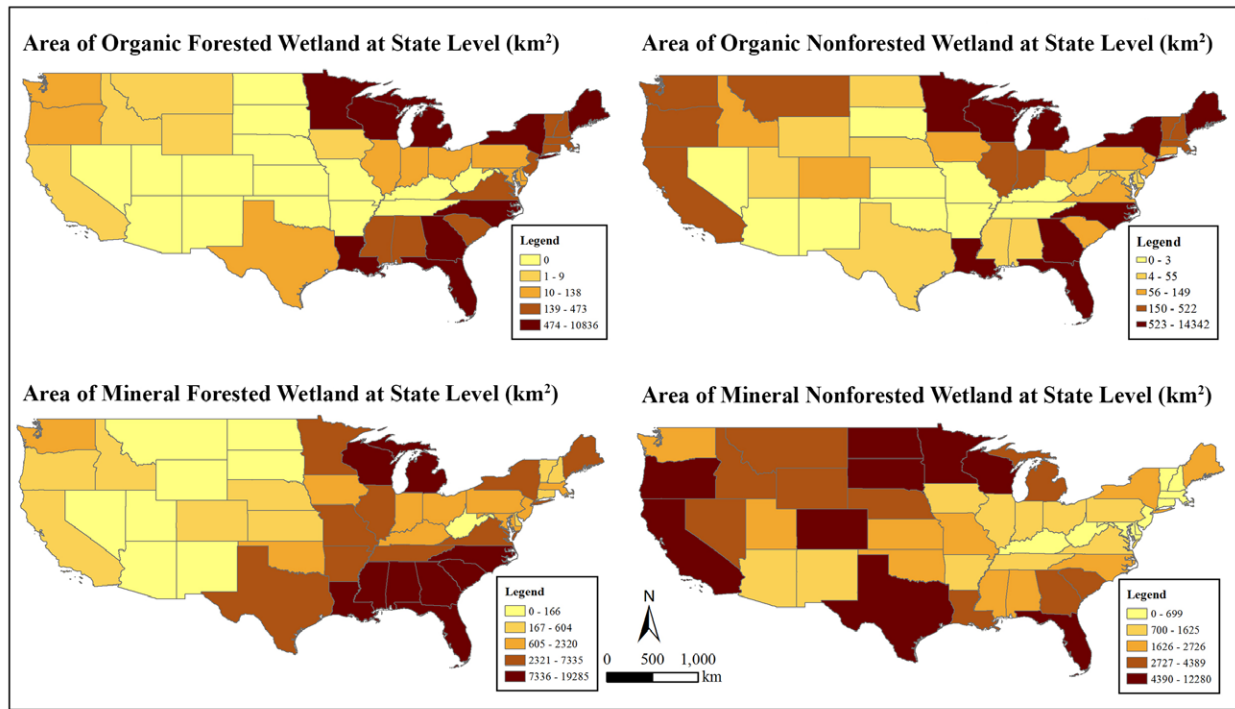


Figure 13A.1. Areal Distribution Among U.S. States of the Four Categories of Freshwater Terrestrial Wetlands. These wetland types are organic forested, organic nonforested, mineral forested, and mineral nonforested.

13A.2.3 Results

Wetland Area

According to NWI data, there are 395,197 km² of terrestrial freshwater wetlands in CONUS, 54% of which are forested and 46% nonforested (see Table 13A.2, this page). The estimate of forested freshwater wetlands is within 2% of the most recent NWI report; the total area of freshwater forested wetlands is calculated as 213,914 km², compared with 208,912 km² for 2009 from Dahl (2011). This area is smaller than the wetland area used in SOCCRI (405,670 km²; CCSP 2007) because that report also included tidal wetlands. Mineral soils compose 79% of the terrestrial wetlands, with 21% being organic or peat soils (see Table 13A.2, this page). The distribution of wetlands among soil (organic and mineral) and vegetation (forest and nonforest) categories among states is presented in Figure 13A.1, this page.

The accuracy of the NWI data is considered to be over 90% for large wetlands (i.e., those > 1 hectare);

Table 13A.2. Area of Forested and Nonforested Terrestrial Wetland and Related Soil Types in the United States

Soil Type	Forested Wetlands (km ²)	Nonforested Wetlands (km ²)	Total (km ²)
Organic Soil	40,823	42,903	83,726
Mineral Soil	173,091	138,381	311,472
Total	213,914	181,283	395,197

uncertainties increase with smaller wetlands (Nichols 1994). Independent field-based studies also have been conducted to evaluate the accuracy of the NWI data for wetland mapping. The reported accuracies ranged from over 90% of overall accuracy in Michigan, Maine, and Massachusetts (see Kudray and Gale 2000; Nichols 1994; Swartwout et al., 1981) to underestimation of wetland area by 39% in Vermont



(see Morrissey and Sweeney 2006). With these issues considered, the NWI data are recognized as a reasonable source for estimating wetland area, particularly at large spatial extents, and thus are the source for national-level reporting.

Wetland Carbon Stock Estimation

Carbon stocks were calculated based on soil carbon content calculated from gSSURGO, forest biomass extracted from the FIA database, and a biomass density factor for nonforest vegetation. Forest vegetation consists of a carbon stock of about 0.878 petagrams of carbon (Pg C), with 79% occurring on mineral soils; nonforest vegetation contributed approximately 0.093 Pg C (see Table 13A.3, this page). Integrating forest biomass and soil carbon pools yields approximately 13.5 Pg C in terrestrial wetlands (see Table 13A.4, this page). The breakdown of carbon within forested and nonforested wetlands and of mineral and organic soils by state is summarized in Table 13A.4.

13A.3 Alaska

13A.3.1 Approach

The NWI and traditional soil surveys of Alaska are not available for the entire state. Fortunately, Clewley et al. (2015) recently published an inventory of wetlands based on remote-sensing data that used the Cowardin Classification system for representing the distribution of wetland types. Similarly, NRCS has produced a gSSURGO dataset for Alaska. Accordingly, those datasets were used as the basis for estimating the terrestrial wetland categories and carbon stocks following the same general approach used for CONUS. The combination of the wetland and carbon stock assessment with the distribution of frozen wetlands is considered to provide a comprehensive assessment of wetlands for the state.

13A.3.2 Data

Table 13A.5, p. 550, presents the principal datasets used in this study that include information on soil, wetlands, soil organic carbon, permafrost, and elevation.

Table 13A.3. Carbon Stock in Forest and Nonforest Biomass Within Organic and Mineral Soil Terrestrial Wetlands^a

Soil Type	Forest Carbon Pool (Pg C)	Nonforest Carbon Pool (Pg C)
Organic Soil	0.185	0.022
Mineral Soil	0.693	0.071
Total	0.878	0.093

Notes

a) Carbon stocks are measured in petagrams of carbon (Pg C) within the conterminous United States.

Table 13A.4. Carbon Stocks Within Organic and Mineral Soil, and Forested and Nonforested Freshwater Wetlands^a

Soil Type	Forested Wetlands (Pg C)	Nonforested Wetlands (Pg C)	Total (Pg C)
Organic Soil	4.45	3.88	8.34
Mineral Soil	3.26	1.94	5.21
Total	7.71	5.82	13.55

Notes

a) Carbon stocks are measured in petagrams of carbon (Pg C) within the conterminous United States.

13A.3.3 Results

Wetland Area

The total area of freshwater wetlands in Alaska, based on the Clewley et al. (2015) database, is 579,645 km² (see Table 13A.6, p. 550). The wetland data were classified from ALOS PALSAR² remote-sensing data using a random forest-based classifier. The data were processed using the adjustment factor employed by Clewley et al. (2015) to calculate the total area of freshwater wetlands, and data that overlapped into Canada were excluded. The overall accuracy of the classification is 84.5% for distinguishing specific wetland types and 94.7% for distinguishing wetlands with uplands (Clewley

² Advanced Land Observing Satellite-1 (ALOS) Phased Array type L-band Synthetic Aperture Radar (PALSAR)



Table 13A.5. Datasets Used to Estimate the Distribution and Carbon Stocks of Alaskan Terrestrial Wetlands^{a-b}

Dataset	Year	Publisher	Download Link
Alaska Wetlands (Clewley et al., 2015)	2007	Alaska Satellite Facility	www.asf.alaska.edu/sar-data/palsar
STATSGO2	2014	U.S. Department of Agriculture (USDA) Natural Resources Conservation Service	www.nrcs.usda.gov/wps/portal/nrcs/detail/soils/survey/geo/?cid=nrcs142p2_053629
Organic Soil Probability	2016	U.S. Geological Survey (USGS) LandCarbon	pubs.er.usgs.gov/publication/pp1826
Forest Biomass	2002	USDA Forest Service Forest Inventory and Analysis	data.fs.usda.gov/geodata/rastergateway/biomass
Probability of Near-Surface 1-m Permafrost	2015	USGS ^a	sciencebase.gov/catalog/item/5602ab5ae4b03bc34f5448b4
STATSGO Depth of Permafrost	2012	USGS ^a	ckan.snap.uaf.edu/dataset/depth-to-permafrost-alaska-landcarbon-project
STATSGO Permafrost Soil	2014	USDA Natural Resources Conservation Service ^b	www.nrcs.usda.gov/wps/portal/nrcs/detail/soils/survey/geo/?cid=nrcs142p2_053629
Alaska State Boundary	2016	U.S. Census Bureau	www.census.gov/geo/maps-data/data/cbf/cbf_state.html
Elevation	1996	USGS	agdc.usgs.gov/data/usgs/erosafo/dem/dem.html

Notes

- a) Provided by Neal Pastick, USGS.
- b) Provided by Steve Campbell, USDA Natural Resources Conservation Service.

et al., 2015). The NWI class was used to aggregate the areas into forested and nonforested types.

Also calculated was the total area of wetlands in Alaska from STATSGO2 data using the percent in hydric soil attribute (“hydric_pct”; i.e., the percent in hydric soil). The total area is 587,143.9 km² based on the STATSGO2 percentage of hydric soils, which is very close to that provided by the Clewley et al. (2015) dataset.

Soil organic carbon data from STATSGO2 were employed to estimate the area of organic soils in Alaska, using the variable named “hydric_org_pct” (i.e., the percent in hydric organic soil) as the basis. This variable was multiplied by the area of map units (polygons) in the STATSGO2 dataset to obtain the area of peatland within each map

Table 13A.6. Area of Four Terrestrial Wetland Types in Alaska

Soil Type	Forested (km ²)	Nonforested (km ²)	Total (km ²)
Organic	9,947	97,111	107,057
Mineral	54,858	417,729	472,587
Total	64,805	514,840	579,645

unit. The total area of peatlands estimated from STATSGO2 using the hydric organic soil attribute is 107,057 km².

Incorporating the distribution of organic soils into the overlay analyses yielded the distribution and area of the four wetland categories (see Figure 13A.2, p. 551). The total area of the four wetland

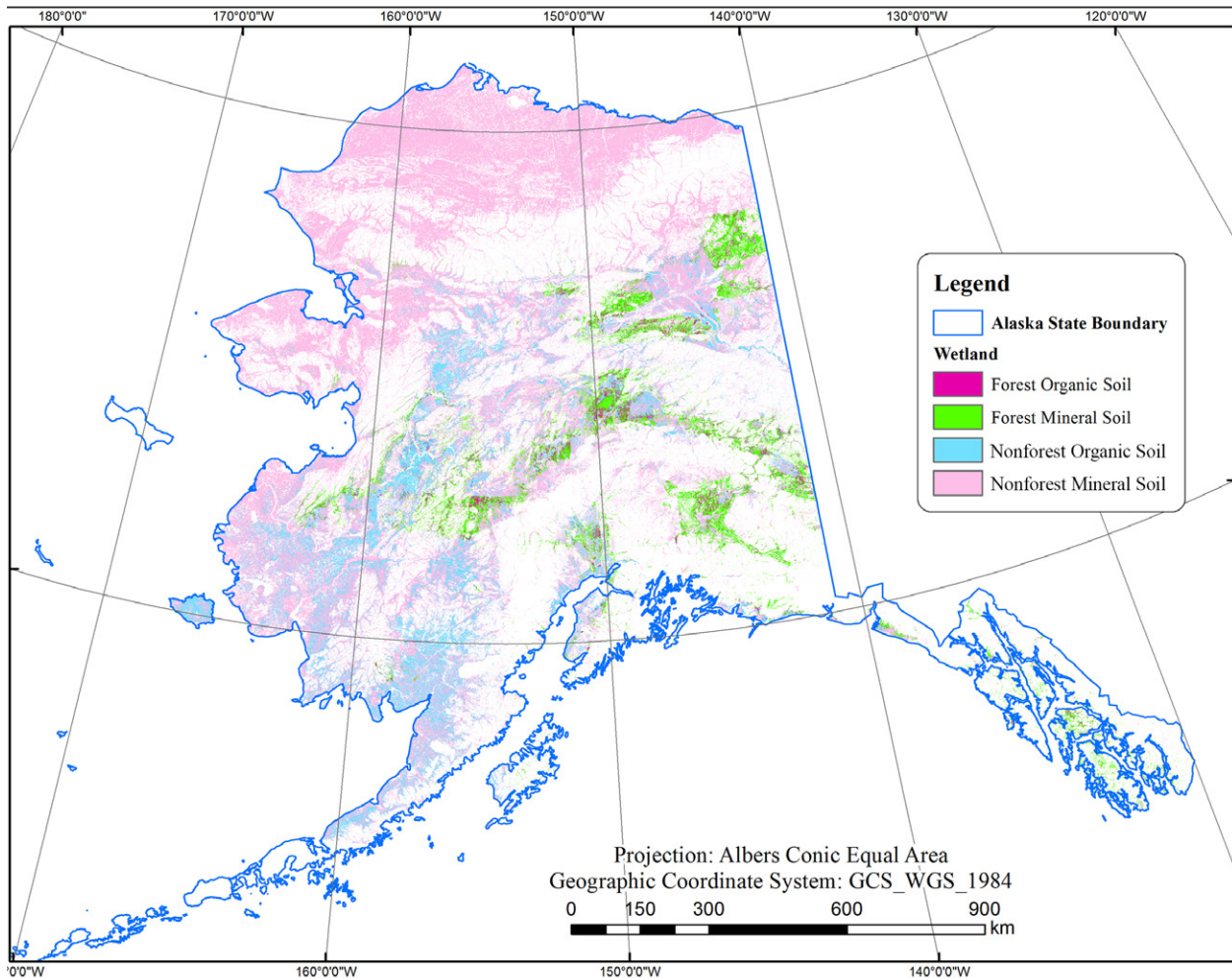


Figure 13A.2. Areal Distribution in Alaska of the Four Categories of Terrestrial Wetlands. These wetland types are forest organic soil, forest mineral soil, nonforest organic soil, and nonforest mineral soil.

categories of freshwater wetlands in Alaska are summarized in Table 13A.6, p. 550.

Assessing the overlap of wetlands and permafrost areas provided a basis for distinguishing carbon stocks. The use of the USGS probability map of permafrost provided a cut-off threshold of 60% to permafrost occurring within 1 m of the surface (with a 30-m spatial resolution). The resultant area of permafrost is 405,891 km², compared with 548,503 km² based on permafrost 2 m in depth from STATSGO2 data. Overlaying the USGS permafrost area with the wetlands shows that the total area of

wetlands within the permafrost region is 267,887 km², which is approximately 46% of the total wetland area. The areas of the four types of freshwater wetlands in Alaska within permafrost or nonpermafrost regions are presented in Table 13A.7, p. 552.

Wetland Carbon Stocks

Ecosystem carbon stocks for the four wetland categories were derived from soil carbon stocks from USDA STATSGO data, biomass carbon data from FIA for forests, and a density factor for nonforested wetlands (see Table 13A.8, p. 552).

**Table 13A.7. Distribution of Wetland Types Among Areas With and Without Permafrost in Alaska**

Soil Type		Forested (km ²)	Nonforested (km ²)	Total (km ²)
Permafrost	Organic	4,199	23,274	27,474
	Mineral	14,696	225,716	240,413
	Total	18,895	248,991	267,887
Nonpermafrost	Organic	5,747	73,836	79,584
	Mineral	40,162	192,013	232,175
	Total	45,910	265,849	311,759

Table 13A.8. Total Carbon Pool of the Four Wetland Categories in Alaska^a

Soil Type	Forested (Pg C)	Nonforested (Pg C)	Total Carbon (Pg C)
Organic	0.70	7.09	7.79
Mineral	2.80	21.21	24.01
Total	3.50	28.31	31.80

Notes

a) Carbon stocks are measured in petagrams of carbon (Pg C).

Partitioning the ecosystem carbon pools among wetlands in permafrost and nonpermafrost zones is provided in Table 13A.9, p. 553. Approximately 46% of the wetland carbon pool occurs within the permafrost areas.

13A.4 Puerto Rico

13A.4.1 Approach

The approaches to quantifying the distribution of terrestrial wetlands and the associated carbon pools for Puerto Rico follow those of CONUS, where a suite of datasets was used, including gSSURGO, NWI, Value-Added Look Up Table Dataset, Cartographic Boundary Shapefile, and FIA Forest Biomass Dataset. An overlay analysis was conducted between NWI and gSSURGO to identify vegetation and soil types for wetlands. Cartographic Boundary identified the boundary of Puerto Rico. The FIA Forest Biomass dataset provided the forest biomass information. Soil

Data Development Tools for ArcGIS were used to extract the soil class of freshwater wetlands.

13A.4.2 Data

Datasets used in this study are summarized in Table 13A.10, p. 553.

13A.4.3 Results

Wetland Area

The total area of terrestrial wetlands derived from NWI data is 311.4 km². However, gSSURGO data coverage was missing for approximately 9.8% of the terrestrial wetland area. Distributing the area of missing soil data among the forested and nonforested categories yields the final area of the four wetland categories (see Table 13A.11, p. 553).

Ecosystem Carbon Pool

Ecosystem carbon pools, including soil and biomass, for freshwater wetlands in Puerto Rico are summarized in Table 13A.12, p. 553.

13A.5 Canada

13A.5.1 Approach

Canadian terrestrial freshwater wetlands were estimated based on a combination of spatial data because there was not a single wetland database that could produce estimates of organic and mineral soil wetlands and of forest and nonforest vegetation.

13A.5.2 Data

Datasets in this study are summarized in Table 13A.13, p. 554.



Table 13A.9. Ecosystem Carbon Pools in Freshwater Wetlands Occurring in Permafrost and Nonpermafrost Areas in Alaska^a

Soil Type		Forested (Pg C)	Nonforested (Pg C)	Total Carbon (Pg C)
Permafrost	Organic	0.27	1.56	1.83
	Mineral	0.83	11.87	12.70
	Total	1.11	13.43	14.53
Nonpermafrost	Organic	0.42	5.54	5.96
	Mineral	1.97	9.34	11.30
	Total	2.39	14.88	17.26

Notes

a) Carbon stocks are measured in petagrams of carbon (Pg C).

Table 13A.10. Datasets Used to Estimate Terrestrial Wetland Area and Carbon Pools in Puerto Rico

Dataset	Year	Provider	Download Link
Gridded Soil Survey Geographic (gSSURGO)	2016	U.S. Department of Agriculture (USDA) Natural Resources Conservation Service	gdg.sc.egov.usda.gov
National Wetlands Inventory	2010	U.S. Fish and Wildlife Service	www.fws.gov/wetlands/Data/State-Downloads.html
Forest Biomass	2008	USDA Forest Service's Forest Inventory and Analysis	data.fs.usda.gov/geodata/rastergateway/biomass
Puerto Rico Boundary	2016	U.S. Census Bureau	www.census.gov/geo/maps-data/data/cbf/cbf_state.html

Table 13A.11. Area of Terrestrial Wetland Categories in Puerto Rico

Soil Type	Forested (km ²)	Nonforested (km ²)	Total (km ²)
Organic Soil	0.67	8.4	9.1
Mineral Soil	49.9	252.3	302.3
Total	50.6	260.7	311.4

13A.5.3 Results

Organic and Mineral Soil in Forested and Nonforested Terrestrial Wetlands in Canada

Organic and mineral soils for forested and nonforested wetlands were estimated by overlaying land-cover datasets (GLWD and North America land-cover data) with soil datasets (FAO soil data, Peatland Database of Canada, and Soil Landscape of Canada). Those analyses routinely underestimated wetland

Table 13A.12. Ecosystem Carbon Pools Among the Four Terrestrial Wetland Categories in Puerto Rico^a

Soil Type	Forested (Pg C)	Nonforested (Pg C)	Total (Pg C)
Organic Soil	0.000	0.001	0.001
Mineral Soil	0.001	0.006	0.007
Total	0.001	0.007	0.008

Notes

a) Carbon pools are measured in petagrams of carbon (Pg C).

area compared with estimates in published reports, especially for organic soils (Tarnocai 2006; Warner 2005; see Table 13A.14, p. 554, for examples of the differences in wetland area based on data sources).



Table 13A.13. Datasets Used in Canadian Terrestrial Wetland Assessment

Code ^a	Dataset	Year	Publisher	Download Link
W₁	North America Land Cover	2010	U.S. Geological Survey	landcover.usgs.gov/nalcms.php
W₂	Global Lakes and Wetlands Database Level 3 (GLWD-3)	2004	World Wild Life Organization; The Center for Environmental Systems Research, University of Kassel, Germany	worldwildlife.org/pages/global-lakes-and-wetlands-database
S₁	FAO/UNESCO ^b Digital Soil Map of the World 3.6	2007	Food and Agriculture Organization of the United Nations	fao.org/geonetwork/srv/en/metadata.show?id=14116
S₂	Soil Landscapes of Canada 3.2	2010	Agriculture and Agri-Food Canada	sis.agr.gc.ca/cansis/nsdb/slc/v3.2/index.html
S₃	Peatlands of Canada	2005	Natural Resources Canada	geogratis.gc.ca/api/en/nrcan-rncan/ess-sst/4e9e791c-ebad-594a-a3ba-14b8b974f239.html

Notes

- a) The *W₁* and *W₂* and *S₁*, *S₂*, and *S₃* abbreviations are used in this and subsequent tables to indicate, respectively, the wetlands and soils datasets outlined here.
- b) Key: FAO, U.N. Food and Agriculture Organization; UNESCO, United Nations Educational, Scientific and Cultural Organization.

Table 13A.14. Areas of Forested Wetland and Nonforested Terrestrial Wetland and Related Soils in Canada^{a-b}

Soil Type	<i>W₁</i> * <i>S₁</i> (km ²)			<i>W₁</i> * <i>S₂</i> (km ²)		
	Forested	Nonforested	Total	Forested	Nonforested	Total
Organic Soil	582,078	194,895	776,973	499,271	35,692	534,963
Mineral Soil	215,794	40,933	256,727	360,249	21,345	381,594
Total	797,872	235,828	1,033,700	859,520	57,037	916,557
Soil Type	<i>W₂</i> * <i>S₁</i> (km ²)			<i>W₂</i> * <i>S₂</i> (km ²)		
	Forested	Nonforested	Total	Forested	Nonforested	Total
Organic Soil	503,810	187,765	691,575	351,529	32,084	383,613
Mineral Soil	161,886	38,960	200,846	193,374	17,685	211,059
Total	665,696	226,725	892,421	544,903	49,769	594,672

Notes

- a) Areas estimated using different data sources.
- b) *W₁*: 2010 North America Land Cover dataset (wetland class available); *W₂*: Global Lakes and Wetlands Database; *S₁*: FAO/UNESCO Digital Soil Map of the World; *S₂*: Soil Landscapes of Canada; *S₃*: Peatlands of Canada dataset. Asterisk (*) denotes the use of multiple datasets (GIS-based overlay analysis applied).



Table 13A.15. Areas of Forested and Nonforested Wetland and Related Soil in Canada from Peatland Dataset (S₃)^a

Soil Type	Forested (km ²)	Nonforested (km ²)	Total (km ²)
Organic Soil	703,785	415,450	1,119,235
Mineral Soil	268,337	103,932	372,270
Total	972,122	519,382	1,491,505

Notes

a) S₃, Peatlands of Canada dataset.

Table 13A.16. Carbon Pools of Forested and Nonforested Wetland and Peat and Mineral Soils in Canada^a

Soil Type	Forested (Pg)	Nonforested (Pg)	Total ^a
Organic Soil	76.7	37.8	114.5
Mineral Soil	5.1	9.5	14.6
Total	81.8	47.3	129.0

Notes

a) Carbon pools are calculated in petagrams (Pg).

Table 13A.17. List of Datasets Used to Assess the Area of Terrestrial Wetlands in Mexico

Dataset	Year	Publisher	Download Link
North America Land Cover	2010	U.S. Geological Survey, Natural Resources Canada, Instituto Nacional de Estadística y Geografía (INEGI), Comisión Nacional para el Conocimiento y Uso de la Biodiversidad (CONABIO), and Comisión Nacional Forestal (CONAFOR)	landcover.usgs.gov/nalcms.php
Mapa Potencial de Humedales	2012	INEGI	www.inegi.org.mx/geo/contenidos/recreat/humedales/datosvec.aspx

Because the accepted area of peatlands is 1,135,610 km² as reported by Tarnocai (2006), it was used as the basis for the total peatland area; the 16,375 km² of permafrost peatlands (Tarnocai et al., 2011) were excluded from the final area table (see Table 13A.15, this page). Wetland-specific soil types from the Peatlands of Canada and the Soil Landscapes of Canada datasets were used to identify mineral and organic soil wetlands. The analysis of wetland area in Canada is based on the Peatlands of Canada database, which was updated from its previous version. The accuracy of the wetland area estimated using this database is equal to or greater than 66%, as suggested by Tarnocai (2009). The distribution of terrestrial freshwater wetlands in Canada is presented in Table 13A.15. For comparison, Warner (2005) reported 1.056 million km² of peatland area (organic soil wetland) for Canada, a difference of 7%.

Carbon Pools

Carbon pools of the Canadian wetlands were calculated using the area carbon density factors for the four wetland categories, derived from CONUS (see Table 13A.16, this page).

13A.6 Mexico

13A.6.1 Approach

An assessment of terrestrial wetlands in Mexico was used as the basis for identifying wetland areas and soil types. The North American Land Cover dataset (see Table 13A.17, this page) and a recent dataset from Mexico were used to segregate the wetlands into vegetation categories. Area carbon density factors were used to develop the estimates of wetland carbon pools.

13A.6.2 Data

The datasets used to estimate the area of terrestrial wetlands in Mexico are presented in Table 13A.17.



Table 13A.18. Area of Freshwater Wetlands in Mexico Categorized by Soils and Vegetation

Soil Type	Forested (km ²)	Nonforested (km ²)	Total (km ²)
Organic Soil	3,394	17,191	20,585
Mineral Soil	5,288	10,320	15,608
Total	8,682	27,511	36,193

13A.6.3 Results

Organic and Mineral Soil in Forested and Nonforested Wetlands in Mexico

This estimate of freshwater wetlands is greater than other reported values (e.g., 31,000 km²; Bridgham et al., 2006). A review of the map units from the Mapa Potencial de Humedales could not ensure that selected wetlands were adequately constrained to

freshwater systems (due to problems with data code translations). Accordingly, the calculated wetland area was reduced by 25% to provide a conservative estimate (see Table 13A.18, this page), thereby reducing the accuracy to at least 75%. The metadata for the database did not provide an estimate of the mapping error.

Acknowledgments

Spatial analyses were conducted at the Center for Applied GIScience, University of North Carolina, Charlotte, by Yu Lan, Jiyang Shi, Wenpeng Feng, Yu Lan, Douglas Shoemaker, Minrui Zheng, and Xiang Zhao. Julie Arnold, USDA Forest Service Southern Research Station, assisted with the literature and preparation of data tables and spreadsheets. Also used were computational facilities at the Portland office of the USDA Natural Resources Conservation Service.



Appendix 13B

Terrestrial Wetland–Atmosphere Exchange of Carbon Dioxide and Methane

Prepared by Carl Trettin,¹ Judy Drexler,² Randall Kolka,¹ Scott Bridgman,³ Sheel Bansal,² Brian Tangen,² Brian Bescoter,⁴ Wenwu Tang,⁵ and Steven Campbell⁶

¹USDA Forest Service; ²U.S. Geological Survey; ³University of Oregon; ⁴Florida Atlantic University; ⁵University of North Carolina, Charlotte; ⁶USDA Natural Resources Conservation Service

13B.1 Introduction

This chapter used published observational studies and recent syntheses to develop the basis for estimating both the net uptake of atmospheric carbon dioxide (CO₂) by terrestrial wetlands, which is equal to negative net ecosystem exchange (NEE), and the net fluxes of methane (CH₄) from terrestrial wetlands to the atmosphere. The primary source documents were the *First State of the Carbon Cycle Report* (SOCCR1; CCSP 2007) and the recent Intergovernmental Panel on Climate Change (IPCC) Wetlands Supplement (IPCC 2013). That information was augmented where possible with additional references. There were very few recent reports of measured NEE in comparison to reports on CH₄ flux. Accordingly, there was reliance on the previously published synthesis, with considerable uncertainty remaining in the NEE estimates. Tropical wetland fluxes were derived from the recent synthesis by Sjögersten et al. (2014).

Section 13B.2, this page, summarizes the observational data used as the basis for the area density flux factors. The flux estimates were based on those data and specific references, depending on the assessment area. Section 13B.3, p. 558, presents the area density flux factors used for each country and region.

Table 13B.1 Average Methane and Net Ecosystem Exchange for Nonforested and Forested Wetlands on Peat Soils^{a-c}

CH ₄ (g CH ₄ -C per m ² per Year)			
Wetland Area	Average	Standard Error	n
Nonforested	23.6	3.1	73
Forested	8.9	5.2	14
NEE (g C per m ² per Year)			
Nonforested	-135.0	42.5	14
Forested	-124.7	43.1	5

Notes

- Negative net ecosystem exchange (NEE) indicates net transfer to the ecosystem.
- See Tables 13B.8 and 13B.9 in Supplement, p. 561, for values and references.
- Key: CH₄, methane; C, carbon; g, gram; n, number of studies.

13B.2 Literature Review

13B.2.1 Peat Soils

The mean CH₄ and NEE are presented in Table 13B.1, this page. The mean CH₄ flux rate for nonforested and forested wetlands are 23.6 and 8.9 grams (g) of CH₄-C per m² per year, respectively. In comparison, the mean CH₄ flux rate used for peatlands in SOCCR1 was 1.9 g CH₄-C per m² per year. The difference in CH₄ flux rates is attributable to the additional references and the wide range in conditions from the reported studies. The mean NEE for the nonforested and forested wetlands are -135.0 and -124.7 g C per m² per year, respectively. However, there are relatively few reports of measured NEE from peatlands; hence, the basis provided by the published studies is relatively weak. For SOCCR1, NEE was estimated on the basis of net changes in soil



and plant carbon, yielding an NEE of -19.0 to -121.0 g C per m^2 per year for northern and temperate peatlands (CCSP 2007). Plant carbon accumulation was considered negligible for the northern biomes, due to the paucity of data. Accordingly, soil carbon accumulation accounted for 100% of the gain in the northern peatlands and 58% in the temperate peatlands.

13B.2.2 Mineral Soils

The mean CH_4 and NEE fluxes for mineral soil wetlands are presented in Table 13B.2, this page. The mean CH_4 flux rate for nonforested and forested wetlands are 26.1 and 26.9 g CH_4 -C per m^2 per year, respectively. In comparison, the mean CH_4 flux rate used for mineral wetlands in SOCCR1 (CCSP 2007) was 6 g CH_4 -C per m^2 per year. As was the case with the peatlands, the variation in CH_4 flux rates is due to the wide range in conditions from the reported studies. The mean NEE for the nonforested areas is -102.1 g C per m^2 per year. There were too few reports of measured NEE for mineral soil forests; hence, another metric was used. In SOCCR1, NEE was estimated on the basis of net changes in soil and plant carbon, yielding an NEE of -17 to -67 g C per m^2 per year, for northern and temperate mineral soil wetlands, respectively (CCSP 2007). For that analysis, plant carbon accumulation was considered negligible for the northern biomes, due in large part to the paucity of data. Accordingly, soil carbon accumulation accounted for 100% of the gain in the northern mineral soil wetlands and 25% in the temperate mineral soil wetlands.

Table 13B.2. Methane and Net Ecosystem Exchange Means and the Associated Standard Errors for Nonforested and Forested Wetlands on Mineral Soils^{a-c}

Wetland Area	Mean	Standard Error	n
CH_4 (g CH_4-C per m^2 per Year)			
Nonforested	26.1	3.6	46
Forested	26.9	7.9	16
NEE (g C per m^2 per Year)			
Nonforested	-102.1	34.4	13
Forested	NA ^d	NA	

Notes

- Negative net ecosystem exchange (NEE) indicates net transfer to the ecosystem.
- See Tables 13B.10 and 13B.11 in Supplement, p. 561, for values and references.
- Key: CH_4 , methane; C, carbon; g, gram; n, number of studies.
- Not applicable.

13B.3 Country and Regional Density Factors

13B.3.1 Conterminous United States

Carbon flux within the conterminous United States (CONUS) was estimated using area carbon flux density factors (see Table 13B.3, this page). The NEE flux density factors are based on the mean for the peat soil nonforested wetland and mineral

Table 13B.3. Flux Density Factors Used to Estimate Net Ecosystem Exchange and Methane Fluxes from Freshwater Wetlands in the Conterminous United States^{a-d}

Flux	Organic Soil		Mineral Soil	
	Forested	Nonforested	Forested	Nonforested
NEE (g CO_2 -C per m^2 per Year)	-120.97 (45.60)	-134.97 (42.53)	-66.99 (23.55)	-102.15 (34.43)
CH_4 (g CH_4 -C per m^2 per Year)	8.90 (5.24)	23.58 (3.13)	26.93 (7.95)	26.09 (3.60)

Notes

- Negative net ecosystem exchange (NEE) indicates net transfer to the ecosystem.
- Standard error in parentheses.
- Source: Appendix 13B Supplement: Carbon Pools and Fluxes, p. 561.
- Key: CO_2 , carbon dioxide; CH_4 , methane; g, gram; C, carbon.



Table 13B.4. Area Density Factors Used to Estimate Net Ecosystem Exchange and Methane Flux from Freshwater Wetlands in Alaska^{a-d}

Flux	Organic		Mineral	
	Forested	Nonforested	Forested	Nonforested
NEE (g CO ₂ -C per m ² per Year)	-56.53 (32.14)	-56.53 (32.14)	-56.53 (32.14)	-56.53 (32.14)
CH ₄ (g CH ₄ -C per m ² per Year)	8.90 (5.24)	23.58 (3.13)	26.93 (7.95)	26.08 (3.60)

Notes

- a) Negative net ecosystem exchange (NEE) indicates net transfer to the ecosystem.
- b) Standard error in parentheses.
- c) Source: Appendix 13B Supplement: Carbon Pools and Fluxes, p. 561.
- d) Key: CO₂, carbon dioxide; CH₄, methane; g, gram; C, carbon.

soil nonforested wetlands (see Tables 13B.1 and 13B.2, p. 557 and p. 558, respectively). To estimate NEE for the forested wetlands, the SOCCR1 values (Bridgham et al., 2007) were used due to the small number of field-based reports. The estimate in SOCCR1 was based on the annual change in soil and plant carbon; the conservative estimate of 50 g C per m² per year sequestered in forests was used for both peat and mineral soil wetlands (Bridgham et al., 2007). The small number of studies that directly measure NEE in wetlands remains a constraint; hence, the segmented approach used by Bridgham et al. (2007) provides a functional basis.

The CH₄ flux density factors are based on the mean of data reported for the four wetland categories (see Section 13B.2, p. 557). These mean flux factors are similar to those used in SOCCR1 (CCSP 2007), where the mean for freshwater wetlands was 5.3 g CH₄-C per m² per year.

13B.3.2 Alaska

The available data for establishing the carbon flux for Alaska is very limited. The area density factor for NEE employs the values reported by He et al. (2016), which are based on simulation results (see Table 13B.4, this page). For the CH₄ flux, the mean values used were derived from the literature compilation (see Section 13B.2, p. 557). In comparison, He et al. (2016) estimated the CH₄ flux at 47.5 g C

Table 13B.5. Area Density Factors Used to Estimate Net Ecosystem Exchange and Methane Flux for Tropical Terrestrial Wetlands^{a-d}

Wetland Type	NEE	CH ₄ Flux
	g C per m ² per Year	
Organic Soil Wetland	-310.3 (152.8)	40.1 (17.1)
Mineral Soil Wetland	-120.8 (218.2)	54.0 (9.7)

Notes

- a) Negative net ecosystem exchange (NEE) indicates net transfer to the ecosystem.
- b) Standard error in parentheses.
- c) Source: Sjögersten et al. (2014).
- d) Key: C, carbon; g, gram; CH₄, methane.

per m² per year, an amount which is almost twice the value used here; the paucity of data determined use of the more conservative CH₄ flux estimate based on field measurement data.

13B.3.3 Puerto Rico

Estimates of NEE and CH₄ fluxes (see Table 13B.5, this page) were obtained using area density factors for mineral and organic soils derived from the synthesis of tropical wetlands provided by Sjögersten et al. (2014). The same area density factors were used for forested and nonforested wetlands.



Table 13B.6. Area Density Factors Used to Estimate Net Ecosystem Exchange and Methane Flux from Freshwater Wetlands in Canada^{a-c}

Flux	Organic		Mineral	
	Forested	Nonforested	Forested	Nonforested
NEE (g CO ₂ -C per m ² per Year)	-47.71 (4.18)	-16.71 (4.18)	-47.98 (12.74)	-102.15 (34.44)
CH ₄ (g CH ₄ -C per m ² per Year)	8.90 (5.24)	23.58 (3.13)	26.93 (7.95)	26.09 (3.60)

Notes

- a) Negative net ecosystem exchange (NEE) indicates net transfer to the ecosystem.
- b) Standard error in parentheses.
- c) Key: CH₄, methane; CO₂, carbon dioxide; g, gram; C, carbon.

13B.3.4 Canada

Carbon flux for Canada was estimated using area carbon flux density factors (see Table 13B.6, this page) calculated on the basis of reported values. The area density factor for NEE in nonforested peatlands and mineral soil wetlands uses the mean reported from measurement studies (see Section 13B.2, p. 557). For forested wetlands, the value reported in SOCCR1 was used, reflecting the soil carbon accretion, to which was added 31 g C per m² per year sequestered in vegetation, an amount which is based on an 18-year assessment of Canadian forests (Stinson et al., 2011). The analyses of Stinson et al. (2011) did not include changes in soils as a result of bryophytes or sedimentation; hence, adding the soil component seemed appropriate because it was the only component used in SOCCR1 (CCSP 2007).

The CH₄ flux density factors are based on the data average reported for the four categories (see Section 13B.2, p. 557). These mean flux factors for peatlands are higher than the factor used in SOCCR1 (2.8 g C per m² per year). For freshwater wetlands, the SOCCR1 CH₄ flux was 5.3 g CH₄-C per m² per year, which is considerably lower than the forested and nonforested values (CCSP 2007).

Table 13B.7. Area Density Factors Used to Estimate Net Ecosystem Exchange and Methane Flux for Mexico^{a-d}

Wetland Type	NEE	CH ₄ Flux
	g C per m ² per Year	
Organic Soil Wetland	-310.3 (152.8)	40.1 (17.1)
Mineral Soil Wetland	-120.8 (218.2)	54.0 (9.7)

Notes

- a) Negative net ecosystem exchange (NEE) indicates net transfer to the ecosystem.
- b) Standard error in parentheses.
- c) Source: Sjögersten et al. (2014).
- d) Key: CH₄, methane; g, gram; C, carbon.

13B.3.5 Mexico

Estimates of NEE and CH₄ fluxes (see Table 13B.7, this page) were obtained using area density factors for mineral and organic soils derived from the synthesis of tropical wetlands developed by Sjögersten et al. (2014). The negative number for NEE indicates net uptake by the ecosystem. The same area density factors were used for forested and nonforested wetlands.



Appendix 13B Supplement: Carbon Pools and Fluxes

Tables 13B.8–13B.11

Table 13B.8. Forested Peatland Area Density Flux Factors ^{a-b}				
Location	Vegetation Type	NEE Emission (g CO ₂ -C per m ² per Year)	CH ₄ Emission (g CH ₄ -C per m ² per Year)	Reference
New York	Forested peatland		0.150	Coles and Yavitt (2004)
Minnesota	Forest bog hummock		2.625	Dise (1993)
Minnesota	Forest bog hollow		10.350	Dise (1993)
Minnesota	Forest bog hollow		3.513	Dise (1992)
Minnesota	Hummock		1.317	Dise (1992)
Wisconsin	Forest bog	-80.0	0.800	Desai et al. (2015)
West Siberia	Pine peatland		0.132	Golovatskaya and Dyukarev (2008)
West Siberia	Stunted pine peatland		0.198	Golovatskaya and Dyukarev (2008)
Southern Germany	Bog	-62.0	5.300	Hommeltenber et al. (2014)
Boreal	Swamp	-256.0		Lu et al. (2017); Lund et al. (2010)
Boreal	Swamp	-195.5		Lu et al. (2017); Sulman et al. (2012); Syed et al. (2006)
Temperate	Bog	-30.0		Lu et al. (2017); Sulman et al. (2012); Syed et al. (2006)
West Virginia	Appalachian bog		74.646	Wieder et al. (1990)
Florida	Swamp		2.026	Villa and Mitsch (2014)
Florida	Swamp		1.661	Villa and Mitsch (2014)
Maryland	Appalachian bog		19.320	Wieder et al. (1990)
West Virginia	<i>Sphagnum</i> /Forest		2.625	Yavitt et al. (1990)

Notes

a) Negative net ecosystem exchange (NEE) indicates net transfer to the ecosystem.

b) Key: CO₂, carbon dioxide; CH₄, methane; g, gram; C, carbon.

Table 13B.9. Nonforested Peatland Area Density Flux Factors^a

Location	Vegetation Type	Annual Flux (CO ₂ g C per m ² per Year)	Annual Flux (CH ₄ g C per m ² per Year)	Reference
Minnesota	Open bog		61.473	After Crill et al. (1988); after Mitsch and Wu (1995)
Minnesota	Natural fen		65.864	After Crill et al. (1988); after Mitsch and Wu (1995)
Minnesota	Acid fen		21.077	After Crill et al. (1988); after Mitsch and Wu (1995)
West Virginia	Mountain bog		51.374	After Gorham (1991); after Crill et al. (1988)
Minnesota	Bog		36.006	After Harriss et al. (1985)
Minnesota	Fen		1.098	After Harriss et al. (1985)
California	Marsh	-412.5	56.300	Anderson et al. (2016)
Minnesota	Open bog		0	Bridgham et al. (1995)
New Hampshire	Poor fen		82.950	Carroll and Crill (1997)
Boreal Canada	Swamp		0.922	Derived from Moore and Roulet (1995)
Boreal Canada	Fen		2.503	Derived from Moore and Roulet (1995)
Boreal Canada	Bog		1.713	Derived from Moore and Roulet (1995)
Minnesota	Fen Lagg		9.450	Dise (1993)
Minnesota	Bog (open bog)		32.325	Dise (1993)
Minnesota	Fen (open poor fen)		49.275	Dise (1993)
Minnesota	Open poor fen		13.173	Dise (1992)
Minnesota	Open bog		3.074	Dise (1992)
Minnesota	Poor fen, control		66.075	Dise and Verry (2001)
Minnesota	Poor fen, ammonium nitrate added		70.255	Dise and Verry (2001)
Minnesota	Poor fen, ammonium sulfate added		44.788	Dise and Verry (2001)
Minnesota	Nonforested		17.250	Dise and Verry (2001)
Wales	Peat monoliths		63.230	Freeman et al. (1993)
New Hampshire	Poor fen		51.975	Frolking and Crill (1994)
West Siberia	Sedge fen		14.490	Golovatskaya and Dyukarev (2008)
Florida	Wet prairie (marl)		5.625	Happell et al. (1994)
Florida	Marsh (marl)		6.131	Happell et al. (1994)
Florida	Marsh (marl)		10.125	Happell et al. (1994)
Florida	Marsh (peat)		9.281	Happell et al. (1994)
Florida	Marsh (peat)		2.644	Happell et al. (1994)
Florida	Marsh (peat)		33.525	Happell et al. (1994)

Continued on next page



(Continued)

Location	Vegetation Type	Annual Flux (CO₂ g C per m² per Year)	Annual Flux (CH₄ g C per m² per Year)	Reference
Florida	Marsh (peat)		4.163	Happell et al. (1994)
Quebec, Canada	Fen		6.225	Helbig et al. (2017)
Florida	Marsh	-44.9		Jimenez et al. (2012)
California	Young restored wetland	-368.0	53.000	Knox et al. (2015)
California	Old restored wetland	-397.0	38.700	Knox et al. (2015)
Washington	Bog		19.950	Lansdown et al. (1992)
Ontario, Canada	Fen		18.825	Lai et al. (2014)
Ontario, Canada	Fen		3.960	Lai et al. (2014)
Ontario, Canada	Fen		10.478	Lai et al. (2014)
Quebec, Canada	Bog	-60.78		Lu et al. (2017); Sulman et al. (2012); Lund et al. (2010)
Ireland	Bog	-47.78		Lu et al. (2017); Koehler et al. (2011)
Sweden	Fen	-58.0		Lu et al. (2017); Pleichel et al. (2014)
Finland	Natural fen		15.324	Nykänen et al. (1995)
Finland	Drained fen		0.132	Nykänen et al. (1995)
Minnesota	Fen	-35.3	16.300	Olsen et al. (2013)
Michigan	Bog		52.650	Shannon and White (1994)
Michigan	Bog		7.650	Shannon and White (1994)
Ontario, Canada	Marsh	-224.0	127.000	Strachan et al. (2015)
Quebec, Canada	Poor fen, control		0.032	Strack and Waddington (2007)
Quebec, Canada	Poor fen, control		39.080	Strack et al. (2004)
Quebec, Canada	Poor fen, with water table drawdown		17.564	Strack et al. (2004)
Northern Sweden	Ombrotrophic bog, hummocks		0.220	Svensson and Rosswall (1984)
Northern Sweden	Ombrotrophic bog, between hummocks		0.615	Svensson and Rosswall (1984)
Northern Sweden	Ombrotrophic bog, shallow depressions		3.381	Svensson and Rosswall (1984)
Northern Sweden	Ombrotrophic bog, deeper depressions		5.313	Svensson and Rosswall (1984)
Northern Sweden	Ombrominerotrophic		11.987	Svensson and Rosswall (1984)
Northern Sweden	Minerotrophic fen		74.163	Svensson and Rosswall (1984)
Western Canada	Bog		1.756	Turetsky et al. (2007)
North America and Europe	Bogs and fens		26.000	Turetsky et al. (2014)

Continued on next page



(Continued)

Table 13B.9. Nonforested Peatland Area Density Flux Factors^a

Location	Vegetation Type	Annual Flux (CO ₂ g C per m ² per Year)	Annual Flux (CH ₄ g C per m ² per Year)	Reference
Minnesota	Bog		0.036	Updegraff et al. (2001)
Florida	Swamp		19.455	Villa and Mitsch (2014)
Northern England	Acidic blanket peat		0.025	Ward et al. (2007)
Maryland	<i>Sphagnum</i> bog		-0.300	Yavitt et al. (1990)
West Virginia	<i>Sphagnum</i> / <i>Eriophorum</i> (poor fen)		1.800	Yavitt et al. (1990)
West Virginia	<i>Sphagnum</i> /Shrub (fen)		0	Yavitt et al. (1993)
West Virginia	<i>Polytrichum</i> /Shrub (fen)		0	Yavitt et al. (1993)
New York	<i>Typha</i> marsh		17.775	Yavitt (1997)
West Virginia	<i>Eriophorum</i>		14.250	Yavitt et al. (1993)
West Virginia	<i>Polytrichum</i>		11.250	Yavitt et al. (1993)
West Virginia	Shrub		1.200	Yavitt et al. (1993)
Alaska	Fen		53.66	Gorham (1991); after Crill et al. (1988)
Ontario, Canada	Mesocosms		0.510	Blodau and Moore (2003)
Quebec, Canada	Gatineau Park		0.020	Buttler et al. (1994)
Alaska	Waterlogged tundra		32.493	Derived from Sebacher et al. (1986)
Alaska	Wet meadows		10.977	Derived from Sebacher et al. (1986)
Alaska	Alpine fen		79.037	Derived from Sebacher et al. (1986)
Florida	Freshwater marsh	106.0		Malone et al. (2014)
Canada	Hummock	-39.814		Waddington et al. (1998)
Canada	Moss sedge	-148.308		Waddington et al. (1998)
Canada	Hollow	-153.285		Waddington et al. (1998)
Canada	Deep hollow	-5.972		Waddington et al. (1998)
Colorado	Fen		40.700	Chimner and Cooper (2003)

Notes

a) Key: CO₂, carbon dioxide; g, gram; C, carbon; CH₄, methane.

Table 13B.10. Mineral Soil Forest Area Density Flux Factors for Methane^a

Vegetation (Species/Community)	Climate Zone	Location	Annual Flux CH ₄ (g C per m ² per Year)	Reference
Temperate	Temperate	Georgia	17.25	Pulliam (1993)
Dwarf cypress	Subtropical	Florida	2.025	Bartlett et al. (1989)
Swamp forest	Subtropical	Florida	18.825	Bartlett et al. (1989)
Hardwood hammock	Subtropical	Florida	0.000	Bartlett et al. (1989)
Cypress swamp, flowing water	Subtropical	Florida	18.300	Harriss and Sebacher (1981)
Cypress swamp, deep water	Subtropical	Georgia	25.200	Harriss and Sebacher (1981)
Cypress swamp, floodplain	Subtropical	South Carolina	2.700	Harriss and Sebacher (1981)
Maple/Gum forested swamp	Temperate	Virginia	0.375	Harriss et al. (1982)
Wetland forest	Temperate	Florida	16.125	Harriss et al. (1988)
Swamp forests	Temperate	Louisiana	39.825	Alford et al. (1997)
Pools forested swamp	Temperate	New York	51.750	Miller and Ghiorso (1999)
Open water swamp	Subtropical	Florida	131.025	Schipper and Reddy (1994)
Waterlily slough	Subtropical	Florida	24.825	Schipper and Reddy (1994)
Lowland shrub and forested wetland	Temperate	Wisconsin	9.300	Werner et al. (2003)
Oak swamp (bank site)	Temperate	Virginia	31.950	Wilson et al. (1989)
Ash tree swamp	Temperate	Virginia	41.475	Wilson et al. (1989)

Notes

a) Key: CH₄, methane; g, gram; C, carbon.

**Table 13B.11. Mineral Soil Nonforested Area Density Flux Factors^a**

Climate Zone	Location	NEE Emission (g CO ₂ -C per m ² per Year)	CH ₄ Emission (g CH ₄ -C per m ² per Year)	Reference
Temperate	Prairie Pothole Region, Canada		4.900	Badiou et al. (2011)
Tropical	Global		41.900	Bartlett and Harriss (1993)
Temperate	Global		32.800	Bartlett and Harriss (1993)
Temperate	Ottawa, Ontario, Canada	-264.0		Bonneville et al. (2008)
Temperate	Ohio	65.4	37.650	Chu et al. (2015)
Temperate	Sanjiang Plain, China		35.100	Ding and Cai (2007)
Temperate	North Dakota		10.650	Gleason et al. (2009)
Temperate	North Florida		23.700	Happell et al. (1994)
Temperate	North Florida		7.500	Happell et al. (1994)
Tropical	South Florida		16.875	Harriss et al. (1988)
Temperate	Denmark		8.250	Herbst et al. (2011)
Tropical	Louisiana		35.100	Holm et al. (2016)
Temperate	Sanjiang Plain, China		22.500	Huang et al. (2010)
Temperate	Sanjiang Plain, China		16.875	Huang et al. (2010)
Tropical	Everglades, Florida	-44.9		Jimenez et al. (2012)
Temperate	Nebraska		60.000	Kim et al. (1999)
Temperate	Nebraska		48.000	Kim et al. (1999)
Temperate	Louisiana	-289.9	35.325	Krauss et al. (2016)
Tropical	Southwest Florida		0.600	Li and Mitsch (2016)
Tropical	Southwest Florida		92.925	Li and Mitsch (2016)
Tropical	Everglades, Florida	-40.24		Malone et al. (2014)
Temperate	North Carolina		0.525	Morse et al. (2012)
Temperate	Ohio		56.850	Nahlik and Mitsch (2010)
Temperate	Minnesota		8.775	Naiman et al. (1991)
Temperate	Minnesota		10.800	Naiman et al. (1991)
Temperate	Colorado		30.525	Neff et al. (1994)
Temperate	Virginia		54.113	Neubauer et al. (2000)
Temperate	Saskatchewan, Canada		24.100	Pennock et al. (2010)
Temperate	Saskatchewan, Canada		26.175	Pennock et al. (2010)
Temperate	Saskatchewan, Canada		18.075	Pennock et al. (2010)
Boreal	Saskatchewan, Canada		10.875	Rask et al. (2002)
Tropical	Everglades, Florida	-49.9		Schedlbauer et al. (2010)
Temperate	Georgia	92.4		Segarra et al. (2013)
Temperate	Minnesota		14.600	Shurpali and Verma (1998)
Temperate	Colorado		7.725	Smith and Lewis (1992)
Temperate	Sanjiang Plain, China		21.675	Song et al. (2003)
Temperate	Sanjiang Plain, China		32.550	Song et al. (2003)

Continued on next page



(Continued)

Table 13B.11. Mineral Soil Nonforested Area Density Flux Factors^a

Climate Zone	Location	NEE Emission (g CO ₂ -C per m ² per Year)	CH ₄ Emission (g CH ₄ -C per m ² per Year)	Reference
Temperate	Sanjiang Plain, China		4.350	Song et al. (2009)
Temperate	Sanjiang Plain, China		0.225	Song et al. (2009)
Temperate	Ottawa, Ontario, Canada	-223.8	127.000	Strachan et al. (2015)
Tropical	Everglades, Florida		39.975	Villa et al. (2014)
Temperate	Colorado		31.275	Wickland et al. (1999)
Temperate	Colorado		23.456	Wickland et al. (1999)
Temperate	Virginia		31.725	Wilson et al. (1989)
Temperate	Virginia		16.988	Wilson et al. (1989)
Temperate	Three Gorges Reservoir, China		0.975	Yang et al. (2012)
Temperate	New York		93.975	Yavitt et al. (1997)
Temperate	New York		13.331	Yavitt et al. (1997)
Temperate	New York		41.906	Yavitt et al. (1997)
Temperate	Maryland and West Virginia		0.281	Yavitt et al. (1990)
Temperate	New York		10.688	Yavitt et al. (1993)
Temperate	New York		8.438	Yavitt et al. (1993)
Temperate	New York		0.900	Yavitt et al. (1993)
Temperate	Czech Republic	-126.3		Lu et al. (2017); Marek et al. (2011)
Boreal	Quebec, Canada	-264.0		Lu et al. (2017); Bonneville et al. (2008)
Boreal	Finland	-37.0		Lu et al. (2017); Lund et al. (2010)
Temperate	China	-61.67		Lu et al. (2017); Yu et al. (2013)
Temperate	Wisconsin	-83.99		Lu et al. (2017); Sulman et al. (2009)

Notes

a) Key: NEE, net ecosystem exchange; CO₂, carbon dioxide; CH₄, methane; g, gram; C, carbon.



14 Inland Waters

Lead Author

David Butman, University of Washington

Contributing Authors

Rob Striegl, U.S. Geological Survey; Sarah Stackpoole, U.S. Geological Survey; Paul del Giorgio, Université du Québec à Montréal; Yves Prairie, Université du Québec à Montréal; Darren Pilcher, Joint Institute for the Study of the Atmosphere and Ocean, University of Washington and NOAA; Peter Raymond, Yale University; Fernando Paz Pellat, Colegio de Postgraduados Montecillo; Javier Alcocer, Universidad Nacional Autónoma de México

Acknowledgments

Raymond G. Najjar (Science Lead), The Pennsylvania State University; Nicholas Ward (Review Editor), Pacific Northwest National Laboratory; Nancy Cavallaro (Federal Liaison), USDA National Institute of Food and Agriculture; Zhiliang Zhu (Federal Liaison), U.S. Geological Survey

Recommended Citation for Chapter

Butman, D., R. Striegl, S. Stackpoole, P. del Giorgio, Y. Prairie, D. Pilcher, P. Raymond, F. Paz Pellat, and J. Alcocer, 2018: Chapter 14: Inland waters. In *Second State of the Carbon Cycle Report (SOCCR2): A Sustained Assessment Report* [Cavallaro, N., G. Shrestha, R. Birdsey, M. A. Mayes, R. G. Najjar, S. C. Reed, P. Romero-Lankao, and Z. Zhu (eds.)]. U.S. Global Change Research Program, Washington, DC, USA, pp. 568-595, <https://doi.org/10.7930/SOCCR2.2018.Ch14>.



KEY FINDINGS

1. The total flux of carbon—which includes gaseous emissions, lateral flux, and burial—from inland waters across the conterminous United States (CONUS) and Alaska is 193 teragrams of carbon (Tg C) per year. The dominant pathway for carbon movement out of inland waters is the emission of carbon dioxide gas across water surfaces of streams, rivers, and lakes (110.1 Tg C per year), a flux not identified in the *First State of the Carbon Cycle Report* (SOCCR1; CCSP 2007). Second to gaseous emissions are the lateral fluxes of carbon through rivers to coastal environments (59.8 Tg C per year). Total carbon burial in lakes and reservoirs represents the smallest flux for CONUS and Alaska (22.5 Tg C per year) (*medium confidence*).
2. Based on estimates presented herein, the carbon flux from inland waters is now understood to be four times larger than estimates presented in SOCCR1. The total flux of carbon from inland waters across North America is estimated to be 507 Tg C per year based on a modeling approach that integrates high-resolution U.S. data and continental-scale estimates of water area, discharge, and carbon emissions. This estimate represents a weighted average of 24 grams of carbon per m² per year of continental area exported and removed through inland waters in North America (*low confidence*).
3. Future research can address critical knowledge gaps and uncertainties related to inland water carbon fluxes. This chapter, for example, does not include methane emissions, which cannot be calculated as precisely as other carbon fluxes because of significant data gaps. Key to reducing uncertainties in estimated carbon fluxes is increased temporal resolution of carbon concentration and discharge sampling to provide better representations of storms and other extreme events for estimates of total inland water carbon fluxes. Improved spatial resolution of sampling also could potentially highlight anthropogenic influences on the quantity and quality of carbon fluxes in inland waters and provide information for land-use planning and management of water resources. Finally, uncertainties could likely be reduced if the community of scientists working in inland waters establishes and adopts standard measurement techniques and protocols similar to those maintained through collaborative efforts of the International Ocean Carbon Coordination Project and relevant governmental agencies from participating nations.

Note: Confidence levels are provided as appropriate for quantitative, but not qualitative, Key Findings and statements.

14.1 Introduction: The Aquatic Carbon Cycle

14.1.1 Inland Waters in the Carbon Cycle

This chapter provides an assessment of the total mass of carbon moving from terrestrial ecosystems into inland waters and places this flux in the context of major carbon loss pathways. Also provided is evidence that the estimated carbon flux through inland waters is poorly constrained, highlighting several opportunities to improve future estimates of carbon flows through aquatic ecosystems. Inland waters are defined in this chapter as open-water systems of lakes, reservoirs, nontidal rivers, and streams (see Ch. 13: Terrestrial Wetlands, p. 507, and Ch. 15: Tidal Wetlands and Estuaries, p. 596, for assessments

of those ecosystems). Carbon within inland waters includes dissolved and particulate species of inorganic and organic carbon. The separation between dissolved and particulate carbon is operational and reflects, in general, a filtration through a 0.2- to 0.7-micrometer (μm) filter, where the larger material is considered particulate within freshwater environments. Using this definition classifies inland water carbon as dissolved organic carbon (DOC), dissolved inorganic carbon (DIC), particulate organic carbon (POC), and particulate inorganic carbon (PIC). Included within the DIC pool is dissolved carbon dioxide (CO_2).

Lakes, ponds, streams, rivers, and reservoirs are both the intermediate environments that transport,

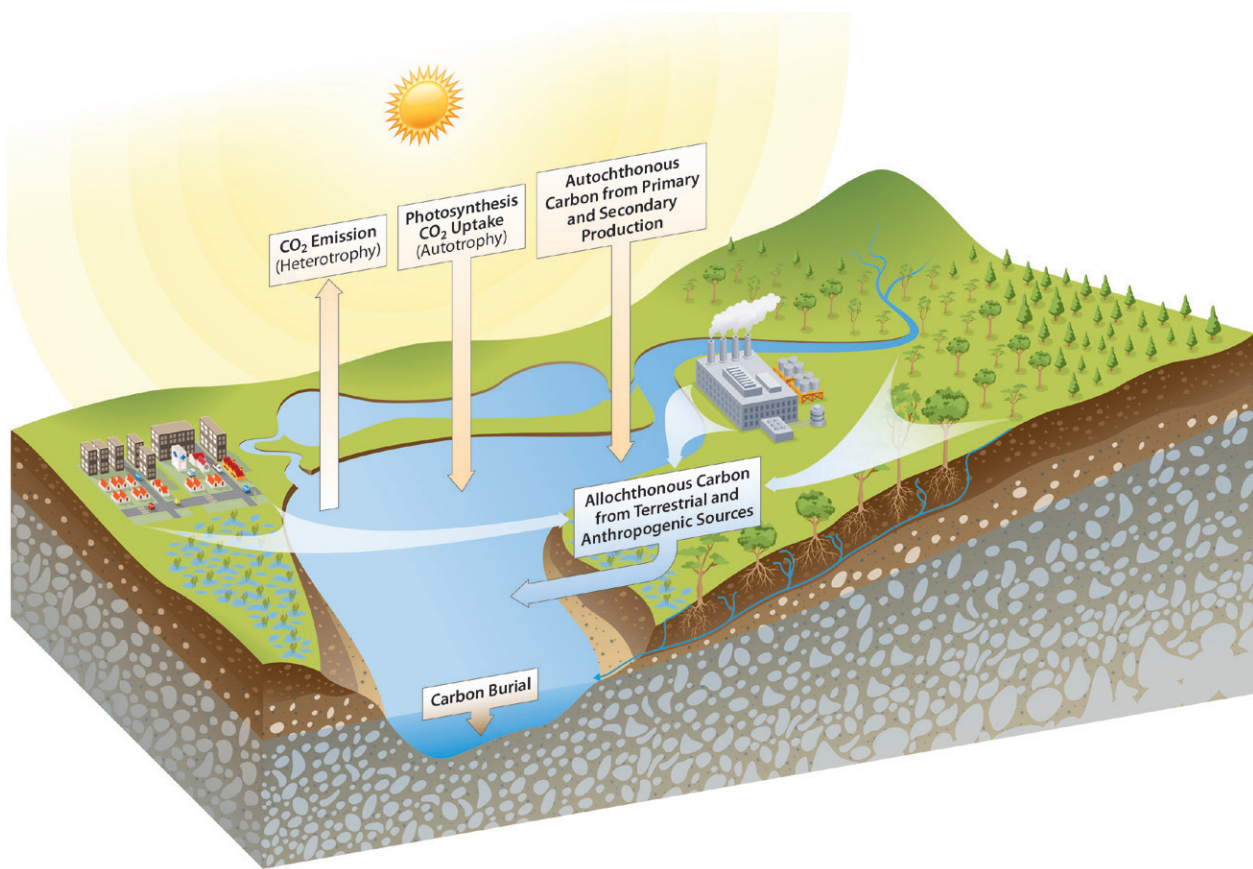


Figure 14.1. Carbon Flux Pathways in Aquatic Environments. Allochthonous carbon represents organic and inorganic carbon, including dissolved carbon dioxide (CO_2), that enters aquatic environments from terrestrial systems. Autochthonous carbon originates from primary and secondary production that uses either atmospheric CO_2 or dissolved inorganic carbon from the aquatic environment. Primary production within autotrophic systems is responsible for the net uptake of atmospheric CO_2 , while respiration and allochthonous inputs of carbon within a heterotrophic system are responsible for a net CO_2 emission to the atmosphere. Burial represents the deposition of autochthonous and allochthonous particulate carbon.

sequester, and transform carbon before it reaches coastal environments (Liu et al., 2010) and dynamic ecosystems that sustain primary and secondary production supporting aquatic metabolism and complex food webs. Inland waters comprise a small fraction of Earth's surface yet play a critical role in the global carbon cycle (Battin et al., 2009b; Butman et al., 2016; Cole et al., 2007; Findlay and Sinsabaugh 2003; Regnier et al., 2013; Tranvik et al., 2009). Over geological timescales, inland waters control long-term sequestration of atmospheric CO_2 through the hydrological transport of inorganic carbon from

terrestrial weathering reactions to coastal and marine carbon "sinks" as dissolved carbonate species (Berner 2004). Today, through anthropogenic land-use change, industrialization, damming, and changes in climate, the ecosystem structure and function of inland waters are changing rapidly. However, as presented in this chapter, the flows of carbon through inland waters represent a combination of both natural and anthropogenic influences, (see Figure 14.1, this page) as the science has not achieved a comprehensive ability to differentiate anthropogenic fluxes from natural fluxes. In the context of the North



American carbon cycle, the science discussed herein addresses current understanding of freshwater carbon cycling from the period since 1990 and highlights the need to focus on better identifying human impacts on the transport and biogeochemical cycling of carbon by inland waters.

14.1.2 Defining Carbon Within Inland Waters

Inland aquatic ecosystems are sites for biogeochemical carbon reactions that result in an exchange of particulate and dissolved carbon, CO₂, and methane (CH₄) among aquatic environments, terrestrial environments, and the atmosphere (Butman and Raymond 2011; Findlay and Sinsabaugh 2003; McCallister and del Giorgio 2012; McDonald et al., 2013; Raymond et al., 2013; Striegl et al., 2012). Carbon species in freshwaters originate from varied sources. Aquatic organic carbon consists of all organic molecules transported to or produced within inland waters and their various organic decomposition products. Inland water organic carbon originates from direct inputs from wastewater, surface runoff (typically, the largest contributor), groundwater, primary and secondary production within the aquatic environment, and atmospheric deposition. Inorganic carbon includes PIC and DIC. The mass balance of DIC in freshwater ecosystems is regulated by biological processes such as photosynthesis (consuming CO₂) and respiration (producing CO₂), along with air-water CO₂ exchange and geochemical reactions, including carbonate precipitation and dissolution (Tobias and Bohlke 2011).

Rivers are conduits that deliver carbon to the coast while maintaining strong CO₂ and CH₄ fluxes to or from the atmosphere (Cole et al., 2007; Stanley et al., 2016; Tranvik et al., 2009). Lakes and reservoirs are sinks of particulate carbon in sediments and also process and remineralize organic carbon to CO₂ and CH₄ gases that are then emitted to the atmosphere (Clow et al., 2015; Teodoru et al., 2012). Autotrophic carbon production in nutrient-enriched lakes and reservoirs can cause inland water bodies to be a sink of atmospheric CO₂ (Clow et al., 2015; Tranvik et al., 2009). The entrapment of sediments

by dams can facilitate aerobic and anaerobic organic carbon oxidation and thus the net production of CO₂ and CH₄ that escape to the atmosphere, with important implications to climate forcing (Crawford and Stanley 2016; Deemer et al., 2016). However, the balances among primary production, total respiration, carbon burial, and carbon gas emission in lakes and reservoirs remain poorly quantified (Arntzen et al., 2013; Teodoru et al., 2012).

Of the roughly 2.9 petagrams of carbon (Pg C) per year that enter inland waters globally, most are emitted as CO₂ across the air-water interface (Butman et al., 2016; Raymond et al., 2013) before ever reaching the ocean (Le Quéré et al., 2014). Recent estimates suggest that inland water surface carbon emissions may exceed 2 Pg C per year (Sawakuchi et al., 2017). In contrast, rivers export to the coastal ocean 0.4 Pg C per year of DIC and between 0.2 and 0.43 Pg C per year of organic carbon (Le Quéré et al., 2014; Ludwig et al., 1996; Raymond et al., 2013; Schlünz and Schneider 2000). However, the biogeochemical processes that produce and sustain both atmospheric carbon emissions and lateral fluxes remain unclear because physical and biological processes vary significantly across freshwater systems and along the hydrological continuum (see Figure 14.2, p. 572; Battin et al., 2008; Hotchkiss et al., 2015).

Carbon fluxes in inland waters are considered in Equation 14.1 in the context of a simple mass balance approach.

Equation 14.1

$$C_{aquatic} = C_{allochthonous} - [C_{emissions} + C_{burial} + C_{export}]$$

The dimensions of this equation are mass carbon (C) per unit time (e.g., Tg C per year) or mass C per unit area per unit time (e.g., units of g C per m² per year), where $C_{aquatic}$ represents the change of carbon stock in inland waters, $C_{allochthonous}$ is the input of allochthonous carbon into inland waters from land, $C_{emissions}$ is the total emissions of CO₂ and CH₄ from the water surface, C_{burial} is the total burial of POC in lakes and reservoirs, and C_{export} is

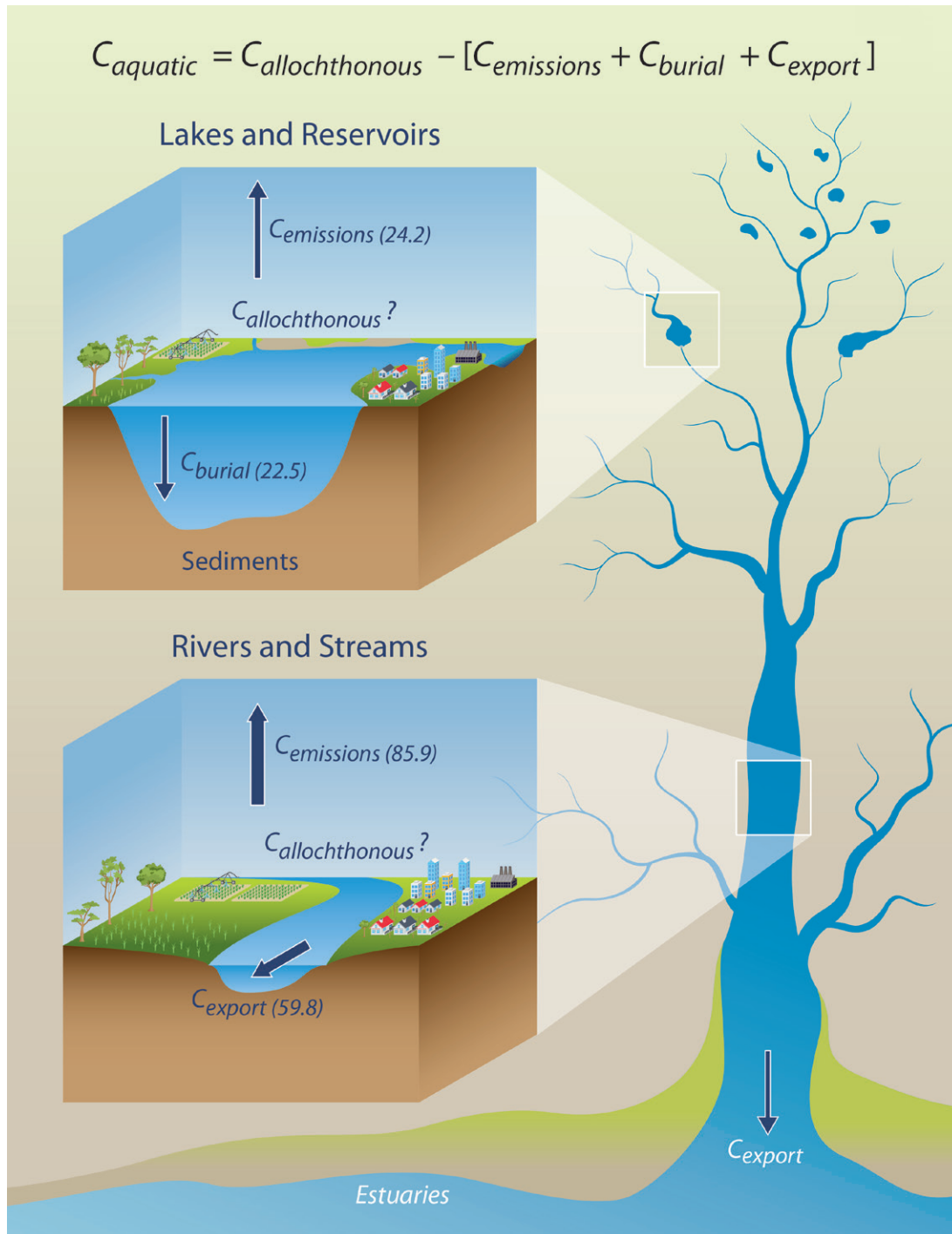


Figure 14.2. Carbon Fluxes from Inland Waters of the Conterminous United States and Alaska. All values represent total fluxes in teragrams of carbon (Tg C) per year. River fluxes represent total carbon fluxes to the point of the head of tide, or the highest flow gaging station not influenced by tidal movement. Individual fluxes from different land uses are not quantified but represented by the mass balance of all aquatic carbon fluxes. The total flux (see Equation 14.1, p. 571) is 193 Tg C per year. Further information regarding estimates of uncertainty are presented in Stackpoole et al. (2017a) and Butman et al. (2016).



the total export of inorganic and organic carbon to coastal systems. For this analysis, estimates of CH_4 emissions are not provided. Furthermore, changes in carbon stocks are assumed to be zero (i.e., assumption of steady state), which is reasonable over long timescales because of the rapid movement and turnover of carbon in lotic (flowing) and lentic (still) ecosystems. Hence, in this chapter, the flux of carbon from inland waters (the terms within brackets in Equation 14.1, p. 571) is assumed to be equivalent to the flux of carbon to inland waters, $C_{\text{terrestrial}}$. The use of this equation implies a fully constrained hydrological system. Adjustments have been made to U.S. flux estimates for carbon originating outside national boundaries.

14.1.3 Inland Waters of the United States and North America

The conterminous United States (CONUS) and Alaska contain over 45 million individual lakes and ponds greater than 0.001 km^2 . Excluding the Laurentian Great Lakes (see Section 14.1.4, p. 574), these lakes and ponds cover an estimated 179,000 to 183,000 km^2 (Butman et al., 2016; Clow et al., 2015; McDonald et al., 2012; Zhu and McGuire 2016) and include more than 87,000 reservoir systems (Clow et al., 2015; Hadjerioua et al., 2012). Streams and rivers in the United States and Alaska are estimated to cover 36,722 km^2 (Butman et al., 2016; Stackpoole et al., 2017b; Zhu and McGuire 2016). Combined, inland waters (except the Great Lakes) cover approximately 1.9% of CONUS and 3.9% of Alaska. Although 30-m resolution map products include inland freshwater bodies $>0.005 \text{ km}^2$ (Feng et al., 2015), large-scale water-surface map products currently do not capture smaller-scale water bodies ($<0.001 \text{ km}^2$), which have been linked with higher greenhouse gas (GHG) emissions rates (Holgerson and Raymond 2016). All stream and river areas in this chapter are estimated by scaling the relationships among discharge and water velocity, water depth, and stream or river width (Melching and Flores 1999; Raymond et al., 2012). Freshwater discharge to the coast of North America is dominated by the Mississippi, St. Lawrence, Mackenzie,

Columbia, and Yukon rivers, which have a combined discharge of $1,500 \text{ km}^3$ per year, about half the total freshwater runoff to the coast of North America (Dai et al., 2009).

The boreal area of North America constitutes one of the most lake-rich regions in the world. In Canada alone, there are an estimated 3.3 million water bodies greater than 0.01 km^2 in surface area and another 5.4 million in the smallest size category ($<0.001 \text{ km}^2$). All Canadian water bodies (excluding the Great Lakes) are estimated to cover 884,000 km^2 , or about 9% of the country's surface. In some large regions of northern Quebec and Ontario, inland waters cover up to 25% of the surface area. In Mexico, surface waters (excluding fluvial systems) are estimated to cover 25,769 km^2 , or 1% of the country's surface, and the total length of streams and rivers is estimated to be 633,000 km (INEGI 2017). The watersheds of Mexico's 33 main rivers cover 565,128 km^2 , and freshwater flow is dominated by the Grijalva and Usumancinta rivers, which drain to the Gulf of Mexico.

There are 87,359 registered dams in the United States (USACE 2016), more than 10,000 dams in Canada (Canadian Dam Association 2018), and 5,163 dams and reservoirs holding approximately 150 km^3 of water in Mexico (CONAGUA 2015). Dam construction in recent years has increased the volume of retained water by about 600% to 700% globally, tripling the transit time of water from land to sea (Vörösmarty et al., 2009). This trend is expected to continue globally with several large damming projects underway (Zarfl et al., 2014). Within the United States, nearly 2,500 dams provide 78 gigawatts (GW) of power; up to 12 GW potentially could be added by leveraging the installed dam capacity currently not being used for energy production (Hadjerioua et al., 2012). The U.S. Pacific Northwest and Southeast have the highest potential for future power generation (Hadjerioua et al., 2012). Reservoirs formed through the damming of rivers alter the natural flux of carbon and the dispersal of sediments (Dean and Gorham 1998), increasing the likelihood that organic carbon will be



remineralized to CH_4 and CO_2 compared to unrestricted conditions (Deemer et al., 2016; Rudd et al., 1993; Teodoru et al., 2012). Thus, the conversion of meandering rivers to a series of reservoirs potentially reduces the transport of carbon to the coast (Hedges et al., 1997), and it may increase the flux of CO_2 and CH_4 to the atmosphere (Deemer et al., 2016; Tranvik et al., 2009; Tremblay et al., 2005).

14.1.4 The Great Lakes

The Laurentian Great Lakes vary between being considered as part of the coastal domain or as inland waters because each of the five lakes is distinct in size and volume. In this chapter, these lakes are considered as inland waters, containing about 18% of the world's supply of surface fresh liquid water and 84% of North America's supply (www.epa.gov/greatlakes/great-lakes-facts-and-figures). Although interconnected, the lakes differ substantially in their physical, biological, and chemical characteristics. The largest, Lake Superior, has an average depth of 147 m and a water retention time of nearly 200 years, while the smallest, Lake Erie, has an average depth of 19 m and a retention time of about 3 years. Productivity ranges from oligotrophic in Lake Superior to eutrophic in Lake Erie. Water chemistry also varies substantially among the lakes, with mean alkalinity ranging from 840 micromoles (μmol) per kg in Lake Superior to 2,181 μmol per kg in Lake Michigan (Phillips et al., 2015).

Despite the large size of the Great Lakes, knowledge of their lakewide carbon cycle is relatively limited. Recent observational and modeling studies have helped elucidate some of the physical and biogeochemical processes governing the seasonal carbon cycle (Atilla et al., 2011; Bennington et al., 2012; Pilcher et al., 2015), but current CO_2 emissions estimates are poorly constrained and are excluded from regional carbon budgets (McDonald et al., 2013). Observations of surface partial pressure of CO_2 ($p\text{CO}_2$) suggest that the Great Lakes are in near equilibrium with the atmosphere on annual timescales but vary seasonally between periods of significant undersaturation and supersaturation (Atilla et al., 2011; Karim et al., 2011; Shao

et al., 2015). Autochthonous carbon from spring and summer productivity is respired at depth and ventilated back to the atmosphere during strong vertical mixing in late fall and winter, limiting burial (Pilcher et al., 2015). However, even highly productive regions, such as western Lake Erie, have been shown to be net sources of carbon to the atmosphere (Shao et al., 2015). Additional data are required to better understand the lakewide response to increasing atmospheric CO_2 and any resulting, decreasing trend in lake pH (Phillips et al., 2015). Further uncertainty arises from a long history of anthropogenic stressors that have significantly affected lakewide ecology and ecosystem services (Allan et al., 2013). A recent example is the proliferation of invasive *Dreissena* mussels throughout most of the Great Lakes. Filter feeding from these mussels coincides with substantial reductions in aquatic primary productivity, which probably has altered the lakewide food web and resulted in unknown impacts to the carbon cycle (Evans et al., 2011; Madenjian et al., 2010).

14.2 Historical Context

14.2.1 Early Understandings

The study of carbon cycling in lakes, streams, and large rivers started in the early part of the last century with the development of the ecosystem concept as a functional unit by which scientists could define the physical, chemical, and biological structure of the world around them. This concept was adapted from terrestrial to aquatic systems through seminal work (Lindeman 1942) partitioning the movement of energy, and as a result carbon, across trophic levels in lakes. A second concept relevant to carbon cycling in inland waters is the tracing of elements through natural systems, which has a long history in geochemistry and had developed prior to the notion of ecology. The convergence of these two concepts that define the interactions among biological, physical, and chemical environments was permanently established by the need to 1) improve water quality from eutrophication of freshwaters by agricultural fertilizer inputs and 2) understand the impacts of acid rain through the exploration of elemental cycling in whole lakes (Johnson and



Vallentyne 1971) and at the watershed scale (Likens 1977). Although carbon remained secondary to the tracing of nutrients and other chemical species, research clearly established that carbon from terrestrial systems provided energy to and influenced the structure of aquatic systems (Pace et al., 2004) and that the boundary between these two systems might not be so discrete. A rich field of ecosystem-based science subsequently developed that expanded dramatically into this century. In an attempt to synthesize carbon dynamics in freshwaters, a group through the National Center for Ecological Analysis and Synthesis produced a seminal paper that highlighted the magnitude of the flows of carbon through freshwaters at the global scale (Cole et al., 2007), laying the foundation for the research that supports this chapter.

14.2.2 First State of the Carbon Cycle Report

The *First State of the Carbon Cycle Report* (SOCCR1) identified rivers and lakes as a net sink of 25 Tg C per year into sediments across North America (CCSP 2007; Pacala et al., 2001; Stallard 1998). The total lateral transfer of carbon (including both DIC and DOC) to the ocean was estimated to be 35 Tg C per year (Pacala et al., 2001) and was considered highly uncertain. These estimates did not include Canada, Mexico, or the Great Lakes because of a lack of available data for each. It is important to note that all estimates for rivers were considered sinks or net transfers of carbon to the coastal environment, as well as storage of carbon in lake and reservoir sediments. Since 2007, the research community has widely accepted that inland aquatic ecosystems also function as an important interface for carbon exchange between terrestrial ecosystems and the atmosphere (Cole et al., 2007; Tranvik et al., 2009). Evidence summarized herein shows that, over short timescales, freshwaters function as sources of atmospheric CO₂. Also provided are improved estimates of burial in lakes and reservoirs and lateral transfer to the coast. The updated budget increases the total carbon fluxes from inland waters by a factor of two over those reported in SOCCR1 (see Table 14.1, p. 576) and alters the

previous perception of inland waters as a sink of atmospheric CO₂. These estimates of inland water fluxes, coupled with a better understanding of flow paths for carbon losses and export from wetland and coastal environments, provide evidence that the majority of terrestrially derived carbon moving through inland waters is released to the atmosphere as CO₂.

14.3 Current Understanding of Carbon Fluxes and Stocks

A more complete accounting of aquatic carbon has been a major advance in aquatic carbon cycle science, specifically the inclusion of CO₂ emissions from rivers and lakes to the atmosphere. Additionally, publications of high-resolution inventories of lake and river surface areas have enabled researchers to more accurately scale up local hydrology and chemistry datasets to regional and continental scales. One of the most important results from these new and rigorous assessments is the documentation of regional variability across Arctic, boreal, temperate, subtropical, and tropical ecosystems in North America.

14.3.1 Carbon Fluxes from U.S. Waters

Contemporary total inland water carbon fluxes from CONUS and Alaska were estimated with comparable datasets and methodologies (Butman et al., 2016; Stackpoole et al., 2016). Total aquatic carbon fluxes represent the sum of 1) lateral transport of DIC and total organic carbon (TOC) from river systems to the coast, 2) CO₂ emissions from rivers and lakes, and 3) carbon burial in sediments. Although burial in lake sediments also has been considered storage at the continental scale, this report considers burial as the removal of carbon from the aqueous environment and thus adds burial to the total flux (see Equation 14.1, p. 571).

The estimated total carbon flux from inland waters in CONUS is 147 Tg C per year (5% and 95%: 80.5 and 219 Tg C presented in Butman et al., 2016). In Alaska, it is 44.5 Tg C per year (31.4 and 52.5 Tg C presented in Stackpoole et al., 2016). These

**Table 14.1. U.S., North American, and Global Annual Carbon Fluxes from Inland Waters^{a-k}**

Source	United States ^a	Canada	Mexico	Great Lakes	North America	Globe (Pg C per Year)
	(Tg C per Year)					
Rivers and Streams						
Lateral Fluxes	59.8***	18.2 (TOC) ^b	ND	ND	105****	0.6–0.7 ^c
Gas Emissions	85.9**	ND	ND	ND	124.5**	0.7–1.8 ^d (2.9) ^e
Lakes and Reservoirs						
Burial	22.5**	ND	ND	2.7* ^h	155**	0.2–0.6 ^f
Gas Emissions	24.2***	ND	ND	ND	122**	0.6 ^g
Inland Aquatic Systems						
Total Carbon Flux	193***	ND	ND	2.3–36* ⁱ	507**	2.1–3.7 (4.9)
Net Carbon Yield (g C per m ² per year)	20.6***	ND	ND	ND	23.2**	16–17 (33)

Notes

- a) Butman et al. (2016); Stackpoole et al. (2016). United States includes the conterminous United States and Alaska.
- b) Clair et al. (2013).
- c) Dai et al. (2012); Meybeck (1982); Seitzinger et al. (2005); Hartmann et al. (2014b); Spitzky and Ittekkot (1991); Syvitski and Milliman (2007); Galy et al. (2015).
- d) Raymond et al. (2013); Lauerwald et al. (2015).
- e) All estimates in parenthesis derived from Sawakuchi et al. (2017).
- f) Battin et al. (2009a); Tranvik et al. (2009).
- g) Aufdenkampe et al. (2011).
- h) Einsele et al. (2001).
- i) McKinley et al. (2011).
- j) All fluxes include inorganic and organic carbon as well as particulate and dissolved species.
- k) Key: Tg C, teragrams of carbon; Pg C, petagrams of carbon; g C, grams of carbon; TOC, total organic carbon; ND, no data; Asterisks indicate that there is 95% confidence that the actual value is within 10% (*****), 25% (****), 50% (***), 100% (**), or >100% (*) of the reported value.

estimates combine for a total flux of about 193 Tg C per year, as presented in Table 14.1, this page. Carbon yields, which represent fluxes normalized by land surface area, are 18.6 g C per m² per year in CONUS and 29 g C per m² per year in Alaska. The higher value for Alaska is most likely related to the higher water surface area found across the state. Combined and weighted by area, the average yield for CONUS and Alaska is 20.6 g C per m² per year.

Rivers dominate total carbon fluxes from inland waters in CONUS and Alaska. Coastal carbon export is 41.5 Tg C per year (5% and 95%: 39.4, 43.5 Tg C) for CONUS and 18.3 Tg C per year

(16.3, 25.0 Tg C) for Alaska. River CO₂ emissions are 69.3 Tg C per year (36.0, 109.6 Tg C) and 16.6 Tg C per year (9.0, 26.3 Tg C), respectively.

Carbon burial in lakes and reservoirs is 20.6 Tg C per year (9.0, 65.1 Tg C) in CONUS and 1.9 Tg C per year (1.3, 2.8 Tg C) in Alaska, lower than the respective river fluxes to the coast. Lake emissions are 16.0 Tg C per year (14.3, 18.7 Tg C) in CONUS and 8.2 Tg C per year (6.1, 11.2 Tg C) in Alaska. Lake CO₂ losses to the atmosphere roughly equal the magnitude of carbon buried in lake sediments in CONUS, but lake CO₂ emissions are much greater relative to carbon burial rates in Alaska.



14.3.2 Carbon Fluxes from Canadian Waters

The Canadian climate and terrestrial landscape are highly heterogeneous, from temperate rainforests to Arctic desert. The transport and processing of carbon in Canada's inland waters are correspondingly variable. Although lake or river carbon cycling has been studied in several regions, significant gaps remain in this report's assessment of country-wide carbon transport and transformation in aquatic systems. The terrestrial carbon export rate to aquatic networks varies from <1 g C per m^2 per year to >20 g C per m^2 per year for both organic and inorganic fractions, though their relative importance is region-specific (Clair et al., 2013). A recent estimate for all the drainage basins in Canada suggests that 18.2 Tg of organic carbon is exported to the coast each year (Clair et al., 2013). Although DIC is the dominant form of carbon export from terrestrial systems in the Prairie provinces, Manitoba, Saskatchewan, and Alberta (Finlay et al., 2010), the balance shifts toward co-equality in Southern Quebec catchments (Li et al., 2015) and to a dominance of organic carbon in the boreal zone (Molot and Dillon 1997; Roulet and Moore 2006). The combined organic and inorganic lateral flux from land to the coast is currently unavailable.

While the vast majority of Canadian lakes and rivers are supersaturated in CO_2 and CH_4 relative to the atmosphere and thus act as sources (Campeau et al., 2014; del Giorgio et al., 1997; Prairie et al., 2002; Teodoru et al., 2009), alkaline and eutrophic systems can act, at least temporarily, as carbon sinks (Finlay et al., 2010). Generally, however, Canadian lakes are net heterotrophic through the degradation of incoming DOC (Vachon et al., 2016), with emission rates of CO_2 and CH_4 from lakes typically varying as an inverse function of lake size (Rasilo et al., 2015; Roehm et al., 2009) and positively with organic matter inputs (del Giorgio et al., 1999). Lakes of northern Quebec have accumulated more carbon per unit area than their surrounding forest soils but less than surrounding peatlands (Heathcote et al., 2015). Lake bathymetric shape and exposure

to oxygen are the primary determinants of carbon accumulation and of the efficiency of burial relative to the carbon supply (Ferland et al., 2014; Teodoru et al., 2012). At the whole-landscape scale, lake sediments account for about 15% of the accumulated carbon (Ferland et al., 2012).

14.3.3 Carbon Fluxes from Mexican Waters

Extensive data on carbon stocks and fluxes do not yet exist for Mexico, but a summary exists of several individual small-scale datasets about Mexican inland water carbon fluxes (Alcocer and Bernal-Brooks 2010). The state of knowledge presented herein regarding carbon cycling in the inland waters of Mexico focuses on lake GHG emissions and burial. Given the tectonic activity of Mexico, there has been an interest in understanding how the carbon emissions of volcanic lakes evolve across space and time. Carbon dioxide emissions from the lake inside El Chichón volcano, Chiapas, reportedly range from 0.005 to 0.016 Tg C per year, or 72,000 to 150,000 g C per m^2 per year (Mazot and Taran 2009; Perez et al., 2011). More recently, research on Lake Alchichica showed that, on average, surface water pCO_2 was below atmospheric pCO_2 for 67% of the year, with an average surface water pCO_2 of 184 microatmospheres (μatm ; Guzmán-Arias et al., 2015). These findings suggest that deep, tropical, and warm monomictic lakes have the potential to take up atmospheric CO_2 through primary production and preserve most of the POC deposited to the sediments, creating important carbon sinks. Emissions of CH_4 may be as important as emissions of CO_2 across regions of Mexico. Although few studies have evaluated the CH_4 emissions from Mexican inland waters, the CH_4 flux from six Mexican lakes is estimated to be about 1.3 ± 0.4 Tg CH_4 per year, which constitutes 20% of Mexico's CH_4 emissions (Gonzalez-Valencia et al., 2013). The total CH_4 flux from 11 aquatic ecosystems in Mexico City was 0.004 Tg CH_4 per year, 3.5% of the CH_4 emissions of the city (Martinez-Cruz et al., 2016). Fully quantifying the importance of anthropogenic inputs of CH_4 -producing organic materials through waste



streams is critical for better constraining these fluxes at the national scale.

Other research on inland water carbon dynamics in Mexico has focused on reservoirs. The CO₂ emissions of the Valle de Bravo reservoir, Estado de Mexico, calculated through the photosynthesis and respiration balance, was 0.34 g C per m² per year (Valdespino-Castillo et al., 2014). Carbon burial has been studied in a few Mexican lakes. A 3-year study determined that the well-characterized system of Lake Alchichica, Puebla, has a carbon burial rate of 25.6 ± 12.3 g C per m² per year (Oseguera-Pérez et al., 2013).

14.3.4 Carbon Fluxes from the Great Lakes

As previously suggested, a comprehensive assessment of carbon fluxes does not yet exist for all of the Laurentian Great Lakes. The best estimates for individual component carbon flux values for the Great Lakes come from Lake Superior. Primary production is estimated to be 5.3 to 9.7 Tg C per year, while respiration is estimated to be significantly greater at 13 to 83 Tg C per year (Cotner et al., 2004; Sterner 2010; Urban et al., 2005). External inputs of 0.68 to 1.03 Tg C per year (Cotner et al., 2004) of organic carbon are too small to account for this imbalance between primary production and respiration, suggesting significant sources of external DIC. However, modeling work suggests that previous respiration estimates were biased high because of spatial heterogeneity and found a much lower value of 5.5 Tg C per year (Bennington et al., 2012). Estimates do not yet exist for the balance between the amount of organic carbon buried in sediments versus the amount exported through rivers or emitted as CO₂ and CH₄. However, total carbon burial across all lakes may be on the order of 2.7 Tg C per year, with an areal sink of 15 g C per m² per year since 1930 (Einsele et al., 2001). Additional research is needed to constrain the fluxes of carbon from the Great Lakes.

14.4 Current and Future Trends

Whether carbon fluxes from inland waters are increasing or decreasing at the national or

continental scale remains unclear. Because carbon export from the terrestrial landscape is tightly linked to discharge, increases in discharge probably will lead to increases in carbon export (Mulholland and Kuenzler 1979). Current studies are arguing for an increase in discharge for many regions of North America, including the U.S. Midwest and New England; however, reductions in precipitation are predicted in the southern and western regions of the United States (Georgakakos et al., 2014). Human water use through irrigation also may be affecting the spatial variability of discharge, with lower discharge in regions of higher irrigation, an effect which may be mitigated by increases in precipitation (Kustu et al., 2011). However, future changes in precipitation that lead to regional drought will reduce the transfer of carbon from the terrestrial ecosystem into the aquatic environment, while simultaneously decreasing the total area of aquatic ecosystems. Other anthropogenic drivers also can impact fluxes. Evidence suggests that DIC fluxes have increased from the Mississippi River over time because of land-management practices associated with liming and irrigation for agriculture, as well as increases in precipitation across portions of the basin (Raymond et al., 2008; Tian et al., 2015). In the United States, about 30 Tg of lime are applied each year, resulting in a potential flux of 7.2 Tg of inorganic carbon per year in the form of bicarbonate, or an actual flux of approximately 5.4 Tg C per year, assuming that 25% is balanced by the export of products from weathering reactions other than carbonic acid (Oh and Raymond 2006). The total U.S. riverine flux of DIC is approximately 35 Tg per year (Stets and Striegl 2012). Thus, liming and fertilizer use may contribute about 15% of total river bicarbonate flux in the United States.

Calculations suggest that DOC export from the Mississippi River has increased since the early 1900s, primarily a result of land-cover change from forest and grasslands to managed agriculture (Ren et al., 2016). Tributaries to the Mississippi have been shown to have decreasing DOC as a result of wetland loss (Duan et al., 2017). However, DOC flux from the Mississippi River to the



Gulf of Mexico did not change from 1997 to 2013 (Stackpoole et al., 2016). Changing concentrations of dissolved CO₂ were identified in nine lakes in the Adirondacks, New York, where six showed significant increases and three showed significant decreases over 18 years (Seekell and Gudasz 2016). The rate of change in both the positive and negative direction was found to be in excess of 12 μatm per year, well outside the rate of increase in the atmosphere. Increasing trends in these lakes were attributed first to basin-scale recovery from acid precipitation, resulting in an increase in soil CO₂ production in systems with little buffering capacity, where CO₂ can be a large contributor of inorganic carbon exported from the catchment. Also attributed were changes in DOC concentrations, export, and remineralization rates within the lake environment (Burns et al., 2006; Seekell and Gudasz 2016). Globally, evidence indicates increases in the concentrations of organic carbon from a number of sources, a phenomenon termed the “browning” of waters. However, studies suggest that these increases are caused by regionally specific factors, including recovery from acid rain; increases in carbon export from soils; and the mobilization of permafrost carbon into stream systems (Evans et al., 2006; Lapierre et al., 2013; Monteith et al., 2007; Roulet and Moore 2006; Tank et al., 2016). Evidence also suggests that the active layer depth in permafrost soil has increased, mobilizing previously frozen carbon stocks (Neff et al., 2006). In addition, warming and related vegetation changes have increased DOC flux from the Mackenzie River to the Arctic Ocean (Tank et al., 2016). However, permafrost thaw and increased groundwater contribution to Arctic rivers also have been linked to increased mineralization of organic carbon in the subsurface and changes in the proportion of DOC and DIC exports in Alaska’s Yukon River basin (Striegl et al., 2005; Walvoord and Striegl 2007). Any decreases in organic carbon export, though, potentially may be offset by increased organic carbon runoff from vegetation change in low-lying regions (Dornblaser and Striegl 2015). The proportion of carbon mobilized under warming conditions

that is mineralized to CO₂ versus exported as DOC remains unknown. Furthermore, research indicates that permafrost thaw also has increased CH₄ emissions since the 1950s as a result of degrading lake shorelines that contribute aged carbon (Walter Anthony et al., 2016). However, these emissions cannot be quantified at the national or continental scales.

Changes in aquatic carbon fluxes are linked directly to the residence time of water in both terrestrial and aquatic environments (Catalán et al., 2016). In particular, as precipitation increases, reducing water residence time, so do organic carbon fluxes from landscapes (Bianchi et al., 2013; Yoon and Raymond 2012). Knowing the contribution of groundwater versus surface water in streams is also important to understand CO₂ fluxes from terrestrial systems (Hotchkiss et al., 2015). The removal of organic carbon in lakes, streams, and rivers is positively related to its residence time (Catalán et al., 2016; Vachon et al., 2016). The half-life of organic carbon in inland waters is about 2.5 years, much shorter than the decades to millennia required for soil systems to completely turn over (Catalán et al., 2016). Some studies hypothesize that increases in precipitation caused by an altered climate will move carbon that would be stored in soils into aquatic environments where remineralization may accelerate the return of organic carbon to the atmosphere as CO₂ in high and temperate latitudes (Drake et al., 2015; Raymond et al., 2016). In addition, the installation or removal of dams will directly affect the quantity and form of carbon in aquatic environments by shifting water residence time, water surface areas, and sediment loads. Predicting how the overall carbon balance will shift across North America remains difficult because of complex interactions between inorganic and organic carbon within aquatic systems and the importance of anthropogenic change at the landscape scale (Butman et al., 2015; Lapierre et al., 2013; Regnier et al., 2013; Solomon et al., 2015; Tank et al., 2016).



14.5 Global, North American, and U.S. Context

14.5.1 A Global Carbon Cycle Perspective

Understanding the fluxes of carbon through inland waters in the context of the global carbon cycle remains an active area of research today. Of particular interest are 1) terrestrial carbon fluxes to inland waters; 2) carbon transformations within inland waters, especially movement into storage reservoirs and the atmosphere; and 3) carbon fluxes to coastal waters and large inland lakes. Using Equation 14.1, p. 571, assessment of components of the inland water carbon cycle can begin at the global, regional, and U.S. scales.

Globally, the component with the least uncertainty is the flux of carbon to coastal waters. Estimates of DOC flux to the coast, for instance, have remained around 0.2 ± 0.05 Pg C per year for the last 30 years, although these estimates often are based on the same underlying dataset (Dai et al., 2012; Meybeck 1982; Seitzinger et al., 2005). The DIC flux of 0.35 Pg C per year has been shown to result from strong linkages between lithology and climate, coupled with better global products for these drivers (Hartmann et al., 2014b). Global estimates of the POC flux to coastal waters have changed because of a large and evolving anthropogenic signal from POC trapping behind dams, with a total flux of 0.15 Pg C per year (Galy et al., 2015; Spitzky and Ittekkot 1991; Syvitski and Milliman 2007). The sum of DOC, DIC, and POC fluxes results in a C_{export} of 0.7 Pg C per year.

New global and ecosystem-specific estimates of CH_4 and CO_2 exchanges with the atmosphere have been facilitated by the growth of databases that capture measurements of these GHGs and by the ability to scale up estimates of inland water area and gas transfer velocity (Abril et al., 2014; Bastviken et al., 2011; Borges et al., 2015; Butman and Raymond 2011; Lauerwald et al., 2015; Raymond et al., 2013). New research suggests that Arctic and boreal lakes and ponds may release 16.5 Tg C per year (Wik et al., 2016), more than double previous

estimates (Bastviken et al., 2011) for a similar range of latitudes. Evidence now shows that lake and river size, topography, land cover, and terrestrial productivity affect the total carbon dynamics in freshwaters (Butman et al., 2016; Holgerson and Raymond 2016; Hotchkiss et al., 2015; Stanley et al., 2016). However, these relationships are based on limited empirical data, and, although progress is being made, a mechanistic understanding that links landscapes to inland water carbon fluxes is still lacking (Hotchkiss et al., 2015). Furthermore, the fluxes of CH_4 and CO_2 per unit area of water surface are extremely high for very small streams and ponds (Holgerson and Raymond 2016), but these systems are not easily detected with remote sensing and have very few high temporal frequency studies (Feng et al., 2015; Koprivnjak et al., 2010).

Carbon dioxide flux from inland waters to the atmosphere ($C_{emissions}$) at the global scale is due to mostly large river systems and currently is estimated at 1.8 to 2.2 Pg C per year (Raymond et al., 2013). Recent data from the Amazon suggest that total global emissions could be as high as 2.9 Pg C per year (Sawakuchi et al., 2017). Carbon burial represents another large removal process for aquatic carbon. Global inland water burial estimates are fairly uncertain, ranging from 0.2 to 0.6 Pg C per year as C_{burial} (Battin et al., 2009b; Tranvik et al., 2009). Assuming that the carbon stock of inland waters is not changing with time and using compiled values only (Raymond et al., 2013) lead to the maximum possible terrestrial input being approximately 3.7 Pg C per year (Raymond et al., 2013), which represents the total carbon needed to balance the loss through coastal export, burial, and gas emissions. Internal primary production and respiration are known contributors to gas emissions, as well as burial. Therefore, verifying this 3.7 Pg C per year currently is not possible due to the diversity of terrestrial and inland water ecosystems, temporal variability of fluxes, and lack of studies of small end-member ecosystems.



14.5.2 Comparison Between Global and U.S. Carbon Fluxes

The fluxes of carbon from the United States (CONUS and Alaska) represent those with the highest confidence reported here and will be evaluated against those at the global scale. A comparison of global versus U.S. estimates of aquatic carbon fluxes shows similar patterns in the relative magnitude of carbon flux pathways. Applying the conservative global estimate for carbon burial of 0.2 Pg C per year (Tranvik et al., 2009), carbon emissions across the air-water interface are 60% of the total flux at the global scale and 63% at the U.S. scale (see Equation 14.1, p. 571, and Figure 14.2, p. 572). In contrast to estimates in SOCCR1, these results suggest that half of all aquatic carbon fluxes are releases of gases to the atmosphere. At the global and U.S. scales, lateral fluxes from land to coasts represent 24% and 26% of the total, respectively. It is important to note that globally, POC entrapment through burial, if assumed to be 0.2 Pg C per year, is nearly 6% of the total flux of carbon from inland waters. This amount increases to 16% if the burial term is considered to be 0.6 Pg C per year (Battin et al., 2009b). The range of estimates for the proportion of carbon entering sediments (i.e., 6% to 16%) globally bounds the more refined modeling for CONUS that suggests burial is 10% of the total.

Global and U.S. CO₂ emissions equal 17 and 13.6 g C per m² per year, respectively, indicating that CO₂ emissions from U.S. inland waters are 20% less than the global average per unit land area. Carbon burial per unit area varies from 1.5 to 4.5 g C per m² per year, very similar to the 1.9 g C per m² per year estimate obtained for CONUS and Alaska. Overall, per unit area, the total carbon flux at the global scale is 25% greater (at 24.8 g C per m² per year) than the 20.6 g C per m² per year estimated for the United States. The discrepancies between the U.S. and global areal fluxes increase if recently estimated values (Sawakuchi et al., 2017) are used for the comparisons (see Table 14.1, p. 576). These discrepancies may be due to differences in methodologies but also may reflect spatial variability in inland

water ecosystem type. For example, the importance of tropical systems for carbon fluxes may drive the distribution of inland water fluxes at the global scale, even though tropical areas represent only a very small fraction of the ecosystems within CONUS.

14.5.3 Regional Differences of U.S. Carbon Fluxes

Carbon fluxes from inland waters differ across regions in CONUS, and the relative contributions of each flux component vary across space (Butman et al., 2016). In particular, lateral fluxes from the eastern portion of the Mississippi River basin are larger than gaseous emissions, while carbon burial dominates lake fluxes in the river's lower basin. Carbon dioxide emissions are dominant in systems that have steep topography and more acidic waters. Emissions of CO₂ are highest in the western regions of the Pacific Northwest, where both rainfall and topography drive large carbon inputs from primary production and topography enhances gas transfer (Butman et al., 2016). Inorganic carbon fluxes in the form of bicarbonate are large within watersheds with large areas of agriculture in the upper Midwest, an effect attributed to agricultural liming (Oh and Raymond 2006). Regional variability in inland water carbon fluxes is driven by the available inputs of carbon from variable land cover, as well as precipitation that facilitates the physical movement of that carbon from groundwater, soils, and wetlands.

14.5.4 North American Carbon Fluxes in Context

Total carbon fluxes from inland waters of North America were estimated using the results of the Regional Carbon Cycle Assessment and Processes (RECCAP) effort (see Table 14.1, p. 576) for emissions and lateral fluxes based on the scaling of empirical data (Hartmann et al., 2009; Mayorga et al., 2010; Raymond et al., 2013). The average burial rate of carbon based on land cover from CONUS and Alaska was used herein for calculations (Clow et al., 2015). The total carbon flux from inland waters is estimated to be 507 Tg C per year. About 48% of this carbon, or 247 Tg per year, consists of emissions across the air-water interface



from both lentic and lotic systems. The lateral flux of carbon to the coast is 105 Tg C per year, or 21% of the total. This estimate compares well with recent results derived from a spatially explicit coupled hydrological-biogeochemical model that suggest 96 (standard deviation 8.9) Tg C per year move laterally to coastal systems in North America (Tian et al., 2015). Finally, the burial of carbon within inland waters is estimated to be nearly 30% of the total flux, at 155 Tg C per year. These estimates are based on modeled export of carbon to coastal systems and broadly scaled estimates for CO₂ emissions derived from sparse datasets at high latitudes (Hartmann et al., 2014a; Raymond et al., 2013) and are considered uncertain.

14.6 Societal Drivers, Impacts, and Carbon Management

Human impacts on carbon movement and processing in inland waters include 1) land-use change that promotes the destabilization of soil carbon and increases erosion (Lal and Pimentel 2008; Quinton et al., 2010; Stallard 1998); 2) altered climate patterns that shift the timing and magnitude of precipitation and hydrological events (Clair and Ehrman 1996; Evans et al., 2007); 3) changes in nutrient and organic matter inputs that alter carbon processing and storage within aquatic environments (Humborg et al., 2004; Mayorga et al., 2010; Seitzinger et al., 2005); and 4) changes in temperature (Nelson and Palmer 2007). These effects are not independent of one another. However, inland waters are inherently difficult to evaluate in the context of carbon management, from either a sequestration or mitigation position. In contrast to forested ecosystems, the chemistry of inland waters changes rapidly on timescales from seconds to days in direct relation to the hydrological regime (Sobczak and Raymond 2015). Furthermore, the sources of carbon within inland waters are poorly characterized across spatial and temporal scales relevant to national-scale management decisions. A robust understanding of the impact that dams have on carbon transformation and fluxes to coastal systems would directly identify the connections between anthropogenic energy

and water resource needs and the carbon cycling of inland waters (Deemer et al., 2016; Maeck et al., 2014; Teodoru et al., 2012). The research community is currently unable to identify whether all dammed systems cause increased carbon emissions, but recent synthesis efforts suggest that CO₂ and CH₄ emissions increase under conditions of high nutrients and with large inputs of terrestrial carbon (Barros et al., 2011; Deemer et al., 2016; Teodoru et al., 2012). Worldwide there are more than 1 million estimated dams (Lehner et al., 2011); of these, over 87,000 have heights >15 m (World Commission on Dams 2000). Research is needed to evaluate the impact that this level of damming has on the aquatic carbon cycle.

14.7 Synthesis, Knowledge Gaps, and Outlook

14.7.1 Summary

Advances in the ability to manipulate large databases of carbon chemistry covering the United States, coupled with new methods for spatial analysis, have enabled new and robust estimates for carbon fluxes from inland waters in CONUS and Alaska. By identifying and including CO₂ emissions, the U.S. fluxes of carbon are estimated to be approximately 193 Tg C per year. These fluxes are dominated by river and stream networks exporting up to 59.8 Tg C per year to the coast and emitting nearly 85.9 Tg C per year as CO₂ to the atmosphere. Availability of data is limited from Mexican inland waters. Deep, tropical, warm monomictic lakes constitute carbon sinks primarily as POC, while shallow, tropical—and mostly eutrophic—lakes are sources of CO₂ and CH₄ to the atmosphere. Further data collection is needed to properly assess carbon cycling within inland waters at the national scale in both Canada and Mexico. However, based on estimates presented here, the carbon flux from inland waters is now understood to be four times larger than estimates presented in SOCCRI.

14.7.2 Key Knowledge Gaps and Current Opportunities

Peer-reviewed and detailed estimates are not currently available for carbon fluxes from inland waters



within Mexico and Canada. Further collaboration is necessary among monitoring efforts in these countries and the United States to properly develop a spatially explicit inland water database on carbon concentration and carbon fluxes across North America. In addition, robust estimates of annual carbon fluxes for the Laurentian Great Lakes are not yet possible, a surprising limitation given their importance as the largest inland waters on Earth. Preliminary data suggest that these systems vary from a net carbon source to the atmosphere in Lake Superior, Lake Michigan, and Lake Huron to a net carbon sink in Lake Erie and Lake Ontario. By combining a box model analysis with a literature review of respiration, river inputs, and burial, McKinley et al. (2011) conclude that the Great Lakes efflux lies between 2.3 and 36 Tg C per year. If future research suggests emissions near 2.3 Tg C per year, then the emission of carbon as CO₂ may be nearly balanced by carbon burial (Einsele et al., 2001). However, if new data suggest significantly higher emissions, such results would increase the importance of the Great Lakes with respect to total carbon fluxes from the United States and Canada. The Great Lakes are heavily affected by anthropogenic disturbance through nutrient enrichment and invasive species, with unknown impacts on carbon cycling.

Also unavailable is a comprehensive estimate for the contribution of CH₄ to carbon emissions for inland waters of North America. Data on CH₄ do not yet exist across space and time to properly scale to national and continental levels, though significant progress is being made (Holgerson and Raymond 2016; Stanley et al., 2016; Wik et al., 2016).

One major methodological advancement in past years is *in situ* probe systems (Baehr and DeGrandpre, 2004). Probes to measure aspects of the carbon cycle are becoming more accurate and affordable (Bastviken et al., 2015; Johnson et al., 2010), and the research community is advancing methodologies to process high-temporal datasets (Downing et al., 2012), identifying the role that storm events may play in carbon fluxes. The possibility now exists to instrument inland water systems

along the aquatic continuum from when water emerges from the terrestrial interface to when it is exported to the coast or large inland lakes. Such instrumentation will facilitate understanding of the transformations of terrestrial carbon during transport to inland waters and the controls on this transport. However, deploying sensor systems alone is not enough to ensure the development of the data needed to reduce uncertainties. The inland water carbon cycle science community must learn from the efforts of organizations like the International Ocean Carbon Coordination Project to develop standard approaches and reference materials for study comparison and reproducibility. Furthermore, future research needs to take advantage of developments in both large- and small-scale data acquisition and should attempt nested watershed studies across scales to understand the carbon cycling within inland water environments. These studies, coupled with new methods to quantify surface waters at the global scale, particularly small streams and ponds, will help further constrain the importance of inland waters to the Earth biogeochemical system under a changing climate (Pekel et al., 2016).

At 193 Tg C per year, the fluxes of carbon through inland waters of the United States are significant. The scaled value of 507 Tg C per year for North America represents an estimate that requires further science to reduce uncertainties. In the context of the overall cycling of carbon among terrestrial, wetland, and aquatic environments, there are important methodological differences that must be considered when using the estimates of carbon flux from inland waters. The aquatic carbon fluxes presented herein are derived from the modeling of fluxes to the coast, lake sediments, and the atmosphere. The quantification of the lateral flux of carbon to estuarine systems is perhaps the most well constrained, as it is derived from long-term monitoring of water flow and decades of direct measurements of carbon concentration. The emission of CO₂ from water surfaces is more uncertain. The difficulty of quantifying this emission is compounded by the ephemeral nature of small streams, along with a lack of detailed spatial information



on their total length and surface area. As suggested in this chapter, small streams and ponds represent a large fraction of the CO₂ emissions from inland waters to the atmosphere, important when scaling fluxes across the United States and the world. Furthermore, apportioning the carbon in an aquatic environment to its source (e.g., autochthonous versus allochthonous) currently is not possible. This gap in understanding removes an ability to differentiate, for example, soil respiration that simply has changed location into an aquatic ecosystem from in-stream respiration.

The importance of erosional fluxes of carbon to North American inland waters also cannot be properly assessed. The lateral transport of soil carbon and the concurrent fluxes of CO₂ returning

to the atmosphere in China suggest that upwards of 45 Tg C per year enter inland waters, thus representing a terrestrial carbon sink (Yue et al., 2016). However, this type of calculation does not fully account for replacement of carbon within soils, the remineralization of organic carbon during transport, direct inputs of inorganic carbon, or the lateral fluxes of dissolved carbon to the coast. Therefore, caution is warranted when including inland waters in a mass balance for total carbon accounting. To fully understand the role that inland waters play across the land-water continuum, studies must be conducted at the watershed scale, coupling terrestrial and inland water processes. These measurements will help constrain future modeling studies that require coupling between hydrology and biogeochemistry.



SUPPORTING EVIDENCE

KEY FINDING 1

The total flux of carbon—which includes gaseous emissions, lateral flux, and burial—from inland waters across the conterminous United States (CONUS) and Alaska is 193 teragrams of carbon (Tg C) per year. The dominant pathway for carbon movement out of inland waters is the emission of carbon dioxide gas across water surfaces of streams, rivers, and lakes (110.1 Tg C per year), a flux not identified in the *First State of the Carbon Cycle Report* (SOCCR1; CCSP 2007). Second to gaseous emissions are the lateral fluxes of carbon through rivers to coastal environments (59.8 Tg C per year). Total carbon burial in lakes and reservoirs represents the smallest flux for CONUS and Alaska (22.5 Tg C per year) (*medium confidence*).

Description of evidence base

Estimates for the export of carbon to U.S. coasts have been well documented through long-term observations (Stets and Striegl 2012) and syntheses (Butman et al., 2016; Stackpoole et al., 2016; Zhu and McGuire 2016). Carbon burial is derived from recent model results (Clow et al., 2015). Gaseous emissions of CO₂ were originally assessed in Butman and Raymond (2011) for streams and rivers and McDonald et al. (2013) for lakes and reservoirs of CONUS only. Previous data do exist to support inland waters as dominated by supersaturated conditions (Striegl et al., 2012; Tranvik et al., 2009).

The finding that the dominant pathway for carbon loss through inland waters is through surface emissions was identified in Richey et al. (2002) and Cole et al. (2007) and quantified for CONUS in (Butman and Raymond 2011). Estimates that support this finding for Alaska are presented in Zhu and McGuire (2016). McDonald et al. (2012) showed that across CONUS, lake carbon burial and lake emissions are similar in magnitude when considered at the national scale, with regional variation based on the input of dissolved inorganic carbon (DIC) to lake systems.

Major uncertainties

Large uncertainties exist for the emission of CO₂ from stream and river systems based on empirical estimates of the gas transfer velocity of CO₂ presented in Raymond et al. (2012). The modeling of gas transfer is poorly constrained under high-flow conditions in steep topography. High levels of uncertainty also exist regarding the temporal dynamics of both lentic and lotic CO₂ emissions (Battin et al., 2008; Striegl et al., 2012; Tranvik et al., 2009), where limited data exist to assess carbon gas concentrations under ice or storm flow conditions.

Uncertainties also exist regarding the use of the empirical model for carbon burial presented in Clow et al. (2015). Limited concentration data exist for lakes in Alaska, and there may be significant bias in the concentrations used to scale lake fluxes across regions (Stackpoole et al., 2017a; Zhu and McGuire 2016). These constraints may result in overestimates of emissions. In addition, limited data on carbon burial exist for northern latitudes, resulting in the use of empirical models derived from samples that do not capture the level of variability that exists across Alaska (Stackpoole et al., 2016).

Assessment of confidence based on evidence and agreement, including short description of nature of evidence and level of agreement

The overall confidence level of medium reflects 1) advancements in inland water spatial representations in a global information system (GIS) format to develop surface areas, 2) completion



of datasets enabling the calculation of lateral fluxes, and 3) advancements in databases relevant to sedimentation rates in U.S. lakes and reservoirs. Confidence is reduced because modeling approaches available to estimate gas transfer velocities used for calculating carbon emissions are limited, and there are few chemical measurements in small stream systems.

Summary sentence or paragraph that integrates the above information

For Key Finding 1, individual flux terms (i.e., lateral flux, CO₂ emission, and carbon burial) each have a medium to high level of certainty. This reflects the high confidence in the spatial representation of the chemical data for CONUS and Alaska, as well as the length of monitoring for water chemistry within CONUS and Alaska.

KEY FINDING 2

Based on estimates presented herein, the carbon flux from inland waters is now understood to be four times larger than estimates presented in SOCCR1. The total flux of carbon from inland waters across North America is estimated to be 507 Tg C per year based on a modeling approach that integrates high-resolution U.S. data and continental-scale estimates of water area, discharge, and carbon emissions. This estimate represents a weighted average of 24 grams of carbon per m² per year of continental area exported and removed through inland waters in North America (*low confidence*).

Description of evidence base

Initial data presented in SOCCR1 did not acknowledge emission of carbon across the air-water interface. The estimate of 507 Tg C per year is based on well-constrained estimates of water discharge presented in Mayorga et al. (2010), Seitzinger et al. (2005), and compared with Dai et al. (2009, 2012). Estimates for the export of carbon modeled with water discharge are provided through the Regional Carbon Cycle Assessment and Processes (RECCAP) effort of the Global Carbon Project. Gaseous emissions of CO₂ are presented in Raymond et al. (2013) based on similar methods presented in Butman and Raymond (2011). Areal rates of carbon flux through inland waters for CONUS and Alaska match those for North America.

Major uncertainties

Estimates and uncertainties to scale the emissions of CO₂ from streams, rivers, and lake systems from CONUS to North America have already been provided. However, the application of CONUS lake carbon burial rates derived from Clow et al. (2015) to the total lake areas from Aufdenkampe et al. (2011) is unique. The methods used an average burial rate of about 110 g C per m² per year, which is lower than those used in recent global estimates for lake and reservoir burial (Battin et al., 2009a). This burial rate is not dynamic and does not fully capture the spatial heterogeneity found across North America (Clow et al., 2015).

Assessment of confidence based on evidence and agreement, including short description of nature of evidence and level of agreement

Overall level of confidence is lower for the region of North America due to the different modeling approach, lack of data that exist in both Canada and Mexico, and the simplified application of U.S. data to a region that covers many different ecosystem types.

**Summary sentence or paragraph that integrates the above information**

For Key Finding 2, confidence is low for estimates of inland aquatic carbon fluxes for North America because of a general lack of data available from Mexico and Canada, including CO₂ emissions or burial estimates. Methods developed for datasets within CONUS were applied to these two regions.

KEY FINDING 3

Future research can address critical knowledge gaps and uncertainties related to inland water carbon fluxes. This chapter, for example, does not include methane emissions, which cannot be calculated as precisely as other carbon fluxes because of significant data gaps. Key to reducing uncertainties in estimated carbon fluxes is increased temporal resolution of carbon concentration and discharge sampling to provide better representations of storms and other extreme events for estimates of total inland water carbon fluxes. Improved spatial resolution of sampling also could potentially highlight anthropogenic influences on the quantity and quality of carbon fluxes in inland waters and provide information for land-use planning and management of water resources. Finally, uncertainties could likely be reduced if the community of scientists working in inland waters establishes and adopts standard measurement techniques and protocols similar to those maintained through collaborative efforts of the International Ocean Carbon Coordination Project and relevant governmental agencies from participating nations.

Description of evidence base

Methane CH₄ emissions can be a significant source of carbon to the atmosphere from Arctic lakes (Wik et al., 2016). Fixed-interval sampling protocols may miss large storm events and may critically bias estimates for total carbon fluxes to the coast (Raymond et al., 2012). Management of water resources in reservoir systems may influence the magnitude of carbon burial and emissions, driving systems to be more or less effective at storing or releasing carbon over time (Deemer et al., 2016).

Major uncertainties

Uncertainties are presented within the evidence base. Major uncertainties include 1) the relative importance of storm events or perturbations in the hydrological cycle to carbon export to coastal systems, 2) the magnitude of CH₄ fluxes over time and across seasonal and latitudinal gradients, 3) the role that management of water resources plays in the movement and storage of carbon over time, and 4) the lack of established protocols for comparable sampling and scaling of carbon emissions across inland waters.

Summary sentence or paragraph that integrates the above information

For Key Finding 3, overall spatial and temporal data are not adequate to estimate the magnitude of CH₄ fluxes from inland waters or to capture the influence of storm events or management on inland water carbon fluxes.



REFERENCES

- Abril, G., J. M. Martinez, L. F. Artigas, P. Moreira-Turcq, M. F. Benedetti, L. Vidal, T. Meziane, J. H. Kim, M. C. Bernardes, N. Savoye, J. Deborde, E. L. Souza, P. Alberic, M. F. Landim de Souza, and F. Roland, 2014: Amazon River carbon dioxide outgassing fuelled by wetlands. *Nature*, **505**(7483), 395-398, doi: 10.1038/nature12797.
- Alcocer, J., and F. W. Bernal-Brooks, 2010: Limnology in Mexico. *Hydrobiologia*, **644**(1), 15-68, doi: 10.1007/s10750-010-0211-1.
- Allan, J. D., P. B. McIntyre, S. D. Smith, B. S. Halpern, G. L. Boyer, A. Buchsbaum, G. A. Burton, Jr., L. M. Campbell, W. L. Chad-derton, J. J. Ciborowski, P. J. Doran, T. Eder, D. M. Infante, L. B. Johnson, C. A. Joseph, A. L. Marino, A. Prusevich, J. G. Read, J. B. Rose, E. S. Rutherford, S. P. Sowa, and A. D. Steinman, 2013: Joint analysis of stressors and ecosystem services to enhance restoration effectiveness. *Proceedings of the National Academy of Sciences USA*, **110**(1), 372-377, doi: 10.1073/pnas.1213841110.
- Arntzen, E. V., B. L. Miller, A. C. O'Toole, S. E. Niehus, and M. C. Richmond, 2013: *Evaluating Greenhouse Gas Emissions from Hydropower Complexes on Large Rivers in Eastern Washington* PNNL-22297. Pacific Northwest National Laboratory. [http://www.pnl.gov/main/publications/external/technical_reports/PNNL-22297.pdf]
- Atilla, N., G. A. McKinley, V. Bennington, M. Baehr, N. Urban, M. DeGrandpre, A. R. Desai, and C. Wu, 2011: Observed variability of Lake Superior $p\text{CO}_2$. *Limnology and Oceanography*, **56**(3), 775-786, doi: 10.4319/lo.2011.56.3.0775.
- Aufdenkampe, A. K., E. Mayorga, P. A. Raymond, J. M. Melack, S. C. Doney, S. R. Alin, R. E. Aalto, and K. Yoo, 2011: Riverine coupling of biogeochemical cycles between land, oceans, and atmosphere. *Frontiers in Ecology and the Environment*, **9**(1), 53-60, doi: 10.1890/100014.
- Baehr, M. M., & DeGrandpre, M. D. (2004). *In situ* $p\text{CO}_2$ and O_2 measurements in a lake during turnover and stratification: Observations and modeling. *Limnology and Oceanography*, **49**(2), 330-340. doi:10.4319/lo.2004.49.2.0330
- Barros, N., J. J. Cole, L. J. Tranvik, Y. T. Prairie, D. Bastviken, V. L. M. Huszar, P. del Giorgio, and F. Roland, 2011: Carbon emission from hydroelectric reservoirs linked to reservoir age and latitude. *Nature Geoscience*, **4**(9), 593-596, doi: 10.1038/ngeo1211.
- Bastviken, D., L. J. Tranvik, J. A. Downing, P. M. Crill, and A. Enrich-Prast, 2011: Freshwater methane emissions offset the continental carbon sink. *Science*, **331**(6013), 50, doi: 10.1126/science.1196808.
- Bastviken, D., I. Sundgren, S. Natchimuthu, H. Reyier, and M. Galfalk, 2015: Technical Note: Cost-efficient approaches to measure carbon dioxide (CO_2) fluxes and concentrations in terrestrial and aquatic environments using mini loggers. *Biogeosciences*, **12**(12), 3849-3859, doi: 10.5194/bg-12-3849-2015.
- Battin, T. J., L. A. Kaplan, S. Findlay, C. S. Hopkinson, E. Marti, A. I. Packman, J. D. Newbold, and F. Sabater, 2008: Biophysical controls on organic carbon fluxes in fluvial networks. *Nature Geoscience*, **1**(2), 95-100, doi: 10.1038/ngeo101.
- Battin, T. J., S. Luysaert, L. A. Kaplan, A. K. Aufdenkampe, A. Richter, and L. J. Tranvik, 2009a: The boundless carbon cycle. *Nature Geoscience*, **2**(9), 598-600, doi: 10.1038/ngeo618.
- Battin, T. J., L. A. Kaplan, S. Findlay, C. S. Hopkinson, E. Marti, A. I. Packman, J. D. Newbold, and F. Sabater, 2009b: Biophysical controls on organic carbon fluxes in fluvial networks. *Nature Geoscience*, **2**(8), 595-595, doi: 10.1038/ngeo602.
- Bennington, V., G. A. McKinley, N. R. Urban, and C. P. McDonald, 2012: Can spatial heterogeneity explain the perceived imbalance in Lake Superior's carbon budget? A model study. *Journal of Geophysical Research: Biogeosciences*, **117**(G3), doi: 10.1029/2011jg001895.
- Berner, R. A., 2004: *The Phanerozoic Carbon Cycle: CO_2 and O_2* . Oxford University Press, 150 pp.
- Bianchi, T. S., F. Garcia-Tigreros, S. A. Yvon-Lewis, M. Shields, H. J. Mills, D. Butman, C. Osburn, P. Raymond, G. C. Shank, S. F. DiMarco, N. Walker, B. K. Reese, R. Mullins-Perry, A. Quigg, G. R. Aiken, and E. L. Grossman, 2013: Enhanced transfer of terrestrially derived carbon to the atmosphere in a flooding event. *Geophysical Research Letters*, **40**(1), 116-122, doi: 10.1029/2012gl054145.
- Borges, A. V., F. Darchambeau, C. R. Teodoru, T. R. Marwick, F. Tamooh, N. Geeraert, F. O. Omengo, F. Guérin, T. Lambert, C. Morana, E. Okuku, and S. Bouillon, 2015: Globally significant greenhouse-gas emissions from African inland waters. *Nature Geoscience*, **8**(8), 637-642, doi: 10.1038/ngeo2486.
- Burns, D. A., M. R. McHale, C. T. Driscoll, and K. M. Roy, 2006: Response of surface water chemistry to reduced levels of acid precipitation: Comparison of trends in two regions of New York, USA. *Hydrological Processes*, **20**(7), 1611-1627, doi: 10.1002/hyp.5961.
- Butman, D., and P. A. Raymond, 2011: Significant efflux of carbon dioxide from streams and rivers in the United States. *Nature Geoscience*, **4**(12), 839-842, doi: 10.1038/ngeo1294.
- Butman, D., S. Stackpoole, E. Stets, C. P. McDonald, D. W. Clow, and R. G. Striegl, 2016: Aquatic carbon cycling in the conterminous United States and implications for terrestrial carbon accounting. *Proceedings of the National Academy of Sciences USA*, **113**(1), 58-63, doi: 10.1073/pnas.1512651112.
- Butman, D. E., H. F. Wilson, R. T. Barnes, M. A. Xenopoulos, and P. A. Raymond, 2015: Increased mobilization of aged carbon to rivers by human disturbance. *Nature Geoscience*, **8**(2), 112-116, doi: 10.1038/ngeo2322.
- Campeau, A., J.-F. Lapierre, D. Vachon, and P. A. del Giorgio, 2014: Regional contribution of CO_2 and CH_4 fluxes from the fluvial network in a lowland boreal landscape of Québec. *Global Biogeochemical Cycles*, **28**(1), 57-69, doi: 10.1002/2013gb004685.
- Canadian Dam Association, 2018: [<https://www.cda.ca/>]



- Catalán, N., R. Marcé, D. N. Kothawala, and L. J. Tranvik, 2016: Organic carbon decomposition rates controlled by water retention time across inland waters. *Nature Geoscience*, **9**(7), 501-504, doi: 10.1038/ngeo2720.
- CCSP, 2007: *First State of the Carbon Cycle Report (SOCCR): The North American Carbon Budget and Implications for the Global Carbon Cycle. A Report by the U.S. Climate Change Science Program and the Subcommittee on Global Change Research*. [A. W. King, L. Dilling, G. P. Zimmerman, D. M. Fairman, R. A. Houghton, G. Marland, A. Z. Rose, and T. J. Wilbanks (eds.)]. National Oceanic and Atmospheric Administration, National Climatic Data Center, Asheville, NC, USA, 242 pp.
- Clair, T. A., and J. M. Ehrman, 1996: Variations in discharge and dissolved organic carbon and nitrogen export from terrestrial basins with changes in climate: A neural network approach. *Limnology and Oceanography*, **41**(5), 921-927, doi: 10.4319/lo.1996.41.5.0921.
- Clair, T. A., I. F. Dennis, and S. Bélanger, 2013: Riverine nitrogen and carbon exports from the Canadian landmass to estuaries. *Biogeochemistry*, **115**(1-3), 195-211, doi: 10.1007/s10533-013-9828-2.
- Clow, D. W., S. M. Stackpoole, K. L. Verdin, D. E. Butman, Z. Zhu, D. P. Krabbenhoft, and R. G. Striegl, 2015: Organic carbon burial in lakes and reservoirs of the conterminous United States. *Environmental Science and Technology*, **49**(13), 7614-7622, doi: 10.1021/acs.est.5b00373.
- Cole, J. J., Y. T. Prairie, N. F. Caraco, W. H. McDowell, L. J. Tranvik, R. G. Striegl, C. M. Duarte, P. Kortelainen, J. A. Downing, J. J. Middelburg, and J. Melack, 2007: Plumbing the global carbon cycle: Integrating inland waters into the terrestrial carbon budget. *Ecosystems*, **10**(1), 171-184, doi: 10.1007/s10021-006-9013-8.
- CONAGUA, 2015: *Estadísticas del Agua en México*. Comisión Nacional del Agua, 295 pp. [<http://files.conagua.gob.mx/conagua/publicaciones/Publicaciones/EAM2015-ALTA.pdf>]
- Cotner, J. B., B. A. Biddanda, W. Makino, and E. Stets, 2004: Organic carbon biogeochemistry of Lake Superior. *Aquatic Ecosystem Health and Management*, **7**(4), 451-464, doi: 10.1080/14634980490513292.
- Crawford, J. T., and E. H. Stanley, 2016: Controls on methane concentrations and fluxes in streams draining human-dominated landscapes. *Ecological Applications*, **26**(5), 1581-1591, doi: 10.1890/15-1330.
- Dai, A., T. Qian, K. E. Trenberth, and J. D. Milliman, 2009: Changes in continental freshwater discharge from 1948 to 2004. *Journal of Climate*, **22**(10), 2773-2792, doi: 10.1175/2008jcli2592.1.
- Dai, M. H., Z. Q. Yin, F. F. Meng, Q. Liu, and W. J. Cai, 2012: Spatial distribution of riverine DOC inputs to the ocean: An updated global synthesis. *Current Opinion in Environmental Sustainability*, **4**(2), 170-178, doi: 10.1016/j.cosust.2012.03.003.
- Dean, W. E., and E. Gorham, 1998: Magnitude and significance of carbon burial in lakes, reservoirs, and peatlands. *Geology*, **26**(6), 535, doi: 10.1130/0091-7613(1998)026<0535:masocb>2.3.co;2.
- Deemer, B. R., J. A. Harrison, S. Li, J. J. Beaulieu, T. DelSontro, N. Barros, J. F. Bezerra-Neto, S. M. Powers, M. A. dos Santos, and J. A. Vonk, 2016: Greenhouse gas emissions from reservoir water surfaces: A new global synthesis. *BioScience*, **66**(11), 949-964, doi: 10.1093/biosci/biw117.
- del Giorgio, P. A., Y. T. Prairie, and D. F. Bird, 1997: Coupling between rates of bacterial production and the abundance of metabolically active bacteria in lakes, enumerated using CTC reduction and flow cytometry. *Microbial Ecology*, **34**(2), 144-154, doi: 10.1007/s002489900044.
- del Giorgio, P. A., J. J. Cole, N. F. Caraco, and R. H. Peters, 1999: Linking planktonic biomass and metabolism to net gas fluxes in northern temperate lakes. *Ecology*, **80**(4), 1422-1431, doi: 10.1890/0012-9658(1999)080[1422:lpbamt]2.0.co;2.
- Dornblaser, M. M., and R. G. Striegl, 2015: Switching predominance of organic versus inorganic carbon exports from an intermediate-size subarctic watershed. *Geophysical Research Letters*, **42**(2), 386-394, doi: 10.1002/2014gl062349.
- Downing, B. D., B. A. Pellerin, B. A. Bergamaschi, J. F. Saraceno, and T. E. C. Kraus, 2012: Seeing the light: The effects of particles, dissolved materials, and temperature on *in situ* measurements of dom fluorescence in rivers and streams. *Limnology and Oceanography: Methods*, **10**(10), 767-775, doi: 10.4319/lom.2012.10.767.
- Drake, T. W., K. P. Wickland, R. G. Spencer, D. M. McKnight, and R. G. Striegl, 2015: Ancient low-molecular-weight organic acids in permafrost fuel rapid carbon dioxide production upon thaw. *Proceedings of the National Academy of Sciences USA*, **112**(45), 13946-13951, doi: 10.1073/pnas.1511705112.
- Duan, S., Y. He, S. S. Kaushal, T. S. Bianchi, N. D. Ward, and L. Guo, 2017: Impact of wetland decline on decreasing dissolved organic carbon concentrations along the Mississippi River continuum. *Frontiers in Marine Science*, **3**(280). doi:10.3389/fmars.2016.00280.
- Einsele, G., J. P. Yan, and M. Hinderer, 2001: Atmospheric carbon burial in modern lake basins and its significance for the global carbon budget. *Global and Planetary Change*, **30**(3-4), 167-195, doi: 10.1016/S0921-8181(01)00105-9.
- Evans, C. D., P. J. Chapman, J. M. Clark, D. T. Monteith, and M. S. Cresser, 2006: Alternative explanations for rising dissolved organic carbon export from organic soils. *Global Change Biology*, **12**(11), 2044-2053, doi: 10.1111/j.1365-2486.2006.01241.x.



- Evans, C. D., C. Freeman, L. G. Cork, D. N. Thomas, B. Reynolds, M. F. Billett, M. H. Garnett, and D. Norris, 2007: Evidence against recent climate-induced destabilisation of soil carbon from ^{14}C analysis of riverine dissolved organic matter. *Geophysical Research Letters*, **34**(7), doi: 10.1029/2007gl029431.
- Evans, M. A., G. Fahnenstiel, and D. Scavia, 2011: Incidental oligotrophication of North American Great Lakes. *Environmental Science and Technology*, **45**(8), 3297-3303, doi: 10.1021/es103892w.
- Feng, M., J. O. Sexton, S. Channan, and J. R. Townshend, 2015: A global, high-resolution (30-m) inland water body dataset for 2000: First results of a topographic-spectral classification algorithm. *International Journal of Digital Earth*, **9**(2), 113-133, doi: 10.1080/17538947.2015.1026420.
- Ferland, M.-E., P. A. del Giorgio, C. R. Teodoru, and Y. T. Prairie, 2012: Long-term C accumulation and total C stocks in boreal lakes in northern Québec. *Global Biogeochemical Cycles*, **26**(4), doi: 10.1029/2011gb004241.
- Ferland, M.-E., Y. T. Prairie, C. Teodoru, and P. A. del Giorgio, 2014: Linking organic carbon sedimentation, burial efficiency, and long-term accumulation in boreal lakes. *Journal of Geophysical Research: Biogeosciences*, **119**(5), 836-847, doi: 10.1002/2013jg002345.
- Findlay, S., and R. L. Sinsabaugh, 2003: *Aquatic Ecosystems: Interactivity of Dissolved Organic Matter*. Academic Press, 512 pp.
- Finlay, K., P. R. Leavitt, A. Patoine, A. Patoine, and B. Wissel, 2010: Magnitudes and controls of organic and inorganic carbon flux through a chain of hard-water lakes on the northern Great Plains. *Limnology and Oceanography*, **55**(4), 1551-1564, doi: 10.4319/lo.2010.55.4.1551.
- Galy, V., B. Peucker-Ehrenbrink, and T. Eglinton, 2015: Global carbon export from the terrestrial biosphere controlled by erosion. *Nature*, **521**(7551), 204-207, doi: 10.1038/nature14400.
- Georgakakos, A., P. Fleming, M. Dettinger, C. Peters-Lidard, Terese (T.C.) Richmond, K. Reckhow, K. White, and D. Yates, 2014: Water resources. In: *Climate Change Impacts in the United States: the Third National Climate Assessment*. [J. M. Melillo, T. T. C. Richmond, and G. W. Yohe (eds.)]. U.S. Global Change Research Program, 69-112. doi:10.7930/J0G44N6T
- Gonzalez-Valencia, R., A. Sepulveda-Jauregui, K. Martinez-Cruz, J. Hoyos-Santillan, L. Dendooven, and F. Thalasso, 2013: Methane emissions from Mexican freshwater bodies: Correlations with water pollution. *Hydrobiologia*, **721**(1), 9-22, doi: 10.1007/s10750-013-1632-4.
- Guzmán-Arias, A. P., J. Alcocer-Durand, M. Merino-Ibarra, F. García-Oliva, J. Ramírez-Zierold, and L. A. Oseguera-Pérez, 2015: Lagos tropicales profundos: ¿fuentes de CO_2 a la atmósfera o sumideros de COP a los sedimentos? In: *Estado Actual del Conocimiento del Ciclo del Carbono y sus Interacciones en México: Síntesis a 2015. Serie Síntesis Nacionales*. [F. Paz Pellat, J. W. González, and R. T. Alamilla (eds.)]. Programa Mexicano del Carbono. Centro del Cambio Global y la Sustentabilidad en el Sureste, A.C. y Centro Internacional de Vinculación y Ense-anza de la Universidad Juárez Autónoma de Tabasco, 473-480 pp.
- Hadjerioua, B., S. C. Kao, Y. Wei, H. Battey, and B. T. Smith, 2012: Non-powered dams: An untapped source of renewable electricity in the USA. *The International Journal on Hydropower and Dams*, **19**(4), 45-48.
- Hartmann, J., R. Lauerwald, and N. Moosdorf, 2014a: A brief overview of the GLObal River Chemistry database, GLORICH. *Procedia Earth and Planetary Science*, **10**, 23-27, doi: 10.1016/j.proeps.2014.08.005.
- Hartmann, J., N. Moosdorf, R. Lauerwald, M. Hinderer, and A. J. West, 2014b: Global chemical weathering and associated P-release—The role of lithology, temperature and soil properties. *Chemical Geology*, **363**, 145-163, doi: 10.1016/j.chemgeo.2013.10.025.
- Hartmann, J., N. Jansen, H. H. Dürr, S. Kempe, and P. Köhler, 2009: Global CO_2 -consumption by chemical weathering: What is the contribution of highly active weathering regions? *Global and Planetary Change*, **69**(4), 185-194, doi: 10.1016/j.gloplacha.2009.07.007.
- Heathcote, A. J., N. J. Anderson, Y. T. Prairie, D. R. Engstrom, and P. A. del Giorgio, 2015: Large increases in carbon burial in northern lakes during the Anthropocene. *Nature Communications*, **6**, 10016, doi: 10.1038/ncomms10016.
- Hedges, J. I., R. G. Keil, and R. Benner, 1997: What happens to terrestrial organic matter in the ocean? *Organic Geochemistry*, **27**(5-6), 195-212, doi: 10.1016/s0146-6380(97)00066-1.
- Holgerson, M. A., and P. A. Raymond, 2016: Large contribution to inland water CO_2 and CH_4 emissions from very small ponds. *Nature Geoscience*, **9**(3), 222-226, doi: 10.1038/ngeo2654.
- Hotchkiss, E. R., R. O. Hall Jr, R. A. Sponseller, D. Butman, J. Klaminder, H. Laudon, M. Rosvall, and J. Karlsson, 2015: Sources of and processes controlling CO_2 emissions change with the size of streams and rivers. *Nature Geoscience*, **8**(9), 696-699, doi: 10.1038/ngeo2507.
- Humborg, C., E. Smedberg, S. Blomqvist, C.-M. Mörrth, J. Brink, L. Rahm, Å. Danielsson, and J. Sahlberg, 2004: Nutrient variations in boreal and subarctic Swedish rivers: Landscape control of land-sea fluxes. *Limnology and Oceanography*, **49**(5), 1871-1883, doi: 10.4319/lo.2004.49.5.1871.



- INEGI, 2017: México en Cifras. Instituto Nacional de Estadística y Geografía. [<http://www.beta.inegi.org.mx/app/areasgeograficas/>]
- Johnson, M. S., M. F. Billett, K. J. Dinsmore, M. Wallin, K. E. Dyson, and R. S. Jassal, 2010: Direct and continuous measurement of dissolved carbon dioxide in freshwater aquatic systems—Method and applications. *Ecohydrology*, **3**(1), 68-78, doi: 10.1002/eco.95.
- Johnson, W. E., and J. R. Vallentyne, 1971: Rationale, background, and development of experimental lake studies in northwestern Ontario. *Journal of the Fisheries Research Board of Canada*, **28**(2), 123-128, doi: 10.1139/f71-026.
- Karim, A., K. Dubois, and J. Veizer, 2011: Carbon and oxygen dynamics in the Laurentian Great Lakes: Implications for the CO₂ flux from terrestrial aquatic systems to the atmosphere. *Chemical Geology*, **281**(1-2), 133-141, doi: 10.1016/j.chemgeo.2010.12.006.
- Koprivnjak, J. F., P. J. Dillon, and L. A. Molot, 2010: Importance of CO₂ evasion from small boreal streams. *Global Biogeochemical Cycles*, **24**, doi: 10.1029/2009gb003723.
- Kustu, M. D., Y. Fan, and M. Rodell, 2011: Possible link between irrigation in the U.S. High Plains and increased summer stream-flow in the Midwest. *Water Resources Research*, **47**(3), doi: 10.1029/2010wr010046.
- Lal, R., and D. Pimentel, 2008: Soil erosion: A carbon sink or source? *Science*, **319**(5866), 1040-1042; author reply 1040-1042, doi: 10.1126/science.319.5866.1040.
- Lapierre, J. F., F. Guillemette, M. Berggren, and P. A. del Giorgio, 2013: Increases in terrestrially derived carbon stimulate organic carbon processing and CO₂ emissions in boreal aquatic ecosystems. *Nature Communications*, **4**, 2972, doi: 10.1038/ncomms3972.
- Lauerwald, R., G. G. Laruelle, J. Hartmann, P. Ciais, and P. A. G. Regnier, 2015: Spatial patterns in CO₂ evasion from the Global River Network. *Global Biogeochemical Cycles*, **29**(5), 534-554, doi: 10.1002/2014gb004941.
- Le Quéré, C., G. P. Peters, R. J. Andres, R. M. Andrew, T. A. Boden, P. Ciais, P. Friedlingstein, R. A. Houghton, G. Marland, R. Moriarty, S. Sitch, P. Tans, A. Arneeth, A. Arvanitis, D. C. E. Bakker, L. Bopp, J. G. Canadell, L. P. Chini, S. C. Doney, A. Harper, I. Harris, J. I. House, A. K. Jain, S. D. Jones, E. Kato, R. F. Keeling, K. Klein Goldewijk, A. Körtzinger, C. Koven, N. Lefèvre, F. Maignan, A. Omar, T. Ono, G. H. Park, B. Pfeil, B. Poulter, M. R. Raupach, P. Regnier, C. Rödenbeck, S. Saito, J. Schwinger, J. Segsneider, B. D. Stocker, T. Takahashi, B. Tilbrook, S. van Heuven, N. Viovy, R. Wanninkhof, A. Wiltshire, and S. Zaehle, 2014: Global carbon budget 2013. *Earth System Science Data*, **6**(1), 235-263, doi: 10.5194/essd-6-235-2014.
- Lehner, B., C. R. Liermann, C. Revenga, C. Vörösmarty, B. Fekete, P. Crouzet, P. Döll, M. Endejan, K. Frenken, J. Magome, C. Nilsson, J. C. Robertson, R. Rödel, N. Sindorf, and D. Wisser, 2011: High-resolution mapping of the world's reservoirs and dams for sustainable river-flow management. *Frontiers in Ecology and the Environment*, **9**(9), 494-502, doi: 10.1890/100125.
- Li, M., P. A. del Giorgio, A. H. Parkes, and Y. T. Prairie, 2015: The relative influence of topography and land cover on inorganic and organic carbon exports from catchments in southern Quebec, Canada. *Journal of Geophysical Research: Biogeosciences*, **120**(12), 2562-2578, doi: 10.1002/2015jg003073.
- Likens, G. E., 1977: *Biogeochemistry of a Forested Ecosystem*. Springer-Verlag, 146 pp.
- Lindeman, R. L., 1942: The trophic-dynamic aspect of ecology. *Ecology*, **23**(4), 399-417, doi: 10.2307/1930126.
- Liu, K.-K., L. Atkinson, R. Quinones, and L. Talaue-McManus, 2010: *Carbon and Nutrient Fluxes in Continental Margins: A Global Synthesis*. Springer Science and Business Media, 744 pp.
- Ludwig, W., J.-L. Probst, and S. Kempe, 1996: Predicting the oceanic input of organic carbon by continental erosion. *Global Biogeochemical Cycles*, **10**(1), 23-41, doi: 10.1029/95gb02925.
- Madenjian, C. P., S. A. Pothoven, P. J. Schneeberger, M. P. Ebener, L. C. Mohr, T. F. Nalepa, and J. R. Bence, 2010: Dreissenid mussels are not a "dead end" in Great Lakes food webs. *Journal of Great Lakes Research*, **36**, 73-77, doi: 10.1016/j.jglr.2009.09.001.
- Maeck, A., H. Hofmann, and A. Lorke, 2014: Pumping methane out of aquatic sediments—Ebullition forcing mechanisms in an impounded river. *Biogeosciences*, **11**(11), 2925-2938, doi: 10.5194/bg-11-2925-2014.
- Martinez-Cruz, K., R. Gonzalez-Valencia, A. Sepulveda-Jauregui, F. Plascencia-Hernandez, Y. Belmonte-Izquierdo, and F. Thalasso, 2016: Methane emission from aquatic ecosystems of Mexico City. *Aquatic Sciences*, doi: 10.1007/s00027-016-0487-y.
- Mayorga, E., S. P. Seitzinger, J. A. Harrison, E. Dumont, A. H. W. Beusen, A. F. Bouwman, B. M. Fekete, C. Kroeze, and G. Van Drecht, 2010: Global Nutrient Export from WaterSheds 2 (NEWS 2): Model development and implementation. *Environmental Modelling and Software*, **25**(7), 837-853, doi: 10.1016/j.envsoft.2010.01.007.
- Mazot, A., and Y. Taran, 2009: CO₂ flux from the volcanic lake of El Chichón (Mexico). *Geofísica Internacional*, **48**(1), 73-83.
- McCallister, S. L., and P. A. del Giorgio, 2012: Evidence for the respiration of ancient terrestrial organic C in northern temperate lakes and streams. *Proceedings of the National Academy of Sciences USA*, **109**(42), 16963-16968, doi: 10.1073/pnas.1207305109.



- McDonald, C. P., J. A. Rover, E. G. Stets, and R. G. Striegl, 2012: The regional abundance and size distribution of lakes and reservoirs in the United States and implications for estimates of global lake extent. *Limnology and Oceanography*, **57**(2), 597-606, doi: 10.4319/lo.2012.57.2.0597.
- McDonald, C. P., E. G. Stets, R. G. Striegl, and D. Butman, 2013: Inorganic carbon loading as a primary driver of dissolved carbon dioxide concentrations in the lakes and reservoirs of the contiguous United States. *Global Biogeochemical Cycles*, **27**(2), 285-295, doi: 10.1002/gbc.20032.
- McKinley, G., N. Urban, V. Bennington, D. Pilcher, and C. McDonald, 2011: Preliminary carbon budgets for the Laurentian Great Lakes. Ocean Carbon and Biogeochemistry News, **4**(2), Spring/Summer 2011. [https://web.who.edu/ocb/wp-content/uploads/sites/43/2016/12/OCB_NEWS_SPR_SUM11.pdf]
- Melching, C. S., and H. E. Flores, 1999: Reaeration equations derived from U.S. Geological Survey database. *Journal of Environmental Engineering*, **125**(5), 407-414, doi: 10.1061/(asce)0733-9372(1999)125:5(407).
- Meybeck, M., 1982: Carbon, nitrogen, and phosphorus transport by world rivers. *American Journal of Science*, **282**(4), 401-450, doi: 10.2475/ajs.282.4.401.
- Molot, L. A., and P. J. Dillon, 1997: Colour — mass balances and colour — dissolved organic carbon relationships in lakes and streams in central Ontario. *Canadian Journal of Fisheries and Aquatic Sciences*, **54**(12), 2789-2795, doi: 10.1139/f97-196.
- Monteith, D. T., J. L. Stoddard, C. D. Evans, H. A. de Wit, M. Forsius, T. Hogasen, A. Wilander, B. L. Skjelkvale, D. S. Jeffries, J. Vuorenmaa, B. Keller, J. Kopacek, and J. Vesely, 2007: Dissolved organic carbon trends resulting from changes in atmospheric deposition chemistry. *Nature*, **450**(7169), 537-540, doi: 10.1038/nature06316.
- Mulholland, P. J., and E. J. Kuenzler, 1979: Organic carbon export from upland and forested wetland watersheds. *Limnology and Oceanography*, **24**(5), 960-966, doi: 10.4319/lo.1979.24.5.0960.
- Neff, J. C., J. C. Finlay, S. A. Zimov, S. P. Davydov, J. J. Carrasco, E. A. G. Schuur, and A. I. Davydova, 2006: Seasonal changes in the age and structure of dissolved organic carbon in Siberian rivers and streams. *Geophysical Research Letters*, **33**(23), doi: 10.1029/2006gl028222.
- Nelson, K. C., and M. A. Palmer, 2007: Stream temperature surges under urbanization and climate change: Data, models, and responses. *Journal of the American Water Resources Association*, **43**(2), 440-452, doi: 10.1111/j.1752-1688.2007.00034.x.
- Oh, N. H., and P. A. Raymond, 2006: Contribution of agricultural liming to riverine bicarbonate export and CO₂ sequestration in the Ohio River Basin. *Global Biogeochemical Cycles*, **20**(3), doi: 10.1029/2005gb002565.
- Oseguera-Pérez, L., A. J. Alcocer-Durand, and B. Hernández-Hernández, 2013: Variación del flujo de carbono orgánico particulado en un lago oligotrófico con dominancia de fitoplancton de talla grande. In: *Estado Actual del Conocimiento del Ciclo del Carbono y sus Interacciones en México: Síntesis a Programa Mexicano del Carbono*. [F. Paz Pellat, J. W. González, M. Bazan, and V. Saynes (eds.)]. Colegio de Posgraduados, Universidad Autónoma de Chapingo e Instituto Tecnológico y de Estudios Superiores de Monterrey, 328-334 pp.
- Palca, S. W., G. C. Hurtt, D. Baker, P. Peylin, R. A. Houghton, R. A. Birdsey, L. Heath, E. T. Sundquist, R. F. Stallard, P. Ciais, P. Moorcroft, J. P. Caspersen, E. Shevliakova, B. Moore, G. Kohlmaier, E. Holland, M. Gloor, M. E. Harmon, S. M. Fan, J. L. Sarmiento, C. L. Goodale, D. Schimel, and C. B. Field, 2001: Consistent land- and atmosphere-based U.S. Carbon sink estimates. *Science*, **292**(5525), 2316-2320, doi: 10.1126/science.1057320.
- Pace, M. L., J. J. Cole, S. R. Carpenter, J. F. Kitchell, J. R. Hodgson, M. C. Van De Bogert, D. L. Bade, E. S. Kritzberg, and D. Bastviken, 2004: Whole-lake carbon-13 additions reveal terrestrial support of aquatic food webs. *Nature*, **427**(6971), 240-243, doi: 10.1038/nature02227.
- Pekel, J. F., A. Cottam, N. Gorelick, and A. S. Belward, 2016: High-resolution mapping of global surface water and its long-term changes. *Nature*, **540**(7633), 418-422, doi: 10.1038/nature20584.
- Perez, N. M., P. A. Hernandez, G. Padilla, D. Nolasco, J. Barrancos, G. Melian, E. Padron, S. Dionis, D. Calvo, F. Rodriguez, K. Notsu, T. Mori, M. Kusakabe, M. C. Arpa, P. Reniva, and M. Ibarra, 2011: Global CO₂ emission from volcanic lakes. *Geology*, **39**(3), 235-238, doi: 10.1130/g31586.1.
- Phillips, J., G. McKinley, V. Bennington, H. Bootsma, D. Pilcher, R. Sterner, and N. Urban, 2015: The potential for CO₂-induced acidification in freshwater: A Great Lakes case study. *Oceanography*, **25**(2), 136-145, doi: 10.5670/oceanog.2015.37.
- Pilcher, D. J., G. A. McKinley, H. A. Bootsma, and V. Bennington, 2015: Physical and biogeochemical mechanisms of internal carbon cycling in Lake Michigan. *Journal of Geophysical Research: Oceans*, **120**(3), 2112-2128, doi: 10.1002/2014jc010594.
- Prairie, Y. T., D. F. Bird, and J. J. Cole, 2002: The summer metabolic balance in the epilimnion of southeastern Quebec lakes. *Limnology and Oceanography*, **47**(1), 316-321, doi: 10.4319/lo.2002.47.1.0316.
- Quinton, J. N., G. Govers, K. Van Oost, and R. D. Bardgett, 2010: The impact of agricultural soil erosion on biogeochemical cycling. *Nature Geoscience*, **3**(5), 311-314, doi: 10.1038/ngeo838.
- Rasilo, T., Y. T. Prairie, and P. A. Del Giorgio, 2015: Large-scale patterns in summer diffusive CH₄ fluxes across boreal lakes, and contribution to diffusive C emissions. *Global Change Biology*, **21**(3), 1124-1139, doi: 10.1111/gcb.12741.



- Raymond, P. A., J. E. Saiers, and W. V. Sobczak, 2016: Hydrological and biogeochemical controls on watershed dissolved organic matter transport: Pulse-shunt concept. *Ecology*, **97**(1), 5-16.
- Raymond, P. A., N. H. Oh, R. E. Turner, and W. Broussard, 2008: Anthropogenically enhanced fluxes of water and carbon from the Mississippi River. *Nature*, **451**(7177), 449-452, doi: 10.1038/nature06505.
- Raymond, P. A., C. J. Zappa, D. Butman, T. L. Bott, J. Potter, P. Mulholland, A. E. Laursen, W. H. McDowell, and D. Newbold, 2012: Scaling the gas transfer velocity and hydraulic geometry in streams and small rivers. *Limnology and Oceanography: Fluids and Environments*, **2**(1), 41-53, doi: 10.1215/21573689-1597669.
- Raymond, P. A., J. Hartmann, R. Lauerwald, S. Sobek, C. McDonald, M. Hoover, D. Butman, R. Striegl, E. Mayorga, C. Humborg, P. Kortelainen, H. Durr, M. Meybeck, P. Ciais, and P. Guth, 2013: Global carbon dioxide emissions from inland waters. *Nature*, **503**(7476), 355-359, doi: 10.1038/nature12760.
- Regnier, P., P. Friedlingstein, P. Ciais, F. T. Mackenzie, N. Gruber, I. A. Janssens, G. G. Laruelle, R. Lauerwald, S. Luyssaert, A. J. Andersson, S. Arndt, C. Arnosti, A. V. Borges, A. W. Dale, A. Gallego-Sala, Y. Godderis, N. Goossens, J. Hartmann, C. Heinze, T. Ilyina, F. Joos, D. E. LaRowe, J. Leifeld, F. J. R. Meysman, G. Munhoven, P. A. Raymond, R. Spahni, P. Suntharalingam, and M. Thullner, 2013: Anthropogenic perturbation of the carbon fluxes from land to ocean. *Nature Geoscience*, **6**(8), 597-607, doi: 10.1038/Ngeo1830.
- Ren, W., H. Tian, W.-J. Cai, S. E. Lohrenz, C. S. Hopkinson, W.-J. Huang, J. Yang, B. Tao, S. Pan, and R. He, 2016: Century-long increasing trend and variability of dissolved organic carbon export from the Mississippi River Basin driven by natural and anthropogenic forcing. *Global Biogeochemical Cycles*, **30**(9), 1288-1299, doi: 10.1002/2016gb005395.
- Richey, J. E., J. M. Melack, A. K. Aufdenkampe, V. M. Ballester, and L. L. Hess, 2002: Outgassing from Amazonian rivers and wetlands as a large tropical source of atmospheric CO₂. *Nature*, **416**(6881), 617-620, doi: 10.1038/416617a.
- Roehm, C. L., Y. T. Prairie, and P. A. del Giorgio, 2009: The pCO₂ dynamics in lakes in the boreal region of northern Québec, Canada. *Global Biogeochemical Cycles*, **23**(3), doi: 10.1029/2008gb0003297.
- Roulet, N., and T. R. Moore, 2006: Environmental chemistry: Browning the waters. *Nature*, **444**(7117), 283-284, doi: 10.1038/444283a.
- Rudd, J. W. M., R. Harris, C. A. Kelly, and R. E. Hecky, 1993: Are hydroelectric reservoirs significant sources of greenhouse gases. *Ambio*, **22**(4), 246-248.
- Sawakuchi, H. O., V. Neu, N. D. Ward, M. d. L. C. Barros, A. M. Valerio, W. Gagne-Maynard, A. C. Cunha, D. F. S. Less, J. E. M. Diniz, D. C. Brito, A. V. Krusche, and J. E. Richey, 2017: Carbon dioxide emissions along the lower Amazon River. *Frontiers in Marine Science*, **4**(76), doi: 10.3389/fmars.2017.00076.
- Schlünz, B., and R. R. Schneider, 2000: Transport of terrestrial organic carbon to the oceans by rivers: Re-estimating flux- and burial rates. *International Journal of Earth Sciences*, **88**(4), 599-606, doi: 10.1007/s005310050290.
- Seekell, D. A., and C. Gudas, 2016: Long-term pCO₂ trends in Adirondack lakes. *Geophysical Research Letters*, **43**(10), 5109-5115, doi: 10.1002/2016gl068939.
- Seitzinger, S. P., J. A. Harrison, E. Dumont, A. H. W. Beusen, and A. F. Bouwman, 2005: Sources and delivery of carbon, nitrogen, and phosphorus to the coastal zone: An Overview of Global Nutrient Export from Watersheds (NEWS) models and their application. *Global Biogeochemical Cycles*, **19**(4), doi: 10.1029/2005gb002606.
- Shao, C., J. Chen, C. A. Stepien, H. Chu, Z. Ouyang, T. B. Bridgeman, K. P. Czajkowski, R. H. Becker, and R. John, 2015: Diurnal to annual changes in latent, sensible heat, and CO₂ fluxes over a Laurentian Great Lake: A case study in Western Lake Erie. *Journal of Geophysical Research: Biogeosciences*, **120**(8), 1587-1604, doi: 10.1002/2015jg003025.
- Sobczak, W. V., and P. A. Raymond, 2015: Watershed hydrology and dissolved organic matter export across time scales: Minute to millennium. *Freshwater Science*, **34**(1), 392-398, doi: 10.1086/679747.
- Solomon, C. T., S. E. Jones, B. C. Weidel, I. Buffam, M. L. Fork, J. Karlsson, S. Larsen, J. T. Lennon, J. S. Read, S. Sadro, and J. E. Saros, 2015: Ecosystem consequences of changing inputs of terrestrial dissolved organic matter to lakes: Current knowledge and future challenges. *Ecosystems*, **18**(3), 376-389, doi: 10.1007/s10021-015-9848-y.
- Spitz, A., and V. Ittekkot, 1991: Dissolved and particulate organic matter in rivers. In: *Ocean Margin Processes in Global Change*, John Wiley & Sons Inc, 5-17 pp.
- Stackpoole, S. M., D. E. Butman, D. W. Clow, K. Verdin, B. V. Gaglioti, and R. G. Striegl, 2016: Carbon burial, transport, and emission from inland aquatic ecosystems of Alaska. In: *Baseline and Projected Future Carbon Storage and Greenhouse-Gas Fluxes in Ecosystems of Alaska*. U.S. Geological Survey Professional Paper #1826. [Z. Zhu and A. D. McGuire (eds.)]. 196 pp. [https://pubs.usgs.gov/pp/1826/pp1826.pdf]
- Stackpoole, S. M., D. E. Butman, D. W. Clow, K. L. Verdin, B. V. Gaglioti, H. Genet, and R. G. Striegl, 2017a: Inland waters and their role in the carbon cycle of Alaska. *Ecological Applications*, **27**(5), 1403-1420, doi: 10.1002/eap.1552.



- Stackpoole, S. M., E. G. Stets, D. W. Clow, D. A. Burns, G. R. Aiken, B. T. Aulenbach, I. F. Creed, R. M. Hirsch, H. Laudon, B. A. Pellerin, and R. G. Striegl, 2017b: Spatial and temporal patterns of dissolved organic matter quantity and quality in the Mississippi River Basin, 1997-2013. *Hydrological Processes*, **31**(4), 902-915, doi: 10.1002/hyp.11072.
- Stallard, R. F., 1998: Terrestrial sedimentation and the carbon cycle: Coupling weathering and erosion to carbon burial. *Global Biogeochemical Cycles*, **12**(2), 231-257, doi: 10.1029/98gb00741.
- Stanley, E. H., N. J. Casson, S. T. Christel, J. T. Crawford, L. C. Loken, and S. K. Oliver, 2016: The ecology of methane in streams and rivers: Patterns, controls, and global significance. *Ecological Monographs*, **86**(2), 146-171, doi: 10.1890/15-1027.
- Sterner, R. W., 2010: *In situ*-measured primary production in Lake Superior. *Journal of Great Lakes Research*, **36**(1), 139-149, doi: 10.1016/j.jglr.2009.12.007.
- Stets, E., and R. Striegl, 2012: Carbon export by rivers draining the conterminous United States. *Inland Waters*, **2**(4), 177-184, doi: 10.5268/iw-2.4.510.
- Striegl, R. G., G. R. Aiken, M. M. Dornblaser, P. A. Raymond, and K. P. Wickland, 2005: A decrease in discharge-normalized DOC export by the Yukon River during summer through autumn. *Geophysical Research Letters*, **32**(21), doi: 10.1029/2005gl024413.
- Striegl, R. G., M. M. Dornblaser, C. P. McDonald, J. R. Rover, and E. G. Stets, 2012: Carbon dioxide and methane emissions from the Yukon River system. *Global Biogeochemical Cycles*, **26**(4), doi: 10.1029/2012gb004306.
- Syvitski, James P. M., and John D. Milliman, 2007: Geology, geography, and humans battle for dominance over the delivery of fluvial sediment to the coastal ocean. *The Journal of Geology*, **115**(1), 1-19, doi: 10.1086/509246.
- Tank, S. E., R. G. Striegl, J. W. McClelland, and S. V. Kokelj, 2016: Multi-decadal increases in dissolved organic carbon and alkalinity flux from the Mackenzie Drainage Basin to the Arctic Ocean. *Environmental Research Letters*, **11**(5), 054015, doi: 10.1088/1748-9326/11/5/054015.
- Teodoru, C. R., P. A. Del Giorgio, Y. T. Prairie, and M. Camire, 2009: Patterns in pCO₂ in boreal streams and rivers of northern Quebec, Canada. *Global Biogeochemical Cycles*, **23**, doi: 10.1029/2008gb003404.
- Teodoru, C. R., J. Bastien, M. C. Bonneville, P. A. del Giorgio, M. Demarty, M. Garneau, J. F. Helie, L. Pelletier, Y. T. Prairie, N. T. Roulet, I. B. Strachan, and A. Tremblay, 2012: The net carbon footprint of a newly created boreal hydroelectric reservoir. *Global Biogeochemical Cycles*, **26**, doi: 10.1029/2011gb004187.
- Tian, H., Q. Yang, R. G. Najjar, W. Ren, M. A. M. Friedrichs, C. S. Hopkinson, and S. Pan, 2015: Anthropogenic and climatic influences on carbon fluxes from eastern North America to the Atlantic Ocean: A process-based modeling study. *Journal of Geophysical Research: Biogeosciences*, **120**(4), 757-772, doi: 10.1002/2014jg002760.
- Tobias, C., and J. K. Bohlke, 2011: Biological and geochemical controls on diel dissolved inorganic carbon cycling in a low-order agricultural stream: Implications for reach scales and beyond. *Chemical Geology*, **283**(1-2), 18-30, doi: 10.1016/j.chemgeo.2010.12.012.
- Tranvik, L. J., J. A. Downing, J. B. Cotner, S. A. Loiselle, R. G. Striegl, T. J. Ballatore, P. Dillon, K. Finlay, K. Fortino, L. B. Knoll, P. L. Kortelainen, T. Kutser, S. Larsen, I. Laurion, D. M. Leech, S. L. McCallister, D. M. McKnight, J. M. Melack, E. Overholt, J. A. Porter, Y. Prairie, W. H. Renwick, F. Roland, B. S. Sherman, D. W. Schindler, S. Sobek, A. Tremblay, M. J. Vanni, A. M. Verschoor, E. von Wachenfeldt, and G. A. Weyhenmeyer, 2009: Lakes and reservoirs as regulators of carbon cycling and climate. *Limnology and Oceanography*, **54**(6), 2298-2314, doi: 10.4319/lo.2009.54.6_part_2.2298.
- Tremblay, A., J. Therrien, B. Hamlin, E. Wichmann, and L. J. LeDrew, 2005: GHG emissions from boreal reservoirs and natural aquatic ecosystems. In: *Greenhouse Gas Emissions — Fluxes and Processes: Hydroelectric Reservoirs and Natural Environments*. [A. Tremblay, L. Varfalvy, C. Roehm, and M. Garneau (eds.)]. Springer Berlin Heidelberg, 209-232 pp. [https://doi.org/10.1007/978-3-540-26643-3_9]
- Urban, N. R., M. T. Auer, S. A. Green, X. Lu, D. S. Apul, K. D. Powell, and L. Bub, 2005: Carbon cycling in Lake Superior. *Journal of Geophysical Research: Oceans*, **110**(C6), doi: 10.1029/2003jc002230.
- USACE, 2016: U.S. Army Corps of Engineers National Inventory of Dams. [http://nid.usace.army.mil/cm_apex/f?p=838:12]
- Vachon, D., J.-F. Lapierre, and P. A. del Giorgio, 2016: Seasonality of photochemical dissolved organic carbon mineralization and its relative contribution to pelagic CO₂ production in northern lakes. *Journal of Geophysical Research: Biogeosciences*, **121**(3), 864-878, doi: 10.1002/2015jg003244.
- Valdespino-Castillo, P. M., M. Merino-Ibarra, J. Jimenez-Contreras, F. S. Castillo-Sandoval, and J. A. Ramirez-Zierold, 2014: Community metabolism in a deep (stratified) tropical reservoir during a period of high water-level fluctuations. *Environmental Monitoring and Assessment*, **186**(10), 6505-6520, doi: 10.1007/s10661-014-3870-y.
- Vörösmarty, C. J., J. Syvitski, J. Day, A. de Sherbinin, L. Giosan, and C. Paola, 2009: Battling to save the world's river deltas. *Bulletin of the Atomic Scientists*, **65**(2), 31-43, doi: 10.2968/065002005.
- Walter Anthony, K., R. Daanen, P. Anthony, T. Schneider von Deimling, C.-L. Ping, J. P. Chanton, and G. Grosse, 2016: Methane emissions proportional to permafrost carbon thawed in Arctic lakes since the 1950s. *Nature Geoscience*, **9**(9), 679-682, doi: 10.1038/ngeo2795.



Walvoord, M. A., and R. G. Striegl, 2007: Increased groundwater to stream discharge from permafrost thawing in the Yukon River Basin: Potential impacts on lateral export of carbon and nitrogen. *Geophysical Research Letters*, **34**(12), doi: 10.1029/2007gl030216.

Wik, M., R. K. Varner, K. W. Anthony, S. MacIntyre, and D. Bastviken, 2016: Climate-sensitive northern lakes and ponds are critical components of methane release. *Nature Geoscience*, **9**(2), 99-105, doi: 10.1038/ngeo2578.

World Commission on Dams, 2000: *Dams and Development: A New Framework for Decision-Making: The report of the World Commission on Dams*. Earthscan Publications Ltd, 404 pp.

Yoon, B., and P. A. Raymond, 2012: Dissolved organic matter export from a forested watershed during Hurricane Irene. *Geophysical Research Letters*, **39**(18), doi: 10.1029/2012gl052785.

Yue, Y., J. Ni, P. Ciais, S. Piao, T. Wang, M. Huang, A. G. Borthwick, T. Li, Y. Wang, A. Chappell, and K. Van Oost, 2016: Lateral transport of soil carbon and land-atmosphere CO₂ flux induced by water erosion in China. *Proceedings of the National Academy of Sciences USA*, **113**(24), 6617-6622, doi: 10.1073/pnas.1523358113.

Zarfl, C., A. E. Lumsdon, J. Berlekamp, L. Tydecks, and K. Tockner, 2014: A global boom in hydropower dam construction. *Aquatic Sciences*, **77**(1), 161-170, doi: 10.1007/s00027-014-0377-0.

Zhu, Z., and A. D. McGuire, 2016: *Baseline and Projected Future Carbon Storage and Greenhouse-Gas Fluxes in Ecosystems of Alaska*. U.S. Geological Survey Professional Paper 1826. [Z. Zhu and A. D. McGuire (eds.)]. 196 pp.



15 Tidal Wetlands and Estuaries

Lead Authors

Lisamarie Windham-Myers, U.S. Geological Survey; Wei-Jun Cai, University of Delaware

Contributing Authors

Simone R. Alin, NOAA Pacific Marine Environmental Laboratory; Andreas Andersson, Scripps Institution of Oceanography; Joseph Crosswell, Commonwealth Scientific and Industrial Research Organisation; Kenneth H. Dunton, University of Texas, Austin; Jose Martin Hernandez-Ayon, Autonomous University of Baja California; Maria Herrmann, The Pennsylvania State University; Audra L. Hinson, Texas A&M University; Charles S. Hopkins, University of Georgia; Jennifer Howard, Conservation International; Xiping Hu, Texas A&M University, Corpus Christi; Sara H. Knox, U.S. Geological Survey; Kevin Kroeger, U.S. Geological Survey; David Lagomasino, University of Maryland; Patrick Megonigal, Smithsonian Environmental Research Center; Raymond G. Najjar, The Pennsylvania State University; May-Linn Paulsen, Scripps Institution of Oceanography; Dorothy Peteet, NASA Goddard Institute for Space Studies; Emily Pidgeon, Conservation International; Karina V. R. Schäfer, Rutgers University; Maria Tzortziou, City University of New York; Zhaohui Aleck Wang, Woods Hole Oceanographic Institution; Elizabeth B. Watson, Drexel University

Acknowledgments

Camille Stagg (Expert Reviewer), U.S. Geological Survey; Raymond G. Najjar (Science Lead), The Pennsylvania State University; Marjorie Friederichs (Review Editor), Virginia Institute of Marine Science; Zhiliang Zhu (Federal Liaison), U.S. Geological Survey. Authors wish to thank their respective funding agencies, including the U.S. Geological Survey LandCarbon Program, NASA Carbon Monitoring System Program (NNH14AY671 for Windham-Myers), and the National Science Foundation Division of Ocean Sciences (OCE 1238212, 1637630, and 1237140 for Hopkins).

Recommended Citation for Chapter

Windham-Myers, L., W.-J. Cai, S. R. Alin, A. Andersson, J. Crosswell, K. H. Dunton, J. M. Hernandez-Ayon, M. Herrmann, A. L. Hinson, C. S. Hopkins, J. Howard, X. Hu, S. H. Knox, K. Kroeger, D. Lagomasino, P. Megonigal, R. G. Najjar, M.-L. Paulsen, D. Peteet, E. Pidgeon, K. V. R. Schäfer, M. Tzortziou, Z. A. Wang, and E. B. Watson, 2018: Chapter 15: Tidal wetlands and estuaries. In *Second State of the Carbon Cycle Report (SOCCR2): A Sustained Assessment Report* [Cavallaro, N., G. Shrestha, R. Birdsey, M. A. Mayes, R. G. Najjar, S. C. Reed, P. Romero-Lankao, and Z. Zhu (eds.)]. U.S. Global Change Research Program, Washington, DC, USA, pp. 596-648, <https://doi.org/10.7930/SOCCR2.2018.Ch15>.



KEY FINDINGS

1. The top 1 m of tidal wetland soils and estuarine sediments of North America contains $1,886 \pm 1,046$ teragrams of carbon (Tg C) (*high confidence, very likely*).
2. Soil carbon accumulation rate (i.e., sediment burial) in North American tidal wetlands is currently 9 ± 5 Tg C per year (*high confidence, likely*), and estuarine carbon burial is 5 ± 3 Tg C per year (*low confidence, likely*).
3. The lateral flux of carbon from tidal wetlands to estuaries is 16 ± 10 Tg C per year for North America (*low confidence, likely*).
4. In North America, tidal wetlands remove 27 ± 13 Tg C per year from the atmosphere, estuaries outgas 10 ± 10 Tg C per year to the atmosphere, and the net uptake by the combined wetland-estuary system is 17 ± 16 Tg C per year (*low confidence, likely*).
5. Research and modeling needs are greatest for understanding responses to accelerated sea level rise; mapping tidal wetland and estuarine extent; and quantifying carbon dioxide and methane exchange with the atmosphere, especially in large, undersampled, and rapidly changing regions (*high confidence, likely*).

Note: Confidence levels are provided as appropriate for quantitative, but not qualitative, Key Findings and statements.

15.1 Introduction

Estuaries and tidal wetlands are dynamic ecosystems that host high biological production and diversity (Bianchi 2006). They receive large amounts of dissolved and particulate carbon and nutrients from rivers and uplands and exchange materials and energy with the ocean. Estuaries and tidal wetlands are often called biogeochemical “reactors” where terrestrial materials are transformed through interactions with the land, ocean, and atmosphere. Work conducted in the past decade has clearly shown that open-water estuaries as a whole can be strong sources of carbon to the atmosphere—both carbon dioxide (CO₂) and methane (CH₄)—despite the fact that how degassing (i.e., gas emissions) rates vary in space and time in many estuaries is unknown (Borges and Abril 2011; Cai 2011). In contrast, tidal wetlands represent a small fraction of the land surface but are among the strongest long-term carbon sinks, per unit area, because of continuous organic carbon accumulation in sediments with rising sea level (Chmura et al., 2003). Estuaries are included here in the *Second State of the Carbon Cycle Report* (SOCCR2) but were not included in the *First State*

of the Carbon Cycle Report’s (SOCCR1; CCSP 2007) assessment of coastal carbon cycling. Estuaries have been reviewed in recent synthesis activities, particularly the Coastal Carbon Synthesis (CCARS; Benway et al., 2016). Tidal wetlands were included in the wetlands chapter of SOCCR1 but are separated from inland wetlands in this SOCCR2 assessment to reflect their unique connections to estuarine and ocean dynamics. Consistently missing from previous fieldwork and syntheses are important annual carbon exchanges (including CO₂ and CH₄ flux) across boundaries of intertidal (hereafter, wetland) and subtidal ecosystems and deeper waters (hereafter, estuarine). As subsystems of an integrated coastal mixing zone, this lack of information limits understanding of the relative roles of wetlands and estuaries in carbon cycling at the critical land-ocean margin. An updated synthesis of current knowledge and gaps in quantifying the magnitude and direction of carbon fluxes in dynamic estuarine environments is presented herein.

According to Perillo and Picollo (1995) and Pritchard (1967), estuaries are commonly defined as “semi-enclosed coastal bodies of water that extend



to the effective limit of tidal influence, within which seawater entering from one or more free connections with the open sea, or any saline coastal body of water, is significantly diluted with fresh water [sic] derived from land drainage, and can sustain euryhaline biological species from either part or the whole of the life cycle.” For the purpose of this report, the landward boundary of estuarine zones is defined as the “head of tide” (i.e., the maximal boundary of tidal expression in surface water elevation) and the shoreward limit of the continental shelf (i.e., the relatively shallow sea that extends to the edge of continental crust). While island coastlines are included in the overall SOCCR2 domain (namely Hawai‘i, Puerto Rico, and the Pacific Islands), due to reliance on recent synthesis products for carbon accounting, the focus herein is exclusively on continental coastlines where stocks and fluxes have been quantified and mapped most comprehensively. Section 15.2, this page, provides a brief historical overview of carbon flux in estuaries and tidal wetlands with an emphasis on coastal processes with global applicability. Section 15.3, p. 601, compiles information on carbon fluxes of estuaries and tidal wetlands of North America in the global context and from regional perspectives. Through literature summaries and data syntheses, Section 15.4, p. 609, provides new estimates of selected fluxes and stocks in tidal wetlands and estuaries of North America. Section 15.5, p. 615, discusses new and relevant coastal carbon observations through indicators, trends, and feedbacks, and Section 15.6, p. 619, reports on management and decisions associated with societal drivers and impacts within the carbon cycle context. Finally, Section 15.7, p. 620, provides a synthesis that summarizes conclusions, gaps in knowledge, and near-future outlooks.

15.2 Historical Context, Overview of Carbon Fluxes and Stocks in Tidal Wetlands and Estuaries

Tidal wetlands and estuaries of North America vary in relative area depending on coastal topography, historic rates of sea level rise, and inputs of suspended solids from land. In drowned river

valleys (e.g., Chesapeake Bay) and fjords (e.g., Puget Sound) that are topographically steep, estuarine habitat is the dominant subsystem (Dalrymple et al., 1992). In contrast, the ratio of tidal wetland area to estuarine area is relatively high (Day et al., 2013), though still less than one (Najjar et al., 2018) along coastal plains.

The land-sea interface that defines the presence of tidal wetlands and estuaries (i.e., river-sea mixing zones) is itself extremely dynamic over broad spatial and temporal scales. The current configuration of tidal wetlands and estuaries is the result of processes that have been occurring since the last glacial maximum, roughly 18,000 years ago. Over the past 6,000 years, when rates of sea level rise slowed to less than 1 mm per year, tidal wetlands increased in size relative to open-water estuaries, as bay bottoms filled with sediments from uplands and tidal wetlands prograded into shallow open-water regions and transgressed across uplands (see Figure 15.1, p. 599; Redfield 1967). Concomitant with increasing sea levels, tidal wetlands maintained their relative elevation as wetland plants trapped suspended sediments from tidal floodwaters, as well as accumulated organic matter in soils. Factors that affect tidal wetland area and relative elevation, through lateral and vertical erosion and accretion, include 1) rate of sea level rise, 2) land subsidence or isostasy (glacial rebound), 3) delivery and deposition of suspended sediment, 4) balance between wetland gross primary production (GPP) and respiration of all autotrophs and heterotrophs (R_{AH}), 5) sediment compaction, and 6) slope of land at the land-water interface (Cahoon 2006).

Tidal wetlands are among the most productive ecosystems on Earth, continuously accumulating organic carbon that results from environmental conditions that inhibit organic matter decomposition. As a result, intact tidal wetlands are capable of storing vast amounts of *autochthonous* organic carbon (i.e., fixed through photosynthesis on site) as well as intercepting and storing *allochthonous* organic carbon (i.e., produced off site, terrigenous; Canuel et al., 2012). Documented carbon-related

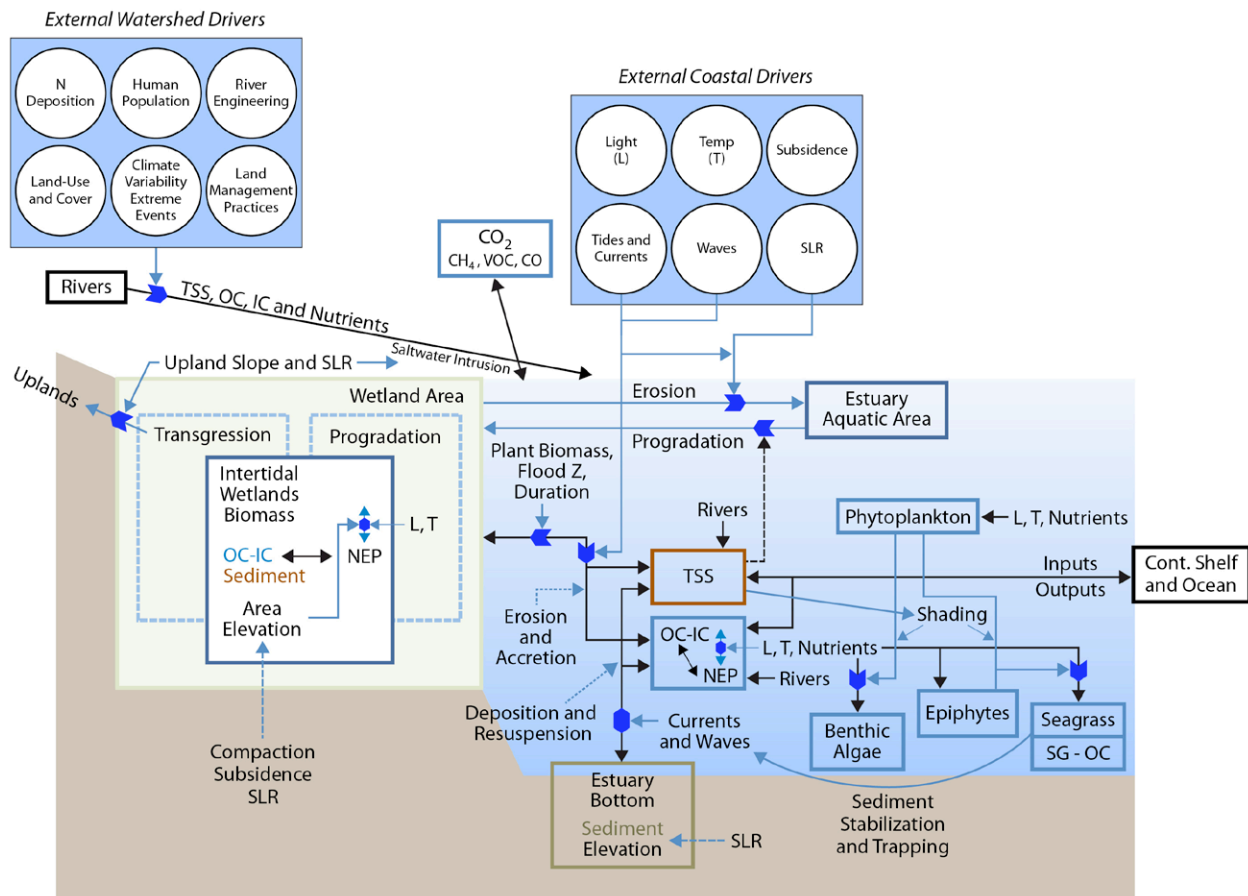


Figure 15.1. Conceptual Model of Coastal Tidal Wetlands and Estuaries and Their Linkages with Adjacent Terrestrial and Oceanic Systems. The drivers, processes, and factors depicted here largely control carbon dynamics in these systems. Net ecosystem production (NEP) is equal to gross primary production minus the sum of heterotrophic and autotrophic respiration. [Key: N, nitrogen; CO₂, carbon dioxide; CH₄, methane; VOC, volatile organic compound; CO, carbon monoxide; L, light; T, temperature; TSS, total suspended solids; OC, organic carbon; IC, inorganic carbon; Z, elevation; SG, seagrass; SLR, sea level rise]

ecosystem benefits, referred to as “services,” include significant uptake and storage of carbon in wetland soils, as well as export to the ocean of organic matter, which increases the productivity of coastal fisheries (Day et al., 2013). Globally, tidal wetlands are strongly variable in age and structure. Some of today’s tidal wetlands have persisted for more than 6,500 years, accumulating to a depth of up to 13 m of tidal peat (Drexler et al., 2009; McKee et al., 2007; Peteet et al., 2006), but some wetlands are young and shallow because of recent human influences that enhanced sediment delivery to nearshore waters. Examples include the colonial-era East Coast

(Kirwan et al., 2011) and gold rush in California (Palaima 2012). Because human development is preferentially concentrated on coastlines, tidal wetlands have been subject to active loss through development pressures. While tidal wetland losses have slowed in the United States, global tidal wetland losses are currently estimated at 0.5% to 3% annually (Pendleton et al., 2012), with estimates depending on the ecosystem, time frame, and methods used in evaluation (Hamilton and Casey 2016; Spalding et al., 2010). Loss of carbon stocks through wetland drainage and erosion remains poorly modeled due to limited mapping and quantification of



initial carbon stock conditions (Chmura 2013). Further, more subtle rates of wetland loss, through drowning or erosion, may be underestimated by remote-sensing techniques insensitive to small-scale changes observed through aerial photography (e.g., Schepers et al., 2017; Watson et al., 2017).

Estuarine waters are a small but productive fraction of coastal waters (Cloern et al., 2014; Wollast 1991). The role of coastal zones as sinks or sources of atmospheric CO₂ is still poorly understood (Borges 2005; Borges et al., 2005; Smith and Hollibaugh 1997), resulting in a lack of consensus toward their role in global carbon budgets (Cai 2011; Wollast 1991; Borges and Abril 2011; Chen et al., 2013). With poorly characterized boundary conditions, estuarine waters have strong upland and ocean-based drivers, leading to strong seasonality in carbon transport and transformation. Geological records suggest that estuarine carbon storage was enhanced in the past 6,000 years and during recent centuries by watershed activities (Colman et al., 2002), but responses were varied. Human activities initially increased the delivery of organic materials to estuaries (e.g., forest clearing) and thus drove them to support higher net respiration (and likely greater sources of atmospheric CO₂); however, more recent human activities (e.g., dam construction and fertilizer use) have greatly reduced sediment and organic matter delivery but increased nutrient fluxes to many estuaries (Bianchi and Allison 2009; Galloway et al., 2008), driving estuarine waters to be less heterotrophic and, possibly, causing more net carbon burial and export to the ocean (Regnier et al., 2013). While North American estuarine conditions vary along coasts according to upstream land use, the most significant human-induced change to estuarine carbon dynamics over the past century is certainly increased nutrient loading (Schlesinger 2009), which has led to eutrophication and hypoxia in estuaries and continental shelves. Eutrophication promotes carbon uptake and pH increase in surface estuarine waters (Borges and Gypens 2010), but it also may enhance acidification when organic matter fixed by photosynthesis is respired. In stratified estuarine waters, respiration-induced CO₂ and poor

buffering capacity could greatly reduce pH and carbonate saturation states to levels much lower than those resulting from the increase of anthropogenic CO₂ in the atmosphere and its subsequent uptake in surface waters (Cai 2011, Cai et al., 2017; Feely et al., 2010). The particularly large pH changes and the difficulty in predicting acidification in estuaries have motivated many scientists to study estuarine acidification in addition to ocean acidification (Duarte et al., 2013).

Estuaries generally have more interannual variability in carbon dynamics than do tidal wetlands, a phenomenon reflecting the balance of exchanges with terrestrial watersheds, tidal wetlands, and the continental shelf (Bauer et al., 2013). Processing of material inputs from land and tidal wetlands determines the autotrophic-heterotrophic balance of the estuary; this processing reflects the biological, chemical, and physical structure of the receiving estuary, as well as the nature of the inputs themselves. The autotrophic-heterotrophic balance of an estuary is especially sensitive to the water residence time (largely a function of freshwater runoff, tidal mixing, and estuarine geometry), the ratio of inputs of organic carbon (primarily from land and tidal wetlands) to inorganic nutrients (primarily from land), the degradability of the organic carbon input (Hopkinson and Vallino 1995; Kemp et al., 1997; Herrmann et al., 2015). The relative abundance of pelagic (i.e., phytoplankton-dominated) versus benthic (i.e., seagrass- or benthic algal-dominated) communities is also a major factor affecting estuarine carbon dynamics. The availability of light is perhaps the major constraint on the distribution of benthic autotrophic communities. Light availability to the benthos depends on estuarine depth and water clarity, which in turn are related to concentrations of suspended solids and phytoplankton in the estuarine water column. In nitrogen-enriched estuarine waters, high-phytoplankton biomass and epiphytic algae decrease light availability to benthic autotrophic communities, sometimes resulting in a complete loss of seagrass habitats (Howarth et al., 2000). In shallow systems, benthic macroalgae often dominate system dynamics. Seagrass, because of its ability to control



wave and current strength, can play a major role in limiting sediment resuspension, thereby maintaining high water clarity (van der Heide et al., 2011). Estuaries typically are heterotrophic and release CO₂ to the atmosphere, largely as a result of their processing of organic carbon inputs from watersheds (Raymond and Bauer 2001) and adjacent tidal wetlands (Bauer et al., 2013; Cai and Wang 1998; Wang and Cai 2004). For example, U.S. Atlantic coastal estuaries as a whole are net heterotrophic (Herrmann et al., 2015); all but three of 42 sites in the U.S. National Estuarine Research Reserve System were net heterotrophic over a year (Caffrey 2004), and a global survey concluded that 66 out of 79 estuaries were net heterotrophic (Borges and Abril 2011). At the same time, estuaries can serve as significant long-term organic carbon sinks through sedimentation of terrestrial inputs and seagrass organic matter burial (Duarte et al., 2005; Hopkinson et al., 2012; McLeod et al., 2011; Nellemann et al., 2009).

15.3 Global, North American, and Regional Context

Similar to the approach used by Benway et al. (2016), this assessment divided the North American coastline into four main subregions (see Figure 15.2, p. 602): the Atlantic Coast (Nova Scotia, Canada, to the southern tip of Florida, United States), the Gulf of Mexico, the Pacific Coast (southernmost Mexico to the Seward Peninsula, United States), and the High-Latitude Coast (the boreal and Arctic coastlines of Alaska and Canada between the Seward Peninsula and Nova Scotia). There are notable differences in carbon cycling among these four major subregions of North America. This section presents a descriptive analysis of those processes by subregion.

15.3.1 Atlantic Coast Estuaries and Tidal Wetlands

Estuaries of the North American Atlantic coast are the most extensive and diverse in structure and function within North America. Relatively shallow and driven primarily by landward influences, they are strongly influenced by freshwater flow and quality from rivers and groundwater. From boreal to

subtropical latitudes, a wide range of biotic activity (e.g., photosynthesis and respiration) is seen from Nova Scotia to Florida.

Atlantic Coast Estuaries

South Atlantic Bight. The South Atlantic Bight (SAB: southern tip of Florida to Cape Hatteras, North Carolina) is a passive, western boundary current margin with broad shelf areas, extensive shoals, and a series of barrier islands, behind which are lagoons. Freshwater delivery in the SAB is through rivers that are nearly evenly located along the coast. These rivers carry high loads of dissolved organic carbon (DOC). Because of short transit times through the estuaries, much of the DOC is discharged onto the shelf, supporting respiration, net heterotrophy (Hopkinson 1985, 1988), and CO₂ degassing on the inner-shelf regions (Jiang et al., 2013). Much is known about the export of organic matter from SAB watersheds. The SAB salt marshes are tremendous sinks of CO₂ and organic carbon from uplands, whereas the estuarine waters are strong sources of CO₂ to the atmosphere—sources that are largely supported by organic matter and dissolved inorganic matter (DIC) export from both wetland saltmarshes and from SAB watersheds (Wang and Cai 2004; Cai 2011; Herrmann et al., 2015; Hopkinson 1988).

Mid-Atlantic Bight and Gulf of Maine. The Mid-Atlantic Bight (MAB: Cape Hatteras, North Carolina, to Cape Cod, Massachusetts) and Gulf of Maine (GOM: Cape Cod to Nova Scotia) are characterized by large estuaries. Inorganic carbon from carbonate weathering and organic matter remineralization accounts for the majority of riverine carbon input to the MAB (Hossler and Bauer 2013; Moosdorf et al., 2011). Generally, aqueous organic matter concentrations are higher in southern MAB rivers and can be more than half the riverine carbon load to estuaries (Stets and Striegl 2012; Tian et al., 2015). Lateral exchange with wetlands is an important carbon input to MAB waters and has been linked to net heterotrophy and air-water CO₂ efflux in narrow, marsh-dominated subestuaries (Baumann et al., 2015; Raymond et al., 2000; Wang



Figure 15.2. Map of the Main Coastal Regions and Associated Drainage Basins of North America. In this chapter, the North American coastline is broken up into four main regions: Atlantic Coast, Gulf of Mexico, Pacific Coast (including the Sea of Cortez, Gulf of Alaska, and Bering Sea), and High Latitudes (including the Chukchi Sea, Beaufort Sea, Hudson Bay, Labrador Sea, and Gulf of Saint Lawrence). [Figure source: Redrawn from U.S. Department of Interior]



et al., 2016). However, larger MAB estuaries can be seasonal or annual sinks for atmospheric CO_2 because of stratification and high rates of internal production (Crosswell et al., 2014; Joesoef et al., 2015). Supporting this result, recent carbon budget studies have estimated that MAB estuaries are near metabolic balance and that total organic carbon (TOC) export to the coastal ocean is about equal to riverine TOC input (Herrmann et al., 2015; Crosswell et al., 2017). The GOM shares many of these traits, but its TOC input is low due to its small catchment area (Najjar et al., 2018).

Atlantic Coast Tidal Wetlands

Despite some similarity in vegetation community composition (e.g., estuarine emergent *Spartina* spp., dominant in saline habitats), Atlantic coast tidal marshes are extensive and topographically varied in structure, from the more patchy, organic-rich GOM and MAB soils to the extensive, mineral-rich plains of the SAB. Biomass stocks of the dominant plant species, *Spartina alterniflora*, show a decrease with latitude (Kirwan et al., 2009), with the notably productive SAB marshes (Gallagher et al., 1980; Schubauer and Hopkinson 1984) exporting large amounts of marsh grass–derived organic matter and CO_2 into the estuaries and nearshore ocean where respiration and degassing occur (Jiang et al., 2008; Wang and Cai 2004). Soil carbon burial is not commensurate with productivity, as increased organic matter decomposition (Kirwan and Blum 2011) may negate any latitudinal productivity gradients. More important than latitudinal patterns for carbon flux accounting are within-watershed patterns of marsh elevation (i.e., low marsh versus high marsh), tidal range (e.g., microtidal eastern Florida versus extreme macrotidal Bay of Fundy), and salinity regimes. Freshwater tidal wetlands (both marsh and forest) make up 21% of tidal wetlands of the eastern United States (Hinson et al., 2017). Localized hotspots for soil carbon stock change also occur along the East Coast because of physical drivers such as sea level rise (Sallenger et al., 2012) and storm-induced erosion (Cahoon 2006). Estimated net ecosystem exchange (NEE) of atmospheric CO_2

from chamber and eddy covariance systems illustrates that vertical fluxes dominate carbon inputs to many East Coast tidal wetlands (Forbrich and Giblin 2015; Kathilankal et al., 2008). Much of this NEE is exported to ocean subsystems in particulate and dissolved forms, with lateral exports of DIC and DOC fluxes representing as much as 80% of annual carbon inputs (Wang and Cai 2004; Wang et al., 2016). Further, the role of groundwater flows in driving carbon fluxes, as well as nutrient fluxes that alter estuarine processes, is varied and poorly understood (Kroeger and Charette 2008; Moore 1996).

15.3.2 Gulf of Mexico Estuaries and Tidal Wetlands

Variability of Gulf of Mexico (GMx) estuaries is due, in part, to the variable forcing at their boundaries, including groundwater (dominating the Mexican coastline), rivers (dominating the U.S. coastline), wind, bathymetry, and ocean currents (e.g., the Loop Current). Gulf of Mexico tidal wetlands share many species but notably are experiencing enhanced mangrove encroachment and land subsidence.

Gulf of Mexico Estuaries

Estuarine GMx environments are microtidal with winds and river flows exerting strong control on water levels. On the extensive subtidal carbonate benthos, extensive seagrass meadows (e.g., *Thalassia*) persist and are known to recover rapidly from disturbance (e.g., Thorhaug et al., 2017). There is a paucity of data on air-water CO_2 flux in GMx estuaries. However, the lower-river portion of the two largest rivers, the Mississippi and the Atchafalaya, are strong sources of CO_2 to the atmosphere because the partial pressure of CO_2 ($p\text{CO}_2$) ranges from about 1,000 microatmospheres (μatm : a unit of pressure defined as 101,325 Pascals or 1.01325 bar) in winter to about 2,200 μatm in summer, but some large bays (e.g., Terrebonne Bay) have substantially lower $p\text{CO}_2$ (Huang et al., 2015). In comparison, despite relatively low $p\text{CO}_2$ (about 500 μatm), a semi-arid lagoonal estuary in northwestern GMx has a CO_2 efflux of 149 ± 40 grams of carbon (g C) per m^2 per year due to windy conditions all year



long (Yao and Hu 2017), an amount comparable to other lagoonal estuaries in the world (Laruelle et al., 2014). A strong climatic gradient from northeast to southwest along the northwestern GMx coast leads to riverine freshwater export decreasing by a factor of two (Montagna et al., 2009), with large interannual variability. This hydrological variability exerts strong control on estuarine CO₂ fluxes in this region.

Gulf of Mexico Tidal Wetlands

As of 2017, 52% of conterminous U.S. tidal wetlands are located within GMx, with Louisiana alone containing 40% of all the saltwater wetlands in the United States (Dahl 2011; Edwards and Proffitt 2003). While the GMx U.S. coastline is dominated by emergent marsh vegetation and the Mexican coastline is dominated by mangrove vegetation (see Table 15.1, this page), a wide range of salinity and geomorphic conditions promote structural diversity throughout GMx from tidal freshwater forests to

floating peatlands to brackish and saline marshes. For the past two decades, other coastlines have been relatively stable in their tidal wetland extent but GMx is experiencing rapid transitions. Though there is active delta building at the Atchafalaya River outflow, tidal wetland conversion to open water (i.e., wetland loss) is common in GMx as a result of land subsidence, coastal storms, sea level rise, nutrient enrichment, and a lack of sediment delivery to compensate for ongoing compaction. The fate of wetland soil carbon following erosion or conversion to open water is poorly understood but important for conducting carbon accounting, particularly in GMx (DeLaune and White 2011; Lane et al., 2016). Climate shifts are also accelerating changes in wetland cover (Gabler et al., 2017), including mangrove encroachment on salt marshes in Texas, Louisiana, and Florida (Krauss et al., 2011; Saintilan et al., 2014).

Table 15.1. Average Values for Ecosystem Extent (km²) by Coast (Atlantic, Pacific, Gulf of Mexico, and Arctic) for North America^a (Includes Combined Mapped Data for Canada, Mexico, and the United States)

Coast	Tidal Freshwater Marsh	Tidal Freshwater Forest	Tidal Brackish and Saline Marsh	Tidal Brackish and Saline Forest	Total Tidal Wetland	Seagrass	Estuarine ^b
Atlantic Coast	539	1,916	7,958	768	11,181	11,889	34,000
Gulf of Mexico	1,612	1,153	9,847	9,899	22,511	20,260	31,900
Pacific Coast	83	188	510	2,642	3,423	1,148	49,000
High Latitudes	ND ^c	ND	1,494	NA ^c	1,494 ^d	1,050	238,800
CONUS	2,234	3,257	18,162	3,165	26,818	23,630	75,040
Alaska	ND	ND	948	NA	948 ^d	405	ND
Canada	ND	ND	546	NA	546 ^d	645	ND
Mexico	ND	ND	153	10,144	10,297 ^d	9,667	ND
North America	2,234 ^d	3,257 ^d	19,809	13,309 ^d	38,609 ^d	34,347	353,700

Notes

- a) Geospatial data sources: CEC 2016; Laruelle et al., 2013; USFWS NWI 2017.
- b) All estimates based on MARGins and CATchments Segmentation (MARCATS) data of Laruelle et al. (2013), except the conterminous United States (CONUS), which is from Bricker et al. (2007). Corresponding MARCATS segment numbers are 10 for the Atlantic Coast; 9 for the Gulf of Mexico; 1, 2, and 3 for the Pacific Coast; and 11, 12, and 13 for High Latitudes.
- c) ND = no data, NA = not applicable.
- d) Indicates missing data from at least one coastal subregion.



Mangroves extend all the way around GMx, with 80% of the total distribution of North American mangroves on the Mexican coastline (50% of which grow on the Campeche, Yucatán, and Quintana Roo coasts). Mangrove carbon sequestration rates can range from 0 to 1,000 g C per m² per year, primarily a result of biomass responses to disturbance status and hydrogeomorphic characteristics of the landscape setting (Adame et al., 2013; Breithaupt et al., 2014; Ezcurra et al., 2016; Marchio et al., 2016). Regular tidal flushing and allochthonous input from river and marine sediments generally provide more favorable conditions for above- and belowground productivity. The belowground components of mangrove forests, such as coarse woody debris, soil, and pneumatophores (i.e., aerial roots), can contribute between 45% and 65% of the total ecosystem respiration (Troxler et al., 2015). Mangroves are similar to all tidal wetlands in that soil carbon pools dominate ecosystem carbon stocks, and carbon burial is an important long-term fate of fixed carbon. For example, despite their short stature, dwarf mangroves may generate greater annual increases in belowground carbon pools than might taller mangroves (Adame et al., 2013; Osland et al., 2012).

Coupled stressors from both human and natural drivers, such as groundwater extraction and sea level rise, currently are altering subtropical tidal wetlands. Soil organic carbon (SOC) stocks face increased rates of mineralization and peat collapse with saline intrusion (Neubauer et al., 2013). Still, total carbon stocks may increase as a result of trends in mangrove expansion into salt marsh habitat (Cavanaugh et al., 2014; Doughty et al., 2015; Krauss et al., 2011; Bianchi et al., 2013). This pattern of expansion is expected to continue with current trends in climate change (e.g., the changes in frequency and intensity of hurricanes and freeze events) and with increasing rates of sea level rise (Barr et al., 2012; Lagomasino et al., 2014; Meeder and Parkinson 2017; Dessu et al., 2018). Dwarf and basin mangroves, which generally have shorter canopies, are most affected by freezing temperatures, while hurricane damage has the strongest impact on fringing mangrove forests along the coasts (Zhang et al., 2016). Freeze and

cold events drive the poleward advancement of mangroves along the eastern coast of Florida and GMx (Cavanaugh et al., 2014; Giri et al., 2011; Saintilan et al., 2014). Though mangroves in these regions may not currently extend past their historical range limits (Giri and Long 2014), the expansion and contraction of the mangrove forest clearly is documented in field and remotely sensed map products.

15.3.3 Pacific Coast Estuaries and Tidal Wetlands

The Pacific (west) coast of North America is seismically active with subduction zones that create steep topography and narrow continental shelves. As such, seasonal coastal winds drive upwelling and downwelling events that can shape biogeochemical cycling along the Pacific continental margin in estuarine waters and tidal wetlands. A more descriptive approach herein reflects the limited representation of Pacific Coast information presented in Appendix 15A, p. 642, as compared with that for the Atlantic and GMx coastlines.

Pacific Coast Estuaries

Estuaries of the Pacific Coast differ from other North American estuaries in that their carbon cycle dynamics tend to be dominated by ocean-sourced rather than river-borne drivers, predisposing many Pacific Coast estuaries and coastal environments to hypoxia and acidified conditions, largely as a result of natural processes (e.g., Chan et al., 2016, 2017; Feely et al., 2010, 2012; Hales et al., 2016). From the Gulf of Alaska south through Puget Sound, glacially formed estuaries have sills that restrict circulation between estuaries and coastal waters, further predisposing deep estuarine waters to hypoxic or anoxic conditions that form in the deep water of these estuaries. Interannual-to-decadal, basin-scale, ocean-climate oscillations such as the Pacific Decadal Oscillation and El Niño Southern Oscillation drive variations in rainfall along the Pacific Coast, which, in turn, controls material export from land to estuaries and subsequently to the coastal ocean. These oscillating climate drivers, as well as stochastic events such as large marine heatwaves, drive interannual variability



in physical and biogeochemical dynamics along the Pacific Coast, with significant effects on estuarine carbon cycle and ecosystem processes (Di Lorenzo and Mantua 2016).

Within spatially large marine ecosystems (LMEs) on the Pacific Coast—Gulf of Alaska, California Current, Gulf of California, and Pacific Central-American Coastal LMEs (lme.noaa.gov)—estuaries represent either globally significant large river systems, such as the Fraser, Columbia, San Joaquin/Sacramento, and Colorado rivers or one of many “small mountainous rivers” (SMRs) with steep watershed terrain and limited continental shelves for delta development. From the Southern California Bight (SCB) south to Panama, lagoons also represent a significant fraction of the semi-enclosed, saline-to-brackish water bodies along the Pacific Coast. Lagoons typically have episodic connection to adjacent coastal ocean areas and lack substantial freshwater input, distinguishing them from estuaries. However, despite the strong along-coast gradients in rainfall and terrestrial input to Pacific Coast lagoons and estuaries, oceanic sources of nutrients and carbon, particularly those delivered via upwelling, play an important or dominant role in carbon cycle dynamics in all systems studied (Camacho-Ibar et al., 2003; Davis et al., 2014; Hernández-Ayón et al., 2007; Steinberg et al., 2010).

Terrestrial inputs to Pacific Coast estuaries vary substantially along the steep rainfall gradient from very wet conditions in the north to arid conditions in southern and Baja California, with precipitation increasing again from central Mexico through Panama. The Global NEWS 2 model estimated terrestrial TOC inputs are approximately 8.5 teragrams of carbon (Tg C) per year to the Gulf of Alaska through northern California, 0.7 Tg C per year to southern and Baja California and the Gulf of California, and 2.8 Tg C per year to Mexico south of Baja California and Central America (Mayorga et al., 2010). The SMRs representing a significant portion of these inputs are similar to the Mississippi River in delivering their freshwater, nutrient, and organic carbon loads directly to the coastal ocean or larger estuarine water

bodies such as Puget Sound or the Strait of Georgia (Johannessen et al., 2003; Wheatcroft et al., 2010).

Phytoplankton productivity estimates across Pacific Coast estuaries from San Francisco Bay to British Columbia reflect an order of magnitude variation in median annual primary production rates, from about 50 g C per m² per year in the Columbia River estuary to 455 to 609 g C per m² per year in the Indian Arm fjord near Vancouver, British Columbia (Cloern et al., 2014). The role of riverborne nutrients is exemplified by the total water column primary production estimate for the Columbia River estuary at 0.030 Tg C per year (Lara-Lara et al., 1990). An air-sea CO₂ exchange study on the Columbia River estuary estimated that the net annual emission is quite small at 12 g C per m² per year (Evans et al., 2012). SCB estuaries are also highly productive but most likely act as sources of CO₂ to the atmosphere and net exporters of dissolved inorganic and organic carbon to the coastal ocean owing to input and decomposition of allochthonous carbon from surrounding land areas. All recent studies from lagoons and estuaries in the San Diego area report estuarine *p*CO₂ levels consistently greater than atmospheric levels (Davidson 2015; Paulsen et al., 2017; see also Southern California Coastal Ocean Observing System: sccoos.org/data/oa). Carbon cycling in lagoons with little or no riverine input is likely to be dominated by upwelling, as in San Quintín Bay, Baja California. Most of San Quintín Bay (85%) acts as a source of CO₂ to the atmosphere (131 g C per m² per year) due to the inflow and outgassing of CO₂-rich upwelled waters from the adjacent ocean. The remaining 15%, composed of *Zostera marina* seagrass beds, shows net uptake of CO₂ and bicarbonate (HCO₃⁻), with *p*CO₂ below atmospheric equilibrium, resulting in a net CO₂ sink of 26 g C per m² per year (Camacho-Ibar et al., 2003; Hernández-Ayón et al., 2007; Muñoz-Anderson et al., 2015; Reimer et al., 2013; Ribas-Ribas et al., 2011). Whereas this Mediterranean climate bay was net autotrophic during the upwelling season in previous decades, it now appears to be net heterotrophic due to import of labile phytoplanktonic carbon generated in the



adjacent ocean during upwelling (Camacho-Ibar et al., 2003). This transition illustrates the potential sensitivity of estuarine, bay, and lagoonal net ecosystem production (NEP) to changes in upwelling intensity and persistence, highlighting the vulnerability to effects of ocean warming or changing coastal stratification on ecosystem metabolism and carbon balance.

Lateral transfers of carbon from estuaries to the coastal ocean are poorly constrained by observations because of the difficulty and expense of making sufficient direct observations to measure this important lateral transfer. Many gaps remain in the understanding of the carbon cycle of Pacific Coast estuaries and lagoons, despite sporadic observations over the last several decades. For example, no systematic information on carbon burial is available and seagrass extent is likely undermapped (CEC 2016). With few exceptions, long-term monitoring time series are inadequate to track changes in terrestrial carbon inputs, primary production, air-sea CO₂ exchange, carbon burial in sediments, and carbon transfers to the coastal ocean that can be expected to result from climate and human-caused environmental changes (Boyer et al., 2006; Canuel et al., 2012). Implementing long-term observations of carbon, oxygen, and nutrient biogeochemistry, along with metrics of ecological response and health, in Pacific Coast estuaries is a priority (Alin et al., 2015).

Pacific Coast Tidal Wetlands

The Pacific Coast is dominated by rocky headlands, broad sand dune complexes, sand beaches, and spits (i.e., sandbars). The area of Pacific Coast tidal wetlands is roughly 628 km² in the United States (NOAA 2015) and at least 2,522 km² in Mexico, predominantly as mangroves (Valderrama-Landeros et al., 2017), perhaps more if shallow water habitats are included (Contreras-Espinosa and Warner 2004). While small but iconic “low-flow” estuaries are distributed sparsely along the coast (e.g., Elkhorn Slough and Tomales Bay), areas of expansive estuarine wetlands are limited to the larger coastal estuaries, where major rivers enter the sea and where embayments are sheltered by sandbars or headlands

(e.g., Coos Bay, Humboldt Bay, and San Diego Bay). San Francisco Bay, which supports the largest extent of coastal wetlands along the Pacific Coast of North America, is a tectonic estuary—a down-dropped graben (i.e., trench) located between parallel north-south trending faults. In Mexico, coastal wetlands are found in association with large barrier-island lagoon complexes where wave energy is reduced by headlands, offshore islands, or the Baja California peninsula, as well as along the Gulf of Tehuantepec, where the continental shelf widens and the winds are intense and offshore (northerly), originating in the Gulf of Campeche across the Isthmus of Tehuantepec. Assuming that published studies of soil carbon accumulation (79 to 300 g C per m² per year (Ezcurra et al., 2016) are broadly representative of U.S. and Mexico coastlines, average estimates of soil carbon sequestration by Pacific estuarine wetlands sum to 0.05 Tg C per year for the United States and 2.67 Tg C per year for Mexico.

Although U.S. Atlantic and GMx coastlines are known to support more organic-rich sediments, rates of carbon burial in tidal wetlands on the Pacific Coast tend to be commensurately high due to high rates of volume gain through sediment accretion. Previous studies have reported accretion rates of 0.20 to 1.7 cm per year in natural marshes along the Pacific Coast of North America (Callaway et al., 2012; Thom 1992; Watson 2004), with many values at the higher end of this range. High rates of sediment accretion are a function of the active Pacific Coast margin, because Pacific coastal watersheds tend to have high relief and support elevated erosion rates while providing limited opportunity for deposition of sediments along lowland floodplains (Walling and Webb 1983). This circumstance leads to high water column–suspended sediment concentrations, often exacerbated by anthropogenic land-use activities, such as agriculture, grazing, logging, and development (Meybeck 2003). Although not ubiquitous due to landscape changes (e.g., Skagit River), high rates of sediment accretion are common and known to promote high carbon burial rates when allochthonous organic carbon derived from upland sources is a sediment constituent



(Ember et al., 1987). Additionally, organic carbon produced *in situ* is more quickly buried in the sediment anoxic zone in high-accumulation environments (Watson 2004).

15.3.4 High-Latitude (Alaskan, Canadian, and Arctic) Estuaries and Tidal Wetlands

High-latitude estuaries (boreal and Arctic) are the youngest estuaries (<1,000 years) but the most subject to coastal erosion and hydrological carbon export from thawing permafrost during the current warming climate. Terrigenous inputs of silt and organic carbon are estimated as dominant sources of carbon flux, but inadequate mapping and measurements limit current estimates of carbon fluxes in high-latitude estuaries and tidal wetlands.

High-Latitude (Arctic) Estuaries

Salinity gradients are a defining feature of the estuarine zones of the Arctic Ocean (McClelland et al., 2012). Further, nearshore ice conditions are changing, erosion of coastlines is increasing, and the duration and intensity of estuarine and ocean acidification events are increasing (Fabry et al., 2009), as also discussed in Ch. 16: Coastal Ocean and Continental Shelves and Ch. 17: Biogeochemical Effects of Rising Atmospheric Carbon Dioxide. Lagoons in the Alaskan Beaufort Sea, bounded by barrier islands to the north and Alaska's Arctic slope to the south, span over 50% of the coast. These lagoons link marine and terrestrial ecosystems and support productive biological communities that provide valuable habitat and feeding grounds for many ecologically and culturally important species. Beaufort Sea lagoons are icebound for approximately 9 months of the year; therefore, the brief summer open-water period is an especially important time for resident animals to build energy reserves (i.e., necessary for spawning and surviving winter months) and for migratory animals to feed in preparation for fall migrations. Recent dramatic declines in ice extent have allowed wave heights to reach unprecedented levels as fetch has increased (AMAP 2011).

These studies highlight the climate linkages along coastal margins of the Arctic, especially how changes in sea ice extent can affect terrestrial processes (Bhatt et al., 2010), controlling coastal erosion and the transport of carbon, water, and nutrients to near-shore estuarine environments (Pickart et al., 2013). Nearshore estuarine environments in the Arctic are critical to a vibrant coastal fishery (von Biela et al., 2012) and also serve as habitat for hundreds of thousands of birds representing over 157 species that breed and raise their young over the short summer period (Brown 2006).

High-Latitude (Arctic) Tidal Wetlands

High-latitude ecosystem carbon flux measurements tend to focus on abundant inland peatlands (see Ch. 11: Arctic and Boreal Carbon, p. 428, and Ch. 13: Terrestrial Wetlands, p. 507), and thus less is known about Arctic and subarctic tidal marshes. However, due to high sedimentation rates, Arctic estuarine wetlands are estimated to sequester carbon at rates up to tenfold higher per area than many other wetlands (Bridgham et al., 2006). In a North American survey of published literature, Chmura et al. (2003) accounted for soil carbon stock only to 50 cm in depth, but some brackish marshes, especially in seismically active regions, have much deeper organic sediments. The Hudson Bay Lowlands tidal marshes are a notably understudied region where soil carbon stocks in the nontidal component alone are estimated to contain 20% of the entire North American soil carbon pool (Packalen et al., 2014). Gulf of Alaska marshes are relatively low salinity or freshwater dominated due to the excess of precipitation over evapotranspiration of the Pacific Northwest, as well as the substantial glacial meltwater that characterizes the region. Still, the large impact of melting glaciers, including the Bering and Malaspina piedmont glaciers (each approximating the size of Rhode Island), is expected to contribute to sea level rise locally, as will thawing river deltas, such as the Yukon-Kuskokwim Delta, that are characterized by discontinuous permafrost.

One of the most important coastal Alaskan marsh systems is the Copper River Delta, a critical habitat



for migratory birds along the Pacific Flyway, which extends for more than 75 km and inland as much as 20 km in some places along the Gulf of Alaska (Thilenius 1990). Although carbon storage estimates in these marsh locations are lacking, extensive research on the uplifted (and buried) peats by Plafker (1965) indicate alternating events of extreme subsidence and uplift (i.e., yo-yo tectonics). For example, the 1964 earthquake raised the entire delta from 1.8 to 3.4 m (Reimnitz 1966). Current studies on peat cores reveal marsh vegetation interspersed with intertidal muds, freshwater coastal forest, and moss peat, which extends to depths greater than 7 m (Plafker 1965). Whereas geological drivers clearly are the primary control on carbon storage in these marshes, the dynamic relationship with vegetation illustrates biological feedbacks as well (e.g., nutrient redistribution; Marsh et al., 2000). Highly dynamic sedge- and rush-dominated marshes are notably resilient to extensive sediment deposition from the Copper River, further ensuring growth of willows and shrubs and contributing to the woody component of buried peats. Whether the areal extent of these wetlands will expand or decline with tectonic impact and regional sea level rise is not known.

15.4 Carbon Fluxes and Stocks in Tidal Wetlands and Estuaries of North America

Literature summaries and data compilations discussed in this section enable estimates to be made of carbon stocks and fluxes in North American tidal wetlands and estuaries. Accuracy in quantifying stocks and fluxes in tidal wetlands and estuaries is a function of the accuracy in estimated area (extent) and in estimated stocks and fluxes per unit area. For North America, estimates involve areas, sediment carbon stocks, and the following fluxes: the net change in the carbon stock of tidal wetland soils, tidal wetland exchange of CO₂ with the atmosphere (i.e., NEE), tidal wetland exchange of CH₄ with the atmosphere, tidal wetland carbon burial, lateral exchange of carbon between tidal wetlands and estuaries, and estuarine outgassing of CO₂. Additionally, because the conterminous United States (CONUS)

contains a more robust estuarine dataset of most stocks and fluxes, a separate analysis is presented for this region that includes estimates of estuarine NEP, burial, and export of organic carbon to shelf waters.

15.4.1 Tidal Wetland and Estuarine Extent

A synthesis of recent compilation efforts is used to estimate the areas of tidal wetlands and estuaries, and the accuracy of these estimates varies among countries of North America (see Table 15.1, p. 604). In CONUS, a tidal wetland distribution is estimated using the full salinity spectrum of tidal wetland habitats mapped by the U.S. Fish and Wildlife Service National Wetlands Inventory (USFWS NWI; Hinson et al., 2017). However, in Mexico and Canada, only saline wetlands are available at a national scale, as mapped by the Commission for Environmental Cooperation (CEC; CEC 2016). Hence, tidal wetland areas in Mexico and Canada are likely underestimated. Estimates for the estuarine area of North America use a global segmentation of the coastal zone and associated watersheds known as MARCATS (MARGins and CATchments Segmentation; Laruelle et al., 2013). The MARCATS product is available globally at a resolution of 0.5 degrees and delineates a total of 45 coastal regions, or MARCATS segments, eight of which are in North America. Some CONUS-only applications use estuarine areas from the National Estuarine Eutrophication Assessment survey (Bricker et al., 2007), which is based on geospatial data from the National Oceanic and Atmospheric Administration (NOAA) Coastal Assessment Framework (NOAA 1985). The Coastal Assessment Framework includes a high-resolution delineation of the U.S. coastline in this area and delineates 115 individual estuarine subsystems. Seagrasses are considered separately because of their distinct sediment carbon stocks, even though they overlap in area with estuaries. Seagrass area across North America is estimated according to CEC (2016), using web-available map layers.

Table 15.1, p. 604, reveals the relative areas of tidal wetlands, estuaries, and seagrasses of North America, in addition to how these ecosystems are distributed by subregion and country. Estuaries of



North America cover about 10 times the area of tidal wetlands. About half the tidal wetlands of North America are salt marsh, a third are mangrove, and the remainder is split roughly between tidal fresh marsh and tidal fresh forest. The high-latitude region is characterized by a large estuarine area, about 60% of North America's total estuarine area, but has only a few percent of the continent's tidal wetland area and seagrass area. The Gulf of Mexico (GMx), on the other hand, is home to most of North America's tidal wetlands and seagrasses, with 58% of each. The Atlantic Coast and GMx each have about 10% of the total estuarine area, and the Atlantic coast has about half the tidal wetland area and seagrass area of GMx. The Pacific Coast is similar to the high-latitude subregion with a relatively small area of tidal wetlands and seagrasses (although these areas may be under-mapped), and it has an estuarine area about 50% greater than that of GMx. Tidal wetlands of North America reside mainly in CONUS (as salt marsh) and Mexico (as mangroves). Similarly, seagrasses are found mainly in coastal waters of CONUS and Mexico. Estuarine area is not available by country, except for CONUS, which is estimated to have 21% of North America's total estuarine area.

15.4.2 Tidal Wetland and Estuarine Stocks

Estimates of tidal wetland and estuarine carbon stock in the upper 1 m of sediment or soil were made by using estimates of the carbon density (mass carbon per unit volume) from large synthetic datasets. Cross-site comparisons of soil carbon stocks in tidal wetlands illustrate very little range in carbon densities in North America both downcore and among tidal wetlands of varied salinity, vegetation structure, and soil types. Hence, for all tidal wetlands except GMx mangroves, a single estimate of carbon density, 27.0 ± 13 kg organic carbon per m^3 , was used based on a comprehensive review of the literature (Chmura 2013; Holmquist et al., 2018a; Morris et al., 2016; Nahlik and Fennessy 2016; Ouyang and Lee 2014). For mangroves in GMx, a value of 31.8 ± 1.3 kg organic carbon per m^3 was used (Sanderman et al., 2018). A review of seagrass SOC densities (CEC 2017; Fourqurean et al., 2012; Kennedy et al., 2010; Thorhaug et al., 2017) revealed more variance

within and between regions, with some notably high soil carbon densities in GMx. Best estimates (and ranges) of 2.0 ± 1.3 kg organic carbon per m^3 were used for the Atlantic Coast and high-latitude subregions, 3.1 ± 2.4 kg organic carbon per m^3 for GMx, and 1.4 ± 1.2 kg organic carbon per m^3 for the Pacific Coast. For organic carbon density in estuarine sediments, a carbon density of 1.0 ± 1.2 kg organic carbon per m^3 was used based on a mean value of organic carbon mass fraction (0.4% organic carbon in waters shallower than 50 m; Premuzic et al., 1982; Kennedy et al., 2010) and a dry bulk density average of 2.6 g per cm^3 from Muller and Suess (1979). The assumed carbon densities and areas led to carbon stocks in the upper 1 m of 1,410, 354, and 122 Tg C for tidal wetlands, estuaries, and seagrasses, respectively, with a total carbon stock of $1,886 \pm 1,046$ Tg C.

Net Change in Tidal Wetland Soil Carbon Stock

An estimate of tidal wetland carbon stock loss could only be made using the loss rate for saltwater wetlands in CONUS, as loss rates in other parts of North America and for tidal fresh wetlands are not available. However, CONUS saltwater wetlands make up the overwhelming majority of North American tidal wetlands (see Table 15.1, p. 604), so applying the CONUS saltwater wetland loss rate to all North American tidal wetlands is not unreasonable. The use of a loss rate of CONUS vegetated saltwater wetlands of 0.18% per year between 1996 and 2010 (Couvillion et al., 2017) and estimated mass of carbon in the upper meter of tidal wetland soils (i.e., 1,362 Tg C) resulted in an overall annualized loss rate of 2.4 Tg C per year. For CONUS only, which holds 1,019 Tg C, the loss rate is 1.8 Tg C per year. Expert judgement assigned 100% errors to these losses because they are deeply uncertain due to annualized episodic events (e.g., Couvillion et al., 2017), difficulty in mapping loss, and difficulty in assessing the rate and fate of carbon from disturbed tidal wetlands (Ward et al., 2017; Lane et al., 2016).

15.4.3 Tidal Wetland and Estuarine Fluxes Tidal Wetland Net Ecosystem Exchange

Presented in Table 15A.1, p. 642, are annual estimates of NEE in North America based on



continuous measurements, focusing primarily on eddy covariance approaches and high-frequency datasets from static chamber deployments to reduce uncertainty. A total of 16 sites were compiled, including restored wetlands, all of which are in CONUS and mostly along the Atlantic Coast. This limited dataset indicates that NEE varies greatly within and among sites, ranging from the highest annual uptakes in a mangrove ecosystem ($-1,200$ g C per m^2 per year) to the greatest annual losses in a mudflat ($1,000$ g C per m^2 per year) and in a sequence of tidal marshes in Alabama (400 to 900 g C per m^2 per year; Wilson et al., 2015). Excluding the restored sites and mudflats from the Hudson-Raritan estuary in New Jersey, as well as the static chamber data from Alabama, the mean NEE at the continuously monitored sites ($n = 11$ of 16) was negative, indicating uptake of atmospheric CO_2 by tidal wetlands. Comparing annual values from the 11 sites (comprising 22 annual datasets) yields coast-specific estimates of NEE: -133 ± 148 g C per m^2 per year on the Pacific (one site, 3 years), -231 ± 79 g C per m^2 per year on the Atlantic (seven sites, 1 to 3 years), and -724 ± 367 g C per m^2 per year in GMx (three sites, 1 to 5 years). Integrating these estimates by area of tidal wetlands on each of North America's three coasts, the NEE estimate is -27 ± 13 Tg C per year. For CONUS only, NEE is -19 ± 10 Tg C per year.

Tidal Wetland Carbon Burial

Rates of carbon burial in wetland soils and sediments are associated with specific temporal scales depending on calculation methods. Typically, carbon burial is calculated as the product of *soil carbon density* (i.e., the mass of carbon stored in soil per unit volume) multiplied by *accretion rate* (i.e., the vertical rate of soil accrual and thus change in volume), which is measured by a variety of dating techniques that span multiple time frames (e.g., marker horizons; radioactive isotopes including those of cesium (^{137}Cs), lead (^{210}Pb), and carbon (^{14}C); pollution chronologies; and pollen stratigraphy). Carbon burial is thus a rate of carbon accumulation in tidal wetland soils over a specific time period (typical units are g C per m^2 per year). This measure integrates all carbon pools

present, both “old” and “new,” and both autochthonous and allochthonous sources.

Table 15.2 lists carbon burial estimates for salt marshes summarized by Ouyang and Lee (2014), excluding short-term accretion cores (e.g., marker horizons). Identified were 125 cores in North America, about half of which are along the Atlantic Coast and the rest roughly spread evenly among the three other subregions. Mean carbon burial estimates vary considerably among the four subregions, with the lowest rates along the Atlantic Coast, intermediate rates along the Pacific Coast, and the highest rates in the high-latitude subregion and GMx. The spatially integrated burial rate was computed for each subregion by multiplying its mean burial rate by its tidal wetland area, thus using an assumption that the salt marsh burial rate applies to tidal freshwater and mangrove systems. The spatially integrated burial rate (± 2 standard errors) across North America is 9.1 ± 4.8 Tg C per year, with more than 75% in GMx, owing to its large tidal wetland area (see Table 15.1, p. 604) and high carbon burial rate (see Table 15.2, p. 612). For CONUS alone, assuming equivalent distributions of rates among coasts and vegetation types, carbon burial is estimated to be 5.5 ± 3.6 Tg C.

Tidal Wetland CH_4 Fluxes

While CH_4 fluxes tend to be negligible from tidal wetlands with high soil salinities, emissions can increase considerably when sulfate availability is lower (as indexed by salinity; Poffenbarger et al., 2011). Based on the higher net radiative impact of CH_4 , climatic benefits of CO_2 uptake and the sequestration illustrated by most of the sites in Table 15A.1, p. 642, may be offset partially by CH_4 release in lower-salinity tidal wetlands (Whiting and Chanton 2001).

Here are reported annual CH_4 fluxes from tidal wetlands across North America (see Table 15A.2, p. 644), with values from studies published in 2011 or earlier taken from Poffenbarger et al. (2011). For studies published after 2011, the same methodology was used as Poffenbarger et al. (2011) in analyzing CH_4 flux data and reporting average annual CH_4



Table 15.2. Carbon Accumulation Rate (CAR) and Associated Data for Tidal Estuarine (Salt and Brackish) Marsh^a

Region	n	Mean CAR ± 2σ ^b (g C per m ² per year)	Regional Tidal Wetland Burial ^c ± 2σ (Tg C per year)
High Latitudes	25	301 ± 155	0.5 ± 0.2
Atlantic Coast	59	126 ± 87	1.4 ± 1.0
Pacific Coast	18	173 ± 92	0.6 ± 0.3
Gulf of Mexico	23	293 ± 210	6.6 ± 4.7
North America	125	236 ± 124	9.1 ± 4.8

Notes

- a) From Ouyang and Lee (2014).
- b) 2σ = 2 standard errors.
- c) Regional burial calculated for all tidal wetland types regardless of salinity or vegetation type.
- d) Key: n, number of sites; g C, grams of carbon; Tg C, teragrams of carbon.

emissions. If CH₄ emissions were measured over all seasons of the year with the annual rate unreported, calculations were made by extracting emission rates from tables and figures and then interpolating between time points. Finally, although this was only the case in a few studies, for short-term studies lasting a few days to months over the growing season, average daily CH₄ emissions were calculated and then converted to annual fluxes using the rate conversion factors determined by Bridgham et al. (2006). The compilation resulted in CH₄ flux measurements at 51 sites in North America.

The compilation, illustrated in Figure 15.3, this page, continues to support the role of salinity as a predictor of CH₄ emissions observed by Poffenbarger et al. (2011). However, there is considerable variability among methods and sites in annual CH₄ emissions in fresh and brackish (i.e., oligohaline and mesohaline) wetlands, indicating the need for further studies to help improve understanding of the drivers and sensitivities of CH₄ fluxes in these common salinity ranges. Tidal wetlands in the salinity range of 0 to 5 practical salinity units (PSU; i.e., fresh-oligohaline) show an average (±2 standard errors) CH₄ emission of 55 ± 48 g CH₄ per m² per year, whereas tidal wetlands in the salinity range of

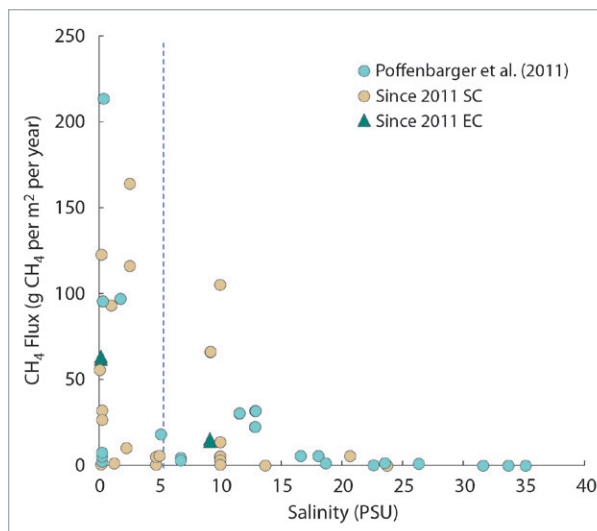


Figure 15.3. Tidal Marsh Methane (CH₄) Emissions Versus Salinity. Approaches to measuring atmospheric CH₄ flux are coded by method as SC (static chamber) and EC (eddy covariance flux tower). CH₄ flux is in grams (g); salinity is in practical salinity units (PSU). The dashed line denotes the demarcation of fresh and oligohaline marshes (0 to 5 PSU) versus mesohaline to saline marshes (5 to 35 PSU).

5 to 38 PSU (i.e., mesohaline to fully saline) emit CH₄ at an average rate of 11 ± 13 g CH₄ per m² per year. The spatially integrated tidal wetland CH₄



emission rate, computed by multiplying the fluxes for fresh-oligohaline and mesohaline-saline systems by their respective areas (5,491 and 33,118 km²; see Table 15.1, p. 604), results in 0.29 ± 0.27 and 0.35 ± 0.43 Tg CH₄ per year, respectively, totaling 0.65 ± 0.48 Tg CH₄ per year (0.49 ± 0.36 Tg C per year) across the entire salinity gradient. Hence, in North America, fresh-oligohaline and mesohaline-saline systems contribute about equally to the total flux, with the former having high per-unit-area flux rates and low area and the latter having low per-unit-area flux rates and high area.

Lateral Fluxes of Carbon from Wetlands to Estuaries

A significant part of tidal wetland and estuarine carbon budgets is the lateral flux from tidal wetlands to estuaries, which is due mainly to tidal flushing. Twelve estimates of TOC (in both dissolved and particulate forms) exchange (per unit area of wetland) in tidal wetlands of the eastern United States were summarized by Herrmann et al. (2015), and the mean value and 2 standard errors derived in that study (185 ± 71 g C per m² per year) were used herein. Similarly, four estimates of DIC exchange in eastern U.S. tidal wetlands were summarized in Najjar et al. (2018), with a mean (± 2 standard errors) of 236 ± 120 g C per m² per year. With only a small number of DIC flux measurements, the error was doubled. Hence, tidal wetland export of total carbon is estimated to be 421 ± 250 g C per m² per year. Applying this to all North American tidal wetlands (see Table 15.1, p. 604) yields a total export of 16 ± 10 Tg C per year; applied to CONUS wetlands only, the estimate of lateral export is 11 ± 7 Tg C per year.

Estuarine CO₂ Outgassing

The SOCCR2 assessment used the global synthesis of Chen et al. (2013), which combined field estimates of outgassing per unit area with the MARCATS areas. Most MARCATS segments were found to be sources of CO₂ to the atmosphere, with the integrated flux over North America at $+10$ Tg C per year (see Table 15.3, this page). Chen et al. (2013) did not provide error estimates, so

Table 15.3. Estuarine CO₂ Outgassing for North America^{a,e}

MARCATS ^b Segment No.	CO ₂ Outgassing ^c (g C per m ² per year)	Number of Systems	CO ₂ Outgassing (Tg C per year)
1	129	3	4.4
2	11	3	0.1
3	174	0	1.1
9	96	2	3.1
10	118	15	4.0
11	-9	1	-0.3
12	-5	1	-0.2
13	-13	0	-2.1
Total North America		25	10.0
Approximate CONUS ^d (2, 9, and 10)		20	7.2

Notes

- Based on the Global Synthesis of Chen et al. (2013).
- MARCATS, MARGins and CATchments Segmentation.
- For regions 3 and 13, where no data were available within the segments, the methods of Chen et al. (2013) were used.
- CONUS, conterminous United States.
- Key: CO₂, carbon dioxide; g C, grams of carbon; Tg C, teragrams of carbon.

expert judgment was used to provide a range. The MARCATS segments in North America contain only 25 individual flux estimates, 15 of which are along the Atlantic coast, and some segments have no measurements at all (in which case data from similar systems were used). There is a possibility of a 100% error in the North American flux, so the estimate was placed at 10 ± 10 Tg C per year. Reduced uncertainty may be possible for distinct regions, but this level of error indicates confidence bounds at a continental scale.

A separate estimate was made of CONUS estuarine outgassing based on the SOCCR2 synthesis of CO₂ flux estimates (see Table 15A.3, p. 647) and the areas from the Coastal Assessment Framework (NOAA 1985). Because only one study was



identified for the Pacific Coast, analysis was limited to the Atlantic and GMx coasts, which contain about 90% of the CONUS estuarine area (see Table 15.1, p. 604). For the Atlantic coast, mean fluxes were first estimated in each of three subregions (GOM, MAB, and SAB) before multiplying by their respective areas. This was done because the outgassing per unit area increases toward the south. This analysis results in an outgassing of 10 ± 6 Tg C per year (best estimate ± 2 standard errors), which is larger (but not significantly so) than the Chen et al. (2013) analysis for the three segments covering CONUS (i.e., 7 Tg C per year). The SOCCR2 synthesis is an improvement over Chen et al. (2013) by being based on a larger flux dataset and more accurate CONUS estuarine areas.

Estuarine CH₄ Emissions

Only a very limited number of studies are known to be available and scalable for estimating net CH₄ emissions in North American estuaries. In their global review, Borges and Abril (2011) report only three within North America (de Angeles and Scranton 1993; Bartlett et al., 1985; Sansone et al., 1998), ranging from 0.16 to 5.6 mg CH₄ per m² per day. Two recent studies with continuous sampling illustrate temporal and spatial variability. Relatively high emissions were observed in the Chesapeake Bay during summer (28.8 mg CH₄ per m² per day;

Gelesh et al., 2016). In the Columbia River estuary (Pfeiffer-Herbert et al., 2016), summer emissions were estimated at 1.6 mg CH₄ per m² per day; 42% of the CH₄ losses were to the atmosphere, 32% were to the ocean, and 25% were to CH₄ oxidation. When scaled to a year, the estuarine CH₄ fluxes from the above studies range from 0.04 to 8 g C per m² per year, which is well below typical CO₂ outgassing rates (e.g., the U.S. Atlantic Coast mean estuarine CO₂ outgassing rate is 104 ± 53 g C per m² per year, see Table 15A.3, p. 647). Thus, estuarine CH₄ outgassing is likely a small fraction of estuarine carbon emissions. To be comparable with North American tidal wetland CH₄ emissions (~ 0.5 Tg CH₄ per year), the mean estuarine CH₄ emissions rate would need to be a conceivable rate of ~ 0.1 g CH₄ m² per year. Unfortunately, the lack of estuarine CH₄ emissions data for North America—and any well-constrained relationship with salinity or other physical parameter—precludes the possibility of making a constrained estimate of estuarine CH₄ emissions for North America.

15.4.4 Total Organic Carbon Budget for Estuaries of the Conterminous United States

The empirical model of Herrmann et al. (2015) was applied to quantify the TOC budget for CONUS estuaries (see Table 15.4, this page). This

Table 15.4. Estuarine Areas and Organic Carbon Regional Budgets for the Conterminous United States^{a,c}

Estuary	Area (km ²)	Riverine + Tidal Wetland Input (Tg C per year)	Net Ecosystem Production (Tg C per year)	Burial (Tg C per year)	Export to Shelf (Tg C per year)
Gulf of Mexico	30,586	12.6 \pm 3.5	-2.2 \pm 0.6	-0.3 \pm 0.1	-10.1 \pm 3.5
Pacific Coast	6,690	1.4 \pm 0.2	0.0 \pm 0.2	-0.2 \pm 0.1	-1.2 \pm 0.2
Atlantic Coast	37,764	5.5 \pm 1.3	-1.8 \pm 1.0	-0.5 \pm 0.3	-3.2 \pm 1.3
CONUS ^b	75,040	19.5 \pm 3.8	-4.0 \pm 1.2	-1.0 \pm 0.3	-14.5 \pm 3.7

Notes

a) Positive values = input of organic carbon to estuaries; negative values = removal of organic carbon from estuaries. Source: model of Herrmann et al. (2015).

b) CONUS, conterminous United States; best estimate and ± 2 standard errors.

c) Key: Tg C, teragrams of carbon.



model takes carbon and nitrogen inputs from a data-constrained watershed model and uses empirical relationships to compute burial and NEP. TOC export to shelf waters is computed by the difference. TOC input from rivers and tidal wetlands to CONUS estuaries is estimated to be 19.5 Tg C per year, with an average of 79% coming from rivers and the rest from tidal wetlands (not shown). Most of the input (74%) is exported from the estuary to the shelf, while 21% is remineralized to CO₂ and 5% is buried in estuarine sediments. Like most estuaries worldwide (Borges and Abril 2011), CONUS estuaries are, in the aggregate, net heterotrophic. However, there are regional differences in NEP, with GMx estuaries remineralizing twice as much of the TOC input as Atlantic estuaries and Pacific estuaries metabolically neutral.

15.4.5 Summary Budgets for Tidal Wetlands and Estuaries

The individual flux estimates above were combined into overall carbon budgets for tidal wetlands and estuaries of CONUS and the rest of North America. CONUS (see Figure 15.4a, this page) has better constraints on the fluxes. Central estimates of CONUS tidal wetland carbon losses and gains are very close to balancing even though they were estimated independently; burial, lateral export, and loss of soil carbon stock are all found to be significant terms of carbon removal that balance carbon uptake from the atmosphere. For the estuarine CONUS balance, riverine carbon delivery at the head of tide was taken from Ch. 14: Inland Waters (41.5 ± 2.0 Tg C per year). Including the tidal wetland delivery (11 ± 7 Tg C per year), CONUS estuaries thus were found to receive a total of 53 ± 7 Tg C per year from upland sources. With about 15% (best estimate) of this input outgassed and only a few percent buried, the resulting net total carbon flux from estuaries to shelf waters is 40 ± 9 Tg C.

The North American carbon budget for tidal wetlands and estuaries (see Figure 15.4b, this page) is similar to the CONUS budget except that most of the fluxes are larger. The net uptake of atmospheric CO₂ by the combined system of tidal wetlands and estuaries is

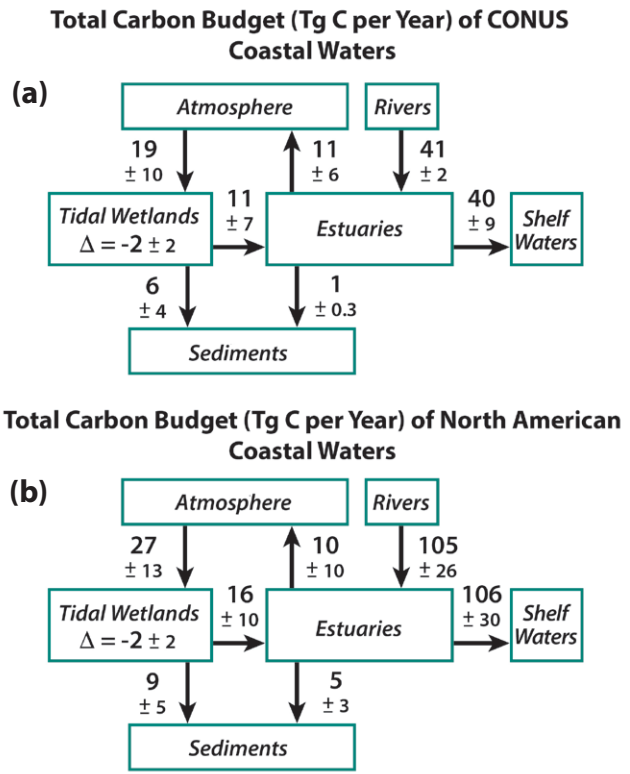


Figure 15.4. Summary Carbon Budgets for Tidal Wetlands and Estuaries. Budgets are given in teragrams of carbon (Tg C) for (a) the conterminous United States (CONUS) and (b) North America, with errors of ± 2 standard errors.

17 ± 16 Tg C per year. The riverine flux of 105 Tg C per year from Ch. 14: Inland Waters was used and assigned an error of 25%. Lacking direct estimates of carbon burial in North American estuaries, the CONUS estimate was used (see Table 15.4, p. 614) and scaled to all North American estuaries; the error is doubled to reflect this extrapolation. The carbon flux from North American estuaries to the shelf waters, estimated as a residual, is 106 ± 30 Tg C per year.

15.5 Indicators, Trends, and Feedbacks

All indications suggest that most North American coastal and estuarine environments, from Canada to Mexico, are changing rapidly as a result of global- and local-scale changes induced by climate alteration and human activities. The sustainability and quality of



estuarine and intertidal wetland habitats, including the magnitude and direction of carbon fluxes, are uncertain, especially due to limited monitoring time series relevant to changing extents and conditions of these habitats. Simulation models have illustrated the long-term sensitivity of coastal carbon fluxes to land-use and management practices while decadal and interannual variations of carbon export are attributable primarily to climate variability and extreme flooding events (Ren et al., 2015; Tian et al., 2015, 2016). Further, tidal wetland sustainability is strongly influenced by human modifications that generally reduce resilience (e.g., groundwater withdrawal, lack of sediment, nutrient loading, and ditching; Kirwan and Megonigal 2013).

Climatic changes affect entire watersheds, so the integration of small changes to terrestrial carbon cycling leads to a significant impact on the quantity, quality, and seasonality of riverine inputs to coastal zones (Bergamaschi et al., 2012; Tian et al., 2016). Within wetlands, accelerating sea level rise and increasing temperature yield a range of responses from enhanced wetland flushing, salinity intrusion, and productivity to enhanced respiration, tidal carbon export, and CH₄ emissions, which have all been postulated. Increased rates of sea level rise may enhance sedimentation and carbon burial rates up to a threshold of marsh resilience, above which erosion processes will dominate (Morris et al., 2016). This effect of accelerated sea level rise on morphology also affects carbon fluxes in shallow estuaries, whereby the loss of barrier islands to erosion will increase tidal mixing.

Estuaries show significant regional drivers of carbon cycling, such as the dominance of land-use change in Atlantic coast (Shih et al., 2010) and GMx (Stets and Striegl 2012) watersheds. In Pacific coast estuaries, ocean drivers (i.e., upwelling patterns) and rainfall variability are dominant controls on carbon fate and CO₂ degassing from Alaska to Mexico. In Arctic regions, along both Pacific and Atlantic coastlines, ice-cover melt and permafrost thaw appear to be critical drivers of wetland extent and estuarine mixing. Tidal wetland carbon dynamics, however,

show more local variability than regional variability, with multivariate drivers of extent and carbon fluxes, such as sediment supply (Day et al., 2013), nutrient supply (Swarzenski et al., 2008), tidal restrictions (Kroeger et al., 2017), and subsurface water or hydrocarbon withdrawal (Kolker et al., 2011). These coastal drivers illustrate the complexity of projecting carbon fluxes and their potential to alter fundamental habitat quality. For example, estuarine acidification is observed along all coastlines with potential stress to shell fisheries (Ekstrom et al., 2015), often with changes in riverine input, circulation, and local biological dynamics more significant than direct atmospherically driven ocean acidification (Salisbury et al., 2008).

Thus, expected changes in climate and land use for the remainder of this century likely will have a major impact on carbon delivery to and processing in tidal wetlands and estuaries. While terrestrial carbon loads likely will continue to drive ecosystem heterotrophy, extreme flooding events might shunt material directly to the continental shelf, thus decreasing processing, transformation, and burial in the estuary and tidal wetlands. Overall, estuarine area likely will increase relative to that of tidal wetlands (Fagherazzi et al., 2013; Mariotti and Fagherazzi 2013; Mariotti et al., 2010), and estuarine production will become more based on phytoplankton relative to benthic algae and macrophytes (Hopkinson et al., 2012). While this trajectory may be reversible (see Cloern et al., 2016), by the end of this century tidal wetland and estuary net CO₂ uptake and storage as organic carbon quite likely will be significantly reduced throughout the United States due to passive and active loss of tidally influenced lands.

15.5.1 Observational Approaches

Coastal observations of carbon stocks and fluxes cross many spatial and temporal scales because of their intersection in multiple contexts: past or future, land or ocean, and managed or unmanaged. A variety of observational approaches has been applied to study tidal wetland habitats and carbon fluxes and exchanges with the atmosphere and adjacent estuarine and ocean waters. Currently



lacking is a standardized, consistent methodology on carbon-relevant wetland mapping, wetland carbon flux monitoring, and repeated assessment. Wetland mapping, inventories, and sampling efforts include the National Wetlands Inventory (USFWS NWI 2017), a national effort to map and classify the wetland resources in the United States (data updated at a rate of 2% per year), using aerial photography and high spatial resolution remote-sensing color infrared imagery. Light detection and ranging, or LIDAR, imagery has been applied to develop high-resolution digital elevation models for wetlands and incorporate those maps into coastal resilience (NOAA 2015) and response mapping (USGS 2018). Satellite optical (e.g., Landsat; see Appendix C: Selected Carbon Cycle Research Observations and Measurement Programs, p. 821) and synthetic aperture radar (SAR) imagery has been used for decades in mapping wetland structure and biomass, with tidal hydrologies potentially interpretable through repeat measures. High-resolution satellite ocean color observations can be used to examine wetland impacts on estuarine carbon dynamics and stocks, which, combined with hydrodynamic models, may provide information on lateral fluxes and wetland contributions to estuarine and coastal carbon budgets, especially in the actively restoring Mississippi-Atchafalaya River Delta. However, existing remote-sensing algorithms could be improved, adding the capability for representing and quantifying carbon-related properties in highly turbid estuarine and nearshore waters (Son et al., 2014). Various ground-based approaches have been applied to validate mapped carbon stocks and inventories. Deep soil cores provide quantification of carbon stocks and, when dated, can provide long-term rates of net carbon accumulation or loss (Callaway et al., 2012). Exchanges of CO_2 and CH_4 between wetlands and the atmosphere have been measured historically using static (closed) chamber systems, but, increasingly, continuous eddy covariance approaches are being deployed (Forbrich and Giblin 2015; Knox et al., 2018). Continuous gas flux measurements (i.e., NEE) over a range of temporal scales (hours to days to seasons to years) can be very effective at

quantifying photosynthesis and respiration in tidal wetlands. An example of observational NEE data from estuarine ecosystems is illustrated in Figure 15.5a, p. 618. Similarly, in Figure 15.5b, p. 618, observational NEE from a tidal wetland ecosystem is shown. Estuarine NEE is typically quantified using measurements of the gradient in partial pressure across the air-water interface in combination with a model of the gas transfer velocity; more direct approaches are needed to reduce uncertainty (e.g., McGillis et al., 2001; Orton et al., 2010). Deployment of automated water quality sondes and optical sensors within channels of tidal wetlands provides a method for continuous bidirectional measurements of physicochemical and optical parameters that can be used as proxies for hydrological carbon concentrations and flux (Wang et al., 2016). These findings emphasize the importance of time-series measurements to provide *in situ* measurements of variability across timescales.

15.5.2 Modeling Approaches

While there have been numerous applications of three-dimensional estuarine biogeochemical models (Azevedo et al., 2014; Feng et al., 2015; Ganju et al., 2012; Irby et al., 2016; Kenov Ascione et al., 2014), none specifically allow integration with hydrological exchange of tidal wetlands. With unstructured meshes that provide topological flexibility, the Finite Volume Community Ocean Model (FVCOM; Chen et al., 2003) and the Semi-implicit Cross-scale Hydroscience Integrated System Model (SCHISM; Ye et al., 2016, 2018) have been successfully applied to wetland-estuarine environments. Currently, there are no biogeochemical models that include accurate parameterizations for the sources and sinks that drive variability in carbon fluxes, amount, and quality at the wetland-estuary interface (e.g., allochthonous sources, photochemical transformation, and viral lysis). Further, coupled biogeochemical-geomorphic models are necessary for full tidal wetland carbon accounting and projection with accelerated sea level rise, but they have yet to be validated successfully (Kirwan et al., 2010). Efforts to

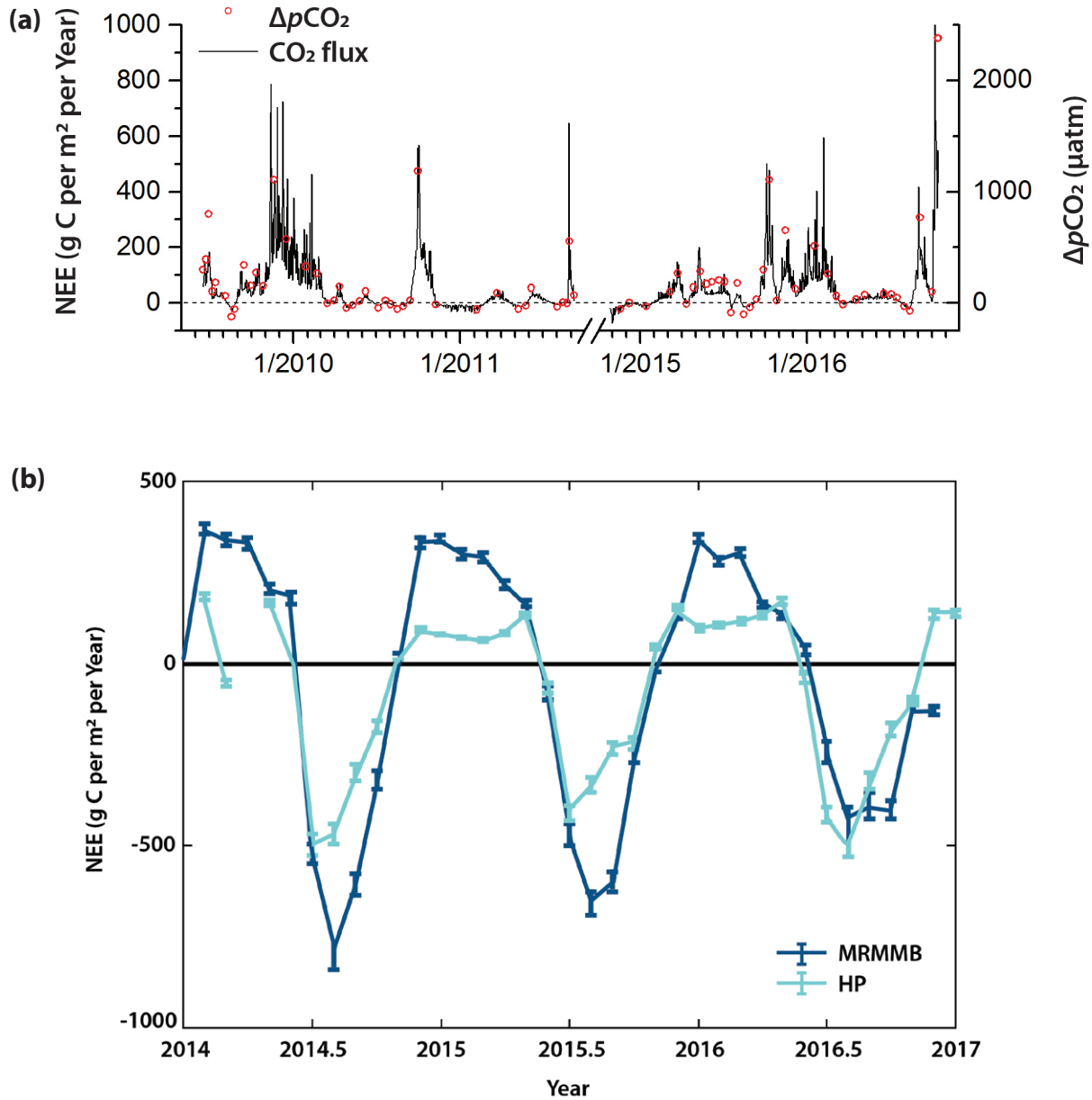


Figure 15.5. Example Observational Net Ecosystem Exchange (NEE) Data from (a) an Estuarine Ecosystem and (b) a Tidal Wetland Ecosystem. (a) NEE of carbon dioxide (CO_2 , black line) and the partial pressure difference of CO_2 ($\Delta p\text{CO}_2$) between air and water (red circles) in the Neuse River Estuary in North Carolina. NEE is positive when flux is from the water to the atmosphere. The $\Delta p\text{CO}_2$ is positive when water $p\text{CO}_2$ is greater than atmospheric $p\text{CO}_2$. Fluxes were estimated using the $p\text{CO}_2$ measured during spatial surveys (Crosswell et al., 2012, 2014; Van Dam et al., 2018) and a gas transfer parameterization based on local wind speed (Jiang et al., 2008). These studies present alternative gas transfer parameterizations and associated errors. (b) Data are from restored coastal tidal wetlands in the New Jersey Meadowlands. The dark blue line represents the Marsh Resource Meadowlands Mitigation Bank (MRMMB; Duman and Schäfer, 2018), and the teal line, the Hawk Property (HP) natural wetland. Error bars are standard deviation of the mean of all measurements during this period (monthly). Key: g C, grams of carbon; μatm , microatmospheres.



couple tidal wetland lateral exchanges with estuarine dynamics are ongoing.

Empirical approaches to modeling include synthetic cross-site comparisons and relationships. The National Wetlands Condition Assessment (U.S. EPA 2016) illustrates homeostasis among tidal wetland soil carbon densities spatially and downcore (Nahlik and Fennessy 2016). National Aeronautics and Space Administration (NASA) synthesis efforts, which include the Wetland-Estuary Transports and Carbon Budgets (WETCARB; NASA 2017b) project and the Blue Carbon Monitoring System (Blue CMS; NASA 2017a) project, have integrated literature-derived field data and national datasets (e.g., USFWS and U.S. Department of Agriculture) and identified key differences and similarities among tidal wetland and estuarine processes for CONUS. These approaches provide boundary conditions for new observations and identify critical knowledge gaps.

Key areas to aid further research and development are:

- Mapping approaches that characterize key drivers of tidal carbon accounting (organic carbon burial and CH₄ production), such as multiple salinity classes, relative elevations, and tidal boundaries;
- Unbiased, landscape-level sampling protocol to quantify sediment carbon stock change in tidal wetlands (similar to U.S. Forest Service Forest Inventory Analysis approaches for carbon accounting);
- Remote-sensing capability suitable for highly turbid estuarine waters;
- Networks for continuous measurements of wetland-atmosphere exchanges (CO₂ and CH₄ emissions) and wetland-ocean exchanges (dissolved and particulate carbon fluxes) and better constraint and linkage of these important fluxes;
- New biogeochemical models that account for critical processes at the wetland-estuary

interface, both ocean drivers (sea level rise) as well as watershed influences (land use); and

- Estuarine gas flux monitoring, including CO₂ and CH₄, especially in large, undersampled, episodic or rapidly changing environments, such as high latitudes (Arctic).

15.6 Societal Drivers, Impacts, and Carbon Management

As land- and freshwater-use changes have an outsized effect on estuarine carbon dynamics, societal drivers are at the heart of future projections for coastal zone carbon cycling. Dissolved carbon inputs are thought to have increased over the past century to Atlantic and GMx estuaries through riverine delivery, largely as a result of agricultural developments (Raymond et al., 2008; Tian et al., 2016). Similarly, delivery of nutrients from agricultural or urban growth and intensification can stimulate primary production in surface waters and respiration in bottom waters, leading to hypoxia and acidification in subsurface estuarine habitats (Cai et al., 2011; Feely et al., 2010; Irby et al., 2018). These human inputs reflect potential pathways for carbon management within estuaries by state, local, or provincial agencies and stakeholders (Chan et al., 2016; Washington State Blue Ribbon Panel on Ocean Acidification 2012). One step removed from carbon are the rich biological resources that have supported human populations on North American estuaries for millennia (e.g., Jackley et al., 2016), which link carbon management to fisheries and ecosystem management processes more broadly (Cooley et al., 2015). As ocean warming and CO₂ uptake drive changes in estuarine circulation, metabolism, and biogeochemistry, myriad changes to estuarine carbon cycles are expected over both short and long timescales, with impacts ranging from direct effects on individual species of ecosystem or economic importance to indirect effects on human health and livelihoods through stimulation of disease vectors (Bednarsek et al., 2017; McCabe et al., 2016; Waldbusser et al., 2014). Broad thinking about societal drivers of carbon cycle change and its ecosystem impacts, as well



as building effective partnerships with diverse stakeholders, will be critical to effective management of estuarine carbon cycle problems over the coming decades (DeFries and Nagendra 2017).

Coastal wetlands in temperate and tropical latitudes are a “directly or indirectly” managed landscape component, with increasing pressures from human stressors and sea level rise. Given their role in linking land, ocean, and atmospheric carbon fluxes, the increasing rate of global wetland loss and degradation is concerning. Tidal wetland areas in the United States have recently experienced relatively low rates of conversion and loss: ~0.2% per year, according to NOAA Coastal Change and Analysis Program (C-CAP) data from 1996 to 2010, with 92% of all loss occurring in Louisiana (Couvillion et al., 2017; Holmquist et al., 2018b). However, direct and indirect conversions of tidal wetlands to drained or impounded land uses continue actively along coastlines globally. In Mexico, 10% of mangrove area has been lost from 1980 to 2015, resulting in CO₂ emissions ranging from 0.4 to 1 Tg C per year (Troche-Souza et al., 2016); while GMx has more mangrove area, loss is high on the Pacific Coast due primarily to anthropogenic land-use changes.

Coastal “blue carbon” ecosystems—tidal marshes, mangroves, and estuarine sea grasses—are characterized by high areal rates of carbon sequestration, low rates of CH₄ and nitrous oxide (N₂O) emissions, and large soil carbon pools (Howard et al., 2017). Because the influence of coastal ecosystems on carbon cycles greatly exceeds their area (Najjar et al., 2018), activities that affect the conservation, degradation, or restoration of these ecosystems have implications for greenhouse gas (GHG) emissions and national GHG accounting (Kennedy et al., 2014). Loss of tidal hydrology likely shifts tidal wetlands from sinks to sources as large soil carbon reservoirs in tidal wetlands can become large sources of CO₂ emissions when disturbed (Pendleton et al., 2012), and freshwater dominance can dramatically impact CH₄ emissions (Kroeger et al., 2017). Further, nitrate pollution can dramatically impact N₂O emissions (Moseman-Valtierra et al., 2011).

In 2013, the Intergovernmental Panel on Climate Change (IPCC) issued guidance on including management of seagrasses, tidal marshes, and mangroves as an anthropogenic carbon flux in national GHG inventories (Kennedy et al., 2014). Currently a number of countries, including the United States, are in the process of implementing these guidelines (U.S. EPA 2017), an action which would be a major step toward reducing uncertainties in national carbon budgets and understanding the roles played by coastal tidal wetland management in national GHG emissions. This new information includes the relatively strong long-term sink for carbon in tidal and subtidal wetland soils, relatively limited CH₄ emissions in saline wetlands, and relatively large GHG emissions associated with wetland loss. In addition to improved knowledge of tidal wetland carbon balance, inclusion of tidal wetlands in the U.S. national GHG inventory provides an opportunity for enhanced estimation of the ecosystem services these wetlands offer to coastal communities. Ongoing research on feedbacks among hydrology, geomorphology, nutrient availability, plant productivity, and microbial activity is needed to understand and manage the impacts of human activities on the GHG balance of these ecosystems.

15.7 Synthesis, Knowledge Gaps, and Outlook

The CCARS synthesis report (Benway et al., 2016) is the most comprehensive attempt to develop a science plan for carbon cycle research of North American coastal systems. While clarifying key regional differences in processes and projections, this synthesis effort also exposed major knowledge gaps and disconnects between measurement and modeling scales. These knowledge gaps are currently being explored by multiple synthesis efforts, and below is a review of some of the major gaps being investigated.

15.7.1 Lateral Exchanges Between Tidal Wetlands and Estuaries

Estimates of lateral fluxes of carbon between tidal wetlands and estuaries are mostly based on discrete sampling events at monthly to seasonal intervals,



with sampling resolution from hourly to one half of a tidal cycle, leaving the majority of time unsampled and thus requiring large interpolation between sampling events and producing substantial uncertainty in export fluxes (Downing et al., 2009; Ganju et al., 2012). A recent estimate of the DIC lateral flux from a pristine intertidal wetland marsh on Cape Cod, Massachusetts, with minute-scale resolution revealed that previous estimates of marsh DIC export—such as those summarized by Najjar et al. (2018) and used here—may be severalfold too low (Wang et al., 2016). Previous studies generally show a positive carbon export from tidal wetlands to estuaries but may not fully resolve the export magnitude and temporal heterogeneity, which, in turn, are controlled by variability in water flux and constituent concentration across timescales from minutes to tidal cycles to years. Such observational gaps extend beyond DIC to include DOC and particulate organic carbon (POC) as well. In particular, the fate of exported POC from eroding marshes, though virtually unknown, is important for carbon accounting. Future studies should be directed to capture appropriate temporal scales of variability of carbon exports from marshes to accurately constrain lateral exchanges.

15.7.2 Coastal Subhabitat Boundaries

The definition of estuarine subhabitat within the coastal ocean is fluid, primarily associated with bottom depth and mixing processes. This boundary may not be mappable, but the absence of a robust definition inhibits future monitoring efforts and projections. Progress has been made in defining estuaries and quantifying their fundamental characteristics (such as residence time) in CONUS via NOAA's Coastal Assessment Framework (NOAA 2017). Such a framework has been essential for scaling up carbon and nitrogen fluxes from limited data (Herrmann et al., 2015; Najjar et al., 2018) and is greatly needed for all of North America. The global estuarine delineation based on MARCATS (Project Geocarbon 2017) has been very helpful, but the coarse resolution (i.e., 0.5 degrees) is a concern. For coastal wetland boundaries, multiple

criteria have been used by different entities: political boundaries, salinity gradients, elevation thresholds, and tidal criteria. This variability has led to great confusion in the literature (e.g., Lu et al., 2017), in agency policies, and in market-based carbon accounting protocols. A strong gap is the lack of a boundary mapped for head of tide. Tidal wetlands, by definition, cross a wide range of salinities (i.e., saline, brackish, and freshwater), with the singular distinction of having a hydroperiod influenced by ocean tides (paraphrased from web link; U.S. EPA 2016). Networks of available data may be useful in monitoring this boundary, as it is a key distinction of carbon dynamics in coastal habitats. These networks include, for example, a NOAA repository of coastal LIDAR; NOAA tide gauge networks; USFWS wetland mapping efforts; and USGS Land Change Monitoring, Assessment, and Prevention (LCMAP; USGS 2017). In the absence of a mapped boundary, spatial accounting of tidal and estuarine extent—current, past, and future—is fraught with uncertainty, with a likely underestimate of at least 50% for freshwater tidal wetlands alone.

15.7.3 Spatial Variability in Burial Rates and in Air-Water Flux

Because of ocean influences and similar processes along coastlines, spatial variability can be much greater within an estuarine and tidal wetland complex than among regions. Tracking the drivers of spatial variability in ecosystem properties—sea level, bathymetry, river flow, elevation, soil properties, and vegetation types—can greatly improve the use of remotely sensed data to validate carbon flux models and their variability between years. Accounting processes generally rely on spatial data, and mapping stocks and fluxes in these spatially dynamic habitats will require improved use of geospatial datasets and, thus, improved attribution of location information with observations. Relative sea level rise is particularly variable in its magnitude and influence. Geomorphic models (e.g., Kirwan and Megonigal 2013; Morris et al., 2016) are improving understanding of the sustainability of wetland carbon storage, showing enhanced carbon sequestration under modest



increases in sea level but rapid carbon emissions after wetland accretion reaches its conditional “tipping point.” Empirically, many GMx wetlands undergoing land subsidence appear to have crossed their threshold of sustainability and are being rapidly eroded or drowned (Couvillion et al., 2017).

15.7.4 Other Greenhouse Gases: CH₄ and N₂O

The bulk of data on CH₄ and N₂O fluxes in tidal wetlands is modeled from pore-water measurements in profile or from atmospheric chamber measurements under static conditions. However, these methods generate an incomplete picture of these dynamic environments and fluid boundaries. The growing network of eddy covariance and other continuous data-rich approaches (“movies” instead of “snapshots”) is improving the understanding of the episodic nature of these processes and emergent thresholds of concern. Nitrous oxide fluxes likely are heightened under enhanced nitrate runoff (i.e., “nitrate saturation”; Firestone and Davidson 1989), but documentation is poor. Further, CH₄ production is likely low when sulfate is available (Poffenbarger et al., 2011), but it is enhanced by increased carbon fixation, such as through global changes that include rising atmospheric CO₂ concentrations or invasions of more productive species (e.g., *Phragmites australis*; Martin and Moseman-Valtierra 2015; Mueller et al., 2016).

Estuarine CH₄ emissions currently appear to be a small fraction of global emissions (i.e., <1%; Borges and Abril 2011), but they may be poised to increase with enhanced rates of methanogenesis in response to organic matter inputs and hypoxia expansion under future conditions (Gelesh et al., 2016). A seaward decrease in near-surface porewater concentrations of CH₄ is observed often, likely due to both increasing sulfate availability and *in situ* water column oxidation. Water column CH₄ and *p*CO₂ are positively correlated in well-mixed estuaries, suggesting *in situ* production from organic matter transferred from surface waters to methane-producing bottom waters (Borges and Abril 2011). Like tidal wetlands, many estimates of emission rates are

modeled from profiles of surface and porewater concentrations of CH₄, but continuous sampling and eddy covariance data likely will reduce uncertainty in emissions and allow better characterization of the physical and biogeochemical processes associated with atmospheric CH₄ emissions.

15.7.5 Regional Gaps

Much assessment has been focused on estuaries along different regions of the Atlantic Coast (e.g., GOM, MAB, and SAB), but modeled carbon fluxes for large estuaries still remain poorly constrained. For example, few measurements of air-water CO₂ flux are available for upscaling within the Chesapeake Bay, the largest East Coast estuary (e.g., Cai et al., 2017).

The Gulf of Mexico also is well studied, but it has surprisingly few gas flux measurements in its tidal wetlands and estuaries (see, however, Holm et al., 2016). One of the most extensive regional monitoring programs, Louisiana’s Coastwide Reference Monitoring System (CRMS 2017), supports GMx soil and vegetation stock change assessments and predictive models through annual records of tidal wetland conditions. These data also help illustrate the wide within-watershed variability in conditions, such as land subsidence (Jankowski et al., 2017), that drive organic carbon accretion, erosion, and mineralization processes. In addition, the Texas Commission on Environmental Quality (TCEQ) has been maintaining quarterly measurements of total alkalinity and pH in all coastal estuaries across the state in the northwestern GMx since 1969 (TCEQ 2017). This dataset may offer insight on multidecadal changes in CO₂ flux that await further investigation.

In contrast, Pacific Coast estuaries lack published carbon cycle measurements with sufficient resolution and duration to afford insight into short- or long-term changes associated with climate or human-caused forcing. Observation and modeling gaps are notably large in the Gulf of Alaska and Central American isthmus regions. For instance, very few studies have addressed CO₂ cycling and air-sea



exchange in lagoons (Ávila-López et al., 2017), a dominant habitat type in the tropical Pacific and the Gulf of California in Mexico. Estimates of air-sea exchange of climate-reactive gases (e.g., CO₂, CH₄, and N₂O) in open waters of Pacific Coast estuaries, along with estimates of primary production and carbon burial, are insufficient for a systematic analysis.

Finally, high-latitude estuaries are experiencing rapid shifts in salinity and seasonality, making relationships between climatic drivers difficult to assess. Some clear data needs for a monitoring framework in Arctic systems include depths of coastal peats along rivers, the sensitivity of productivity to rising temperatures and longer growing seasons, terrestrial carbon fluxes (including DOC and DIC), and the long-term prognosis for coastal erosion rates due to relative sea level rise.

Carbon stock and flux data from Pacific Islands, Puerto Rico, and Hawai'i are not included in this chapter because of their limited datasets (Fagan and MacKenzie 2007; MacKenzie et al., 2012) and the inability to extrapolate their data in space and time. Emerging carbon assessments may be useful for upscaling (Selmants et al., 2017), but the necessary measurements are lacking to estimate carbon

fluxes of similar confidence as reported herein for continental coastlines. Hence, there is a clear need for studies of carbon cycling in the coastal environments of Pacific Islands, Puerto Rico, and Hawai'i.

15.7.6 Outlook and Conclusion

Current outlooks and understanding of tidal wetland and estuarine carbon cycling are represented herein, recognizing that synthetic and novel research activities are ongoing. The current state of knowledge represented is sufficient to identify predictable processes and responses, but uncertainty in modeling is higher when applied at continental scales and across datasets of varied confidence. Whereas coastal habitats have distinct responses to myriad global changes, regional and temporal drivers of carbon exchanges and internal processing remain critical knowledge gaps. Monitoring advances, such as high-frequency field data, remotely sensed imagery, and data integration platforms, may shed light on the carbon dynamics at the land-ocean margin and provide the clarity needed to close continental-scale carbon budgets. Improved confidence in projected changes of coastal carbon storage and processing is needed for contributing to more effective policy and management decisions in coastal communities and nationally within North America.



SUPPORTING EVIDENCE

KEY FINDING 1

The top 1 m of tidal wetland soils and estuarine sediments of North America contains $1,886 \pm 1,046$ teragrams of carbon (Tg C) (*high confidence, very likely*).

Description of evidence base

Several sources were available to verify the extent of intertidal wetland and subtidal habitats in North America for Key Finding 1. First, the U.S. Fish and Wildlife Service National Wetlands Inventory (USFWS NWI 2017) is a conservative but definitive source due to inclusion of tidal modifiers to clarify hydrology. Second, a synthesis of Mexican, Canadian, and U.S. saline coastal habitats was provided by the Commission for Environmental Cooperation (CEC 2016). For carbon density in intertidal wetland environments, a synthesis of datasets from tidal wetland habitats reviewed (Chmura et al., 2003; Ouyang and Lee 2014; Holmquist et al., 2018a) found a very narrow distribution measured in kilograms (kg; 27.0 ± 13.0 kg C per m^3) in wetland carbon stocks across North American tidal wetlands, regardless of salinity or vegetation type, as did a national dataset review (28.0 ± 7.8 ; Nahlik and Fennessy 2016). A global synthesis (Sanderman et al., 2018) provided data to synthesize a new estimate for Mexico's mangroves (31.8 ± 1.3 kg C per m^3). For carbon stocks in seagrass environments, synthetic data from literature reviews reporting bulk density and organic carbon along 1-m profiles were used for coast-specific estimates: 2.0 ± 1.3 for the Atlantic Coast, 3.1 ± 2.4 for the Gulf of Mexico coast, 1.4 ± 1.2 for the Pacific Coast, and 2.0 for boreal and Arctic regions. For carbon density in estuarine open-water sediments, coastal regions played no clear role and geomorphic settings were not available (Smith et al., 2015), so a mean of 1.0 kg per m^3 was chosen, using a literature-based average for total organic carbon (TOC) content (0.4% organic carbon; range 0.17% to 2%; Premuzic et al., 1982; Kennedy et al., 2010) coupled with a literature average of percentage of dry bulk densities (2.6 g C per cm^3 ; Muller and Suess 1979).

Major uncertainties

Uncertainties vary for each subhabitat, and these data likely represent an underestimate of total stocks, which may be many meters deep. For tidal wetland soils to 1 m in depth, the primary uncertainty is in underestimates of mapped boundaries, with, for example, no accounting of freshwater tidal systems in either Mexico or Canada, and likely undercounting of freshwater tidal wetlands in the United States. For seagrass, the spatial data are conservative estimates of located and documented habitat, although seagrass populations can shift boundaries rapidly and potentially there are far more currently unmapped seagrass beds in North America. For estuarine spatial data, the boundaries are constrained by bathymetry maps, which generally are more uncertain in higher latitudes. In contrast, carbon densities have narrow ranges in tidal wetland and estuarine soils but a skewed representation in seagrass soils, a difference which may be due to limited sampling in northern latitudes.

Assessment of confidence based on evidence and agreement, including short description of nature of evidence and level of agreement

There is theoretical and empirical convergence on tidal marsh carbon densities but a likely bias to underrepresenting tidal freshwater habitats. Further, seagrass carbon densities show a wider range and an apparent latitudinal gradient of decreasing carbon density from tropical to temperate



environments. Geomorphic variability (e.g., shallow waters versus fjords) in estuarine sediments may reduce uncertainty in stock assessments, but map layers are not available for North America.

Estimated likelihood of impact or consequence, including short description of basis of estimate

The likely impact of information is high because it has not been synthesized previously at the continental scale.

Summary sentence or paragraph that integrates the above information

For Key Finding 1, although sediment carbon densities in tidal wetlands are high with a narrow range and carbon densities in subtidal habitats are substantially lower with a wider range, there are still underrepresented samples from high-latitude regions, especially tidal forested wetlands and subtidal seagrasses. Further, the data reported thus far are limited to documented tidal habitats, although there is an appreciation that large areas are likely missing for freshwater tidal marsh and for seagrass extent.

KEY FINDING 2

Soil carbon accumulation rate (i.e., sediment burial) in North American tidal wetlands is currently 9 ± 5 Tg C per year (*high confidence, likely*), and estuarine carbon burial is 5 ± 3 Tg C per year (*low confidence, likely*).

Description of evidence base

Carbon burial, which accounts for all carbon accumulated in coastal sediments over an annual time period, has been documented for Key Finding 2, with geological approaches in multiple studies. Accumulation of carbon stock over a period of time using a marker horizon is relevant to specific periods of time by the method used (e.g., recent years, marker horizons, and radioisotope tracers of different decay rates). The data reported here refer to isotopes of cesium (^{137}Cs) and lead (^{210}Pb) dates alone, thus representing long-term average annual accretion rates for the past 50 years (since 1963). Rates of burial (Ouyang and Lee 2014; $n = 125$ samples) provide a range for comparison with other reviews that do account for mangrove subhabitats. No significant differences in carbon burial are detected for habitat types by salinity or vegetation type when comparing with Chmura et al. (2003) or with Breithaupt et al. (2014). Estuarine carbon burial is estimated for CONUS using the model of Herrmann et al. (2015) and scaled to all of North America using estimates of estuarine area.

Major uncertainties

Carbon burial rate is a bulk measure of multiple processes, both old and new carbon inputs as well as both autochthonous and allochthonous sources. As such, carbon burial through those processes has varied drivers, with different dominating processes across the landscape. Overestimation is possible when accretion of mineral sediment brings lower carbon densities than equilibrium conditions. Underestimates are possible when accretion is reported at historic rates and not adjusted for current rates of sea level rise. Mapped areas are a likely underestimate because they do not include freshwater tidal marshes in Canada or Alaska. Further, high uncertainties are associated with wide ranges of rates through different dating approaches. Estuarine carbon burial rate uncertainties stem from errors in the model of Herrmann et al. (2015) and, more



importantly, the scaling of CONUS results to all of North America. Particularly problematic is the lack of rigorous mapping of estuarine extent outside of CONUS.

Assessment of confidence based on evidence and agreement, including short description of nature of evidence and level of agreement

Because mapping limitations and 50-year averages of tidal wetland carbon accumulation are inferred rather than being the current rates under accelerated sea level rise, these estimates likely are lower than the actual rates of burial. Thus, while these data represent measured rates, this analysis relies on a fairly small range of locations and a small subset of available published data. Estuarine burial rates are not confident because Canada and Mexico have limited data applicable to the modeling strategy of Herrmann et al. (2015).

Estimated likelihood of impact or consequence, including short description of basis of estimate

The likely impact of the information on tidal wetland and estuarine burial is high, as it has not yet been synthesized at the continental scale.

Summary sentence or paragraph that integrates the above information

For Key Finding 2, burial of carbon sourced from within wetlands and from terrestrial sources is similar among regions and wetland types, driven primarily by accretion rates, which are tied to geomorphic feedbacks with sea level rise. Burial of carbon in estuaries is linked most closely to residence time and total nitrogen input.

KEY FINDING 3

The lateral flux of carbon from tidal wetlands to estuaries is 16 ± 10 Tg C per year for North America (*low confidence, likely*).

Description of evidence base

In Key Finding 3, 16 studies were conducted to quantify the lateral flux of organic carbon (12 studies) and inorganic carbon (4 studies) from tidal wetlands to estuaries at individual locations. The organic carbon flux studies are summarized in Herrmann et al. (2015) and the inorganic carbon flux studies are summarized in Najjar et al. (2018). These studies were scaled to all of North America using estimates of tidal wetland area.

Major uncertainties

The major uncertainty in this Key Finding is the limited spatial and temporal extents of the 16 individual flux measurements. Tidal wetlands are highly heterogeneous and vary in their processing of carbon on a wide variety of timescales. Hence, tidal wetlands are likely to have been undersampled in terms of lateral exchanges. However, tidal wetlands consistently export carbon and the range of estimates is less than an order of magnitude.

Assessment of confidence based on evidence and agreement, including short description of nature of evidence and level of agreement

The low confidence is due to the limited number of measurements and time periods. There is appreciation, however, that at a continental scale, there is a strong likelihood that tidal wetlands export carbon to estuaries, although the magnitude of the flux is highly uncertain.



Estimated likelihood of impact or consequence, including short description of basis of estimate

This flux represents 60% (best estimate) of the net uptake of atmospheric carbon by tidal wetlands. Per knowledge gained, this is the first such estimate for North America.

Summary sentence or paragraph that integrates the above information

For Key Finding 3, there is enough information to make a first-order estimate of the flux of carbon from tidal wetlands to estuaries for North America as a whole, and there is high confidence in the order of magnitude of the flux. The high heterogeneity of tidal wetland systems and limited field data prevent a more accurate estimate of the flux.

KEY FINDING 4

In North America, tidal wetlands remove 27 ± 13 Tg C per year from the atmosphere, estuaries outgas 10 ± 10 Tg C per year to the atmosphere, and the net uptake by the combined wetland-estuary system is 17 ± 16 Tg C per year (*low confidence, likely*).

Description of evidence base

The uptake of atmospheric carbon dioxide (CO₂) by tidal wetlands is assessed for Key Finding 4 by net ecosystem exchange (NEE) estimates from eddy covariance measurements. It is similar to an alternative estimate of uptake that assumes uptake as the sum of burial (8 Tg C) and lateral export (16 Tg C). Burial and lateral exports are discussed in the supporting evidence for Key Findings 2 and 3. Estuarine outgassing is based on studies of individual estuary summaries (Chen et al., 2013) and estuarine areas (Laruelle et al., 2013). The flux of the combined system is a simple sum of the fluxes from tidal wetlands and estuaries and compounded error.

Major uncertainties

The major uncertainties in this Key Finding are the limited spatial and temporal extents of tidal wetland atmospheric flux measurements, burial, lateral flux, and estuarine outgassing measurements. Estuarine outgassing uncertainties also stem from the low spatial resolution of the datasets used to estimate areas.

Assessment of confidence based on evidence and agreement, including short description of nature of evidence and level of agreement

There is low confidence on this calculation at the scale of North America. The low confidence is due to the residual between competing fluxes; on the one hand, there is strong likelihood that tidal wetlands take up CO₂ from the atmosphere and estuaries outgas CO₂ to the atmosphere and, on the other hand, that there is large uncertainty in the magnitude of each, assessments which stem from the high spatial and temporal variability of these systems and the limited field data. The fate of carbon released from tidal wetland degradation remains unknown.

Estimated likelihood of impact or consequence, including short description of basis of estimate

These are not major fluxes in the carbon budget of North America, but they are regionally important. Accounting for current knowledge, such estimates are the first for North America.



Summary sentence or paragraph that integrates the above information

For Key Finding 4, there is enough information to make first-order estimates of the exchange of atmospheric CO₂ with tidal wetlands and estuaries for North America as a whole. The high heterogeneity of these systems and limited field data prevent a more accurate estimate of the flux.

KEY FINDING 5

Research and modeling needs are greatest for understanding responses to accelerated sea level rise; mapping tidal wetland and estuarine extent; and quantifying carbon dioxide and methane exchange with the atmosphere, especially in large, undersampled, and rapidly changing regions (*high confidence, likely*).

Description of evidence base

Tidal wetland and estuarine area are first-order drivers of the spatially integrated flux (e.g., in units of Tg C per year) of all carbon fluxes in these ecosystems. The lack of an accurate quantification of tidal wetland and estuarine area, particularly in Canada and Mexico, is thus a major gap in understanding the role of tidal wetlands and estuaries in the carbon cycling of North America. Carbon cycle research is largely motivated by the impact of greenhouse gases on climate and how climate change affects fluxes of these gases to the atmosphere from terrestrial and aquatic systems. However, the database of tidal wetland and estuarine CO₂ and CH₄ exchanges with the atmosphere is severely limited. In particular, direct estimates of these fluxes are rare. Furthermore, some of the most poorly sampled regions are those that are changing the most rapidly (e.g., the Arctic).

Major uncertainties

There are few uncertainties in Key Finding 5 because there is a clear lack of data on extent and atmospheric exchange.

Assessment of confidence based on evidence and agreement, including short description of nature of evidence and level of agreement

Confidence is high in Key Finding 5 because systematic studies (with error estimates) of tidal wetlands and estuaries are extremely limited. Very few direct estimates of exchanges of atmospheric CO₂ and CH₄ with tidal wetlands and estuaries exist. While research needs are present in other aspects of the tidal wetland and estuarine carbon cycling, these needs are unlikely to be more pressing than the needs for quantifying area and gas exchange with the atmosphere.

Estimated likelihood of impact or consequence, including short description of basis of estimate

Key Finding 5 is not an estimate but a recommendation. It could impact future research on tidal wetland and estuarine carbon cycling in North America.

Summary sentence or paragraph that integrates the above information

Key Finding 5 synthesizes the existing research on tidal wetland and estuarine carbon cycling in North America, providing a future direction for research in this area.



REFERENCES

- Adame, M. F., J. B. Kauffman, I. Medina, J. N. Gamboa, O. Torres, J. P. Caamal, M. Reza, and J. A. Herrera-Silveira, 2013: Carbon stocks of tropical coastal wetlands within the karstic landscape of the Mexican Caribbean. *PLOS One*, **8**(2), e56569, doi: 10.1371/journal.pone.0056569.
- Alin, S., R. Brainard, N. Price, J. Newton, A. Cohen, W. Peterson, E. DeCarlo, E. Shadwick, S. Noakes, and N. Bednaršek, 2015: Characterizing the natural system: Toward sustained, integrated coastal ocean acidification observing networks to facilitate resource management and decision support. *Oceanography*, **25**(2), 92-107, doi: 10.5670/oceanog.2015.34.
- AMAP, 2011: *Snow, Water, Ice and Permafrost in the Arctic (SWIPA)*. Climate change and the cryosphere, Arctic Monitoring and Assessment Programme, 538 pp.
- Artigas, F., J. Y. Shin, C. Hobbie, A. Marti-Donati, K. V. R. Schäfer, and I. Pechmann, 2015: Long term carbon storage potential and CO₂ sink strength of a restored salt marsh in New Jersey. *Agricultural and Forest Meteorology*, **200**, 313-321, doi: 10.1016/j.agrformet.2014.09.012.
- Ávila-López, M. C., J. M. Hernández-Ayón, V. F. Camacho-Ibar, A. F. Bermúdez, A. Mejía-Trejo, I. Pacheco-Ruiz, and J. M. Sandoval-Gil, 2017: Air-water CO₂ fluxes and net ecosystem production changes in a Baja California coastal lagoon during the anomalous North Pacific warm condition. *Estuaries and Coasts*, **40**(3), 792-806, doi: 10.1007/s12237-016-0178-x.
- Azevedo, I. C., A. A. Bordalo, and P. Duarte, 2014: Influence of freshwater inflow variability on the Douro Estuary primary productivity: A modelling study. *Ecological Modelling*, **272**, 1-15, doi: 10.1016/j.ecolmodel.2013.09.010.
- Barr, J. G., V. Engel, J. D. Fuentes, J. C. Zieman, T. L. O'Halloran, T. J. Smith, and G. H. Anderson, 2010: Controls on mangrove forest-atmosphere carbon dioxide exchanges in western Everglades National Park. *Journal of Geophysical Research: Biogeosciences*, **115**(G2), doi: 10.1029/2009JG001186.
- Barr, J. G., V. Engel, T. J. Smith, and J. D. Fuentes, 2012: Hurricane disturbance and recovery of energy balance, CO₂ fluxes and canopy structure in a mangrove forest of the Florida Everglades. *Agricultural and Forest Meteorology*, **153**, 54-66, doi: 10.1016/j.agrformet.2011.07.022.
- Bartlett, K. B., D. S. Bartlett, R. C. Harriss, and D. I. Sebacher, 1987: Methane emissions along a salt marsh salinity gradient. *Biogeochemistry*, **4**(3), 183-202, doi: 10.1007/bf02187365.
- Bartlett, K. B., R. C. Harriss, and D. I. Sebacher, 1985: Methane flux from coastal salt marshes. *Journal of Geophysical Research: Atmospheres*, **90**(D3), 5710-5720, doi: 10.1029/JD090iD03p05710.
- Bauer, J. E., W. J. Cai, P. A. Raymond, T. S. Bianchi, C. S. Hopkinson, and P. A. Regnier, 2013: The changing carbon cycle of the coastal ocean. *Nature*, **504**(7478), 61-70, doi: 10.1038/nature12857.
- Baumann, H., R. B. Wallace, T. Tagliaferri, and C. J. Gobler, 2015: Large natural pH, CO₂ and O₂ fluctuations in a temperate tidal salt marsh on diel, seasonal, and interannual time scales. *Estuaries and Coasts*, **38**(1), 220-231, doi: 10.1007/s12237-014-9800-y.
- Bednarsek, N., R. A. Feely, N. Tolimieri, A. J. Hermann, S. A. Siedlecki, G. G. Waldbusser, P. McElhany, S. R. Alin, T. Klinger, B. Moore-Maley, and H. O. Portner, 2017: Exposure history determines pteropod vulnerability to ocean acidification along the U.S. west coast. *Scientific Reports*, **7**(1), 4526, doi: 10.1038/s41598-017-03934-z.
- Benway, H., S. Alin, E. Boyer, W.-J. Cai, P. Coble, J. Cross, M. Friedrichs, M. Goñi, P. Griffith, M. Herrmann, S. Lohrenz, J. Mathis, G. McKinley, R. Najjar, C. Pilskaln, S. Siedlecki, and R. L. Smith, 2016: *A Science Plan for Carbon Cycle Research in North American Coastal Waters. Report of the Coastal Carbon Synthesis (CCARS) Community Workshop, August 19-21, 2014*. Ocean Carbon and Biogeochemistry Program and North American Carbon Program, 84 pp. [<https://www.us-ocb.org/coastal-carbon-synthesis-ccars/>]
- Bergamaschi, B. A., R. A. Smith, M. J. Sauer, and J. S. Shih, 2012: Terrestrial fluxes of sediments and nutrients to Pacific coastal waters and their effects on coastal carbon storage rates. In: *Baseline and Projected Future Carbon Storage and Greenhouse-Gas Fluxes in Ecosystems of the Western United States*. [Z. Zhu and B. Reed (eds.)]. U.S. Department of the Interior. U.S. Geological Survey Professional Paper 1797, 143-158 pp. [<https://pubs.usgs.gov/pp/1797/>]
- Bergamaschi, B., and L. Windham-Myers, 2018: Published data. AmeriFlux US-Srr Suisun marsh - Rush Ranch. doi: 10.17190/AMF/1418685.
- Bhatt, U. S., D. A. Walker, M. K. Reynolds, J. C. Comiso, H. E. Epstein, G. Jia, R. Gens, J. E. Pinzon, C. J. Tucker, C. E. Tweedie, and P. J. Webber, 2010: Circumpolar Arctic tundra vegetation change is linked to sea ice decline. *Earth Interactions*, **14**(8), 1-20, doi: 10.1175/2010ei315.1.
- Bianchi, T. S., 2006: *Biogeochemistry of Estuaries*. Oxford University Press, 720 pp.
- Bianchi, T. S., and M. A. Allison, 2009: Large-river delta-front estuaries as natural "recorders" of global environmental change. *Proceedings of the National Academy of Sciences USA*, **106**(20), 8085-8092, doi: 10.1073/pnas.0812878106.
- Bianchi, T. S., M. A. Allison, J. Zhao, X. Li, R. S. Comeaux, R. A. Feagin, and R. W. Kulawardhana, 2013: Historical reconstruction of mangrove expansion in the Gulf of Mexico: Linking climate change with carbon sequestration in coastal wetlands. *Estuarine, Coastal and Shelf Science*, **119**, 7-16, doi: 10.1016/j.eccs.2012.12.007.



- Borges, A. V., 2005: Do we have enough pieces of the jigsaw to integrate CO₂ fluxes in the coastal ocean? *Estuaries*, **28**(1), 3-27, doi: 10.1007/bf02732750.
- Borges, A. V., and G. Abril, 2011: Carbon dioxide and methane dynamics in estuaries. In: *Treatise on Estuarine and Coastal Science*. [E. Wolanski and D. McLusky (eds.)]. Academic Press, 119-161 pp.
- Borges, A. V., and N. Gypens, 2010: Carbonate chemistry in the coastal zone responds more strongly to eutrophication than ocean acidification. *Limnology and Oceanography*, **55**(1), 346-353, doi: 10.4319/lo.2010.55.1.0346.
- Borges, A. V., B. Delille, and M. Frankignoulle, 2005: Budgeting sinks and sources of CO₂ in the coastal ocean: Diversity of ecosystems counts. *Geophysical Research Letters*, **32**(14), doi: 10.1029/2005gl023053.
- Boyer, E. W., R. W. Howarth, J. N. Galloway, F. J. Dentener, P. A. Green, and C. J. Vörösmarty, 2006: Riverine nitrogen export from the continents to the coasts. *Global Biogeochemical Cycles*, **20**(1), doi: 10.1029/2005gb002537.
- Breithaupt, J. L., J. M. Smoak, T. J. Smith, and C. J. Sanders, 2014: Temporal variability of carbon and nutrient burial, sediment accretion, and mass accumulation over the past century in a carbonate platform mangrove forest of the Florida Everglades. *Journal of Geophysical Research: Biogeosciences*, **119**(10), 2032-2048, doi: 10.1002/2014jg002715.
- Bricker, S., B. Longstaff, W. Dennison, A. Jones, K. Boicourt, C. Wicks, and J. Woerner, 2007: *Effects of Nutrient Enrichment in the Nation's Estuaries: A Decade of Change. National Estuarine Eutrophication Assessment Update*. NOAA's National Centers for Coastal Ocean Science, 328 pp. [[https://yosemite.epa.gov/oa/EAB_Web_Docket.nsf/\(Filings\)/3BE82A42C7ED8C3585257B-120059CB8A/\\$File/Opposition%20to%20Petition%20for%20Review%20-%20Ex.%2010%20Part1...23.53.pdf](https://yosemite.epa.gov/oa/EAB_Web_Docket.nsf/(Filings)/3BE82A42C7ED8C3585257B-120059CB8A/$File/Opposition%20to%20Petition%20for%20Review%20-%20Ex.%2010%20Part1...23.53.pdf)]
- Bridgman, S. D., J. P. Megonigal, J. K. Keller, N. B. Bliss, and C. Trettin, 2006: The carbon balance of North American wetlands. *Wetlands*, **26**(4), 889-916, doi: 10.1672/0277-5212(2006)26[889:tcbona]2.0.co;2.
- Brown, S. C., 2006: *Arctic Wings: Birds of the Arctic National Wildlife Refuge*. Mountaineers Books. Seattle, WA.
- Caffrey, J. M., 2004: Factors controlling net ecosystem metabolism in U.S. estuaries. *Estuaries*, **27**(1), 90-101, doi: 10.1007/bf02803563.
- Cahoon, D. R., 2006: A review of major storm impacts on coastal wetland elevations. *Estuaries and Coasts*, **29**(6), 889-898, doi: 10.1007/bf02798648.
- Cai, W. J., 2011: Estuarine and coastal ocean carbon paradox: CO₂ sinks or sites of terrestrial carbon incineration? *Annual Review of Marine Science*, **3**, 123-145, doi: 10.1146/annurev-marine-120709-142723.
- Cai, W. J., and Y. Wang, 1998: The chemistry, fluxes, and sources of carbon dioxide in the estuarine waters of the Satilla and Altamaha Rivers, Georgia. *Limnology and Oceanography*, **43**(4), 657-668, doi: 10.4319/lo.1998.43.4.0657.
- Cai, W. J., W. J. Huang, G. W. Luther, 3rd, D. Pierrot, M. Li, J. Testa, M. Xue, A. Joesoef, R. Mann, J. Brodeur, Y. Y. Xu, B. Chen, N. Hussain, G. G. Waldbusser, J. Cornwell, and W. M. Kemp, 2017: Redox reactions and weak buffering capacity lead to acidification in the Chesapeake Bay. *Nature Communications*, **8**(1), 369, doi: 10.1038/s41467-017-00417-7.
- Cai, W.-J., X. Hu, W.-J. Huang, M. C. Murrell, J. C. Lehrter, S. E. Lohrenz, W.-C. Chou, W. Zhai, J. T. Hollibaugh, Y. Wang, P. Zhao, X. Guo, K. Gundersen, M. Dai, and G.-C. Gong, 2011: Acidification of subsurface coastal waters enhanced by eutrophication. *Nature Geoscience*, **4**(11), 766-770, doi: 10.1038/ngeo1297.
- Callaway, J. C., E. L. Borgnis, R. E. Turner, and C. S. Milan, 2012: Carbon sequestration and sediment accretion in San Francisco Bay tidal wetlands. *Estuaries and Coasts*, **35**(5), 1163-1181, doi: 10.1007/s12237-012-9508-9.
- Camacho-Ibar, V. F., J. D. Carriquiry, and S. V. Smith, 2003: Non-conservative P and N fluxes and net ecosystem production in San Quintin Bay, México. *Estuaries*, **26**(5), 1220-1237, doi: 10.1007/bf02803626.
- Canuel, E. A., S. S. Cammer, H. A. McIntosh, and C. R. Pondell, 2012: Climate change impacts on the organic carbon cycle at the land-ocean interface. *Annual Review of Earth and Planetary Sciences*, **40**(1), 685-711, doi: 10.1146/annurev-earth-042711-105511.
- Cavanaugh, K. C., J. R. Kellner, A. J. Forde, D. S. Gruner, J. D. Parker, W. Rodriguez, and I. C. Feller, 2014: Poleward expansion of mangroves is a threshold response to decreased frequency of extreme cold events. *Proceedings of the National Academy of Sciences USA*, **111**(2), 723-727, doi: 10.1073/pnas.1315800111.
- CCSP, 2007: *First State of the Carbon Cycle Report (SOCCR): The North American Carbon Budget and Implications for the Global Carbon Cycle. A Report by the U.S. Climate Change Science Program and the Subcommittee on Global Change Research*. [A. W. King, L. Dilling, G. P. Zimmerman, D. M. Fairman, R. A. Houghton, G. Marland, A. Z. Rose, and T. J. Wilbanks (eds.)]. National Oceanic and Atmospheric Administration, National Climatic Data Center, Asheville, NC, USA, 242 pp.
- CEC, 2016: *North American Blue Carbon, 2015 Map Files*. Commission for Environmental Cooperation. [<http://www.cec.org/tools-and-resources/map-files/north-american-blue-carbon-2017>]



- CEC, 2017: *Seagrass Sediment Sampling Protocol and Field Study Montreal, Canada*. Commission for Environmental Cooperation, 48 pp.
- Chan, F., A. B. Boehm, J. A. Barth, E. A. Chornesky, A. G. Dickson, R. A. Feely, B. Hales, T. M. Hill, G. Hofmann, D. Ianson, T. Klinger, J. Largier, J. Newton, T. F. Pedersen, G. N. Somero, M. Sutula, W. W. Wakefield, G. G. Waldbusser, S. B. Weisberg, and E. A. Whiteman, 2016: *The West Coast Ocean Acidification and Hypoxia Science Panel: Major Findings, Recommendations, and Actions*. California Ocean Science Trust. [<http://westcoastoah.org/wp-content/uploads/2016/04/OAH-Panel-Key-Findings-Recommendations-and-Actions-4.4.16-FINAL.pdf>]
- Chan, F., J. A. Barth, C. A. Blanchette, R. H. Byrne, F. Chavez, O. Cheriton, R. A. Feely, G. Friederich, B. Gaylord, T. Gouhier, S. Hacker, T. Hill, G. Hofmann, M. A. McManus, B. A. Menge, K. J. Nielsen, A. Russell, E. Sanford, J. Sevdjian, and L. Washburn, 2017: Persistent spatial structuring of coastal ocean acidification in the California current system. *Scientific Reports*, **7**(1), 2526, doi: 10.1038/s41598-017-02777-y.
- Chen, C. T. A., T. H. Huang, Y. C. Chen, Y. Bai, X. He, and Y. Kang, 2013: Air-sea exchanges of CO₂ in the world's coastal seas. *Biogeosciences*, **10**(10), 6509-6544, doi: 10.5194/bg-10-6509-2013.
- Chen, C., H. Liu, and R. C. Beardsley, 2003: An unstructured grid, finite-volume, three-dimensional, primitive equations ocean model: Application to coastal ocean and estuaries. *Journal of Atmospheric and Oceanic Technology*, **20**(1), 159-186, doi: 10.1175/1520-0426(2003)020<0159:augfvt>2.0.co;2.
- Chmura, G. L., 2013: What do we need to assess the sustainability of the tidal salt marsh carbon sink? *Ocean and Coastal Management*, **83**, 25-31, doi: 10.1016/j.ocecoaman.2011.09.006.
- Chmura, G. L., L. Kellman, L. van Ardenne, and G. R. Guntenspergen, 2016: Greenhouse gas fluxes from salt marshes exposed to chronic nutrient enrichment. *PLOS One*, **11**(2), e0149937, doi: 10.1371/journal.pone.0149937.
- Chmura, G. L., S. C. Anisfeld, D. R. Cahoon, and J. C. Lynch, 2003: Global carbon sequestration in tidal, saline wetland soils. *Global Biogeochemical Cycles*, **17**(4), doi: 10.1029/2002gb001917.
- Cloern, J. E., S. Q. Foster, and A. E. Kleckner, 2014: Phytoplankton primary production in the world's estuarine-coastal ecosystems. *Biogeosciences*, **11**(9), 2477-2501, doi: 10.5194/bg-11-2477-2014.
- Cloern, J., A. Robinson, L. Grenier, R. Grossinger, K. Boyer, J. Burau, E. Canuel, J. DeGeorge, J. Drexler, C. Enright, E. Howe, R. Kneib, A. Mueller-Solger, R. Naiman, J. Pinckney, S. Safran, D. Schoellhamer, and C. Simenstad, 2016: Primary production in the Delta: Then and now. *San Francisco Estuary and Watershed Science*, **14**(3), doi: 10.15447/sfews.2016v14iss3art1.
- Colman, S. M., P. C. Baucom, J. F. Bratton, T. M. Cronin, J. P. McGeehin, D. Willard, A. R. Zimmerman, and P. R. Vogt, 2002: Radiocarbon dating, chronologic framework, and changes in accumulation rates of Holocene estuarine sediments from Chesapeake Bay. *Quaternary Research*, **57**(1), 58-70, doi: 10.1006/qres.2001.2285.
- Contreras-Espinosa, F., and B. G. Warner, 2004: Ecosystem characteristics and management considerations for coastal wetlands in Mexico. *Hydrobiologia*, **511**(1), 233-245, doi: 10.1023/b:hydr.0000014097.74263.54.
- Cooley, S., E. Jewett, J. Reichert, L. Robbins, G. Shrestha, D. Wiczorek, and S. Weisberg, 2015: Getting ocean acidification on decision makers' to-do lists: Dissecting the process through case studies. *Oceanography*, **25**(2), 198-211, doi: 10.5670/oceanog.2015.42.
- Couvillion, B. R., H. Beck, D. Schoolmaster, and M. Fischer, 2017: Land area change in coastal Louisiana (1932 to 2016). *Scientific Investigations Map 3381*, doi: 10.3133/sim3381. [<http://pubs.er.usgs.gov/publication/sim3381>]
- CRMS, 2017: *Louisiana Coastwide Reference Monitoring System*. [<https://www.lacoast.gov/crms2/home.aspx>]
- Crosswell, J. R., I. C. Anderson, J. W. Stanhope, B. Van Dam, M. J. Brush, S. Ensign, M. F. Piehler, B. McKee, M. Bost, and H. W. Paerl, 2017: Carbon budget of a shallow, lagoonal estuary: Transformations and source-sink dynamics along the river-estuary-ocean continuum. *Limnology and Oceanography*, **62**(5), S29-S45, doi: 10.1002/lno.10631.
- Crosswell, J. R., M. S. Wetz, B. Hales, and H. W. Paerl, 2012: Air-water CO₂ fluxes in the microtidal Neuse River Estuary, North Carolina. *Journal of Geophysical Research: Oceans*, **117**, C08017, doi: 10.1029/2012jc007925.
- Crosswell, J. R., M. S. Wetz, B. Hales, and H. W. Paerl, 2014: Extensive CO₂ emissions from shallow coastal waters during passage of Hurricane Irene (August 2011) over the Mid-Atlantic coast of the U.S.A. *Limnology and Oceanography*, **59**(5), 1651-1665, doi: 10.4319/lno.2014.59.5.1651.
- Dahl, T. E. 2011: *Status and Trends of Wetlands in the Conterminous United States 2004 to 2009*. U.S. Department of the Interior; Fish and Wildlife Service, Washington, D.C. 108 pp.
- Dalrymple, R. W., B. A. Zaitlin, and R. Boyd, 1992: Estuarine facies models; conceptual basis and stratigraphic implications. *Journal of Sedimentary Research*, **62**(6), 1130-1146, doi: 10.1306/d4267a69-2b26-11d7-8648000102c1865d.
- Davidson, C. W., 2015: *Spatial and Temporal Variability of Coastal Carbonate Chemistry in the Southern California Region*. M.S. Thesis, Earth Sciences, University of California San Diego, 37 pp.



- Davis, K. A., N. S. Banas, S. N. Giddings, S. A. Siedlecki, P. MacCready, E. J. Lessard, R. M. Kudela, and B. M. Hickey, 2014: Estuary-enhanced upwelling of marine nutrients fuels coastal productivity in the U.S. Pacific Northwest. *Journal of Geophysical Research: Oceans*, **119**(12), 8778-8799, doi: 10.1002/2014jc010248.
- Day, J., W. Kemp, A. Yanez-Arancibia, and B. C. Crump, 2013: *Estuarine Ecology, 2nd edition*. Wiley-Blackwell 568 pp.
- de Angelis, M. A., and M. I. Scranton, 1993: Fate of methane in the Hudson River and Estuary. *Global Biogeochemical Cycles*, **7**(3), 509-523, doi: 10.1029/93gb01636.
- DeFries, R., and H. Nagendra, 2017: Ecosystem management as a wicked problem. *Science*, **356**(6335), 265-270, doi: 10.1126/science.aal1950.
- DeLaune, R. D., and J. R. White, 2011: Will coastal wetlands continue to sequester carbon in response to an increase in global sea level?: A case study of the rapidly subsiding Mississippi River Deltaic Plain. *Climatic Change*, **110**(1-2), 297-314, doi: 10.1007/s10584-011-0089-6.
- DeLaune, R. D., C. J. Smith, and W. H. Patrick, 1983: Methane release from Gulf Coast wetlands. *Tellus B*, **35B**(1), 8-15, doi: 10.1111/j.1600-0889.1983.tb00002.x.
- Dessu, S. B., R. M. Price, T. G. Troxler, and J. S. Kominoski, 2018: Effects of sea-level rise and freshwater management on long-term water levels and water quality in the Florida Coastal Everglades. *Journal of Environmental Management*, **211**, 164-176, doi: 10.1016/j.jenvman.2018.01.025.
- Di Lorenzo, E., and N. Mantua, 2016: Multi-year persistence of the 2014/15 North Pacific Marine Heatwave. *Nature Climate Change*, **6**(11), 1042-1047, doi: 10.1038/nclimate3082.
- Doughty, C. L., J. A. Langley, W. S. Walker, I. C. Feller, R. Schaub, and S. K. Chapman, 2015: Mangrove range expansion rapidly increases coastal wetland carbon storage. *Estuaries and Coasts*, **39**(2), 385-396, doi: 10.1007/s12237-015-9993-8.
- Downing, B. D., E. Boss, B. A. Bergamaschi, J. A. Fleck, M. A. Lionberger, N. K. Ganju, D. H. Schoellhamer, and R. Fujii, 2009: Quantifying fluxes and characterizing compositional changes of dissolved organic matter in aquatic systems in situ using combined acoustic and optical measurements. *Limnology and Oceanography: Methods*, **7**(1), 119-131, doi: 10.4319/lom.2009.7.119.
- Drexler, J. Z., C. S. de Fontaine, and T. A. Brown, 2009: Peat accretion histories during the past 6,000 years in marshes of the Sacramento-San Joaquin Delta, CA, USA. *Estuaries and Coasts*, **32**(5), 871-892, doi: 10.1007/s12237-009-9202-8.
- Duarte, C. M., I. E. Hendriks, T. S. Moore, Y. S. Olsen, A. Steckbauer, L. Ramajo, J. Carstensen, J. A. Trotter, and M. McCulloch, 2013: Is ocean acidification an open-ocean syndrome? Understanding anthropogenic impacts on seawater pH. *Estuaries and Coasts*, **36**(2), 221-236, doi: 10.1007/s12237-013-9594-3.
- Duarte, C. M., J. J. Middelburg, and N. Caraco, 2005: Major role of marine vegetation on the oceanic carbon cycle. *Biogeosciences*, **2**(1), 1-8, doi: 10.5194/bg-2-1-2005.
- Duman, T., and K. V. R. Schäfer, 2018: Partitioning net ecosystem carbon exchange of native and invasive plant communities by vegetation cover in an urban tidal wetland in the New Jersey Meadowlands (USA). *Ecological Engineering*, **114**, 16-24, doi: 10.1016/j.ecoleng.2017.08.031.
- Edwards, K. R., and C. E. Proffitt, 2003: Comparison of wetland structural characteristics between created and natural salt marshes in southwest Louisiana, USA. *Wetlands*, **23**(2), 344-356, doi: 10.1672/10-20.
- Ekstrom, J. A., L. Suatoni, S. R. Cooley, L. H. Pendleton, G. G. Waldbusser, J. E. Cinner, J. Ritter, C. Langdon, R. van Hooidonk, D. Gledhill, K. Wellman, M. W. Beck, L. M. Brander, D. Rittschof, C. Doherty, P. E. T. Edwards, and R. Portela, 2015: Vulnerability and adaptation of US shellfisheries to ocean acidification. *Nature Climate Change*, **5**(3), 207-214, doi: 10.1038/nclimate2508.
- Ember, L. M., D. F. Williams, and J. T. Morris, 1987: Processes that influence carbon isotope variations in salt-marsh sediments. *Marine Ecology Progress Series*, **36**(1), 33-42, doi: DOI 10.3354/meps036033.
- Evans, W., B. Hales, P. G. Strutton, and D. Ianson, 2012: Sea-air CO₂ fluxes in the Western Canadian coastal ocean. *Progress in Oceanography*, **101**(1), 78-91, doi: 10.1016/j.pcean.2012.01.003.
- Ezcurra, P., E. Ezcurra, P. P. Garcillan, M. T. Costa, and O. Aburto-Oropeza, 2016: Coastal landforms and accumulation of mangrove peat increase carbon sequestration and storage. *Proceedings of the National Academy of Sciences USA*, **113**(16), 4404-4409, doi: 10.1073/pnas.1519774113.
- Fabry, V., J. McClintock, J. Mathis, and J. Grebeier, 2009: Ocean acidification at high latitudes: The bellwether. *Oceanography*, **22**(4), 160-171, doi: 10.5670/oceanog.2009.105.
- Fagan, K. E., and F. T. Mackenzie, 2007: Air-sea CO₂ exchange in a subtropical estuarine-coral reef system, Kaneohe Bay, Oahu, Hawaii. *Marine Chemistry*, **106**(1-2), 174-191, doi: 10.1016/j.marchem.2007.01.016.
- Fagherazzi, S., G. Mariotti, P. Wiberg, and K. McGlathery, 2013: Marsh collapse does not require sea level rise. *Oceanography*, **26**(3), 70-77, doi: 10.5670/oceanog.2013.47.
- Feely, R. A., S. R. Alin, J. Newton, C. L. Sabine, M. Warner, A. Devol, C. Krembs, and C. Maloy, 2010: The combined effects of ocean acidification, mixing, and respiration on pH and carbonate saturation in an urbanized estuary. *Estuarine, Coastal and Shelf Science*, **88**(4), 442-449, doi: 10.1016/j.jecss.2010.05.004.



- Feely, R. A., T. Klinger, J. A. Newton, and M. Chadsey, 2012: *Scientific Summary of Ocean Acidification in Washington State Marine Waters*. National Oceanic and Atmospheric Administration Oceanic and Atmospheric Research Division Special Report.
- Feng, Y., M. A. M., Friedrichs, J., Wilkin, H., Tian, Q., Yang, E. E., Hofmann, J. D., Wiggert, R. R., Hood, 2015: Chesapeake Bay nitrogen fluxes derived from a land-estuarine-ocean biogeochemical modeling system: Model description, evaluation and nitrogen budgets. *Journal of Geophysical Research: Biogeosciences*, **120**, 1666-1695, doi:10.1002/2015JG002931.
- Firestone, M., and E. Davidson, 1989: Microbiological basis of NO and N₂O production and consumption in soil. In: *Exchange of Trace Gases between terrestrial Ecosystems and the Atmosphere* **47**, [M. O. Andreae and D. S. Schimel (eds.)]. John Wiley and Sons Ltd., 7-21 pp.
- Forbrich, I., and A. E. Giblin, 2015: Marsh-atmosphere CO₂ exchange in a New England salt marsh. *Journal of Geophysical Research: Biogeosciences*, **120**(9), 1825-1838, doi: 10.1002/2015jg003044.
- Fourqurean, J. W., C. M. Duarte, H. Kennedy, N. Marbà, M. Holmer, M. A. Mateo, E. T. Apostolaki, G. A. Kendrick, D. Krause-Jensen, K. J. McGlathery, and O. Serrano, 2012: Seagrass ecosystems as a globally significant carbon stock. *Nature Geoscience*, **5**(7), 505-509, doi: 10.1038/ngeo1477.
- Gabler, C. A., M. J. Osland, J. B. Grace, C. L. Stagg, R. H. Day, S. B. Hartley, N. M. Enwright, A. S. From, M. L. McCoy, and J. L. McLeod, 2017: Macroclimatic change expected to transform coastal wetland ecosystems this century. *Nature Climate Change*, **7**(2), 142-147, doi: 10.1038/nclimate3203.
- Gallagher, J. L., R. J. Reimold, R. A. Linthurst, and W. J. Pfeiffer, 1980: Aerial production, mortality, and mineral accumulation-export dynamics in *Spartina alterniflora* and *Juncus roemerianus* plant stands in a Georgia salt marsh. *Ecology*, **61**(2), 303-312, doi: 10.2307/1935189.
- Galloway, J. N., A. R. Townsend, J. W. Erisman, M. Bekunda, Z. Cai, J. R. Freney, L. A. Martinelli, S. P. Seitzinger, and M. A. Sutton, 2008: Transformation of the nitrogen cycle: Recent trends, questions, and potential solutions. *Science*, **320**(5878), 889-892, doi: 10.1126/science.1136674.
- Ganju, N. K., M. Hayn, S.-N. Chen, R. W. Howarth, P. J. Dickhudt, A. L. Aretxabaleta, and R. Marino, 2012: Tidal and groundwater fluxes to a shallow, microtidal estuary: Constraining inputs through field observations and hydrodynamic modeling. *Estuaries and Coasts*, **35**(5), 1285-1298, doi: 10.1007/s12237-012-9515-x.
- Gelesh, L., K. Marshall, W. Boicourt, and L. Lapham, 2016: Methane concentrations increase in bottom waters during summertime anoxia in the highly eutrophic estuary, Chesapeake Bay, U.S.A. *Limnology and Oceanography*, **61**(S1), S253-S266, doi: 10.1002/lno.10272.
- Giri, C. P., and J. Long, 2014: Mangrove reemergence in the northernmost range limit of Eastern Florida. *Proceedings of the National Academy of Sciences USA*, **111**(15), E1447-1448, doi: 10.1073/pnas.1400687111.
- Giri, C., E. Ochieng, L. L. Tieszen, Z. Zhu, A. Singh, T. Loveland, J. Masek, and N. Duke, 2011: Status and distribution of mangrove forests of the world using Earth observation satellite data. *Global Ecology and Biogeography*, **20**(1), 154-159, doi: 10.1111/j.1466-8238.2010.00584.x.
- Hales, B., A. Suhrbier, G. G. Waldbusser, R. A. Feely, and J. A. Newton, 2016: The carbonate chemistry of the "fattening line," Willapa Bay, 2011–2014. *Estuaries and Coasts*, **40**(1), 173-186, doi: 10.1007/s12237-016-0136-7.
- Hamilton, S. E., and D. Casey, 2016: Creation of a high spatio-temporal resolution global database of Continuous Mangrove Forest Cover for the 21st century (CGMFC-21). *Global Ecology and Biogeography*, **25**(6), 729-738, doi: 10.1111/geb.12449.
- Hernández-Ayón, J. M., V. F. Camacho-Ibar, A. Mejía-Trejo, and A. Cabello-Pasini, 2007: Variabilidad del CO₂ total durante eventos de surgencia en bahía de san quintín, Baja California Mexico. In: *Carbono en Ecosistemas Acuáticos de México*. Secretaría de Medio Ambiente y Recursos Naturales Instituto Nacional de Ecología Centro de Investigaciones Científicas y de Educación de Ensenada, 187-200 pp.
- Herrmann, M., R. G. Najjar, W. M. Kemp, R. B. Alexander, E. W. Boyer, W.-J. Cai, P. C. Griffith, K. D. Kroeger, S. L. McCallister, and R. A. Smith, 2015: Net ecosystem production and organic carbon balance of U.S. east coast estuaries: A synthesis approach. *Global Biogeochemical Cycles*, **29**(1), 96-111, doi: 10.1002/2013gb004736.
- Hinson, A. L., R. A. Feagin, M. Eriksson, R. G. Najjar, M. Herrmann, T. S. Bianchi, M. Kemp, J. A. Hutchings, S. Crooks, and T. Boutton, 2017: The spatial distribution of soil organic carbon in tidal wetland soils of the continental United States. *Global Change Biology*, 1-13, doi: 10.1111/gcb.13811.
- Holm, G. O., B. C. Perez, D. E. McWhorter, K. W. Krauss, D. J. Johnson, R. C. Raynie, and C. J. Killebrew, 2016: Ecosystem level methane fluxes from tidal freshwater and brackish marshes of the Mississippi River Delta: Implications for coastal wetland carbon projects. *Wetlands*, **36**(3), 401-413, doi: 10.1007/s13157-016-0746-7.
- Holmquist, J. R., L. Windham-Myers, N. Bliss, S. Crooks, J. T. Morris, J. P. Megonigal, T. Troxler, D. Weller, J. Callaway, J. Drexler, M. C. Ferner, M. E. Gonneea, K. D. Kroeger, L. Schile-Beers, I. Woo, K. Buffington, J. Breithaupt, B. M. Boyd, L. N. Brown, N. Dix, L. Hice, B. P. Horton, G. M. MacDonald, R. P. Moyer, W. Reay, T. Shaw, E. Smith, J. M. Smoak, C. Sommerfield, K. Thorne, D. Velinsky, E. Watson, K. W. Grimes, and M. Woodrey, 2018a: Accuracy and precision of tidal wetland soil carbon mapping in the conterminous United States. *Scientific Reports*, **8**(1), 9478, doi: 10.1038/s41598-018-26948-7.



- Holmquist, J., L. Windham-Myers, B. Bernal, K. B. Byrd, S. Crooks, M. E. Gonnee, N. Herold, S. H. Knox, K. D. Kroeger, J. McCombs, J. P. Megonigal, L. Meng, J. T. Morris, A. E. Sutton-Grier, T. G. Troxler, and D. E. Weller, 2018b: Uncertainty in United States coastal wetland greenhouse gas inventoring. *Environmental Research Letters*, 105350, doi: 10.1088/1748-9326/aae157.
- Hopkinson, C. S., 1985: Shallow-water benthic and pelagic metabolism. *Marine Biology*, **87**(1), 19-32, doi: 10.1007/bf00397002.
- Hopkinson, C. S., 1988: Patterns of organic carbon exchange between coastal ecosystems. In: *Coastal-Offshore Ecosystem Interactions*. Proceedings of a symposium sponsored by SCOR, UNESCO, San Francisco Society, California Sea Grant program, and the U.S. Department of Interior, Mineral Management Service held at San Francisco State University, Tiburon, California, April 7–22, 1986. [B. O. Jansson (ed.)]. Springer Berlin Heidelberg, 122-154 pp.
- Hopkinson, C. S., and J. J. Vallino, 1995: The relationships among man's activities in watersheds and estuaries: A model of runoff effects on patterns of estuarine community metabolism. *Estuaries*, **18**(4), 598, doi: 10.2307/1352380.
- Hopkinson, C. S., W.-J. Cai, and X. Hu, 2012: Carbon sequestration in wetland dominated coastal systems—a global sink of rapidly diminishing magnitude. *Current Opinion in Environmental Sustainability*, **4**(2), 186-194, doi: 10.1016/j.cosust.2012.03.005.
- Hossler, K., and J. E. Bauer, 2013: Amounts, isotopic character, and ages of organic and inorganic carbon exported from rivers to ocean margins: 1. Estimates of terrestrial losses and inputs to the Middle Atlantic Bight. *Global Biogeochemical Cycles*, **27**(2), 331-346, doi: 10.1002/gbc.20033.
- Howard, J., A. Sutton-Grier, D. Herr, J. Kleypas, E. Landis, E. McLeod, E. Pidgeon, and S. Simpson, 2017: Clarifying the role of coastal and marine systems in climate mitigation. *Frontiers in Ecology and the Environment*, **15**(1), 42-50, doi: 10.1002/fee.1451.
- Howarth, R. W., D. Anderson, J. Cloern, C. Elfring, C. Hopkinson, B. Lapointe, T. Malone, N. Marcus, K. McGlathery, A. Sharpley, and D. Walker, 2000: Nutrient pollution of coastal rivers, bays and seas. *Issues in Ecology*, **7**, 1-15.
- Huang, W. J., W. J. Cai, Y. Wang, S. E. Lohrenz, and M. C. Murrell, 2015: The carbon dioxide system on the Mississippi River-dominated continental shelf in the Northern Gulf of Mexico: 1. Distribution and air-sea CO₂ flux. *Journal of Geophysical Research: Oceans*, **120**(3), 1429-1445, doi: 10.1002/2014JC010498.
- Hunt, C. W., J. E. Salisbury, and D. Vandemark, 2014: CO₂ input dynamics and air-sea exchange in a large New England estuary. *Estuaries and Coasts*, **37**(5), 1078-1091, doi: 10.1007/s12237-013-9749-2.
- Hunt, C. W., J. E. Salisbury, and D. Vandemark, 2011: Contribution of non-carbonate anions to total alkalinity and overestimation of pCO₂ in New England and New Brunswick rivers. *Biogeosciences*, **8**(10), 3069-3076, doi: 10.5194/bg-8-3069-2011.
- Irby, I. D., M. A. M. Friedrichs, C. T. Friedrichs, A. J. Bever, R. R. Hood, L. W. J. Lanerolle, M. Li, L. Linker, M. E. Scully, K. Sellner, J. Shen, J. Testa, H. Wang, P. Wang, and M. Xia, 2016: Challenges associated with modeling low-oxygen waters in Chesapeake Bay: A multiple model comparison. *Biogeosciences*, **13**(7), 2011-2028, doi: 10.5194/bg-13-2011-2016.
- Irby, I. D., M. A. M. Friedrichs, F. Da, and K. E. Hinson, 2018: The competing impacts of climate change and nutrient reductions on dissolved oxygen in Chesapeake Bay. *Biogeosciences*, **15**(9), 2649-2668, doi: 10.5194/bg-15-2649-2018.
- Jackley, J., L. Gardner, A. F. Djunaedi, and A. K. Salomon, 2016: Ancient clam gardens, traditional management portfolios, and the resilience of coupled human-ocean systems. *Ecology and Society*, **21**(4), doi: 10.5751/es-08747-210420.
- Jankowski, K. L., T. E. Tornqvist, and A. M. Fernandes, 2017: Vulnerability of Louisiana's coastal wetlands to present-day rates of relative sea-level rise. *Nature Communications*, **8**, 14792, doi: 10.1038/ncomms14792.
- Jiang, L. Q., W. J. Cai, Y. Wang, and J. E. Bauer, 2013: Influence of terrestrial inputs on continental shelf carbon dioxide. *Biogeosciences*, **10**(2), 839-849, doi: 10.5194/bg-10-839-2013.
- Jiang, L.-Q., W.-J. Cai, and Y. Wang, 2008: A comparative study of carbon dioxide degassing in river- and marine-dominated estuaries. *Limnology and Oceanography*, **53**(6), 2603-2615, doi: 10.4319/lo.2008.53.6.2603.
- Joesoef, A., W. J. Huang, Y. Gao, and W. J. Cai, 2015: Air-water fluxes and sources of carbon dioxide in the Delaware Estuary: Spatial and seasonal variability. *Biogeosciences*, **12**(20), 6085-6101, doi: 10.5194/bg-12-6085-2015.
- Johannessen, S. C., R. W. Macdonald, and D. W. Paton, 2003: A sediment and organic carbon budget for the greater Strait of Georgia. *Estuarine, Coastal and Shelf Science*, **56**(3-4), 845-860, doi: 10.1016/s0272-7714(02)00303-7.
- Kathilankal, J. C., T. J. Mozdzer, J. D. Fuentes, P. D'Odorico, K. J. McGlathery, and J. C. Zieman, 2008: Tidal influences on carbon assimilation by a salt marsh. *Environmental Research Letters*, **3**(4), 044010, doi: 10.1088/1748-9326/3/4/044010.
- Kelley, C. A., C. S. Martens, and W. Ussler, 1995: Methane dynamics across a tidally flooded riverbank margin. *Limnology and Oceanography*, **40**(6), 1112-1129, doi: 10.4319/lo.1995.40.6.1112.
- Kemp, W. M., E. M. Smith, M. Marvin-DiPasquale, and W. R. Boynton, 1997: Organic carbon balance and net ecosystem metabolism in Chesapeake Bay. *Marine Ecology Progress Series*, **150**, 229-248, doi: 10.3354/meps150229.
- Kennedy, H., D. M. Alongi, A. Karim, G. Chen, G. L. Chmura, S. Crooks, J. G. Kairo, B. Liao, and G. Lin, 2014: Coastal Wetlands. In: *2013 Supplement to the 2006 Intergovernmental Panel on Climate Change Guidelines for National Greenhouse Gas Inventories: Wetlands*. [T. Hiraishi, T. Krug, K. Tanabe, N. Srivastava, J. Baasansuren, M. Fukuda, et al. (eds.)]. Switzerland, pp 4.1-4.55.



- Kennedy, H., J. Beggins, C. M. Duarte, J. W. Fourqurean, M. Holmer, N. Marbà, and J. J. Middelburg, 2010: Seagrass sediments as a global carbon sink: Isotopic constraints. *Global Biogeochemical Cycles*, **24**(4), doi: 10.1029/2010gb003848.
- Kenov Ascione, I., F. Campuzano, G. Franz, R. Fernandes, C. Viegas, J. Sobrinho, H. de Pablo, A. Amaral, L. Pinto, M. Mateus, and R. Neves, 2014: Advances in modeling of water quality in estuaries. In: *Remote Sensing and Modeling: Advances in Coastal and Marine Resources*. [C. W. Finkl and C. Makowski (eds.)]. Coastal Research Library 9. Springer, 237-276 pp.
- Kirwan, M. L., A. B. Murray, J. P. Donnelly, and D. R. Corbett, 2011: Rapid wetland expansion during European settlement and its implication for marsh survival under modern sediment delivery rates. *Geology*, **39**(5), 507-510, doi: 10.1130/g31789.1.
- Kirwan, M. L., and J. P. Megonigal, 2013: Tidal wetland stability in the face of human impacts and sea-level rise. *Nature*, **504**(7478), 53-60, doi: 10.1038/nature12856.
- Kirwan, M. L., and L. K. Blum, 2011: Enhanced decomposition offsets enhanced productivity and soil carbon accumulation in coastal wetlands responding to climate change. *Biogeosciences*, **8**(4), 987-993.
- Kirwan, M. L., G. R. Guntenspergen, A. D'Alpaos, J. T. Morris, S. M. Mudd, and S. Temmerman, 2010: Limits on the adaptability of coastal marshes to rising sea level. *Geophysical Research Letters*, **37**(23), doi: 10.1029/2010gl045489.
- Kirwan, M. L., G. R. Guntenspergen, and J. T. Morris, 2009: Latitudinal trends in *Spartina alterniflora* productivity and the response of coastal marshes to global change. *Global Change Biology*, **15**(8), 1982-1989, doi: 10.1111/j.1365-2486.2008.01834.x.
- Knox, S. H., L. Windham-Myers, F. Anderson, C. Sturtevant, and B. Bergamaschi, 2018: Direct and indirect effects of tides on ecosystem-scale CO₂ exchange in a brackish tidal marsh in Northern California. *Journal of Geophysical Research: Biogeosciences*, **123**(3), 787-806, doi: 10.1002/2017JG004048.
- Kolker, A. S., M. A. Allison, and S. Hameed, 2011: An evaluation of subsidence rates and sea-level variability in the Northern Gulf of Mexico. *Geophysical Research Letters*, **38**(21), doi: 10.1029/2011gl049458.
- Kone, Y. J. M., and A. V. Borges, 2008: Dissolved inorganic carbon dynamics in the waters surrounding forested mangroves of the Ca Mau Province (Vietnam). *Estuarine, Coastal and Shelf Science*, **77**(3), 409-421, doi: 10.1016/j.ecss.2007.10.001.
- Krauss, K. W., A. S. From, T. W. Doyle, T. J. Doyle, and M. J. Barry, 2011: Sea-level rise and landscape change influence mangrove encroachment onto marsh in the Ten Thousand Islands Region of Florida, USA. *Journal of Coastal Conservation*, **15**(4), 629-638, doi: 10.1007/s11852-011-0153-4.
- Krauss, K. W., and J. L. Whitbeck, 2011: Soil greenhouse gas fluxes during wetland forest retreat along the Lower Savannah River, Georgia (USA). *Wetlands*, **32**(1), 73-81, doi: 10.1007/s13157-011-0246-8.
- Krauss, K. W., G. O. Holm, B. C. Perez, D. E. McWhorter, N. Cormier, R. F. Moss, D. J. Johnson, S. C. Neubauer, and R. C. Raynie, 2016: Component greenhouse gas fluxes and radiative balance from two deltaic marshes in Louisiana: Pairing chamber techniques and eddy covariance. *Journal of Geophysical Research: Biogeosciences*, **121**(6), 1503-1521, doi: 10.1002/2015JG003224.
- Kroeger, K. D., and M. A. Charette, 2008: Nitrogen biogeochemistry of submarine groundwater discharge. *Limnology and Oceanography*, **53**(3), 1025-1039, doi: 10.4319/lo.2008.53.3.1025.
- Kroeger, K. D., S. Crooks, S. Moseman-Valtierra, and J. Tang, 2017: Restoring tides to reduce methane emissions in impounded wetlands: A new and potent blue carbon climate change intervention. *Scientific Reports*, **7**(1), 11914, doi: 10.1038/s41598-017-12138-4.
- Lagomasino, D., R. M. Price, D. Whitman, P. K. E. Campbell, and A. Melesse, 2014: Estimating major ion and nutrient concentrations in mangrove estuaries in Everglades National Park using leaf and satellite reflectance. *Remote Sensing of Environment*, **154**, 202-218, doi: 10.1016/j.rse.2014.08.022.
- Lane, R. R., S. K. Mack, J. W. Day, R. D. DeLaune, M. J. Madison, and P. R. Precht, 2016: Fate of soil organic carbon during wetland loss. *Wetlands*, **36**(6), 1167-1181, doi: 10.1007/s13157-016-0834-8.
- Lara-Lara, J. R., B. E. Frey, and F. L. Small, 1990: Primary production in the Columbia River Estuary I. Spatial temporal variability of properties. *Pacific Science*, **44**(1), 17-37.
- Laruelle, G. G., H. H. Dürr, R. Lauerwald, J. Hartmann, C. P. Slomp, N. Goossens, and P. A. G. Regnier, 2013: Global multi-scale segmentation of continental and coastal waters from the watersheds to the continental margins. *Hydrology and Earth System Sciences*, **17**(5), 2029-2051, doi: 10.5194/hess-17-2029-2013.
- Laruelle, G. G., R. Lauerwald, B. Pfeil, and P. Regnier, 2014: Regionalized global budget of the CO₂ exchange at the air-water interface in continental shelf seas. *Global Biogeochemical Cycles*, **28**(11), 1199-1214, doi: 10.1002/2014gb004832.
- Lu, W., J. Xiao, F. Liu, Y. Zhang, C. Liu, and G. Lin, 2017: Contrasting ecosystem CO₂ fluxes of inland and coastal wetlands: A meta-analysis of eddy covariance data. *Global Change Biology*, **23**(3), 1180-1198, doi: 10.1111/gcb.13424.
- Mackenzie, F. T., E. H. De Carlo, and A. Lerman, 2012: Coupled C, N, P, and O biogeochemical cycling at the land-ocean interface. In: *Biogeochemistry*, Vol. 5. Elsevier Inc., 26 pp.
- Magenheimer, J. F., T. R. Moore, G. L. Chmura, and R. J. Daoust, 1996: Methane and carbon dioxide flux from a macrotidal salt marsh, Bay of Fundy, New Brunswick. *Estuaries*, **19**(1), 139, doi: 10.2307/1352658.



- Marchio, D., M. Savarese, B. Bovard, and W. Mitsch, 2016: Carbon sequestration and sedimentation in mangrove swamps influenced by hydrogeomorphic conditions and urbanization in southwest Florida. *Forests*, **7**(6), 116, doi: 10.3390/f7060116.
- Mariotti, G., and S. Fagherazzi, 2013: Critical width of tidal flats triggers marsh collapse in the absence of sea-level rise. *Proceedings of the National Academy of Sciences USA*, **110**(14), 5353-5356, doi: 10.1073/pnas.1219600110.
- Mariotti, G., S. Fagherazzi, P. L. Wiberg, K. J. McGlathery, L. Carniello, and A. Defina, 2010: Influence of storm surges and sea level on shallow tidal basin erosive processes. *Journal of Geophysical Research*, **115**(C11), doi: 10.1029/2009jc005892.
- Marsh, A. L., K. A. Becraft, and G. A. Somorjai, 2005: Methane dissociative adsorption on the Pt(111) surface over the 300–500 K temperature and 1–10 Torr pressure ranges. *The Journal of Physical Chemistry B*, **109**(28), 13619-13622, doi: 10.1021/jp051718+.
- Marsh, A. S., J. A. Arnone, B. T. Bormann, and J. C. Gordon, 2000: The role of equestum in nutrient cycling in an Alaskan shrub wetland. *Journal of Ecology*, **88**(6), 999-1011, doi: 10.1046/j.1365-2745.2000.00520.x.
- Martin, R. M., and S. Moseman-Valtierra, 2015: Greenhouse gas fluxes vary between *Phragmites australis* and native vegetation zones in coastal wetlands along a salinity gradient. *Wetlands*, **35**(6), 1021-1031, doi: 10.1007/s13157-015-0690-y.
- Mayorga, E., S. P. Seitzinger, J. A. Harrison, E. Dumont, A. H. W. Beusen, A. F. Bouwman, B. M. Fekete, C. Kroeze, and G. Van Drecht, 2010: Global nutrient export from WaterSheds 2 (NEWS 2): Model development and implementation. *Environmental Modelling and Software*, **25**(7), 837-853, doi: 10.1016/j.envsoft.2010.01.007.
- McCabe, R. M., B. M. Hickey, R. M. Kudela, K. A. Lefebvre, N. G. Adams, B. D. Bill, F. M. Gulland, R. E. Thomson, W. P. Cochlan, and V. L. Trainer, 2016: An unprecedented coast-wide toxic algal bloom linked to anomalous ocean conditions. *Geophysical Research Letters*, **43**(19), 10366-10376, doi: 10.1002/2016GL070023.
- McClelland, J. W., R. M. Holmes, K. H. Dunton, and R. W. Macdonald, 2012: The Arctic Ocean estuary. *Estuaries and Coasts*, **35**(2), 353-368, doi: 10.1007/s12237-010-9357-3.
- McGillis, W. R., J. B. Edson, J. E. Hare, and C. W. Fairall, 2001: Direct covariance air-sea CO₂ fluxes. *Journal of Geophysical Research: Oceans*, **106**(C8), 16729-16745, doi: 10.1029/2000jc000506.
- McKee, K. L., D. R. Cahoon, and I. C. Feller, 2007: Caribbean mangroves adjust to rising sea level through biotic controls on change in soil elevation. *Global Ecology and Biogeography*, **16**(5), 545-556, doi: 10.1111/j.1466-8238.2007.00317.x.
- McLeod, E., G. L. Chmura, S. Bouillon, R. Salm, M. Björk, C. M. Duarte, C. E. Lovelock, W. H. Schlesinger, and B. R. Silliman, 2011: A blueprint for blue carbon: Toward an improved understanding of the role of vegetated coastal habitats in sequestering CO₂. *Frontiers in Ecology and the Environment*, **9**(10), 552-560, doi: 10.1890/110004.
- Meeder, J. F., and R. W. Parkinson, 2017: SE Saline Everglades transgressive sedimentation in response to historic acceleration in sea-level rise: A viable marker for the base of the Anthropocene? *Journal of Coastal Research*, **34**2, 490-497, doi: 10.2112/jcoastres-d-17-00031.1.
- Megonigal, J. P., and W. H. Schlesinger, 2002: Methane-limited methanotrophy in tidal freshwater swamps. *Global Biogeochemical Cycles*, **16**(4), 35-1 to 35-10, doi: 10.1029/2001GB001594.
- Meybeck, M., 2003: Global analysis of river systems: From Earth system controls to anthropocene syndromes. *Philosophical Transactions of the Royal Society B. Biological Sciences*, **358**(1440), 1935-1955, doi: 10.1098/rstb.2003.1379.
- Montagna, P. A., J. Brenner, J. Gibeau, and S. Morehead, 2009: Coastal impacts. In: *The Impact of Global Warming on Texas*. [J. Schmandt, J. Clarkson, and G. R. North (eds.)]. University of Texas Press, Austin, TX, 318 pp.
- Moore, W. S., 1996: Large groundwater inputs to coastal waters revealed by ²²⁶Ra enrichments. *Nature*, **380**(6575), 612-614, doi: 10.1038/380612a0.
- Moosdorf, N., J. Hartmann, R. Lauerwald, B. Hagedorn, and S. Kempe, 2011: Atmospheric CO₂ consumption by chemical weathering in North America. *Geochimica et Cosmochimica Acta*, **75**(24), 7829-7854, doi: 10.1016/j.gca.2011.10.007.
- Morris, J. T., D. C. Barber, J. C. Callaway, R. Chambers, S. C. Hagen, C. S. Hopkinson, B. J. Johnson, P. Megonigal, S. C. Neubauer, T. Troxler, and C. Wigand, 2016: Contributions of organic and inorganic matter to sediment volume and accretion in tidal wetlands at steady state. *Earths Future*, **4**(4), 110-121, doi: 10.1002/2015EF000334.
- Moseman-Valtierra, S., O. I. Abdul-Aziz, J. Tang, K. S. Ishtiaq, K. Morkeski, J. Mora, R. K. Quinn, R. M. Martin, K. Egan, E. Q. Brannon, J. Carey, and K. D. Kroeger, 2016: Carbon dioxide fluxes reflect plant zonation and belowground biomass in a coastal marsh. *Ecosphere*, **7**(11), e01560, doi: 10.1002/ecs2.1560.
- Moseman-Valtierra, S., R. Gonzalez, K. D. Kroeger, J. Tang, W. C. Chao, J. Crusius, J. Bratton, A. Green, and J. Shelton, 2011: Short-term nitrogen additions can shift a coastal wetland from a sink to a source of N₂O. *Atmospheric Environment*, **45**(26), 4390-4397, doi: 10.1016/j.atmosenv.2011.05.046.
- Mueller, P., R. N. Hager, J. E. Meschter, T. J. Mozdzer, J. A. Langley, K. Jensen, and J. P. Megonigal, 2016: Complex invader-ecosystem interactions and seasonality mediate the impact of non-native phragmites on CH₄ emissions. *Biological Invasions*, **18**(9), 2635-2647, doi: 10.1007/s10530-016-1093-6.



- Müller, P. J., and E. Suess, 1979: Productivity, sedimentation rate, and sedimentary organic matter in the oceans—I. Organic carbon preservation. *Deep Sea Research Part A. Oceanographic Research Papers*, **26**(12), 1347-1362, doi: 10.1016/0198-0149(79)90003-7.
- Munoz-Anderson, M. A., J. R. Lara-Lara, S. Alvarez-Borrego, C. Bazan-Guzman, and M. de la Cruz-Orozco, 2015: Water-air carbon fluxes in the coastal upwelling zone off Northern Baja California. *Ciencias Marinas*, **41**(2), 157-168, doi: 10.7773/cm.v41i2.2484.
- Nahlik, A. M., and M. S. Fennessy, 2016: Carbon storage in US wetlands. *Nature Communications*, **7**, 13835, doi: 10.1038/ncomms13835.
- Najjar, R. G., M. Herrmann, R. Alexander, E. W. Boyer, D. J. Burdige, D. Butman, W. J. Cai, E. A. Canuel, R. F. Chen, M. A. M. Friedrichs, R. A. Feagin, P. C. Griffith, A. L. Hinson, J. R. Holmquist, X. Hu, W. M. Kemp, K. D. Kroeger, A. Mannino, S. L. McCallister, W. R. McGillis, M. R. Mulholland, C. H. Pilskaln, J. Salisbury, S. R. Signorini, P. St-Laurent, H. Tian, M. Tzortziou, P. Vlahos, Z. A. Wang, and R. C. Zimmerman, 2018: Carbon budget of tidal wetlands, estuaries, and shelf waters of Eastern North America. *Global Biogeochemical Cycles*, **32**(3), 389-416, doi: 10.1002/2017gb005790.
- NASA, 2017a: National Aeronautics and Space Administration, Blue Carbon Monitoring System. [<https://water.usgs.gov/nrp/blue-carbon/nasa-blue-cms/>]
- NASA, 2017b: National Aeronautics and Space Administration, Wetland-Estuary Transports and Carbon Budgets (WETCARB) project. [https://cce.nasa.gov/cgi-bin/cce/cce_profile.pl?project_group_id=3165]
- Nellemann, C., E. Corcoran, C. Duarte, L. Vales, C. Fonseca, and G. Grimsditch, 2009: *Blue Carbon - The Role of Healthy Oceans in Binding Carbon*. GRID-Arendal: United Nations Environment Programme. [<https://www.grida.no/publications/145>]
- Neubauer, S. C., R. B. Franklin, and D. J. Berrier, 2013: Saltwater intrusion into tidal freshwater marshes alters the biogeochemical processing of organic carbon. *Biogeosciences*, **10**(12), 8171-8183, doi: 10.5194/bg-10-8171-2013.
- Neubauer, S. C., W. D. Miller, and I. C. Anderson, 2000: Carbon cycling in a tidal freshwater marsh ecosystem: A carbon gas flux study. *Marine Ecology Progress Series*, **199**, 13-30.
- NOAA, 1985: *National Estuarine Inventory Data Atlas. Volume 1: Physical and Hydrologic Characteristics*. National Ocean Service, National Oceanic and Atmospheric Administration. [https://www.greateratlantic.fisheries.noaa.gov/habitat/publications/national_estuarine_inventory_-_ne_region1.pdf]
- NOAA, 2015: *Land Cover Atlas*. Coastal Change Analysis Program (C-CAP) Regional Land Cover. National Oceanic and Atmospheric Administration, Office for Coastal Management. Charleston, SC, NOAA Office for Coastal Management. [<https://www.coast.noaa.gov/ccapftp>]
- NOAA, 2017: National Oceanic and Atmospheric Administration Office for Coastal Management, Digital Coast. [<https://coast.noaa.gov/digitalcoast/>]
- Orton, P. M., W. R. McGillis, and C. J. Zappa, 2010: Sea breeze forcing of estuary turbulence and air-water CO₂ exchange. *Geophysical Research Letters*, **37**(13), doi: 10.1029/2010gl043159.
- Osland, M. J., A. C. Spivak, J. A. Nestlerode, J. M. Lessmann, A. E. Almario, P. T. Heitmuller, M. J. Russell, K. W. Krauss, F. Alvarez, D. D. Dantin, J. E. Harvey, A. S. From, N. Cormier, and C. L. Stagg, 2012: Ecosystem development after mangrove wetland creation: Plant-soil change across a 20-year chronosequence. *Ecosystems*, **15**(5), 848-866, doi: 10.1007/s10021-012-9551-1.
- Ouyang, X., and S. Y. Lee, 2014: Updated estimates of carbon accumulation rates in coastal marsh sediments. *Biogeosciences*, **11**(18), 5057-5071, doi: 10.5194/bg-11-5057-2014.
- Packalen, M. S., S. A. Finkelstein, and J. W. McLaughlin, 2014: Carbon storage and potential methane production in the Hudson Bay lowlands since mid-Holocene peat initiation. *Nature Communications*, **5**, 4078, doi: 10.1038/ncomms5078.
- Palaima, A., 2012: *Ecology, Conservation, and Restoration of Tidal Marshes: The San Francisco Estuary*. University of California Press, 288 pp.
- Paulsen M.-L., A. J. Andersson, L. Aluwihare, T. Cyronak, S. D'Angelo, C. Davidson, H. Elwany, S. Giddings, M. Harvey, H. Page, M. Porrachia, and S. Schroeter, 2017: Temporal changes in seawater carbonate chemistry and carbon export from a Southern California estuary. *Estuaries and Coasts*, **41**(4), 1050-1068, doi: 10.1007/s12237-017-0345-8.
- Pendleton, L., D. C. Donato, B. C. Murray, S. Crooks, W. A. Jenkins, S. Sifleet, C. Craft, J. W. Fourqurean, J. B. Kauffman, N. Marba, P. Megonigal, E. Pidgeon, D. Herr, D. Gordon, and A. Baldera, 2012: Estimating global "blue carbon" emissions from conversion and degradation of vegetated coastal ecosystems. *PLOS One*, **7**(9), e43542, doi: 10.1371/journal.pone.0043542.
- Perillo, G. M. E., and M. C. Picollo, 1995: Definition and geomorphologic classification of estuaries. In: *Introduction to Estuary Studies*. [M. C. Picollo, G. M. E. Perillo, and Pino-Quivira (eds.)].
- Peteet, D., D. Pederson, D. Kurdyla, and T. Guilderson, 2006: Hudson River paleoecology from marshes. In: *Hudson River Fishes and their Environment*. [J. R. Waldman, K. E. Limburg, and D. Strayer (eds.)]. American Fisheries Society Monograph 113-128 pp.
- Pfeiffer-Herbert, A. S., F. G. Prahl, B. Hales, J. A. Lerczak, S. D. Pierce, and M. D. Levine, 2016: High resolution sampling of methane transport in the Columbia River near-field plume: Implications for sources and sinks in a river-dominated estuary. *Limnology and Oceanography*, **61**(S1), S204-S220, doi: 10.1002/lno.10221.



- Pickart, R. S., L. M. Schulze, G. W. K. Moore, M. A. Charette, K. R. Arrigo, G. van Dijken, and S. L. Danielson, 2013: Long-term trends of upwelling and impacts on primary productivity in the Alaskan Beaufort Sea. *Deep Sea Research Part I: Oceanographic Research Papers*, **79**, 106-121, doi: 10.1016/j.dsr.2013.05.003.
- Plafker, G., 1965: Tectonic deformation associated with the 1964 Alaska earthquake: The earthquake of 27 March 1964 resulted in observable crustal deformation of unprecedented areal extent. *Science*, **148**(3678), 1675-1687, doi: 10.1126/science.148.3678.1675.
- Poffenbarger, H. J., B. A. Needelman, and J. P. Megonigal, 2011: Salinity influence on methane emissions from tidal marshes. *Wetlands*, **31**(5), 831-842, doi: 10.1007/s13157-011-0197-0.
- Premuzic, E. T., C. M. Benkovitz, J. S. Gaffney, and J. J. Walsh, 1982: The nature and distribution of organic matter in the surface sediments of world oceans and seas. *Organic Geochemistry*, **4**(2), 63-77, doi: 10.1016/0146-6380(82)90009-2.
- Pritchard, D. W., 1967: What is an estuary: Physical viewpoint. In: *Estuaries*. [G. H. Lauff (ed.)]. American Association for the Advancement of Science, Washington, D.C. Publication No. 83, pp. 3-5.
- Project Geocarbon, 2017: Operational global carbon observing system. [http://www.geocarbon.net/images/phocadownload/geocarbon_deliverable3.1.pdf]
- Raymond, P. A., and C. S. Hopkins, 2003: Ecosystem modulation of dissolved carbon age in a temperate marsh-dominated estuary. *Ecosystems*, **6**(7), 694-705, doi: 10.1007/s10021-002-0213-6.
- Raymond, P. A., and J. E. Bauer, 2001: Use of ¹⁴C and ¹³C natural abundances for evaluating riverine, estuarine, and coastal DOC and POC sources and cycling: A review and synthesis. *Organic Geochemistry*, **32**(4), 469-485, doi: 10.1016/s0146-6380(00)00190-x.
- Raymond, P. A., J. E. Bauer, and J. J. Cole, 2000: Atmospheric CO₂ evasion, dissolved inorganic carbon production, and net heterotrophy in the York River estuary. *Limnology and Oceanography*, **45**(8), 1707-1717, doi: 10.4319/lo.2000.45.8.1707.
- Raymond, P. A., N. H. Oh, R. E. Turner, and W. Broussard, 2008: Anthropogenically enhanced fluxes of water and carbon from the Mississippi River. *Nature*, **451**(7177), 449-452, doi: 10.1038/nature06505.
- Redfield, A. C., 1967: The ontogeny of a salt marsh estuary. In: *Estuaries*. [G. H. Lauff (ed.)]. American Association for the Advancement of Science, Washington, D.C. Publication No. 83.
- Regnier, P., P. Friedlingstein, P. Ciais, F. T. Mackenzie, N. Gruber, I. A. Janssens, G. G. Laruelle, R. Lauerwald, S. Luyssaert, A. J. Andersson, S. Arndt, C. Arnosti, A. V. Borges, A. W. Dale, A. Gallego-Sala, Y. Goddérís, N. Goossens, J. Hartmann, C. Heinze, T. Ilyina, F. Joos, D. E. LaRowe, J. Leifeld, F. J. R. Meysman, G. Munhoven, P. A. Raymond, R. Spahni, P. Suntharalingam, and M. Thullner, 2013: Anthropogenic perturbation of the carbon fluxes from land to ocean. *Nature Geoscience*, **6**(8), 597-607, doi: 10.1038/ngeo1830.
- Reid, M. C., R. Tripathee, K. V. R. Schäfer, and P. R. Jaffé, 2013: Tidal marsh methane dynamics: Difference in seasonal lags in emissions driven by storage in vegetated versus unvegetated sediments. *Journal of Geophysical Research: Biogeosciences*, **118**(4), 1802-1813, doi: 10.1002/2013JG002438.
- Reimer, J. J., R. Vargas, S. V. Smith, R. Lara-Lara, G. Gaxiola-Castro, J. Martín Hernández-Ayón, A. Castro, M. Escoto-Rodríguez, and J. Martínez-Osuna, 2013: Air-sea CO₂ fluxes in the near-shore and intertidal zones influenced by the California current. *Journal of Geophysical Research: Oceans*, **118**(10), 4795-4810, doi: 10.1002/jgrc.20319.
- Reimnitz, E., 1966: *Late Quaternary History and Sedimentation of the Copper River Delta and Vicinity*, Alaska. Ph.D. Thesis, University of California San Diego, CA, 160 pp.
- Ren, W., H. Tian, B. Tao, J. Yang, S. Pan, W. J. Cai, S. E. Lohrenz, R. He, and C. S. Hopkins, 2015: Large increase in dissolved inorganic carbon flux from the Mississippi River to Gulf of Mexico due to climatic and anthropogenic changes over the 21st century. *Journal of Geophysical Research: Biogeosciences*, **120**(4), 724-736, doi: 10.1002/2014JG002761.
- Ribas-Ribas, M., J. M. Hernández-Ayón, V. F. Camacho-Ibar, A. Cabello-Pasini, A. Mejía-Trejo, R. Durazo, S. Galindo-Bect, A. J. Souza, J. M. Forja, and A. Siqueiros-Valencia, 2011: Effects of upwelling, tides and biological processes on the inorganic carbon system of a coastal lagoon in Baja, California. *Estuarine, Coastal and Shelf Science*, **95**(4), 367-376, doi: 10.1016/j.ecss.2011.09.017.
- Saintilan, N., N. C. Wilson, K. Rogers, A. Rajkaran, and K. W. Krauss, 2014: Mangrove expansion and salt marsh decline at mangrove poleward limits. *Global Change Biology*, **20**(1), 147-157, doi: 10.1111/gcb.12341.
- Salisbury, J., M. Green, C. Hunt, and J. Campbell, 2008: Coastal acidification by rivers: A threat to shellfish? *Eos, Transactions American Geophysical Union*, **89**(50), 513-513, doi: 10.1029/2008eo500001.
- Sallenger Jr, A. H., K. S. Doran, and P. A. Howd, 2012: Hotspot of accelerated sea-level rise on the Atlantic coast of North America. *Nature Climate Change*, **2**, 884, doi: 10.1038/nclimate1597.
- Sanderman, J., T. Hengl, G. Fiske, K. Solvik, M. F. Adame, L. Benson, J. J. Bukoski, P. Carnell, M. Cifuentes-Jara, D. Donato, C. Duncan, E. M. Eid, P. zu Ermgassen, C. J. E. Lewis, P. I. Macreadie, L. Glass, S. Gress, S. L. Jardine, T. G. Jones, E. N. Nsombo, M. M. Rahman, C. J. Sanders, M. Spalding, and E. Landis, 2018: A global map of mangrove forest soil carbon at 30 m spatial resolution. *Environmental Research Letters*, **13**(5), 055002.
- Sansone, F. J., T. M. Rust, and S. V. Smith, 1998: Methane distribution and cycling in Tomales Bay, California. *Estuaries*, **21**(1), 66, doi: 10.2307/1352547.



- Schäfer, K. V. R., R. Tripathee, F. Artigas, T. H. Morin, and G. Bohrer, 2014: Carbon dioxide fluxes of an urban tidal marsh in the Hudson-Raritan Estuary. *Journal of Geophysical Research: Biogeosciences*, **119**(11), 2065-2081, doi: 10.1002/2014jg002703.
- Schepers, L., M. Kirwan, G. Guntenspergen, and S. Temmerman, 2017: Spatio-temporal development of vegetation die-off in a submerging coastal marsh. *Limnology and Oceanography*, **62**(1), 137-150, doi: 10.1002/lno.10381.
- Schlesinger, W. H., 2009: On the fate of anthropogenic nitrogen. *Proceedings of the National Academy of Sciences USA*, **106**(1), 203-208, doi: 10.1073/pnas.08110193105.
- Schubauer, J. P., and C. S. Hopkins, 1984: Above- and below-ground emergent macrophyte production and turnover in a coastal marsh ecosystem, Georgia. *Limnology and Oceanography*, **29**(5), 1052-1065, doi: 10.4319/lo.1984.29.5.1052.
- Segarra, K. E. A., V. Samarkin, E. King, C. Meile, and S. B. Joye, 2013: Seasonal variations of methane fluxes from an unvegetated tidal freshwater mudflat (Hammersmith Creek, GA). *Biogeochemistry*, **115**(1-3), 349-361, doi: 10.1007/s10533-013-9840-6.
- Selmants, P. C., C. P. Giardina, J. D. Jacobi, and Z. Zhu, 2017: *Baseline and Projected Future Carbon Storage and Carbon Fluxes in Ecosystems of Hawai'i*. U.S. Geological Survey Professional Paper 1834, 134 pp, doi: 10.3133/pp1834.
- Shih, J. S., R. Alexander, R. A. Smith, E. W. Boyer, G. E. Schwarz, and S. Chung, 2010: *An Initial Sparrow Model of Land Use and In-Stream Controls on Total Organic Carbon in Streams of the Conterminous United States*. U.S. Geological Survey Open File Report 1276. [<https://pubs.usgs.gov/of/2010/1276/of2010-1276.pdf>]
- Smith, R. W., T. S. Bianchi, M. Allison, C. Savage, and V. Galy, 2015: High rates of organic carbon burial in fjord sediments globally. *Nature Geoscience*, **8**(6), 450-453, doi: 10.1038/ngeo2421.
- Smith, S. V., and J. T. Hollibaugh, 1997: Annual cycle and interannual variability of ecosystem metabolism in a temperate climate embayment. *Ecological Monographs*, **67**(4), 509-533, doi: 10.1890/0012-9615(1997)067[0509:acaivo]2.0.co;2.
- Son, S., M. Wang, and L. W. Harding, 2014: Satellite-measured net primary production in the Chesapeake Bay. *Remote Sensing of Environment*, **144**, 109-119, doi: 10.1016/j.rse.2014.01.018.
- Spalding, M., M. Kainuma, and L. Collins, 2010: *World Atlas of Mangroves*. Earthscan, 319 pp. [<https://books.google.com/books?id=wzSckulW9SQc>]
- Steinberg, P. D., M. T. Brett, J. S. Bechtold, J. E. Richey, L. M. Porensky, and S. N. Smith, 2010: The influence of watershed characteristics on nitrogen export to and marine fate in Hood Canal, Washington, USA. *Biogeochemistry*, **106**(3), 415-433, doi: 10.1007/s10533-010-9521-7.
- Stets, E., and R. Striegl, 2012: Carbon export by rivers draining the conterminous United States. *Inland Waters*, **2**(4), 177-184, doi: 10.5268/iw-2.4.510.
- Swarzenski, C. M., T. W. Doyle, B. Fry, and T. G. Hargis, 2008: Biogeochemical response of organic-rich freshwater marshes in the Louisiana Delta Plain to chronic river water influx. *Biogeochemistry*, **90**(1), 49-63, doi: 10.1007/s10533-008-9230-7.
- TCEQ, 2017: Texas Commission on Environmental Quality. [<https://www.tceq.texas.gov/waterquality/>]
- Thilenius, J. F., 1990: Woody plant succession on earthquake-uplifted coastal wetlands of the Copper River Delta, Alaska. *Forest Ecology and Management*, **33-34**, 439-462, doi: 10.1016/0378-1127(90)90209-t.
- Thom, R. M., 1992: Accretion rates of low intertidal salt marshes in the Pacific Northwest. *Wetlands*, **12**(3), 147-156, doi: 10.1007/bf03160603.
- Thorhaug, A., H. M. Poulos, J. Lopez-Portillo, T. C. W. Ku, and G. P. Berlyn, 2017: Seagrass blue carbon dynamics in the Gulf of Mexico: Stocks, losses from anthropogenic disturbance, and gains through seagrass restoration. *Science of the Total Environment*, **605-606**, 626-636, doi: 10.1016/j.scitotenv.2017.06.189.
- Tian, H., W. Ren, J. Yang, B. Tao, W.-J. Cai, S. E. Lohrenz, C. S. Hopkins, M. Liu, Q. Yang, C. Lu, B. Zhang, K. Banger, S. Pan, R. He, and Z. Xue, 2015: Climate extremes dominating seasonal and interannual variations in carbon export from the Mississippi River Basin. *Global Biogeochemical Cycles*, **29**(9), 1333-1347, doi: 10.1002/2014gb005068.
- Tian, X., B. Sohngen, J. B. Kim, S. Ohrel, and J. Cole, 2016: Global climate change impacts on forests and markets. *Environmental Research Letters*, **11**(3), 035011, doi: 10.1088/1748-9326/11/3/035011.
- Troche-Souza, C., M. T. Rodríguez-Zúñiga, S. Velázquez-Salazar, L. Valderrama-Landeros, E. Villeda-Chávez, A. Alcántara-Maya, B. Vázquez-Balderas, M. I. Cruz-López y R. Ressler, 2016: *Manglares de México: Extensión, Distribución y Monitoreo (1970/1980 - 2015)*. Comisión Nacional para el Conocimiento y Uso de la Biodiversidad, México. D. F., México.
- Troxler, T. G., J. G. Barr, J. D. Fuentes, V. Engel, G. Anderson, C. Sanchez, D. Lagomasino, R. Price, and S. E. Davis, 2015: Component-specific dynamics of riverine mangrove CO₂ efflux in the Florida Coastal Everglades. *Agricultural and Forest Meteorology*, **213**, 273-282, doi: 10.1016/j.agrformet.2014.12.012.
- U.S. EPA, 2016: *Inventory of U.S. Greenhouse Gas Emissions and Sinks: 1990-2014*. U.S. Environmental Protection Agency. EPA 430-R-16-002. [<https://www.epa.gov/sites/production/files/2016-04/documents/us-ghg-inventory-2016-main-text.pdf>]



- U.S. EPA, 2017: *Avoiding and Reducing Long-Term Risks of Climate Change: A Technical Report for the Fourth National Climate Assessment*. U.S. Environmental Protection Agency. EPA 430-R-17-00.
- USFWS NWI, 2017. *U.S. Fish and Wildlife Service National Wetlands Inventory Product Summary*. U.S. Fish and Wildlife Service. [<https://www.fws.gov/wetlands/Data/Wetlands-Product-Summary.html>]
- USGS, 2018: *U.S. Geological Survey Coastal Change Hazards Portal*. U.S. Geological Survey. [<https://marine.usgs.gov/coastalchange-hazardsportal>]
- USGS, 2017: *U.S. Geological Survey Land Change Monitoring, Assessment, and Projection Initiative*. U.S. Geological Survey. [<https://eros.usgs.gov/doi-remote-sensing-activities/2015/land-change-monitoring-assessment-and-projection>]
- Valderrama Landeros L. H., M. T. Rodríguez-Zúñiga, C. Troche Souza, S. Velázquez Salazar, E. Villeda Chávez, J. A. Alcántara Maya, B. Vázquez Balderas, M. I. Cruz López, and R. Ressler, 2017: Manglares de México: Actualización y exploración de los datos del sistema de monitoreo 1970/1980-2015. Comisión Nacional para el Conocimiento y Uso de la Biodiversidad. Ciudad de México. [http://www.biodiversidad.gob.mx/ecosistemas/manglares2013/pdf/manglares_mexico_2015.pdf]
- van Dam, B. R., J. R. Crosswell, I. C. Anderson, and H. W. Paerl, 2018: Watershed-scale drivers of air-water CO₂ exchanges in two lagoonal North Carolina (USA) estuaries. *Journal of Geophysical Research: Biogeosciences*, **123**(1), 271-287, doi: 10.1002/2017JG004243.
- van der Heide, T., E. H. van Nes, M. M. van Katwijk, H. Olf, and A. J. Smolders, 2011: Positive feedbacks in seagrass ecosystems: Evidence from large-scale empirical data. *PLOS One*, **6**(1), e16504, doi: 10.1371/journal.pone.0016504.
- von Biela, V. R., C. E. Zimmerman, B. R. Cohn, and J. M. Welker, 2012: Terrestrial and marine trophic pathways support young-of-year growth in a nearshore Arctic fish. *Polar Biology*, **36**(1), 137-146, doi: 10.1007/s00300-012-1244-x.
- Waldbusser, G. G., B. Hales, C. J. Langdon, B. A. Haley, P. Schrader, E. L. Brunner, M. W. Gray, C. A. Miller, and I. Gimenez, 2014: Saturation-state sensitivity of marine bivalve larvae to ocean acidification. *Nature Climate Change*, **5**(3), 273-280, doi: 10.1038/nclimate2479.
- Walling, D. E., and B. W. Webb, 1983: Patterns of sediment yield. In: *Background to Palaeohydrology. A Perspective*. pp. 69-100.
- Wang, Z. A., and W.-J. Cai, 2004: Carbon dioxide degassing and inorganic carbon export from a marsh-dominated estuary (the Duplin River): A marsh CO₂ pump. *Limnology and Oceanography*, **49**(2), 341-354, doi: 10.4319/lo.2004.49.2.0341.
- Wang, Z. A., K. D. Kroeger, N. K. Ganju, M. E. Gonnee, and S. N. Chu, 2016: Intertidal salt marshes as an important source of inorganic carbon to the coastal ocean. *Limnology and Oceanography*, **61**(5), 1916-1931, doi: 10.1002/lno.10347.
- Ward, N. D., T. S. Bianchi, P. M. Medeiros, M. Seidel, J. E. Richey, R. G. Keil, and H. O. Sawakuchi, 2017: Where carbon goes when water flows: Carbon cycling across the aquatic continuum. *Frontiers in Marine Science*, **4**, doi: 10.3389/fmars.2017.00007.
- Washington State Blue Ribbon Panel on Ocean Acidification, 2012: *Ocean Acidification: From Knowledge to Action, Washington State's Strategic Response*. Publication no. 12-01-015. [H. Adelman and L. W. Binder (eds.)]. Washington Department of Ecology, Olympia, Washington. [<https://fortress.wa.gov/ecy/publications/documents/1201015.pdf>]
- Watson, E. B., 2004: Changing elevation, accretion, and tidal marsh plant assemblages in a south San Francisco bay tidal marsh. *Estuaries*, **27**(4), 684-698, doi: 10.1007/bf02907653.
- Watson, E. B., C. Wigand, E. W. Davey, H. M. Andrews, J. Bishop, and K. B. Raposa, 2017: Wetland loss patterns and inundation-productivity relationships prognosticate widespread salt marsh loss for southern New England. *Estuaries and Coasts*, **40**(3), 662-681, doi: 10.1007/s12237-016-0069-1.
- Weston, N. B., S. C. Neubauer, D. J. Velinsky, and M. A. Vile, 2014: Net ecosystem carbon exchange and the greenhouse gas balance of tidal marshes along an estuarine salinity gradient. *Biogeochemistry*, **120**(1-3), 163-189, doi: 10.1007/s10533-014-9989-7.
- Wheatcroft, R. A., M. A. Goñi, J. A. Hatten, G. B. Pasternack, and J. A. Warrick, 2010: The role of effective discharge in the ocean delivery of particulate organic carbon by small, mountainous river systems. *Limnology and Oceanography*, **55**(1), 161-171, doi: 10.4319/lo.2010.55.1.0161.
- Whiting, G. J., and J. P. Chanton, 2001: Greenhouse carbon balance of wetlands: Methane emission versus carbon sequestration. *Tellus B*, **53**(5), 521-528, doi: 10.1034/j.1600-0889.2001.530501.x.
- Wilson, B. J., B. Mortazavi, and R. P. Kiene, 2015: Spatial and temporal variability in carbon dioxide and methane exchange at three coastal marshes along a salinity gradient in a northern Gulf of Mexico estuary. *Biogeochemistry*, **123**(3), 329-347, doi: 10.1007/s10533-015-0085-4.
- Wollast R., 1991: The coastal carbon cycle: Fluxes, sources and sinks. In: *Ocean Margin Processes in Global Change*. [R. F. C. Mantoura, J.-M. Martin, and R. Wollast (eds.)]. J. Wiley & Sons, Chichester, pp. 365-382.
- Yao, H., and X. Hu, 2017: Responses of carbonate system and CO₂ flux to extended drought and intense flooding in a semiarid subtropical estuary. *Limnology and Oceanography*, **62**(S1), S112-S130, doi: 10.1002/lno.10646.



Ye, F., Y. J. Zhang, H. V. Wang, M. A. M. Friedrichs, I. D. Irby, E. Alteljevich, A. Valle-Levinson, Z. Wang, H. Huang, J. Shen, and J. Du, 2018: A 3D unstructured-grid model for Chesapeake Bay: Importance of bathymetry. *Ocean Modelling*, **127**, 16-39, doi: 10.1016/j.ocemod.2018.05.002.

Ye, F., Y. J. Zhang, M. A. M. Friedrichs, H. V. Wang, I. D. Irby, J. Shen, and Z. Wang, 2016: A 3D, cross-scale, baroclinic model with implicit vertical transport for the upper Chesapeake Bay and its tributaries. *Ocean Modelling*, **107**, 82-96, doi: 10.1016/j.ocemod.2016.10.004.

Zhang, J. Z., and C. J. Fischer, 2014: Carbon dynamics of Florida Bay: Spatiotemporal patterns and biological control. *Environmental Science and Technology*, **48**(16), 9161-9169, doi: 10.1021/es500510z.

Zhang, K., B. Thapa, M. Ross, and D. Gann, 2016: Remote sensing of seasonal changes and disturbances in mangrove forest: A case study from South Florida. *Ecosphere*, **7**(6), e01366, doi: 10.1002/ecs2.1366.



Appendix 15A

Supplemental Data Tables

Table 15A.1. Summary of North American Carbon Dioxide Exchange Between Tidal Wetlands and the Atmosphere (Net Ecosystem Exchange ^a) from Continuous Measurements ^b					
System Name and Type	Location	EC/SC	Year	NEE (g C per m ² per year)	Source
Pacific Coast					
Rush Ranch, Suisun Bay, brackish marsh	California	EC	2014–2015	14	Bergamaschi and Windham-Myers (2018)
			2015–2016	–190	
			2016–2017	–222	
Atlantic Coast					
Plum Island, salt marsh	Massachusetts	EC	2012	–255.6	Forbrich and Giblin (2015)
			2013	–336.0	
			2014	–279.6	
Waquoit Bay, salt marsh	Massachusetts	SC	2015	–160.0	Moseman-Valtierra et al. (2016)
Hudson-Raritan Estuary, restored salt marsh	New Jersey	EC	2009	984 ^c	Schäfer et al. (2014)
			2011	–64.8	
			2012	–309.6	
Hudson-Raritan Estuary, restored salt marsh	New Jersey	EC	2011–2012	–213.6	Artigas et al. (2015)
Delaware Bay, tidal fresh marsh	New Jersey	SC	2007	–256.8	Weston et al. (2014)
			2008	61.2	
Delaware Bay, oligohaline marsh	New Jersey	SC	2007	93.6	Weston et al. (2014)
			2008	–45.6	
Delaware Bay, mesohaline marsh	New Jersey	SC	2007	–115.2	Weston et al. (2014)
			2008	–171.6	
Fowling Point, salt marsh	Virginia	SC	2007	–129.6	Kathilankal et al. (2008)

Continued on next page



(Continued)

Table 15A.1. Summary of North American Carbon Dioxide Exchange Between Tidal Wetlands and the Atmosphere (Net Ecosystem Exchange^a) from Continuous Measurements^b					
System Name and Type	Location	EC/SC	Year	NEE (g C per m² per year)	Source
Springfield Creek, tidal fresh marsh	South Carolina	SC	2009	-295.2	Neubauer et al. (2013)
Gulf of Mexico					
Pointe-aux-Chenes, brackish marsh	Louisiana	EC	2011	-337.2	Holm et al. (2016)
Salvador, tidal fresh marsh	Louisiana	EC	2011	170.4	Holm et al. (2016)
Florida Bay, mangrove	Florida	EC	2004	-1172.4	Barr et al. (2010); Barr et al. (2012)
			2005	-1176	
			2007	-823.2	
			2008	-806.4	
			2009	-926.4	
Mobile Bay, tidal fresh marsh	Alabama	SC	2011	893.4	Wilson et al. (2015)
Mobile Bay, brackish marsh	Alabama	SC	2011	517.8	Wilson et al. (2015)
Mobile Bay, salt marsh	Alabama	SC	2011	410.2	Wilson et al. (2015)

Notes

a) NEE, Net ecosystem exchange; g C, grams of carbon.

b) Continuous measurements: eddy covariance (EC) or static chamber (SC). Positive values = atmospheric carbon dioxide (CO₂) source. Negative values = atmospheric CO₂ sink. Annual estimate (mean) provided.

c) Mudflat habitat (very little data available in literature).



Table 15A.2. Tidal Wetland Methane Flux by Discrete Static Chamber Data or Continuous Eddy Covariance^a Data

Site Name	Location	Year	EC/SC	Salinity (PSU) ^b	CH ₄ Flux (g C per m ² per year) ^c	Reference
Atlantic Coast						
Upland edge	New Brunswick	1993	SC	23.5	1.0	Magenheimer et al. (1996)
High marsh				31.6	0.2	
Middle marsh				33.7	0.2	
Low marsh				35.1	0.2	
Dipper Harbour	New Brunswick	2011–2012	SC	23.7	0.1	Chmura et al. (2016)
Kouchibouguac				13.7	0.0	
Creek Bank	Virginia	1981–1983	SC	18.7	0.9	Bartlett et al. (1985)
High marsh				22.6	0.3	
Short <i>Spartina</i>				26.3	1.0	
Site 1	Virginia	1983–1984	SC	5.1	13.7	Bartlett et al. (1987)
Site 2		1983–1984	SC	12.8	16.8	
Site 3		1983–1984	SC	16.6	4.2	
Sweet Hall	Virginia	1996–1997	SC	0.25	72.0	Neubauer et al. (2000)
C ₃ Ambient CO ₂	Maryland	1998–1999	SC	6.8	3.5	Marsh et al. (2005)
C ₄ Ambient CO ₂	Maryland	1998–1999	SC	6.8	2.5	
Tidal freshwater marsh	Delaware	2007	SC	0.25	20.0	Weston et al. (2014)
Oligohaline marsh		2008		0.25	24.0	
Mesohaline marsh		2007		2.5	123.0	
		2008		2.5	87.0	
		2007		10	-5.0	
		2008		10	-2.0	
Wildlife	Maryland	2008	SC	11.6	23.0	Poffenbarger et al. (2011)
Barbados	Maryland	2008	SC	12.9	24.0	

Continued on next page



(Continued)

Table 15A.2. Tidal Wetland Methane Flux by Discrete Static Chamber Data or Continuous Eddy Covariance ^a Data						
Site Name	Location	Year	EC/SC	Salinity (PSU ^b)	CH ₄ Flux (g C per m ² per year) ^c	Reference
Vegetated low marsh	New Jersey	2012	SC	5	4.3	Reid et al., (2013)
Mud flat		2012	SC	5	3.8	
Fox Creek Marsh	Maryland	2013–2014	SC	10	79.1	Mueller et al. (2016)
Kirkpatrick Marsh				10	3.9	
				10	0.8	
				10	10.1	
				10	3.4	
				10	2.3	
GI Near Bank	North Carolina	1990–1991	SC	0.25	6.2	Kelley et al. (1995)
GI Far Bank				0.25	4.3	
UF Near Bank				0.25	3.8	
UF Far Bank				0.25	2.6	
Lower site	North Carolina	1994–1995	SC	0.25	1.0	Meronigal and Schlesinger (2002)
Upper site				0.25	1.4	
Upper	Georgia	2006–2007	SC	0.2	0.8	Krauss and Whitbeck (2011)
Middle	Georgia	2006–2007	SC	1.3	1.0	
Lower	Georgia	2006–2007	SC	4.7	1.0	
Georgia Coastal Ecosystems LTER ^d	Georgia	2008–2009	SC	1	69.8	Segarra et al. (2013)
Brookgreen Gardens	South Carolina	2009	SC	0.05	42.0	Neubauer et al. (2013)
Gulf of Mexico						
Fresh	Louisiana	1980–1981	SC	0.4	160.0	DeLaune et al. (1983)
Brackish				1.8	73.0	
Salt Marsh				18.1	4.3	

Continued on next page



(Continued)

Table 15A.2. Tidal Wetland Methane Flux by Discrete Static Chamber Data or Continuous Eddy Covariance ^a Data						
Site Name	Location	Year	EC/SC	Salinity (PSU ^b)	CH ₄ Flux (g C per m ² per year) ^c	Reference
Brackish marsh Freshwater marsh	Louisiana	2012	EC	9.15	10.4	Holm et al. (2016)
		2012	EC	0.23	47.3	
		2013	EC	0.23	46.2	
Brackish marsh Freshwater marsh	Louisiana	2012–2013	EC	9.15	11.1	Krauss et al. (2016)
			SC	9.15	49.6	
			EC	0.23	47.1	
			SC	0.23	91.9	
Week’s Bay Dog River Dauphin Island	Alabama	2012–2013	SC	2.3	7.9	Wilson et al. (2015)
				4.7	3.9	
				20.7	4.3	

Notes

- a) CH₄, methane; CO₂, carbon dioxide; SC, static chamber; EC, eddy covariance; g C, grams of carbon.
- b) Salinity values in bold indicate porewater salinity; otherwise, channel salinity is reported (where PSU = practical salinity units). When salinity was not reported for tidal freshwater wetlands, a value of 0.25 was assigned, which represents the midpoint of their salinity range (0 to 0.5) by definition.
- c) Positive values = atmospheric CH₄ source. Negative values = atmospheric CH₄ sink. Annual estimate provided.
- d) LTER, Long-term ecological research.



Table 15A.3. Estuarine Carbon Dioxide Outgassing (Emissions) for the U.S. Pacific Coast, Atlantic Coast, ^a and Gulf of Mexico Regions ^{b,c}						
System Name	Location	Subregion	Source	CO ₂ Flux (g C per m ² per year) ^c	CO ₂ Flux Integral (Tg C per year)	
Pacific Coast: Northwest						
Columbia River	Oregon, WA	Northwest	Evans et al. (2012)	12	NA ^d	
Atlantic Coast: Gulf of Maine (GOM) Subregion^a						
Bellamy Estuary	Massachusetts, USA	GOM	Hunt et al. (2011)	55		
Cocheco Estuary	Massachusetts, USA	GOM	Hunt et al. (2011)	44		
Great Bay	Massachusetts, USA	GOM	Hunt et al. (2011)	43		
Kennebec Estuary	Massachusetts, USA	GOM	Hunt et al. (2014)	30		
Little Bay	Massachusetts, USA	GOM	Hunt et al. (2011)	48		
Oyster Estuary	Massachusetts, USA	GOM	Hunt et al. (2011)	48		
Parker River	Massachusetts, USA	GOM	Raymond and Hopkinson (2003)	13		
				Mean	40	0.22
				Standard error	5	0.03
Atlantic Coast: Mid-Atlantic Bight (MAB) Subregion^a						
Delaware River	Delaware/ New Jersey, USA	MAB	Joeseof et al. (2015)	29		
York River	Virginia, USA	MAB	Raymond et al. (2000)	67		
				Mean	48	1.0
				Standard error	19	0.4
Atlantic Coast: South Atlantic Bight (SAB) Subregion^a						
Altamaha Sound	Georgia, USA	SAB	Jiang et al. (2008)	322		
Doboy Sound	Georgia, USA	SAB	Jiang et al. (2008)	143		
Duplin River	Georgia, USA	SAB	Wang and Cai (2004)	256		
Neuse River	N. Carolina, USA	SAB	Crosswell et al. (2012); Crosswell et al. (2014)	-68		
Pamlico Sound	N. Carolina, USA	SAB	Crosswell et al. (2014)	-180		
Sapelo Sound	Georgia, USA	SAB	Jiang et al. (2008)	126		

Continued on next page



(Continued)

Table 15A.3. Estuarine Carbon Dioxide Outgassing (Emissions) for the U.S. Pacific Coast, Atlantic Coast,^a and Gulf of Mexico Regions^{b,c}					
System Name	Location	Subregion	Source	CO₂ Flux (g C per m² per year)^c	CO₂ Flux Integral (Tg C per year)
Satilla River	Georgia, USA	SAB	Cai and Wang (1998)	510	
				Mean	158
				Standard error	1.1
Atlantic Coast Totals					
				Mean	3.1
				Standard error	1.1
Gulf of Mexico (GMx)					
Atchafalaya River	Louisiana, USA	GMx	Huang et al. (2015)	504	
Florida Bay	Florida, USA	GMx	Zhang and Fischer (2014)	47	
Mission-Aransas Estuary	Texas, USA	GMx	Yao and Hu (2017)	149	
Mississippi River	Louisiana, USA	GMx	Huang et al. (2015)	444	
Shark River	Florida, USA	GMx	Kone and Borges (2008)	192	
Terrebonne Bay	Louisiana, USA	GMx	Huang et al. (2015)	-4	
				Mean	6.8
				Standard error	2.6
Atlantic Coast and Gulf of Mexico Totals					
				Mean	9.9
				Standard error	2.8

Notes

- a) The Atlantic Coast is subdivided into three subregions: Gulf of Maine, Mid-Atlantic Bight, and South Atlantic Bight.
- b) Positive values = atmospheric CO₂ source; negative values = atmospheric CO₂ sink. A spatially representative annual CO₂ flux integral is not calculated for the Pacific Coast due to the presence of only one study and limited seasonal sampling.
- c) CO₂, carbon dioxide; g C, grams of carbon; Tg C, teragrams of carbon.
- d) NA (or blank): Not assessed.



16 Coastal Ocean and Continental Shelves

Lead Author

Katja Fennel, Dalhousie University

Contributing Authors

Simone R. Alin, NOAA Pacific Marine Environmental Laboratory; Leticia Barbero, NOAA Atlantic Oceanographic and Meteorological Laboratory; Wiley Evans, Hakai Institute; Timothée Bourgeois, Dalhousie University; Sarah R. Cooley, Ocean Conservancy; John Dunne, NOAA Geophysical Fluid Dynamics Laboratory; Richard A. Feely, NOAA Pacific Marine Environmental Laboratory; Jose Martin Hernandez-Ayon, Autonomous University of Baja California; Chuanmin Hu, University of South Florida; Xinpeng Hu, Texas A&M University, Corpus Christi; Steven E. Lohrenz, University of Massachusetts, Dartmouth; Frank Muller-Karger, University of South Florida; Raymond G. Najjar, The Pennsylvania State University; Lisa Robbins, University of South Florida; Joellen Russell, University of Arizona; Elizabeth H. Shadwick, College of William & Mary; Samantha Siedlecki, University of Connecticut; Nadja Steiner, Fisheries and Oceans Canada; Daniela Turk, Dalhousie University; Penny Vlahos, University of Connecticut; Zhaohui Aleck Wang, Woods Hole Oceanographic Institution

Acknowledgments

Raymond G. Najjar (Science Lead), The Pennsylvania State University; Marjorie Friederichs (Review Editor), Virginia Institute of Marine Science; Erica H. Ombres (Federal Liaison), NOAA Ocean Acidification Program; Laura Lorenzoni (Federal Liaison), NASA Earth Science Division

Recommended Citation for Chapter

Fennel, K., S. R. Alin, L. Barbero, W. Evans, T. Bourgeois, S. R. Cooley, J. Dunne, R. A. Feely, J. M. Hernandez-Ayon, C. Hu, X. Hu, S. E. Lohrenz, F. Muller-Karger, R. G. Najjar, L. Robbins, J. Russell, E. H. Shadwick, S. Siedlecki, N. Steiner, D. Turk, P. Vlahos, and Z. A. Wang, 2018: Chapter 16: Coastal ocean and continental shelves. In *Second State of the Carbon Cycle Report (SOCCR2): A Sustained Assessment Report* [Cavallaro, N., G. Shrestha, R. Birdsey, M. A. Mayes, R. G. Najjar, S. C. Reed, P. Romero-Lankao, and Z. Zhu (eds.)]. U.S. Global Change Research Program, Washington, DC, USA, pp. 649-688, <https://doi.org/10.7930/SOCCR2.2018.Ch16>.



KEY FINDINGS

1. Observing networks and high-resolution models are now available to construct coastal carbon budgets. Efforts have focused primarily on quantifying the net air-sea exchange of carbon dioxide (CO₂), but some studies have estimated other key fluxes, such as the exchange between shelves and the open ocean.
2. Available estimates of air-sea carbon fluxes, based on more than a decade of observations, indicate that the North American margins act as a net sink for atmospheric CO₂. This net uptake is driven primarily by fluxes in the high-latitude regions. The estimated magnitude of the net flux is 160 ± 80 teragrams of carbon per year (*medium confidence*) for the North American Exclusive Economic Zone, a number that is not well constrained.
3. The increasing concentration of CO₂ in coastal and open-ocean waters leads to ocean acidification. Corrosive conditions in the subsurface occur regularly in Arctic coastal waters, which are naturally prone to low pH, and North Pacific coastal waters, where upwelling of deep, carbon-rich waters has intensified and, in combination with the uptake of anthropogenic carbon, leads to low seawater pH and aragonite saturation states in spring, summer, and early fall (*very high confidence, very likely*).
4. Expanded monitoring, more complete syntheses of available observations, and extension of existing model capabilities are required to provide more reliable coastal carbon budgets, projections of future states of the coastal ocean, and quantification of anthropogenic carbon contributions.

Note: Confidence levels are provided as appropriate for quantitative, but not qualitative, Key Findings and statements.

16.1 Introduction

Along ocean margins, the atmospheric, terrestrial, sedimentary, and deep-ocean carbon reservoirs meet, resulting in quantitatively significant carbon exchanges. Anthropogenic activities lead to secular trends in these exchanges. The drivers underlying these trends include rising atmospheric carbon dioxide (CO₂) levels, climate-driven changes in atmospheric forcing (e.g., winds and heat fluxes) and the hydrological cycle (e.g., freshwater input from rivers), and changes in riverine and atmospheric nutrient inputs from agricultural activities and fossil fuel burning. The collective impact of these factors on carbon processing and exchanges along ocean margins is complex and difficult to quantify (Regnier et al., 2013).

This chapter focuses on two particularly pressing issues within the much broader topic of carbon cycling along ocean margins: 1) the uptake of atmospheric CO₂ and subsequent export to the deep ocean and 2) patterns and drivers of coastal ocean acidification. The first is relevant to overall

quantification of the ocean's uptake of CO₂. The second is directly relevant to coastal ecosystem health, fisheries, and aquaculture.

Two different terms will be used here when referring to ocean margins: 1) the coastal ocean, defined in this report as nonestuarine waters within 200 nautical miles (370 km) of the coast, and 2) continental shelves, which refer to the submerged margins of the continental plates, operationally defined here as regions with water depths shallower than 200 m (indicated in gray in Figure 16.1, p. 651). Although the two definitions overlap, there are important reasons for considering both. Along passive margins with broad shelves like the North American Atlantic Coast, the continental shelf is the relevant spatial unit for discussing carbon fluxes. Along active margins with narrow shelves, such as the North American Pacific Coast, a larger region than just the shelf needs to be considered to meaningfully discuss coastal carbon dynamics. The 370-km limit chosen here to define the coastal ocean was recommended by Hales et al. (2008) and corresponds to the Exclusive

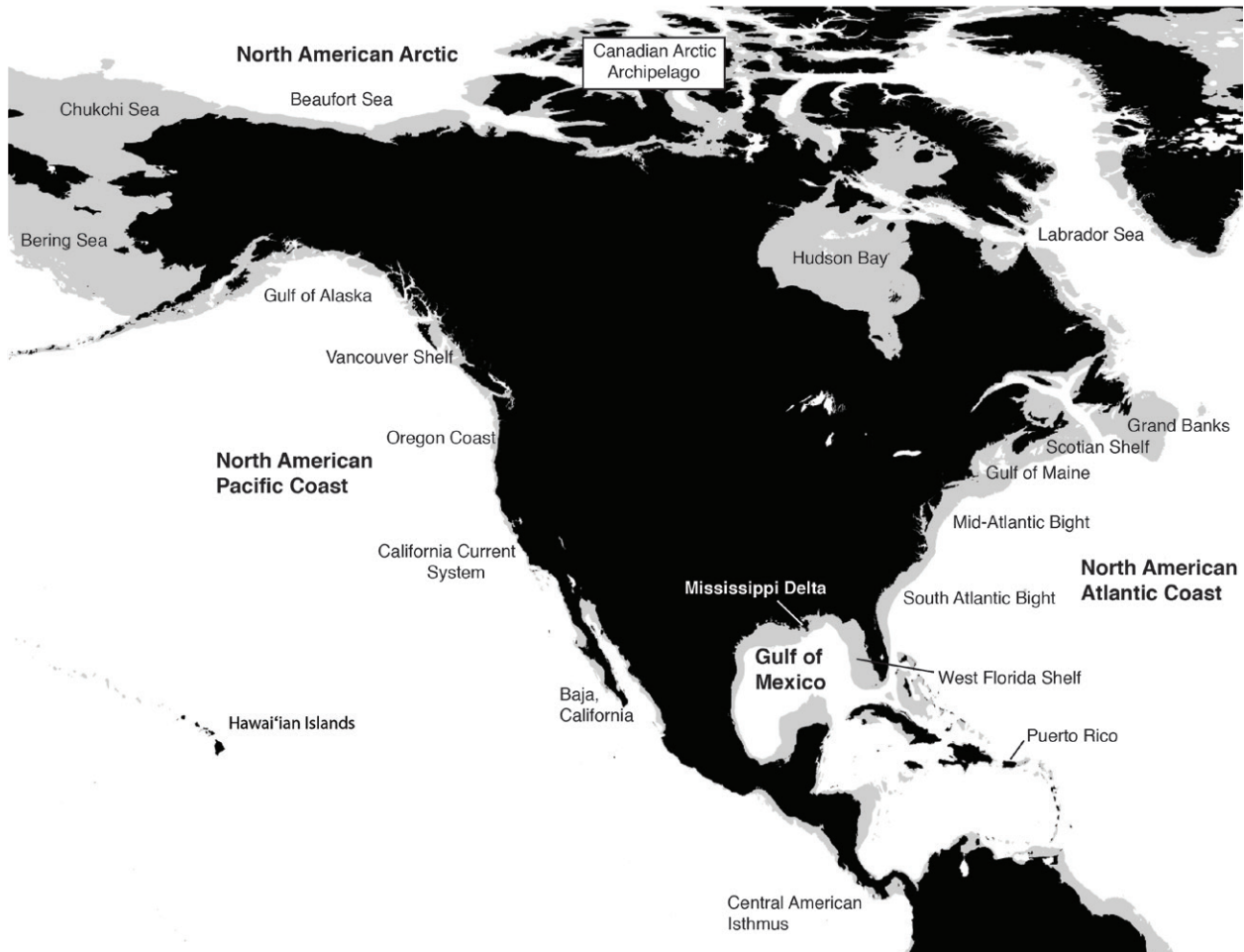


Figure 16.1. North American Shelf Seas. These seas (in gray) are defined as waters with bottom depths less than 200 m.

Economic Zone (EEZ, the region where a nation can claim exclusive rights for fishing, drilling, and other economic activities). Worth noting here is that ocean CO₂ uptake or loss is not credited to any nation under Intergovernmental Panel on Climate Change (IPCC) CO₂ accounting; instead, ocean uptake is viewed as an internationally shared public commons.

This chapter builds on and extends several previous synthesis and planning activities, including a report by the North American Continental Margins Working Group (Hales et al., 2008), the *First State of the Carbon Cycle Report* (SOCCR1; CCSP 2007; Chavez et al., 2007), and activities within the North

American coastal interim synthesis (Benway et al., 2016; Alin et al., 2012; Najjar et al., 2012; Mathis and Bates 2010; Robbins et al., 2009). SOCCR1 (Chavez et al., 2007) concluded that carbon fluxes for North American ocean margins were not well quantified because of insufficient observations and the complexity and highly localized spatial variability of coastal carbon dynamics. The report was inconclusive as to whether North American coastal waters act as an overall source or sink of atmospheric CO₂.

The objective here is to provide a review and synthesis of recent findings with respect to coastal carbon uptake and ocean acidification for the margins of North America. Summarized first are the key



variables and fluxes relevant to carbon budgets for coastal waters, followed by descriptions of 1) the mechanisms by which carbon can be removed from the atmospheric reservoir and 2) the means for quantifying the resulting carbon removal (see Section 16.2, this page). Next presented is available research relevant to carbon budgets for North American coastal waters by region, along with an assessment of whether enough information is available to derive robust estimates of carbon export to the open ocean (see Section 16.3, p. 655). Climate-driven trends in coastal carbon fluxes and coastal ocean acidification are then discussed (see Section 16.4, p. 669), followed by conclusions (see Section 16.5, p. 673).

16.2 Current Understanding of Carbon Fluxes and Stocks

Carbon is present in various inorganic and organic forms in coastal waters (see Figure 16.2, p. 653). Dissolved inorganic species include aqueous CO_2 (a combination of dissolved CO_2 and carbonic acid), bicarbonate and carbonate ions, and methane (CH_4); the first three carbon species are collectively referred to as dissolved inorganic carbon or DIC. The major particulate inorganic species is calcium carbonate (CaCO_3), also referred to as particulate inorganic carbon (PIC). Carbon is also present in various dissolved and particulate organic forms (DOC and POC). In shelf waters, the reduced carbon pool or total organic carbon pool (TOC) represents roughly 2% to 5% of the total carbon stock (Liu et al., 2010), and DOC constitutes more than 90% to 95% of this TOC (Vlahos et al., 2002).

Carbon is constantly transferred among these different pools and exchanged across the interfaces that demarcate coastal waters: the land-ocean interface, the air-sea interface, and the interface between coastal and open-ocean waters (see Figure 16.2, p. 653). The internal carbon transformations within coastal regions include photosynthetic primary production, respiration, transfers between lower and higher trophic levels of the food web, exchanges between sediment and overlying water, biogeochemical processes in the sediment, and the formation and dissolution of CaCO_3 . Major internal

transformations are the conversion of DIC into organic carbon (POC and DOC), through primary production, and respiration throughout the water column, returning most of the organic carbon into inorganic forms (primarily DIC). Some POC settles out of the water column and becomes incorporated into the sediments where most of this material is respired through a range of different redox processes that produce DIC and, under certain circumstances, CH_4 (i.e., in the relative absence of electron acceptors other than CO_2). Both DIC and CH_4 are released back into the overlying water. POC that is not respired (referred to as refractory POC) can be buried in sediments and stored for a very long time. Some organisms form internal or external body structures of CaCO_3 , which either dissolve or become incorporated into the sediments and are buried. This discussion will refer to long-term storage of buried POC and PIC in coastal sediments as permanent burial.

A major carbon exchange process along the ocean margin is the flux of CO_2 across the air-sea interface. The annual cycle of this flux is driven by 1) seawater warming and cooling, which affects CO_2 solubility; 2) the under- or oversaturation of CO_2 resulting from primary production, respiration, and CaCO_3 precipitation and dissolution; 3) the transport of DIC to and from the ocean surface (e.g., upwelling and convection); and 4) factors that influence the resistance to gas exchange across the air-sea interface (e.g., winds, sea ice extent, and surface films). The annual cycles of primary production, respiration, and air-sea CO_2 flux tend to be of larger magnitude and more variable in coastal waters than in the open ocean (Bauer et al., 2013; Liu et al., 2010; Muller-Karger et al., 2005; Thunell et al., 2007; Xue et al., 2016) and more pronounced in high latitudes. Other important exchange fluxes are organic and inorganic carbon inputs from land via rivers and estuaries (see Ch. 15: Tidal Wetlands and Estuaries, p. 596), from tidal wetlands, and exchanges between the coastal and open oceans across the continental shelf break or the operationally defined open-ocean boundary of the coastal ocean. Net removal of carbon from direct interaction with the atmospheric

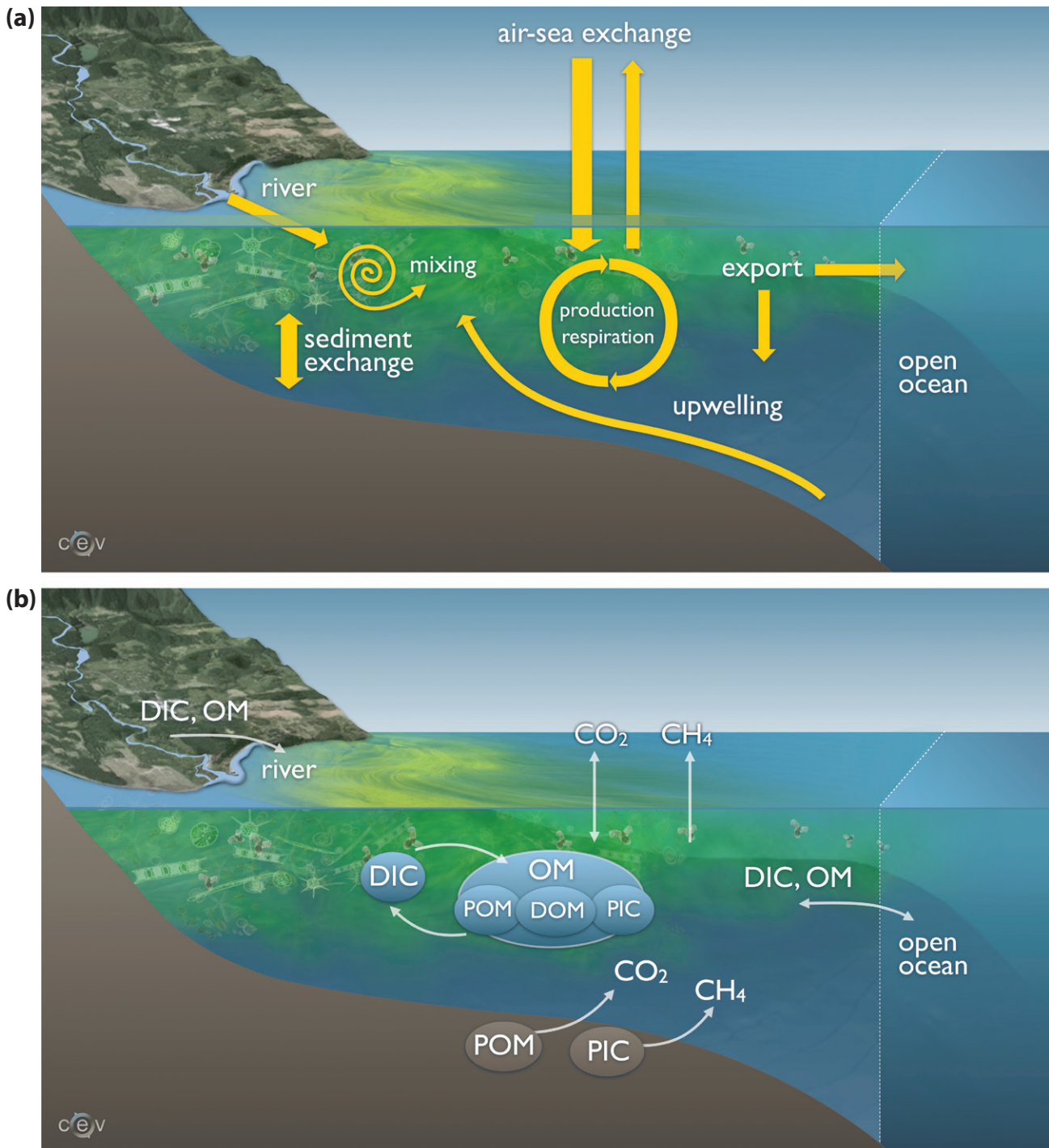


Figure 16.2. Major Coastal Carbon Pools and Fluxes. (a) Carbon in various forms (e.g., CO₂, carbon dioxide; CH₄, methane) is transferred among different pools and exchanged across interfaces between land, air, and ocean in coastal regions. (b) Carbon forms include dissolved inorganic carbon (DIC), organic matter (OM), particulate organic matter (POM), dissolved organic matter (DOM), and particulate inorganic matter (PIC). [Figure sources: Simone Alin, National Oceanic and Atmospheric Administration; Hunter Hadaway, University of Washington Center for Environmental Visualization; and Katja Fennel, Dalhousie University.]



reservoir can occur by export to the deep ocean or by permanent burial in coastal sediments.

Although continental shelves make up only 7% to 10% of the global ocean surface area, they are estimated to contribute up to 30% of primary production, 30% to 50% of inorganic carbon burial, and 80% of organic carbon burial (Dunne et al., 2007; Gattuso et al., 1998). As such, continental shelves have been argued to contribute disproportionately to the oceanic uptake of CO₂ (Cai 2011; Liu et al., 2010; Muller-Karger et al., 2005).

Carbon export, referring to the flux of organic and inorganic carbon from coastal waters to the deep ocean, can occur through the so-called “Continental Shelf Pump”—a term coined by Tsunogai et al. (1999) after they observed a large uptake of atmospheric CO₂ in the East China Sea. There are two distinct mechanisms underlying the Continental Shelf Pump (Fennel 2010). The first is physical in nature and thought to operate in mid- and high-latitude systems. In winter, shelf water is cooled more strongly than surface water in the adjacent open ocean because the former is not subject to deep convection. The colder shelf water is denser and experiences a larger influx of atmospheric CO₂; both density and the solubility of CO₂ increase with decreasing temperature. If this dense and carbon-rich water is transported off the shelf, it will sink due to its higher density, and the associated carbon will be exported to the deep ocean. The second mechanism relies on biological processes that concentrate carbon below the seasonal pycnocline (i.e., photosynthetic production of organic carbon and subsequent sinking). If the carbon-rich water below the seasonal pycnocline is moved off the shelf horizontally, carbon potentially could be exported if this water is transported or mixed below the seasonal thermocline. The depth to which the shelf-derived carbon can be exported will be different for POC, which will sink, and DOC and DIC, which primarily would be advected laterally. Both mechanisms for carbon export critically depend on physical transport of carbon-rich water off the shelf.

Carbon export flux from coastal waters to the deep ocean cannot be quantified easily or accurately through direct observation. Thus, the only available estimates of such export are indirect, using mass balances of POC and dissolved oxygen (Hales et al., 2006), mass balances of DOC (Barrón and Duarte 2015; Vlahos et al., 2002), mass balances of TOC and DIC (Najjar et al., 2018), and model estimates (Izett and Fennel 2018a, 2018b; Bourgeois et al., 2016; Fennel and Wilkin 2009; Fiechter et al., 2014; Mannino et al., 2016; Turi et al., 2014; Xue et al., 2013). If the total carbon inventory in a coastal system can be considered constant over a sufficiently long timescale (i.e., on the order of years), inferring carbon export is possible from using the sum of all other exchange fluxes across the system’s interfaces over that same period. Export to the open ocean must balance the influx of carbon from land and wetlands, its net exchange across the air-sea interface, lateral exchange caused by advection, and any removal through permanent sediment burial. The accuracy of the inferred export flux directly depends on the accuracy of the other flux estimates and of the assumption of a constant carbon inventory. Quantifying internal transformation processes (e.g., respiration and primary and secondary production) does not directly enter this budgeting approach but can elucidate the processes that drive fluxes across interfaces.

Current estimates of carbon fluxes across coastal interfaces come with significant uncertainties (Regnier et al., 2013; Birdsey et al., 2009). These uncertainties are caused by a combination of 1) small-scale temporal and spatial variability, which is undersampled by currently available means of direct observation, and 2) regional heterogeneity, which makes scaling up observations from one region to larger areas difficult. Contributing to variability in regional carbon budgets and export are geographical differences arising from variations in shelf width, the presence or absence of large rivers, seasonal ice cover, and latitude through its modulation of annual temperature and productivity cycles and of hydrography due to the rotation of the Earth (Sharples et al., 2017). Section 16.3, p. 655, describes the regional characteristics of North American



coastal waters and how these characteristics influence carbon dynamics. Available estimates of carbon fluxes are compiled in an attempt to estimate export.

The motivation for quantifying permanent burial of carbon and export of carbon from coastal waters to the deep ocean is that both processes remove CO₂ from the atmospheric reservoir. A more relevant but harder to obtain quantity in this context is the burial or export of anthropogenic carbon. The anthropogenic component of a given carbon flux is defined as the difference between its preindustrial and present-day fluxes. Thus, present-day carbon fluxes represent a superposition of the anthropogenic flux component and the natural background flux. Only total fluxes—the sum of anthropogenic and background fluxes—can be observed directly. Distinction between anthropogenic fluxes and the natural background is difficult to assess for coastal ocean fluxes and has to rely on process-based arguments and models (Regnier et al., 2013). Observation-based estimates of the global open ocean's anthropogenic uptake have been made by Sabine et al. (2004), Sabine and Tanhua (2010), and Carter et al. (2017). Bourgeois et al. (2016) were the first to estimate coastal anthropogenic carbon uptake in their global model. Their estimates are presented in some detail in Section 16.3.5, p. 665.

16.3 Coastal Carbon Fluxes Around North America

16.3.1 North American Atlantic Coast

The North American Atlantic Coast borders on a wide, geologically passive margin shelf that extends from the southern tip of Florida to the continental shelf of the Labrador Sea (see Figure 16.1, p. 651). The shelf is several hundreds of kilometers wide in the north (Labrador shelf and Grand Banks) but narrows progressively toward the south in the Middle Atlantic Bight (MAB), which is between Cape Cod and Cape Hatteras, and the South Atlantic Bight (SAB), which is south of Cape Hatteras. The SAB shelf width measures only several tens of kilometers. Two major semi-enclosed bodies of water are the Gulf of Maine (GOM) and Gulf of

St. Lawrence. Important rivers and estuaries north of Cape Hatteras include the St. Lawrence River and Estuary, the Hudson River, Long Island Sound, Delaware Bay, and Chesapeake Bay. South of Cape Hatteras, the coastline is characterized by small rivers and marshes. The SAB is influenced by the Gulf Stream, which flows northeastward along the shelf edge before detaching at Cape Hatteras and meandering eastward into the open North Atlantic Ocean. North of Cape Hatteras, shelf circulation is influenced by the confluence of the southwestward-flowing fresh and cold shelf-break current (a limb of the Labrador Current) and the warm and salty Gulf Stream (Loder et al., 1998). Because shelf waters north of Cape Hatteras are sourced from the Labrador Sea, they are relatively cold, fresh, and carbon rich, while slope waters (those located between the shelf break and the northern wall of the Gulf Stream) are a mixture of Labrador Current and Gulf Stream water. Exchange between the shelf and open ocean across the shelf break is impeded by the presence of the Gulf Stream south of Cape Hatteras and by shelf-break jets and fronts north of Cape Hatteras.

Air-sea fluxes of CO₂ exhibit a large-scale latitudinal gradient along the North American Atlantic Coast and significant seasonal and interannual variability. The net flux on the Scotian Shelf remains controversial. Shadwick et al. (2010), combining *in situ* and satellite observations, reported a large source of CO₂ to the atmosphere of 8.3 ± 6.6 grams of carbon (g C) per m² per year. In contrast, Signorini et al. (2013) estimated a relatively large sink of atmospheric CO₂, 14 ± 3.2 g C per m² per year, when using *in situ* data alone and a much smaller uptake, 5.0 ± 4.3 g C per m² per year, from a combination of *in situ* and satellite observations. The open GOM is a weak net source of 4.6 ± 3.1 g C per m² per year according to Vandemark et al. (2011) but with significant interannual variability, while Signorini et al. (2013) estimate the region to be neutral. The shallow, tidally mixed GOM regions (i.e., Georges Bank and Nantucket Shoals) are thought to be sinks, however (see Table 16.1, p. 657; Signorini et al., 2013). The MAB and SAB are net sinks. Observation-based



estimates for the MAB include sinks of 13 ± 8.3 g C per m^2 per year (DeGrandpre et al., 2002) and 13 ± 3.2 g C per m^2 per year (Signorini et al., 2013). Estimates for the SAB include sinks of 5.8 ± 2.5 g C per m^2 per year (Jiang et al., 2008) and 8.2 ± 2.9 g C per m^2 per year (Signorini et al., 2013). The change from neutral or occasional net source in the Scotian Shelf and GOM regions to net sink in the MAB arises because the properties of shelf water are modified during its southwestward flow by air-sea exchange, inflows of riverine and estuarine waters (Salisbury et al., 2008b, 2009), and exchange with the open North Atlantic across the shelf break (Cai et al., 2010a; Wang et al., 2013). Outgassing of CO_2 on the Scotian Shelf is driven primarily by warming of cold, carbon-rich shelf water, which still carries a pronounced signature of its Labrador Sea origin. The GOM, which is deeper than the Scotian Shelf and the MAB and connected to the open North Atlantic through a relatively deep channel, is characterized by a mixture of cold, carbon-rich shelf waters and warmer, saltier slope waters. Shelf water in the MAB is sourced from the GOM and thus is a mixture of shelf and slope water.

Shelf water in the SAB is distinct from that in the MAB and has almost no trace of Labrador Current water; instead, its characteristics are similar to those of the Gulf Stream, but its carbon signature is modified by significant organic and inorganic carbon and alkalinity inputs from coastal marshes (Cai et al., 2003; Jiang et al., 2013; Wang and Cai 2004; Wang et al., 2005). Herrmann et al. (2015) estimated that 59% of the 3.4 teragrams of carbon (Tg C) per year of organic carbon exported from U.S. East Coast estuaries is from the SAB. The subsequent respiration of this organic matter and direct outgassing of marsh-derived carbon make the nearshore regions a significant CO_2 source almost year-round. Despite the carbon inputs from marshes, uptake of CO_2 on the mid- and outer shelf during the winter months is large enough to balance CO_2 outgassing in the other seasons and on the inner shelf, making the SAB overall a weak net sink (Jiang et al., 2008).

North of Cape Hatteras, CO_2 dynamics are characterized by strong seasonality with solubility-driven uptake by cooling in winter and biologically driven uptake in spring followed by outgassing in summer and fall due to warming and respiration of organic matter (DeGrandpre et al., 2002; Shadwick et al., 2010, 2011; Signorini et al., 2013; Vandemark et al., 2011; Wang et al., 2013). Hydrography and CO_2 dynamics on the Scotian Shelf are influenced by the significant freshwater input from the St. Lawrence River. Riverine inputs of carbon and nutrients are relatively small in the GOM but can cause local phytoplankton blooms, CO_2 drawdown, and low-pH conditions (Salisbury et al., 2008a, 2009). Riverine and estuarine inputs become more important in the MAB with discharges from the Chesapeake Bay and the Delaware, Hudson, and Connecticut rivers (Wang et al., 2013). South of Cape Hatteras, seasonal phytoplankton blooms do not occur regularly and biologically driven CO_2 uptake is less pronounced than that further north (Wang et al., 2013), although sporadic phytoplankton blooms do occur because of intrusions of high-nutrient subsurface Gulf Stream water (Wang et al., 2005, 2013). The influence of riverine inputs is small and localized in the SAB (Cai and Wang 1998; Wang and Cai 2004; Wang et al., 2005).

Regional biogeochemical models reproduce the large-scale patterns of air-sea CO_2 flux with oceanic uptake increasing from the SAB to the GOM (Cahill et al., 2016; Fennel et al., 2008; Previdi et al., 2009). These model studies elucidate the magnitude and sources of interannual variability as well as long-term trends in air-sea CO_2 fluxes. Previdi et al. (2009) investigated opposite phases of the North Atlantic Oscillation (NAO) and found that the simulated air-sea flux in the MAB and GOM was 25% lower in a high-NAO year compared with that in a low-NAO year. In the MAB, the decrease resulted primarily from changes in wind forcing, while in the GOM, changes in surface temperature and new production were more important. Cahill et al. (2016) investigated the impact of future, climate-driven warming and trends in atmospheric forcing (primarily wind) on air-sea CO_2 flux (without considering the



Table 16.1. Regional Estimates of Net Air-Sea Carbon Dioxide Exchange from Observations and Regional Models^{a,b}

Region	Area (km ²)	Air-Sea Exchange		Observation-Based Estimate or Model	Reference
		g C per m ² per year ^{a,b}	Tg C per year ^{a,b}		
North American Atlantic Coast (NAAC)					
Scotian Shelf	2.2 × 10 ⁵	8.3 ± 6.6	1.8	Combination of <i>in situ</i> and satellite observations (10-year average, 1999–2008)	Shadwick et al. (2010)
	1.28 × 10 ⁵	−14 ± 3.2	−1.9	Observation-based estimate (reference year, 2004)	Signorini et al. (2013); using Ho et al. (2011) gas transfer param.
		−5.0 ± 4.3	−0.64	Combination of <i>in situ</i> and satellite observations (reference year, 2004)	Signorini et al. (2013); using Ho et al. (2011) gas transfer param.
	1.2 × 10 ⁵	−28 ± 0.72	−3.3	Model (2-year average, 2004–2005)	Fennel and Wilkin (2009)
Gulf of Maine (without Georges Bank and Nantucket Shoals)	1.28 × 10 ⁵	0.48 ± 2.6	0.061	Observation-based estimate (reference year, 2004)	Signorini et al. (2013); using Ho et al. (2011) gas transfer param.
		0.12 ± 0.96	0.015	Combination of <i>in situ</i> and satellite observations (reference year, 2004)	Signorini et al. (2013); using Ho et al. (2011) gas transfer param.
		4.6 ± 3.1	0.58	Observation-based estimate (5-year mean, 2004–2008)	Vandemark et al. (2011)
Georges Bank and Nantucket Shoals	0.58 × 10 ⁵	−8.5 ± 2.6	−0.49	Observation-based estimate (reference year, 2004)	Signorini et al. (2013); using Ho et al. (2011) gas transfer param.
		−16 ± 2.9	−0.95	Combination of <i>in situ</i> and satellite observations (reference year, 2004)	Signorini et al. (2013); using Ho et al. (2011) gas transfer param.
Gulf of Maine (with Georges Bank and Nantucket Shoals)	1.7 × 10 ⁵	−20 ± 4.9	−3.4	Model (2-year average, 2004–2005)	Fennel and Wilkin (2009)
	0.87 × 10 ⁵	−27 ± 8.4	−1.9	Model (4-year average, 2004–2007)	Cahill et al. (2016)

Continued on next page



(Continued)

Table 16.1. Regional Estimates of Net Air-Sea Carbon Dioxide Exchange from Observations and Regional Models ^{a,b}					
Region	Area (km ²)	Air-Sea Exchange		Observation-Based Estimate or Model	Reference
		g C per m ² per year ^{a,b}	Tg C per year ^{a,b}		
Mid-Atlantic Bight (MAB)	1.25 × 10 ⁵	-13 ± 8.3	-1.6	Observation-based estimate	DeGrandpre et al. (2002)
		-14	-1.8	Model (2004)	Fennel et al. (2008)
	0.93 × 10 ⁵	-13 ± 3.2	-1.2	Observation-based estimate (reference year, 2004)	Signorini et al. (2013); using Ho et al. (2011) gas transfer param.
		-21 ± 2.3	-2.0	Combination of <i>in situ</i> and satellite observations (reference year, 2004)	Signorini et al. (2013); using Ho et al. (2011) gas transfer param.
	0.86 × 10 ⁵	-11 ± 2.6	-0.92	Model (2-year average, 2004–2005)	Fennel and Wilkin (2009)
1.15 × 10 ⁵	-14 ± 2.4	-1.7	Model (4-year average, 2004–2007)	Cahill et al. (2016)	
South Atlantic Bight (SAB)	1.02 × 10 ⁵	-5.8 ± 2.5	-0.59	Observation-based estimate	Jiang et al. (2008)
		-8.2 ± 2.9	-0.83	Observation-based estimate (reference year, 2004)	Signorini et al. (2013); using Ho et al. (2011) gas transfer param.
		-8.0 ± 1.9	-0.82	Combination of <i>in situ</i> and satellite observations (reference year, 2004)	Signorini et al. (2013); using Ho et al. (2011) gas transfer param.
	0.92 × 10 ⁵	-6 ± 2.4	-0.55	Model (4-year average, 2004–2007)	Cahill et al. (2016)
Gulf of Mexico (GMx)					
Whole Gulf of Mexico	15.6 × 10 ⁵	-2.3 ± 0.96	-3.6	Observation-based estimate	Robbins et al. (2014)
		-8.5 ± 6.5	-13	Model (7-year average, 2005–2010)	Xue et al. (2016)
Open Gulf of Mexico	10.1 × 10 ⁵	-5.8 ± 0.84	-5.8	Observation-based estimate	Robbins et al. (2014)
		-12 ± 5.5	-13	Model (7-year average, 2005–2010)	Xue et al. (2016)
West Florida Shelf	1.5 × 10 ⁵	4.4 ± 1.3	0.67	Observation-based estimate	Robbins et al. (2014)
		4.6 ± 0.58	0.68	Model (7-year average, 2005–2010)	Xue et al. (2016)

Continued on next page



(Continued)

Region	Area (km ²)	Air-Sea Exchange		Observation-Based Estimate or Model	Reference
		g C per m ² per year ^{a,b}	Tg C per year ^{a,b}		
Northern Gulf of Mexico	1.5 × 10 ⁵	-5.3 ± 4.4	-0.79	Observation-based estimate	Robbins et al. (2014)
		-3.8 ± 8.9	-0.58	Model (7-year average, 2005–2010)	Xue et al. (2016)
	unknown	-11 ± 44		Observation-based estimate	Huang et al. (2015)
	unknown	-13 ± 3.6		Combination of <i>in situ</i> and satellite observations	Lohrenz et al. (2018)
Western Gulf of Mexico	0.8 × 10 ⁵	2.2 ± 0.6	0.17	Observation-based estimate	Robbins et al. (2014)
		4.1 ± 3.8	0.33	Model (7-year average, 2005–2010)	Xue et al. (2016)
Mexico Shelf	1.8 × 10 ⁵	-1.1 ± 0.6	-0.19	Observation-based estimate	Robbins et al. (2014)
		-2.3 ± 4.2	-0.41	Model (7-year average, 2005–2010)	Xue et al. (2016)
North America Pacific Coast (NAPC)					
Gulf of Alaska	3 × 10 ⁶	-11	-36	Observations, climatology of 1991–2011, 0 to 400 km offshore	Evans and Mathis (2013)
British Columbia coastal ocean		-35		Observations, 1995–2001	Evans et al. (2012)
British Columbia Vancouver Island shelf		-6		Model, annual average	Ianson and Allen (2002)
Oregon Shelf		-3.6 ± 82		Observations inshore of 200-m isobath	Evans et al. (2011)
Oregon Shelf		-88		Observations	Hales et al. (2005)
50° to 22°N	1.76 × 10 ⁶	-7.9	-14	Satellite-based prediction of <i>p</i> CO ₂ and satellite-based wind speed, within 370 km of coast	Hales et al. (2012)
35° to 40°N			0.6	Model, 0 to 100 km from coast, 1999–2005	Fiechter et al. (2014)
40° to 45°N			-0.4	Model, 0 to 100 km from the coast, 1999–2005	Fiechter et al. (2014)

Continued on next page



(Continued)

Table 16.1. Regional Estimates of Net Air-Sea Carbon Dioxide Exchange from Observations and Regional Models^{a,b}

Region	Area (km ²)	Air-Sea Exchange		Observation-Based Estimate or Model	Reference
		g C per m ² per year ^{a,b}	Tg C per year ^{a,b}		
30° to 46°N	1.49 × 10 ⁶	0.6 ± 2.4	0.9±3.6	Model, 0 to 800 km from the coast, 12-year simulation with climatological forcing	Turi et al. (2014)
North American Arctic (NAA)					
Chukchi Sea	2.9 × 10 ⁵	-15	-4.4	Observations	Evans et al. (2015b)
	5.95 × 10 ⁵	-175 ± 44	-38 ± 7	Observations	Bates et al. (2006)
	5.95 × 10 ⁵	-35	-12.1	Observations	Gao et al. (2012)
		-17 ± 17		Satellite-based prediction of pCO ₂ and satellite-based wind speed	Yasunaka et al. (2016)
Beaufort Sea (Amundsen Gulf)		-14		Observations	Shadwick et al. (2011)
Beaufort Sea (Cape Bathurst Polynya)		-44 ± 28		Observations	Else et al. (2013)
Beaufort Sea	9.2 × 10 ⁵	-4.4	-4.0	Observations	Evans et al. (2015b)
Beaufort Sea		-10 ± 15		Observations	Mucci et al. (2010)
Western Arctic Coastal Ocean	1.2 × 10 ⁶	-8.8 ± 4.8	-11 ± 5.7	Observations	Evans et al. (2015b)
Hudson Bay	7.32 × 10 ⁵	-3.2 ± 1.8	-0.58 ± 0.3	Observations	Else et al. (2008)
Bering Sea	6.94 × 10 ⁵	-9.6	-6.7	Observations	Cross et al. (2014a)
		-5.3	-3.7	Observations	Takahashi et al. (2009)

Notes

- a) Positive fluxes indicate a source to the atmosphere.
 b) C, carbon; CO₂, carbon dioxide; Tg, teragrams; g, grams; 1 Tg = 10¹² g.

atmospheric increase in CO₂). Their results suggest that warming and changes in atmospheric forcing have modest impacts on air-sea CO₂ flux in the MAB and GOM compared with that in the SAB where surface warming turns the region from a net sink into a net source of CO₂ to the atmosphere. Model studies also illustrate the effects of interactions between biogeochemical transformations in the sediment and the overlying water column on carbon fluxes. For example, Fennel et al. (2008) showed that the

effective alkalinity flux resulting from denitrification in sediments of the North American Atlantic Coast reduces the simulated ocean uptake of CO₂ by 6% compared to a simulation without sediment denitrification.

The passive-margin sediments along the Atlantic coast have not been considered an area of significant CH₄ release until recently (Brothers et al., 2013; Phrampus and Hornbach 2012; Skarke et al., 2014). Phrampus and Hornbach (2012) predicted that



massive seepage of CH₄ from upper-slope sediments is occurring in response to warming of intermediate-depth Gulf Stream waters. Brothers et al. (2013) and Skarke et al. (2014) documented widespread CH₄ plumes in the water column and attributed them to gas hydrate degradation. Estimated CH₄ efflux from the sediment in this region ranges from 1.5×10^{-5} to 1.8×10^{-4} Tg CH₄ per year, where the uncertainty range reflects different assumptions underlying the conversion from CH₄ plume observations to seepage rates. The fraction of the released CH₄ that escapes to the atmosphere remains uncertain (Phrampus and Hornbach 2012).

16.3.2 North American Pacific Coast

The North American Pacific Coast extends from Panama to the Gulf of Alaska and is an active margin with varying shelf widths (see Figure 16.1, p. 651). The continental shelf is narrow along the coasts of California, Oregon, and Washington, with a width on the order of 10 km but widening significantly in the Gulf of Alaska, where shelves extend up to 200 km offshore. In the Gulf of Alaska, freshwater and tidal influences strongly affect cross-shelf exchange, and the shelf is dominated by downwelling circulation. The region from Vancouver Island to Baja California is a classic eastern boundary current upwelling region influenced by the California Current System (Chavez et al., 2017). Winds drive a coastal upwelling circulation characterized by equatorward flow in the California Current and by coastal jets and their associated eddies and fronts that extend offshore, particularly off the coasts of Baja California, California, Washington, and Oregon. The northern California Current System experiences strong freshwater influences and seasonality in wind forcing that diminish in the southern part of the system. In addition to the Columbia River and the Fraser River, a variety of small mountainous rivers, with highly variable discharge, supply freshwater. The Central American Isthmus runs from Panama to the southern tip of Baja California and experiences intense and persistent wind events, large eddies, and high waves that combine to produce upwelling and strong nearshore mixing (Chapa-Balcorta et al., 2015; Franco et al., 2014). In addition to alongshore

winds, strong seasonal wind jets that pass through the Central American cordillera create upwelling “hotspots” and drive production during boreal winter months in the gulfs of Tehuantepec, Papagayo, and Panama (Chapa-Balcorta et al., 2015; Chelton et al., 2000a, 2000b; Gaxiola-Castro and Muller-Karger 1998; Lluch-Cota et al., 1997). The California Current brings water from the North Pacific southward into the southern California and Central American Isthmus regions, while the California Undercurrent transports equatorial waters northward in the subsurface.

The net exchange of CO₂ with the atmosphere across the North American Pacific Coast is characterized by strong spatial and temporal variation and reflects complex interactions between biological uptake of nutrients and degassing of nutrient- and carbon-rich upwelled waters. A growing number of coastal air-sea flux studies have used extrapolation techniques to estimate fluxes across the coastal ocean on regional to continental scales. Observation-based studies of air-sea CO₂ flux suggest that estimates for the coastal ocean from Baja California to the Gulf of Alaska range from a weak to moderate sink of atmospheric CO₂ over this broad longitudinal range. Central California coastal waters have long been understood to have near-neutral air-sea CO₂ exchange because of their large and counter-balancing periods of efflux during upwelling conditions and influx during periods of relaxation and high primary productivity; this pattern is strongly modulated by El Niño–La Niña conditions (Friederich et al., 2002). Hales et al. (2005) used seasonal data to estimate an uptake of 88 g C per m² per year by Oregon coastal waters, which is about 15 times larger than the global mean of 6 g C per m² per year. Using data with greater temporal coverage, Evans et al. (2011) showed how large flux events can significantly alter the estimation of net exchanges for the Oregon shelf. After capturing a large and short-lived efflux event, their annual estimate was outgassing of 3.1 ± 82 g C per m² per year for this same region. The disparity illustrates the importance of basing regional flux estimates on observations that are well resolved in time and space. Capitalizing on



the increased and more uniform spatiotemporal coverage of satellite data, Hales et al. (2012) estimated an annual mean uptake of 7.9 g C per m² per year between 22° and 50°N within 370 km offshore. The most northern estimates for the North American Pacific Coast by Evans et al. (2012) and Evans and Mathis (2013) determined influxes of 26 g C per m² per year for British Columbian coastal waters shoreward of the 500-m isobath and 18 g C per m² per year for Gulf of Alaska coastal waters shoreward of the 1500-m isobath.

Models for the upwelling region (Fiechter et al., 2014; Turi et al., 2014) reproduce the pattern of CO₂ outgassing nearshore and CO₂ uptake further offshore. They also illustrate the intense eddy-driven variability nearshore. Turi et al. (2014) simulate a weak source of 0.6 ± 2.4 g C per m² per year for the region from 30° to 46°N, extending 800 km of shore, an amount which is inconsistent with the observations of Hales et al. (2012) that describe the same region as a sink of 7.9 g C per m² per year. Fiechter et al. (2014) simulate a source of atmospheric CO₂ of 0.6 Tg C per year for the region from 35° to 45°N within 600 km of shore, an estimate which is in contrast to the observation-based estimate of a 14 Tg C sink published by Hales et al. (2012). Both models simulate strong outgassing within the first 100 km of shore, driven by intense upwelling of nutrient- and carbon-rich water, compensated by biologically driven CO₂ uptake from the atmosphere as upwelled nutrients are consumed by photosynthesis during subsequent offshore advection within several hundreds of kilometers of the coast. The disagreement in mean simulated fluxes may result partly from different choices of averaging region and period and differences in model forcing, such as the climatological forcing in Turi et al. (2014) versus realistic variability in Fiechter et al. (2014). Notable, however, is that observations for the Oregon shelf by Evans et al. (2015a) showed intense summer upwelling that led to strong outgassing with pronounced variability in air-sea fluxes but found only weak stimulation of primary production. The research team hypothesized that nutrient-rich waters might be

subducted offshore at convergent surface temperature fronts before nutrients are fully consumed by primary producers.

Less is known about the air-sea flux of CH₄ along the North American Pacific Coast margin. Recent studies inventoried sedimentary sources of CH₄ hydrates, derived from terrestrial and coastal primary production, and suggested that extensive deposits along the Cascadia margin are beginning to destabilize because of warming (Hautala et al., 2014; Johnson et al., 2015).

Cross-shelf exchange of carbon occurs in the California Current System mostly in response to wind-driven circulation and eddies, but river plumes and tides also have been shown to increase offshore transport in the northern part of the system (Barth et al., 2002; Hales et al., 2006). Uncertainties in published estimates are high, ranging from very small (Ianson and Allen 2002; Pennington et al., 2010) to very high fractions of primary production (Hales et al., 2005; Turi et al., 2014), again as a result of the region's large spatial and temporal variability.

16.3.3 Gulf of Mexico

The Gulf of Mexico (GMx) is a semi-enclosed marginal sea at the southern coast of the conterminous United States. The passive margin shelves of its northern portion are relatively wide (up to 250 km west of Florida), but, in contrast to shelf waters of the North American Atlantic Coast, those of the GMx are not separated from open-ocean waters by shelf-break fronts or currents. Ocean water enters the Gulf mainly through the Yucatan Channel, where it forms the northeastward meandering Loop Current (LC), which sheds anticyclonic eddies and exits the Gulf through the Florida Straits (Muller-Karger et al., 2015; Rivas et al., 2005). While shelf circulation is influenced primarily by local wind and buoyancy forcing, outer-shelf regions are at times influenced by LC eddies that impinge on and interact with the shelf (Lohrenz and Verity 2004). Riverine input is substantial in the northern GMx, where the Mississippi-Atchafalaya River System delivers large loads of freshwater, nutrients, and sediments.



Observational estimates indicate that the GMx, as a whole, is a weak net sink of atmospheric CO₂ with an annual average of 2.3 ± 0.96 g C per m² per year (Robbins et al., 2014). Robbins et al. (2014) also provide flux estimates, as follows, for smaller shelf regions, namely, the West Florida Shelf, the northern Gulf shelf, the western Gulf shelf, and the Mexico shelf. The West Florida Shelf and western Gulf shelf act as sources to the atmosphere, with estimated annual average fluxes of 4.4 ± 1.3 and 2.2 ± 0.6 g C per m² per year, respectively. The northern Gulf acts as a sink, with an estimated flux of 5.3 ± 4.4 g C per m² per year, and the Mexican shelf is almost neutral, with an estimated flux of 1.1 ± 0.6 g C per m² per year. Huang et al. (2015) estimated a larger uptake on the northern Gulf shelf of 11 ± 44 g C per m² per year (i.e., about twice the estimate of Robbins et al., 2014) and reported a much larger uncertainty. In an analysis that combines satellite and *in situ* observations, Lohrenz et al. (2018) estimated a similar uptake for the northern GMx of 13 ± 3.6 g C per m² per year. The overall carbon exchanges in the Gulf vary significantly from year to year because of inter-annual variability in wind, temperature, and precipitation (Muller-Karger et al., 2015).

Model-simulated air-sea CO₂ fluxes by Xue et al. (2016) agree relatively well with the estimates of Robbins et al. (2014), reproducing the same spatial pattern though their simulated Gulf-wide uptake of 8.5 ± 6.5 g C per m² per year is larger. This discrepancy results largely from a greater simulated sink in the open Gulf. Also, the uncertainty estimates of the model-simulated fluxes by Xue et al. (2016) are much larger than those of Robbins et al. (2014); the latter might be too optimistic in reporting uncertainties of the flux estimates.

Overall, the various observation- and model-derived estimates for Gulf regions agree in terms of their broad patterns, but existing discrepancies and, at times, large uncertainties indicate that current estimates need further refinement.

Quantitative understanding of CH₄ dynamics in GMx coastal and oceanic environments is limited.

Solomon et al. (2009) speculated that deep CH₄ hydrate seeps in the Gulf potentially are a significant CH₄ source to the atmosphere. They estimated ocean-atmosphere fluxes from seep plumes of $1,150 \pm 790$ to $38,000 \pm 21,000$ g CH₄ per m² per day compared with 2.2 ± 2.0 to 41 ± 8.2 g CH₄ per m² per day for background sites. Subsequent acoustic analyses of bubble plume characteristics question the finding that CH₄ bubbles make their way to the surface (Weber et al., 2014), and the fate of CH₄ emissions from seeps and their overall contribution to atmospheric CH₄ remain uncertain.

16.3.4 North American Arctic

The North American Arctic coastal ocean comprises broad (~300 km) shallow shelves in the Bering and Chukchi seas, the narrower (<100-km) Beaufort Sea shelf, the Hudson Bay, and the extensive Canadian Arctic Archipelago (CAA). Shelf water enters these regions from the North Pacific and follows a large-scale pathway from its entrance into the North American Arctic through the Bering Strait via the Chukchi and Beaufort seas into the CAA and, ultimately, the North Atlantic (Carmack et al., 2006, 2015). Hudson Bay receives significant inputs of freshwater (Dery et al., 2005). Except for the southernmost Bering Sea, most of the coastal region is covered with sea ice from about October to June. Areas of persistent multiyear sea ice at the northernmost extent of the CAA are rapidly declining (Stroeve et al., 2012). Reoccurring polynyas (i.e., holes in the ice) are found in all three of its major regions (Smith and Barber 2007). The North American Arctic is sparsely populated with communities heavily reliant on subsistence fishing and hunting; the rapid regional changes associated with global warming are affecting these communities. Globally, the pace of increasing air temperatures is the highest in the North American Arctic and adjacent Arctic regions, resulting in significant reductions in both summer and winter sea ice cover that profoundly affect the marine ecosystems across the northern extent of the continent (Moore and Stabeno 2015; Steiner et al., 2015).

Coastal waters in the North American Arctic have been described consistently as a net sink for



atmospheric CO₂ (Bates et al., 2006, 2011; Chen et al., 2013; Cross et al., 2014a; Dai et al., 2013; Else et al., 2008; Evans et al., 2015b; Laruelle et al., 2014; Mucci et al., 2010; Shadwick et al., 2011). This general trait is caused by low surface water *p*CO₂, the partial pressure of CO₂, relative to the atmosphere during ice-free months. These levels are set by the combination of low water temperatures and seasonally high rates of both ice-associated and open-water primary production (Cai et al., 2010b, 2014; Steiner et al., 2014), as well as by limited gas exchange through sea ice relative to open water (Butterworth and Miller 2016; Rutgers van der Loeff et al., 2014) during winter months when under-ice *p*CO₂ is higher. Suppressed gas exchange through sea ice has been a source of debate within the Arctic CO₂ flux community, likely a result of inconsistencies between methodologies and the challenge of data collection in such a harsh environment, particularly during winter. The typical approach of calculating air-sea CO₂ flux (from measured air-sea *p*CO₂ differences and gas transfer rates parameterized using wind speed relationships) can differ markedly from flux estimations determined by eddy correlations. The latter suggest high rates of CO₂ exchange relative to open-water fluxes (Else et al., 2011). Three arguments indicate that the high, initial eddy correlation-based fluxes may be overestimates: 1) the potential for unaccounted CO₂ and water vapor cross-correlation possibly affecting the measurement (Landwehr et al., 2014); 2) independent analysis of the ²²²Radon isotope showing near-zero gas exchange in areas covered by sea ice (Rutgers van der Loeff et al., 2014); and 3) recent demonstration of dampened gas-transfer velocities via concurrent, properly corrected eddy covariance-based fluxes and air-sea *p*CO₂ difference measurements in the Antarctic marginal ice zone supporting linear scaling methods that calculate fluxes using percent sea ice cover (Butterworth and Miller 2016).

However, despite the dampening effect of sea ice, its permeability is a known function of temperature (Golden et al., 2007). Therefore, as Arctic winter temperatures continue to rise, the role of wintertime air-ice CO₂ exchange may become increasingly

important because rising temperatures may allow some degree of exchange to take place. To date, measurements of wintertime exchange have been limited to very few studies (Else et al., 2011, 2013; Miller et al., 2015). In recent years, the role of sea ice growth and decay has been shown to significantly affect the air-sea CO₂ flux (Rysgaard et al., 2007, 2009). During sea ice formation, brine rejection forms dense high-saline water that is exported from the surface layer. This process alters the ratio of total alkalinity to sea ice DIC and the underlying seawater, because DIC is a component of the brine whereas total alkalinity precipitates in the brine channels as a form of CaCO₃ known as ikaite (Dieckmann et al., 2008; Rysgaard et al., 2013). During sea ice decay, ikaite dissolves, leading to excess total alkalinity relative to DIC and undersaturation of CO₂ in meltwater.

Estimates of air-sea CO₂ flux in the Chukchi and Beaufort seas, Hudson Bay, and the western CAA all indicate atmospheric CO₂ uptake (Bates et al., 2006; Else et al., 2008, 2013; Gao et al., 2012; Mucci et al., 2010; Semiletov et al., 2007; Shadwick et al., 2011; see Table 16.1, p. 657) with significantly higher uptake over the broad and productive Chukchi shelf. A recent synthesis of a decade of coastal ocean data collected within 400 km of land determined an annual mean uptake of 8.8 g C per m² per year (Evans et al., 2015b). Variability in wind patterns and sea ice cover affects the water column structure and connectivity between the surface ocean and overlying atmosphere, thus influencing the magnitude of air-sea CO₂ exchange.

With regard to Arctic CH₄ fluxes, much more is known about the emission potential, distribution, and functioning of terrestrial sources (McGuire et al., 2009); knowledge of marine CH₄ sources is developing slowly due to sparse observations and the logistical challenges of Arctic marine research. The largest marine CH₄ source in the Arctic is dissociation of gas hydrates stored in continental margin sediments (Parmentier et al., 2013, 2015). As sea ice continues to retreat and ocean waters warm, CH₄ hydrate stability is expected to decrease



Table 16.2. Regional Estimates of Net Air-Sea Carbon Dioxide Exchange from Two Data Syntheses and a Process-Based Model for the MARCATS Regions^{a,b}

MARCATS Segment No. ^b	MARCATS System ^b	Class	Shelf Area (10 ³ km ²)	Chen et al. (2013)	Laruelle et al. (2014)	Bourgeois et al. (2016)
				Flux ^{a,b} (Tg C per year)	Flux ^{a,b} (Tg C per year)	Flux ^{a,b} (Tg C per year)
1	Northeastern Pacific	Subpolar	460	-19	-6.8	-10 ± 0.82
2	California Current	Eastern Boundary Current	210	-5.7	-0.13	-0.48 ± 0.15
3	Tropical Eastern Pacific	Tropical	200	-0.1	0.19	-0.22 ± 0.095
9	Gulf of Mexico	Marginal Sea	540	-1.3	-2.1	-4.5 ± 0.63
10	Florida Upwelling	Western Boundary Current	860	-11	-2.7	-15 ± 1.3
11	Labrador Sea	Subpolar	400	-10	-19	-8.8 ± 1.2
12	Hudson Bay	Marginal Sea	1100	11	NA	-3.8 ± 3.4
13	Canadian Arctic Archipelago	Polar	1200	-57	-14	-6.2 ± 0.75
	Total		4900	-94	-44	-49

Notes

a) Positive fluxes indicate a source to the atmosphere.

b) MARCATS, MARGins and CATchments Segmentation; C, carbon; CO₂, carbon dioxide; Tg, teragrams; g, gram; Tg = 10¹² g

with potentially large and long-term implications. An additional potential marine CH₄ source, unique to polar settings, is release from subsea permafrost layers, with fluxes from thawed sediments reported to be orders of magnitude higher than fluxes from adjacent frozen sediments (Shakhova et al., 2015).

16.3.5 Summary Estimates for CO₂ Uptake by North American Coastal Waters

Despite the variability in regional estimates discussed above and summarized in Table 16.1, p. 657, North American coastal waters clearly act as a net sink of atmospheric carbon. Because of discrepancies among studies, these various regional estimates would be difficult to combine into one number with any confidence. Instead, this chapter

considers estimates of net air-sea CO₂ exchange in North American coastal waters from two global data syntheses (Chen et al., 2013; Laruelle et al., 2014) and a process-based global model (Bourgeois et al., 2016; see Table 16.2, this page). The data syntheses use a global segmentation of the coastal zone and associated watersheds known as MARCATS (MARGins and CATchments Segmentation; Laruelle et al., 2013), which, at a resolution of 0.5°, delineates a total of 45 coastal segments, eight of which surround North America. The data synthesis of Chen et al. (2013) is a summary of individual studies, whereas Laruelle et al. (2014) analyze the Surface Ocean CO₂ Atlas 2.0 database (Bakker et al., 2014) to derive regional estimates. The data syntheses of Chen et al. (2013) and Laruelle et al. (2014)



estimate the North American coastal uptake to be 94.4 and 44.5 Tg C per year, respectively, and the process-based model of Bourgeois et al. (2016) estimates an uptake of 48.8 Tg C per year (see Table 16.2, p. 665). Although there are significant regional discrepancies between the latter two estimates for the eastern tropical Pacific Ocean (i.e., the Central American Isthmus), the GMx, the Florida Upwelling region (actually covering the eastern United States), the Labrador Sea, and the CAA, the overall flux estimates for North America are in close agreement. This, and the fact that Laruelle et al. (2014) used a consistent methodology to estimate air-sea CO₂ flux, builds some confidence in these numbers.

The net CO₂ flux and its anthropogenic component from the process-based global model of Bourgeois et al. (2016) are also reported for a regional decomposition of the EEZs of the United States, Canada, and Mexico (see Table 16.3, this page) in Table 16.4, p. 667. The model simulates a net uptake of CO₂ in North American EEZ coastal waters (excluding the EEZ of the Hawaiian and other islands) of 160 Tg C per year with an anthropogenic flux contribution of 59 Tg C per year. This chapter adopts 160 Tg C per year as the net uptake by coastal waters of North America, excluding tidal wetlands and estuaries. Unfortunately, there are no formal error estimates for this uptake. Instead, estimates adopted here project an error by first noting that the Bourgeois et al. (2016) model is in good agreement with the more recent of the two observation-based estimates for the MARCATS regions of North America. Furthermore, the error estimate for the uptake by continental shelves globally is about 25%, with the North American MARCATS regions having mainly “fair” data quality (Laruelle et al., 2014). Hence, assuming an error of ±50% for the uptake by North American EEZ waters seems reasonable.

16.3.6 Summary Carbon Budget for North American Coastal Waters

Combining the atmospheric CO₂ uptake estimate with estimates of carbon transport from land and carbon burial in ocean sediments enables a first attempt at constructing a carbon budget for the

Table 16.3. Subregions of the Combined Exclusive Economic Zone of Canada, the United States, and Mexico^a

Region Number	Area (10 ³ km ²)	Acronym	Name
1	500	MAB	Mid-Atlantic Bight
2	160	GOM	Gulf of Maine
3	220	SS	Scotian Shelf
4	860	GStL	Gulf of St. Lawrence and Grand Banks
5	1,100	LS	Labrador Shelf
6	1,200	HB	Hudson Bay
7	1,000	CAA	Canadian Arctic Archipelago
8	950	BCS	Beaufort and Chukchi Seas
9	2,200	BS	Bering Sea
10	1,500	GAK	Gulf of Alaska
11	460	CCSN	Northern California Current System
12	640	CCSC	Central California Current System
13	1,200	CCSS	Southern California Current System
14	1,400	Isthmus	Isthmus
15	1,600	GMx	Gulf of Mexico and Yucatan Peninsula
16	500	SAB	South Atlantic Bight
17	7,500	Islands	Hawai'i and other Pacific and Caribbean islands

Notes

a) Area is calculated for the mask that was used to define subregions for averaging.

North American EEZ (see Table 16.5, p. 668). Carbon delivery to the coastal ocean from land via rivers and from tidal wetlands after estuarine processing (i.e., CO₂ outgassing and carbon burial in estuaries) is estimated to be 106 ± 30 Tg C per year (see Ch. 15:



Table 16.4. Estimates of Carbon Burial and Primary Production,^a Net Primary Production (NPP),^b and Simulated NPP and Air-Sea Exchange of Carbon Dioxide^c for the Exclusive Economic Zone Decomposition in Table 16.2^{d,e,g}

Region ^f	Carbon Burial ^a		Satellite NPP ^a		Satellite NPP ^b	NPP from Global Model ^c		Air-Sea Exchange of CO ₂ ^c	
	g C per m ² per year	Tg C per year	g C per m ² per year	Tg C per year	Tg C per year	g C per m ² per year	Tg C per year	g C per m ² per year	Tg C per year
1, MAB	23	101	360	170	170	260	120	31 (14)	15 (6.8)
2, GOM	46	5.5	490	58	81	180	26	33 (7.1)	4.9 (1.1)
3, SS	9.8	2.0	300	63	64	170	43	33 (11)	8.2 (2.8)
4, GStL	16	11	260	190	230	150	130	24 (6.5)	21 (5.6)
5, LS	2.3	2.3	120	120	70	82	88	33 (9.5)	36 (10)
6, HB	19	17.1	144	130	13	130	150	-0.48 (1.4)	-0.50 (1.7)
7, CAA	2.6	1.6	42	26	Not available	19	20	4.1 (0.96)	4.3 (0.96)
8, BCS	12	10	120	110	Not available	49	47	8.0 (1.2)	7.6 (1.1)
9, BS	17	34	240	490	470	130	270	13 (4.0)	28 (8.6)
10, GAK	7.2	10.0	260	360	420	130	210	19 (4.6)	29 (7.1)
11, CCSN	6.1	2.54	270	110	150	160	73	9.4 (4.2)	4.3 (1.9)
12, CCSC	1.2	0.65	260	150	210	170	110	1.1 (4.4)	0.72 (2.9)
13, CCSS	0.99	1.1	210	230	280	150	190	-4.3 (3.1)	-5.5 (4.0)
14, Isthmus	0.42	0.53	230	300	210	150	200	-2.3 (3.6)	-3.2 (4.9)
15, GMx	6.2	8.7	250	350	390	220	360	4.8 (3.7)	7.9 (6.2)
16, SAB	5.4	2.4	210	92	110	260	130	9.7 (6.6)	5.0 (3.4)
17, Islands	0.0055	0.041	120	890	580	80	620	-1.4 (4.1)	-11 (31)
Total	NA	120	NA	3,400	NA	NA	2,800	NA	150 (100)
Total w/o 17	NA	120	NA	2,500	NA	NA	2,200	NA	160 (59)

Notes

a) Dunne et al. (2007).

b) Balcom and Continental Shelf Associates (2011).

c) Bourgeois et al. (2016).

d) Included in carbon dioxide (CO₂) exchange estimates are total and anthropogenic fluxes calculated by averaging the model years 1993–2012. Here all fluxes are relative to the coastal ocean reservoir (i.e., positive fluxes are a source to the coastal ocean, while negative fluxes are a sink).

e) NPP, net primary production; g, grams; C, carbon; Tg, teragrams.

f) See Table 16.3, p. 666, for region descriptions.

g) Key: g C, grams of carbon; Tg C, teragrams of carbon.



Tidal Wetlands and Estuaries, p. 596). Estimates of carbon burial, based on the method of Dunne et al. (2007) for the regional decomposition of the North American EEZ, are reported in Table 16.4, p. 667, with a total flux of 120 Tg C per year. Here these fluxes are considered to be an upper bound because they are substantially larger than other estimates. The Dunne et al. (2007) global estimates of organic carbon burial in waters shallower than 200 m are 19 ± 9 g C per m^2 per year, much larger than the estimates of 6 and 1 g C per m^2 per year by Chen (2004) and Muller-Karger et al. (2005), respectively, although areas are slightly different in the three studies. The organic carbon burial estimates of Dunne et al. (2007) for the GOM, MAB, and SAB (see Table 16.4, p. 667) are larger by factors of 8, 17, and 3, respectively, than the best estimates of the empirical model of Najjar et al. (2018). However, due to different definitions of the boundary between coastal waters and the open ocean, the combined area of the GOM, MAB, and SAB in Najjar et al. (2018) is about a third of that in Dunne et al. (2007). Finally, Dunne et al. (2007) estimated the organic carbon burial in Hudson Bay to be 19 g C per m^2 per year, compared to a mean estimate of 1.5 ± 0.7 g C per m^2 per year of burial from sediment cores (Kuzyk et al., 2009). Given these results, SOCCR2 considers the estimates of Dunne et al. (2007) to be an upper bound and assumes that a reasonable lower bound is about an order of magnitude smaller, thus placing the North American organic carbon burial estimate at 65 ± 55 Tg C per year.

If these estimates of net air-sea flux, carbon burial, and carbon input from land are accurate, then the residual must be balanced by an increase in carbon inventory in coastal waters and a net transfer of carbon from coastal to open-ocean waters. In their global compilation, Regnier et al. (2013) report an increase in the coastal carbon inventory of 50 Tg C per year, which is a quarter of their estimated anthropogenic carbon uptake by air-sea exchange in the coastal waters of 200 Tg C per year. The latter estimate is uncertain. In their global modeling study, which did not account for anthropogenic changes in carbon delivery from land, Bourgeois et al. (2016) estimated an accumulation

Table 16.5. Approximate Summary Carbon Budget for the Exclusive Economic Zone of North America^{a-d}

Process	Flux (Tg C per year) ^{b,d}
Input from land	106 ± 30
Uptake from atmosphere	160 ± 80
Burial	-65 ± 55
DIC ^c accumulation in coastal waters	-50 ± 25
Inferred open-ocean export (residual)	-151 ± 105

Notes

- a) Exclusive Economic Zone (EEZ) excludes EEZs of the Hawaiian and other islands.
- b) Positive fluxes are a source to the coastal ocean, while negative fluxes are a sink.
- c) The accumulation of dissolved inorganic carbon (DIC) is reported with a negative sign to illustrate that all fluxes balance.
- d) Tg C, teragrams of carbon.

of carbon in the coastal ocean of 30 Tg C per year. This amount is a third of their estimated uptake of anthropogenic carbon from air-sea gas exchange in the coastal ocean of 100 Tg C per year and approximately half of their estimated cross-shelf export of anthropogenic carbon of 70 Tg C per year. The rate of carbon accumulation in the North American EEZ from the model of Bourgeois et al. (2016) is 50 Tg C per year (see Table 16.5, this page). Here again, this chapter assumes an uncertainty of $\pm 50\%$. The residual of 151 ± 105 Tg C per year is the inferred export of carbon to the open ocean (see Table 16.5, this page). The fact that the error in this residual is large in absolute and relative terms emphasizes the need for more accurate carbon budgets for coastal waters of North America. The challenge, however, is that many of these terms are small compared to internal carbon cycling in coastal waters, which is dominated by primary production and respiration. Two separate estimates of primary production (see Table 16.4, p. 667) are in broad agreement and reveal that terms in the Table 16.5 budget are just a few percent of primary



production. This also emphasizes that small changes in carbon cycling in coastal waters can result in large changes in atmospheric uptake and transport to the open ocean.

16.4 Climate Trends and Feedbacks

16.4.1 Trends in Coastal Carbon Fluxes

Important questions with respect to coastal carbon fluxes include:

- What is the anthropogenic component of the CO₂ sink?
- How will the coastal ocean change as a CO₂ sink?
- How will changing climate and other forcings affect the total and anthropogenic flux proportions?

As stated in Section 16.2, p. 652, when considering the ocean's role in sequestering anthropogenic carbon, the relevant component is anthropogenic flux, not the total uptake flux. Neither quantifying the anthropogenic carbon flux component nor predicting its future trend is straightforward. Here the likely trends in total carbon fluxes are described; by definition, changes in total carbon fluxes imply changes in anthropogenic fluxes as well.

A direct effect of increasing atmospheric CO₂ will be an increase in net uptake by the coastal ocean. In addition to rising atmospheric CO₂ levels, changes in climate forcings (i.e., surface heat fluxes, winds, and freshwater input) may affect carbon fluxes in North American coastal waters. Ocean warming reduces the solubility of gases and thus directly affects gas concentrations near the surface; this likely will decrease the net air-sea flux of CO₂ by reducing the undersaturation of CO₂ (see Cahill et al., 2016, for the North American Atlantic Coast). Surface temperature increases also strengthen vertical stratification and thus impede vertical mixing, effects which will affect upward diffusion of nutrients and DIC. Enhanced stratification, therefore, could lead to decreases in both biologically driven carbon uptake and CO₂ outgassing. However, model projections for the northern GMx show that the direct effect of increasing atmospheric

CO₂ overwhelms the other more secondary effects (Laurent et al., 2018). Furthermore, temperature trends in coastal waters around North America show complex patterns with some regions having cooled from 1982 to 1997 followed by warming from 1997 to 2013 (e.g., the MAB), some regions having warmed from 1982 to 1997 followed by cooling from 1997 to 2013 (e.g., the SAB and Gulf of Alaska), and other regions showing no consistent warming from 1982 to 2013 (e.g., the NAA; Liao et al., 2015). Temperature anomalies from a time series in the central California Current System show warm surface waters for the decade prior to 1997 followed by a prolonged cooler period until the strong surface warming associated with a marine heatwave and the 2015 to 2016 El Niño interrupted the cool anomalies (Chavez et al., 2017). However, deeper waters in the California Undercurrent have shown a multidecadal trend (1980 to 2012) toward warmer, saltier, lower-oxygen, and higher-CO₂ waters at a depth associated with increased northward transport of Pacific equatorial waters (Meinvielle and Johnson 2013).

Some studies suggest that trends in the air-sea $p\text{CO}_2$ gradient ($\Delta p\text{CO}_2$) are indicative of a strengthening or weakening of the net CO₂ uptake by shelf systems, where an increasing $\Delta p\text{CO}_2$, implying that ocean $p\text{CO}_2$ rises more slowly than atmospheric $p\text{CO}_2$, corresponds to increased net uptake and cross-shelf export (Laruelle et al., 2018). In their observation-based analysis of decadal trends in shelf $p\text{CO}_2$, Laruelle et al. (2018) found that coastal waters lag compared to the rise in atmospheric CO₂ in most regions. For North American coastal waters, they found that the MAB has an increase in $\Delta p\text{CO}_2$ of 1.9 ± 3.1 microatmospheres (μatm) per year, a finding which means that in this region surface ocean $p\text{CO}_2$ does not increase or else increases at a rate that is substantially slower than in the atmosphere. For the shelves of the Labrador Sea, the Vancouver Shelf, and the SAB, they found rates of 0.68 ± 0.61 μatm per year, 0.83 ± 1.7 μatm per year, and 0.51 ± 0.74 μatm per year, respectively, implying that surface ocean $p\text{CO}_2$ does not increase or increases at a slower rate than atmospheric CO₂. The only North



American coastal region that exhibits a negative trend is the Bering Sea, with $-1.1 \pm 0.74 \mu\text{atm}$ per year, meaning that surface ocean $p\text{CO}_2$ increases at a faster rate than in the atmosphere. Laruelle et al. (2018) concluded that the lag in coastal ocean $p\text{CO}_2$ increase compared to that in the atmosphere in most regions indicates an enhancement in the coastal uptake and export of atmospheric CO_2 , although they did not investigate alternative explanations.

Trends in coastal ocean uptake of $p\text{CO}_2$ are highly variable regionally and result from a complex interplay of factors. In coastal upwelling systems, surface warming will increase the horizontal gradient between cold, freshly upwelled source waters and warm, offshore surface water, leading to a greater tendency for the subduction of upwelled water at offshore surface temperature fronts during periods of persistent and strong upwelling-favorable winds. The cumulative effect of these processes for the North American Pacific Coast may be greater and more persistent CO_2 outgassing nearshore and lower productivity offshore as upwelled nitrate is exported before it can be used by the phytoplankton community (Evans et al., 2015a). Rates of warming clearly are faster in higher latitudes, but predicting the net effect of these warming-induced changes in the North American Arctic is not easy. Furthermore, warming in the Arctic leads to reductions in ice cover and longer ice-free periods, both of which directly affect air-sea gas exchange (Bates and Mathis 2009). Another profound effect of Arctic warming is the melting of permafrost, which leads to the release of large quantities of CH_4 to the atmosphere, from both the land surface and the coastal ocean (Crabeck et al., 2014; Parmentier et al., 2013).

Changes in wind stress also directly affect air-sea gas fluxes because stronger winds intensify gas exchange. For example, for the North American Atlantic Coast, changes in wind stress were shown to significantly modify air-sea fluxes (Cahill et al., 2016; Previdi et al., 2009). Large-scale changes in wind patterns also affect ocean circulation with a range of implications (Bakun 1990). Upwelling-favorable winds along the North American Pacific Coast have intensified

in recent years, especially in the northern parts of the upwelling regimes (García-Reyes et al., 2015; Rykaczewski and Checkley 2008; Rykaczewski et al., 2015; Sydeman et al., 2014), a change which has led to 1) shoaling of subsurface nutrient-rich waters (Aksnesa and Ohman 2009; Bograd et al., 2015), 2) increased productivity (Chavez et al., 2011, 2017; Jacox et al., 2015; Kahru et al., 2015), 3) higher DIC delivery to the surface (Turi et al., 2016), and 4) declining oxygen levels (Crawford and Peña 2016; Peterson et al., 2013; Bograd et al., 2015). In the North American Arctic, late-season air-sea CO_2 fluxes may become increasingly more directed toward the atmosphere as Arctic low-pressure systems with storm-force winds occur more often over open water, thus ventilating CO_2 respired from the high organic carbon loading of the shallow shelf (Evans et al., 2015b; Hauri et al., 2013; Steiner et al., 2013) and affecting net annual exchanges. The intense warming observed across the North American Arctic also influences mid-latitude weather patterns (Kim et al., 2014), with probable cascading effects on CO_2 exchanges through adjustments in the wind field.

16.4.2 Acidification Trends in North America's Coastal Ocean

Increasing atmospheric CO_2 emissions lead to rising atmospheric CO_2 levels (see Figure 16.3, p. 671) and a net ocean uptake of CO_2 . Since about 1750, the ocean has absorbed 27% of anthropogenic CO_2 emissions to the atmosphere from fossil fuel burning, cement production, and land-use changes (Canadell et al., 2007; Le Quéré et al., 2015; Sabine and Tanhua 2010). As a result of this uptake, the surface ocean $p\text{CO}_2$ has increased (see Figure 16.3, p. 671) and oceanic pH, carbonate ion concentration, and carbonate saturation state have decreased (Caldeira and Wickett 2003; Feely et al., 2004, 2009; Orr et al., 2005). Commonly called ocean acidification, this suite of chemical changes is defined more precisely as “any reduction in the pH of the ocean over an extended period, typically decades or longer, that is caused primarily by uptake of CO_2 from the atmosphere but also can be caused by other chemical additions or subtractions from the ocean” (IPCC 2011, p. 37). In addition to uptake of

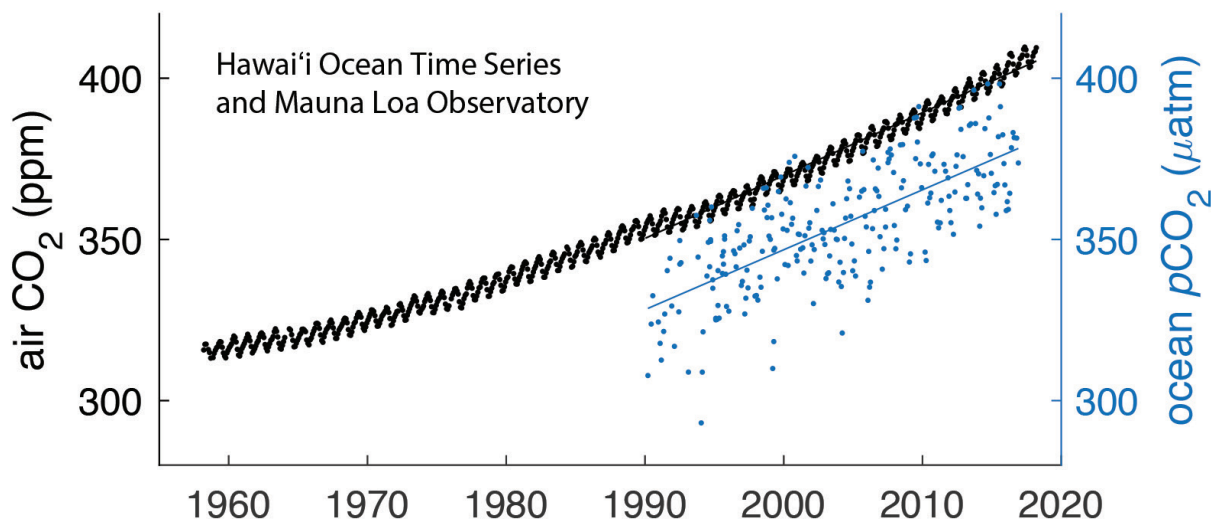


Figure 16.3. Trends in Measured Atmospheric Carbon Dioxide (CO_2) and Surface Ocean Partial Pressure of CO_2 ($p\text{CO}_2$). Black dots represent atmospheric CO_2 measured in parts per million (ppm) at the Mauna Loa Observatory in Hawai'i beginning in 1958. Surface ocean $p\text{CO}_2$ data (blue dots) are measured in microatmospheres (μatm) from the Hawai'i Ocean Time-series (HOT) station near Hawai'i (see Figure 16.4, p. 672, for site location). Black and blue lines indicate linear trends after 1990. Atmospheric CO_2 increased by 1.86 ppm per year; surface ocean $p\text{CO}_2$ increased by 1.95 μatm per year. [Data sources: Mauna Loa, www.esrl.noaa.gov/gmd/ccgg/trends/data.html; HOT, hahana.soest.hawaii.edu/hot/hot-dogs/interface.html.]

CO_2 from the atmosphere, variations in DIC concentrations and thus pH can be caused by biological production and respiration. Ocean acidification can significantly affect growth, metabolism, and life cycles of marine organisms (Fabry et al., 2008; Gattuso and Hansson 2011; Somero et al., 2016) and most directly affects marine calcifiers, organisms that precipitate CaCO_3 to form internal or external body structures. When the carbonate saturation state decreases below the equilibrium point for carbonate precipitation or dissolution, conditions are said to be corrosive, or damaging, to marine calcifiers. These conditions make it more difficult for calcifying organisms to form shells or skeletons, perform metabolic functions, and survive.

Acidification trends in open-ocean surface waters tend to occur at a rate that is commensurate with the rate of the increase in atmospheric CO_2 (see, for example, trends of atmospheric CO_2 in comparison to surface ocean $p\text{CO}_2$ at the Hawai'i Ocean Time-series in Figure 16.3, this page). Acidification

in coastal waters is more variable because of a combination of changes in circulation and upwelling, larger-amplitude seasonal signals in production and respiration than in the open ocean, and atmospheric CO_2 uptake (see Figure 16.4, p. 672; Feely et al., 2008, 2016, 2018; Chavez et al., 2017). In many coastal regions, $p\text{CO}_2$ rises more slowly than in the open ocean (see Section 16.4.1, p. 669; Laruelle et al., 2018). Along the North American Pacific Coast, climate-driven changes in upwelling circulation result in coastal acidification events. As mentioned in Section 16.4.1, upwelling-favorable winds along this coast have intensified over recent years, especially in the northern parts of the upwelling regimes (García-Reyes et al., 2015; McClatchie et al., 2016; Rykaczewski and Checkley 2008; Rykaczewski et al., 2015; Sydeman et al., 2014). Intensified upwelling supplies deep water to the shelf that is rich in DIC and nutrients but poor in oxygen. Ocean acidification and hypoxia thus are strongly linked ecosystem stressors because

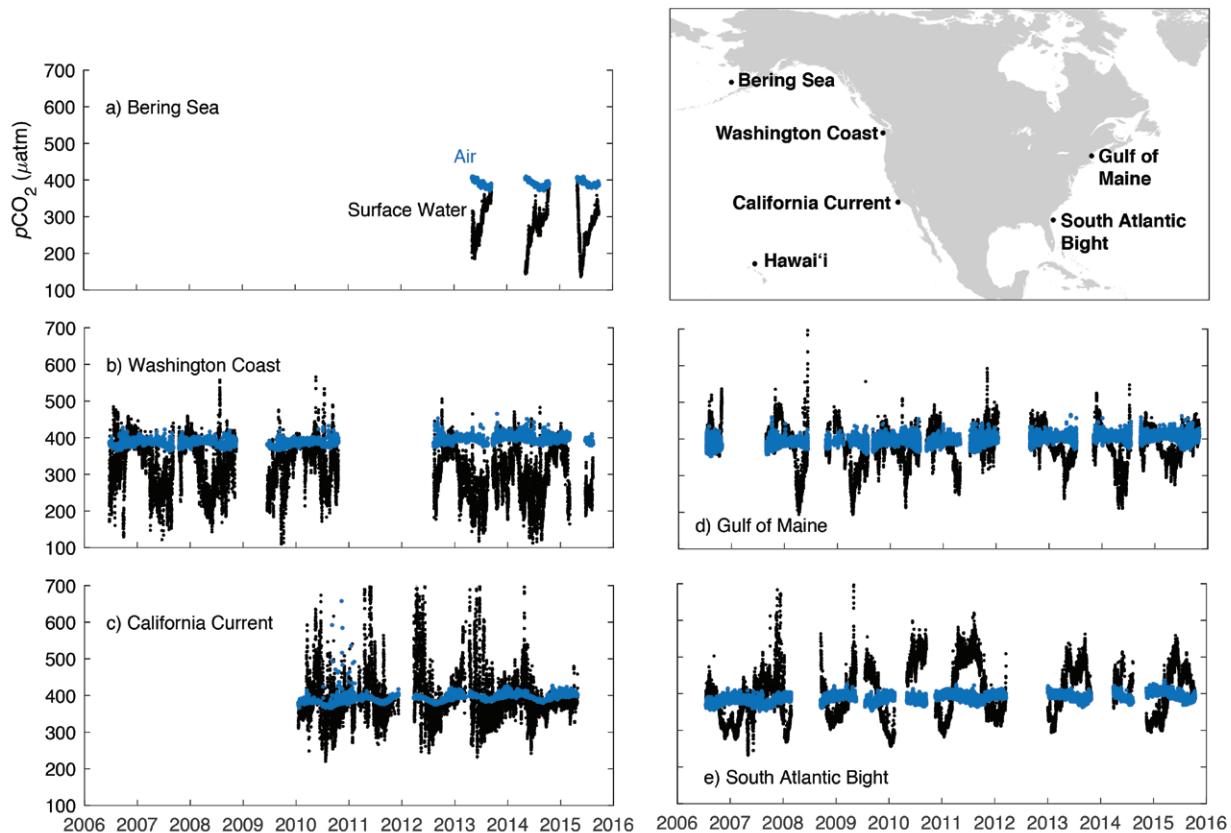


Figure 16.4. Partial Pressure of Carbon Dioxide ($p\text{CO}_2$) Data for the Surface Ocean (black) and Overlying Atmosphere (blue) at Five Coastal Sites. Data are in microatmospheres (μatm); map shows mooring locations. [Data sources: Bering Sea (mooring M2), Cross et al., 2014b. Washington coast (Cape Elizabeth mooring), Mathis et al., 2013. California Current (mooring CCE2), Sutton et al., 2012. Coastal Western Gulf of Maine mooring, Sutton et al., 2013. South Atlantic Bight (Gray's Reef mooring), Sutton et al., 2011.]

low-oxygen, high- CO_2 conditions derive from the microbial respiration of organic matter (Chan et al., 2016; Feely et al., 2008, 2016, 2018). In the northern California Current System, $p\text{CO}_2$, pH, and aragonite saturation reach levels known to be harmful to ecologically and economically important species during the summer upwelling season (see Ch. 17: Biogeochemical Effects of Rising Atmospheric Carbon Dioxide, p. 690; Barton et al., 2012, 2015; Bednaršek et al., 2014, 2016, 2017; Feely et al., 2008, 2016; Harris et al., 2013). In the Gulf of Alaska, aragonite saturation drops to near saturation values during the winter months when deep mixing occurs and surface ocean $p\text{CO}_2$ exceeds atmospheric $p\text{CO}_2$ (Evans and Mathis 2013). Along the Pacific Coast,

50% of shelf waters are projected to experience year-long undersaturation by 2050 (Gruber et al., 2012; Hauri et al., 2013; Turi et al., 2016).

Polar regions are naturally prone to acidification because of their low temperatures (Orr et al., 2005; Steinacher et al., 2009). In many Arctic coastal regions, pH and carbonate saturation state are naturally low relative to lower-latitude coastal settings. These low levels result from higher CO_2 solubility, the influence of multiple sources of freshwater (e.g., riverine, glacial melt, and sea ice melt) with varying CO_2 chemistries, and the high respiratory DIC content in bottom waters. The Beaufort and Chukchi Sea continental shelves experience inflows of naturally corrosive Pacific seawater with pH as low



as 7.6 (Mathis et al., 2011). The main contributing factor to the relatively high rates of acidification in polar waters is retreating sea ice, which adds melt-water from multiyear ice and increases the surface area of open water, thereby enhancing the uptake of atmospheric CO₂ (Cai et al., 2010b; Steiner et al., 2013). These factors, in combination with increasing atmospheric CO₂ levels, have set a faster pace of ocean acidification in the Arctic than projected trends in other coastal regions (Feely et al., 2009; Mathis et al., 2015a). Models predict annual average aragonite undersaturation (i.e., favoring dissolution) for the Bering Sea and the Chukchi Sea by 2070 and 2030, respectively (Mathis et al., 2015a). The Beaufort Sea upper halocline and deep waters now regularly show aragonite undersaturation (Mathis et al., 2015a; Miller et al., 2014). These chemical seawater signatures are propagated via M'Clure Strait and Amundsen Gulf into the CAA and beyond (Azetsu-Scott et al., 2010; Turk et al., 2016; Yamamoto-Kawai et al., 2013). Model projections based on the IPCC high-CO₂ emissions scenario, Representative Concentration Pathway 8.5 (RCP8.5), suggest the Beaufort Sea surface water will become undersaturated with respect to aragonite around 2025 (Steinacher et al., 2009; Steiner et al., 2014). As these conditions intensify, negative impacts on calcifying marine organisms are expected to become a critical issue, reshaping ecosystems and fisheries across the North American Arctic domain (Mathis et al., 2015b; Moore and Stabeno 2015).

In the northern GMx, surface aragonite saturation states typically range from 3.6 to 4.5 and are thus well above the dissolution threshold (Wang et al., 2013; Wanninkhof et al., 2015). Here excessive nutrient inputs from the Mississippi River result in hypoxia and eutrophication-induced acidification of near-bottom waters (Cai et al., 2011; Laurent et al., 2017). Similar to the California Current System, low-oxygen and high-CO₂ conditions coincide and derive from microbial respiration of organic matter (Cai et al., 2011; Laurent et al., 2017; Feely et al., 2018). Currently, aragonite saturation states are around 2 in hypoxic bottom waters and thus well above the saturation threshold. Projections suggest that aragonite

saturation states of these near-bottom waters will drop below the saturation threshold near the end of this century (Cai et al., 2011; Laurent et al., 2018).

Recent studies indicate that the northern regions of the North American Atlantic Coast (the MAB and GOM) are more prone to acidification than the SAB (Wang et al., 2013; Wanninkhof et al., 2015). Coastal waters in this region have, on average, lower pH and lower aragonite saturation states than more southern coastal regions. These properties are driven primarily by a decrease in mean total alkalinity of shelf water from the SAB northward to the GOM. Seasonal undersaturation of aragonite in subsurface water is occurring in the GOM with photosynthesis and respiration playing a major role in controlling the seasonal variability of aragonite saturation states; dissolution of aragonite might already occur in fall and winter (Wang et al., 2017). With a significant shellfish industry, the GOM displays the lowest pH and aragonite saturation levels along the East Coast in summer (Wang et al., 2013).

16.5 Conclusions

The research community has made tremendous progress in improving understanding and constraining rates of carbon cycling in coastal waters since SOCCR1 (CCSP 2007), primarily because of a greatly expanded suite of observations, process studies, and models. However, quantification of many coastal carbon fluxes remains a significant challenge. Carbon is constantly exchanged across the air-sea interface as well as the interfaces between land and coastal ocean, coastal and open-ocean waters, and water and sediment. Net exchange fluxes and trends are relatively small signals masked by a large and fluctuating background. At present, most of these fluxes are not quantified well enough to derive well-constrained carbon budgets for North American coastal waters or to project how those fluxes will change in the future due to various drivers.

This chapter focused primarily on the role of ocean margins in sequestering atmospheric CO₂ and coastal ocean acidification. In the coastal ocean, a net removal of carbon from direct interaction with



the atmospheric reservoir can occur by export of dissolved or particulate carbon to the deep ocean or by permanent burial in sediments. Neither of these is easily observed or well quantified. The best-observed flux is gas exchange across the air-sea interface, although extracting the small net flux and its trend from a variable background remains a challenge. Ultimately, the removal of anthropogenic carbon is the relevant quantity for assessing the contribution of ocean margins to the uptake of anthropogenic carbon; however, the separation of anthropogenic fluxes from the natural background is thus far elusive for coastal waters.

Estimates of air-sea CO₂ fluxes currently provide the best evidence for the contribution of coastal waters to overall carbon uptake by the ocean. In the broad shelf system of the North American Atlantic Coast, shelf water is separated from the adjacent open ocean by persistent shelf break currents and density fronts. Available estimates suggest that the overall North American Atlantic Coast is a weak sink, with some subregions acting as sources (e.g., nearshore regions of the SAB), while others are either neutral (Scotian Shelf and GOM) or act as weak sinks (MAB and outer SAB). Large sections of the narrow shelf of the North American Pacific Coast are dominated by upwelling circulation, which leads to strong CO₂ outgassing near the coast. However, compensating for this outgassing is biologically driven uptake from upwelled nutrients further offshore. Recent estimates are consistent in suggesting that the region is a weak to moderate sink of atmospheric CO₂. The relatively wide shelves in the GMx are considered a weak net sink, with the West Florida Shelf and the western Gulf shelf acting as sources; the Mexico shelf being neutral; and only the northern shelf a clear sink that is driven largely by anthropogenic nutrient inputs from the Mississippi River. The wide, seasonally ice-covered shelves in the North American Arctic consistently are acting as a sink for atmospheric CO₂. The low surface-water *p*CO₂ in this region primarily results from low water temperatures and the decreased uptake of atmospheric CO₂ during a significant fraction of the year because of seasonal ice cover. Overall, North American coastal waters act as a sink, but regional variations and uncertainties are large.

Several drivers influence secular trends in coastal carbon fluxes and will continue to do so in the future. These drivers include rising atmospheric CO₂ levels, changes in atmosphere-ocean interactions (e.g., wind forcing and heat fluxes), changes in the hydrological cycle, and anthropogenic perturbations of global nutrient cycling (particularly, the nitrogen cycle). Coastal surface *p*CO₂ clearly does not closely track atmospheric *p*CO₂. Although there are a number of plausible mechanisms for potential future changes in coastal carbon uptake, the total effect cannot be predicted with any confidence. Regional model studies are beginning to address these challenges.

A major concern is coastal acidification, which can affect the growth, metabolism, and life cycles of many marine organisms, specifically calcifiers, and can trigger cascading ecosystem-scale effects. Most vulnerable are those organisms that precipitate aragonite, one of the more soluble forms of biogenic CaCO₃ in the ocean. Aragonite saturation states are routinely below saturation (i.e., favoring dissolution) in North American Arctic coastal waters. In the North American Pacific Coast region, atmospheric CO₂ uptake in combination with intensified upwelling that brings low-pH, low-oxygen water onto the shelves leads to aragonite levels below the saturation threshold in large portions of the subsurface waters. In the northern GMx, aragonite saturation states are well above the dissolution threshold. Although eutrophication-induced acidification occurs in bottom waters influenced by Mississippi River inputs of nutrients and freshwater, saturation levels remain well above the dissolution threshold.

Given the importance of coastal margins, both in contributing to carbon budgets and in the societal benefits they provide, further efforts to improve assessments of the carbon cycle in these regions are paramount. Critical needs are maintaining and expanding existing coastal observing programs, continuing national and international coordination and integration of observations, increasing development of modeling capabilities, and addressing stakeholder needs.



SUPPORTING EVIDENCE

KEY FINDING 1

Observing networks and high-resolution models are now available to construct coastal carbon budgets. Efforts have focused primarily on quantifying the net air-sea exchange of carbon dioxide (CO_2), but some studies have estimated other key fluxes, such as the exchange between shelves and the open ocean.

Description of evidence base

Observing networks are in place along the Atlantic, Pacific, and Arctic coasts of North America and the U.S. Gulf Coast (Alin et al., 2015; Bates et al., 2006, 2011; Cai et al., 2010a; Chen et al., 2013; Cross et al., 2014a; Dai et al., 2013; DeGrandpre et al., 2002; Evans et al., 2011, 2012, 2015b; Hales et al., 2005, 2012; Jiang et al., 2008; Mucci et al., 2010; Najjar et al., 2018; Robbins et al., 2009, 2014; Salisbury et al., 2008b, 2009; Shadwick et al., 2010, 2011; Vandemark et al., 2011; Wang et al., 2013, 2017).

Regional models are in place for the same regions (Cahill et al., 2016; Fennel et al., 2008; Fiechter et al., 2014; Pilcher et al., 2018; Previdi et al., 2009; Turi et al., 2014; Xue et al., 2016).

The emphasis on quantifying air-sea exchange is illustrated by the fact that the references listed in Table 16.1, p. 657, all provide an estimate of this flux, but few provide estimates of other fluxes. Few studies exist that do provide estimates of carbon exchange between shelves and open ocean; they include Fennel and Wilkin (2009), Barth et al. (2002), Hales et al. (2006), Xue et al. (2016), and Najjar et al. (2018).

Major uncertainties

This key message essentially contains statements of fact. Hence, this statement is not considered uncertain.

KEY FINDING 2

Available estimates of air-sea carbon fluxes, based on more than a decade of observations, indicate that the North American margins act as a net sink for atmospheric CO_2 . This net uptake is driven primarily by fluxes in the high-latitude regions. The estimated magnitude of the net flux is 160 ± 80 teragrams of carbon per year (*medium confidence*) for the North American Exclusive Economic Zone, a number that is not well constrained.

Description of evidence base

This statement is supported by the numbers summarized in Tables 16.1, p. 657, and 16.2, p. 665. Consistent reports of outgassing exist only for the Gulf of Maine (GOM), where the net flux is almost neutral, and the West Florida Shelf. Contradictory reports exist for the Scotian Shelf. Everywhere else the net flux is reported as net uptake (i.e., sink), although with large uncertainties. Three independent studies also provide estimates of net air-sea CO_2 exchange in North American coastal waters. Two are global data syntheses (Chen et al., 2013; Laruelle et al., 2014), and one is from a process-based global model (Bourgeois et al., 2016; see Table 16.2, p. 665). The model of Bourgeois et al. (2016) estimates a net air-sea CO_2 flux of 160 teragrams of carbon



(Tg C) per year for the North American Exclusive Economic Zone (EEZ). The estimate is that the uncertainty is 50%.

These individual estimates cannot be combined because of discrepancies in numbers and gaps in coverage.

Major uncertainties

The consistency among studies pointing at North American coastal waters as a sink provides confidence, although each individual estimate is uncertain.

Assessment of confidence based on evidence and agreement, including short description of nature of evidence and level of agreement

The statement that North American coastal waters act as a sink overall can be made with high confidence and reflects the fact that studies are consistent in supporting this conclusion, even though each number itself comes with a large uncertainty. The overall uptake estimate is uncertain; hence, there is high confidence in stating that this flux estimate is poorly constrained.

Summary sentence or paragraph that integrates the above information

The consistency of many independent estimates reporting coastal uptake of atmospheric CO₂ builds confidence that these waters indeed act as a sink.

KEY FINDING 3

The increasing concentration of CO₂ in coastal and open-ocean waters leads to ocean acidification. Corrosive conditions in the subsurface occur regularly in Arctic coastal waters, which are naturally prone to low pH, and North Pacific coastal waters, where upwelling of deep, carbon-rich waters has intensified and, in combination with the uptake of anthropogenic carbon, leads to low seawater pH and aragonite saturation states in spring, summer, and early fall (*very high confidence, very likely*).

Description of evidence base

In Arctic coastal waters, pH and carbonate saturation state are naturally low (Cai et al., 2010b; Mathis et al., 2011; Steiner et al., 2013). The pace of ocean acidification is faster in the Arctic than in other coastal and open-ocean regions (Fabry et al., 2009; Feely et al., 2009; Mathis et al., 2015a). The Beaufort Sea upper halocline and deep waters now regularly show aragonite undersaturation (Mathis et al., 2015a; Miller et al., 2014). These chemical seawater signatures are propagated via M'Clure Strait and Amundsen Gulf into the Canadian Archipelago and beyond (Azetsu-Scott et al., 2010; Turk et al., 2016; Yamamoto-Kawai et al., 2013). Variability in the carbon content of freshwater end members also has been shown to contribute to undersaturation events in coastal waters of the Gulf of Alaska region (Siedlecki et al., 2017; Evans et al., 2014)

In the North America Pacific Coast (NAPC) region, anthropogenic CO₂ uptake combined with climate-driven changes in upwelling circulation result in coastal acidification events. Upwelling-favorable winds along the NAPC have intensified over recent years, especially in the northern parts of the upwelling regimes (García-Reyes et al., 2015; McClatchie et al., 2016; Rykaczewski and Checkley 2008; Rykaczewski et al., 2015; Sydeman et al., 2014). In the northern California Current System, pCO₂ (partial pressure of CO₂), pH, and aragonite saturation



reach levels known to be harmful to ecologically and economically important species during the summer upwelling season (see Ch. 17: Biogeochemical Effects of Rising Atmospheric Carbon Dioxide, p. 690; Barton et al., 2012, 2015; Bednaršek et al., 2014, 2016, 2017; Feely et al., 2008, 2016, 2018; Harris et al., 2013; Siedlecki et al., 2016).

Major uncertainties

Statement is well supported by the literature. No major uncertainties.

Assessment of confidence based on evidence and agreement, including short description of nature of evidence and level of agreement

Statement is well supported by the literature. No major uncertainties.

Estimated likelihood of impact or consequence, including short description of basis of estimate

Corrosive waters have been observed in the Arctic and North Pacific coastal regions (Feely et al., 2008, 2016; Mathis et al., 2015a; Miller et al., 2014). A more comprehensive list of references is given in the description above and in the chapter body.

Summary sentence or paragraph that integrates the above information

Statement that corrosive waters regularly occur is well supported by the literature because these conditions have been directly observed. There are no major uncertainties.

KEY FINDING 4

Expanded monitoring, more complete syntheses of available observations, and extension of existing model capabilities are required to provide more reliable coastal carbon budgets, projections of future states of the coastal ocean, and quantification of anthropogenic carbon contributions.

Description of evidence base

The underlying motivation for constructing complete carbon budgets for coastal waters is that permanent burial of carbon in coastal sediments and export of carbon from coastal waters to the deep ocean both remove anthropogenic carbon from the atmospheric reservoir. The relevant carbon flux in this context is the burial or export of anthropogenic carbon, not total burial or export. Only total fluxes can be observed directly. Distinction between anthropogenic fluxes and the natural background has not been attempted in regional observational or modeling studies, because more comprehensive accounting than is available for carbon fluxes and improved modeling capabilities would be needed. The study by Bourgeois et al. (2016) is the first to estimate coastal anthropogenic carbon uptake in a global model. The estimated net air-sea exchange of CO₂ from this global model is reported for a regional decomposition of the EEZs of the United States, Canada, and Mexico in Table 16.3, p. 666. The model simulates a net uptake of CO₂ in North American coastal waters that is of similar magnitude to estimates of organic carbon burial and riverine carbon input, but the latter two numbers are uncertain because they are each taken from one individual study and not corroborated by multiple references. However, the similar magnitudes of these numbers illustrate that current coastal carbon budgets are uncertain and that constraining just the air-sea gas exchange will not be sufficient to quantify the export of anthropogenic carbon by coastal processes.



Major uncertainties

This report's synthesis of the current literature shows that the magnitudes of several significant components of coastal carbon budgets are currently uncertain.

Summary sentence or paragraph that integrates the above information

The synthesis in this chapter shows that coastal carbon budgets and anthropogenic contributions to the underlying fluxes are currently uncertain. Thus, more observations and modeling efforts could reduce these uncertainties.



REFERENCES

- Aksnesa, D. L., and M. D. Ohman, 2009: Multi-decadal shoaling of the euphotic zone in the Southern sector of the California current system. *Limnology and Oceanography*, **54**(4), 1272-1281, doi: 10.4319/lo.2009.54.4.1272.
- Alin, S., R. Brainard, N. Price, J. Newton, A. Cohen, W. Peterson, E. DeCarlo, E. Shadwick, S. Noakes, and N. Bednaršek, 2015: Characterizing the natural system: Toward sustained, integrated coastal ocean acidification observing networks to facilitate resource management and decision support. *Oceanography*, **25**(2), 92-107, doi: 10.5670/oceanog.2015.34.
- Alin, S., S. Siedlecki, B. Hales, J. Mathis, W. Evans, M. Stukel, G. Gaxiola-Castro, J. M. Hernandez-Ayon, L. Juranek, M. Goñi, G. Turi, J. Needoba, E. Mayorga, Z. Lachkar, N. Gruber, J. Hartmann, N. Moosdorf, R. Feely, and F. Chavez, 2012: Coastal carbon synthesis for the continental shelf of the North American Pacific coast (NAPC): Preliminary results. *Ocean Carbon and Biogeochemistry News*, **5**(1).
- Azetsu-Scott, K., A. Clarke, K. Falkner, J. Hamilton, E. P. Jones, C. Lee, B. Petrie, S. Prinsenberg, M. Starr, and P. Yeats, 2010: Calcium carbonate saturation states in the waters of the Canadian Arctic archipelago and the Labrador Sea. *Journal of Geophysical Research*, **115**(C11), doi: 10.1029/2009jc005917.
- Bakker, D. C. E., B. Pfeil, K. Smith, S. Hankin, A. Olsen, S. R. Alin, C. Cosca, S. Harasawa, A. Kozyr, Y. Nojiri, K. M. O'Brien, U. Schuster, M. Telszewski, B. Tilbrook, C. Wada, J. Akl, L. Barbero, N. R. Bates, J. Boutin, Y. Bozec, W. J. Cai, R. D. Castle, F. P. Chavez, L. Chen, M. Chierici, K. Currie, H. J. W. de Baar, W. Evans, R. A. Feely, A. Fransson, Z. Gao, B. Hales, N. J. Hardman-Mountford, M. Hoppema, W. J. Huang, C. W. Hunt, B. Huss, T. Ichikawa, T. Johannessen, E. M. Jones, S. D. Jones, S. Jutterström, V. Kitidis, A. Körtzinger, P. Landschützer, S. K. Lauvset, N. Lefèvre, A. B. Manke, J. T. Mathis, L. Merlivat, N. Metzl, A. Murata, T. Newberger, A. M. Omar, T. Ono, G. H. Park, K. Paterson, D. Pierrot, A. F. Ríos, C. L. Sabine, S. Saito, J. Salisbury, V. V. S. S. Sarma, R. Schlitzer, R. Sieger, I. Skjelvan, T. Steinhoff, K. F. Sullivan, H. Sun, A. J. Sutton, T. Suzuki, C. Sweeney, T. Takahashi, J. Tjiputra, N. Tsurushima, S. M. A. C. van Heuven, D. Vandemark, P. Vlahos, D. W. R. Wallace, R. Wanninkhof, and A. J. Watson, 2014: An update to the Surface Ocean CO₂ Atlas (SOCAT version 2). *Earth System Science Data*, **6**(1), 69-90, doi: 10.5194/essd-6-69-2014.
- Bakun, A., 1990: Global climate change and intensification of coastal ocean upwelling. *Science*, **247**(4939), 198-201, doi: 10.1126/science.247.4939.198.
- Balcom, B. J., and Continental Shelf Associates, Inc., 2011: *Net Primary Productivity (NPP) and Associated Parameters for the U.S. Outer Continental Shelf Waters, 1998-2009 Version 1*. National Oceanographic Data Center, NOAA. Dataset. [https://catalog.data.gov/dataset/net-primary-productivity-npp-and-associated-parameters-for-the-u-s-outer-continental-shelf-wate]
- Barrón, C., and C. M. Duarte, 2015: Dissolved organic carbon pools and export from the coastal ocean. *Global Biogeochemical Cycles*, **29**(10), 1725-1738, doi: 10.1002/2014gb005056.
- Barth, J. A., T. J. Cowles, P. M. Kosro, R. K. Shearman, A. Huyer, and R. L. Smith, 2002: Injection of carbon from the shelf to offshore beneath the euphotic zone in the California current. *Journal of Geophysical Research*, **107**(C6), doi: 10.1029/2001jc000956.
- Barton, A., B. Hales, G. G. Waldbusser, C. Langdon, and R. A. Feely, 2012: The Pacific Oyster, *Crassostrea gigas*, shows negative correlation to naturally elevated carbon dioxide levels: Implications for near-term ocean acidification effects. *Limnology and Oceanography*, **57**(3), 698-710, doi: 10.4319/lo.2012.57.3.0698.
- Barton, A., G. Waldbusser, R. Feely, S. Weisberg, J. Newton, B. Hales, S. Cudd, B. Eudeline, C. Langdon, I. Jefferds, T. King, A. Suhrbier, and K. McLaughlin, 2015: Impacts of coastal acidification on the Pacific Northwest shellfish industry and adaptation strategies implemented in response. *Oceanography*, **25**(2), 146-159, doi: 10.5670/oceanog.2015.38.
- Bates, N., W.-J. Cai, and J. Mathis, 2011: The ocean carbon cycle in the Western Arctic Ocean: Distributions and air-sea fluxes of carbon dioxide. *Oceanography*, **24**(3), 186-201, doi: 10.5670/oceanog.2011.71.
- Bates, N. R., 2006: Air-sea CO₂ fluxes and the continental shelf pump of carbon in the Chukchi Sea adjacent to the Arctic Ocean. *Journal of Geophysical Research*, **111**(C10), C10013, doi: 10.1029/2005jc003083.
- Bates, N. R., and J. T. Mathis, 2009: The Arctic Ocean marine carbon cycle: Evaluation of air-sea CO₂ exchanges, ocean acidification impacts and potential feedbacks. *Biogeosciences*, **6**(11), 2433-2459, doi: 10.5194/bg-6-2433-2009.
- Bates, N. R., S. B. Moran, D. A. Hansell, and J. T. Mathis, 2006: An increasing CO₂ sink in the Arctic Ocean due to sea-ice loss. *Geophysical Research Letters*, **33**(23), doi: 10.1029/2006gl027028.
- Bauer, J. E., W. J. Cai, P. Raymond, T. S. Bianchi, C. S. Hopkinson, and P. Regnier, 2013: The changing carbon cycle of the coastal ocean. *Nature*, **504**(7478), 61-70, doi: 10.1038/nature12857.
- Bednaršek, N., C. J. Harvey, I. C. Kaplan, R. A. Feely, and J. Možina, 2016: Pteropods on the edge: Cumulative effects of ocean acidification, warming, and deoxygenation. *Progress in Oceanography*, **145**, 1-24, doi: 10.1016/j.pocean.2016.04.002.
- Bednaršek, N., R. A. Feely, J. C. Reum, B. Peterson, J. Menkel, S. R. Alin, and B. Hales, 2014: *Limacina helicina* shell dissolution as an indicator of declining habitat suitability owing to ocean acidification in the California current ecosystem. *Proceedings of the Royal Society B: Biological Sciences*, **281**(1785), 20140123, doi: 10.1098/rspb.2014.0123.



- Benaršek, N., R. A. Feely, N. Tolimieri, A. J. Hermann, S. A. Siedlecki, G. G. Waldbusser, P. McElhany, S. R. Alin, T. Klinger, B. Moore-Maley, and H. O. Pörtner, 2017: Exposure history determines pteropod vulnerability to ocean acidification along the U.S. West Coast. *Scientific Reports*, **7**, 4526, doi: 10.1038/s41598-017-03934-z.
- Benway, H., S. Alin, E. Boyer, W. Cai, J., P. Coble, J. Cross, M. Friedrichs, M. Goñi, P. Griffith, M. Herrmann, S. Lohrenz, J. Mathis, G. McKinley, R. Najjar, C. Pilskaln, S. Siedlecki, and R. L. Smith, 2016: A science plan for carbon cycle research in North American coastal waters. In: *Coastal CARbon Synthesis (CCARS) Community Workshop, August 19-21, 2014*, doi:10.1575/1912/7777.
- Birdsey, R., A. N. Bates, M. Behrenfeld, K. Davis, S. C. Doney, R. Feely, D. Hansell, L. Heath, E. Kasischke, H. Kheshgi, B. Law, C. Lee, A. D. McGuire, P. Raymond, and C. J. Tucker, 2009: Carbon cycle observations: Gaps threaten climate mitigation policies. *Eos, Transactions American Geophysical Union*, **90**(34), 292-293, doi: 10.1029/2009EO340005.
- Bograd, S. J., M. Pozo Buil, E. DiLorenzo, C. G. Castro, I. D. Schroeder, R. Goericke, C. R. Anderson, C. Benitez-Nelson, and F. A. Whitney, 2015: Changes in source waters to the Southern California Bight. *Deep-Sea Research Part II: Topical Studies in Oceanography*, **112**, 42–52, doi: 10.1016/j.dsr2.2014.04.009.
- Bourgeois, T., J. C. Orr, L. Resplandy, J. Terhaar, C. Ethé, M. Gehlen, and L. Bopp, 2016: Coastal-ocean uptake of anthropogenic carbon. *Biogeosciences*, **13**(14), 4167-4185, doi: 10.5194/bg-13-4167-2016.
- Brothers, L. L., C. L. Van Dover, C. R. German, C. L. Kaiser, D. R. Yoerger, C. D. Ruppel, E. Lobecker, A. D. Skarke, and J. K. S. Wagner, 2013: Evidence for extensive methane venting on the southeastern U.S. Atlantic margin. *Geology*, **41**(7), 807-810, doi: 10.1130/g34217.1.
- Butterworth, B. J., and S. D. Miller, 2016: Air-sea exchange of carbon dioxide in the Southern Ocean and Antarctic marginal ice zone. *Geophysical Research Letters*, **43**(13), 7223-7230, doi: 10.1002/2016gl069581.
- Cahill, B., J. Wilkin, K. Fennel, D. Vandemark, and M. A. M. Friedrichs, 2016: Interannual and seasonal variabilities in air-sea CO₂ fluxes along the U.S. eastern continental shelf and their sensitivity to increasing air temperatures and variable winds. *Journal of Geophysical Research: Biogeosciences*, **121**(2), 295-311, doi: 10.1002/2015jg002939.
- Cai, W.-J., and Y. Wang, 1998: The chemistry, fluxes, and sources of carbon dioxide in the estuarine waters of the Satilla and Altamaha Rivers, Georgia. *Limnology and Oceanography*, **43**(4), 657-668, doi: 10.4319/lo.1998.43.4.0657.
- Cai, W.-J., Z. A. Wang, and Y. Wang, 2003: The role of marsh-dominated heterotrophic continental margins in transport of CO₂ between the atmosphere, the land-sea interface and the ocean. *Geophysical Research Letters*, **30**(16), doi: 10.1029/2003gl017633.
- Cai, W.-J., X. Hu, W.-J. Huang, L.-Q. Jiang, Y. Wang, T.-H. Peng, and X. Zhang, 2010a: Alkalinity distribution in the western North Atlantic Ocean margins. *Journal of Geophysical Research*, **115**(C8), doi: 10.1029/2009jc005482.
- Cai, W.-J., L. Chen, B. Chen, Z. Gao, S. H. Lee, J. Chen, D. Pierrot, K. Sullivan, Y. Wang, X. Hu, W. J. Huang, Y. Zhang, S. Xu, A. Murata, J. M. Grebmeier, E. P. Jones, and H. Zhang, 2010b: Decrease in the CO₂ uptake capacity in an ice-free Arctic Ocean basin. *Science*, **329**(5991), 556-559, doi: 10.1126/science.1189338.
- Cai, W.-J., N. R. Bates, L. Guo, L. G. Anderson, J. T. Mathis, R. Wanninkhof, D. A. Hansell, L. Chen, and I. P. Semiletov, 2014: Carbon fluxes across boundaries in the Pacific Arctic region in a changing environment. In: *The Pacific Arctic Region: Ecosystem Status and Trends in a Rapidly Changing Environment*. [J. M. Grebmeier and W. Maslowski (eds.)]. Springer, 199-222 pp.
- Cai, W.-J., X. Hu, W.-J. Huang, M. C. Murrell, J. C. Lehrter, S. E. Lohrenz, W.-C. Chou, W. Zhai, J. T. Hollibaugh, Y. Wang, P. Zhao, X. Guo, K. Gundersen, M. Dai, and G.-C. Gong, 2011: Acidification of subsurface coastal waters enhanced by eutrophication. *Nature Geoscience*, **4**(11), 766-770, doi: 10.1038/ngeo1297.
- Cai, W. J., 2011: Estuarine and coastal ocean carbon paradox: CO₂ sinks or sites of terrestrial carbon incineration? *Annual Review of Marine Science*, **3**, 123-145, doi: 10.1146/annurev-marine-120709-142723.
- Caldeira, K., and M. E. Wickett, 2003: Oceanography: Anthropogenic carbon and Ocean pH. *Nature*, **425**(6956), 365, doi: 10.1038/425365a.
- Canadell, J. G., C. Le Quéré, M. R. Raupach, C. B. Field, E. T. Buitenhuis, P. Ciais, T. J. Conway, N. P. Gillett, R. A. Houghton, and G. Marland, 2007: Contributions to accelerating atmospheric CO₂ growth from economic activity, carbon intensity, and efficiency of natural sinks. *Proceedings of the National Academy of Sciences USA*, **104**(47), 18866-18870, doi: 10.1073/pnas.0702737104.
- Carmack, E., P. Winsor, and W. Williams, 2015: The contiguous panarctic riverine coastal domain: A unifying concept. *Progress in Oceanography*, **139**, 13-23, doi: 10.1016/j.pocean.2015.07.014.
- Carmack, E., D. Barber, J. Christensen, R. Macdonald, B. Rudels, and E. Sakshaug, 2006: Climate variability and physical forcing of the food webs and the carbon budget on panarctic shelves. *Progress in Oceanography*, **71**(2-4), 145-181, doi: 10.1016/j.pocean.2006.10.005.
- Carter, B. R., R. A. Feely, S. Mecking, J. N. Cross, A. M. Macdonald, S. A. Siedlecki, L. D. Talley, C. L. Sabine, F. J. Millero, J. H. Swift, A. G. Dickson, and K. B. Rodgers, 2017: Two decades of Pacific anthropogenic carbon storage and ocean acidification along Global Ocean Ship-based Hydrographic Investigations Program sections P16 and P02. *Global Biogeochemical Cycles*, **31**(2), 306–327, doi: 10.1002/2016GB005485.



- CCSP, 2007: *First State of the Carbon Cycle Report (SOCCR): The North American Carbon Budget and Implications for the Global Carbon Cycle. A Report by the U.S. Climate Change Science Program and the Subcommittee on Global Change Research*. [A. W. King, L. Dilling, G. P. Zimmerman, D. M. Fairman, R. A. Houghton, G. Marland, A. Z. Rose, and T. J. Wilbanks (eds.)]. National Oceanic and Atmospheric Administration, National Climatic Data Center, Asheville, NC, USA, 242 pp.
- Chan, F., A. B. Boehm, J. A. Barth, E. A. Chornesky, A. G. Dickson, R. A. Feely, B. Hales, T. M. Hill, G. Hofmann, D. Ianson, T. Klinger, J. Largier, J. Newton, T. F. Pedersen, G. N. Somero, M. Sutula, W. W. Wakefield, G. G. Waldbusser, S. B. Weisberg, and E. A. Whitman, 2016: *The West Coast Ocean Acidification and Hypoxia Science Panel: Major Findings, Recommendations, and Actions*. California Ocean Science Trust. [<http://westcoastcoastoh.org/wp-content/uploads/2016/04/OAH-Panel-Key-Findings-Recommendations-and-Actions-4.4.16-FINAL.pdf>]
- Chapa-Balcorta, C., J. M. Hernandez-Ayon, R. Durazo, E. Beier, S. R. Alin, and A. López-Pérez, 2015: Influence of post-Tehuano oceanographic processes in the dynamics of the CO₂ system in the Gulf of Tehuantepec, Mexico. *Journal of Geophysical Research: Oceans*, **120**(12), 7752-7770, doi: 10.1002/2015jc011249.
- Chavez, F. P., T. Takahashi, W. J. Cai, G. E. Friederich, B. Hales, R. Wanninkhof, and R. A. Feely, 2007: Coastal oceans. In: *First State of the Carbon Cycle Report (SOCCR): The North American Carbon Budget and Implications for the Global Carbon Cycle. A Report by the U.S. Climate Change Science Program and the Subcommittee on Global Change Research*. [A. King, W. L. Dilling, G. P. Zimmerman, D. M. Fairman, R. A. Houghton, G. Marland, A. Z. Rose, and T. J. Wilbanks (eds.)]. National Oceanic and Atmospheric Administration, National Climatic Data Center, Asheville, NC, USA, 157-166 pp.
- Chavez, F. P., M. Messie, and J. T. Pennington, 2011: Marine primary production in relation to climate variability and change. *Annual Review of Marine Science*, **3**, 227-260, doi: 10.1146/annurev.marine.010908.163917.
- Chavez, F. P., J. T. Pennington, R. P. Michisaki, M. Blum, G. M. Chavez, J. Friederich, B. Jones, R. Herlien, B. Kieft, B. Hobson, A. S. Ren, J. Ryan, J. C. Sevadjian, C. Wahl, K. R. Walz, K. Yamahara, G. E. Friederich, and M. Messié, 2017: Climate variability and change: Response of a coastal ocean ecosystem. *Oceanography*, **30**(4), 128-145, doi: 10.5670/oceanog.2017.429.
- Chelton, D. B., M. H. Freilich, and S. K. Esbensen, 2000a: Satellite observations of the wind jets off the Pacific Coast of Central America. Part I: Case studies and statistical characteristics. *Monthly Weather Review*, **128**(7), 1993-2018, doi: 10.1175/1520-0493(2000)128<1993:sootwj>2.0.co;2.
- Chelton, D. B., M. H. Freilich, and S. K. Esbensen, 2000b: Satellite observations of the wind jets off the Pacific Coast of Central America. Part II: Regional relationships and dynamical considerations. *Monthly Weather Review*, **128**(7), 2019-2043, doi: 10.1175/1520-0493(2000)128<2019:sootwj>2.0.co;2.
- Chen, C. T. A., 2004: Exchange of carbon in the coastal seas. In: *The Global Carbon Cycle: Integrating Human, Climate and the Natural World*. [C. B. Field and M. R. Raupach (eds.)]. SCOPE, Washington, DC, pp. 341-351.
- Chen, C. T. A., T. H. Huang, Y. C. Chen, Y. Bai, X. He, and Y. Kang, 2013: Air-sea exchanges of CO₂ in the world's coastal seas. *Biogeosciences*, **10**(10), 6509-6544, doi: 10.5194/bg-10-6509-2013.
- Crabeck, O., B. Delille, D. Thomas, N. X. Geilfus, S. Rysgaard, and J. L. Tison, 2014: CO₂ and CH₄ in sea ice from a subarctic fjord under influence of riverine input. *Biogeosciences*, **11**(23), 6525-6538, doi: 10.5194/bg-11-6525-2014.
- Crawford, W. R., and M. A. Peña, 2016: Decadal trends in oxygen concentration in subsurface waters of the north-east Pacific Ocean. *Atmosphere-Ocean*, **54**(2), 171-192, doi: 10.1080/07055900.2016.1158145.
- Cross, J. N., J. T. Mathis, K. E. Frey, C. E. Cosca, S. L. Danielson, N. R. Bates, R. A. Feely, T. Takahashi, and W. Evans, 2014a: Annual sea-air CO₂ fluxes in the Bering Sea: Insights from new autumn and winter observations of a seasonally ice-covered continental shelf. *Journal of Geophysical Research: Oceans*, **119**(10), 6693-6708, doi: 10.1002/2013jc009579.
- Cross, J., J. Mathis, N. Monacci, S. Musielewicz, S. Maenner, and J. Osborne, 2014b. *High-Resolution Ocean and Atmosphere pCO₂ Time-series Measurements from Mooring M2_164W_57N (NCEI Accession 0157599)*. Carbon Dioxide Information Analysis Center, U.S. Department of Energy, Oak Ridge National Laboratory, Oak Ridge, Tenn. doi: 10.3334/CDIAC/OTG.TSM_M2_164W_57N.
- Dai, M., Z. Cao, X. Guo, W. Zhai, Z. Liu, Z. Yin, Y. Xu, J. Gan, J. Hu, and C. Du, 2013: Why are some marginal seas sources of atmospheric CO₂? *Geophysical Research Letters*, **40**(10), 2154-2158, doi: 10.1002/grl.50390.
- DeGrandpre, M. D., G. J. Olbu, C. M. Beatty, and T. R. Hammar, 2002: Air-sea CO₂ fluxes on the US Middle Atlantic Bight. *Deep Sea Research Part II: Topical Studies in Oceanography*, **49**(20), 4355-4367, doi: 10.1016/s0967-0645(02)00122-4.
- Déry, S. J., M. Stieglitz, E. C. McKenna, and E. F. Wood, 2005: Characteristics and trends of river discharge into Hudson, James, and Ungava Bays, 1964-2000. *Journal of Climate*, **18**, 2540-2557, doi: 10.1175/JCLI3440.1.
- Dieckmann, G. S., G. Nehrke, S. Papadimitriou, J. Göttlicher, R. Steininger, H. Kennedy, D. Wolf-Gladrow, and D. N. Thomas, 2008: Calcium carbonate as ikaite crystals in Antarctic sea ice. *Geophysical Research Letters*, **35**(8), doi: 10.1029/2008gl033540.
- Dunne, J. P., J. L. Sarmiento, and A. Gnanadesikan, 2007: A synthesis of global particle export from the surface ocean and cycling through the ocean interior and on the seafloor. *Global Biogeochemical Cycles*, **21**(4), doi: 10.1029/2006gb002907.



- Else, B. G. T., T. N. Papakyriakou, M. A. Granskog, and J. J. Yackel, 2008: Observations of sea surface $f\text{CO}_2$ distributions and estimated air-sea CO_2 fluxes in the Hudson Bay region (Canada) during the open water season. *Journal of Geophysical Research-Oceans*, **113**, C08026, doi:10.1029/2007jc004389.
- Else, B. G. T., T. N. Papakyriakou, R. J. Galley, W. M. Drennan, L. A. Miller, and H. Thomas, 2011: Wintertime CO_2 fluxes in an Arctic polynya using eddy covariance: Evidence for enhanced air-sea gas transfer during ice formation. *Journal of Geophysical Research*, **116**, doi: 10.1029/2010jc006760.
- Else, B. G. T., T. N. Papakyriakou, M. G. Asplin, D. G. Barber, R. J. Galley, L. A. Miller, and A. Mucci, 2013: Annual cycle of air-sea CO_2 exchange in an Arctic polynya region. *Global Biogeochemical Cycles*, **27**(2), 388-398, doi: 10.1002/gbc.20016.
- Evans, W., and J. T. Mathis, 2013: The Gulf of Alaska coastal ocean as an atmospheric CO_2 sink. *Continental Shelf Research*, **65**, 52-63, doi: 10.1016/j.csr.2013.06.013.
- Evans, W., B. Hales, and P. G. Strutton, 2011: Seasonal cycle of surface ocean $p\text{CO}_2$ on the Oregon shelf. *Journal of Geophysical Research*, **116**(C5), doi: 10.1029/2010jc006625.
- Evans, W., B. Hales, P. G. Strutton, and D. Ianson, 2012: Sea-air CO_2 fluxes in the Western Canadian coastal ocean. *Progress in Oceanography*, **101**(1), 78-91, doi: 10.1016/j.pocean.2012.01.003.
- Evans, W., B. Hales, P. G. Strutton, R. K. Shearman, and J. A. Barth, 2015a: Failure to bloom: Intense upwelling results in negligible phytoplankton response and prolonged CO_2 outgassing over the Oregon Shelf. *Journal of Geophysical Research: Oceans*, **120**(3), 1446-1461, doi: 10.1002/2014jc010580.
- Evans, W., J. T. Mathis, J. N. Cross, N. R. Bates, K. E. Frey, B. G. T. Else, T. N. Papakyriakou, M. D. DeGrandpre, F. Islam, W.-J. Cai, B. Chen, M. Yamamoto-Kawai, E. Carmack, W. J. Williams, and T. Takahashi, 2015b: Sea-air CO_2 exchange in the western Arctic coastal ocean. *Global Biogeochemical Cycles*, **29**(8), 1190-1209, doi: 10.1002/2015gb005153.
- Evans, W., J. T. Mathis, and J. N. Cross, 2014: Calcium carbonate corrosivity in an Alaskan inland sea. *Biogeosciences*, **11**(2), 365-379, doi: 10.5194/bg-11-365-2014.
- Fabry, V., J. McClintock, J. Mathis, and J. Grebmeier, 2009: Ocean acidification at high latitudes: The bellwether. *Oceanography*, **22**(4), 160-171, doi: 10.5670/oceanog.2009.105.
- Fabry, V. J., B. A. Seibel, R. A. Feely, and J. C. Orr, 2008: Impacts of ocean acidification on marine fauna and ecosystem processes. *ICES Journal of Marine Science*, **65**(3), 414-432, doi: 10.1093/icesjms/fsn048.
- Feely, R. A., S. C. Doney, and S. R. Cooley, 2009: Ocean acidification: Present conditions and future changes in a high- CO_2 world. *Oceanography*, **22**(4), 36-47, doi: 10.5670/oceanog.2009.95.
- Feely, R. A., C. L. Sabine, J. M. Hernandez-Ayon, D. Ianson, and B. Hales, 2008: Evidence for upwelling of corrosive "acidified" water onto the continental shelf. *Science*, **320**(5882), 1490-1492, doi: 10.1126/science.1155676.
- Feely, R. A., C. L. Sabine, K. Lee, W. Berelson, J. Kleypas, V. J. Fabry, and F. J. Millero, 2004: Impact of anthropogenic CO_2 on the CaCO_3 system in the oceans. *Science*, **305**(5682), 362-366, doi: 10.1126/science.1097329.
- Feely, R. A., S. R. Alin, B. Carter, N. Bednaršek, B. Hales, F. Chan, T. M. Hill, B. Gaylord, E. Sanford, R. H. Byrne, C. L. Sabine, D. Greeley, and L. Juranek, 2016: Chemical and biological impacts of ocean acidification along the west coast of North America. *Estuarine, Coastal and Shelf Science*, doi: 10.1016/j.ecss.2016.08.043.
- Feely, R. A., R. R. Okazaki, W.-J. Cai, N. Bednaršek, S. R. Alin, R. H. Byrne, and A. Fassbender, 2018: The combined effects of acidification and hypoxia on pH and aragonite saturation in the coastal waters of the Californian Current Ecosystem and the northern Gulf of Mexico. *Continental Shelf Research*, **152**, 50-60, doi: 10.1016/j.csr.2017.11.002.
- Fennel, K., 2010: The role of continental shelves in nitrogen and carbon cycling: Northwestern North Atlantic case study. *Ocean Science*, **6**(2), 539-548, doi: 10.5194/os-6-539-2010.
- Fennel, K., and J. Wilkin, 2009: Quantifying biological carbon export for the northwest North Atlantic continental shelves. *Geophysical Research Letters*, **36**(18), doi: 10.1029/2009gl039818.
- Fennel, K., J. Wilkin, M. Previdi, and R. Najjar, 2008: Denitrification effects on air-sea CO_2 flux in the coastal ocean: Simulations for the northwest North Atlantic. *Geophysical Research Letters*, **35**(24), doi: 10.1029/2008gl036147.
- Fiechter, J., E. N. Curchitser, C. A. Edwards, F. Chai, N. L. Goebel, and F. P. Chavez, 2014: Air-sea CO_2 fluxes in the California current: Impacts of model resolution and coastal topography. *Global Biogeochemical Cycles*, **28**(4), 371-385, doi: 10.1002/2013gb004683.
- Franco, A. C., J. M. Hernández-Ayón, E. Beier, V. Garçon, H. Maske, A. Paulmier, J. Färber-Lorda, R. Castro, and R. Sosa-Ávalos, 2014: Air-sea CO_2 fluxes above the stratified oxygen minimum zone in the coastal region off Mexico. *Journal of Geophysical Research: Oceans*, **119**(5), 2923-2937, doi: 10.1002/2013jc009337.
- Friederich, G. E., P. M. Walz, M. G. Burczynski, and F. P. Chavez, 2002: Inorganic carbon in the central California upwelling system during the 1997-1999 El Niño-La Niña event. *Progress in Oceanography*, **54**(1-4), 185-203, doi: 10.1016/s0079-6611(02)00049-6.
- Gao, Z., L. Chen, H. Sun, B. Chen, and W.-J. Cai, 2012: Distributions and air-sea fluxes of carbon dioxide in the western Arctic Ocean. *Deep Sea Research Part II: Topical Studies in Oceanography*, **81-84**, 46-52, doi: 10.1016/j.dsr2.2012.08.021.



- García-Reyes, M., W. J. Sydeman, D. S. Schoeman, R. R. Rykaczewski, B. A. Black, A. J. Smit, and S. J. Bograd, 2015: Under pressure: Climate change, upwelling, and eastern boundary upwelling ecosystems. *Frontiers in Marine Science*, **2**, doi: 10.3389/fmars.2015.00109.
- Gattuso, J. P., and L. Hansson, (eds.) 2011: *Ocean Acidification*. Oxford University Press, New York, NY, USA, 326 pp.
- Gattuso, J. P., M. Frankignoulle, and R. Wollast, 1998: Carbon and carbonate metabolism in coastal aquatic ecosystems. *Annual Review of Ecology and Systematics*, **29**(1), 405-434, doi: 10.1146/annurev.ecolsys.29.1.405.
- Gaxiola-Castro, G., and F. E. Muller-Karger, 1998: Seasonal phytoplankton pigment variability in the Eastern Tropical Pacific Ocean as determined by CZCS imagery. In: *Remote Sensing Tropical Pacific Ocean by Satellites*. [R. A. Brown (ed.)]. Pan Ocean Remote Sensing Conference, 1998. Earth Ocean and Space Pty. Ltd., 271-277 pp.
- Golden, K. M., H. Eicken, A. L. Heaton, J. Miner, D. J. Pringle, and J. Zhu, 2007: Thermal evolution of permeability and microstructure in sea ice. *Geophysical Research Letters*, **34**(16), doi: 10.1029/2007gl030447.
- Gruber, N., C. Hauri, Z. Lachkar, D. Loher, T. L. Frolicher, and G. K. Plattner, 2012: Rapid progression of ocean acidification in the California Current System. *Science*, **337**(6091), 220-223, doi: 10.1126/science.1216773.
- Hales, B., T. Takahashi, and L. Bandstra, 2005: Atmospheric CO₂ uptake by a coastal upwelling system. *Global Biogeochemical Cycles*, **19**(1), doi: 10.1029/2004gb002295.
- Hales, B., L. Karp-Boss, A. Perlin, and P. A. Wheeler, 2006: Oxygen production and carbon sequestration in an upwelling coastal margin. *Global Biogeochemical Cycles*, **20**(3), doi: 10.1029/2005gb002517.
- Hales, B., W.-J. Cai, B. G. Mitchell, C. L. Sabine, and O. Schofield (eds.), 2008: *North American Continental Margins: A Synthesis and Planning Workshop. Report of the North American Continental Margins Working Group for the U.S. Carbon Cycle Scientific Steering Group and Interagency Working Group*. U.S. Carbon Cycle Science Program, 110 pp. [<http://www.globalchange.gov/browse/reports/north-american-continental-margins-synthesis-and-planning-workshop>]
- Hales, B., P. G. Stratton, M. Saraceno, R. Letelier, T. Takahashi, R. Feely, C. Sabine, and F. Chavez, 2012: Satellite-based prediction of pCO₂ in coastal waters of the eastern North Pacific. *Progress in Oceanography*, **103**, 1-15, doi: 10.1016/j.pocean.2012.03.001.
- Harris, K. E., M. D. DeGrandpre, and B. Hales, 2013: Aragonite saturation state dynamics in a coastal upwelling zone. *Geophysical Research Letters*, **40**(11), 2720-2725, doi: 10.1002/grl.50460.
- Hauri, C., P. Winsor, L. W. Juraneck, A. M. P. McDonnell, T. Takahashi, and J. T. Mathis, 2013: Wind-driven mixing causes a reduction in the strength of the continental shelf carbon pump in the Chukchi Sea. *Geophysical Research Letters*, **40**(22), S932-S936, doi: 10.1002/2013gl058267.
- Hautala, S. L., E. A. Solomon, H. P. Johnson, R. N. Harris, and U. K. Miller, 2014: Dissociation of Cascadia margin gas hydrates in response to contemporary ocean warming. *Geophysical Research Letters*, **41**(23), 8486-8494, doi: 10.1002/2014gl061606.
- Herrmann, M., R. G. Najjar, W. M. Kemp, R. B. Alexander, E. W. Boyer, W.-J. Cai, P. C. Griffith, K. D. Kroeger, S. L. McCallister, and R. A. Smith, 2015: Net ecosystem production and organic carbon balance of U.S. east coast estuaries: A synthesis approach. *Global Biogeochemical Cycles*, **29**(1), 96-111, doi: 10.1002/2013gb004736.
- Ho, D. T., R. Wanninkhof, P. Schlosser, D. S. Ullman, D. Hebert, and K. F. Sullivan, 2011: Toward a universal relationship between wind speed and gas exchange: Gas transfer velocities measured With ³He/SF₆ during the Southern Ocean Gas Exchange Experiment. *Journal of Geophysical Research*, **116**(C4), doi: 10.1029/2010jc006854.
- Huang, W. J., W. J. Cai, Y. Wang, S. E. Lohrenz, and M. C. Murrell, 2015: The carbon dioxide system on the Mississippi River-dominated continental shelf in the Northern Gulf of Mexico: 1. Distribution and air-sea CO₂ flux. *Journal of Geophysical Research: Oceans*, **120**(3), 1429-1445, doi: 10.1002/2014JC010498.
- Ianson, D., and S. E. Allen, 2002: A two-dimensional nitrogen and carbon flux model in a coastal upwelling region. *Global Biogeochemical Cycles*, **16**, doi: 10.1029/gb001451.
- IPCC, 2011: *Workshop Report of the Intergovernmental Panel on Climate Change Workshop on Impacts of Ocean Acidification on Marine Biology and Ecosystems*. [C. B. Field, V. Barros, T. F. Stocker, D. Qin, K. J. Mach, G.-K. Plattner, M. D. Mastrandrea, M. Tignor, and K. L. Eb (eds.)]. IPCC Working Group II Technical Support Unit, Carnegie Institution, Stanford, California, United States of America, 164 pp.
- Izett, J. and K. Fennel, 2018a: Estimating the cross-shelf export of riverine materials, Part 1: General relationships from an idealized numerical model. *Global Biogeochemical Cycles*, **32**, 160-175, doi:10.1002/2017GB005667.
- Izett, J. and K. Fennel, 2018b: Estimating the cross-shelf export of riverine materials, Part 2: Estimates of global freshwater and nutrient export. *Global Biogeochemical Cycles*, **32**, 176-186, doi:10.1002/2017GB005668.
- Jacox, M. G., S. J. Bograd, E. L. Hazen, and J. Fiechter, 2015: Sensitivity of the California current nutrient supply to wind, heat, and remote ocean forcing. *Geophysical Research Letters*, **42**(14), S950-S957, doi: 10.1002/2015gl065147.



- Jiang, L.-Q., W.-J. Cai, R. Wanninkhof, Y. Wang, and H. Lüger, 2008: Air-sea CO₂ fluxes on the U.S. South Atlantic Bight: Spatial and seasonal variability. *Journal of Geophysical Research*, **113**(C7), doi: 10.1029/2007jc004366.
- Jiang, L. Q., W. J. Cai, Y. Wang, and J. E. Bauer, 2013: Influence of terrestrial inputs on continental shelf carbon dioxide. *Biogeosciences*, **10**(2), 839-849, doi: 10.5194/bg-10-839-2013.
- Johnson, H. P., U. K. Miller, M. S. Salmi, and E. A. Solomon, 2015: Analysis of bubble plume distributions to evaluate methane hydrate decomposition on the continental slope. *Geochemistry, Geophysics, Geosystems*, **16**(11), 3825-3839, doi: 10.1002/2015gc005955.
- Kahru, M., Z. Lee, R. M. Kudela, M. Manzano-Sarabia, and B. Greg Mitchell, 2015: Multi-satellite time series of inherent optical properties in the California current. *Deep Sea Research Part II: Topical Studies in Oceanography*, **112**, 91-106, doi: 10.1016/j.dsr2.2013.07.023.
- Kim, B. M., S. W. Son, S. K. Min, J. H. Jeong, S. J. Kim, X. Zhang, T. Shim, and J. H. Yoon, 2014: Weakening of the stratospheric polar vortex by Arctic sea-ice loss. *Nature Communications*, **5**, 4646, doi: 10.1038/ncomms5646.
- Kuzyk, Z. Z. A., R. W. Macdonald, S. C. Johannessen, C. Gobeil, and G. A. Stern, 2009: Towards a sediment and organic carbon budget for Hudson Bay. *Marine Geology*, **264**(3-4), 190-208, doi: 10.1016/j.margeo.2009.05.006.
- Landwehr, S., S. D. Miller, M. J. Smith, E. S. Saltzman, and B. Ward, 2014: Analysis of the PKT correction for direct CO₂ flux measurements over the ocean. *Atmospheric Chemistry and Physics*, **14**(7), 3361-3372, doi: 10.5194/acp-14-3361-2014.
- Laruelle, G. G., W.-J. Cai, X. Hu, N. Gruber, F. T. Mackenzie, and P. Regnier, 2018: Continental shelves as a variable but increasing global sink for atmospheric carbon dioxide. *Nature Communications*, **9**, 454, doi: 10.1038/s41467-017-02738-z.
- Laruelle, G. G., R. Lauerwald, B. Pfeil, and P. Regnier, 2014: Regionalized global budget of the CO₂ exchange at the air-water interface in continental shelf seas. *Global Biogeochemical Cycles*, **28**(11), 1199-1214, doi: 10.1002/2014gb004832.
- Laruelle, G. G., H. H. Dürr, R. Lauerwald, J. Hartmann, C. P. Slomp, N. Goossens, and P. A. G. Regnier, 2013: Global multi-scale segmentation of continental and coastal waters from the watersheds to the continental margins. *Hydrology and Earth System Sciences*, **17**(5), 2029-2051, doi: 10.5194/hess-17-2029-2013.
- Laurent, A., K. Fennel, W.-J. Cai, W.-J. Huang, L. Barbero, and R. Wanninkhof, 2017: Eutrophication-induced acidification of coastal waters in the northern Gulf of Mexico: Insights into origin and processes from a coupled physical-biogeochemical model. *Geophysical Research Letters*, **44**(2), 946-956, doi: 10.1002/2016gl071881.
- Laurent, A., K. Fennel, D. S. Ko, J. Lehrter, 2018: Climate change projected to exacerbate impacts of coastal eutrophication in the northern Gulf of Mexico. *Journal of Geophysical Research-Oceans*, **123**, 3408-3426, doi: 10.1002/2017JC013583.
- Le Quéré, C., R. Moriarty, R. M. Andrew, J. G. Canadell, S. Sitch, J. I. Korsbakken, P. Friedlingstein, G. P. Peters, R. J. Andres, T. A. Boden, R. A. Houghton, J. I. House, R. F. Keeling, P. Tans, A. Arneth, D. C. E. Bakker, L. Barbero, L. Bopp, J. Chang, F. Chevallier, L. P. Chini, P. Ciais, M. Fader, R. A. Feely, T. Gkritzalis, I. Harris, J. Hauck, T. Ilyina, A. K. Jain, E. Kato, V. Kitidis, K. Klein Goldewijk, C. Koven, P. Landschützer, S. K. Lauvset, N. Lefèvre, A. Lenton, I. D. Lima, N. Metz, F. Millero, D. R. Munro, A. Murata, J. E. M. S. Nabel, S. Nakaoka, Y. Nojiri, K. O'Brien, A. Olsen, T. Ono, F. F. Pérez, B. Pfeil, D. Pierrot, B. Poulter, G. Rehder, C. Rödenbeck, S. Saito, U. Schuster, J. Schwinger, R. Séférian, T. Steinhoff, B. D. Stocker, A. J. Sutton, T. Takahashi, B. Tilbrook, I. T. van der Laan-Luijkx, G. R. van der Werf, S. van Heuven, D. Vandemark, N. Viovy, A. Wiltshire, S. Zaehle, and N. Zeng, 2015: Global carbon budget 2015. *Earth System Science Data*, **7**(2), 349-396, doi: 10.5194/essd-7-349-2015.
- Liao, E., W. Lu, X.-H. Yan, Y. Jiang, and A. Kidwell, 2015: The coastal ocean response to the global warming acceleration and hiatus. *Scientific Reports*, **5**, 16630, doi: 10.1038/srep16630.
- Liu, K., K. L. Atkinson, R. A. Quinones, and L. Talaue-McManus, 2010: *Carbon and Nutrient Fluxes in Continental Margins: A Global Synthesis*. Springer.
- Lluch-Cota S. E., S. Alvarez-Borrego, E. Santamaría-del-Angel, F. E. Muller-Karger, and S. Hernández-Vázquez, 1997: El Golfo de Tehuantepec y áreas adyacentes: Variación espacio-temporal de pigmentos forosintéticos derivados de satélite. *Ciencias Marinas*, **23**(3):329-340.
- Loder, J. W., B. Petrie, and G. Gawarkiewicz, 1998: The coastal ocean off northeastern North America: A large-scale view. In: *The Sea*. [A. R. Robinson and K. H. Brink (eds.)]. John Wiley & Sons, Inc., New York, NY, 105-133 pp.
- Lohrenz, S., and P. Verity, 2004: Regional oceanography: Southeastern United States and Gulf of Mexico. In: *The Sea: Ideas and Observations on Progress in the Study of Seas. Volume 14. Interdisciplinary Regional Studies and Syntheses*. [A. R. Robinson and K. H. Brink (eds.)], 169-224 pp.
- Lohrenz, S. E., W.-J. Cai, W.-J. Huang, X. Guo, R. He, Z. Xue, K. Fennel, S. Chakraborty, S. Howden, and H. Tian, 2018: Satellite estimation of coastal pCO₂ and air-sea flux of carbon dioxide in the Northern Gulf of Mexico. *Remote Sensing of Environment*, **207**, 71-83.
- Mannino, A., S. R. Signorini, M. G. Novak, J. Wilkin, M. A. M. Friedrichs, and R. G. Najjar, 2016: Dissolved organic carbon fluxes in the Middle Atlantic Bight: An integrated approach based on satellite data and ocean model products. *Journal of Geophysical Research: Biogeosciences*, **121**(2), 312-336, doi: 10.1002/2015jg003031.



- Mathis, J., A. Sutton, C. Sabine, S. Musielewicz, and S. Maenner. 2013. *High-Resolution Ocean and Atmosphere pCO₂ Time-Series Measurements from Mooring WA_125W_47N (NODC Accession 0115322)*. Carbon Dioxide Information Analysis Center, U.S. Department of Energy, Oak Ridge National Laboratory, Oak Ridge, Tenn. doi:10.3334/CDIAC/OTG.TSM_WA_125W_47N.
- Mathis, J. T., and N. R. Bates, 2010: The marine carbon cycle of the Arctic Ocean: Some thoughts about the controls on air-sea CO₂ exchanges and responses to ocean acidification. *Ocean Carbon and Biogeochemistry News*, **3**(2), 1-5.
- Mathis, J. T., J. N. Cross, and N. R. Bates, 2011: Coupling primary production and terrestrial runoff to ocean acidification and carbonate mineral suppression in the Eastern Bering Sea. *Journal of Geophysical Research*, **116**(C2), doi: 10.1029/2010jc006453.
- Mathis, J. T., J. N. Cross, W. Evans, and S. C. Doney, 2015a: Ocean acidification in the surface waters of the Pacific-Arctic boundary regions. *Oceanography*, **25**(2), 122-135, doi: 10.5670/oceanog.2015.36.
- Mathis, J. T., S. R. Cooley, N. Lucey, S. Colt, J. Ekstrom, T. Hurst, C. Hauri, W. Evans, J. N. Cross, and R. A. Feely, 2015b: Ocean acidification risk assessment for Alaska's fishery sector. *Progress in Oceanography*, **136**, 71-91, doi: 10.1016/j.pocean.2014.07.001.
- McClatchie, S., A. R. Thompson, S. R. Alin, S. Siedlecki, W. Watson, and S. J. Bograd, 2016: The influence of Pacific equatorial water on fish diversity in the Southern California Current System. *Journal of Geophysical Research: Oceans*, **121**(8), 6121-6136, doi: 10.1002/2016jc011672.
- McGuire, A. D., L. G. Anderson, T. R. Christensen, S. Dallimore, L. Guo, D. J. Hayes, M. Heimann, T. D. Lorenson, R. W. Macdonald, and N. Roulet, 2009: Sensitivity of the carbon cycle in the Arctic to climate change. *Ecological Monographs*, **79**(4), 523-555, doi: 10.1890/08-2025.1.
- Meinville, M., and G. C. Johnson, 2013: Decadal water-property trends in the California Undercurrent, with implications for ocean acidification. *Journal of Geophysical Research: Oceans*, **118**(12), 6687-6703, doi: 10.1002/2013JC009299.
- Miller, L. A., R. W. Macdonald, F. McLaughlin, A. Mucci, M. Yamamoto-Kawai, K. E. Giesbrecht, and W. J. Williams, 2014: Changes in the marine carbonate system of the Western Arctic: Patterns in a rescued data set. *Polar Research*, **33**(0), doi: 10.3402/polar.v33.20577.
- Miller, L. A., F. Fripiat, B. G. T. Else, J. S. Bowman, K. A. Brown, R. E. Collins, M. Ewert, A. Fransson, M. Gosselin, D. Lannuzel, K. M. Meiners, C. Michel, J. Nishioka, D. Nomura, S. Papadimitriou, L. M. Russell, L. L. Sørensen, D. N. Thomas, J.-L. Tison, M. A. van Leeuwe, M. Vancoppenolle, E. W. Wolff, and J. Zhou, 2015: Methods for biogeochemical studies of sea ice: The state of the art, caveats, and recommendations. *Elementa: Science of the Anthropocene*, **3**, 000038, doi: 10.12952/journal.elementa.000038.
- Moore, S. E., and P. J. Stabeno, 2015: Synthesis of Arctic Research (SOAR) in marine ecosystems of the Pacific Arctic. *Progress in Oceanography*, **136**, 1-11, doi: 10.1016/j.pocean.2015.05.017.
- Mucci, A., B. Lansard, L. A. Miller, and T. N. Papakyriakou, 2010: CO₂ fluxes across the air-sea interface in the Southeastern Beaufort Sea: Ice-free period. *Journal of Geophysical Research*, **115**(C4), doi: 10.1029/2009jc005330.
- Muller-Karger, F. E., R. Varela, R. Thunell, R. Luerssen, C. M. Hu, and J. J. Walsh, 2005: The importance of continental margins in the global carbon cycle. *Geophysical Research Letters*, **32**(1), doi: 10.1029/2004gl021346.
- Muller-Karger, F. E., J. P. Smith, S. Werner, R. Chen, M. Roffer, Y. Y. Liu, B. Muhling, D. Lindo-Atichati, J. Lamkin, S. Cerdeira-Estrada, and D. B. Enfield, 2015: Natural variability of surface oceanographic conditions in the offshore Gulf of Mexico. *Progress in Oceanography*, **134**, 54-76, doi: 10.1016/j.pocean.2014.12.007.
- Najjar, R. G., M. Friedrichs, and W. J. Cai, 2012: *Report of the U.S. East Coast Carbon Cycle Synthesis Workshop, January 19-20, 2012*. Ocean Carbon and Biogeochemistry Program and North American Carbon Program. 34 pp. [https://www.us-ocb.org/wp-content/uploads/sites/43/2017/02/East_coast_syn_report_FINAL.pdf]
- Najjar, R. G., M. Herrmann, R. Alexander, E. W. Boyer, D. J. Burdige, D. Butman, W.-J. Cai, E. A. Canuel, R. F. Chen, M. A. M. Friedrichs, R. A. Feagin, P. C. Griffith, A. L. Hinson, J. R. Holmquist, X. Hu, W. M. Kemp, K. D. Kroeger, A. Mannino, S. L. McCallister, W. R. McGillis, M. R. Mulholland, C. H. Pilskaln, J. Salisbury, S. R. Signorini, P. St-Laurent, H. Tian, M. Tzortziou, P. Vlahos, Z. A. Wang, and R. C. Zimmerman, 2018: Carbon budget of tidal wetlands, estuaries, and shelf waters of eastern North America. *Global Biogeochemical Cycles*, **32**, 389-416, doi: 10.1002/2017GB005790.
- Orr, J. C., V. J. Fabry, O. Aumont, L. Bopp, S. C. Doney, R. A. Feely, A. Gnanadesikan, N. Gruber, A. Ishida, F. Joos, R. M. Key, K. Lindsay, E. Maier-Reimer, R. Matear, P. Monfray, A. Mouchet, R. G. Najjar, G. K. Plattner, K. B. Rodgers, C. L. Sabine, J. L. Sarmiento, R. Schlitzer, R. D. Slater, I. J. Totterdell, M. F. Weirig, Y. Yamanaka, and A. Yool, 2005: Anthropogenic ocean acidification over the twenty-first century and its impact on calcifying organisms. *Nature*, **437**(7059), 681-686, doi: 10.1038/nature04095.
- Parmentier, F.-J. W., A. Silyakova, A. Biastoch, K. Kretschmer, and G. Panieri, 2015: Natural marine methane sources in the Arctic. *AMAP Assessment 2015: Methane as an Arctic Climate Forcer*. Arctic Monitoring and Assessment Programme. 139 pp. [<https://www.amap.no/documents/doc/amap-assessment-2015-methane-as-an-arctic-climate-forcer/1285>]
- Parmentier, F.-J. W., T. R. Christensen, L. L. Sørensen, S. Rysgaard, A. D. McGuire, P. A. Miller, and D. A. Walker, 2013: The impact of lower sea-ice extent on Arctic greenhouse-gas exchange. *Nature Climate Change*, **3**(3), 195-202, doi: 10.1038/nclimate1784.



- Pennington, J. T., G. E. Friedrich, C. G. Castro, C. A. Collins, W. W. Evans, and F. P. Chavez, 2010: The northern and central California upwelling coastal upwelling system. In: *Carbon and Nutrient Fluxes in Continental Margins: A Global Synthesis*. [K.-K. Liu, L. Atkinson, R. A. Quiñones, and L. Talua-McManus (eds.)]. Springer, 29-43 pp.
- Peterson, J. O., C. A. Morgan, W. T. Peterson, and E. D. Lorenzo, 2013: Seasonal and interannual variation in the extent of hypoxia in the Northern California current from 1998-2012. *Limnology and Oceanography*, **58**(6), 2279-2292, doi: 10.4319/lo.2013.58.6.2279.
- Phrampus, B. J., and M. J. Hornbach, 2012: Recent changes to the gulf stream causing widespread gas hydrate destabilization. *Nature*, **490**(7421), 527-530, doi: 10.1038/nature11528.
- Pilcher, D. J., S. A. Siedlecki, A. J. Hermann, K. O. Coyle, J. T. Mathis, and W. Evans, 2018: Simulated impact of glacial runoff on CO₂ uptake in the Gulf of Alaska. *Geophysical Research Letters*, **45**, 880-890. doi: 10.1002/2017GL075910
- Previdi, M., K. Fennel, J. Wilkin, and D. Haidvogel, 2009: Interannual variability in atmospheric CO₂ uptake on the northeast U.S. continental shelf. *Journal of Geophysical Research*, **114**(G4), doi: 10.1029/2008jg000881.
- Regnier, P., P. Friedlingstein, P. Ciais, F. T. Mackenzie, N. Gruber, I. A. Janssens, G. G. Laruelle, R. Lauerwald, S. Luyssaert, A. J. Andersson, S. Arndt, C. Arnosti, A. V. Borges, A. W. Dale, A. Gallego-Sala, Y. Goddérís, N. Goossens, J. Hartmann, C. Heinze, T. Ilyina, F. Joos, D. E. LaRowe, J. Leifeld, F. J. R. Meysman, G. Munhoven, P. A. Raymond, R. Spahni, P. Suntharalingam, and M. Thullner, 2013: Anthropogenic perturbation of the carbon fluxes from land to ocean. *Nature Geoscience*, **6**(8), 597-607, doi: 10.1038/ngeo1830.
- Rivas, D., A. Badan, and J. Ochoa, 2005: The ventilation of the deep Gulf of Mexico. *Journal of Physical Oceanography*, **35**(10), 1763-1781, doi: 10.1175/jpo2786.1.
- Robbins, L. L., R. Wanninkhof, L. Barbero, X. Hu, S. Mitra, S. Yvon-Lewis, W. Cai, W. Huang, and T. Ryerson, 2009: Air-sea exchange. *Report of the U.S. Gulf of Mexico Carbon Cycle Synthesis Workshop*. Ocean Carbon and Biogeochemistry Program and North American Carbon Program. 63 pp.
- Robbins, L. L., R. Wanninkhof, L. Barbero, X. Hu, S. Mitra, S. Yvon-Lewis, W.-J. Cai, W.-J. Huang, and T. Ryerson, 2014: Air-sea exchange. 2014. *Report of The U.S. Gulf of Mexico Carbon Cycle Synthesis Workshop, March 27-28, 2013*. [H. M. Benway and P. G. Coble (eds.)]. Ocean Carbon and Biogeochemistry Program and North American Carbon Program, 17-23 pp. [https://www.us-ocb.org/wp-content/uploads/sites/43/2017/01/GMx_report_FINAL.pdf]
- Rutgers van der Loeff, M. M., N. Cassar, M. Nicolaus, B. Rabe, and I. Stimac, 2014: The influence of sea ice cover on air-sea gas exchange estimated with radon-222 profiles. *Journal of Geophysical Research: Oceans*, **119**(5), 2735-2751, doi: 10.1002/2013jc009321.
- Rykaczewski, R. R., and D. M. Checkley, Jr., 2008: Influence of ocean winds on the pelagic ecosystem in upwelling regions. *Proceedings of the National Academy of Sciences USA*, **105**(6), 1965-1970, doi: 10.1073/pnas.0711777105.
- Rykaczewski, R. R., J. P. Dunne, W. J. Sydeman, M. García-Reyes, B. A. Black, and S. J. Bograd, 2015: Poleward displacement of coastal upwelling-favorable winds in the ocean's eastern boundary currents through the 21st century. *Geophysical Research Letters*, **42**(15), 6424-6431, doi: 10.1002/2015gl064694.
- Rysgaard, S., R. N. Glud, M. K. Sejr, J. Bendtsen, and P. B. Christensen, 2007: Inorganic carbon transport during sea ice growth and decay: A carbon pump in polar seas. *Journal of Geophysical Research*, **112**(C3), doi: 10.1029/2006jc003572.
- Rysgaard, S., J. Bendtsen, L. T. Pedersen, H. Ramløv, and R. N. Glud, 2009: Increased CO₂ uptake due to sea ice growth and decay in the Nordic Seas. *Journal of Geophysical Research*, **114**(C9), doi: 10.1029/2008jc005088.
- Rysgaard, S., D. H. Søgaard, M. Cooper, M. Pücko, K. Lennert, T. N. Papakyriakou, F. Wang, N. X. Geilfus, R. N. Glud, J. Ehn, D. F. McGinnis, K. Attard, J. Sievers, J. W. Deming, and D. Barber, 2013: Ikaite crystal distribution in winter sea ice and implications for CO₂ system dynamics. *The Cryosphere*, **7**(2), 707-718, doi: 10.5194/tc-7-707-2013.
- Sabine, C. L., and T. Tanhua, 2010: Estimation of anthropogenic CO₂ inventories in the ocean. *Annual Review of Marine Science*, **2**, 175-198, doi: 10.1146/annurev-marine-120308-080947.
- Sabine, C. L., R. A. Feely, N. Gruber, R. M. Key, K. Lee, J. L. Bullister, R. Wanninkhof, C. S. Wong, D. W. Wallace, B. Tilbrook, F. J. Millero, T. H. Peng, A. Kozyr, T. Ono, and A. F. Rios, 2004: The oceanic sink for anthropogenic CO₂. *Science*, **305**(5682), 367-371, doi: 10.1126/science.1097403.
- Salisbury, J., D. Vandemark, C. Hunt, J. Campbell, B. Jonsson, A. Mahadevan, W. McGillis, and H. Xue, 2009: Episodic riverine influence on surface DIC in the coastal Gulf of Maine. *Estuarine, Coastal and Shelf Science*, **82**(1), 108-118, doi: 10.1016/j.ecss.2008.12.021.
- Salisbury, J., M. Green, C. Hunt, and J. Campbell, 2008a: Coastal acidification by rivers: A threat to shellfish? *Eos Transactions*, **89**(50), 513-513, doi: 10.1029/2008eo500001.
- Salisbury, J. E., D. Vandemark, C. W. Hunt, J. W. Campbell, W. R. McGillis, and W. H. McDowell, 2008b: Seasonal observations of surface waters in two Gulf of Maine estuary-plume systems: Relationships between watershed attributes, optical measurements and surface pCO₂. *Estuarine, Coastal and Shelf Science*, **77**(2), 245-252, doi: 10.1016/j.ecss.2007.09.033.
- Semiletov, I. P., I. I. Pipko, I. Repina, and N. E. Shakhova, 2007: Carbonate chemistry dynamics and carbon dioxide fluxes across the atmosphere-ice-water interfaces in the Arctic Ocean: Pacific sector of the Arctic. *Journal of Marine Systems*, **66**(1-4), 204-226, doi: 10.1016/j.jmarsys.2006.05.012.



- Shadwick, E. H., H. Thomas, A. Comeau, S. E. Craig, C. W. Hunt, and J. E. Salisbury, 2010: Air-sea CO₂ fluxes on the Scotian Shelf: Seasonal to multi-annual variability. *Biogeosciences*, **7**(11), 3851-3867, doi: 10.5194/bg-7-3851-2010.
- Shadwick, E. H., H. Thomas, M. Chierici, B. Else, A. Fransson, C. Michel, L. A. Miller, A. Mucci, A. Niemi, T. N. Papakyriakou, and J. É. Tremblay, 2011: Seasonal variability of the inorganic carbon system in the Amundsen Gulf region of the Southeastern Beaufort Sea. *Limnology and Oceanography*, **56**(1), 303-322, doi: 10.4319/lo.2011.56.1.0303.
- Shakhova, N. E., I. Semiletov, V. Sergienko, L. Lobkovsky, V. Yusupov, A. Salyuk, A. Salomatin, D. Chernykh, D. Kosmach, G. Panteleev, D. Nicolsky, V. Samarkin, S. Joye, A. Charkin, O. Dudarev, A. Meluzov, and O. Gustafsson, 2015: The East Siberian Arctic shelf: Towards further assessment of permafrost-related methane fluxes and role of sea ice. *Philosophical Transactions of the Royal Society A: Mathematical, Physical and Engineering Sciences*, **373**(2051), doi: 10.1098/rsta.2014.0451.
- Sharples, J., J. J. Middelburg, K. Fennel, and T. D. Jickells, 2017: What proportion of riverine nutrients reaches the open ocean? *Global Biogeochemical Cycles*, **31**(1), 39-58, doi: 10.1002/2016gb005483.
- Siedlecki, S. A., D. J. Pilcher, A. J. Hermann, K. Coyle, and J. Mathis, 2017: The importance of freshwater to spatial variability of aragonite saturation state in the Gulf of Alaska. *Journal of Geophysical Research: Oceans*, **122**, doi: 10.1002/2017JC012791.
- Siedlecki, S. A., I. C. Kaplan, A. J. Hermann, T. T. Nguyen, N. A. Bond, J. A. Newton, G. D. Williams, W. T. Peterson, S. R. Alin, and R. A. Feely, 2016: Experiments with Seasonal Forecasts of ocean conditions for the Northern region of the California Current upwelling system. *Scientific Reports*, **6**, 27203, doi: 10.1038/srep27203.
- Signorini, S. R., A. Mannino, R. G. Najjar, M. A. M. Friedrichs, W.-J. Cai, J. Salisbury, Z. A. Wang, H. Thomas, and E. Shadwick, 2013: Surface ocean pCO₂ seasonality and sea-air CO₂ flux estimates for the North American East Coast. *Journal of Geophysical Research: Oceans*, **118**(10), 5439-5460, doi: 10.1002/jgrc.20369.
- Skarke, A., C. Ruppel, M. Kodis, D. Brothers, and E. Lobecker, 2014: Widespread methane leakage from the sea floor on the northern US Atlantic Margin. *Nature Geoscience*, **7**(9), 657-661, doi: 10.1038/ngeo2232.
- Smith, W. O., Jr., and D. G. Barber, 2007: *Polynyas: Windows to the World*. Elsevier Oceanography Series Vol. 1.17, Elsevier, Oxford, UK, 458 pp.
- Solomon, E. A., M. Kastner, I. R. MacDonald, and I. Leifer, 2009: Considerable methane fluxes to the atmosphere from hydrocarbon seeps in the Gulf of Mexico. *Nature Geoscience*, **2**(8), 561-565, doi: 10.1038/ngeo574.
- Somero, G. N., J. M. Beers, F. Chan, T. M. Hill, T. Klinger, and S. Y. Litvin, 2016: What changes in the carbonate system, oxygen, and temperature portend for the northeastern Pacific Ocean: A physiological perspective. *BioScience*, **66**(1), 14-26, doi: 10.1093/biosci/biv162.
- Steinacher, M., F. Joos, T. L. Frölicher, G. K. Plattner, and S. C. Doney, 2009: Imminent ocean acidification in the Arctic projected with the NCAR global coupled carbon cycle-climate model. *Biogeosciences*, **6**(4), 515-533, doi: 10.5194/bg-6-515-2009.
- Steiner, N., K. Azetsu-Scott, J. Hamilton, K. Hedges, X. Hu, M. Y. Janjua, D. Lavoie, J. Loder, H. Melling, A. Merzouk, W. Perrie, I. Peterson, M. Scarratt, T. Sou, and R. Tallmann, 2015: Observed trends and climate projections affecting marine ecosystems in the Canadian Arctic. *Environmental Reviews*, **23**(2), 191-239, doi: 10.1139/er-2014-0066.
- Steiner, N. S., W. G. Lee, and J. R. Christian, 2013: Enhanced gas fluxes in small sea ice leads and cracks: Effects on CO₂ exchange and ocean acidification. *Journal of Geophysical Research: Oceans*, **118**(3), 1195-1205, doi: 10.1002/jgrc.20100.
- Steiner, N. S., J. R. Christian, K. D. Six, A. Yamamoto, and M. Yamamoto-Kawai, 2014: Future ocean acidification in the Canada basin and surrounding Arctic ocean from CMIP5 Earth system models. *Journal of Geophysical Research: Oceans*, **119**(1), 332-347, doi: 10.1002/2013jc009069.
- Stroeve, J. C., M. C. Serreze, M. M. Holland, J. E. Kay, J. Malanik, and A. P. Barrett, 2012: The Arctic's rapidly declining sea ice cover: A research synthesis. *Climatic Change*, **110**, 1005-1027, doi: 10.1007/s10584-011-0101-1.
- Sutton, A., C. Sabine, W.-J. Cai, S. Noakes, S. Musielewicz, S. Maenner, C. Dietrich, R. Bott, and J. Osborne, 2011. *High-Resolution Ocean and Atmosphere pCO₂ Time-Series Measurements from Mooring GraysRf_81W_31N (NODC Accession 0109904)*. Carbon Dioxide Information Analysis Center, U.S. Department of Energy, Oak Ridge National Laboratory, Oak Ridge, Tenn. doi: 10.3334/CDIAC/OTG.TSM_GRAYS-RF_81W_31N.
- Sutton, A., C. Sabine, U. Send, M. Ohman, S. Musielewicz, S. Maenner, C. Dietrich, R. Bott, and J. Osborne, 2012: *High-Resolution Ocean and Atmosphere pCO₂ Time-Series Measurements from Mooring CCE2_121W_34N (NODC Accession 0084099)*. Version 4.4. National Oceanographic Data Center, NOAA. Dataset. doi: 10.3334/CDIAC/OTG.TSM_CCE2_121W_34N.
- Sutton, A., C. Sabine, J. Salisbury, D. Vandemark, S. Musielewicz, S. Maenner, C. Dietrich, R. Bott, and J. Osborne, 2013. *High-Resolution Ocean and Atmosphere pCO₂ Time-Series Measurements from Mooring NH_70W_43N (NODC Accession 0115402)*. Carbon Dioxide Information Analysis Center, U.S. Department of Energy, Oak Ridge National Laboratory, Oak Ridge, Tenn. doi: 10.3334/CDIAC/OTG.TSM_NH_70W_43N.



- Sydean, W. J., M. Garcia-Reyes, D. S. Schoeman, R. R. Rykaczewski, S. A. Thompson, B. A. Black, and S. J. Bograd, 2014: Climate change. Climate change and wind intensification in coastal upwelling ecosystems. *Science*, **345**(6192), 77-80, doi: 10.1126/science.1251635.
- Takahashi, T., S. C. Sutherland, R. Wanninkhof, C. Sweeney, R. A. Feely, D. W. Chipman, B. Hales, G. Friederich, F. Chavez, C. Sabine, A. Watson, D. C. E. Bakker, U. Schuster, N. Metzl, H. Yoshikawa-Inoue, M. Ishii, T. Midorikawa, Y. Nojiri, A. Körtzinger, T. Steinhoff, M. Hoppema, J. Olafsson, T. S. Arnarson, B. Tilbrook, T. Johannessen, A. Olsen, R. Bellerby, C. S. Wong, B. Delille, N. R. Bates, and H. J. W. de Baar, 2009: Climatological mean and decadal change in surface ocean $p\text{CO}_2$, and net sea-air CO_2 flux over the global oceans. *Deep Sea Research Part II: Topical Studies in Oceanography*, **56**(8-10), 554-577, doi: 10.1016/j.dsr2.2008.12.009.
- Thunell, R., C. Benitez-Nelson, R. Varela, Y. Astor, and F. Muller-Karger, 2007: Particulate organic carbon fluxes along upwelling-dominated continental margins: Rates and mechanisms. *Global Biogeochemical Cycles*, **21**(1), doi: 10.1029/2006gb002793.
- Tsunogai, S., S. Watanabe, and T. Sato, 1999: Is there a "continental shelf pump" for the absorption of atmospheric CO_2 ? *Tellus B: Chemical and Physical Meteorology*, **51**(3), doi: 10.3402/tellusb.v51i3.16468.
- Turi, G., Z. Lachkar, and N. Gruber, 2014: Spatiotemporal variability and drivers of $p\text{CO}_2$ and air-sea CO_2 fluxes in the California Current System: An eddy-resolving modeling study. *Biogeosciences*, **11**(3), 671-690, doi: 10.5194/bg-11-671-2014.
- Turi, G., Z. Lachkar, N. Gruber, and M. Münnich, 2016: Climatic modulation of recent trends in ocean acidification in the California Current System. *Environmental Research Letters*, **11**(1), 014007, doi: 10.1088/1748-9326/11/1/014007.
- Turk, D., J. M. Bedard, W. J. Burt, S. Vagle, H. Thomas, K. Azetsu-Scott, W. R. McGillis, S. J. Iverson, and D. W. R. Wallace, 2016: Inorganic carbon in a high latitude estuary-fjord system in Canada's eastern Arctic. *Estuarine, Coastal and Shelf Science*, **178**, 137-147, doi: 10.1016/j.ecss.2016.06.006.
- Vandemark, D., J. E. Salisbury, C. W. Hunt, S. M. Shellito, J. D. Irish, W. R. McGillis, C. L. Sabine, and S. M. Maenner, 2011: Temporal and spatial dynamics of CO_2 air-sea flux in the Gulf of Maine. *Journal of Geophysical Research*, **116**(C1), doi: 10.1029/2010jc006408.
- Vlahos, P., R. F. Chen, and D. J. Repeta, 2002: Dissolved organic carbon in the Mid-Atlantic Bight. *Deep Sea Research Part II: Topical Studies in Oceanography*, **49**(20), 4369-4385, doi: 10.1016/s0967-0645(02)00167-4.
- Wang, Z. A., and W.-J. Cai, 2004: Carbon dioxide degassing and inorganic carbon export from a marsh-dominated estuary (the Duplin River): A marsh CO_2 pump. *Limnology and Oceanography*, **49**(2), 341-354, doi: 10.4319/lo.2004.49.2.0341.
- Wang, Z. A., W.-J. Cai, Y. Wang, and H. Ji, 2005: The Southeastern Continental Shelf of the United States as an atmospheric CO_2 source and an exporter of inorganic carbon to the ocean. *Continental Shelf Research*, **25**(16), 1917-1941, doi: 10.1016/j.csr.2005.04.004.
- Wang, Z. A., G. L. Lawson, C. H. Pilskaln, and A. E. Maas, 2017. Seasonal controls of aragonite saturation states in the Gulf of Maine. *Journal of Geophysical Research: Oceans* **122**: 372-389. doi: 10.1002/2016jc012373.
- Wang, Z. A., R. Wanninkhof, W.-J. Cai, R. H. Byrne, X. Hu, T.-H. Peng, and W.-J. Huang, 2013: The marine inorganic carbon system along the Gulf of Mexico and Atlantic coasts of the United States: Insights from a transregional coastal carbon study. *Limnology and Oceanography*, **58**(1), 325-342, doi: 10.4319/lo.2013.58.1.0325.
- Wanninkhof, R., L. Barbero, R. Byrne, W. J. Cai, W. J. Huang, J. Z. Zhang, M. Baringer, and C. Langdon, 2015: Ocean acidification along the Gulf Coast and East coast of the USA. *Continental Shelf Research*, **98**, 54-71, doi: 10.1016/j.csr.2015.02.008.
- Weber, T. C., L. Mayer, K. Jerram, J. Beaudoin, Y. Rzhanov, and D. Lovalvo, 2014: Acoustic estimates of methane gas flux from the seabed in a 6000 km² region in the northern Gulf of Mexico. *Geochemistry, Geophysics, Geosystems*, **15**(5), 1911-1925, doi: 10.1002/2014gc005271.
- Xue, Z., R. He, K. Fennel, W. J. Cai, S. Lohrenz, and C. Hopkinson, 2013: Modeling ocean circulation and biogeochemical variability in the Gulf of Mexico. *Biogeosciences*, **10**(11), 7219-7234, doi: 10.5194/bg-10-7219-2013.
- Xue, Z., R. He, K. Fennel, W.-J. Cai, S. Lohrenz, W.-J. Huang, H. Tian, W. Ren, and Z. Zang, 2016: Modeling $p\text{CO}_2$ variability in the Gulf of Mexico. *Biogeosciences*, **13**(15), 4359-4377, doi: 10.5194/bg-13-4359-2016.
- Yamamoto-Kawai, M., F. McLaughlin, and E. Carmack, 2013: Ocean acidification in the three oceans surrounding northern North America. *Journal of Geophysical Research: Oceans*, **118**(11), 6274-6284, doi: 10.1002/2013jc009157.
- Yasunaka, S., A. Murata, E. Watanabe, M. Chierici, A. Fransson, S. van Heuven, M. Hoppema, M. Ishii, T. Johannessen, N. Kosugi, S. K. Lauvset, J. T. Mathis, S. Nishino, A. M. Omar, A. Olsen, D. Sasano, T. Takahashi, and R. Wanninkhof, 2016: Mapping of the air-sea CO_2 flux in the Arctic Ocean and its adjacent seas: Basin-wide distribution and seasonal to interannual variability. *Polar Science*, **10**(3), 323-334, doi: 10.1016/j.polar.2016.03.006.